The Synthesis and Characterisation of Polydentate/Polyamine Phosphonate Complexes of Cobalt(III) and Their Imine Precursors

A thesis submitted in partial fulfilment of the requirements

for the Degree of **Doctor of Philosophy** in **Bioinorganic Chemistry** at the **University of Canterbury**

by

Nneka Daniel Ekekwe

Supervisors: Professor Richard Hartshorn

Dr. Jan Wikaira

2019

Abstract

This thesis reports the synthesis and characterisation of polydentate/polyamine phosphonate complexes of cobalt(III) and their imine precursors. The complexes prepared during this project have been characterised by a range of techniques, including: $^{13}C\{^{1}H\}$, $^{31}P\{^{1}H\}$, and ^{1}H NMR spectroscopy; UV-visible spectroscopy; mass spectrometry; infra-red spectroscopy; elemental analysis; and single crystal X-ray structure determination. A total of seventeen single crystal X-ray structure determinations have been performed during these studies.

Pre-coordinated cobalt(III) complexes were reacted with phosphonate ($RC(O)P(O)(OCH_3)OH$) ligands where R is either a methyl (CH_3) group or a phenyl (C_6H_5) group. The cyclisation of the phosphonate ligand caused by the nucleophilic attack of a deprotonated primary amine (adjacent to the donor atom of the phosphonate ligand) on the pendant carbonyl group of the phosphonate ligand, lead to the formation of a carbinolamine. The dehydration of the carbinolamine yields an imine. Triazaundecane-1,11-diamine (tetraen), N′-[2-(2-aminoethylamino)ethyl]ethane-1,2-diamine (trien), and ethane-1,2-diamine (en) were each first coordinated to cobalt(III) to form the initial complexes with other monodentate ligand(s).

These polydentate imine phosphonate complexes of cobalt(III) were converted to their amine derivatives through borohydride reduction. Some carboxylate amine derivatives were also prepared.

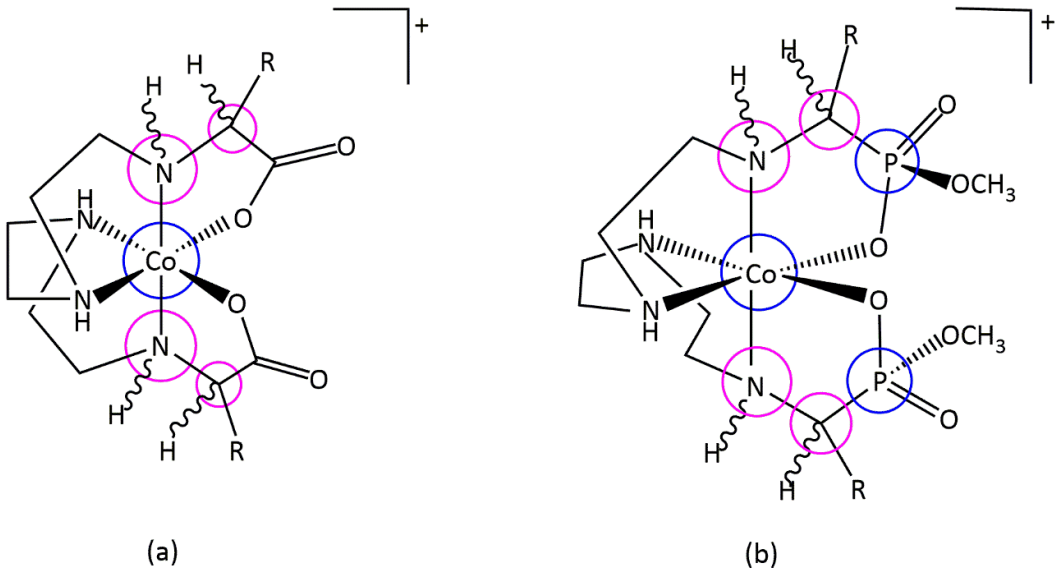

Trien systems with a: carboxylates; b: phosphonates. New stereogenic centres are highlighted in purple while blue highlights already existing stereogenic centres before the reduction reaction.

The introduction of two more stereogenic centres in the phosphonate trien system (b), for example, gives rise to more stereoisomers (diastereomeric pairs) in the product mixture. However, due to the presence of a C_2 axis of rotation which could be retained in the product molecule, the number of stereoisomers observed in the NMR spectra will be limited. This is also because some combinations of absolute configuration from a symmetrical trien system such as that shown below, will be equivalent owing to the limitation placed on the formation of all the possible diastereoisomers by the presence of a C_2 axis in some of the molecules in a given mixture.

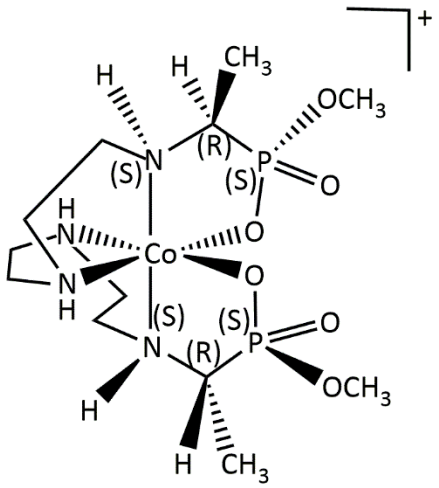

Δ*mffm*(*SRSSRS*)

The Δ*mffm*(*SRSSRS*) diastereoisomer of a trien polyamine system with phosphonates. The stereochemistry around the metal centre is Δ*mffm*. The top half of the molecule has the stereochemistry *S*, *R* and *S* around the phosphorus, α-carbon atom and amine centre respectively. The lower half of the molecule is similar to the top half by the presence of a C_2 axis of rotation.

If the initial polydentate wrapping around the metal centre and the configurations at the phosphorus centres are retained, twenty stereoisomers (ten diastereoisomeric pairs) could therefore be formed from the reduction reaction of the trien systems. Two more pairs of diastereoisomers are expected to be formed for each stereoisomer if the phosphorus centres are not kept constant, making a total of forty stereoisomers (twenty diastereoisomers). Four pairs of diastereoisomers were observed by NMR in the product mixture from the trien system.

Esterification of these phosphonate and carboxylate amine complexes led to the active ester chelates that were used for the synthesis of the cobalt(III) mediated short peptides and amides. The reagents used included benzylamine, diamines such as ethane-1,2-diamine, amino acid methyl esters, amino acid ethyl esters and a novel dipeptide made in the Hartshorn laboratory.

This work is an extension of the established carboxylate chemistry to phosphonate (and some new carboxylate) systems to make complexes like $[Co(trien)(P(O)(OCH_3))_2(Gly\text{-}(OTS)Pro\text{-}OCH_3)_2]^{3+}$. Peptide synthesis on the metal was discovered when β_2–$[Co(trien)(glyOEt)Cl](ClO_4)_2$ was treated with glyOEt in an non aqueous environment.

The chelated esters condense readily with amino acid esters, amines and small peptides. The reaction mechanism for the phosphonate systems is hypothesised to go through a trigonal bipyramidal intermediate (after the nucleophilic attack of the N-terminal of an incoming species on the phosphoryl P atom) which leads to the peptide or amide. No activation of the peptide-forming step is required.

In the absence of other nucleophiles, water attacks the positive centre, the phosphoryl P atom, resulting in hydrolysis of the ester and formation of a 2+ species.

This carboxylate and phosphonate cobalt(III) method does not only provide an alternative route to peptide synthesis, it also provides both N-terminal protection (necessary for preventing any reaction with activated carboxylate/phosphonate species) and phosphoryl-O activation (for directing the nucleophilic attack by the N-terminal of the incoming amino acid to the phosphoryl-P of the complex) in one system and makes coloured compounds which are generally water soluble.

Acknowledgements

I wish to say a big thank you to Professor Richard Hartshorn, my senior supervisor for his acceptance and guidance throughout the course of this study.

A heart felt appreciation goes to Dr. Jan Wikaira (my second supervisor) for being a “Mother” to all of us in the Hartshorn group and especially to me. That will not go without mentioning the relentless assistance provided by Dr. Matt. Polson beyond X-ray crystallography, from the start to the end of this journey. All of the single crystal X-ray structures included in this thesis have been “mattified”.

Thanks to TETFUND Nigeria for funding the first three years of my study. And to the chemistry department for paying some of my tuition fees.

Thanks, are also due to Dr. Marie Squire and Dr. Amanda Inglis for their assistance with NMR experiments as well as Mass Spec. experiments. I will always remember your help with chemistry and life questions.

Thanks to Associate Professor Sarah Masters for making sure that I finished. Thanks to Associate Professor Sally Gaw for being a guardian not only to me but to my children too. Thanks to Professor Greg Russell for taking us as family. Thanks to Professor Ian Shaw for advice along the way. Thanks to Associate Professor Vladimir Golovko for letting me borrow equipment from his laboratory. Thanks to Professor Owen Curnow for all the lectures on NMR. Thanks to Associate Professor Chris Fitchett for his X-ray lectures. Thanks to Professor Paul Kruger for his transition metal chemistry lectures. Thanks to Associate Professor Deb for grooming us as teaching assistants for the undergraduate laboratories.

Thanks to Dr. Nathan Alexander for being the coolest boss I have ever had. And to Dr. Anthea Lees (and Lauren) for becoming family to me.

Thanks to Mike Van der Colk for letting me use the rotatory evaporators in the old laboratories and for being a good team mate during my role as a laboratory technician in the undergraduate laboratories. Thanks to Rob Stainthorpe too for all those helpful conversations. Thanks to Wayne MacKay and to Nick Oliver for their technical expertise in fixing and maintaining our laboratory instruments and for ensuing we can carry on with chemistry safely. Special thanks to Rob McGregor for making me a lot of columns and other glassware for my experiments.

Thanks to Gill Ellis and Laurie Anderson for making sure we have all the chemicals and other laboratory wares we need to do science.

Thanks to John Davis for help with IT and related stuff. Thanks to all of SPCS administrative staff who work in the background for all of us. Thanks to Professor Rudi Marquez for being part of the positive change the school (SPCS) is experiencing.

Thanks to Aunty Philippa Drayton and Uncle Jim Nieman for being our NZ family and for editing this thesis too. Thanks to Grandma Addie and Grandpa Pete (and the entire Malcolm family) for adopting us as family.

Thanks to Dr. Lebe Nnanna for inspiring me to start my doctorate study and for providing me with resources like internet access, library subscriptions, journal subscriptions and relevant others to get this journey started.

Thanks to Nick Scullin of the Engineering and Physical Sciences (EPS) library for blocking a lot of calendar sessions to format this thesis. I could not have done it without your help.

Thanks to Team Hartshorn – Shirley, Josh, Sarah, and Rajika and to all the past students. Thanks to the Marquez group (Ricardo, Zach, Hector and Kim) for being great lab mates.

Thanks to all the current chemistry, biochemistry and environmental chemistry post graduate students in Ernest Rutherford (ER) and to all the friends I have made along the way, I do not have enough space to fill in all the names.

Thanks to Dr. Kelly Dombroski for standing beside me since I got to NZ and for letting me pull her hair while birthing James. Thanks to Rhonda Powell for being a mother to my children while I rested at the hospital after James' birth. Thanks to Karen Whittaker for making sure I stayed sane throughout this journey. Thanks to Dr. Jennifer Bufford and Jenny Stevenson for looking after my children while I attended an ACS conference in the US. And to Sarah Gingrich for standing by in case we did not get home as scheduled. Thanks to Dr. Chinwe Erike for taking care of my children so I could get some rest. I love you all.

Thanks to my wonderful mother, Ebere Udeka for going beyond her circumstances to get me this far and to my siblings Kay, Jane, Nene, and Emeka for being the best family anyone can have or ask for.

Thanks to my sisters-in-law, Olekanma Ekekwe-Kauffman and Chidinma Nzeako, for always being there for us. Thanks to Kingsley Ochiabuto for his motivations when I felt like giving up.

Thanks to my children: Favour, Daniella, Valerie, Hadassah, and James – you all rock! Words fail me to express my gratitude to you guys. You are all amazing. Thanks for putting up with my absences. I will make up for those. A hearty thank you goes to my husband, Daniel, for filling in the gap.

"Now to Him who is able to do immeasurably more than we can ask or imagine, according to His power that is at work within us, be the glory forever more. Amen."

Dedication

This thesis is dedicated to my parents: my mother, Ebere Udeka, who did all she could to see that I went to school against all odds, and to my father (Late Eme Udeka) who taught me how to read and write in English.

Table of Contents

List of Figures

List of Tables

List of Abbreviations

$^{13}C\{^{1}H\}$	Proton decoupled Carbon-13 NMR
$^{31}P\{^{1}H\}$	Proton decoupled Phosphorus-31 NMR
AA	Amino Acid
CIP	Cahn, Ingold and Prelog
en	Ethane-1,2-diamine
f or *fac*	Facial
Gly	Glycinate
IR	Infra-Red frequency light
m or *mer*	Meridional
M	mol/L
MHz	Megahertz
NMR	Nuclear Magnetic Resonance
OTs	Tosylate
ppm	Parts Per Million
Pro	Proline
R_1	Reliability factor
rac	Racemic
T	Temperature
tetraen	Triazaundecane-1,11-diamine
trien	N,N'-bis(2-aminoethyl)ethane-1,2-diamine
TSP	3-(trimethylsilyl)propionic 2,2,3,3-d_4 acid, sodium salt
U	Cell volume
UV	Ultra-Violet light

vis.	Visible
Z	Number of asymmetric units per cell
δ	chemical shift
ε_{max}	Extinction coefficient at maximum absorbance
λ_{max}	Wavelength at maximum absorbance

Chapter 1. Introduction

1.1 Introduction

During Alfred Werner's doctoral study around 1886, he argued that the stereochemistry of nitrogen must be characterised by a tetrahedron which should yield optical isomers.[1]

Ten years later, Pope and Peachey[2] published experimental proof of asymmetric nitrogen. At the time Werner published his revolutionary paper titled "contribution to the constitution of inorganic compounds", he had not performed a single experiment in the field of coordination chemistry.[3] Werner dreamed about his coordination theory after preparing lectures on inorganic chemistry.[4] Werner's revolutionary theory was actually based on experimental data collected by Sophus Mads Jørgensen.[1]

The beautiful colours of the *flavo*, *croceo*, *luteo*, *purpureo*, *roseo*, *praseo* and *violeo* compounds[5-8] were the attraction for chemists in the mid – 19th century[1] and continues to be to date.

The concept of coordination number was introduced by Werner as the number of groups around the central metal atom alongside the assumption that ligands could be replaced by other groups. Six (octahedral, for example, Co(III)) and four (square – planar, for example, Pt(II)) are the most frequent coordination numbers. Werner resolved through his remarkable stereochemical perception that the arrangement of ligands around a central metal atom must lead to stereoisomers. Consequently, *croceo* and *violeo* salts became *cis* and *trans* isomers of an octahedral complex.

1.2 Chirality and Nomenclature in Octahedral Complexes

Stereochemistry is the part of science that deals with structure and reactivity in three dimensions. When different compounds have the same molecular formula, they are called isomers. When these isomers differ only in the way the atoms are oriented in space but are like each other with respect to the connectivity of the atoms, then they are called stereoisomers.[9] Stereoisomers that are not mirror images of each other are called diastereoisomers.[9] Stereochemistry has played a vital role in the evolution of modern coordination theory since its advent in 1893.[10]

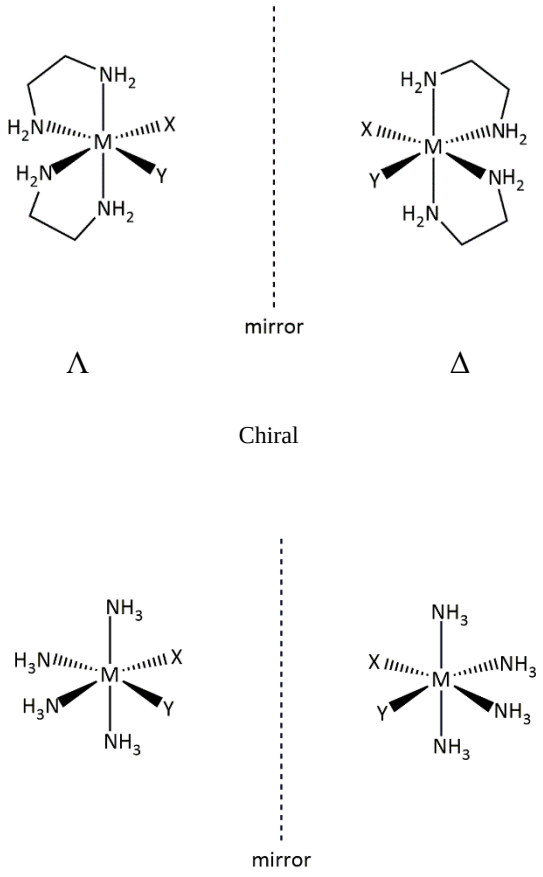

Figure 1.1 **Top**: stereoisomers of the chiral *cis*-$[M(en)_2XY]^+$ complexes originally postulated by Werner in 1899. Two non-superimposable mirror images (enantiomers). **Bottom**: The "parent" complex $[M(NH_3)_4XY]^+$ is achiral.[11] The line represents a mirror.

In 1899, Alfred Werner first predicted that if six-coordinate metal complexes possessed octahedral geometries, then species containing chelating ligands such as ethane-1,2-diamine (en) of stoichiometry *cis*-$[M(en)_2XY]$ should exist as mirror image forms or enantiomers (Fig.1.1)[12]. The stereochemical descriptors Δ and Λ refer to right and left handed enantiomers respectively.

Werner's triumph in establishing his coordination theory was based on his ability[13, 14] to resolve the enantiomers of cis-$[Co(en)_2(NH_3)X]^{2+}$ (X = Cl, Br; en = ethane-1,2-diamine) and $[Co(en)_3]^{3+}$. A molecule is chiral if it is non-superimposable on its mirror image.[15] The significance of chirality is best shown with the dramatic differences that can be observed in the activities of different enantiomers of chiral drugs.[16]

The arrangement of chelate rings about a central metal ion (helicity) and that of unidentate ligands (configuration) around the metal centre[17] are the two most studied ways through which an octahedral coordination compound can attain chirality[10].

Most helical chains are easy to recognise but it is not always simple to identify a chiral compound by checking whether it is superimposable on its mirror image or not.[18] Symmetry considerations help by offering a condition that a chiral molecular species must lack an improper (S_n) axis of symmetry[18] in the same way that the lack of an inversion centre, *i* (S_2), and the plane of symmetry, σ (S_1), both make up a common criterion used for identifying chiral species. However, there are a few species in the literature[18] which are achiral despite lacking an inversion centre, *i*, and plane of symmetry, σ, because they have higher order S_n symmetry elements. One of the systems of identifying chiral compounds is based on the use of X-ray crystallographic methods.

In 1949, Bijvoet[19] laid the foundation for the use of crystallographic methods in the determination of absolute configurations.[11] It is known that phase information is lost in the crystallographic method which means that absolute configurations cannot be determined. However, it was demonstrated[19] that for compounds with heavy atoms, anomalous dispersion can be used to regain the phase information and hence the absolute configuration when the absolute configuration of sodium rubidium tartrate was determined in 1951.[11] In 1955, Saito used the method to show that the enantiomer of $[Co(en)_3]^{3+}$ that rotated plane polarised light at the sodium-D line to the right (D-(+)-$[Co(en)_3]^{3+}$) possessed the Λ absolute configuration.[20] The use of the Flack[21] parameter to confirm absolute configuration is now routine[22, 23], where a measure of the inversion-distinguishing power of a diffraction experiment is afforded by the reciprocal of the standard uncertainty of the Flack parameter. Empirical and calculational methods to establish the relationships between the optical properties and the configuration have been developed.[11]

A series of chiral phosphorus(V) anions with a high tendency to form ion pairs with aromatic rich cations in non-solvating solvents are currently in use[11] for separating diastereoisomeric pairs on a preparative scale for complexes such as $[FeL_3]^{2+}$ (L = diimine ligand), $[CuL_2]^{2+}$ (L = 2-substituted-1,10-phenantroline) and dicobalt(II) helicates. Lacour developed these phosphorus anions based on the Pfeiffer effect. The Pfeiffer effect refers to an enrichment of one enantiomer in a racemic mixture of a labile coordination compound in the presence of ancillary non-labile chiral components.[24]

Pfeiffer was Werner's student. In the course of his career, he noticed that the addition of 1,10-phenanthroline (achiral) to a solution containing zinc sulfate (achiral) and cinchonine hydrochloride resulted in a change in the optical rotation. The expected product of the reaction

was racemic $[Zn(phen)_3]^{2+}$ and the change in optical activity was compatible with the formation of an excess of one of the two enantiomers of the $[Zn(phen)_3]^{2+}$ cation.[25] Analogous effects were observed with nickel(II), cobalt(II) and iron(II) compounds.[25]

These non-covalent interactions between chiral compounds were applied for analytical and preparative purposes either to differentiate and separate enantiomers of coordination compounds or to enrich them. The question of whether the use of chiral ligands will allow the diastereoselective synthesis of coordination compounds or not, then arose.[11]

Werner was one of the first to investigate the use of chiral ligands in his studies of the coordination characteristics of racemic propane-1,2-diamine (pn).[26] The chirality and asymmetric nature of the pn ligand (Fig. 1.2) introduced an additional complexity (Fig. 1.3) to the analysis of the stereoisomers.

Figure 1.2 Enantiopure propane-1, 2-diamine (pn) ligands (R and S)

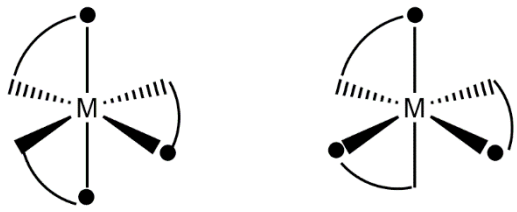

Λ*mer* Λ*fac*

mer-Λ-[M(R-pn)$_3$] and mer-Δ-[M(S-pn)$_3$]

mer-Λ-[M(S-pn)$_3$] and mer-Δ-[M(R-pn)$_3$]

fac-Λ-[M(R-pn)$_3$] and fac-Δ-[M(S-pn)$_3$]

fac-Λ-[M(S-pn)$_3$] and fac-Δ-[M(R-pn)$_3$]

Figure 1.3 Meridional (mer) and facial (fac) stereoisomers. The filled circle represents the amine attached to C1. Eight possible stereoisomers obtained with pure R- or S-pn complexes. Complexes of the same colour are enantiomers (all stereodescriptors inverted); all other relationships are diastereoisomers.[11]

Figure 1.3 also shows an analysis of the stereoisomers expected if enantiopure R-pn or S-pn is used. The situation is considerably more intricate if racemic pn is used. The heterochiral complexes with two *R* and one *S*, or two *S* and one *R* ligand can exist in various isomers depending on the *cis*/*trans* relationship of the R and S ligands and a total of 24 stereoisomers are possible.[11]

The *fac*/*mer* system of nomenclature was proposed by Saito[20] for hexadentate ligands. In that system, tridentate segments of the coordinated polyamine chain are labelled *mer* (*m*) or *fac* (*f*), depending on whether the segment is wrapped around the edge (meridian) or face of the octahedron. Thus, isomer **A** in Fig. 1.4 would be *fac*, *fac*-$[CoCl_2(trien)]^+$ (or *ff*-$[CoCl_2(trien)]^+$) and isomer **B** (Fig. 1.4) would be *fac*, *mer* (or *fm*) isomer. *trans*-tetraamines such as **C** would be assigned *mer*, *mer* (or *mm*)[27] where trien stands for (N′-[2-(2-aminoethylamino)ethyl]ethane-1,2-diamine).

As investigations into the chemistry of more complicated complexes such as $[CoX_2(trien)]^{n+}$ evolved, the distinct contrast between the isomers formed in terms of their spectroscopic properties[28] prompted the next phase of the research. The α and β system of nomenclature was introduced (Fig. 1.4).

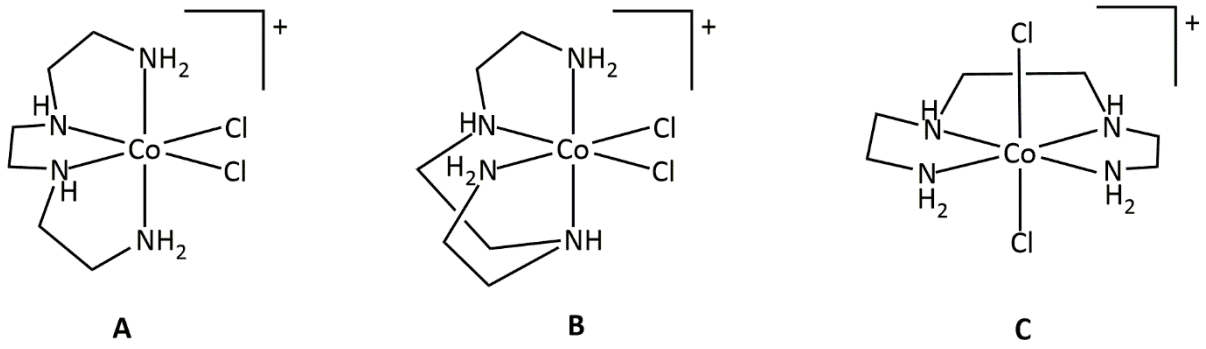

Figure 1.4 The two violet *cis* isomers of $[CoCl_2(trien)]^+$, **A** and **B** were called α and β[28]. The green *trans* isomer, **C**, is identical to the green *trans*-bis(ethane-1,2-diamine) system.

The α isomer was shown to be **A** and the β form to be **B**. Since then, the α/β nomenclature has been extended so that complexes with fully folded linear tetradentate ligands are known as the α isomer, and all those with only one fold are assigned as the β isomer.[29, 30]

House and Garner[31] reported the geometric configurations of $[Co(tetraen)Cl]^{2+}$ complexes as those presented in Fig. 1.5, where tetraen stands for triazaundecane-1,11-diamine.The α/β nomenclature was used for their descriptions. There was a lot of confusion with respect to the asymmetry or otherwise of the four geometric isomers of $[M(tetraen)Cl]^{2+}$ in an octahedral complex prior to their investigation. Due to the ready chemical interconvertibility observed[31], House and Garner proposed that the α- and β-$[Co(tetraen)Cl]^{2+}$ isomers are related to one another either as **I** and **II** or **III** and **IV**. They suggested that the α and β forms were **I** and **II**, respectively.[31]

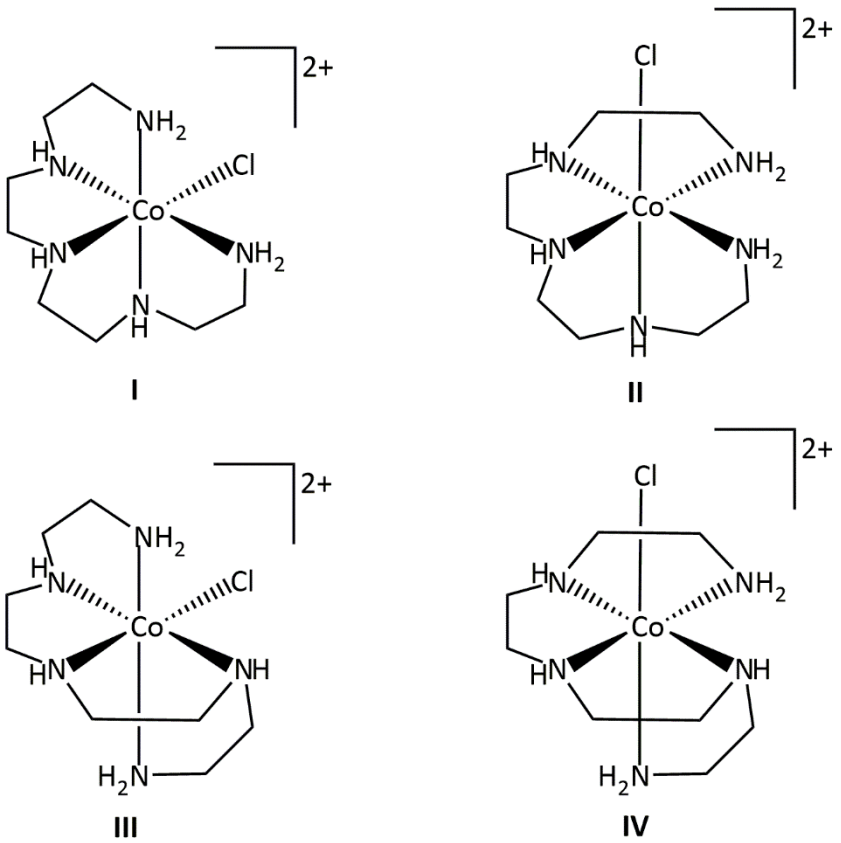

Figure 1.5 House and Garner's[31] illustration of the possible geometric isomers of $[Co(tetraen)Cl]^{2+}$; Probably I is the α-isomer and II is the β-isomer[31].

Saito's[20] system of nomenclature where the octahedral topology is given significant consideration in order to aid visualisation of isomers was extended by Hartshorn and House[27] in their proposal for the description of the diastereoisomers that result from wrapping polydentate ligands around an octahedral metal ion. More details of the Hartshorn and House[27]method shall be discussed later.

Linear tetradentate ligands have the ability to wrap around an octahedral metal ion to form some topological isomers which have so far been identified with the Λ and Δ configurations. However, that system of nomenclature fails to address the differences that could be generated between similar systems by having the protons (or other substituents) attached to coordinated secondary amines (or other donors) adopting alternate positions in space relative to the rest of the ligand.[27] Fig. 1.6 shows the possible isomers that could be produced from the $[CoCl_2(trien)]^+$ system highlighting both previous and Hartshorn and House's[27] system of nomenclature. The isomers shown in Fig. 1.6 could exist for a symmetrical ligand; if the ligand is asymmetrical, further outcomes from its wrapping around the metal ion will arise.

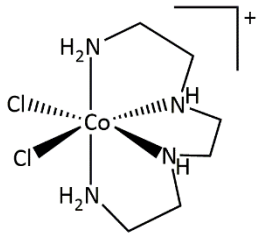

Δ-α-[$CoCl_2$(trien)]$^+$

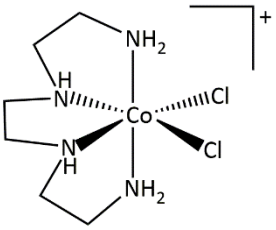

Λ-α-[$CoCl_2$(trien)]$^+$

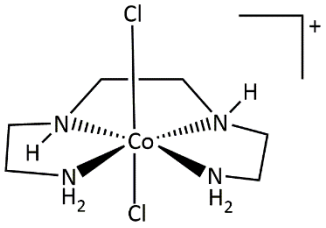

SS-*trans*-[$CoCl_2$(trien)]$^+$

Δ-*ff*-[$CoCl_2$(trien)]$^+$

Λ-*ff*-[$CoCl_2$(trien)]$^+$

SS-m_sm_a-[$CoCl_2$(trien)]$^+$

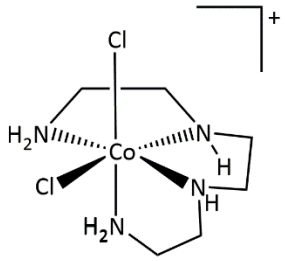

Λ-β-(S)-[$CoCl_2$(trien)]$^+$

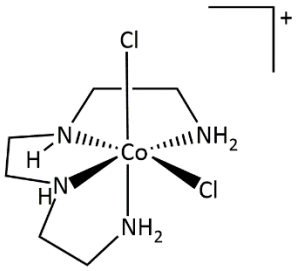

Δ-β-(R)-[$CoCl_2$(trien)]$^+$

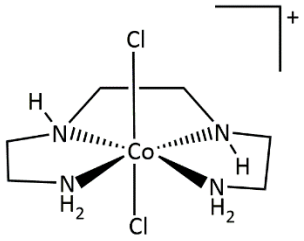

RR-*trans*-[$CoCl_2$(trien)]$^+$

Λ-*fm*$_s$-[$CoCl_2$(trien)]$^+$

Δ-*fm*$_s$-[$CoCl_2$(trien)]$^+$

RR-m_sm_a-[$CoCl_2$(trien)]$^+$

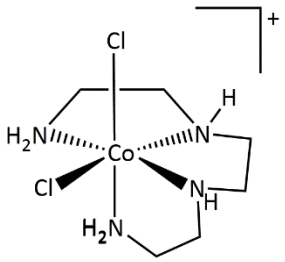

Λ-β-(R)-[$CoCl_2$(trien)]$^+$

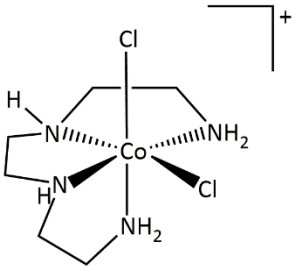

Δ-β-(S)-[$CoCl_2$(trien)]$^+$

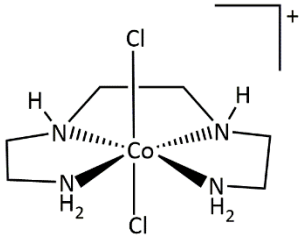

meso-*trans*-[$CoCl_2$(trien)]$^+$

Λ-*fm*$_a$-[$CoCl_2$(trien)]$^+$

Δ-*fm*$_a$-[$CoCl_2$(trien)]$^+$

m_sm_s-[$CoCl_2$(trien)]$^+$

Figure 1.6 The nine isomers of [Co(trien)Cl_2]$^+$ and two nomenclature systems.[27]

Hartshorn and House[27] also reiterated the use of letter codes for indicating the location of ligands (except for those assigned with the lowest priority) in a given complex. Ligands which are *trans* to a primary donor are designated as *p*; secondary donor, *s*; tertiary donor, *t*; unsaturated donor, *u*; another ligand, *x*. That way, complexes of pentadentate ligands will have only one extra ligand, and only one site in which it can be placed, and so would require no

notation.[27] For tetradentate ligands, the locations for the two remaining ligands in a complex can be undoubtedly[27] defined using one letter from the *p*, *s*, *t*, *u* notation. If the other ligands are the same, there is no need to define their locations. Octahedral complexes with tridentate ligands will need three other ligands to fill up the other sites of the octahedron. If the tridentate ligand has the *fac* configuration, it becomes essential to designate the positions of two of these additional ligands in relation to the rest of the complex. Hartshorn and House proposed that the *p*, *s*, *t*, *u* notation can be employed for the two highest ranking ligands based on the Cahn, Ingold and Prelog (CIP) rules.[27] Ambiguity in the *p*, *s*, *t*, *u* notation can be resolved by adding the donor number of the *trans* group as a subscript, where necessary (Fig. 1.7).

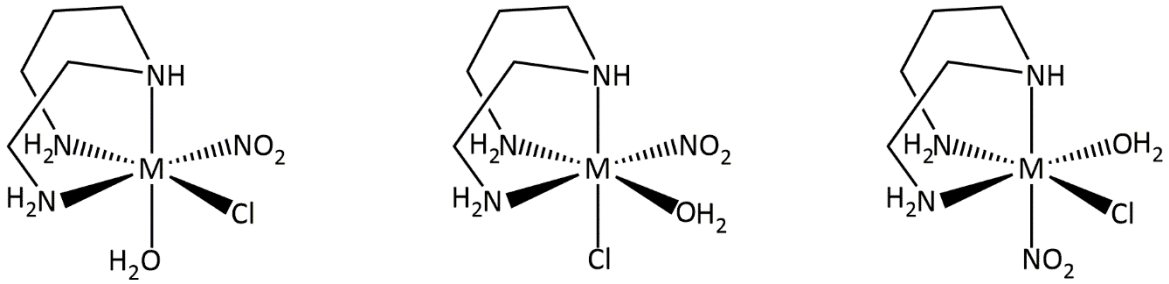

p_3s-*f*-isomer sp_3-*f*-isomer p_3p_1-*f*-isomer

Figure 1.7 Some of the isomers available in complexes of a tridentate ligand and three monodentate ligands. The CIP priority order is Cl > OH_2 > NO_2, so that the first prefixed letter refers to the location of the Cl ligand and the second to that of the OH_2 ligand. The subscripts in the ligand location portion of the prefix are used in order to resolve any ambiguity that may arise if the donor number of the *trans* ligand is not specified. Donor numbers in the Hartshorn and House nomenclature allow the isomers to be uniquely described.[27]

For those compounds where the distribution of donor atoms around the coordination centre is the origin of chirality, Chemical Abstracts Service introduced[32] in 1972 a unified system of stereochemical notation, based on the Cahn, Ingold and Prelog (CIP) standard sequence rule.[33] Although the "chirality symbols C (clockwise) and A (anti-clockwise) could also be used by observing the priming principles given in priming subrule a", the Δ/Λ convention was retained[32] for octahedral complexes of the tris(chelate) or *cis*-bis(chelate) type.

The application of the priming rule[34], for instance, for complexes of the type *fac*-$[M(AB)_3]$ (i.e. (OC-6-22)-$[M(AB)_3]$, Fig. 1.8 lead to two different stereochemical descriptors with opposite chirality symbols for a single stereoisomer, depending on which chelate is primed (or doubly primed).[10]

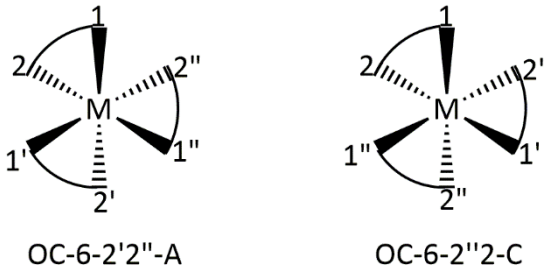

Figure 1.8 Possibilities after applying the priming convention for *fac*-[M(AB)$_3$][10]

Currently, the chirality symbols C and A are used[35] by Chemical Abstracts for octahedral complexes, except in the case of tris(chelate) or *cis*-bis(chelate) species, where the Δ/Λ stereochemical descriptors are to be used. These rules were adopted in the "Red Book" on inorganic nomenclature published in 1990[36] and kept afterwards.[34] All notation systems have always kept apart the chirality of the ligands themselves (the R/S kind) from the handedness around the coordination centre.[10]

Herrero and Usón[10] proposed using the helicity descriptors (Δ or Λ) for octahedral coordination compounds where dissymmetry is generated from the skew orientation of chelate rings. This they did by taking into account only two alternate chelate rings.[37] Their proposal retained the diverse sources of handedness as expressed by the three different sets of chirality symbols: the *R*/*S*, A/C, and Δ/Λ conventions. These three sets of chirality symbols account for the six ways by which an octahedral coordination compound can gain dissymmetry, as outlined by Hawkins.[17, 38] A lot of emphasis was placed on the metal centre by Herrero and Usón[10], distinguishing between chirality generated from the distribution of inequivalent donor atoms (A/C), and that attributed to the helicity of the chelate rings (Δ/Λ). However, for several cases, their method did not maintain the chirality symbol that has been formerly assigned to each of the systems they used.[10]

IUPAC recommends that in order to describe the configuration of coordination complexes, three points must be considered;

1) The coordination geometry – the number and location of donor atoms
2) Relative configuration – where the ligands are placed relative to each other around the central metal ion
3) Absolute configuration – which enantiomer is being identified

Once the coordination geometry has been established (OC-6 for an octahedron, for example), and the relative configuration determined, a *configuration index* is used to label the positions of the ligating atoms on the vertices of the polyhedron. The donor atoms are assigned priority numbers based on the CIP standard rules.[39]

For octahedral systems, there are two digits that determine the configuration index. The first digit is the priority number of the ligating atom *trans* to the ligating atom with priority number 1. This defines the reference axis. The second digit is the priority number of the ligating atom *trans* to the most preferred ligating atom in the plane perpendicular to the reference axis (Fig. 1.9). Unfortunately, configuration indices for closely related complexes can be very different thereby masking interpretation of the stereochemical course of a reaction.[39]

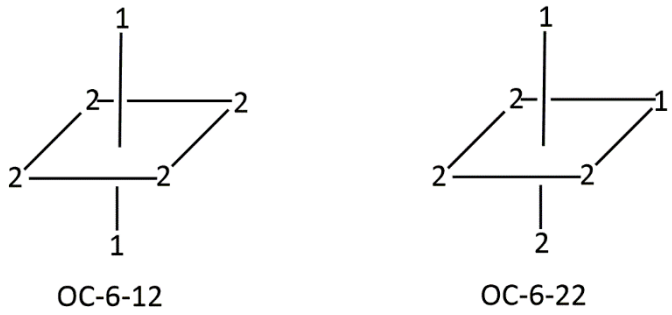

Figure 1.9 Example of an octahedral complex of the form $[MA_4B_2]$ with the configuration index assigned (where A and B have CIP priority 2 and 1 respectively)[39]

Hartshorn and House'[27] method for identifying and distinguishing between the diastereoisomers that result from wrapping polydentate ligands around octahedral metal ions is not only so straight-forward that even beginners could use it, but also conveys the most appropriate stereochemical description to such isomers. The system defines the coordination of polydentate ligands in terms of the relative positioning, facial (*f*) or meridional (*m*), of groups of three neighbouring donor atoms in a six-coordinate complex.[40] The orientation of the proton (or another substituent) on a meridional N atom relative to other donors in the ligand is designated using a subscripted *s* (*syn*) or *a* (*anti*) descriptor. Once the polyamine backbone chain has been identified and the first two donors in the backbone chain put into adjacent coordination sites on the octahedron, the link between them is thereafter drawn. The *m*/*f* folding description is then followed to locate each subsequent donor with respect to already existing ones, adding the ligand framework at each step. Substituents on the donor groups are then added as stated by the bracketed, subscript and superscript instructions.[27] An example extracted

from Blackman's review[40] of the coordination chemistry of acyclic pentadentate pentaamine ligands is shown in Figure 1.10.

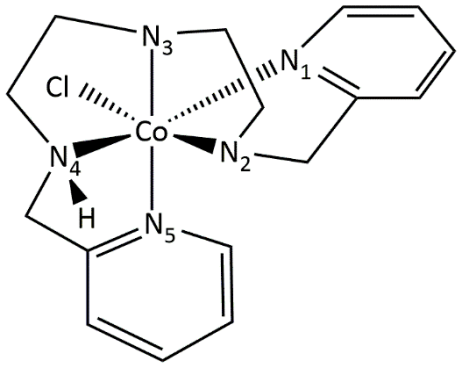

Figure 1.10: The *ffm*$_s$-[Co(**21**)Cl]$^{2+}$ cation, with all H atoms, except that bonded to N_4, removed for clarity. N_1, N_2 and N_3 atoms are facial (f), relative to each other. The N_2, N_3 and N_4 atoms are facial (f) relative to each other, and the N_3, N_4 and N_5 atoms are meridional (m) relative to each other. The proton on N_4, points away from the chlorido ligand (but towards the N_5 donor), making it *syn* to the rest of the pentadentate ligand and therefore requiring an $_s$ descriptor.[40]

The Hartshorn and House'[27] method is the system of nomenclature adopted in this thesis. The basic Δ/Λ descriptors shall be used to express the helicity of the chelate rings around the cobalt(III) metal centre while chirality at the tetrahedral phosphonate groups of these complexes shall be described using the *R*/*S* convention based on the CIP rules.

Diastereoisomers can be characterised using NMR techniques[11, 41] based on their different chemical and magnetic environments. The diamagnetic property of cobalt(III) ion means that its compounds can be studied using NMR techniques. The NMR tool has been used extensively in this project for the characterisation of the compounds synthesised.

The compounds synthesised in this project are racemic mixtures and making enantiomerically pure compounds is not part of the scope of this research. All the crystal structures obtained occurred in centrosymmetric space groups. Therefore, each time a refined structure is shown, the absolute configuration of that diastereoisomer (as shown) would be stated. However, the presence of the other diastereoisomer (with the opposite absolute configuration) in the unit cell must also be considered. Thus, for every isomer shown, its enantiomer is also present in the unit cell.

Cobalt(III) complexes (d^6) are usually low-spin octahedral and kinetically inert. Metal complexes that undergo reactions with $t_{1/2} \leq 1$ min are described as being kinetically labile. If the reaction takes significantly longer than this, the complex is kinetically inert[18]. The kinetic inertness of cobalt(III) complexes allows isomers to be separated and isolated. Complicated

ligands have been coordinated to cobalt(III) metal centres and further reactions carried out on the complexes generated thereof. The inertness of these cobalt(III) complexes have enabled the isolation and characterisation of stereoisomers where possible.

The colours of these complexes also provided visual guides as to the completion or not of the chemical reactions employed for the syntheses of the compounds described in this thesis.

1.3 Previous Research: The Carboxylate Chemistry

The origins of ligand design lie in Werner's recognition of the stereogenic consequences of chelating ligands such as ethane-1,2-diamine in his classical studies leading to the isolation of chiral complexes.[42] A particularly powerful tool in Werner's technical armoury was the recognition that certain combinations of ligands would yield chiral complexes if the geometry were octahedral.[11] The key to modern coordination chemistry is the ability to design ligands with particular properties to enforce a specific coordination mode onto a metal centre.[42]

Sargeson *et al*[43-47]., synthesised cobalt(III)-amine complexes containing N-bound aminoacetone, aminoacetophenone and aminoacetaldehyde in the course of a program aimed at carrying out organic reactions on metal ions. They discovered that in the free state, all these organic compounds did undergo intermolecular condensation reactions readily between the amine and carbonyl groups. Those facile intermolecular reactions were inhibited by the irreversible coordination of their amine groups to the cobalt(III) moiety, since the metal ion consumes the lone pair of electrons on the free amine group and ligand exchange is negligible.[48] However, deprotonation of an adjacent coordinated amine centre allowed the developed amide ion to attack the carbonyl group to form a chelate ring.[48]

It was revealed[48] that the $[Co(NH_3)_5(NH_2CH_2COCH_3)]^{3+}$ ion undergoes an intramolecular base-catalysed cyclisation reaction to produce a coordinated carbinolamine which undergoes a slower base-catalysed dehydration to yield a chelated imine.

Investigations[48] into the stereoselectivity and regioselectivity of such reactions in systems which permit more than one possible cyclisation pathway started with molecules such as aminoacetaldehyde coordinated to a trien cobalt(III) moiety with the structure shown as Fig. 1.11.

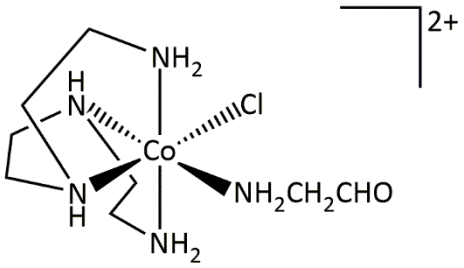

Figure 1.11 The structure of a molecule used to study the stereoselectivity and regioselectivity of the intramolecular condensation reaction of aminoacetaldehyde with a deprotonated adjacent amine through more than one possible cyclisation pathway.

Regioselective and stereoselective synthetic methods have been employed[45, 49-55] to yield a restricted number of isomers from complexes generated from polyamine ligands. Coordinating these multidentate ligands around the cobalt(III) metal centre places further control over the otherwise daunting number of isomers that could be created from such systems.

Carboxylate imine complexes have previously been made in the Hartshorn group using condensation reactions between pyruvate ligands and pre-coordinated polyamine ligands through template reactions. Templating directs the regioselectivity of a chemical reaction. For example, coordination of the polyamine ligand tetraen, around cobalt(III) metal centre (**1**) in Figure 1.12 determines which primary or secondary amine would be available for attack upon the target molecule. The secondary amine *trans* to the incoming ligand cannot react because it is on the other side of the molecule. The possible intermediates formed during the reaction have been schematised in Fig. 1.13 - 1.14.

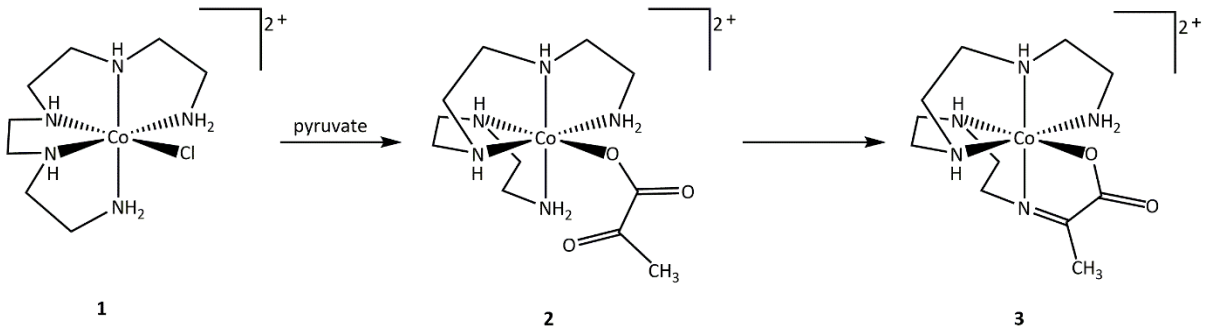

Figure 1.12 Ligand exchange-condensation sequence to imine complexes of cobalt(III).[53]

Once the pyruvate replaces the chloride ligand of the complex (**2**) (Fig. 1.13), one of the primary amines would undergo deprotonation by the mild base (2,6-lutidine) used for these

condensation reactions. The other primary amine can also be deprotonated. The nucleophile thus generated attacks the pendant carbonyl group of the new ligand. A carbinolamine (**2b** or **2c**) is formed. It is the dehydration of a carbinolamine that yields an imine (**3**).

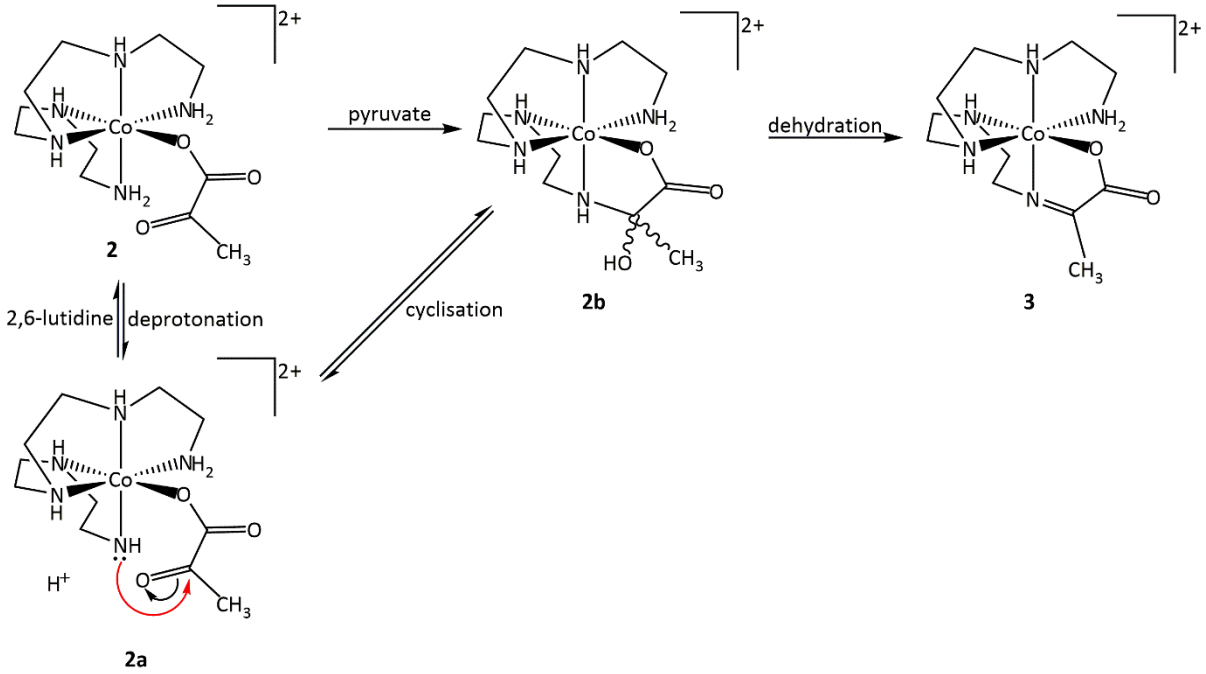

Figure 1.13 Schematic for formation of the carbinolamine and its dehydration.

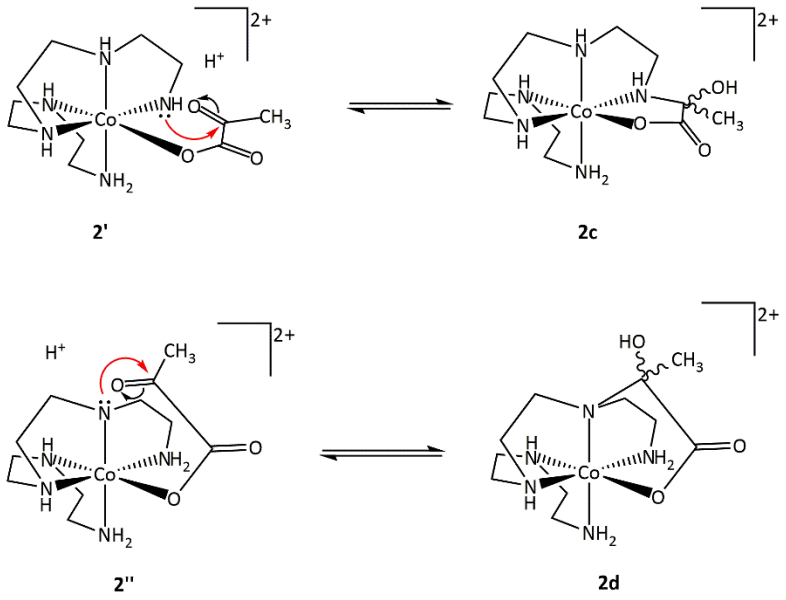

Figure 1.14 Schematic for other isomeric possibilities from the pyruvate reaction. **2c** is a non-planar carbinolamine which would not dehydrate; **2d** cannot dehydrate too.

It has been demonstrated that in cases where the dehydration is prohibited because the imine donor is not at the centre of a meridional ligand fragment, the polyamine ligand wrapping would have to be re-arranged (Fig. 1.15) to effect dehydration.[53] The reaction could also occur at the meridional secondary amine as in **2d** in Fig. 1.14. However, the dehydration for the imine formation cannot occur in that arrangement because the meridional nitrogen atom (in **2d**) has used up all of its valence electrons.

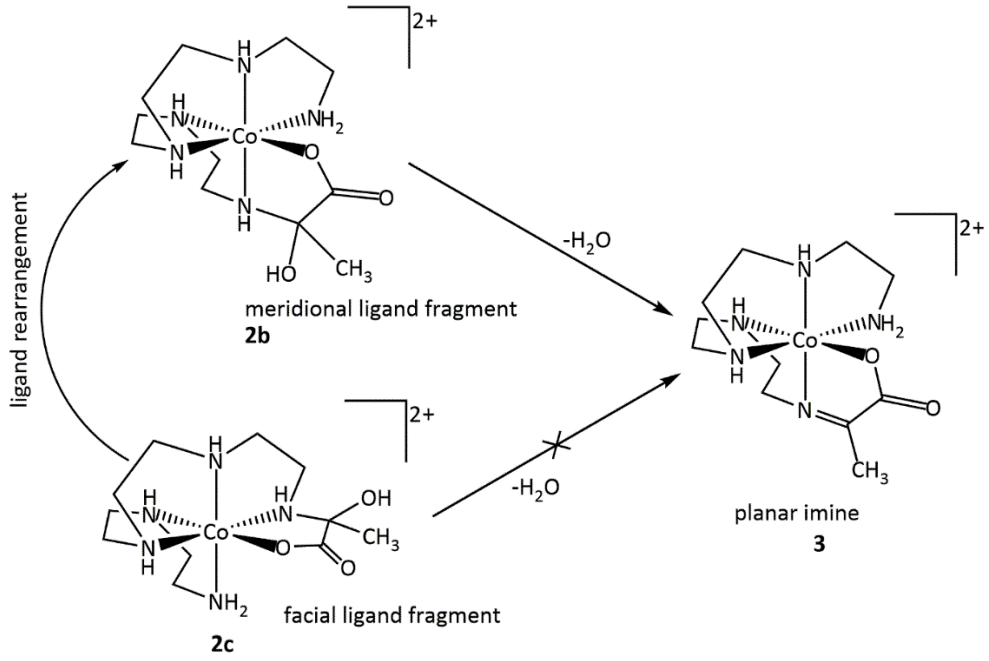

Figure 1.15 Carbinolamine formation and dehydration to yield an imine.

One of the ways through which isomerisation can occur in octahedral complexes containing only chelating ligands, is *via* a dissociative pathway wherein a donor atom detaches from the complex, thereby forming a five-coordinate intermediate. Since the energy difference between a square pyramidal and trigonal bipyramidal intermediate is very small, and once the latter has been formed, it is extremely easy to interchange axial and equatorial groups *via* pseudo-rotation (Fig. 1.16). The detached group has the opportunity to return to the metal creating either a species identical to the starting compound, or its isomer.[56]

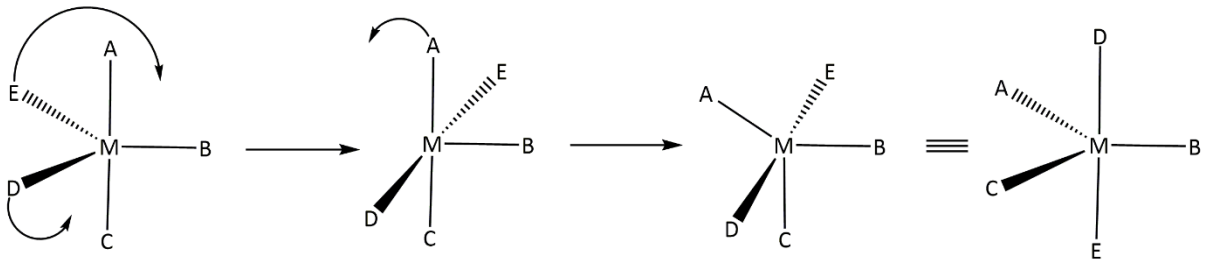

Figure 1.16 Pseudo-rotation or Berry rotation in a trigonal bipyramidal intermediate[56]

The geometry that the polydentate ligand adopts around the metal ion influences both the regiochemistry of the reaction and its stereochemical outcome. It is the ability of the carbinolamine (formed from the cyclization) to dehydrate to yield an imine that determines what arrangement the atoms will adopt around the octahedron. Thus, imine complexes have been formed through a ligand exchange-condensation sequence as shown in Figure 1.12 coupled with reversibility of any cyclisation with secondary amines and rearrangements/reversibility for the wrong primary amine. This geometrical constraint associated with the presence of the planar imine group restricts the number of wrappings available to the polydentate ligand[54]. It is the ability of the polyamine to change its wrapping around the central metal ion, along with the reversibility of carbinolamine formation that facilitates the formation of a particular isomer.

Therefore, control can be gained over the numerous isomers that would originally result from systems of the type shown in Figure 1.12.

It has been reported[53] that the stereoselectivity of this condensation reaction (Fig. 1.12) yields only the imine complex (**3**) and its enantiomer even when three different pairs of diastereoisomers of the starting material (**1**) were used. Therefore, in this project, a mixture of isomers has been used as starting material for the condensation reactions to produce new phosphonate imine complexes of cobalt(III). However, it is expected that the stereogenicity of the tetrahedral phosphorus centre would make these new systems more complicated.

Imines are excellent ligands and they provide ready routes to their amine derivatives by reduction. The reduction of the carboxylate imine complexes synthesised previously in the Hartshorn group has been done mostly by using sodium borohydride, among other reducing agents.

It has been reported[55] that the process by which borohydride adds hydrogen to a double bond leads to the addition of dihydrogen in an *anti*-arrangement.[9, 50, 53, 57-62] This mechanism therefore relates the configuration introduced at the reduced imine nitrogen to that of the adjacent α-carbon atom, which is set by the direction of hydride attack on the imine. However, epimerisation of the hydrogen on the meridional nitrogen atom cannot be excluded given that the reduction reaction is performed in a carbonate buffer.[55] Wilson-Coutts *et al*,[52] reported that the mixture of isomers obtained after shorter times in the buffer system was the result of exchange/isomerisation of the N-H groups of the major isomer isolated (A*RSSR*, C*SRRS*-$[Co(A_2trien)]^+$), with no C-H exchange observed.

There was an initial assumption that if the meridional nitrogen atom retains its original configuration and if the stereogenicity of the amine adjacent to the α-carbon atom is correlated to that nitrogen's stereogenicity, then only two diastereoisomers should form from the tetraen systems (Fig. 1.17). However, more than two diastereoisomers have been observed[39, 55] from these systems, confirming the exchange/isomerisation of the N-H groups.

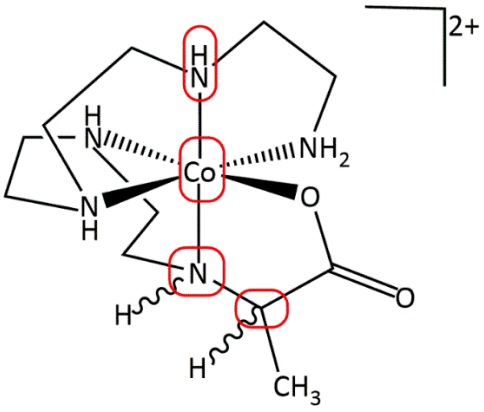

Figure 1.17 A tetraen polyamine system. Stereogenic centres have been highlighted in red[39].

Studies[39, 52, 57] done with a range of imine-acidato ligands demonstrated the selectivity of the hydride attack. The borohydride attack occurred on the more hindered (the amine face as in Fig. 1.18) face of the imine-acidato ligands. For the new phosphonate systems, there is very little steric hindrance to either face of the imine as opposed to the carboxylate systems.

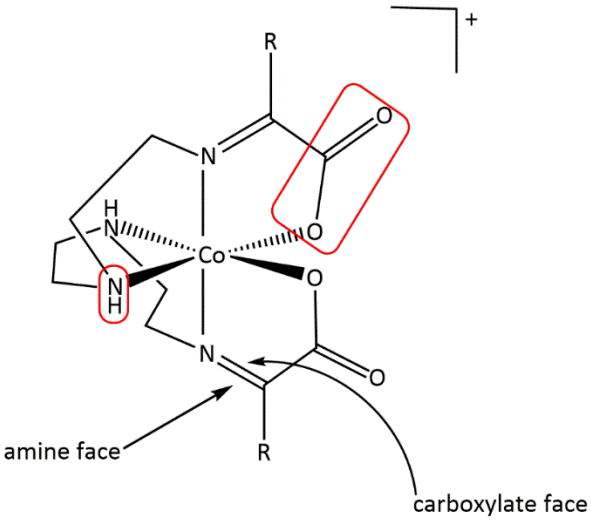

Figure 1.18 Possible faces of the hydride attack[39] shown on a di-imine complex with the trien polyamine.

Work done[50] using various hydride reagents also gave evidence of the facial selectivity. A di-hydrogen bonding interaction occurring between the amine proton of the polyamine backbone adjacent to the imine and a hydride on the borohydride anion was therefore postulated[39] on the argument that the interaction would lead to the preference for the amine face during the hydride delivery (Fig. 1.19).

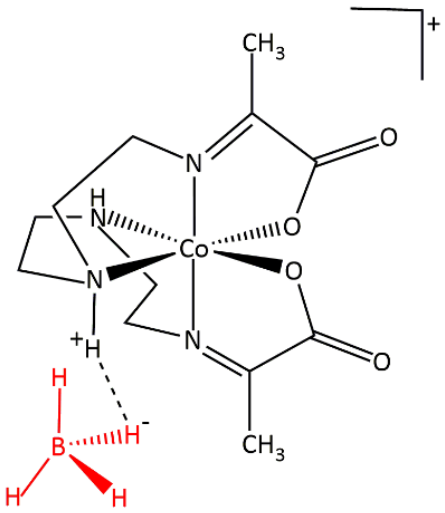

Figure 1.19 Schematic of hydride delivery as postulated by the Hartshorn group[39]. Red highlight shows the BH_4^- anion.

On the other hand, the delivery of the hydride occurring from the carbonyl face (Fig. 1.20) may be hindered by the electrostatic repulsion between the two δ^- fragments.[39]

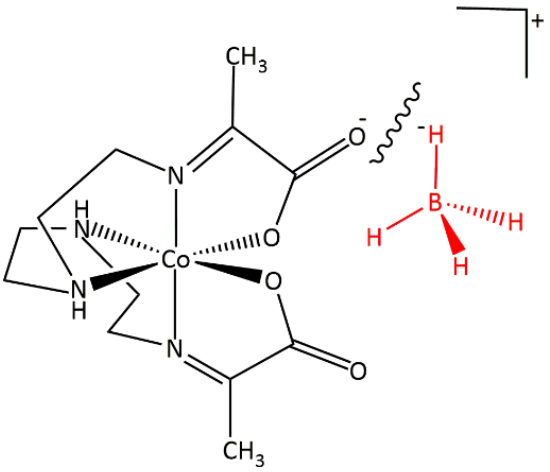

Figure 1.20 Schematic of the repulsion during hydride delivery from the carbonyl face[39].

X-ray crystallographic characterisation of some isolated products supported the hypothesis[39] by showing that the structure from the major (dominant) isomer was one where the hydrogen atoms on the α-carbon atom had been added on the amine face of the imine . Single-crystal X-ray and NMR results from research in the Hartshorn group[39, 52, 55] have shown that only a few of the possible stereoisomers are formed in a significant yield in a given mixture. For the trien systems, it was found that one of the symmetrical isomers (and its enantiomer) where the hydrogen atoms located on the two α-carbon atoms were positioned on the amine face of each meridional ligand fragment dominated the isomer mixture.

The asymmetric molecules are expected to be part of the minor isomers in the mixture. NMR spectra from the asymmetric molecules should have more resonance peaks than for those of the symmetrical molecules. This would primarily be as a result of the different chemical environments where the protons on the two α-carbon atoms would be; one would be located on the amine face whereas the other should be on the carboxylate face of the molecule. Another presentation for asymmetry of one of these molecules from the trien systems is that which occurs from having the configuration of the hydrogen atom on the adjacent amine *anti* for one chelate ring and *syn* for the other chelate ring (Fig. 1.21), while the hydrogen atom on each of the α-carbon atoms is located on the amine face of the meridional ligand fragment. That was the case for one of the minor isomers isolated in the literature[39] where the hydrogen atom of the amine adjacent to the α-carbon atom was placed on the carboxylate face.

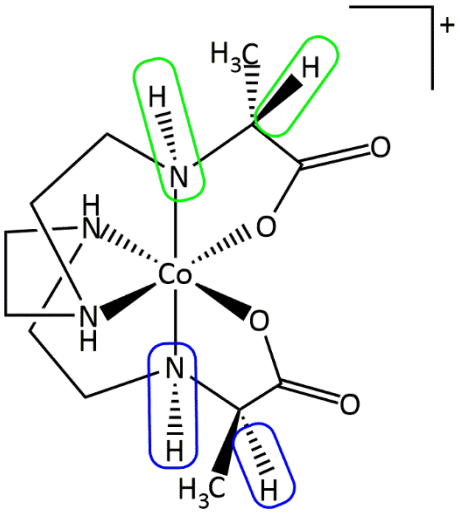

Figure 1.21 Schematic of the *anti*-configuration (green) and the *syn* configuration (blue) of protons using a trien carboxylate system.

The *anti*/*syn* occurrence is related to the selectivity of the observed reaction, where all the isomers seen in any amount from the reduction had the hydride on the same face.

These amino acid complexes can easily be converted into chelated esters through esterification reactions (Fig. 1.22) using methyl trifluoromethanesulfonate (methyl triflate). The ester chelate has been reported to condense readily with amino acid esters and small peptides[63, 64] to form peptides on the metal.

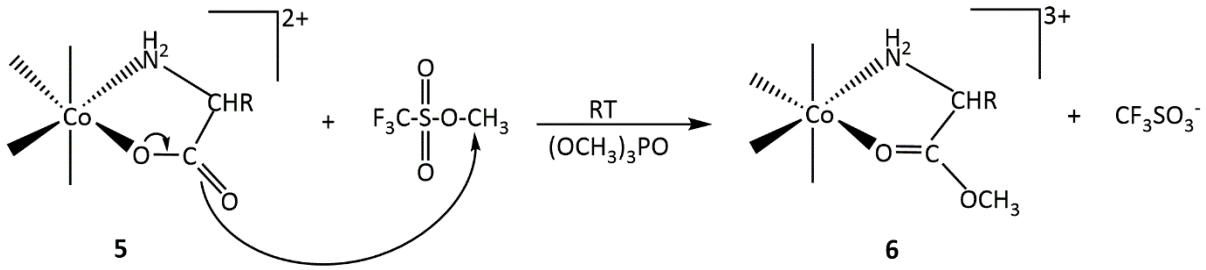

Figure 1.22 Esterification of the chelated amino acid to yield the active ester chelate[65]

Clark et al.[66] suggested that the reaction schematised in Fig. 1.23 could provide an important alternative to the active ester method for the synthesis of peptides. The cobalt(III) moiety provides a sterically robust protecting group for the amino terminus. It can subsequently be easily removed by reduction to the labile cobalt(II) oxidation state thereby freeing up the polydentate peptide. It has been shown that coordination to the cobalt(III) metal centre

significantly activates the carbonyl group of the polydentate amino acid toward addition of another amino acid or peptide.

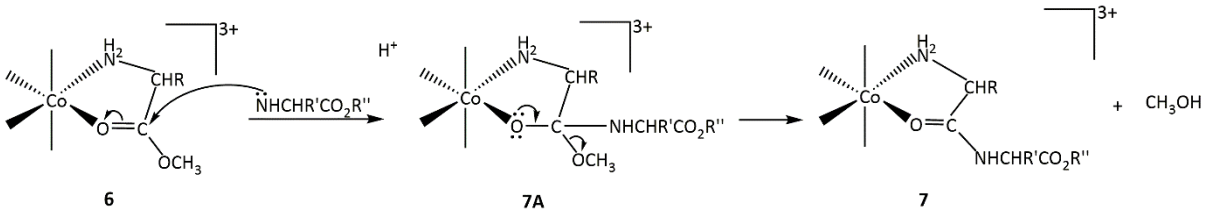

Figure 1.23 Cobalt(III)-mediated peptide synthesis coupling reaction.[66]

Amino acid methyl esters were used for most of the reactions. The chirality of the incoming amino acid methyl ester did not affect the rate of the coupling reaction. The rate of reaction greatly depends on the stereogenic nature of the chelated amino acid ester as well as the nucleophile of the incoming amino acid methyl ester.[67] Therefore, Sutton and Buckingham postulated that these coupling reactions could be selective. However, epimerization at the asymmetric α-carbon centre poses a problem when compared with conventional routes. The reaction schematized in Fig. 1.23 is reported to be quantitative provided no moisture is present.[67]

Investigations into the possibility of using chelated esters of the type shown in Fig. 1.24 for the N-terminal synthesis of peptides as well as for probing the mechanisms of ester hydrolysis and exchange began in the early 1960s.

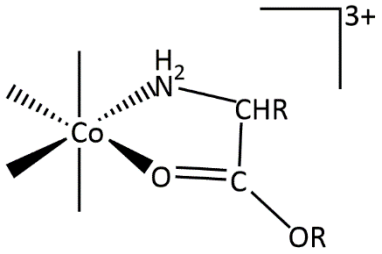

Figure 1.24 Cobalt(III) chelated ester (R is methyl, ethyl or isopropyl ester)

The studies have shown that hydrolysis of the directly activated esters of the type shown in Fig. 1.24 (where R is methyl, ethyl or isopropyl ester) is accelerated by about 10^6 times by the cobalt(III) metal centre.[47, 63-75] In the absence of other nucleophiles, water attacks the electrophilic or partially positive centre, the carbonyl carbon, resulting in hydrolysis of the ester

and formation of a 2+ species[72, 73] followed by the expulsion of the alkoxyl group. Oxygen-18 exchange data was used to establish that it is the acyl-oxygen (Fig. 1.25) bond that breaks.[69, 75]

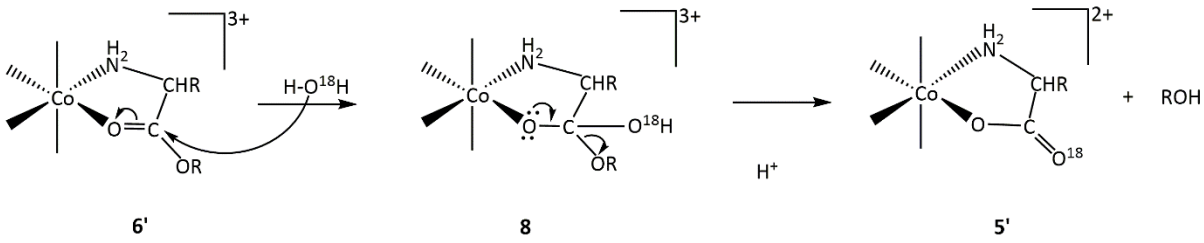

6' 8 5'

Figure 1.25 Cobalt(III)-promoted hydrolysis of an ester chelate by the nucleophilic attack of water[47] through a tetrahedral intermediate (**8**).

Peptide synthesis on the metal was discovered when β_2–[Co(trien)(glyOEt)Cl]$(ClO_4)_2$ was treated with glyOEt in an non aqueous environment.[76] The significance of using cobalt(III) stems from the relative kinetic inertness it offers. This provides a greater likelihood for the identification of reaction intermediates which could facilitate the differentiation of reaction pathways and subsequently help establish reaction mechanisms.

1.4 Extending the Carboxylate Chemistry: Phosphonates; Analogues of Carboxylates

Phosphonates are a class of organophosphorus compounds (OPs) with carbon-phosphorus (C-P) bonds. The (C-P) bond that defines these molecules is a key driver of their potent antimicrobial activities.[77] The C-P bond also plays a big role in their stability against enzymatic degradation.[77] Synthetic phosphonates are known to mimic the polar functional groups of enzyme substrates.[77] The strong structural relationship to natural compounds and high stability, contribute to the activity of this class of compounds as antimetabolites and also as competitors for the active sites of enzymes or cellular receptors.[78] Aminophosphonates, for example, can recognize the active centres of enzymes, and by creating relevant complexes with the metal ions within such centres, perform their inhibition.[78] Bisphosphonates are structural analogues of pyrophosphate. They have been established as a significant class of drugs for the treatment

of diverse diseases linked with excessive bone resorption, including Paget's disease of the bone, myeloma, bone metastases, and osteoporosis.[79]

The diverse application of the phosphonate function is driven by its four combined features[78], namely:

- Tetrahedral geometry
- Ability to form electrostatic interactions
- Ability to form hydrogen bonds
- Capacity to attach to various metal ions

Acetylcholinesterase (AChE) catalyses the hydrolysis of the neurotransmitter acetylcholine (ACh) to choline and acetic acid. Among the most potent and well studied irreversible AChE inhibitors are the organophosphates (OP). The chemical warfare agents Sarin and VX (Fig. 1.26) are analogues[80] of the neurotransmitter acetylcholine (ACh). The acute toxicity of organophosphorus compounds has been related to their irreversible inactivation of acetylcholine esterase (AChE). This arises from their non-reversible phosphorylation of esterases in the central nervous system. The mechanism of action of Sarin has been schematised in Fig. 1.27.

After AChE inhibition and increase in the level of acetylcholine in the nervous system, the excess of acetylcholine triggers seizure activity.[81] Once the seizures are initiated, the noncholinergic systems are gradually engaged and a series of biochemical events lead to the release of excessive amounts of glutamate, which damages nearby neurons.[81] This may lead to death through activation of N-methyl-D-aspartate (NMDA) receptors, accumulation of calcium, activation of catabolic enzymes and cellular death.[81]

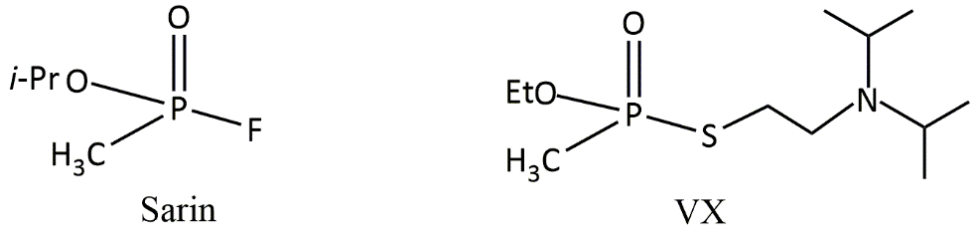

Figure 1.26 Chemical warfare agents

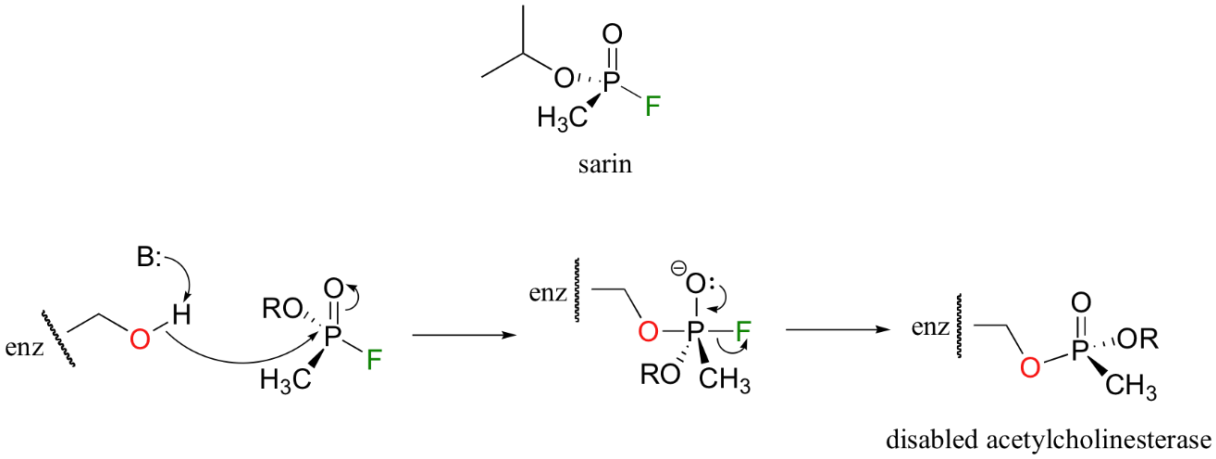

Figure 1.27 the mechanism of action of sarin as a nerve agent.[81, 82]

During neurotransmission, (Fig. 1.28) ACh is released from the nerve into the synaptic cleft and binds to ACh receptors on the post-synaptic membrane, relaying the signal from the nerve. AChE, also located on the post-synaptic membrane, terminates the signal transmission by hydrolysing ACh. The liberated choline from the ACh decomposition is taken up again by the pre-synaptic nerve and the neurotransmitter is synthesised by combining with acetyl-CoA through the action of cholineacetyltransferase.

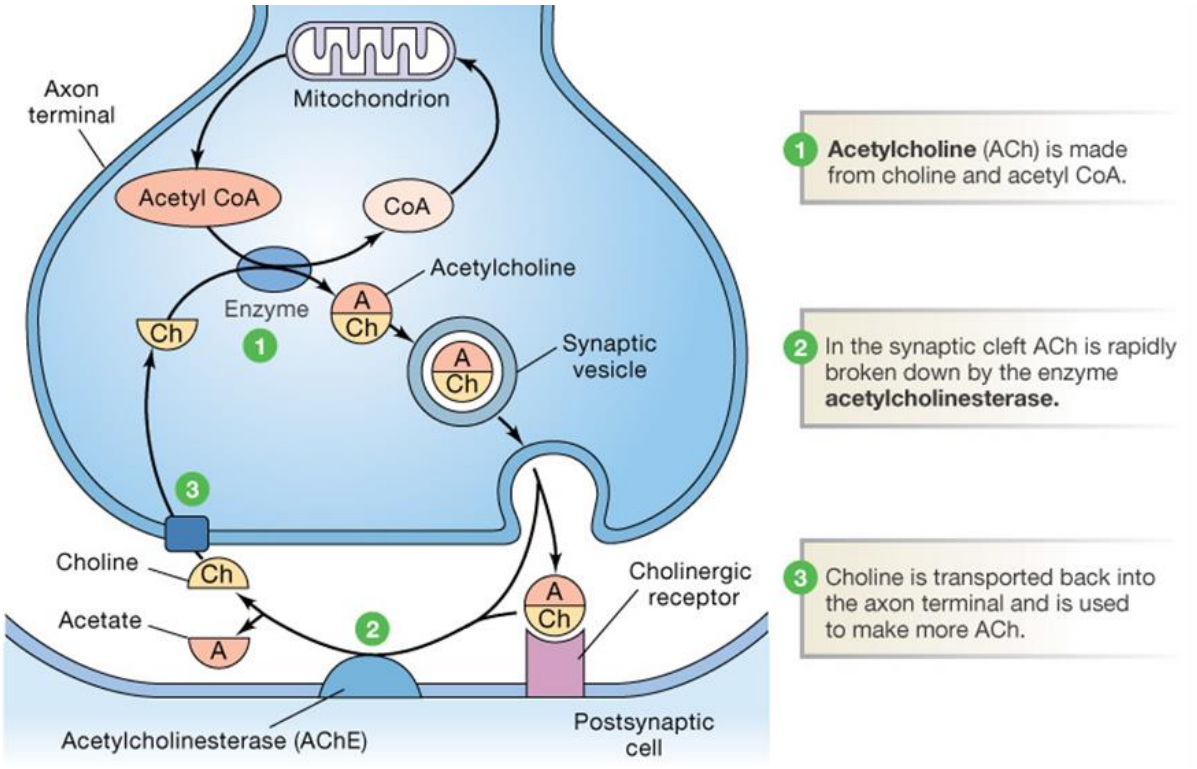

Figure 1.28 Acetylcholinesterase, a neurotransmitter. (Source: https://peaknootropics.com)

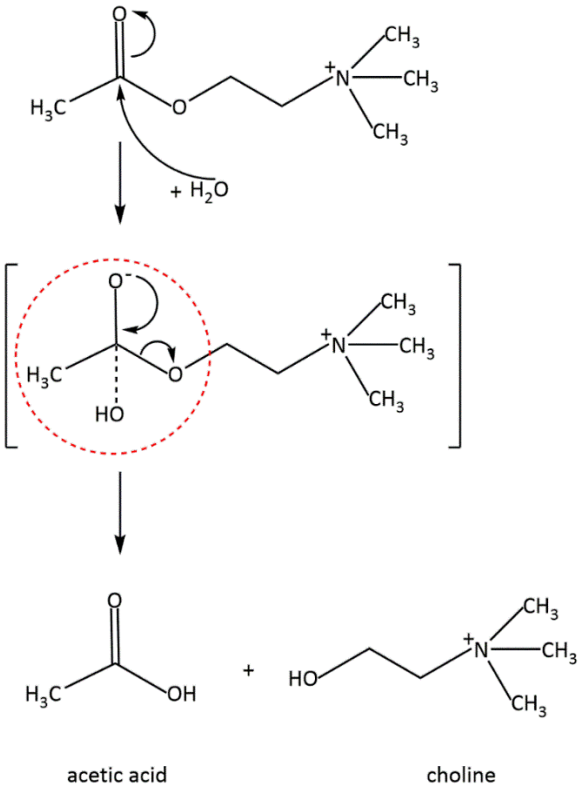

Figure 1.29 A scheme of the hydrolysis of acetylcholine through a tetrahedral intermediate (circled with red dotted lines) that resembles phosphonates

Figure 1.29 schematises the hydrolysis of acetylcholine through a tetrahedral intermediate (circled with red dotted lines). Phosphonates resemble these carboxylate tetrahedal intermediates and so could be used as analogues of the carboxylates in biochemical processes.

Organophosphorus compounds are also in use as antiviral agents, antibiotics (Fosfomysin, used to treat urinary tract infections), herbicides (the most widely used one being glyphosate,) and insecticides. Figure 1.30 shows Fosfomycin and Glyphosate.

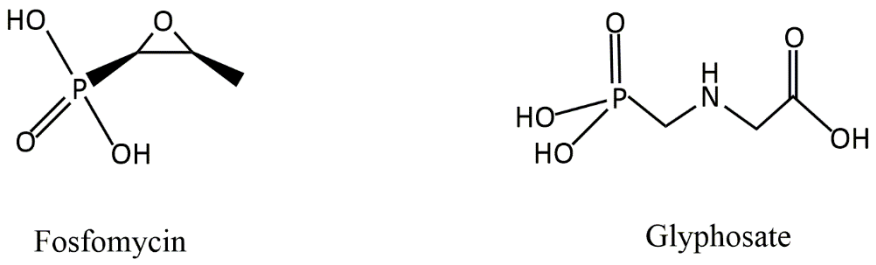

Figure 1.30 Fosfomycin (antibiotic) and glyphosate (herbicide)

The human immunodeficiency virus type-1 protease (HIV-1 PR) is a member of aspartyl retroviral proteases and plays an important role in viral replication.[83] Phosphonamidates have been very effective inhibitors of metalloproteases (carboxypeptidase A, thermolysin)[84-86]; however, because of their instability under acidic conditions, they were originally not considered as viable aspartyl protease inhibitors. Hence, the more stable tetrahedral phosphinates/phosphonates have been used.[87-90] However, McLeod[91] *et al*., demonstrated that a tetrahedral phosphonamidate moiety of the form shown as Fig. 1.31 can inhibit the HIV-1 PR.[91] The monomethyl alkylation of the phosphonamidate moiety was shown[91] to provide the element which stabilises the peptide bond from longer periods of exposure to acidic conditions (where aspartyl proteases exhibit optimum activity).

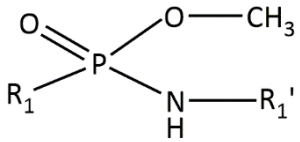

Figure 1.31 General structure of phosphonamidate esters, R_1 and R_1' represent amino acids

The advantageous features of replacing the scissile amide bond are that (1) the nitrogen atom is retained as an important element of the scissile amide bond and depending on the R′ amino acid, an extra hydrogen bond, (2) the methylated phosphonamidate is not susceptible to acid hydrolysis, and (3) there is no overall charge carried within the isosteric replacement, which could assist cell penetration.

Phosphonate ligands similar to that shown in Fig. 1.32 where R is either a methyl (CH_3) or a phenyl (C_6H_5) group, have been synthesized (as analogues of ketocarboxylic acids (Fig. 1.33) and used to generate new systems of cobalt(III) mediated short peptides and amides.

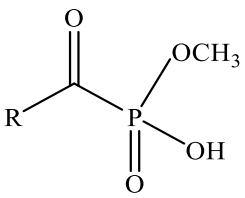

Figure 1.32 Phosphonate ester

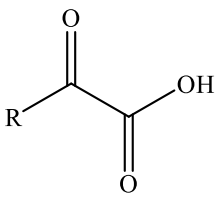

Figure 1.33 Ketocarboxylic acid

References

1. Ernst, K. H.; Wild, F. R.; Blacque, O.; Berke, H., Alfred Werner's coordination chemistry: New insights from old samples. *Angewandte Chemie International Edition* **2011,** *50* (46), 10780-10787.

2. Pope, W. J.; Peachey, S. J., CXIV—Asymmetric optically active nitrogen compounds. Dextro-and lævo-α-benzylphenylallylmethylammonium iodides and bromides. *Journal of the Chemical Society, Transactions* **1899,** *75*, 1127-1131.

3. Kauffman, G. B., *Classics in Coordination Chemistry Part I: The selected papers of Alfred Werner*. Dover Publications: 1968.

4. Berl, E., Some personal recollections of Alfred Werner. *Journal of Chemical Education* **1942,** *19* (4), 153.

5. Kauffman, G. B., Early Experimental Studies of Cobalt-Ammines. *History of Science* **1977,** *68* (3), 392-403.

6. Spingler, B.; Scanavy-Grigorieff, M.; Werner, A.; Berke, H.; Lippard, S. J., Crystal Structure Determination of a (μ-Amido)(μ-hydroxo)(μ-superoxo) dicobalt (III) Complex from the Werner Collection. *Inorganic Chemistry* **2001,** *40* (5), 1065-1066.

7. Fremy, E., Untersuchungen über das Kobalt. *Journal für Praktische Chemie* **1852,** *57* (1), 81-106.

8. Black, D. S. C.; Hartshorn, A., Ligand design and synthesis. *Coordination Chemistry Reviews* **1973,** *9* (3-4), 219-274.

9. Morrison, R. T.; Boyd, R. N., *Organic Chemistry, (1983)*. Fourth ed.; Allyn and Bacon, Inc.: Newton, Massachusetts, 1983; p 637.

10. Herrero, S.; Usón, M. A., Stereochemical nomenclature for octahedral coordination compounds containing polydentate ligands: a comprehensive proposal. *Dalton Transactions* **2008,** (37), 4993-4998.

11. Constable, E. C., Stereogenic metal centres–from Werner to supramolecular chemistry. *Chemical Society Reviews* **2013,** *42* (4), 1637-1651.

12. Kauffman, G. B., Alfred werner's research on structural isomerism. *Coordination Chemistry Reviews* **1973,** *11* (2), 161-188.

13. Werner, A., Zur kenntnis des asymmetrischen kobaltatoms. I. *Berichte der deutschen chemischen Gesellschaft* **1911,** *44* (2), 1887-1898.

14. Werner, A., Zur Kenntnis des asymmetrischen Kobaltatoms. V. *Berichte der deutschen chemischen Gesellschaft* **1912,** *45* (1), 121-130.

15. Moss, G. P., Basic Terminology of Stereochemistry (IUPAC Recommendations 1996) *Pure and Applied Chemistry* **1996,** *68* (12), 2193-2222.

16. Caner, H.; Groner, E.; Levy, L.; Agranat, I., Trends in the development of chiral drugs. *Drug Discovery Today* **2004,** *3* (9), 105-110.

17. Hawkins, C. J., *Absolute configuration of metal complexes*. Krieger Pub Co: 1971.

18. Catherine, E., Housecroft and Alan G. Sharpe. *Inorganic Chemistry (3rd Edition), Pearson Education Limited* **2008**.

19. Bijvoet, J.; Peerdeman, A.; Van Bommel, A., Determination of the absolute configuration of optically active compounds by means of X-rays. *Nature* **1951,** *168* (4268), 271.

20. Saito, Y.; Nakatsu, K.; Shiro, M.; Kuroya, H., Determination of the absolute configuration of optically active complex ion,$[Coen_3]^{3+}$, by means of X-rays. *Acta Crystallographica* **1955,** *8* (11), 729-730.

21. Flack, H., On enantiomorph-polarity estimation. *Acta Crystallographica Section A: Foundations of Crystallography* **1983,** *39* (6), 876-881.

22. Flack, H. D.; Bernardinelli, G., The use of X-ray crystallography to determine absolute configuration. *Chirality: The Pharmacological, Biological, Chemical Consequences of Molecular Asymmetry* **2008,** *20* (5), 681-690.

23. Flack, H.; Bernardinelli, G., Absolute structure and absolute configuration. *Acta Crystallographica Section A: Foundations of Crystallography* **1999,** *55* (5), 908-915.

24. Gillard, R.; Williams, P., Origins of the Pfeiffer effect. *International Reviews in Physical Chemistry* **1986,** *5* (2-3), 301-305.

25. Pfeiffer, P.; Quehl, K., Über einen neuen Effekt in Lösungen optisch-aktiver Substanzen (I. Mitteil.). *Berichte der deutschen chemischen Gesellschaft* **1931,** *64* (10), 2667-2671.

26. Werner, A., Über eine neue Isomerieart bei Kobaltverbindungen und Verbindungen mit asymmetrischem Kobalt und Kohlenstoff. *Helvetica Chimica Acta* **1918,** *1* (1), 5-32.

27. Hartshorn, R. M.; House, D. A., A simple method for identifying and distinguishing between the diastereoisomers that result from wrapping polydentate ligands around octahedral metal ions. *Journal of the Chemical Society, Dalton Transactions* **1998,** (15), 2577-2588.

28. Sargeson, A.; Searle, G., The Absolute Configurations of Disubstituted Cobalt (III) Triethylenetetramine Complexes. *Inorganic Chemistry* **1965,** *4* (1), 45-52.

29. Garnett, P.; Watts, D. W.; Legg, J. I., Existence of the. beta.-cis configuration of chelated ethylenediamine-N, N'-diacetate. *Inorganic Chemistry* **1969,** *8* (11), 2534-2534.

30. Coleman, P. F.; Legg, J. I.; Steele, J., Nuclear magnetic resonance study of the beta-cis-ethylenediamine-N, N'-diacetatocobalt (III) chelate system. *Inorganic Chemistry* **1970,** *9* (4), 937-944.

31. House, D.; Garner, C. S., Transition Metal Complexes of Tetraethylenepentamine. I. Preparation, Properties, and Geometric Configuration of α- and β-Chlorotetraethylenepentaminecobalt (III) Tetrachlorozincate (II) and the α Chromium (III) Analog. *Inorganic Chemistry* **1966,** *5* (12), 2097-2102.

32. Brown, M. F.; Cook, B. R.; Sloan, T. E., Stereochemical notation in coordination chemistry. Mononuclear complexes. *Inorganic Chemistry* **1975,** *14* (6), 1273-1278.

33. Cahn, R.; Ingold, C.; Prelog, V., Convention for тг-complexes. *Angewandte Chemie International Edition. England* **1966,** *5*, 394.

34. Damhus, T.; Hartshorn, R.; Hutton, A., Nomenclature of inorganic chemistry: IUPAC recommendations 2005. *CHEMISTRY International* **2005**.

35. Chemical Abstracts Index Guide. *Chemical Abstracts Service American Chemical Society* **1992,** *Appendix IV* (Part 203, Section III).

36. Leigh, G. J., *Nomenclature of inorganic chemistry: recommendations 1990*. Blackwell scientific publications Oxford: 1990.

37. Herrero, S.; Usón, M. A., A straightforward method for assigning stereochemical Λ/Δ descriptors to octahedral coordination compounds. *Journal of chemical education* **1995,** *72* (12), 1065.

38. Hawkins, C.; Larsen, E., Absolute Configuration of Octahedral Metal Complexes: The Octant Sign. *Acta Chemica Scandinavica* **1965,** *19* (1), 185-190.

39. Wilson-Coutts, S. M. The Synthesis and Configuration of Some Polydentate Amino Acid Complexes of Cobalt (III). A thesis submitted in partial fulfiment of the requirements for a Master of Science degree in Chemistry at the University of Canterbury, 2009.

40. Blackman, A. G., The coordination chemistry of acyclic pentadentate pentaamine ligands. *Polyhedron* **2019,** *161*, 1-33.

41. Baum, G.; Constable, E. C.; Fenske, D.; Housecroft, C. E.; Kulke, T.; Neuburger, M.; Zehnder, M., Regio-and diastereo-selective formation of dicopper (I) and disilver (I) double helicates with chiral 6-substituted 2, 2′: 6′, 2″-terpyridines. *Journal of the Chemical Society, Dalton Transactions* **2000,** (6), 945-959.

42. Constable, E. C.; Housecroft, C. E., Coordination chemistry: the scientific legacy of Alfred Werner. *Chemical Society Reviews* **2013,** *42* (4), 1429-1439.

43. Harrowfield, J. M.; Sargeson, A., Synthesis and reactivity of coordinated imines derived from 2-keto acids. *Journal of the American Chemical Society* **1979,** *101* (6), 1514-1520.

44. Harrowfield, J. M.; Sargeson, A., Reactions of coordinated nucleophiles. Intramolecular imine formation. *Journal of the American Chemical Society* **1974,** *96* (8), 2634-2635.

45. Golding, B.; Harrowfield, J. M.; Sargeson, A., Intramolecular chelation via imines. Stereoselective synthesis of s-chloro-3-(2-aminoethyl)-1, 8-diamino-3, 6-diazaoctanecobalt (III) ion. *Journal of the American Chemical Society* **1974,** *96* (9), 3003-3004.

46. Bell, J. D.; Gainsford, A. R.; Golding, B. T.; Herlt, A. J.; Sargeson, A. M., X-Ray structure and stereoselective intramolecular synthesis of a novel quadridentate complex. *Journal of the Chemical Society, Chemical Communications* **1974,** (23), 980-981.

47. Buckingham, D.; Dekkers, J.; Sargeson, A.; Wein, M., Hydrolysis and aminolysis of metal ion activated esters. Nucleophilic paths and properties of the tetrahedral intermediate. *Journal of the American Chemical Society* **1972,** *94* (11), 4032-4034.

48. Gainsford, A.; Pizer, R.; Sargeson, A.; Whimp, P., Intramolecular carbinolamine and imine formation with cobalt (III)-amine complexes. Synthesis, structure, and reactivity. *Journal of the American Chemical Society* **1981,** *103* (4), 792-805.

49. Gainsford, A.; Sargeson, A., Stereoselective and regioselective condensation reactions of coordinated aminoacetone. *Australian Journal of Chemistry* **1978,** *31* (8), 1679-1688.

50. Hartshorn, R. M. Reactions of chelated ligands. A thesis submitted in partial fulfilment of the requirements for the degree of Doctor of Philosophy in Chemistry at the Australian National University 1989.

51. Sargeson, A. M.; Searle, G. H., The stereochemistry and preparation of triethylenetetraamine-disubstituted cobalt (III) complexes. *Inorganic Chemistry* **1967,** *6* (4), 787-796.

52. Wilson-Coutts, S. M.; Browne, J. M.; Marsh, L. C.; Polson, M. I.; Hartshorn, R. M., High diastereoselectivity in borohydride reductions of coordinated imines. *Dalton Transactions* **2012,** *41* (5), 1591-1596.

53. Browne, J. M.; Wikaira, J.; Fitchett, C. M.; Hartshorn, R. M., Polydentate ligand construction: intramolecular condensation reactions in the synthesis of imine-containing ligands. *Journal of the Chemical Society, Dalton Transactions* **2002,** (10), 2227-2234.

54. Browne, J. M.; Wikaira, J.; Hartshorn, R. M., Polydentate ligand construction: a re-examination of an intramolecular condensation reaction. *Journal of the Chemical Society, Dalton Transactions* **2001,** (23), 3513-3519.

55. Browne, J. M. Intramolecular Condensation Reactions of Cobalt (III) Complexes. A Thesis Submitted in Partial Fulfilment of the Requirements for the Degree of Master of Science in Chemistry at the University of Canterbury, University of Canterbury, 2000.

56. McCleverty, J., *Chemistry of the first-row transition metals*. 1st ed.; Oxford University Press: 1999; Vol. 71, p 96.

57. Pearce, D. A.; Hartshorn, R. M.; Sargeson, A. M., Facile reduction of coordinated α-imino acids to amino acids by dithionite and borohydride. *Journal of the Chemical Society, Dalton Transactions* **2002,** (8), 1747-1752.

58. Lewis, E. A.; Smith, J. R. L.; Walton, P. H.; Archibald, S. J.; Foxon, S. P.; Giblin, G. M., Tuning the metal-based redox potentials of manganese cis, cis-1, 3, 5-triaminocyclohexane complexes. *Journal of the Chemical Society, Dalton Transactions* **2001,** (8), 1159-1161.

59. Colpas, G. J.; Hamstra, B. J.; Kampf, J. W.; Pecoraro, V. L., The preparation of VO^{3+} and VO^{2+} complexes using hydrolytically stable, asymmetric ligands derived from Schiff base precursors. *Inorganic Chemistry* **1994,** *33* (21), 4669-4675.

60. Noble, A.; Olguín, J.; Clérac, R.; Brooker, S., Doubly Pyrazolate-Bridged Dinuclear Complexes of a Highly Constrained Bis-terdentate Ligand: Observation of a [High Spin-Low Spin] State for $[FeII_2(PMAP)_2][SbF_6]_2 \cdot 2.25(C_3H_8O)$(PMAP= 3, 5-bis {[N-(2-pyridylmethyl) amino]-methyl}-1 H-pyrazolate). *Inorganic chemistry* **2010,** *49* (10), 4560-4569.

61. Cook, D. F.; Curtis, N. F.; Rickard, C. E.; Waters, J. M., Compounds of nickel (II) with 5SR, 7RS, 12SR, 14SR-5, 12-dimethyl-7, 14-diphenyl-1, 4, 8, 11-tetraazacyclotetradecane, rmL_2: The structures of [Ni (rmL_2)](ClO_4) $2 \cdot 0.5\ H_2O$ and cis-[Ni (rmL_2)(acac)]ClO_4. *Polyhedron* **2005,** *24* (18), 3022-3031.

62. Price, J. R.; Clegg, J. K.; Fenton, R. R.; Lindoy, L. F.; McMurtrie, J. C.; Meehan, G. V.; Parkin, A.; Perkins, D.; Turner, P., Copper (I) Templated Synthesis of a 2, 2′-Bipyridine Derived 2-Catenane: Synthetic, Modelling, and X-ray Studies. *Australian journal of chemistry* **2009,** *62* (9), 1014-1019.

63. Buckingham, D. A.; Marzilli, L. G.; Sargeson, A. M., Peptide bond formation and subsequent hydrolysis at a cobalt (III) center. *Journal of the American Chemical Society* **1967,** *89* (11), 2772-2773.

64. Buckingham, D. A.; Marzilli, L. G.; Sargeson, A. M., N-Terminal addition of glycine to amino acid and peptide esters activated by the cobalt (III) ion. *Journal of the American Chemical Society* **1967,** *89* (17), 4539-4540.

65. Buckingham, D. A.; Davis, C.; Foster, D.; Sargeson, A. M., Cobalt (III)-promoted hydrolysis of chelated glycine amides, glycylglycine, and glycylglycine esters. Kinetics and mechanism. *Journal of the American Chemical Society* **1970,** *92* (19), 5571-5579.

66. Clark, C.; Tasker, R.; Buckingham, D.; Knighton, D.; Harding, D.; Hancock, W., Cobalt (III)-mediated peptide synthesis. 1. Cobalt (III)-activated amino acid methyl esters and the synthesis of dipeptides. *Journal of the American Chemical Society* **1981,** *103* (23), 7023-7025.

67. Sutton, P. A.; Buckingham, D. A., Cobalt (III)-promoted hydrolysis of amino acid esters and peptides and the synthesis of small peptides. *Accounts of Chemical Research* **1987,** *20* (10), 357-364.

68. Bodanszky, M., Synthesis of peptides by aminolysis of nitrophenyl esters. *Nature* **1955,** *175* (4459), 685-685.

69. Buckingham, D. A.; Foster, D.; Sargeson, A., Cobalt (III)-promoted hydrolysis of chelated glycine esters. Kinetics, anion competition, and oxygen-18 exchange studies. *Journal of the American Chemical Society* **1968,** *90* (22), 6032-6040.

70. Collman, J. P.; Kimura, E., Formation of peptide bonds in the coordination sphere of cobalt (III). *Journal of the American Chemical Society* **1967,** *89* (24), 6096-6103.

71. Lawson, P. J.; McCarthy, M. G.; Sargeson, A. M., Cobalt (III)-promoted syntheses of the amino acids (RS)-2-cyclopropylglycine and (R)-and (S)-proline. *Journal of the American Chemical Society* **1982,** *104* (24), 6710-6716.

72. Wu, Y.-L.; Busch, D. H., Reactions of coordinated ligands. XX. Cobalt (III)-promoted hydrolysis of glycine tert-butyl ester. *Journal of the American Chemical Society* **1970,** *92* (11), 3326-3332.

73. Alexander, M. D.; Busch, D. H., Reactions of Coordinated Ligands. XIII. Cobalt (III)-Promoted Hydrolysis of Glycine Esters. *Journal of the American Chemical Society* **1966,** *88* (6), 1130-1138.

74. Baraniak, E.; Buckingham, D.; Clark, C.; Moynihan, B.; Sargeson, A., Cobalt (III)-promoted hydrolysis of esters. Hydrolysis of chelated and monodentate. beta.-alanine isopropyl ester and interconversions via hydrolysis intermediates. *Inorganic Chemistry* **1986,** *25* (19), 3466-3478.

75. Browne, R. J.; Buckingham, D. A.; Clark, C. R.; Sutton, P. A., The Cobalt (III)-Promoted Synthesis of Small Peptides. *Advances in Inorganic Chemistry* **1999,** *49*, 307-373.

76. Buckingham, D.; Marzilli, L.; Sargeson, A., Racemization and Deuteration at the Asymmetric Nitrogen Center of the N-Methylethylenediaminetetraamminecobalt (III) Ion. *Journal of the American Chemical Society* **1967,** *89* (4), 825-830.

77. Horsman, G. P.; Zechel, D. L., Phosphonate biochemistry. *Chemical Reviews* **2016,** *117* (8), 5704-5783.

78. Galezowska, J.; Gumienna-Kontecka, E., Phosphonates, their complexes and bio-applications: A spectrum of surprising diversity. *Coordination Chemistry Reviews* **2012,** *256* (1), 105-124.

79. Russell, R. G. G., Bisphosphonates: mode of action and pharmacology. *Pediatrics* **2007,** *119* (Supplement 2), S150-S162.

80. Dutta, S.; Malla, R. K.; Bandyopadhyay, S.; Spilling, C. D.; Dupureur, C. M., Synthesis and kinetic analysis of some phosphonate analogs of cyclophostin as

inhibitors of human acetylcholinesterase. *Bioorganic Medicinal Chemistry* **2010,** *18* (6), 2265-2274.

81. Bajgar, J., Organophosphates/nerve agent poisoning: mechanism of action, diagnosis, prophylaxis, and treatment. *Adv Clin Chem* **2004,** *38* (1), 151-216.

82. Colovic, M. B.; Krstic, D. Z.; Lazarevic-Pasti, T. D.; Bondzic, A. M.; Vasic, V. M., Acetylcholinesterase inhibitors: pharmacology and toxicology. *Current neuropharmacology* **2013,** *11* (3), 315-335.

83. Skalka, A. M., Retroviral proteases: first glimpses at the anatomy of a processing machine. *Cell* **1989,** *56* (6), 911-913.

84. Jacobsen, N. E.; Bartlett, P. A., A phosphonamidate dipeptide analog as an inhibitor of carboxypeptidase A. *Journal of the American Chemical Society* **1981,** *103* (3), 654-657.

85. Christianson, D. W.; Lipscomb, W. N., Comparison of carboxypeptidase A and thermolysin: inhibition by phosphonamidates. *Journal of the American Chemical Society* **1988,** *110* (16), 5560-5565.

86. Bartlett, P. A.; Marlowe, C. K., Phosphonamidates as transition-state analog inhibitors of thermolysin. *Biochemistry* **1983,** *22* (20), 4618-4624.

87. Grobelny, D.; Wondrak, E. M.; Galardy, R. E.; Oroszlan, S., Selective phosphinate transition-state analogue inhibitors of the protease of human immunodeficiency virus. *Biochemical biophysical research communications* **1990,** *169* (3), 1111-1116.

88. Dreyer, G. B.; Metcalf, B. W.; Tomaszek, T. A.; Carr, T. J.; Chandler, A. C.; Hyland, L.; Fakhoury, S. A.; Magaard, V. W.; Moore, M. L.; Strickler, J. E., Inhibition of human immunodeficiency virus 1 protease in vitro: rational design of substrate analogue inhibitors. *Proceedings of the National Academy of Sciences* **1989,** *86* (24), 9752-9756.

89. Bartlett, P. A.; Hanson, J. E.; Giannousis, P. P., Potent inhibition of pepsin and penicillopepsin by phosphorus-containing peptide analogs. *The Journal of Organic Chemistry* **1990,** *55* (26), 6268-6274.

90. Bartlett, P. A.; Kezer, W. B., Phosphinic acid dipeptide analogs: potent, slow-binding inhibitors of aspartic peptidases. *Journal of the American Chemical Society* **1984,** *106* (15), 4282-4283.

91. McLeod, D. A.; Brinkworth, R. I.; Ashley, J. A.; Janda, K. D.; Wirsching, P., Phosphonamidates and phosphonamidate esters as HIV-1 protease inhibitors. *Bioorganic Medicinal Chemistry Letters* **1991,** *1* (11), 653-658.

Chapter 2. Polydentate Imine Phosphonate Complexes of Cobalt(III)

2.1 Introduction

The coordination chemistry of cobalt(III) is well known. One application is its use as a template for reactions within the coordination sphere of the metal ion. Templating becomes very useful when seeking to minimise stereochemical complexity.[28, 45, 49, 53, 92-94] The significance of the complexes of cobalt(III) lies in the inherent substitutional inertness which facilitates their isolation and characterization of the various isomeric products.[95] Most cobalt(III) complexes occur in the octahedral geometry.

Coordination of the polyamine ligand, triazaundecane-1,11-diamine (tetraen), around cobalt(III) metal centre, shown in Figure 2.1 determines which primary or secondary amines would be available for attack upon the target molecule. The secondary amine *trans* to the incoming ligand cannot react because it is on the wrong side of the molecule.

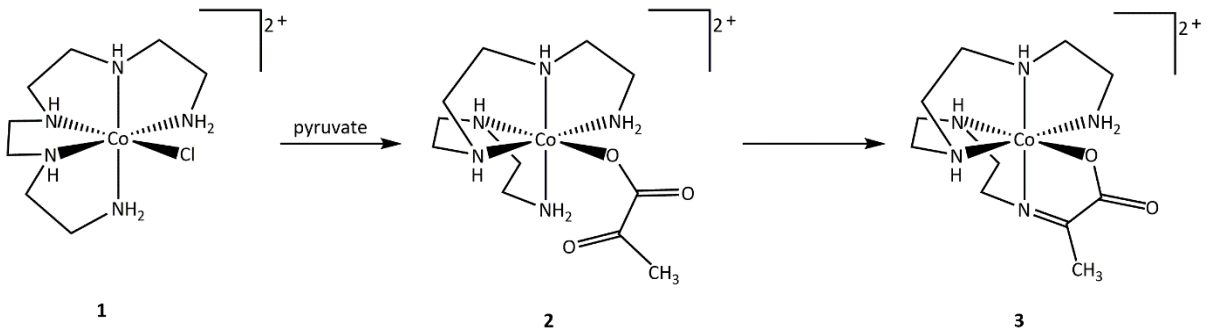

Figure 2.1 Ligand exchange-condensation sequence to imine complexes of cobalt(III).[53]

Once the pyruvate replaces the chloride ligand of the complex, one of the primary amines would undergo deprotonation by the mild base (2,6-lutidine) used for these condensation reactions. The other primary amine can also be deprotonated. The nucleophile thus generated attacks the pendant carbonyl group of the new ligand. A carbinolamine **2b (**Fig. 2.2) or **2c (**Fig. 2.3 and Fig. 2.4) is formed. It is the dehydration of a carbinolamine that yields an imine. It has been demonstrated that in cases where the dehydration is prohibited because the imine donor is not at the centre of a meridional ligand fragment (from the reaction occurring at the other primary amine site), the polyamine ligand wrapping would have to be re-arranged to effect dehydration[53] (Figure 2.4). The reaction could also occur at the meridional secondary amine as in **2d** in Fig. 2.3. However, the dehydration for the imine formation cannot occur in that arrangement because the meridional nitrogen atom (in **2d**) has used up all of its valence electrons.

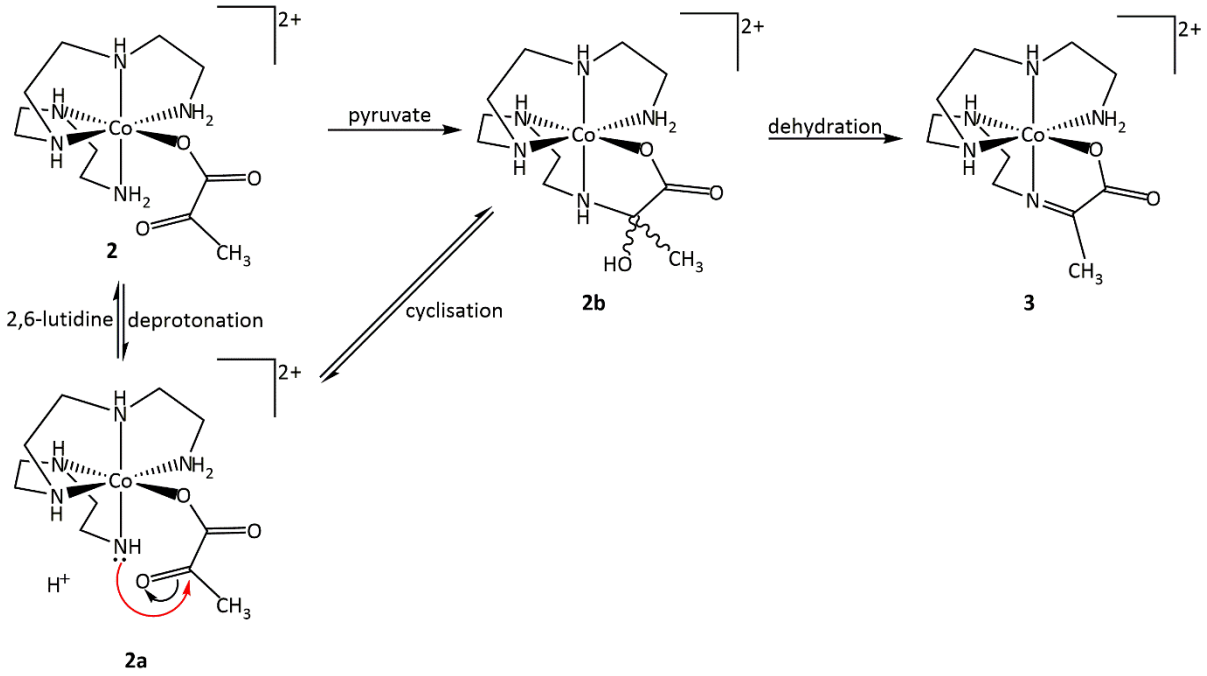

Figure 2.2 Schematic for formation of one of the carbinolamines and its dehydration

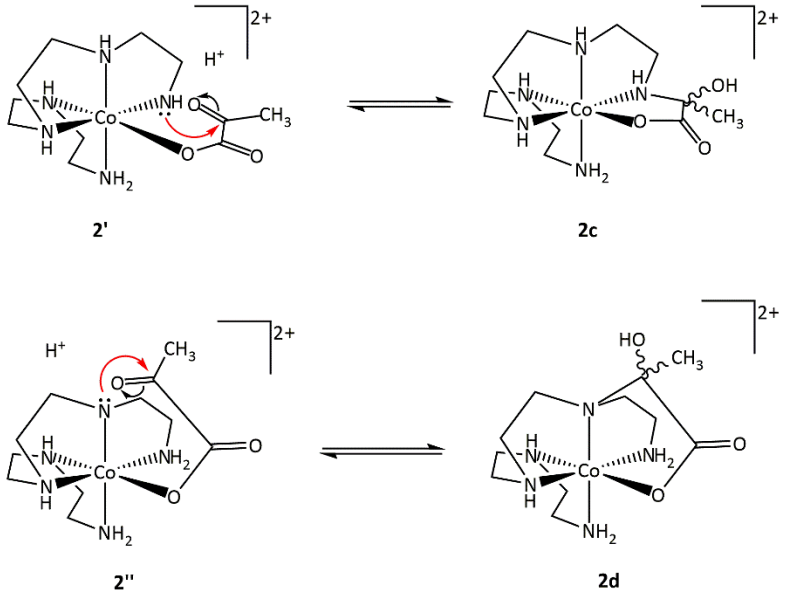

Figure 2.3 Schematic for other isomeric possibilities from the pyruvate reaction. **2c** is a non-planar carbinolamine which would not dehydrate; **2d** cannot dehydrate too.

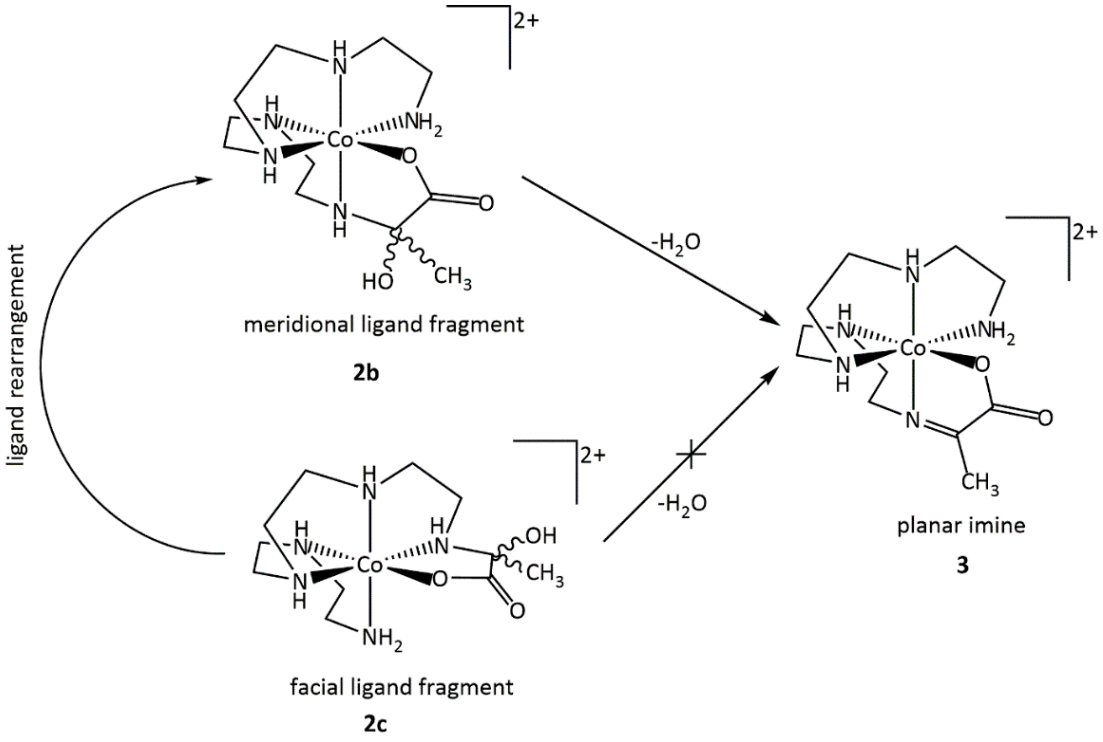

Figure 2.4 Ligand rearrangement of one of the possible carbinolamines and dehydration to yield an imine

The geometry that the polydentate ligand adopts around the metal ion influences both the regiochemistry of the reaction and its stereochemical outcome. It is the ability of the carbinolamine (formed from the cyclization) to dehydrate to yield an imine that determines what arrangement the atoms will adopt around the octahedron. Thus, imine complexes have been formed through a ligand exchange-condensation sequence as shown in Figure 2.1 coupled with reversibility of any cyclisation with secondary amines and rearrangements/reversibility for the wrong primary amine. Imines are excellent ligands and they provide ready routes to their amine derivatives by reduction.

This geometrical constraint associated with the presence of the imine group restricts the number of wrappings available to the newly synthesised polydentate ligand[54]. It is the ability of the polyamine to change its wrapping around the central metal ion that facilitates the formation of a particular isomer. Therefore, control can be gained over the otherwise daunting number of isomers that would originally result from systems of the type shown in Figure 2.1.

It has been reported[53] that the stereoselectivity of this condensation reaction yields only the imine complex (**3**) as shown in Figures 2.1, 2.2 and 2.4 and its enantiomer, even when three different pairs of diastereoisomers of the starting material (**1**) were used. This current research

explores the use of phosphonates (Fig. 2.5) as analogues of carboxylates (Fig. 2.6) in similar systems.

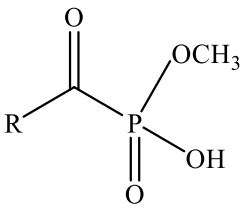

Figure 2.5 Phosphonate ester

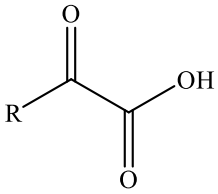

Figure 2.6 Ketocarboxylic acid

Phosphonates are a class of organophosphorus compounds with carbon-phosphorus (C-P) bonds. A lot of phosphonates are biologically active (for example Fig. 2.7), as has been discussed in the introductory chapter.

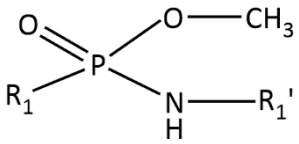

Figure 2.7 General structure of phosphonamidate esters (inhibitors of the HIV-1 PR[91]); R_1 and R_1' represent amino acids.

Phosphonate ligands similar to that shown in Fig. 2.5 where R is either a methyl (CH_3) or a phenyl (C_6H_5) group, have been synthesized and used to generate new systems of polydentate phosphonate imine complexes of cobalt(III) and the results are reported herein.

2.2 Experimental

2.2.1 Materials and Methods

$[Co(tetraen)Cl]ZnCl_4$ and $[Co(en)_2Cl_2]Cl$ were prepared according to literature methods [46,96]. $[Co(trien)Cl_2]Cl$[97] was obtained from the Hartshorn laboratory. Monosodium salts of acetyl phosphonates were made by a combination of both Kabachnik[98] and Dixon's[99] methods. Reagent grade chemicals (or better) obtained from Sigma-Aldrich were used without further purification, unless otherwise specified. Sephadex SPC 25 120 cation exchange resin and Dowex 50WX2 100-200 mesh were washed before use as for chromatographic separations. Column dimensions are given as height × diameter. A Büchi rotary evaporator equipped with a diaphragm vacuum pump and water bath was used to concentrate solutions under reduced pressure.

Single crystal X-ray data of these phosphonate imine complexes of cobalt(III) were obtained. A suitable crystal was selected and mounted on a nylon loop in perfluorinated PEG on a SuperNova, Dual, Cu at zero, Atlas diffractometer. The crystal was kept at 120 K during data collection. Determination, refinement of cell parameters and absorption corrections were made using CrysAlisPro.[100] Using Olex2[101], each structure was solved with the ShelXT[102] structure solution program using Intrinsic Phasing and refined with the ShelXL[103] program using Least Squares minimisation on wR_2.

Numerical face indexed absorption corrections were done on all structures unless otherwise stated.

All non-hydrogen atoms were refined anisotropically, except in some cases where disorder was modelled. Hydrogen atoms bonded to carbon atoms were added in calculated positions and refined using a riding model with fixed isotropic thermal parameters (applying a multiplier factor of 1.2 or 1.5 to that of the parent atom, for aromatic carbons and for all other carbons, respectively). However, the positions of hydrogen atoms bonded to nitrogen and oxygen atoms were located in the residual electron density map, the distance to the parent atom fixed at 0.86 Å using DFIX and their thermal parameters fixed by a multiplier factor of 1.5 that of the parent atom. Methyl groups were refined as an idealised tetrahedron and were free to rotate.

Unit cell parameters and details of the data collection for each crystal structure included in this chapter are given in the Appendix 2.

2.2.2 General Procedure for The Synthesis of Phosphonate Imine Complexes of Cobalt(III)

A cobalt(III) polyamine complex of choice is first synthesized[31, 51, 96]. Depending on whether the cobalt complex had one or two labile ligands, one equivalent of the complex typically on a 1 - 2 g scale was mixed with either two (for one labile ligand) or four (for two labile ligands) equivalents of the monosodium salt of an acyl phosphonate ligand. A mixture was thereafter made with two or four equivalents respectively of the mild base 2,6-lutidine, in excess methanol (about 250 mL) and heated at reflux for 48 h. A precipitate sometimes developed over the reflux period. The resulting mixture was cooled to room temperature and the methanol was removed on a rotary evaporator at 40 °C. The crude mixture was made up to 1 L with reverse osmosis (RO) water and loaded onto a Sephadex SPC 25 120 mesh cation exchange resin column (48 cm x 5 cm). The loaded column is first washed with 1 L of RO water, then

subsequently eluted with 0.05-1.0 M NaCl. The major fraction was usually the first to elute followed by one or two minor fractions. The salt laden solution of each fraction was collected and taken to dryness on a rotary evaporator.

2.2.3 Desalting and Salting Out Procedure

Desalting was achieved by dissolving the dried sample (2-3 g) in 50 mL aliquots of methanol. Since NaCl is sparingly soluble in methanol, the product dissolves, leaving most of the salt on the walls of the flask. Filtration and evaporation of the methanolic solution under vacuum was repeated with less methanol for each repeat until the solution had little or no salt. The crude material obtained after this procedure is usually still contaminated with NaCl.

The resulting residue was isolated as the tetrachloridozincate salt by dissolving the crude product (about 1.5 g) in a minimum amount of methanol (<100 mL), warming the solution on a water bath, and methanolic zinc chloride (0.34 g; 2.5 mmol of $ZnCl_2$ in 5 mL of methanol) was slowly added to the hot solution until a precipitate formed. The solution was cooled and filtered before characterisation.

2.2.4 Measurements

NMR spectra were measured on an Agilent NMRS-400 spectrometer. ^{1}H, $^{13}C\{^{1}H\}$ and $^{31}P\{^{1}H\}$ NMR were recorded in deuterium oxide solution. Chemical shifts are reported in parts per million (ppm) from 3-(trimethylsilyl)propionic 2,2,3,3-d_4 acid, sodium salt (TSP) (^{1}H, ^{13}C δ 0 ppm) as an internal standard and from 10% H_3PO_4 (^{31}P, δ 0 ppm) as an external standard in ^{31}P NMR. Infra-red spectra were recorded using Bruker's ALPHA with a platinum-ATR disc. Electronic spectra were recorded in water using CARY100Bio UV-Visible spectrophotometer from 200-800 nm at room temperature whereas mass spectrometry measurements were obtained using UltiMate 3000 mass spectrometer. Elemental analyses were performed by the Campbell Microanalytical Laboratory (University of Otago, NZ).

2.2.5 Syntheses

Procedure 1

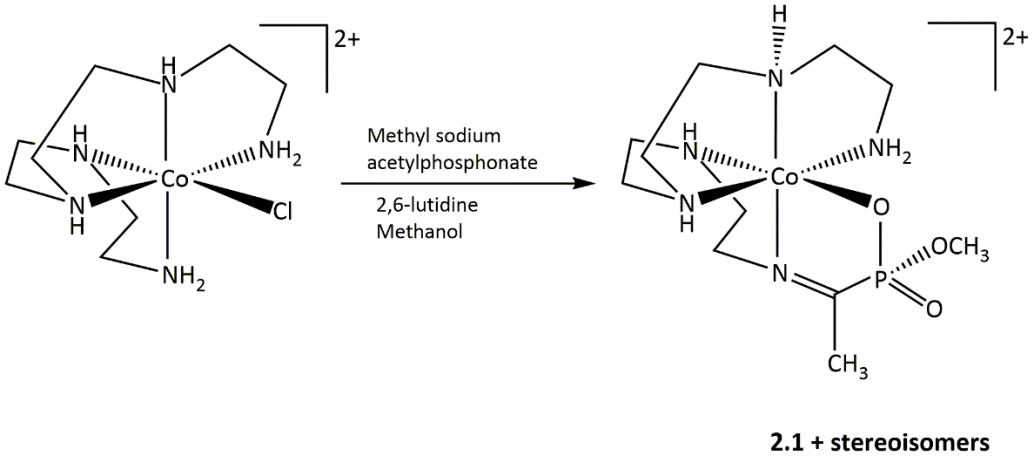

Figure 2.8 Reaction scheme for procedure 1

A mixture of [Co(tetraen)Cl]$ZnCl_4$ (1.23 g, 2.5 mmol), methyl sodium acetylphosphonate (0.93 g, 5.5 mmol) and 2,6-lutidine (0.59 g, 5.5 mmol) in 250 mL of methanol were heated at reflux for 48 h. A reddish-brown precipitate developed over this time. The mixture was cooled to room temperature and the methanol was removed on a rotary evaporator at 40 °C. The crude product was dissolved in 1 L of RO water and loaded onto a Sephadex SPC 25 column. The column was pre-washed with RO water and eluted with 0.05-1.0 M NaCl. One major orange fraction was separated from two minor ones and was collected. NaCl was removed from the fraction according to the desalting procedure outlined in section 2.2.3. This major product (0.97 g including NaCl) was shown to be a mixture of stereoisomers by NMR.

^{1}H NMR (ppm): 2.59 - 2.66 (C**H$_2$**-CH_2-N=C, m), 2.70 (C**H$_3$** , d, $^3J^{HP}$ = 12 Hz), 2.76 (C**H$_2$**-CH_2-N=C, m), 2.84 - 2.88 (C**H$_2$**-CH_2-N=C, m), 3.0 - 3.15 (C**H$_2$**-NH and C**H$_2$**–NH_2, m), 3.16 - 3.26 (C**H$_2$**-NH and C**H$_2$**–NH_2, m), 3.28 - 3.46 (NH_2-CH_2-C**H$_2$**-NH, m), 3.54 - 3.59 (NH_2-CH_2-C**H$_2$**-NH, m), 3.83 (OC**H$_3$** , d, $^3J^{HP}$ = 12 Hz), 3.86 (OC**H$_3$**, d, $^3J^{HP}$ = 8 Hz), 3.88 (OC**H$_3$**, d, $^3J^{HP}$ = 8 Hz), 4.23 - 4.38 (C**H$_2$**-N=C, m); ^{31}P{^{1}H} NMR (ppm): 28.73, 28.92, 29.29, 29.40 (**P**-OCH_3); ^{13}C{^{1}H} NMR (ppm): 193.11 (**C**=N, d, $^1J^{CP}$ = 176.1 Hz), 192.96 (**C**=N, d, $^1J^{CP}$ = 176.0 Hz), 58.48 (H_2**C**-N=C), 57.64 (O**C**H_3, d, $^2J^{CP}$ = 9.9 Hz), 57.58 (O**C**H_3, d, $^2J^{CP}$ = 9.1 Hz), 56.98 (**C**H_2-CH_2-N=C, d, $^4J^{CP}$ = 6.8 Hz), 56.59 (**C**H_2 adj. NH), 56.26 (**C**H_2-NH-CH_2), 56.09 (NH_2-CH_2-

CH$_2$), 52.99 (**C**H$_2$ adj. NH, d, $^4J^{CP}$ = 3.0 Hz), 52.47 (NH$_2$-**C**H$_2$), 51.13 (**C**H$_2$-CH$_2$-NH, d, $^5J^{CP}$ = 10.6 Hz) 23.37 (**C**H$_3$, d, $^2J^{CP}$ = 17.5 Hz), 23.38 (**C**H$_3$, d, $^2J^{CP}$ = 17.5 Hz).

IR spectrum (cm^{-1}): 1632 (C=N), 3251 (NH and NH$_2$).

Anal. Calcd. for $C_{11}H_{27}Cl_4CoN_5O_3PZn \cdot 0.5CH_3OH \cdot H_2O$ (%): C, 22.71; H, 4.82; N, 11.52. Found: C, 22.52; H, 4.81; N, 11.87.

Electronic spectrum λ_{max} (ε_{max}): 471 nm (150 Lmol^{-1}cm^{-1}); ESIMS: *m/z* = 183.5 ([M]$^{2+}$ 100%), 184.0 ([M]$^{2+}$ 15%), 184.5 ([M]$^{2+}$ 2%).

The isomer **2.1** was recrystallized by diffusing acetone into a 0.1 M HCl solution of the tetrachloridozincate salt of the mixture.

Crystal Data for $C_{11}H_{27}Cl_4CoN_5O_3PZn$ (*M* =574.44 g/mol): triclinic, space group P$\bar{1}$ (no. 2), *a* = 8.1037(5) Å, *b* = 10.2097(8) Å, *c* = 14.1124(7) Å, α = 101.636(5)°, β = 91.405(4)°, γ = 111.759(6)°, *V* = 1055.79(13) Å^3, *Z* = 2, *T* = 120.01(10) K, μ(CuKα) = 13.130 mm^{-1}, *Dcalc* = 1.807 g/cm^3, 7094 reflections measured (6.432° ≤ 2Θ ≤ 142.566°), 4047 unique (R_{int} = 0.0546, R_{sigma} = 0.0589) which were used in all calculations. The final R_1 was 0.0383 (I > 2σ(I)) and wR_2 was 0.0954 (all data).

Procedure 2

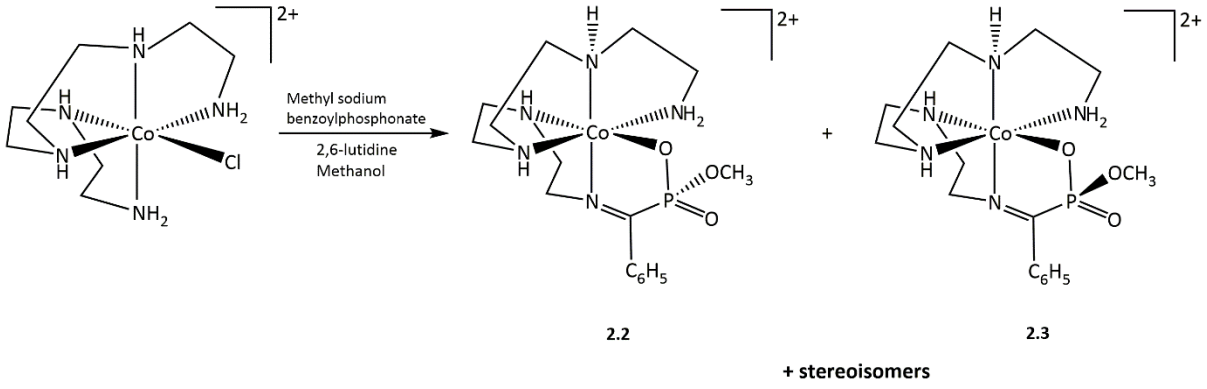

Figure 2.9 Reaction scheme for procedure 2

A mixture of [Co(tetraen)Cl]ZnCl$_4$ (1.23 g, 2.5 mmol), methyl sodium benzoylphosphonate (1.22 g, 5.5 mmol) and 2,6-lutidine (0.59 g, 5.5 mmol) in 250 mL of methanol were heated at reflux for 48 h. A reddish-brown precipitate developed over this time. The mixture was cooled to room temperature and the methanol was removed on a rotary evaporator at 40 °C. The crude

product was dissolved in 1 L of RO water and loaded onto a Sephadex SPC 25 column. The column was pre-washed with RO water and elution commenced with 0.05 M NaCl. The major fraction was orange and eluted with 0.2 M NaCl. NaCl was removed from the fraction according to the desalting procedure outlined in section 2.2.3. Compound **2.2** was from this major fraction. The minor fraction gave compound **2.3**. Characterisation of the major fraction is given below.

^{1}H NMR (ppm): 2.69 - 2.86 (C**H$_2$**-CH$_2$-N=C, m), 3.05 - 3.18 (C**H$_2$**-NH and –C**H$_2$**–NH$_2$, m), 3.25 - 3.36 (C**H$_2$**-NH and –C**H$_2$**–NH$_2$, m), 3.49 (OC**H$_3$**, d, $^{3}J^{HP}$ = 12 Hz), 3.55 (OC**H$_3$**, d,$^{3}J^{HP}$ = 12 Hz), 3.77 (OC**H$_3$**, d, $^{3}J^{HP}$ = 12 Hz), 3.82 (OC**H$_3$**, d, $^{3}J^{HP}$ = 12 Hz), 4.21 – 4.27 (C**H$_2$**-N=C, m), 4.30 - 4.38 (C**H$_2$**-N=C, m), 4.44 – 4.52 (N**H**, m), 4.63 – 4.71 (N**H**, m), 7.70 – 7.75 (C$_6$**H$_5$**, m), 7.83 (C$_6$**H$_5$**, m); ^{31}P{^{1}H} NMR (ppm): 26.82, 27.18, 27.53, 27.77, 28.19, 28.74 (**P**-OCH$_3$); ^{13}C{^{1}H} NMR (ppm): 190.65 (**C**=N, d, $^{1}J^{CP}$ = 176.8 Hz), 189.83 (**C**=N, d, $^{1}J^{CP}$ = 173.7 Hz), 134.67, 134.56, 134.15 (**C**-C=N), 131.09, 130.90 (**C**$_6$H$_5$(para)), 129.20, 129.16 (**C**$_6$H$_5$(ortho)), 128.39, 128.36 (**C**$_6$H$_5$(meta)), 58.75, 58.70 (H$_2$**C**-N=C), 58.02, 57.88, 57.86, 57.80, 57.68, 57.61, (O**C**H$_3$, m), 56.56 (**C**H$_2$-CH$_2$-N=C, m), 54.28, 54.16 (**C**H$_2$-NH), 53.17, 53.13 (**C**H$_2$-NH-CH$_2$), 52.58, 52.54 (NH$_2$-CH$_2$-**C**H$_2$), 51.77 (NH$_2$-**C**H$_2$), (51.18, 51.08 (**C**H$_2$-CH$_2$-NH, d, $^{5}J^{CP}$ = 10.6 Hz).

IR spectrum (cm^{-1}): 1630 (C=N), 3257 (NH and NH$_2$).

Anal. Calcd. for C$_{16}$H$_{29}$Cl$_4$CoN$_5$O$_3$PZn·2H$_2$O (%): C, 28.56; H, 4.94; N, 10.41. Found: C, 28.65; H, 4.75; N, 10.34.

Electronic spectrum λ_{max} (ε_{max}): 467 nm (160 Lmol^{-1}cm^{-1}); ESIMS: *m/z* = 214.57 ([M]$^{2+}$ 100%), 215.07 ([M]$^{2+}$ 25%), 215.57 ([M]$^{2+}$ 2%).

Crystals of **2.2** from fraction 1 of procedure 2 were grown by vapour diffusion of acetone mixed with tetrahydrofuran and methanol into a 0.1 M HCl solution of the ZnCl$_4$ salt of the mixture.

Crystal Data: C$_{16}$H$_{29}$Cl$_4$CoN$_5$O$_3$PZn (*M* =636.51 g/mol): monoclinic, space group P2$_1$/n (no. 14), *a* = 14.0250(7) Å, *b* = 12.6934(6) Å, *c* = 17.1301(9) Å, β = 109.877(6)°, *V* = 2867.9(3) Å^3, *Z* = 4, *T* = 120.00(10) K, μ(CuKα) = 9.730 mm^{-1}, *Dcalc* = 1.474 g/cm^3, 20367 reflections measured (7.072° ≤ 2Θ ≤ 144.094°), 5634 unique (R_{int} = 0.0393, R_{sigma} = 0.0358) which were used in all calculations. The final R_1 was 0.0305 (I > 2σ(I)) and wR_2 was 0.0780 (all data).

Crystals of **2.3** from fraction 2 of procedure 2 were grown by vapour diffusion of acetone only into a 0.1 M HCl solution of the ZnCl$_4$ salt of the mixture.

Crystal Data: $C_{16}H_{31}Cl_4CoN_5O_4PZn$ (M =683.54 g/mol): triclinic, space group P$\bar{1}$ (no. 2), a = 9.2402(4) Å, b = 11.9830(5) Å, c = 13.8865(4) Å, α = 114.763(4)°, β = 102.300(3)°, γ = 90.166(4)°, V = 1356.78(10) Å^3, Z = 2, T = 120.00(10) K, μ(CuKα) = 10.387 mm^{-1}, *Dcalc* = 1.673 g/cm^3, 24037 reflections measured (7.214° ≤ 2Θ ≤ 153.484°), 5622 unique (R_{int} = 0.0464, R_{sigma} = 0.0370) which were used in all calculations. The final R_1 was 0.0391 (I > 2σ(I)) and wR_2 was 0.1093 (all data).

Procedure 3

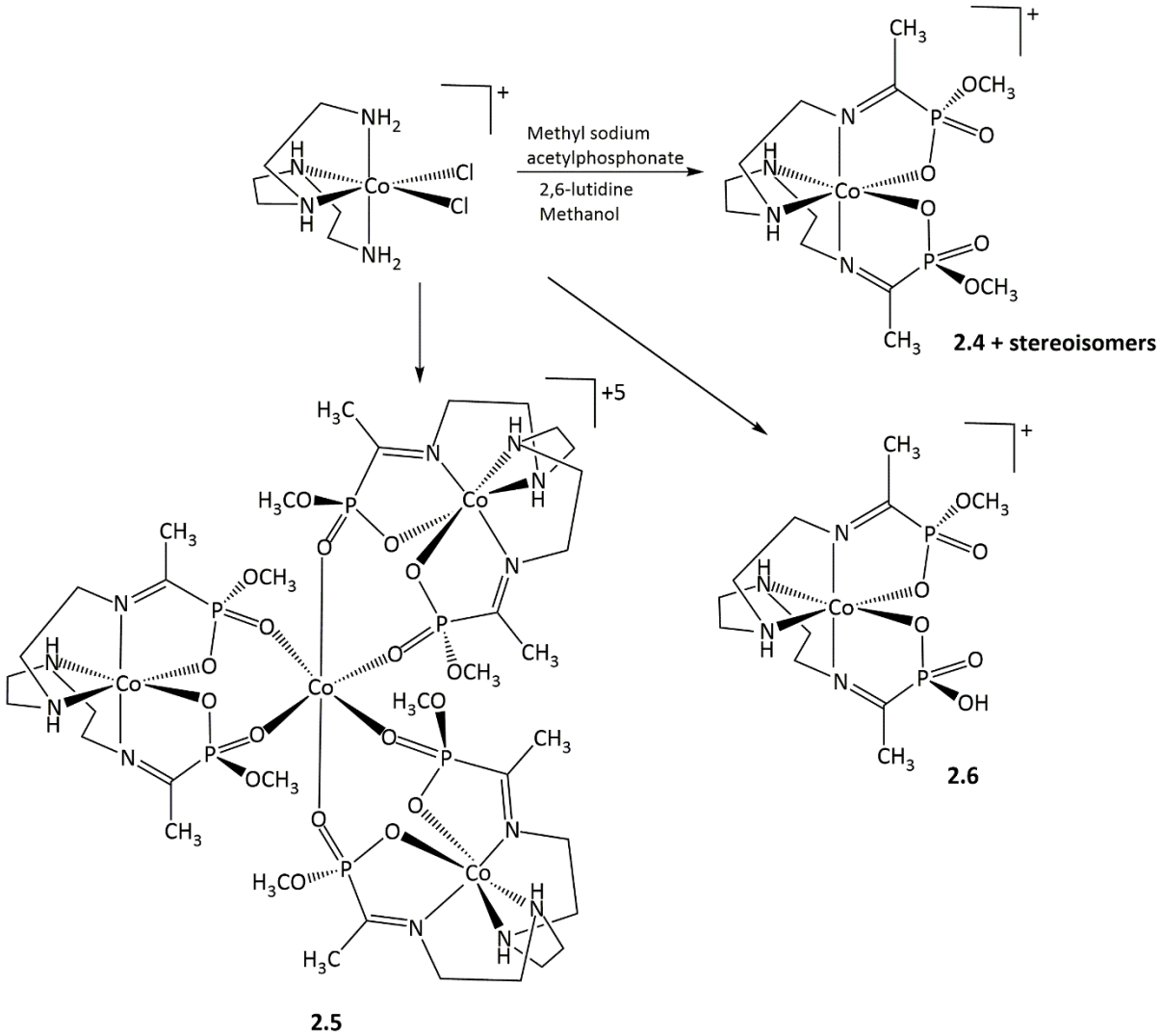

Figure 2.10 Reaction scheme for procedure 3

[Co(trien)Cl$_2$]Cl (1.38 g, 5.0 mmol), methyl sodium acetylphosphonate (3.38 g, 20.0 mmol) and 2,6-lutidine (2.14 g, 20.0 mmol) in 250 mL of methanol were mixed together and refluxed for 48 h. No precipitate formed over this time. The resulting red solution was cooled to room

temperature and the methanol removed on a rotary evaporator at 40 °C. The gel-like crude mixture was made up to 1 L with RO water (to give a purple red solution) and loaded onto an Sephadex SPC 25 column. Two fractions (a major and minor one) eluted with 0.05 M NaCl. NMR showed the minor second fraction was contaminated with 2,6-lutidine. Separation of the minor fraction on a second Sephadex SPC 25 column, yielded two fractions after elution with 0.05 M NaCl.

Fraction 1: ^{1}H NMR (ppm): 2.74 (C**H$_2$**-CH$_2$-N=C, m), 2.80 (C**H$_3$** , d, $^{3}J^{HP}$ = 9.6 Hz), 2.83 (C**H$_3$**, d, $^{3}J^{HP}$ = 9.6 Hz), 3.16 (C**H$_2$** adj. NH, m), 3.26 - 3.31 (C**H$_2$**-N=C, m), 3.69 (OC**H$_3$**, d,$^{3}J^{HP}$ = 12 Hz), 3.85 (OC**H$_3$**, d,$^{3}J^{HP}$ = 12 Hz), 4.3 - 4.6 (N**H**); ^{31}P{^{1}H} NMR (ppm): 29.61, 31.18 (**P**-OCH$_3$); ^{13}C{^{1}H} NMR (ppm): 192.33 (**C**=N, d, $^{1}J^{CP}$ = 178 Hz), 192.44 (**C**=N, d, $^{1}J^{CP}$ = 176 Hz), 57.70 (H$_2$**C**-N=C), 57.46 (**C**H$_2$ adj. NH), 57.26 (**C**H$_2$-CH$_2$-N=C), 57.07 (O**C**H$_3$, d, $^{2}J^{CP}$ = 6.1 Hz), 57.105 (O**C**H$_3$, d, $^{2}J^{CP}$ = 5.0 Hz), 23.18 (**C**H$_3$, d, $^{2}J^{CP}$ = 18 Hz), 23.30 (**C**H$_3$, d, $^{2}J^{CP}$ = 18 Hz).

IR spectrum (cm^{-1}): 1636 (C=N), 3292 (NH and NH$_2$).

Electronic spectrum λ_{max} (ε_{max}): 480 nm (140 Lmol^{-1}cm^{-1}); ESIMS: *m/z* = 443.07 ([M]$^{+}$ 100%), 444.07 ([M]$^{+}$ 25%), 445.07 ([M]$^{+}$ 2%).

Fraction 2: ^{1}H NMR (ppm): 2.70 (C**H$_2$**-CH$_2$-N=C, m), 2.82 (C**H$_3$**, d, $^{3}J^{HP}$ = 10 Hz), 3.11 (C**H$_2$**-NH, m), 3.2 (C**H$_2$**-N=C, m), 3.8 (OC**H$_3$**, d, $^{3}J^{HP}$ = 10.8 Hz), 4.3 – 4.6 (N**H**); ^{31}P{^{1}H} NMR (ppm): 30.97 (**P**-OCH$_3$); ^{13}C{^{1}H} NMR (ppm): 192.365 (**C**=N, d, $^{1}J^{CP}$ = 177 Hz), 57.70 (H$_2$**C**-N=C), 57.43 (**C**H$_2$-NH), 57.31 (**C**H$_2$-CH$_2$-N=C), 57.05 (O**C**H$_3$, d, $^{2}J^{cP}$ = 6.1 Hz), 23.24 (**C**H$_3$, d, $^{2}J^{CP}$ = 17.4 Hz).

Electronic spectrum λ_{max} (ε_{max}): 480 nm (140 Lmol^{-1}cm^{-1}); ESIMS: *m/z* = 443.07 ([M]$^{+}$100%), 444.07 ([M]$^{+}$ 25%), 445.07 ([M]$^{+}$ 2%).

Crystals of **2.5** formed upon addition of methanolic zinc chloride into a saturated methanolic solution of the mixture from the scale up experiment of procedure 3.

Crystal Data: $C_{37}H_{82}N_{12}O_{19}P_6Cl_{13}Co_4Zn_3$ (*M* =2077.64 g/mol): trigonal, space group R3c (no. 161), *a* = 15.3207(4) Å, *c* = 57.5738(13) Å, *V* = 11703.4(7) Å^3, *Z* = 6, *T* = 120.02(10) K, μ(CuKα) = 13.335 mm^{-1}, *Dcalc* = 1.769 g/cm^3, 19386 reflections measured (7.336° ≤ 2Θ ≤ 145.274°), 4433 unique (R_{int} = 0.0375, R_{sigma} = 0.0253) which were used in all calculations. The final R_1 was 0.0452 (I > 2σ(I)) and wR_2 was 0.1341 (all data).

Crystals of **2.6** were grown by vapour diffusion of acetone only into a 0.1 M HCl solution of the $ZnCl_4$ salt of a mixture obtained from another experiment (like procedure 3) carried out at the method development stage of this project, where a DOWEX column was used and eluted with 0.1 M HCl. Compound **2.6** is a partially hydrolysed molecule (hydrolysed on one of its phosphonate arms).

Crystal Data: $C_{10.75}H_{31.25}ClCoN_4Na_{0.25}O_{10}P_2$ (M =538.71 g/mol): triclinic, space group $P\bar{1}$ (no. 2), a = 7.9320(3) Å, b = 10.4761(6) Å, c = 13.6775(6) Å, α = 83.882(4)°, β = 87.529(4)°, γ = 73.459(4)°, V = 1083.21(9) Å^3, Z = 2, T = 120.00(12) K, μ(CuKα) = 9.306 mm^{-1}, *Dcalc* = 1.652 g/cm^3, 21835 reflections measured (8.848° ≤ 2Θ ≤ 147.484°), 4366 unique (R_{int} = 0.0616, R_{sigma} = 0.0382) which were used in all calculations. The final R_1 was 0.0398 (I > 2σ(I)) and wR_2 was 0.0989 (all data).

Procedure 4

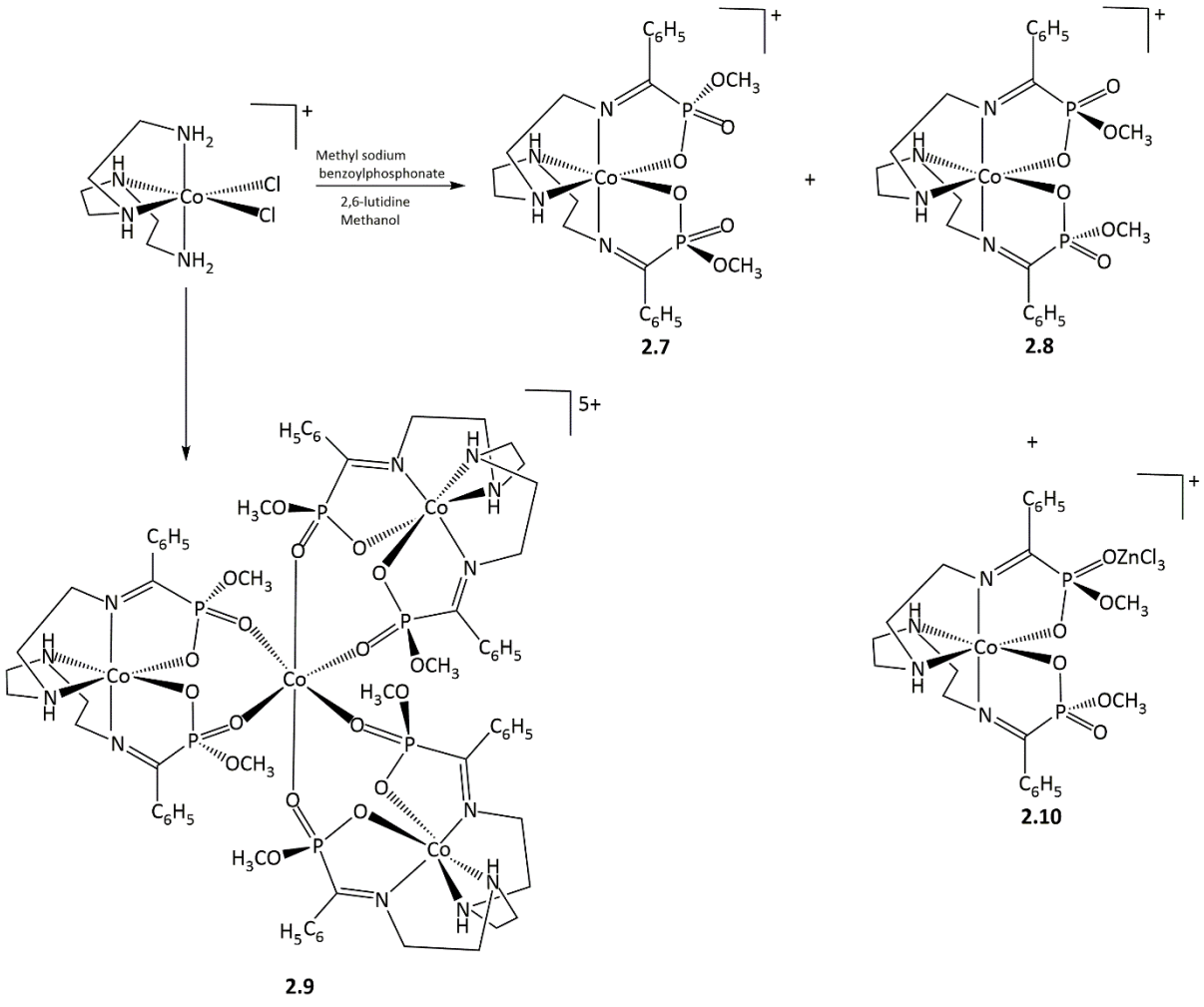

Figure 2.11 Reaction scheme for procedure 4

A mixture of $[Co(trien)Cl_2]Cl$ (1.38 g, 5.0 mmol), methyl sodium benzoylphosphonate (4.44 g, 20.0 mmol) and 2,6-lutidine (2.14 g, 20.0 mmol) in 250 mL of methanol were heated at reflux for 48 h. No precipitate formed over this time. The resulting red solution was cooled to room temperature and the methanol was removed on a rotary evaporator at 40 °C. The gel-like crude mixture was dissolved in 1 L of RO water to give a purple/red solution and loaded onto a Sephadex SPC 25 column. No clear separation was observed for this mixture, therefore the front and tail portions of the widened fraction were collected when the column was eluted with 0.05 M NaCl, as carefully as possible.

As with the product mixture from procedure 3, the tail portion of the product mixture from procedure 4 was also contaminated with 2,6-lutidine. A second Sephadex SPC 25 column, yielded two fractions after elution with 0.05 M NaCl. The resulting fractions were evaporated to dryness and isolated as tetrachloridozincate salts according to the procedure outlined in section 2.2.3.

Fraction 1: ^{1}H NMR (ppm): 2.72 – 2.94 (C**H**$_2$-CH_2-N=C, m), 3.24 – 3.34 (C**H**$_2$ adj. NH, m), 3.51 (OC**H**$_3$, d, $^{3}J^{HP}$ = 11.2 Hz), 3.52 (OC**H**$_3$, d, $^{3}J^{HP}$ = 10.8 Hz), 3.81 (OC**H**$_3$, d, $^{3}J^{HP}$ = 10.8 Hz), 3.84 (OC**H**$_3$, d, $^{3}J^{HP}$ = 12 Hz), 4.46 – 4.64 (C**H**$_2$-N=C, m), 7.72 – 7.85 (C_6**H**$_5$, m), 7.95, 7.97 (C_6**H**$_5$, m); ^{31}P{^{1}H} NMR (ppm): 27.52, 27.99, 30.19, 30.43 (**P**-OCH_3); ^{13}C{^{1}H} NMR (ppm): 189.10 (**C**=N, d, $^{1}J^{CP}$ = 175.3 Hz), 189.32 (**C**=N, d, $^{1}J^{CP}$ = 176 Hz), 135.86, 136.03 (**C**$_6H_5$(para)), 133.88 (quaternary C, d, $^{2}J^{CP}$ = 19 Hz), 134.03 (quaternary C, d, $^{2}J^{CP}$ = 18.2 Hz), 132.24, 132.39 (**C**$_6H_5$(meta), 130.43 (**C**$_6H_5$(ortho), d, $^{3}J^{CP}$ = 3.8 Hz), 130.96 (**C**$_6H_5$(ortho), d, $^{3}J^{CP}$ = 3.8 Hz), 59.49 (H_2**C**-N=C, d, $^{3}J^{CP}$ = 14.4 Hz), 59.65 (H_2**C**-N=C, d, $^{3}J^{CP}$ = 15.6 Hz), 58.11, 58.31 (**C**H_2 adj. NH), 57.99, 58.03 (**C**H_2-CH_2-N=C), 57.64 (O**C**H_3, d, $^{2}J^{CP}$ = 6.8 Hz), 56.98 (O**C**H_3, d, $^{2}J^{CP}$ = 6.9 Hz).

IR spectrum (cm^{-1}): 1635 (C=N), 3300 (NH and NH_2).

Anal. Calcd. for $C_{22}H_{30}N_4O_6P_2Cl_4CoZn$ (%): C, 34.61; H, 3.97; N, 7.34. Found: C, 34.62; H, 4.04; N, 7.31.

Electronic spectrum λ_{max} (ε_{max}): 486 nm (100 $Lmol^{-1}cm^{-1}$); ESIMS: *m/z* = 567.09 ($[M]^+$ 100%), 568.10 ($[M]^+$ 33%), 569.10 ($[M]^+$ 3%).

Fraction 2: ^{1}H NMR (ppm): 2.76 (C**H**$_2$-CH_2-N=C, m), 2.79 (C**H**$_2$-CH_2-N=C, m), 2.93 (C**H**$_2$-NH, m), 3.27 (C**H**$_2$-N=C, m), 3.51 (OC**H**$_3$, d, $^{3}J^{HP}$ = 12 Hz), 4.45 – 4.51 (N**H**, m), 7.74 – 7.79 (C_6**H**$_5$, m), 7.96 (C_6**H**$_5$, m); ^{31}P{^{1}H} NMR (ppm): 27.98 (**P**-OCH_3); ^{13}C{^{1}H} NMR (ppm):

189.11 (**C**=N, d, $^{1}J^{CP}$ = 175.3 Hz), 135.98, (**C**$_6$H$_5$(para)), 133.94 (quaternary C, d, $^{2}J^{CP}$ = 18.9 Hz), 132.22, (**C**$_6$H$_5$(meta), 130.91 (**C**$_6$H$_5$(ortho), d, $^{3}J^{CP}$ = 3.8 Hz), 59.43 (H$_2$**C**-N=C, d, $^{3}J^{CP}$ = 13.7 Hz), 58.09 (**C**H$_2$ adj. NH), 57.91 (**C**H$_2$-CH$_2$-N=C), 57.54 (O**C**H$_3$, d, $^{2}J^{CP}$ = 6.8 Hz);

Electronic spectrum λ_{max} (ε_{max}): 477 nm (90 Lmol^{-1}cm^{-1}); ESIMS: *m/z* = 567.09 ([M]$^+$ 100%), 568.10 ([M]$^+$ 33%), 569.10 ([M]$^+$ 3%).

Crystals of **2.7** (from fraction 2 of procedure 4) formed upon addition of methanolic zinc chloride into a saturated methanolic solution of the mixture.

Crystal Data: $C_{22}H_{33}ClCoN_4O_8P_2$ (*M* =637.84 g/mol): triclinic, space group P$\bar{1}$ (no. 2), *a* = 10.916(5) Å, *b* = 11.057(5) Å, *c* = 12.931(10) Å, α = 69.11(6)°, β = 68.43(6)°, γ = 78.12(4)°, *V* = 1351.0(16) Å^3, *Z* = 4, *T* = 120.01(10) K, μ(CuKα) = 7.480 mm^{-1}, *Dcalc* = 1.570 g/cm^3, 6547 reflections measured (7.73° ≤ 2Θ ≤ 152.85°), 4521 unique (R_{int} = 0.2341, R_{sigma} = 0.4843) which were used in all calculations. The final R_1 was 0.1010 (I > 2σ(I)) and wR_2 was 0.4582 (all data).

Crystals of **2.8** from fraction 1 of procedure 4 formed upon addition of methanolic zinc chloride into a saturated methanolic solution of the mixture.

Crystal Data: $C_{22}H_{30}Cl_4CoN_4O_6P_2Zn$ (*M* =774.54 g/mol): monoclinic, space group P2$_1$/c (no. 14), *a* = 12.2218(11) Å, *b* = 21.1027(17) Å, *c* = 14.5092(14) Å, β = 113.241(11)°, *V* = 3438.5(6) Å^3, *Z* = 4, *T* = 120.01(10) K, μ(CuKα) = 8.716 mm^{-1}, *Dcalc* = 1.496 g/cm^3, 31523 reflections measured (7.844° ≤ 2Θ ≤ 147.55°), 6948 unique (R_{int} = 0.0978, R_{sigma} = 0.0813) which were used in all calculations. The final R_1 was 0.0915 (I > 2σ(I)) and wR_2 was 0.2903 (all data).

Crystals of **2.9** from fraction 2 of procedure 4 were grown by vapour diffusion of acetone mixed with tetrahydrofuran into a 0.1 M HCl solution of the $ZnCl_4$ salt of the mixture.

Crystal Data: $C_{66}H_{90}Cl_{12}Co_4N_{12}O_{18}P_6Zn_3$ (*M* =2382.57 g/mol): trigonal, space group R3c (no. 161), *a* = 15.3774(10) Å, *c* = 75.3092(18) Å, *V* = 15422(2) Å^3, *Z* = 5.99994, *T* = 120.01(10) K, μ(CuKα) = 9.966 mm^{-1}, *Dcalc* = 1.539 g/cm^3, 16210 reflections measured (7.04° ≤ 2Θ ≤ 144.276°), 5600 unique (R_{int} = 0.0347, R_{sigma} = 0.0340) which were used in all calculations. The final R_1 was 0.0709 (I > 2σ(I)) and wR_2 was 0.2610 (all data).

Crystals of **2.10** from fraction 2 of procedure 4 formed after some days during refrigeration of a saturated methanolic solution of the mixture containing methanolic zinc chloride.

Crystal Data: $C_{22}H_{30}Cl_3CoN_4O_{6.4}P_2Zn$ (*M* =745.49 g/mol): monoclinic, space group $P2_1/n$ (no. 14), *a* = 11.7896(7) Å, *b* = 22.3431(13) Å, *c* = 12.2658(6) Å, *β* = 96.699(5)°, *V* = 3209.0(3) Å^3, *Z* = 4, *T* = 120.00(10) K, μ(CuKα) = 8.577 mm^{-1}, *Dcalc* = 1.543 g/cm^3, 31474 reflections measured (7.914° ≤ 2Θ ≤ 145.966°), 6407 unique (R_{int} = 0.0813, R_{sigma} = 0.0549) which were used in all calculations. The final R_1 was 0.0698 (I > 2σ(I)) and wR_2 was 0.2018 (all data).

Procedure 5

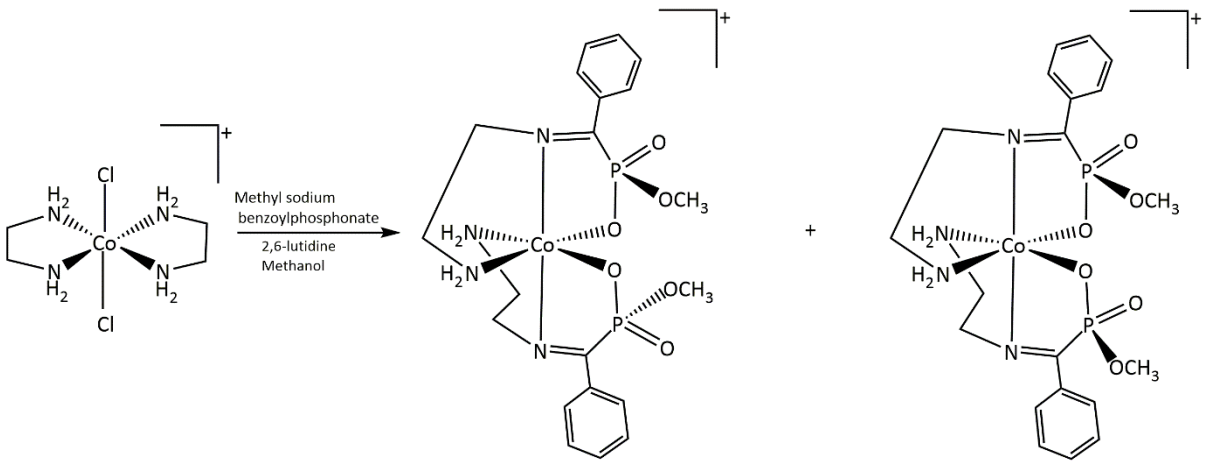

Figure 2.12 Reaction scheme for procedure 5

A mixture of $[Co(en)_2Cl_2]Cl$ (3.0 g, 0.01 mol), methyl sodium benzoylphosphonate (9.0 g, 0.04 mol) and 2,6-lutidine (4.5 g, 0.04 mol) in 450 mL of methanol were heated at reflux for 48 h. No precipitate formed over this time. Methanolic $ZnCl_2$ was added to the resulting red solution while hot and then left to cool to room temperature. The methanol was removed on a rotary evaporator at 40 °C. The gel-like crude mixture was made dissolved in 1 L of RO water (to give a red/orange solution) and adsorbed onto a Sephadex SPC 25 column. No clear separation was observed for this mixture, therefore the front and tail portions of the widened fraction were collected when the column was eluted with 0.05 M NaCl and were evaporated to dryness on a rotary evaporator.

Fraction 1: ^{1}H NMR (ppm): 2.82 – 2.89 (C**H**$_2$–NH$_2$, m), 3.68 (OC**H**$_3$, d, $^3J^{HP}$ = 12 Hz), 3.67 (OC**H**$_3$, d, $^3J^{HP}$ = 12 Hz), 3.54 (OC**H**$_3$, d, $^3J^{HP}$ = 12 Hz), 3.55 (OC**H**$_3$, d, $^3J^{HP}$ = 12 Hz), 4.47 – 4.58 (C**H**$_2$-N=C, m), 7.72 – 7.78 (C$_6$**H**$_5$, m), 7.86 - 7.93 (C$_6$**H**$_5$, m); $^{31}P\{^1H\}$ NMR (ppm): 28.63, 28.94, 30.50, 30.55 (**P**-OCH$_3$); $^{13}C\{^1H\}$ NMR (ppm): 188.18 (**C**=N, d, $^1J^{CP}$ = 176 Hz), 188.14

(**C**=N, d, $^{1}J^{CP}$ = 176 Hz), 188.10 (**C**=N, d, $^{1}J^{CP}$ = 174 Hz), 135.915 (**C**$_6$H$_5$(para)), 133.89 (quaternary C, d, $^{2}J^{CP}$ = 18 Hz), 133.88 (quaternary C, d, $^{2}J^{CP}$ = 18 Hz), 132.40, 132.38, 132.33 (**C**$_6$H$_5$(meta), 130.88 (**C**$_6$H$_5$(ortho), d, $^{3}J^{CP}$ = 3 Hz), 130.81 (**C**$_6$H$_5$(ortho), d, $^{3}J^{CP}$ = 3 Hz), 130.67 (**C**$_6$H$_5$(ortho), d, $^{3}J^{CP}$ = 3 Hz), 130.58 (**C**$_6$H$_5$(ortho), d, $^{3}J^{CP}$ = 3 Hz), 60.35 (H$_2$**C**-N=C, d, $^{3}J^{CP}$ = 13 Hz), 60.12 (H$_2$**C**-N=C, d, $^{3}J^{CP}$ = 14 Hz), 60.11 (H$_2$**C**-N=C, d, $^{3}J^{CP}$ = 14 Hz), 58.11, 58.31 (**C**H$_2$ adj. NH), 57.99, 58.03 (**C**H$_2$-CH$_2$-N=C), 57.57 (O**C**H$_3$, d, $^{2}J^{CP}$ = 6 Hz), 57.27 (O**C**H$_3$, d, $^{2}J^{CP}$ = 6 Hz), 57.50 (O**C**H$_3$, d, $^{2}J^{CP}$ = 6 Hz);

IR spectrum (cm^{-1}): 1629 (C=N), 3293 (NH and NH$_2$).

Electronic spectrum λ_{max} (ε_{max}): 472 nm (90 Lmol^{-1}cm^{-1}); ESIMS: *m/z* = 541.08 ([M]$^+$ 100%), 542.08 ([M]$^+$ 33%), 543.09 ([M]$^+$ 3%).

Crystals of **2.11** formed in the NMR tube used for the sample characterization of fraction 1 off the column, in the presence of the reference salt TSP.

Crystal Data: $C_{20}H_{30}ClCoN_4O_7P_2$ (*M* =594.80 g/mol): monoclinic, space group $P2_1/c$ (no. 14), *a* = 14.7930(4) Å, *b* = 11.6061(3) Å, *c* = 14.8838(5) Å, β = 104.573(3)°, *V* = 2473.17(13) Å^3, *Z* = 4, *T* = 120.00(10) K, μ(CuKα) = 8.093 mm^{-1}, *Dcalc* = 1.597 g/cm^3, 33260 reflections measured (9.786° ≤ 2Θ ≤ 153.778°), 5188 unique (R_{int} = 0.0434, R_{sigma} = 0.0233) which were used in all calculations. The final R_1 was 0.0383 (I > 2σ(I)) and wR_2 was 0.0993 (all data).

Fraction 2: ^{1}H NMR (ppm): 2.82 – 2.89 (C**H$_2$**–NH$_2$, m), 3.68 (OC**H$_3$**, d, $^{3}J^{HP}$ = 12Hz), 3.67 (OC**H$_3$**, d, $^{3}J^{HP}$ = 12 Hz), 3.55 (OC**H$_3$**, d, $^{3}J^{HP}$ = 12 Hz), 3.54 (OC**H$_3$**, d, $^{3}J^{HP}$ = 12 Hz), 4.47 – 4.58 (C**H$_2$**-N=C, m), 7.72 – 7.78 (C$_6$**H$_5$**, m), 7.86 - 7.93 (C$_6$**H$_5$**, m); ^{31}P{^{1}H} NMR (ppm): 28.63, 28.94, 30.50, 30.55 (**P**-OCH$_3$); ^{13}C{^{1}H} NMR (ppm): 188.18 (**C**=N, d, $^{1}J^{CP}$ = 176 Hz), 188.14 (**C**=N, d, $^{1}J^{CP}$ = 176 Hz), 188.00 (**C**=N, d, $^{1}J^{CP}$ = 174 Hz), 135.95, 135.88 (**C**$_6$H$_5$(para)), 133.99 (quaternary C, d, $^{2}J^{CP}$ = 18 Hz), 133.88 (quaternary C, d, $^{2}J^{CP}$ = 18 Hz), 132.40, 132.38, 132.33 (**C**$_6$H$_5$(meta), 130.88 (**C**$_6$H$_5$(ortho), d, $^{3}J^{CP}$ = 3 Hz), 130.81 (**C**$_6$H$_5$(ortho), d, $^{3}J^{CP}$ = 3 Hz), 130.67 (**C**$_6$H$_5$(ortho), d, $^{3}J^{CP}$ = 3 Hz), 130.58 (**C**$_6$H$_5$(ortho), d, $^{3}J^{CP}$ = 3 Hz), 60.35 (H$_2$**C**-N=C, d, $^{3}J^{CP}$ = 13 Hz), 60.12 (H$_2$**C**-N=C, d, $^{3}J^{CP}$ = 14 Hz), 60.11 (H$_2$**C**-N=C, d, $^{3}J^{CP}$ = 14 Hz), 58.11, 58.31 (**C**H$_2$ adj. NH), 57.99, 58.03 (**C**H$_2$-CH$_2$-N=C), 57.57 (O**C**H$_3$, d, $^{2}J^{CP}$ = 6 Hz), 57.27 (O**C**H$_3$, d, $^{2}J^{CP}$ = 6 Hz), 57.50 (O**C**H$_3$, d, $^{2}J^{CP}$ = 6 Hz);

Crystals of **2.12** formed during desalting from a saturated methanolic solution of fraction 2 off the column at 4 °C in the fridge.

Crystal Data: $C_{20}H_{30}ClCoN_4O_7P_2$ (*M* =594.80 g/mol): triclinic, space group PĪ (no. 2), *a* = 9.0001(3) Å, *b* = 9.5389(3) Å, *c* = 15.3957(4) Å, *α* = 86.716(2)°, *β* = 76.364(3)°, *γ* = 82.605(3)°, *V* = 1273.30(7) Å^3, *Z* = 2, *T* = 120.01(10) K, μ(CuKα) = 7.860 mm^{-1}, *Dcalc* = 1.551 g/cm^3, 6527 reflections measured (9.352° ≤ 2Θ ≤ 121.548°), 3840 unique (R_{int} = 0.0482, R_{sigma} = 0.0361) which were used in all calculations. The final R_1 was 0.0456 (I > 2σ(I)) and wR_2 was 0.1253 (all data).

Crystals of **2.13** from the product mixture of procedure 5 also formed during desalting from a saturated methanolic solution of fraction 2 off the column at 4 ℃ in the fridge.

Crystal Data: $C_{21}H_{32}ClCoN_4O_7P_2$ (*M* =608.82 g/mol): triclinic, space group PĪ (no. 2), *a* = 10.7865(6) Å, *b* = 11.5463(7) Å, *c* = 12.4136(5) Å, *α* = 103.013(4)°, *β* = 98.655(4)°, *γ* = 114.250(5)°, *V* = 1321.05(13) Å^3, *Z* = 2, *T* = 120.00(10) K, μ(CuKα) = 7.589 mm^{-1}, *Dcalc* = 1.531 g/cm^3, 20145 reflections measured (7.6° ≤ 2Θ ≤ 154.712°), 5344 unique (R_{int} = 0.0917, R_{sigma} = 0.0638) which were used in all calculations. The final R_1 was 0.0658 (I > 2σ(I)) and wR_2 was 0.2283 (all data).

Procedure 6

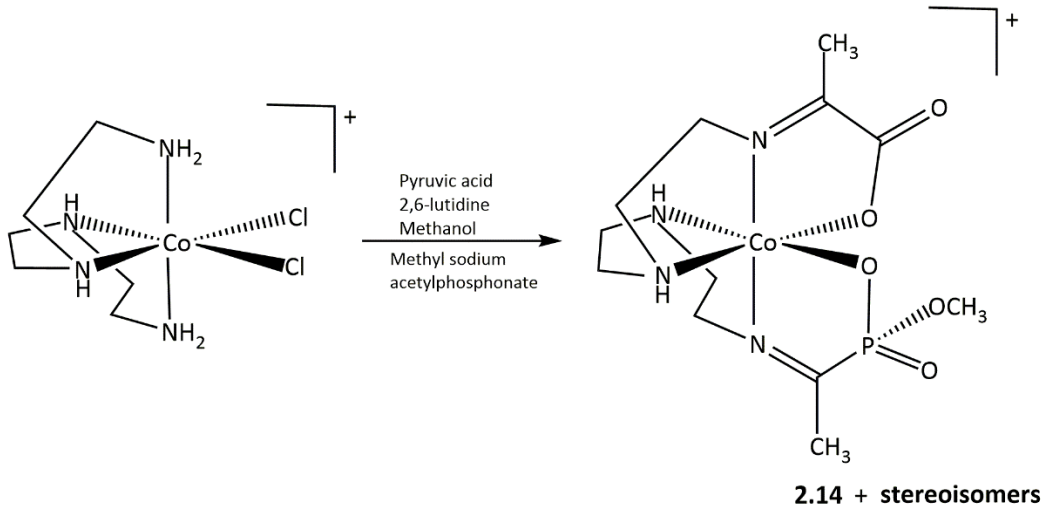

Figure 2.13 Reaction scheme for procedure 6

[Co(trien)Cl_2]Cl (11.05 g, 40.0 mmol), pyruvic acid (14.08 g; 120.0 mmol) and 2,6-lutidine (2.14 g, 20.0 mmol) in 400 mL of methanol were mixed and refluxed for 12 h. A precipitate formed during this time. After 12 h, methyl sodium acetylphosphonate (7.96 g; 47.1 mmol)

was added to the mixture and the solution was diluted to 600 mL with methanol and refluxed for a further 24 h. All precipitate disappeared over the 24 h reflux period. The resulting red solution was cooled to room temperature and the methanol removed on a rotary evaporator at 40 °C. The crude mixture was dissolved in 2 L of RO water and loaded onto a Sephadex SPC 25 column.

Fraction 1: ^{1}H NMR (ppm): 2.70, 2.71 (C**H**$_3$, overlapped singlets), 2.72 - 2.76 (C**H**$_2$-CH$_2$-N=C, m), 2.79 (C**H**$_3$, d, $^{3}J^{HP}$ = 8 Hz), 2.84 – 2.89 (C**H**$_2$-CH$_2$-N=C, m), 2.97 – 3.03 (C**H**$_2$-NH, m), 3.11 – 3.28 (C**H**$_2$-NH, m), 3.41 – 3.52 (C**H**$_2$-N=C, m), 3.61 (OC**H**$_3$, d,$^{3}J^{HP}$ = 12 Hz), 3.82 (OC**H**$_3$, d,$^{3}J^{HP}$ = 12 Hz), 4.36 (N**H,** m), 4.55 – 4.67 (N**H,** m); ^{31}P{^{1}H} NMR (ppm): 29.51, 30.87 (**P**-OCH$_3$); ^{13}C{^{1}H} NMR (ppm): 191.39 (**C**=N, d, $^{1}J^{CP}$ = 175 Hz), 191.41 (**C**=N, d, $^{1}J^{CP}$ = 175 Hz), 184.00 (O=C-**C**=N), 175.95 (**C**OOM), 58.21, 58.03 (H$_2$**C**-N=C on the phosphonate arm), 55.85, 55.50 (H$_2$**C**-N=C on the carboxylate arm), 57.43, 57.38 (**C**H$_2$-NH), 57.58, 57.55 (**C**H$_2$-CH$_2$-N=C on the phosphonate arm), 57.30, 57.27 (**C**H$_2$-CH$_2$-N=C on the carboxylate arm), 57.14 (O**C**H$_3$, d, $^{2}J^{CP}$ = 12 Hz), 57.09 (O**C**H$_3$, d, $^{2}J^{CP}$ = 10 Hz), 22.99 (**C**H$_3$ on the phosphonate arm, d, $^{2}J^{CP}$ = 18 Hz), 23.02 (**C**H$_3$ on the phosphonate arm, d, $^{2}J^{CP}$ = 18 Hz), 21.74, 21.55 (**C**H$_3$ on the carboxylate arm) .

IR spectrum (cm^{-1}): 1636 (C=N), 3287 (NH and NH$_2$).

Electronic spectrum λ_{max} (ε_{max}): 468 nm (170 Lmol^{-1}cm^{-1}); ESIMS: *m/z* = 393.07 ([M]$^{+}$ 100%), 394.08 ([M]$^{+}$ 25%), 395.08 ([M]$^{+}$ 2%).

Crystals of **2.14** from fraction 1 of procedure 6 formed upon addition of methanolic zinc chloride into a saturated methanolic solution of the mixture.

Crystal Data: $C_{24.75}H_{49.25}Cl_4Co_2N_8O_{10.75}P_2Zn$ (*M* =1018.29 g/mol): monoclinic, space group P2$_1$/n (no. 14), *a* = 21.196(2) Å, *b* = 12.4743(4) Å, *c* = 26.969(3) Å, *β* = 144.03(2)°, *V* = 4188.8(15) Å^3, *Z* = 4, *T* = 120.00(10) K, μ(CuKα) = 10.388 mm^{-1}, *Dcalc* = 1.615 g/cm^3, 45134 reflections measured (8.226° ≤ 2Θ ≤ 139.048°), 7795 unique (R_{int} = 0.0808, R_{sigma} = 0.0428) which were used in all calculations. The final R_1 was 0.1512 (I > 2σ(I)) and wR_2 was 0.3288 (all data).

Fraction 2: ^{1}H NMR (ppm): 2.68, 2.69 (C**H**$_3$, overlapped singlets), 2.74 – 2.76 (C**H**$_2$-CH$_2$-N=C, m), 2.80 (C**H**$_3$, overlapped doublets, $^{3}J^{HP}$ = 8 Hz), 2.85 – 2.88 (C**H**$_2$-CH$_2$-N=C, m), 2.97 – 3.01 (C**H**$_2$-CH$_2$-N=C, m), 3.08 – 3.27 (C**H**$_2$-NH, m), 3.41 – 3.49 (C**H**$_2$-N=C, m), 3.61 (OC**H**$_3$, d,$^{3}J^{HP}$ = 12 Hz), 3.82 (OC**H**$_3$, d,$^{3}J^{HP}$ = 12 Hz), 4.35 (N**H**, m), 4.52 – 4.69 (N**H**, m); ^{31}P{^{1}H}

NMR (ppm): 29.51, 30.87 (**P**-OCH_3); $^{13}C\{^1H\}$ NMR (ppm): 191.37 (**C**=N, d, $^1J^{CP}$ = 176 Hz), 191.46 (**C**=N, d, $^1J^{CP}$ = 178 Hz), 184.01 (O=C-**C**=N), 183.07 (O=C-**C**=N), 175.99 (**C**OOM), 58.21, 58.06, 58.04 (H_2**C**-N=C on the phosphonate arm), 57.59, 57.54, 57.44 (H_2**C**-N=C on the carboxylate arm), 57.38, (**C**H_2-NH), 57.14, 57.06 (**C**H_2-CH_2-N=C on the phosphonate arm), 55.93, 55.87, 55.52 (**C**H_2-CH_2-N=C on the carboxylate arm), 57.28 (O**C**H_3, d, $^2J^{CP}$ = 9 Hz), 57.25 (O**C**H_3, d, $^2J^{CP}$ = 10 Hz), 23.07 (**C**H_3 on the phosphonate arm, d, $^2J^{CP}$ = 18 Hz), 23.03 (**C**H_3 on the phosphonate arm, d, $^2J^{CP}$ = 18 Hz), 21.60, 21.35 (**C**H_3 on the carboxylate arm).

2.3 Results and Discussion

2.3.1 Crystal Structure Determinations of the Imine Complexes

In the following sections, a crystallographic mean plane analysis was used to confirm planarity of the imines in the X-ray structures obtained. Given six atoms Co, C, N=C, P and C as shown in Fig. 2.14, where the C=N double bond is the central part and the four other atoms are attached to the C and the N, a crystallographic plane can be applied.

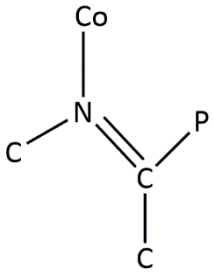

Figure 2.14 A mean plane goes through these six atoms for the mean plane analysis.

A crystallographic mean plane is made to go through these six atoms and the distance between the component atoms and that plane is measured. This distance in Angströms (Å) gives a measure of the deviations from that plane in the imines. The measurement was done for each imine bond present in a molecular structure.

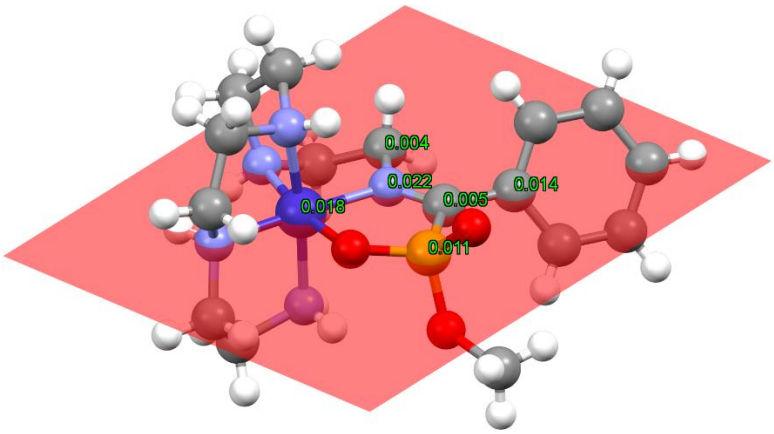

Figure 2.15 An example of a crystallographic mean plane analysis using compound **2.2**

The Hartshorn and House[27] system of nomenclature has been used for expressing the configurations of these complexes with respect to the polydentate wrapping around the metal ion. The Cahn, Ingold and Prelog[33] (CIP) rules have been applied at the phosphorus centres to express their chirality.

All the crystal structures obtained from this chapter occurred in centrosymmetric space groups. Therefore, each time a refined structure is shown, the absolute configuration of that diastereoisomer (as shown) would be stated. However, the presence of the other enantiomer (with the opposite absolute configuration) in the unit cell must also be considered. Thus, for every isomer shown, its enantiomer is also present in the unit cell.

Compound 2.1

The crystal structure of the clear orange coloured plates of **2.1** was solved in the triclinic space group P$\bar{1}$ and is shown in Figure 2.16. This isomer was recrystallised by diffusing acetone into a 0.1 M HCl solution of the tetrachloridozincate salt of the mixture.

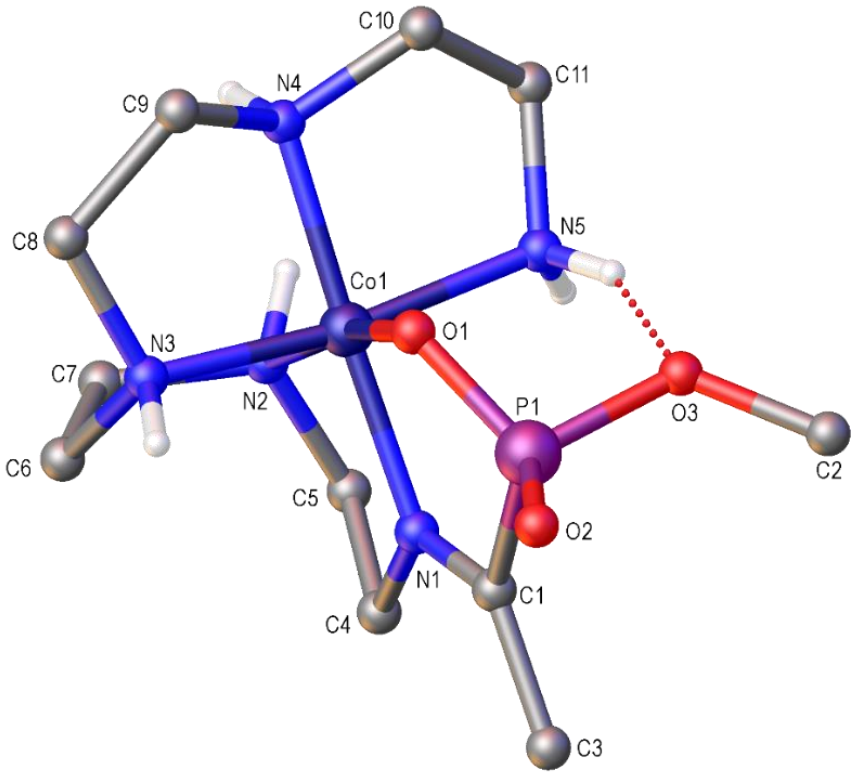

Figure 2.16 The crystal structure of **2.1** (Δ*mffm*$_a$(*R*)) from procedure 1. Most hydrogens and $ZnCl_4$ have been omitted for clarity.

The refined structure shows a cobalt(III) metal ion in octahedral coordination with a primary amine, three secondary amines, one imine group and an oxygen of the phosphonate arm. The polydentate wrapping around the metal centre has been assigned as Δ*mffm*$_a$. This form of wrapping where the orientation of the proton on the meridional nitrogen points away from the rest of the fold is the same as observed for similar complexes isolated in the Hartshorn group [55] and in the wider literature[53, 104-122]. A search of the Cambridge Crystallographic Database showed more than 98% of the compounds with similar folds (where three N atoms are in a meridional arrangement) around a cobalt(III) metal ion have this configuration. Compounds **2.2** and **2.3** also have the orientation of the protons on their meridional nitrogen atoms pointing away from the rest of the fold.

The chirality at the phosphorus stereogenic centre of **2.1** has been presented as the *R* isomer. In this orientation, the methoxy group of the phosphorus centre is close to N5 and away from N3 of the polyamine fold.

The other two isomers isolated from the benzoyl phosphonate (R = C_6H_5) derivative (compounds **2.2** and **2.3**) have been shown as their Δ*S* and Λ*R* forms respectively, with respect to the phosphorus centre. Whereas **2.2** is equivalent to **2.1**with respect to the orientation of the phosphorus centre (with the methoxy group close to N5 and away from N3), compound **2.3** has a different orientation at its phosphorus centre with the methoxy group close to N3 as opposed to N5 in the other tetraen derivatives.

The structural solution for compound **2.1** also reveals a hydrogen bond interaction between one of the hydrogen atoms of N5 (the primary amine) and O3. The presence of an imine bond between N1 and C1 is confirmed by the shorter C=N bond length of 1.285 (4) Å in comparison with the other C-N bonds (about 1.494 (5) Å) shown in Figure 2.14 and in examples from literature. [53, 54] The length of the bond between P1 and O2 (1.485 (2) Å) corresponds to a double bond in contrast to P1-O3 and P1-O1 with lengths of 1.593 (3) Å and 1.525 (2) Å respectively. The planarity of the imine has been confirmed through mean plane analysis.

Compound 2.2

Crystals of **2.2** formed from fraction 1 and were grown through vapour diffusion of acetone mixed with tetrahydrofuran and methanol into a 0.1 M HCl solution of the $ZnCl_4$ salt of the mixture.

The structure of **2.2** shown in Figure 2.17 was solved in the monoclinic space group $P2_1/n$.

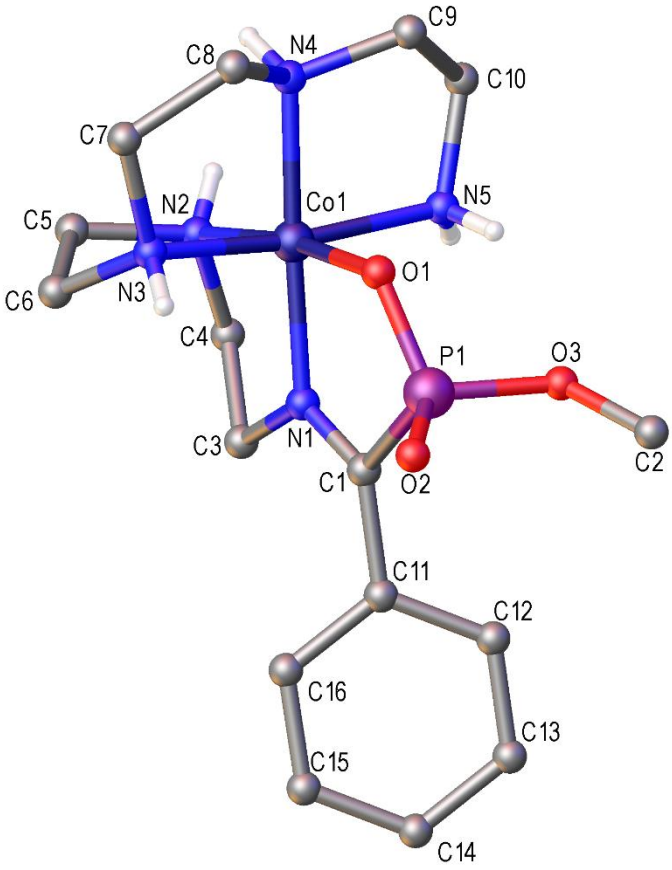

Figure 2.17 The crystal structure **2.2** (Δ*mffm*$_a$(*R*)) from procedure 2. Non-hetero atoms and $ZnCl_4$ have been omitted for clarity.

The structure shows octahedral geometry with an oxygen of the phosphonate arm, an imine group, three secondary amines and a primary amine coordinated to the central cobalt(III) ion. The N1-C1 bond length of 1.279 (3) Å confirms the presence of an imine bond. The other C-N bonds in the structure range from 1.477 (3) Å to 1.498 (3) Å, in line with other structures in this project as well as in the examples from literature.[53, 54] P1-O2 is a double bond (1.4754 (17) Å) whereas P1-O3 is a single bond at 1.5809 (17) Å. The planarity of the imine fragment has been confirmed by applying mean plane analysis. The polydentate wrapping around the metal centre has been assigned as Δ*mffm*$_a$. This form of wrapping is the same observed for the tetraen based carboxylates isolated[55] in the literature as well as for compounds **2.1** and **2.3**. Chirality at the phosphorus centre has been assigned the *R* configuration. In this orientation, the methoxy group of the phosphorus centre is close to N5 of the polyamine fold and away from N3, as in

compound **2.1**. The absolute configuration of the structure shown in Fig. 2.17 is therefore Δ*mffm*$_a$(*R*).

Compound 2.3

The XRD structure of the irregular shaped orange crystals of **2.3** was solved in the triclinic space group P$\bar{1}$ and is shown in Figure 2.18. The solution shows a cobalt(III) metal ion in an octahedral coordination. Three coordination sites are occupied by secondary amines, one by an imine group and the two others have been occupied by an oxygen atom of the phosphonate arm and a primary amine group. The polydentate wrapping around the metal ion has the Δ*mffm* configuration with the meridional nitrogen pointing away from the rest of the fold thus giving the Δ*mffm*$_a$ assignment similar to the compounds isolated from previous research and also for compounds **2.1** and **2.2**. The phosphorus stereogenic centre has been assigned the *S* configuration. This orientation places the methoxy group of the phosphorus centre close to N3 and away from N5. Therefore, the overall absolute configuration for the isomer of compound **2.3** as shown in Fig. 2.18 is Δ*mffm*$_a$(*S*).

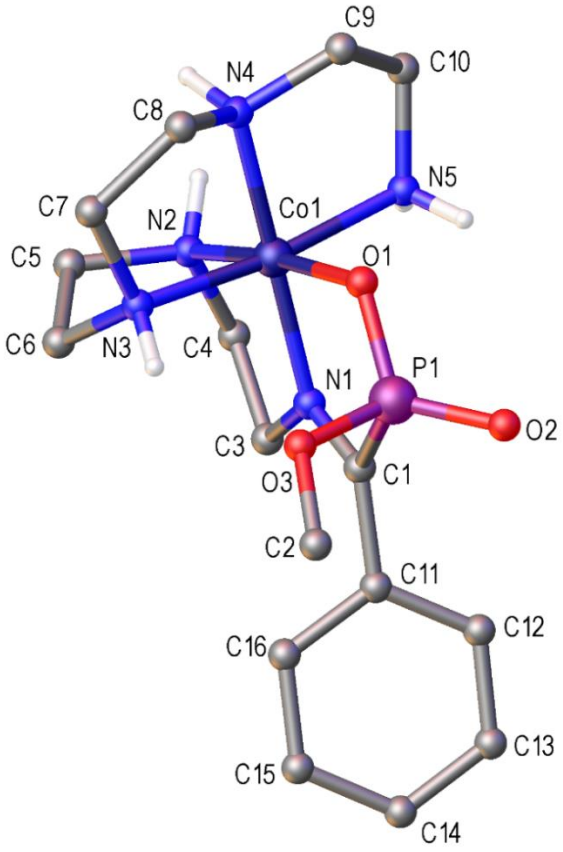

Figure 2.18 The crystal structure of **2.3** (Δ*mffm*$_a$(*S*)) from procedure 2. Non hetero atoms, $ZnCl_4$ and water have been omitted for clarity.

The presence of an imine bond between N1 and C1 is confirmed by the bond length of 1.284 (4) Å in contrast to other C-N bonds in the structure with bond lengths of approximately 1.492 (4) Å. The planarity of the imine has been confirmed by applying mean plane analysis.

Compound 2.5

The structure of **2.5**, solved in the trigonal space group R3c, is shown in Figure 2.19 (grown structure) and Figure 2.20 (asymmetric unit only).

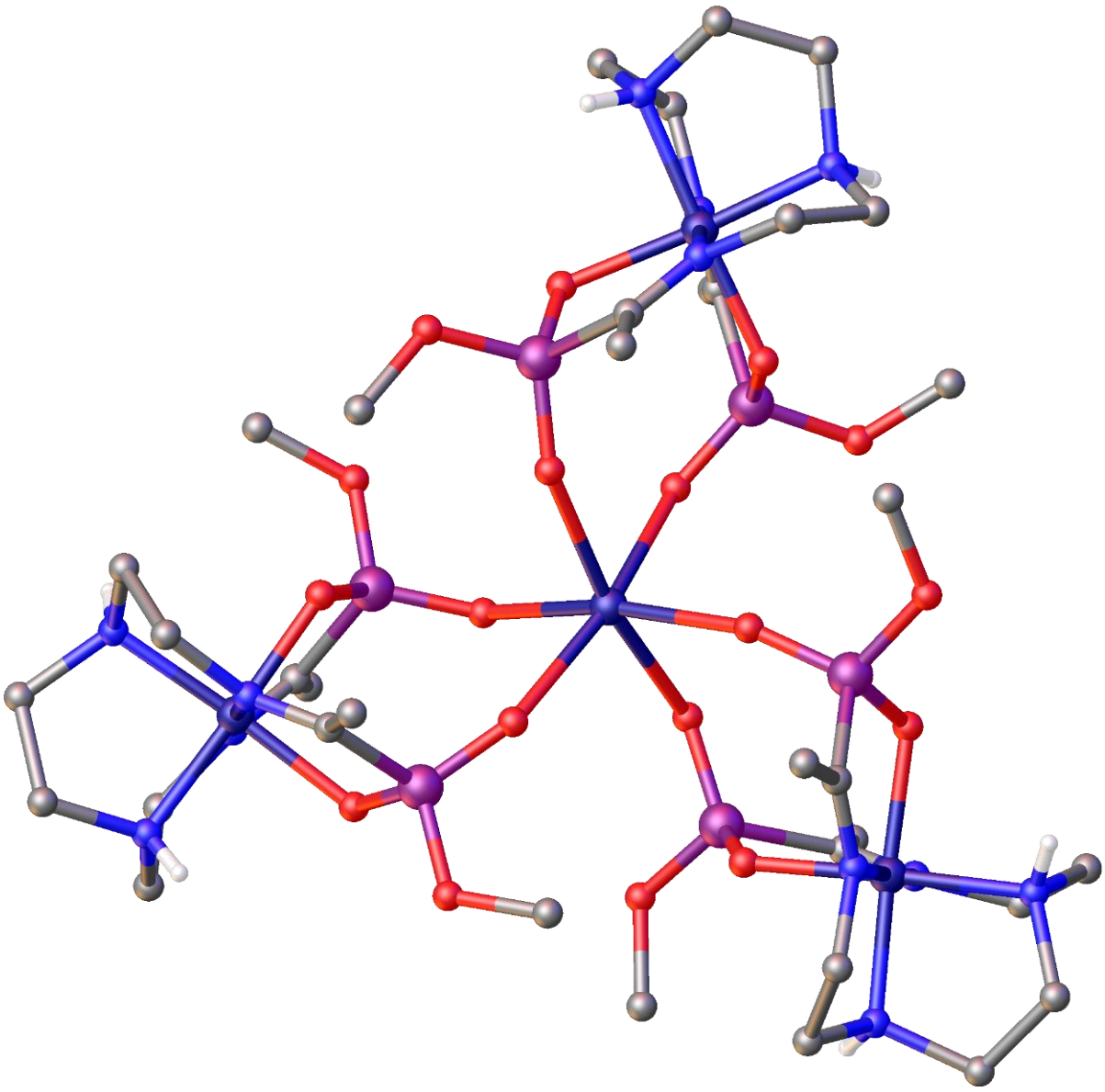

Figure 2.19 The complex unit of **2.5** from procedure 3. Non-hetero atoms, methanol and anions have been omitted for clarity.

This model shows a tetranuclear complex (Figure 2.19) with a cobalt(II) ion at the centre of three phosphonate imine complexes of cobalt(III). The complex ligands are coordinated to the

central metal ion in a distorted octahedral geometry. The asymmetric unit of this structure is shown in Figure 2.20. The presence of two imine bonds in each complexed ligand has been confirmed by the shorter bond lengths for C=N of 1.274 (10) Å for N1-C1 and 1.288 (11) Å for N4-C3 in contrast to other C-N bonds with lengths ranging from 1.462 (9) Å to 1.500 (10) Å. The planarity of the two imine bonds was confirmed by applying mean plane analyses.

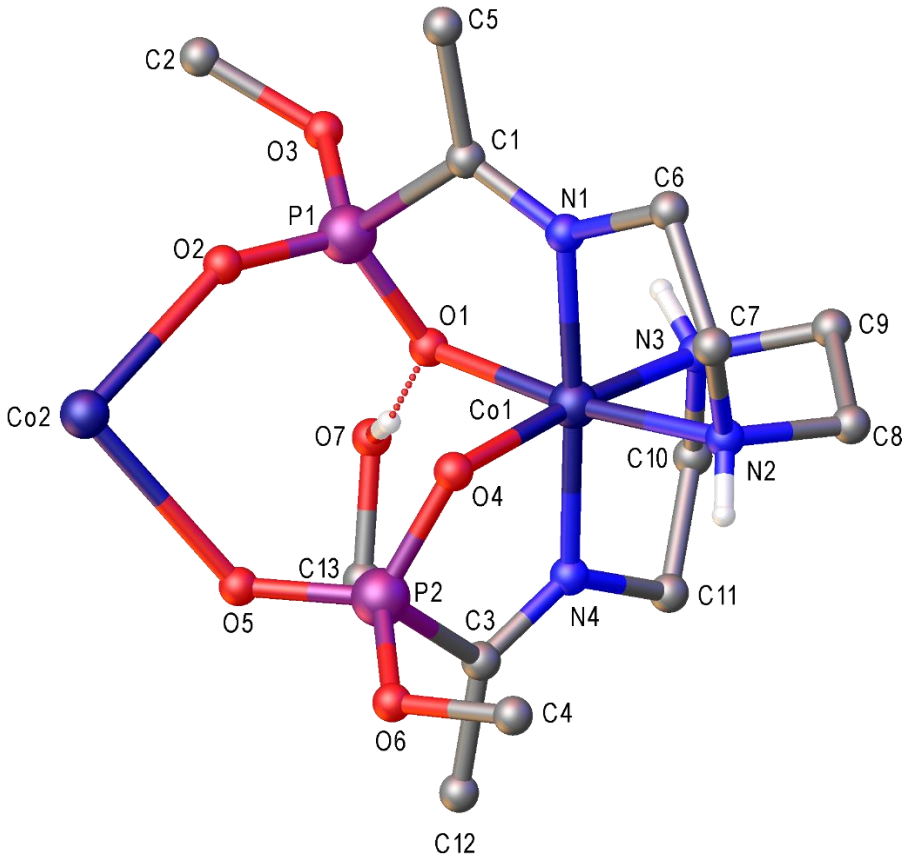

Figure 2.20 The asymmetric unit of a trimer (**2.5**) from procedure 3. A chloride anion, three 0.3($ZnCl_4$) molecules and non-hetero atoms have been omitted for clarity.

The bond lengths for Co1 and its ligands (≈ 1.93 Å) correspond with those expected for an octahedral geometry. However, the bond lengths observed from Co2 to its ligands (2.274 (6) Å - 2.398 (6) Å) are outside of this normal range. Typical Co-O bond lengths were around 1.93 Å in the literature.[6, 39, 55] Cobalt(II) complexes found in the literature had Co-O bond lengths

ranging from 1.959 Å to 1.985 Å.[123] Few cases had bond lengths of 2.034 to 2.166 for Co-O bonds and those were for distorted tetrahedral cobalt(II) centres.[123] Therefore, Co2 has been assigned as the +2 oxidation state of the metal *i.e* cobalt(II).

Consideration was given to the possibility of having a zinc(II) ion in the centre of the tetranuclear complex because zinc(II) ions were present in the reaction mixture. One major reason for this consideration was because of the experimental procedure through which the tetranuclear complex was generated. However, when the cobalt(II) metal ion was replaced by a zinc(II) ion during the process of the structural modelling, the reliability (R_1) factor was higher for the zinc(II) choice. Since the R_1 factor measures the agreement between a crystallographic model and its experimental X-ray data, the cobalt(II) ion choice was made for the central metal ion in the tetranuclear complex.

The 04-Co1-O1 bond angle in Figure 2.19 is 92.9 (2)° in the octahedral complex ligands whereas the O2-Co2-O5 bond angles present in the distorted octahedral complex ranges from 77.1 (2)° to 165.9 (2)°.

Compound 2.6

These dark red irregular shaped crystals of **2.6** formed from a fraction 1 mixture and its structural solution is shown in Figure 2.21 and was solved in the triclinic space group PĪ.

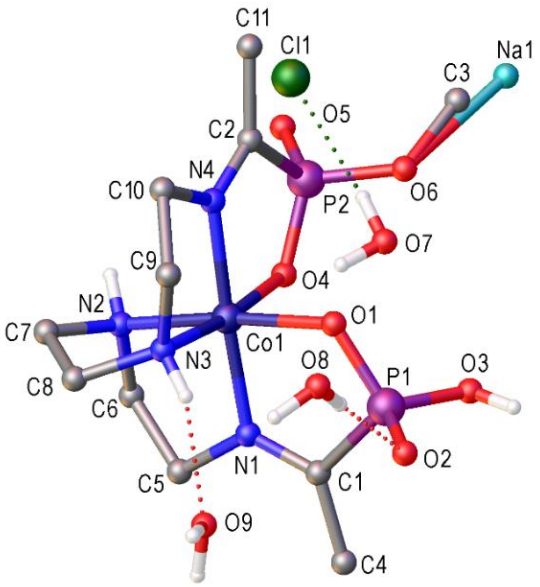

Figure 2.21 The crystal structure of **2.6** (Δ*mffm*(*R*) diastereoisomer) from procedure 3. Non-hetero atoms, an anion and four water molecules have been omitted for clarity.

The cobalt(III) metal centre is coordinated in an octahedral geometry to two oxygens with two secondary amines in the same plane. The six-coordinate geometry is completed by two imine groups *trans* to each other around the metal centre. The configuration of this diastereoisomer is Δ*mffm*(*R*); its enantiomer is also present in the product mixture. The polydentate wrapping around the metal centre resembles that for the complexes isolated from previous research[39, 55] in the Hartshorn group and also the rest of the trien based complexes isolated in this project. Stereogenicity at P2 (which has a methoxy group) is *R*. In this orientation, the methoxy group points away from N2 in contrast to the orientation at the P2 centre of compound **2.5**, where the methoxy group points towards N2.

The imine bonds have been confirmed by their shorter bond lengths of 1.283 (3) and 1.280 (3) Å in contrast to 1.471 (3) Å to 1.500 (3) Å for the rest of the C-N bonds in the structure as well as in literature.[53, 54] The planarity of the imines was also confirmed through mean plane analysis as outlined earlier. Two compounds co-crystallised with one being the OCH_3 and the other ONa, in a 75:25 ratio. The extended packing interactions in the X-ray structural model made chemical sense with a sodium atom in that position (O6). A disorder has therefore been modelled to show a sodium atom with a carbon atom for O6. This molecule has been partially hydrolysed on one of its phosphonate arms. The hydrolysis was also confirmed by mass spectrometry. Details of the hydrolysis can be found in chapter 4 of this thesis. During the method development stage of this research, it was discovered that these imine complexes of cobalt(III) hydrolyse at their ester groups under strongly acidic conditions. Hydrogen bonding interactions have been shown in the structure between the complex (through N3's H and O2) and solvent molecules and also between the counter ion and one of the water molecules found in the asymmetric unit. (Fig. 2.21).

Compound 2.7

Crystals of **2.7** from fraction 1 of procedure 4 formed upon addition of methanolic zinc chloride into a saturated methanolic solution of the mixture. The structure shown in Figure 2.22 was solved in the triclinic space group $P\bar{1}$. The R_1 value for this model is poor (10.10 %). That could be attributed to the low intensity of reflections obtained from the tiny crystals of the mixture. Therefore, bond angles and lengths will not be discussed. The structure has been included for comparison (section 2.3.2) and to show connectivity only.

The configuration of this diastereoisomer (as shown in Fig. 2.22) with respect to the polydentate wrapping around the metal ion (Δ*mffm*) is similar to literature[39, 55] complexes of

the carboxylate systems. Chirality at the two phosphorus stereogenic centres P1 and P2 has been shown as *S* and *R* respectively for the Δ isomer shown in Fig. 2.22.

The methoxy group at P1 points away from N3 whereas the methoxy group at P2 points towards N2.

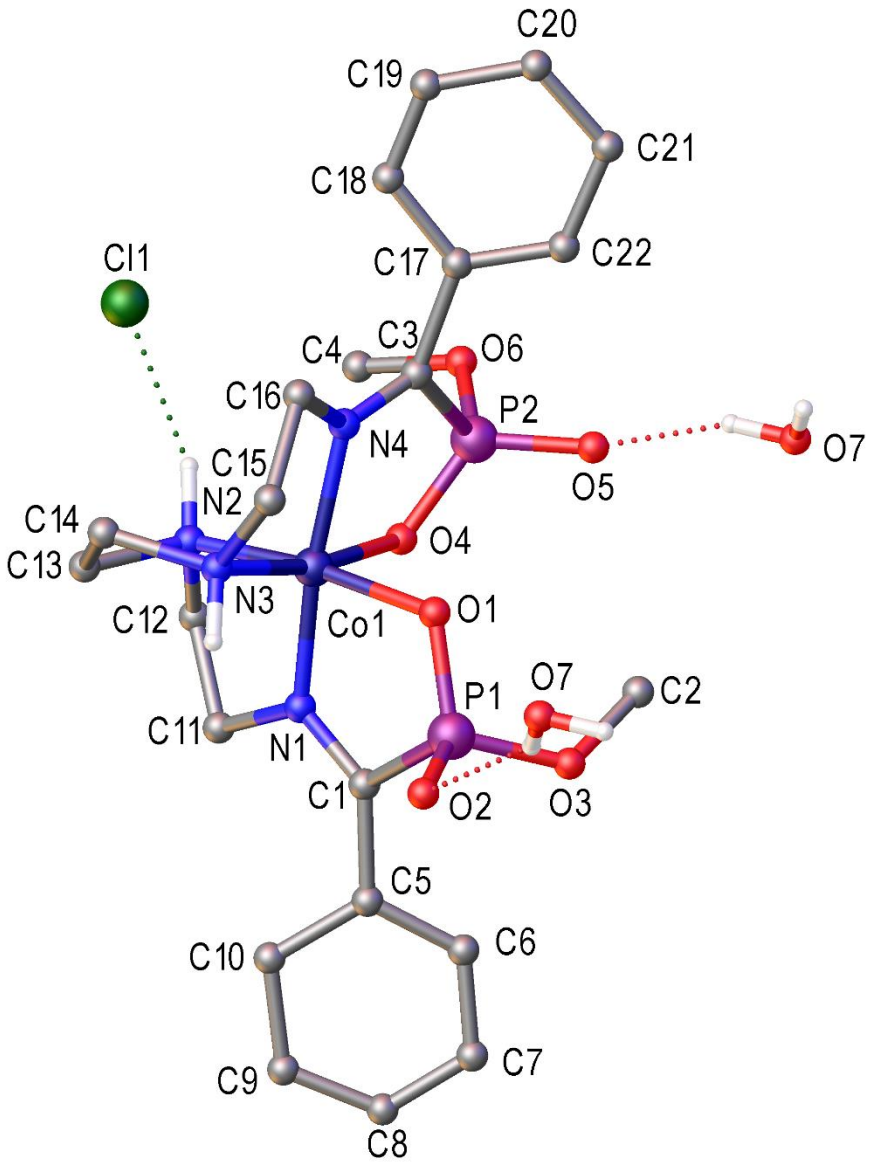

Figure 2.22 The crystal structure of **2.7** (Δ*mffm*(*SR*)) from procedure 4. Non-hetero atoms and $ZnCl_4$ have been omitted for clarity.

Compound 2.8

The structure shown in Figure 2.23 was solved in the monoclinic space group $P2_1/c$. It shows an octahedral geometry for the coordination of a cobalt(III) ion with two secondary amines, two oxygens and two imine groups *trans* to each other around the metal core. The structure has the Δ*mffm* configuration similar to the others with respect to the polyamine fold. The two phosphorus stereogenic centres both have the *R* configurations for the Δ isomer, giving a Δ*RR* isomer in contrast to **2.7** which is an Δ*SR* isomer considering the phosphorus centres. The methoxy group on each of the phosphorus centres in **2.8** points away from the donor group (N2 or N3) perpendicular to the imine plane in each case.

The imine bonds have been confirmed by their shorter lengths of 1.268 (9) Å for C1-N1 and 1.267 (9) Å for C3-N4. Other C-N bond lengths in the structure were around 1.489 (8) Å and for similar structures in literature.[39, 53-55] The planarity of both imines was confirmed by applying mean plane analyses. The methoxy group on P2 was disordered over two positions in a 50:50 ratio.

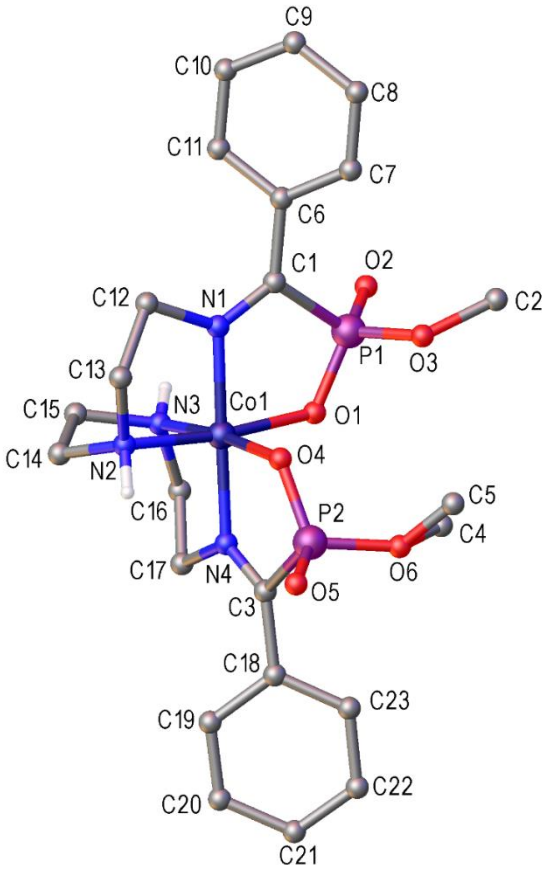

Figure 2.23 The crystal structure of **2.8** (Δ*mffm*(*RR*)) from procedure 4. Non-hetero atoms and a water molecule have been omitted for clarity.

Compound 2.9

The structure of **2.9** was solved in the trigonal space group R3c and is shown in Figure 2.24. Figure 2.25 shows its asymmetric unit.

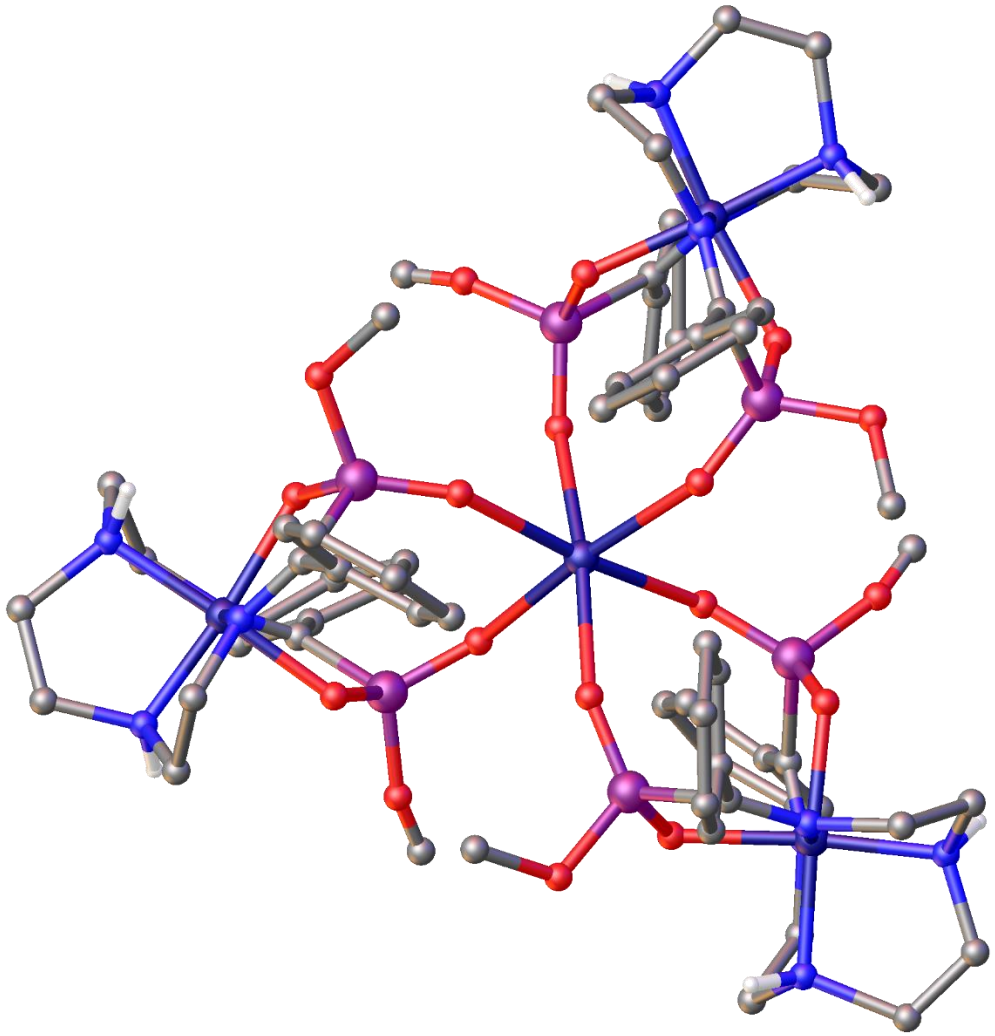

Figure 2.24 The complex unit of **2.9** from procedure 4. Non-hetero atoms and $ZnCl_4$ molecules have been omitted for clarity.

The distorted octahedral geometry of this tetranuclear structural model (Figure 2.24) resembles that seen in compound **2.5** from procedure 3 (Figure 2.19) in terms of the coordination around the central cobalt(II) ion as well as their bond lengths and angles. However, while the methoxy

group on P2 points towards N2 in compound **2.5**, the methoxy group on P2 points away from N2 in compound **2.9**. Both methoxy groups on P1 of **2.5** and **2.9** point away from N3.

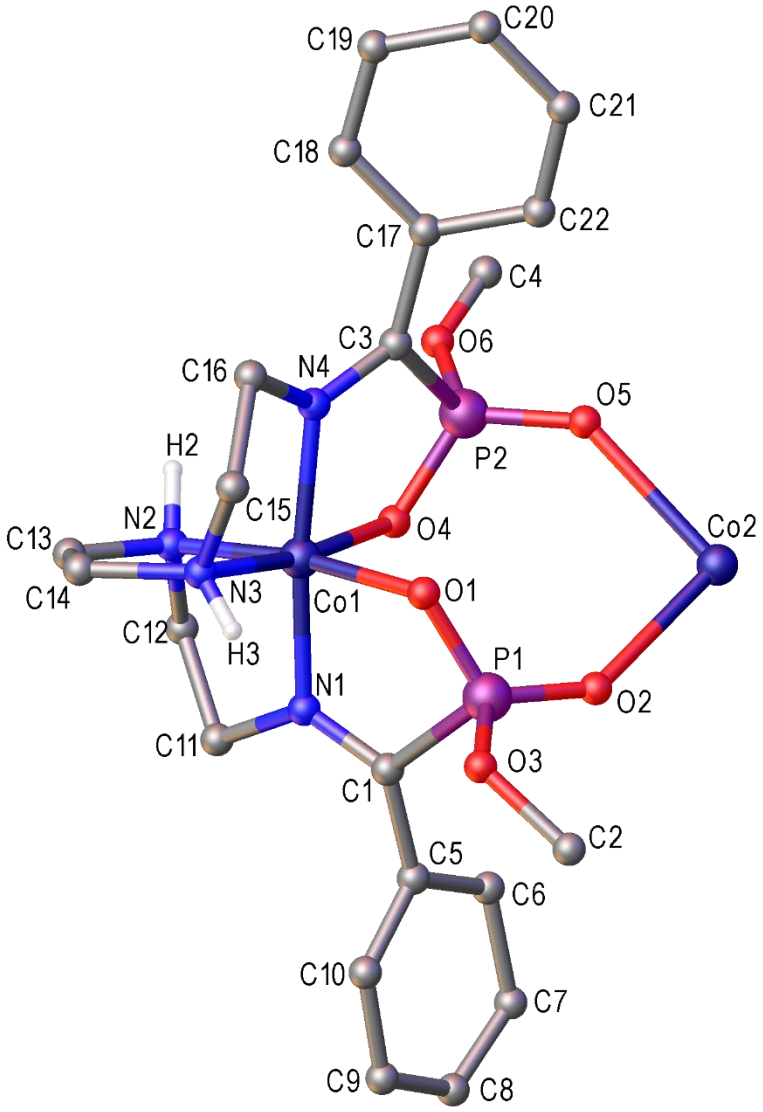

Figure 2.25 The asymmetric unit of **2.9** from procedure 4. Non-hetero atoms and $ZnCl_4$ counter ions have been omitted for clarity.

The presence of two imine bonds have been confirmed by the shorter bond lengths for C=N of about 1.30 (3) Å in contrast to the other C-N bond lengths of about 1.49 (3) Å. Mean plane analyses were used to confirm the planarity of the imines.

Compound 2.10

The structure of **2.10** was solved in the monoclinic space group $P2_1/n$ and is shown in Figure 2.26.

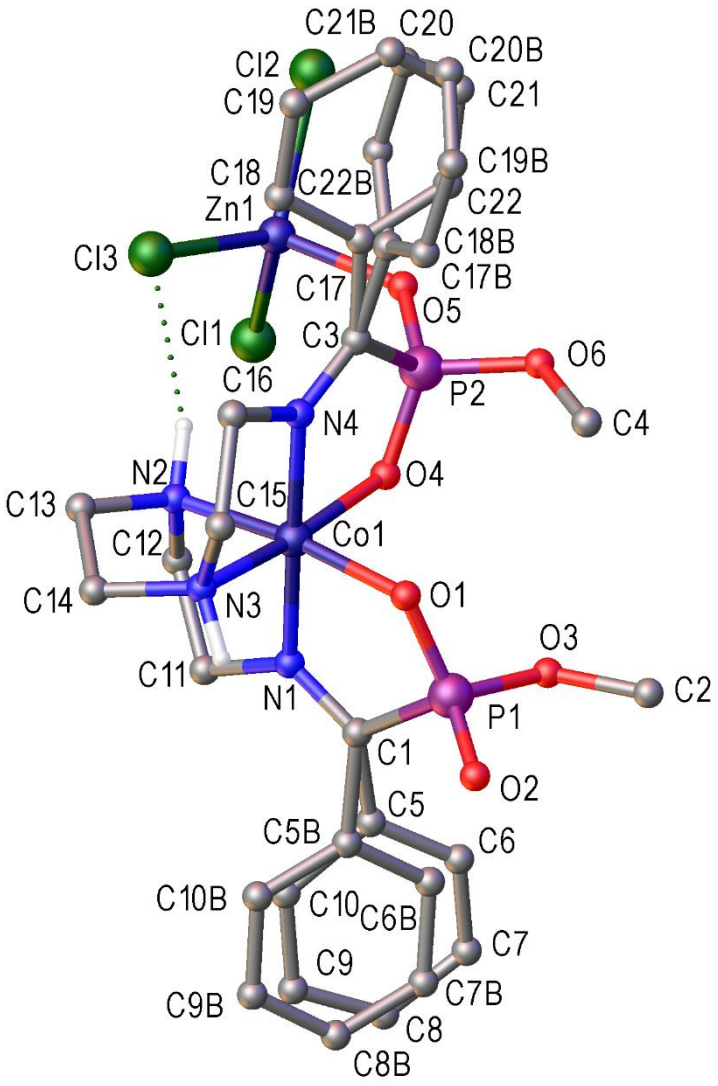

Figure 2.26 The crystal structure of **2.10** (Δ*mffm*(*RR*)**)** from procedure 4. Non-hetero atoms and solvent molecules have been omitted for clarity. Disorder is shown.

The cobalt(III) metal ion is coordinated in an octahedral geometry to two imine groups, two oxygens that are *cis* to each other around the metal centre and adjacent to two secondary amine groups also *cis* to each other. Once again, the Δ*mffm* configuration is being observed. The two phosphorus centres have different groups on them which will influence the standard CIP

priority rules usually applied for the assignment of the *S* or *R* isomer. Therefore, P2 bearing the $OZnCl_3$ (as well as a methyl ester) has the *R* configuration as in P1. Thus, considering the phosphorus stereogenic centres, the structure shown is an Δ*RR* isomer. At each phosphorus centre, the methoxy group points away from the donor group perpendicular to the imine plane in each case.

This crystal structure shows the $ZnCl_2$ introduced to isolate the product as the $ZnCl_4^{-2}$ salt has directly bonded with the cobalt(III) complex as $ZnCl_3^-$, through one of the free oxygens on a phosphonate arm of the complex. This unexpected coordination of $ZnCl_3^-$ to O to form a Zn-O bond has been seen in the literature.[124] The structure also has a hydrogen bond (shown in Fig. 2.26) between the hydrogen on N2 (a secondary amine) and Cl3 of the $ZnCl_3$ moiety. The imine bonds (C1=N1 and C3=N4) have been confirmed by their shorter bond lengths of 1.286 (8) Å and 1.277 (9) Å in contrast to 1.489 (8) Å for the other C-N bonds in the structure and in literature.[53, 54] The planarity of both imines was confirmed by applying mean plane analyses. The distance between C1 and the plane was 0.053 Å whereas C3 was 0.050 Å off the plane. Disorder in the two phenyl rings has been modelled in the structure shown in Fig. 2.26 as the phenyl rings occupying two different positions. The extended packing diagram for this structural model gave no indication of any significant intermolecular interactions.

Compound 2.11

Crystals of **2.11** formed in the NMR tube (in the presence of the TSP reference salt) used for the sample characterisation of fraction 1 of its mixture. The helicity of the fold was assigned a left handedness with the descriptor Λ while the wrapping of the polydentate ligand around the metal ion has been assigned an *mm* descriptor, by following the system of nomenclature discussed in chapter 1 of this thesis.

This Λ*mm* structure was solved in the monoclinic space group of $P2_1/c$ and is shown in Fig. 2.27. Chirality at P1 is *R* and is the same in P2. Therefore, this isomer has been assigned the *RR* configuration with respect to the phosphorus stereogenic centres, giving the shown structure an absolute configuration of Λ*mm*(*RR*). Its enantiomer is also present in the mixture.

While the two other isolated compounds based on the en ligand have the same configuration (Λ*mm*) around their cobalt(III) centres, compound **2.13** has the *RR* configuration with respect to its phosphorus centres whereas **2.12** has the *RS* configuration.

The bond lengths and angles in compounds **2.11** and **2.13** were similar to each other. However, the compounds crystallised in different space groups.

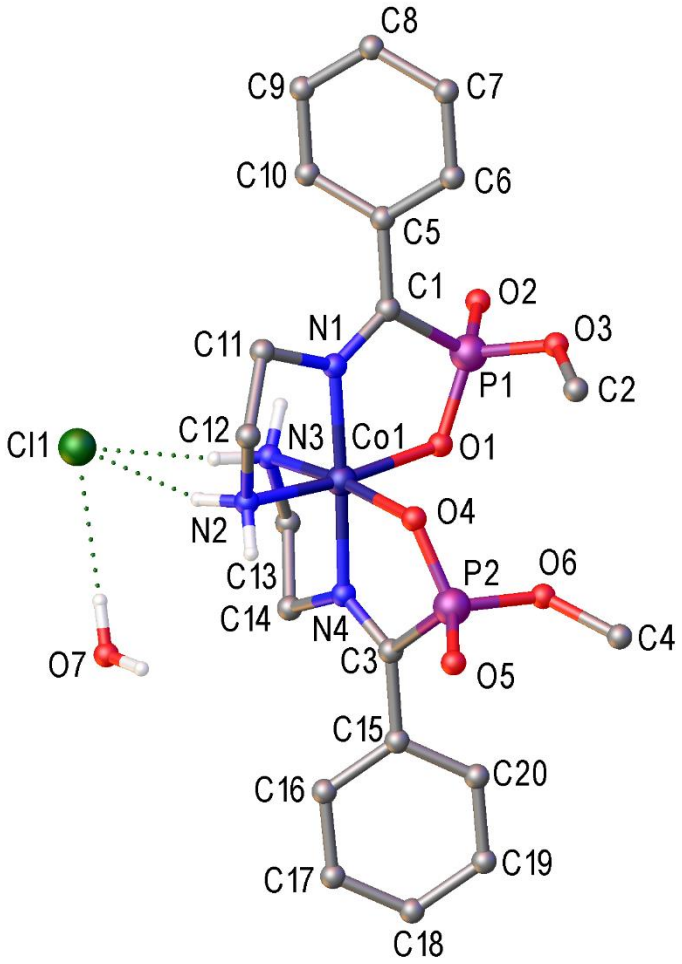

Figure 2.27 The crystal structure of **2.11** (Λ*mm*(*RR*))from procedure 5. Non-hetero atoms have been omitted for clarity.

The imine carbon bonds for compound **2.11** were shorter (1.283 (3) – 1.284 (3) Å) than expected for a single bond (1.48 Å) and matched other C=N double bonds (1.27 Å).[53-55] The planarity of the imines was confirmed through the mean plane analysis. Three hydrogen bonds are shown in Fig. 2.27 extending from the chloride anion to one hydrogen each on N2, N3 and the water molecule in the asymmetric unit.

Compound 2.12

The crystal structure of compound **2.12** from procedure 5 was solved in the triclinic space group PĪ and is shown in Figure 2.28. The crystals were formed in a saturated methanolic solution of fraction 2 at 4°C. The complex has an octahedral geometry with a cobalt(III) ion at the centre. The configuration around the cobalt(III) centre is Λ*mm* and *RS* for P2 and P1

respectively. While the methoxy group on P2 points away from N2, the methoxy group on P1 points towards N3, unlike in compounds **2.11** and **2.13** where all the methoxy groups point away from N2 and N3, as the case may be.

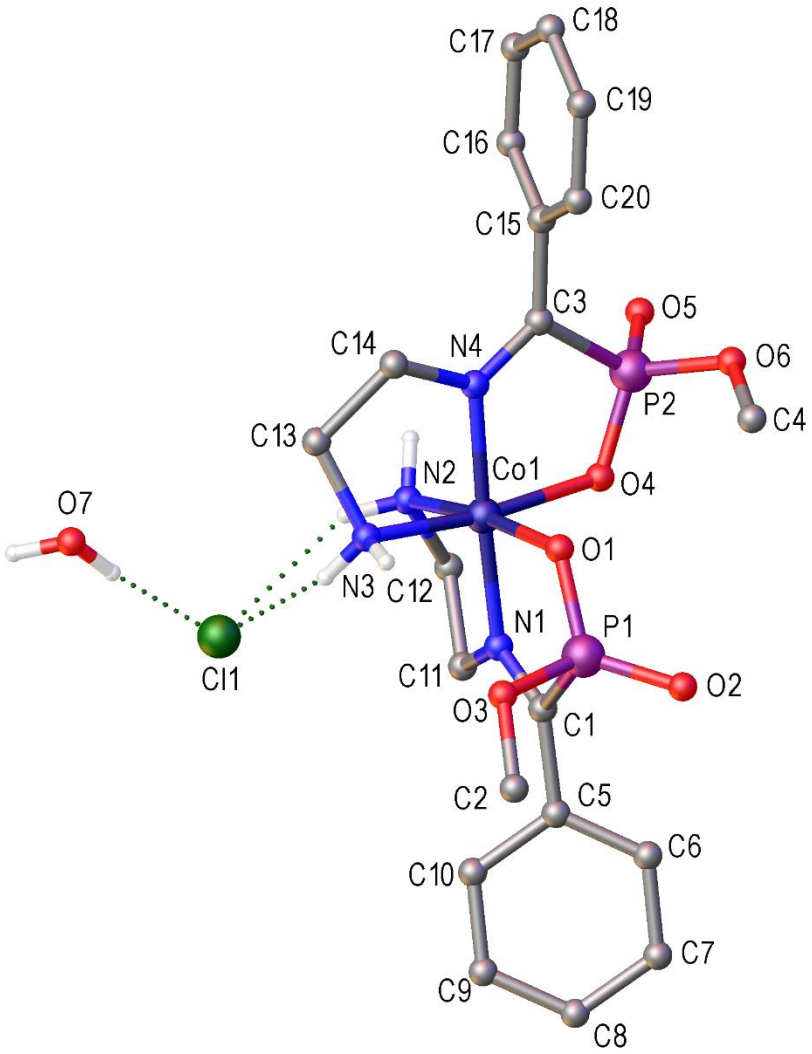

Figure 2.28 The crystal structure of **2.12** (Λ*mm*(*RS*)) from procedure 5. Non-hetero atoms have been omitted for clarity.

The presence of these two imine groups have been confirmed by their shorter bonds of 1.279 (4) and 1.281 (4) Å. The other C-N bond lengths range from 1.475 (4) Å to 1.490 (4) Å. The planarity of both imines was confirmed by applying mean plane analyses. Three hydrogen bonds have been shown in Fig. 2.28. Two of these interactions are between the chloride anion and two hydrogens, one from N2 and N3 respectively. The other hydrogen bond is shown between the anion and a hydrogen atom from the water molecule in the asymmetric unit.

Compound 2.13

Crystals of **2.13** were also formed in a saturated methanolic solution of fraction 2 at 4°C. The crystal structure was solved in the triclinic space group $P\bar{1}$ and is shown in Figure 2.29.

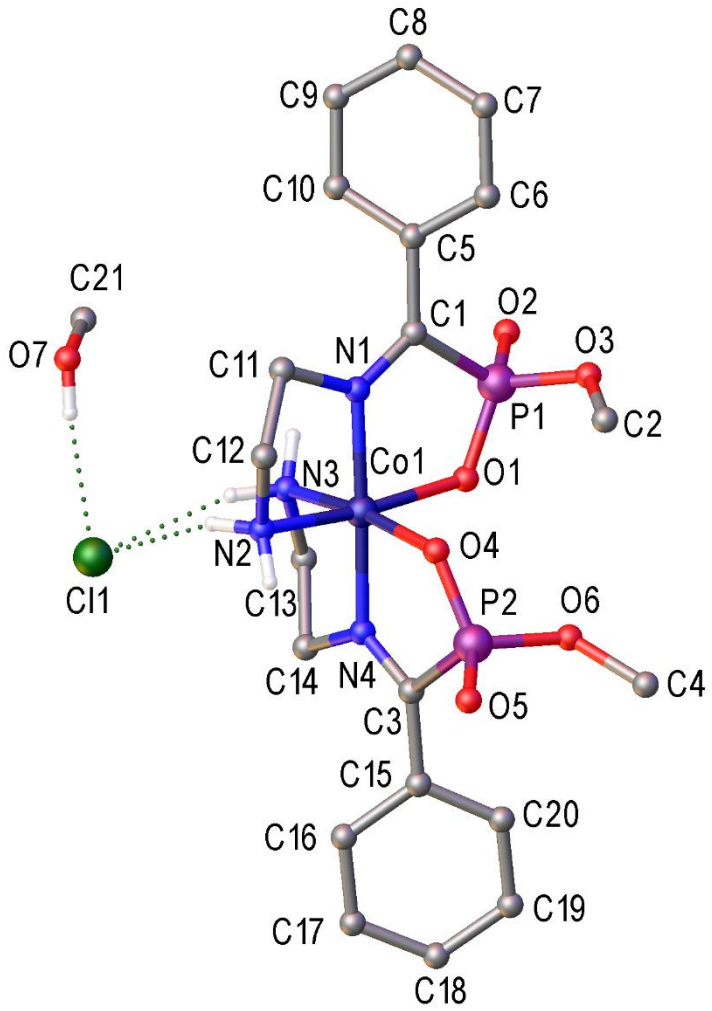

Figure 2.29 The crystal structure of **2.13** (Λ*mm*(*RR*)) from procedure 5. Non-hetero atoms have been omitted for clarity.

The cobalt(III) metal ion at the centre of the octahedron is coordinated to two primary amines, two oxygens from the phosphonate arms and two imine groups. The two oxygens are *cis* to each other and adjacent to the primary amines which are also *cis* to each other. The two imine groups are *trans* to each other with respect to the metal centre. The wrapping of the polydentate ligand around the metal centre has the Λ*mm* configuration. The chirality at P1 is the same as at

P2, thus this diastereoisomer is an *RR* one with respect to the phosphorus stereogenic centres. The structure shown as Fig. 2.13 thus has an absolute configuration of Λ*mm(RR).*

The imine bonds carbon bonds were shorter (1.286 (6) - 1.290 (6) Å) than expected for a single bond (about 1.48 Å) and matched other C=N double bonds (1.27 Å).[53-55] The planarity of both imine bonds was confirmed by applying mean plane analyses. The distance between C1 and the plane was 0.013 Å whereas C3 was 0.016 Å off the plane. Hydrogen bonds are shown in Fig. 2.29 between the chloride anion and a hydrogen each from the two primary amines, N2 and N3 as well as between the chloride anion and the hydrogen on the alcohol end of methanol found in the asymmetric unit.

Compound 2.14

The Δ*mffm* structure (with respect to the polyamine fold around the metal centre) of **2.14** was solved in the monoclinic space group $P2_1/n$ with two molecules in the asymmetric unit, as shown in Figure 2.30. Chirality at the phosphorus centre has been assigned the *R* configuration with the methoxy group pointing away from N3. The structure resembles those from the carboxylate systems isolated from previous research[55] in the Hartshorn group as well in the current project.

The ordered imine bonds N1=C1, N4=C3 and N5=C13 have an average bond length of 1.273 (18) Å, whereas N8=C15 has a bond length of 1.21 (2) Å. The shorter bond length has been attributed to the disorder in that structure. The planarity of both imines was confirmed by applying mean plane analyses.

No intermolecular contact was observed between the two independent molecules. Ignoring the disorder modelled on the bottom structure in Figure 2.30, the two structures are related by a pseudo plane of inversion. The bottom structure is disordered and has been modelled with the phosphonate arm occupying two positions, where one phosphorus atom has a higher occupancy of 75% leaving the other one there 25% of the time. The methyl group from the 50% occupancy methanol, competes with the 25% occupancy methyl group of the ester on P2A.

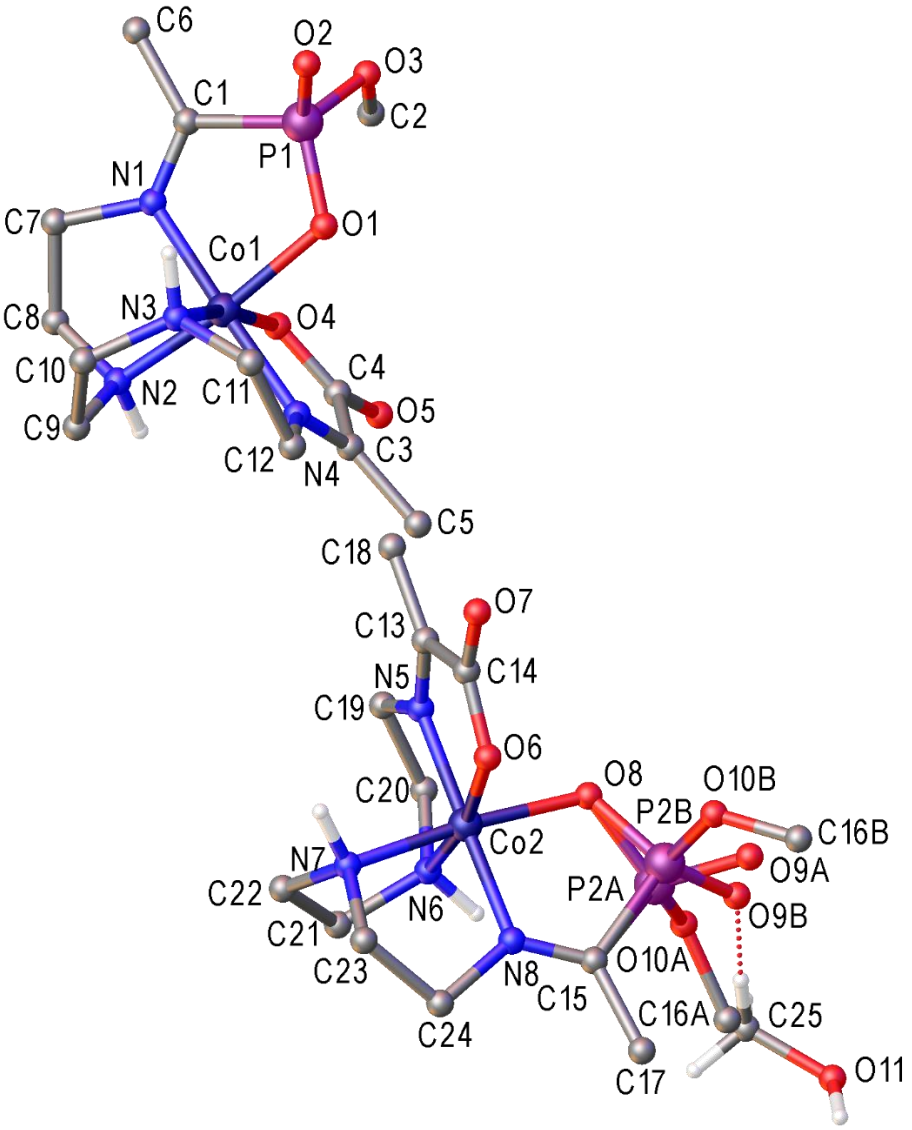

Figure 2.30 The asymmetric unit of compound **2.14**. Non-hetero atoms and $ZnCl_4$ have been omitted for clarity.

The configurations of the two components at the disordered P2 are different. While the A labelled methoxy component points slightly towards N6 (Fig. 2.32), the B methoxy component points away from N6. The B component has higher occupancy than the A component.

The orientation at the phosphorus centre where the methoxy group points away from donor groups perpendicular to the imine plane is dominant across all isolated compounds in this chapter.

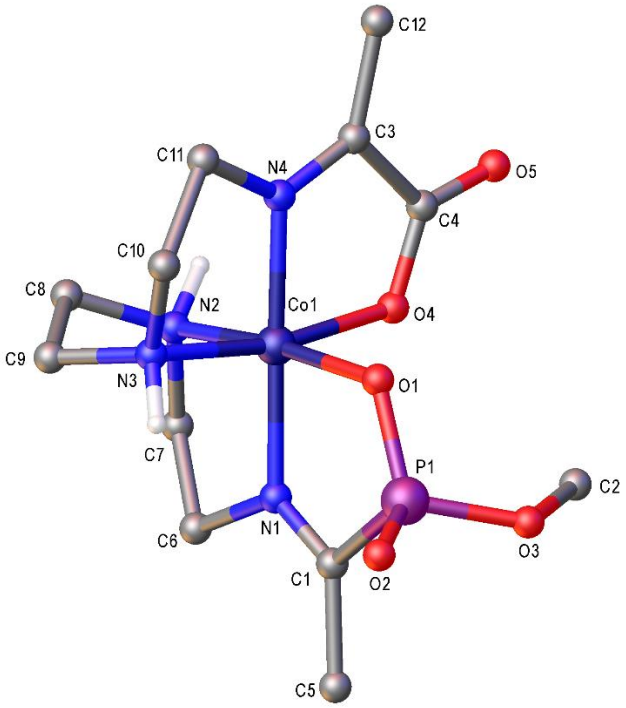

Figure 2.31 One of the molecules (Δ*mffm*(*R*)) in the asymmetric unit in Figure 2.30. Non-hetero atoms and other molecules have been omitted for clarity.

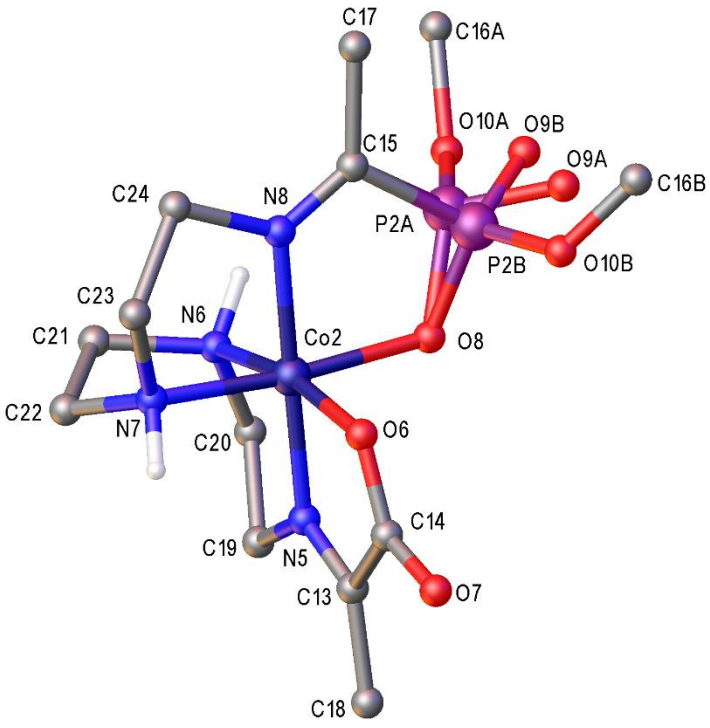

Figure 2.32 One of the molecules in the asymmetric unit in Figure 2.30. Non-hetero atoms and other molecules have been omitted for clarity.

2.3.2 Formation of The Imine Complexes

This chapter showcases new complexes formed from phosphonate ligands condensed around cobalt(III) metal centres already pre-coordinated to polyamine ligands.

The most common method for preparing imines is the traditional reaction of aldehydes (H_2NR'' and ketones (R_2CO) with amines. This method was first discovered by Schiff, the reason for which imines are often referred to as Schiff bases[125]. It is generally carried out by in organic synthesis by refluxing the carbonyl compound and amine while separating water as it is formed (equation 1). Since the reaction (equation 1) is in equilibrium, increasing the amount of the solvent used can shift the equilibrium position to the right, to make more of the products. However, that is not the case for the complexes; a large volume of solvent (methanol) was used for the purpose of solving the issue of low solubility of the starting complexes. More solvent reduced the reaction time with more complexes being dissolved. The length of the reactions (48 hours) is important as the carbinolamine intermediate species need time to rearrange into a geometry suitable for the formation of a planar imine.

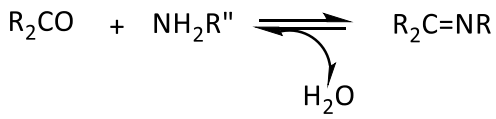

Figure 2.33 General method for the preparation of imines.

The crude product of the reaction gives a mixture of isomers (confirmed by NMR), which can be separated using ion exchange chromatography, mostly using Sephadex SPC 25 resin. The intricacy of a given product mixture depends on the polyamine starting material used. The trien and en based compounds were expected to have less complicated NMR spectra due to the presence of a C_2 axis of rotation in some of their coordination complexes. However, this expectation is only valid for when the symmetry element is retained in the product molecules. The tetraen based complexes having only one phosphonate appear to be simpler in terms of isomer complexity. However, the presence of the meridional N-H configuration makes the potential isomer complexity similar to that of the complexes derived from the trien polyamine ligand but with different origins. All the same, the regioselectivity of the condensation reaction restricts the number of isomers that could be formed from all the systems here reported.

Chirality at the cobalt(III) centre, the meridional nitrogen (where applicable) and at the phosphorus centre(s) give rise to isomerism in these complexes. Isolation of single isomers was achieved in some cases but in the majority, mixtures of isomers were obtained. Elemental analyses obtained from such mixtures showed that there could be only a small amount of non-stereoisomer material contents.

The standard synthetic procedure for the construction of polydentate ligands of our type uses intramolecular condensation reactions between a polyamine ligand and a keto acid ligand. Acylphosphonates have been applied as analogues of carboxylates in the current project. The Hartshorn group [53, 54, 75] and others [45, 46, 48, 49, 126] have reported the processes that lead to similar products in a stepwise manner. Their findings can be extrapolated to these current systems. Thus, one can propose that following the initial substitution of the chloride ligand of the starting complex (Fig. 2.1), the carbon of the pendant carbonyl group of the phosphonate ligand, cyclizes with one of the primary amines to form a carbinolamine. If this carbinolamine is not held in a position that would allow dehydration to occur to yield an imine, then the complex could undergo ligand re-arrangement. The imine donor and the two adjacent donor atoms must be part of a meridional ligand fragment, forming a 5-membered chelate ring, for the dehydration to occur.

Browne *et al.*[53] demonstrated the possibility of carrying out these condensation reactions at more than one site in the same molecule using pyruvate and 2-ketoglutarate ligands. Here the carboxylate chemistry has been extended by using phosphonate ligands and in one case both pyruvate and phosphonate ligands have simultaneously been coordinated unto the same cobalt(III) centre (procedure 6).

Complexes containing two imine acid fragments (procedures 3 to 5) were made by utilizing four equivalents[53] of keto-phosphonate acids to achieve a double condensation reaction. An excess of the incoming ligand was used for the formation of the desired products as a result of optimisation. On one or two occasions during the course of this project, the use of less than the stated excess yielded compounds that had only condensed on one site. The presence of a second imine group in such products further limits the possible number of isomers obtainable from such systems. It has been reported that this geometrical constraint guarantees that only two stereoisomers exist for the double condensation products of the carboxylates and they are enantiomers.[53]

No attempt was made to resolve enantiomers in this project.

Tetraen Based Mono Imine Phosphonate Complexes of Cobalt(III)

Compounds from procedures 1 and 2 were made by reacting two equivalents of keto phosphonate acids with only one equivalent of the pre-coordinated polyamine (triazaundecane-1,11-diamine). The complex formed (**2.1** or **2.2** or **2.3**) contains two major stereogenic centres in each molecule; cobalt(III) and phosphorus respectively. For these mono imine complexes, there is the possibility of epimerization of the protons of a secondary amine and that could increase the total number of stereogenic centres in a particular molecule and consequently result in further isomeric possibilities. A minor isomer in the literature, wherein the only difference between it and the major isomer was in the configuration of the proton of a secondary amine, has been reported for the carboxylate analogues.[53]

Two pairs of diastereoisomers were originally expected in every crude mixture of these mono imine complexes of cobalt(III), considering the wrapping of the polydentate ligand around the metal ion and the chirality at the phosphorus centres only: (Δ*R* and Δ*S*) and (Λ*R* and Λ*S*), where (Δ*R* and Λ*S*) and (Δ*S* and Λ*R*) are enantiomers. There is also the possibility of having more isomers in the product mixtures derived from these tetraen based complexes because of the chirality at the meridional nitrogen (*mer*-N) atom *trans* to the imine donor. Hartshorn and House's nomenclature[27] of using *anti*/*syn* descriptors has made it easier to describe such topological differences between stereoisomers. The hydrogens on the facial secondary amines are fixed by the fold of the polyamine backbone and are usually in opposite directions from each other (the *anti*/*syn* relationship has been explained in chapter 1). Therefore, the meridional N's hydrogen could either point towards the rest of the polyamine fold, where it would be assigned the *syn* configuration, or pointed away from the rest of the fold, to give the *anti* configuration.

All the compounds (**2.1**, **2.2** and **2.3**) isolated from the tetraen derivatives have presented in the *anti* configuration (with respect to their *mer*-NH's) confirmed by X-ray crystallographic techniques and schematised in Fig. 2.34. This observation aligns with the literature[55] from previous research in the Hartshorn group and in the wider literature. [53, 104-122] It seems uncommon to have the *mer*-N-H pointing towards the rest of the polyamine fold. Therefore, the initial potential issue of the possibility of having more isomers in the product mixtures derived from these tetraen based complexes due to the chirality at the *mer*-N atom, shall be ruled out. Two pairs of diastereoisomers are thus expected from the product mixture.

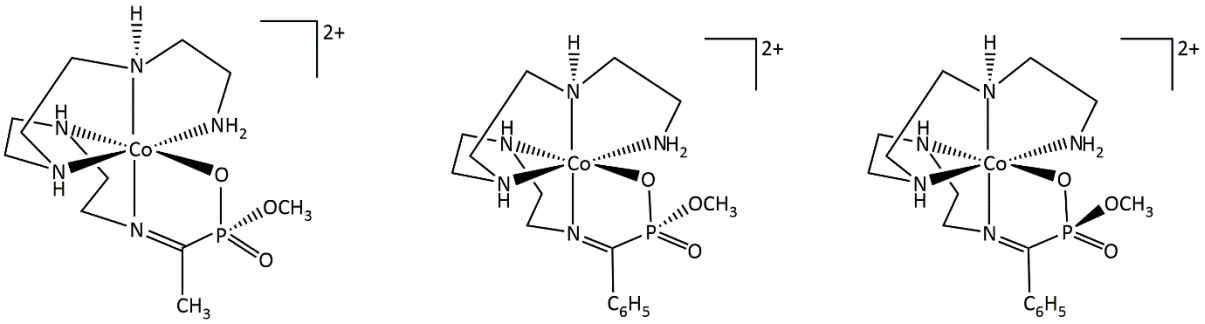

2.1 (Δ*mffm*$_a$(*R*)) **2.2** (Δ*mffm*$_a$(*R*)) **2.3** (Δ*mffm*$_a$(*S*))

Figure 2.34 Isolated isomers from the tetraen polyamine ligand

The diastereoisomers are expected to be observed in an NMR spectrum (Figures 2.35-2.39) as sets of signals because of their different relative configurations.

X-ray crystallography (Fig. 2.16 – 2.18) revealed that when the configuration is *R* at the phosphorus centre of these tetraen derivatives, the methoxy group points towards one of the donor group perpendicular to the plane of the imine (the primary amine labelled N5). On the other hand, when the configuration is *S*, the methoxy group points away from N5. It is expected that the difference in chemical environments experienced by the methoxy protons due to the configuration at the phosphorus centre, would translate to different chemical shifts for the protons on different stereoisomers (diastereoisomers, in this case).

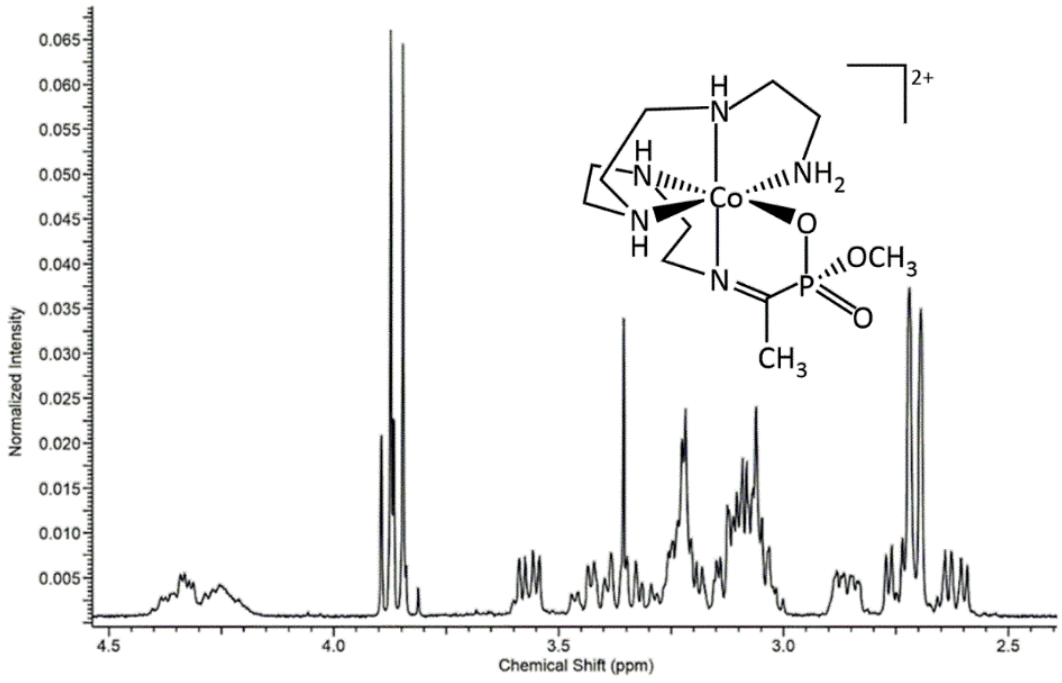

Figure 2.35 ^{1}H NMR spectrum from procedure 1 product mixture showing sets of doublets.

Because phosphorus occurs only as its NMR active ^{31}P, coupling interactions are observed between the phosphorus and other NMR active nuclei in ^{1}H, $^{13}C\{^{1}H\}$ and ^{31}P NMR spectroscopy experiments. This interaction is seen as doublets in the ^{1}H and $^{13}C\{^{1}H\}$ NMR spectra. However, because the phosphorus experiments were all proton decoupled, the phosphorus signals appeared only as singlets in the $^{31}P\{^{1}H\}$ spectra shown in this publication.

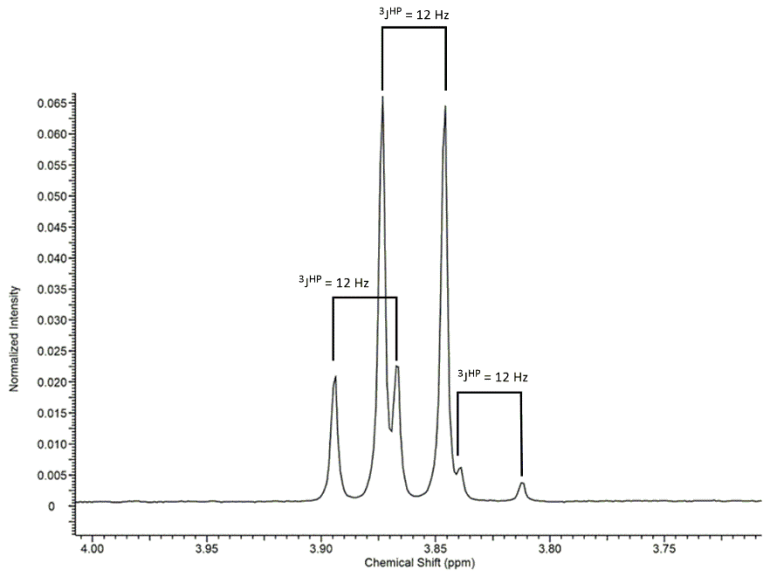

Figure 2.36 Methoxy region of the ^{1}H NMR spectrum from procedure 1 product mixture showing three sets of doublets.

Figure 2.36 shows three sets of doublets in the methoxy region of the ^{1}H spectrum. Integral values show these isomers are in the ratio of 3:1:0.5. Integration also confirmed that all the methyl groups on all three components of the mixture resonated as one broad doublet at 2.7 ppm of the spectrum shown in Fig. 2.35. The most intense doublet in the methoxy region (3.85 ppm) belongs to the major isomer in the mixture. The two other sets are minor isomers. The ^{31}P NMR spectrum (Fig. 2.37), implies the presence of yet another doublet in this spectrum which could have been overlapped by the highly intense peak. The integral values from the phosphorus NMR spectrum (2:1:0.1:0.05) did not quite match those from the ^{1}H spectrum (3:1:0.5). That could be attributed to integration errors from peak overlap.

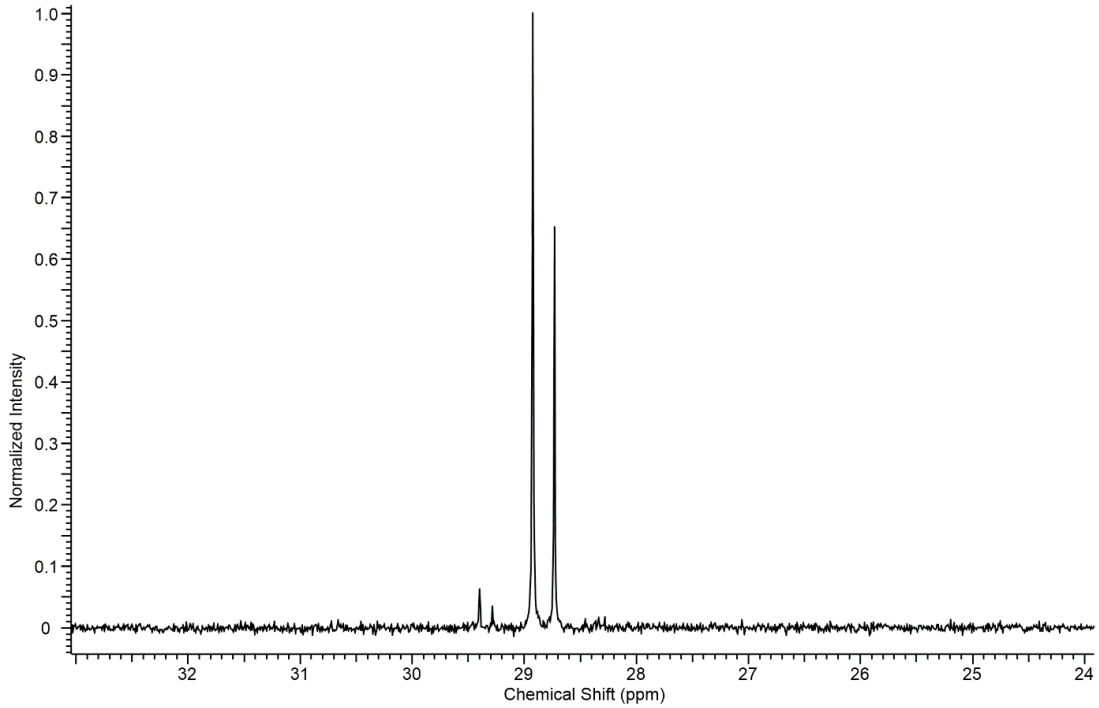

Figure 2.37 $^{31}P\{1H\}$ NMR spectrum from procedure 1 showing at least four signals with the ratio of 2:1:0.1:0.05

One set of the diastereoisomers has been isolated (**2.1**), recrystallized and its X-ray structure shown in Figure 2.16. The structure shown has the Δ*mffm*$_a$ configuration around the metal ion and an *R* configuration around the phosphorus centre, giving it an absolute configuration of Δ*mffm*$_a$(*R*). Its enantiomer (Λ*mffm*$_a$(*S*)) is also present in the mixture.

The two diastereoisomers (**2.2** and **2.3**) isolated from procedure 2 have also been characterised by X-ray diffraction and Figures 2.17 and 2.18 show their respective structural solutions. While all the compounds had the Δ*mffm*$_a$ configuration with respect to the polydentate fold, compound **2.2** has an *R* configuration like compound **2.1** but in contrast to **2.3** which has an *S* configuration at its phosphorus stereogenic centre.

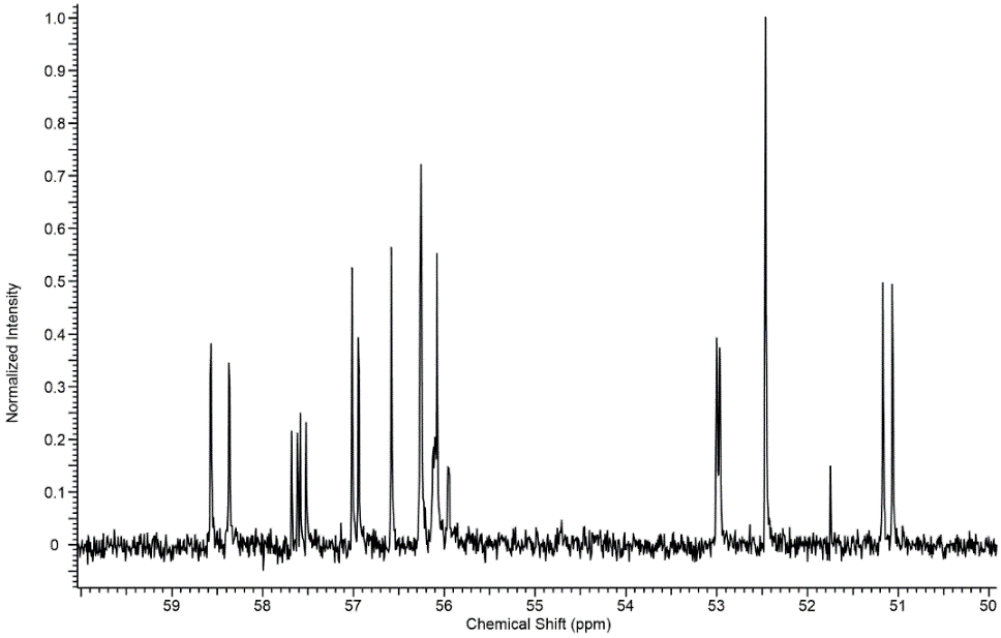

Figure 2.38 Methylene and methoxy region of the $^{13}C\{^{1}H\}$ NMR spectrum from procedure 1 showing sets of doublets.

A region of the $^{13}C\{^{1}H\}$ spectrum (Figure 2.38) from procedure 1 presents two sets of peaks for the methylene and methoxy regions shown. The evidence of coupling between the phosphorus and carbon nuclei is seen as doublets (two sets) in the methoxy (57.5 ppm in Fig. 2.38) as well as the imine (187 ppm in Fig. 2.39) regions of different spectra for these complexes.

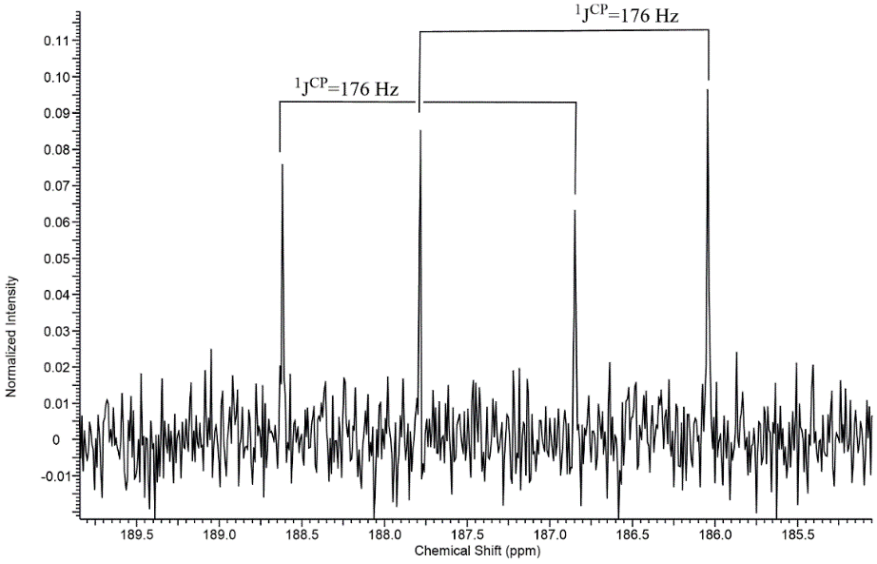

Figure 2.39 Imine region of the $^{13}C\{^{1}H\}$ NMR spectrum from procedure 2 showing two sets of doublets and their coupling constants.

From the X-ray structure of compound **2.1**, the methoxy group of the phosphonate points towards N5, a donor group perpendicular to the plane of the imine but away from N3. The presence of one major doublet in the methyl region of the ^{1}H NMR spectrum (Fig. 2.35) and the cluster of doublets around the 3.8 ppm methoxy region of the same spectrum, suggests that all the species present in the product mixture from where **2.1** was recrystallised may have similar configurations at the phosphonate arm of the complex. All the diastereoisomers present were also expected to have their *mer*-N-H's in the *anti* configuration, given that it is the most common presentation observed in this project and in the literature. However, if that was not the case, then it can be speculated that the other (minor) diastereoisomers present in the product mixture of procedure 1 could have been generated from isomers with their *mer*-N-H's in the *syn* configuration.

Extending this argument to the product mixture from procedure 2 from which compounds **2.2** and **2.3** were isolated, it can be proposed that given the difference in chemical shifts observed in the NMR spectra (Fig. 2.39 - 2.41), the configuration at the phosphorus centres of the diastereoisomers present in the product mixtures must be different. The isolated compounds, **2.2** and **2.3** had different configurations at their phosphorus centres, confirmed by X-ray crystallography. While compound **2.2** had its methoxy group pointing towards N5 but away from N3 (*R*), **2.3** presented with its methoxy group pointing away from N5 but towards N3 (*S*).

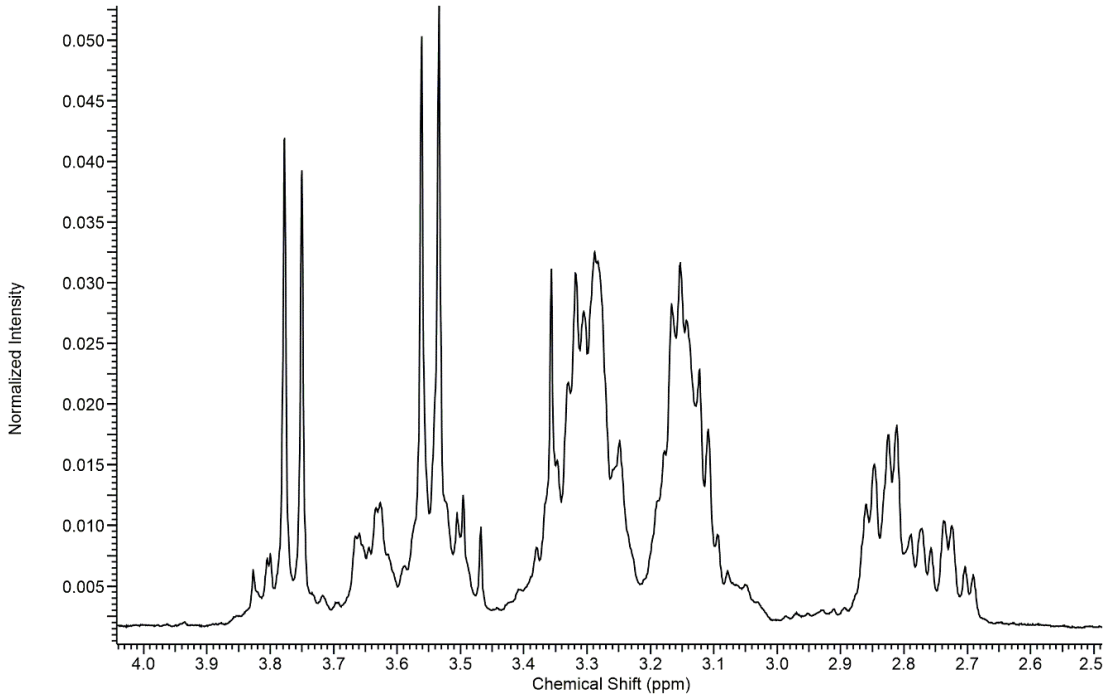

Figure 2.40 ^{1}H NMR spectrum from procedure 2 product mixture showing methoxy and methylene regions only.

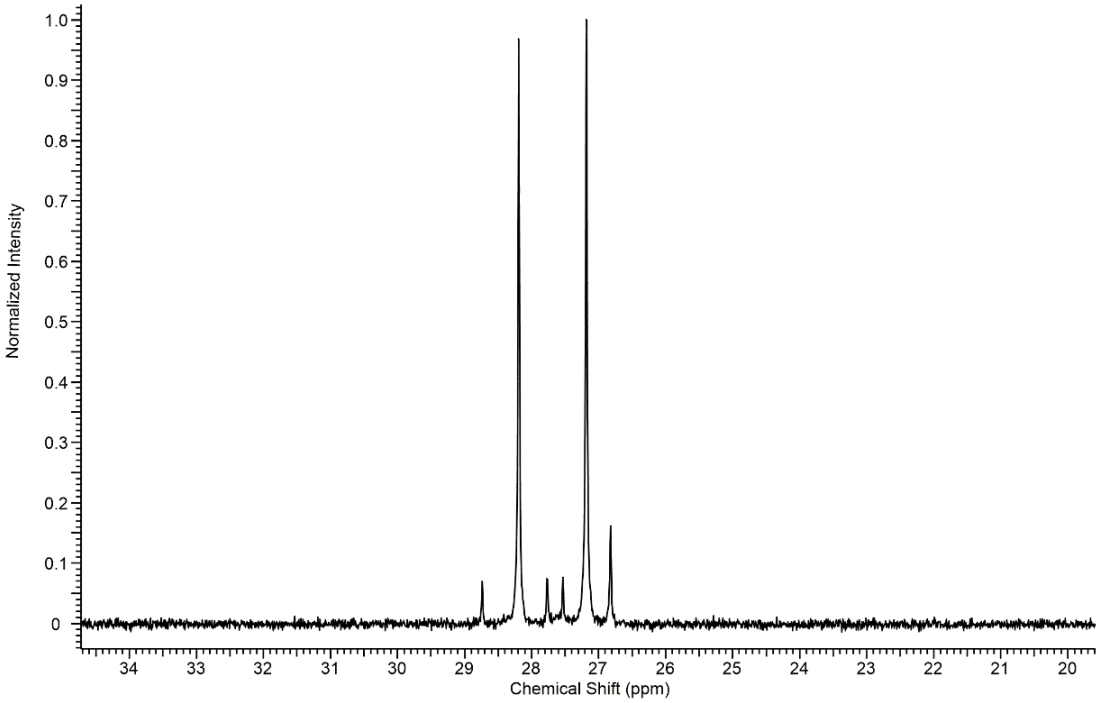

Figure 2.41 $^{31}P\{^{1}H\}$ NMR spectrum from procedure 2 showing six signals with the ratio of 0.05:0.87:0.07:0.07:1.0:0.16

In each case (where R = CH_3 or C_6H_5), these tetraen derivatives have formed two major pairs of diastereoisomers with other minor diastereoisomers present in the mixture. The minor diastereoisomers could be as a result of isomers with their *mer*-N-H's in the *syn* configuration.

Trien Based Di-Imine Phosphonate Complexes of Cobalt(III)

Compounds from procedures 3 and 4 were made by reacting four equivalents of keto phosphonate acid with only one equivalent of the pre-coordinated polyamine (N′-[2-(2-aminoethylamino)ethyl]ethane-1,2-diamine). A two-fold excess amount of the phosphonates was used (as suggested from previous research in the group) since there are two possible condensation sites for these complexes.

Four pairs of diastereoisomers are expected for the di-imine complexes: Δ*RS* & Δ*SR*, Δ*RR* & Δ*SS* and Λ*RS* & Λ*SR*, Λ*RR* & Λ*SS*, where Δ*RS* & Λ*SR* and Δ*SR* & Λ*RS* are enantiomers. Δ*RR* & Λ*SS* and Λ*RR* & Δ*SS* are also enantiomers. The helicity of the polyamine ligand around the cobalt(III) metal centre and the chirality of the phosphorus centre yield either a symmetrical molecule (Δ*RR* & Δ*SS*, Λ*RR* & Λ*SS*) or an unsymmetrical one (Δ*RS* & Δ*SR*, Λ*RS* & Λ*SR*), considering the presence or absence of a C_2 axis of rotation in a given molecule.

A closer look at the methoxy region (around 3.7 ppm) of the proton spectrum shown in Fig. 2.42 reveals three sets of doublets with the integral ratio of 1:2:1 respectively. The most intense

doublet has been assigned to a symmetrical molecule where all the methoxy protons are equivalent and hence resonate in the same frequency.

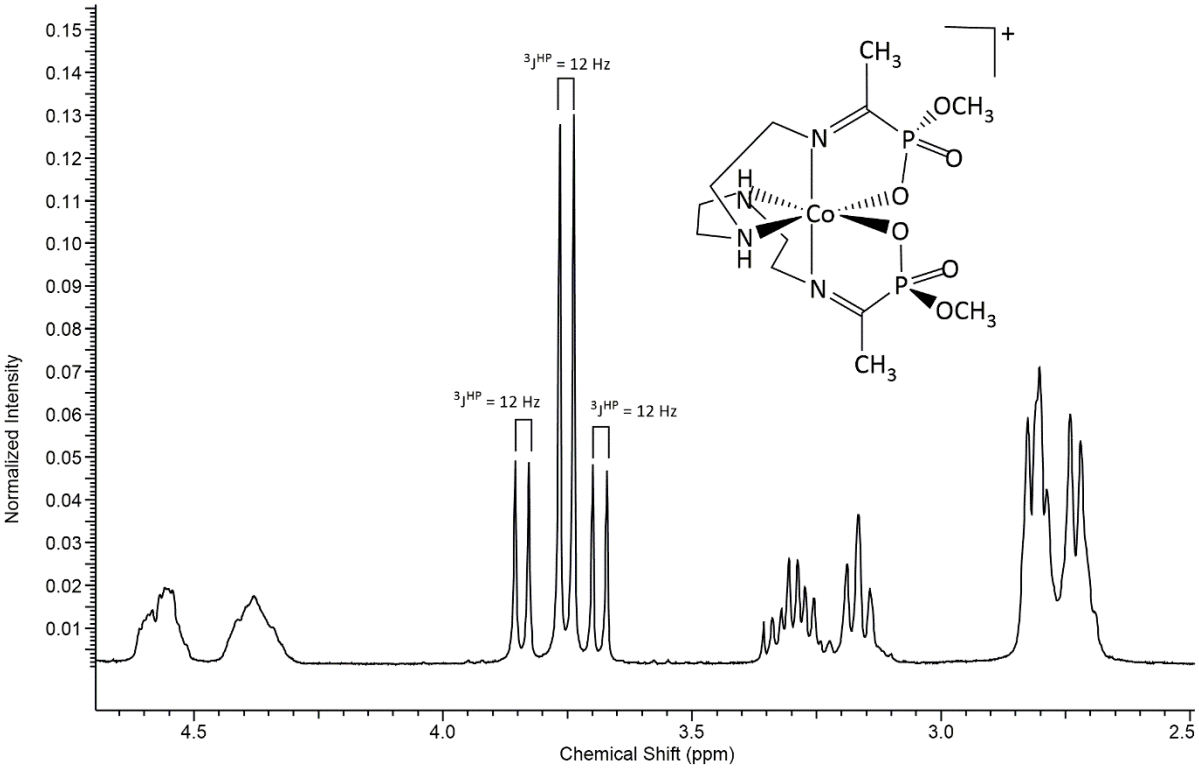

Figure 2.42 ^{1}H NMR spectrum of the first fraction of procedure 3 showing one of the constituent molecules. Integral ratio of the three doublets was 1:3:1 respectively.

The two less intense doublets have subsequently been assigned to an unsymmetrical molecule in which the two phosphorus centres have different configurations. This assignment was based on the integral values obtained from the spectrum coupled with the low likelihood of two other symmetrical isomers being there in the same amount, while also recognising that there are only two C_2 symmetrical diastereoisomers and one of them had already been assigned. The ratio of the integral values was 1:3:1 for the methoxy doublets, respectively.

Occurring in an *R* or *S* configuration, with respect to the phosphorus stereogenic centre, depends on the helicity (Δ or Λ) of the cobalt(III) centre. For these trien derivatives, there are only two other amines (both of them secondary amines) occupying two sites of the octahedron among other donors. If we choose one of the helicity options Δ, it will imply that the methoxy group points either towards the donor group perpendicular to their respective imine plane (in an *S* configuration) or away from it (in an *R* configuration). This difference in the local electron density means the protons will resonate at different frequencies. It is unclear which

configuration produces which resonance since NOE experimental results failed to distinguish them. However, based on information collated from ^{1}H NMR spectra of these complexes, it can be postulated that the Δ*S* configuration at the phosphorus centre makes the methoxy protons resonate at a slightly lower chemical shift (upfield) compared with the Δ*R* configuration which may cause the methoxy protons to resonate more downfield. This difference in chemical shifts could be attributed to the different chemical environments, where proximity to an amine donor could result to greater shielding from the external magnetic field and consequently, upfield signals.

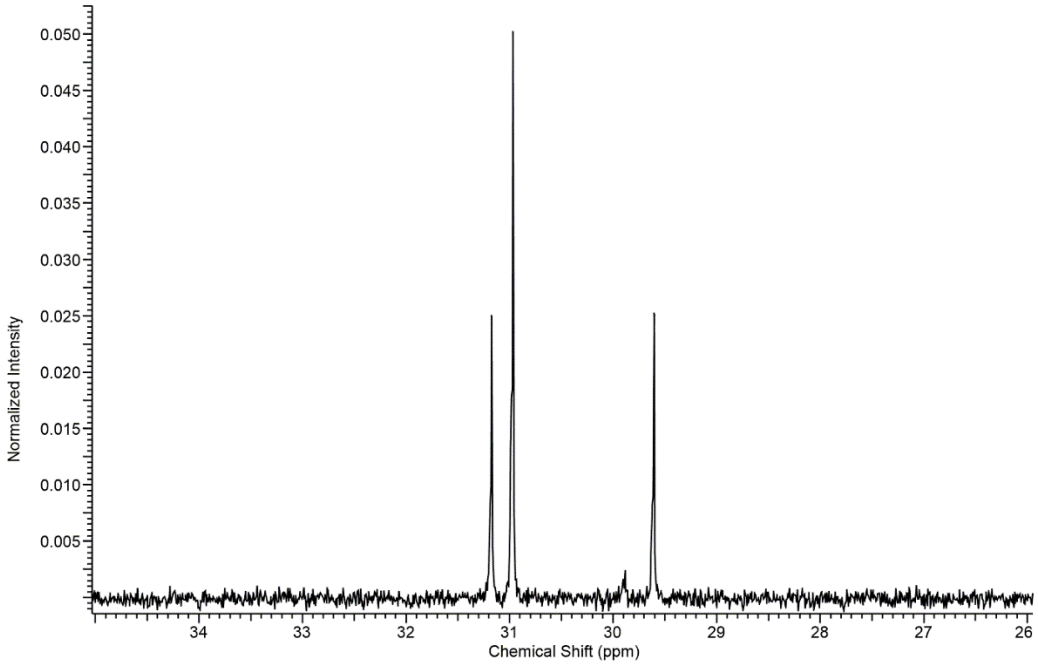

Figure 2.43 ^{31}P{1H} NMR of the first fraction of procedure 3 (integral ratio is 1:2:1).

The ^{31}P{^{1}H} NMR (Figure 2.43) validated the ^{1}H NMR by showing three peaks (integral ratio 1:2:1) which correspond to three different P nuclei: two from the unsymmetrical molecule and one from the symmetrical one. As with the protons, the phosphorus nuclei are in slightly different chemical environments with respect to the configuration at the P stereogenic centre. Two symmetrical Δ*RR* (**2.8** (Fig. 2.23) and **2.10** (Fig. 2.26)) and an unsymmetrical Δ*SR* (**2.7** (Fig. 2.22)) products of procedure 4 were isolated and some regions of their NMR spectra are shown in Figures 2.44 - 2.46.

These NMR spectra show that complete isolation of isomers through column chromatography was not achieved, with each band dominated by the major isomer present in that fraction and the other isomer(s) present as minor components of the mixture.

Figure 2.45 is the ^{1}H NMR spectrum obtained for the product mixture from procedure 4 prior to the separation of its constituents.

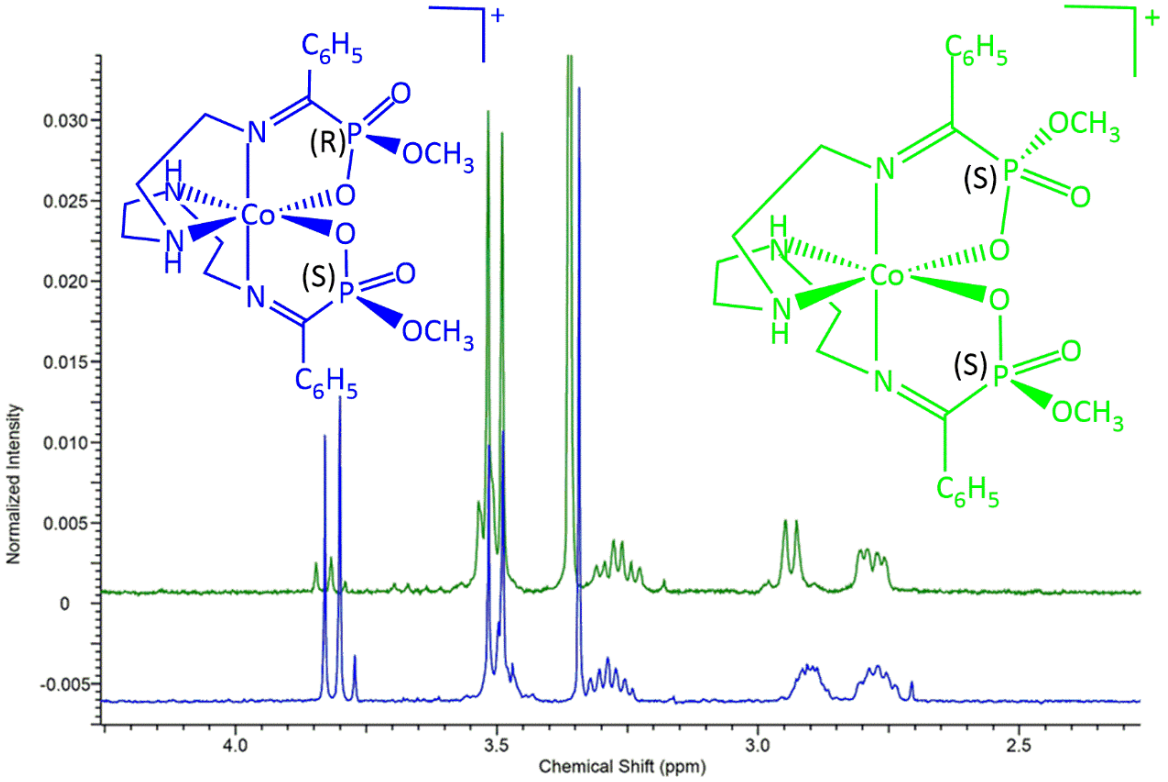

Figure 2.44 Overlaid spectra of ^{1}H NMR of chromatographic fractions from procedure 4.

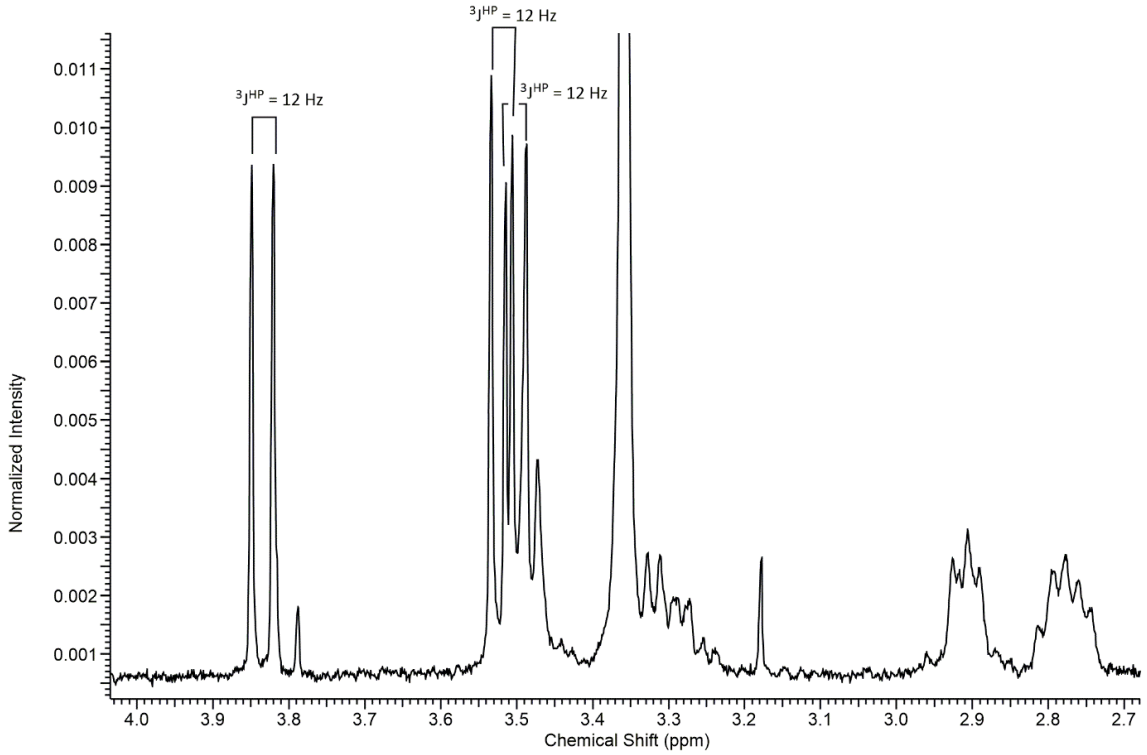

Figure 2.45 Regional ^{1}H NMR spectrum of the product mixture (1:1:1 (2:1) integral ratio) from procedure 4 before separation.

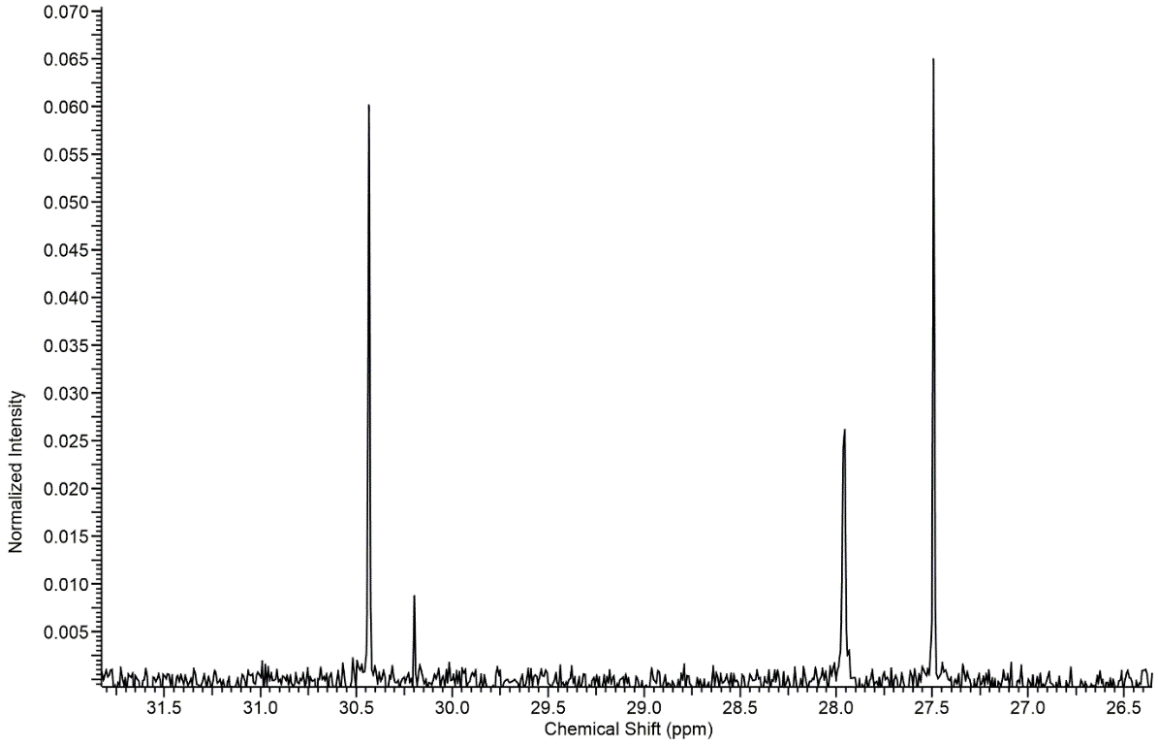

Figure 2.46 ^{31}P{^{1}H} NMR of the crude product mixture from procedure 4 before separation.

The $^{31}P\{^{1}H\}$ NMR shown in Fig. 2.46 shows there are four chemically different phosphorus centres present in the mixture from procedure 4 before the isolation of its constituents. Integration showed the ratio of 1:0.12:0.81:1.05 from left to right for all four signals. Roughly the two main components are in the mixture in the ratio of 2:1. This ratio aligns with that obtained from the ^{1}H NMR (Fig. 2.45) of this same mixture. The ^{1}H NMR spectrum has three major doublets which have been highlighted (showing their coupling constants) in the methoxy region. There are also two minor doublets in that region of the spectrum, which are not very obvious due to overlap. Two of the signals (27.52 and 30.43 ppm) from the $^{31}P\{^{1}H\}$ NMR spectrum shown in Fig. 2.46 have been assigned to an unsymmetrical molecule where the two phosphorus centres are in different chemical environments. The peak at 27.99 ppm has been assigned to a symmetrical molecule. The minor signal in the 30 ppm region could be attributed to a minor diastereoisomer. These spectra also suggest that the unsymmetrical molecules dominate the product mixture from procedure 4.

So far, it appears from NMR data that the symmetrical molecules dominate the methyl system of these trien derivatives whereas the unsymmetrical molecules dominate the phenyl system. There is no explanation as to why this may be the case.

X-ray crystallography showed two symmetrical compounds were isolated (**2.8**; Δ*mffm*(*RR*) (Fig. 2.23) and **2.10**; Δ*mffm*(*RR*) (Fig. 2.26)) and an unsymmetrical isomer (**2.7**; Δ*mffm*(*SR*) (Fig. 2.22)) from the phenyl system.

The C_2 axis (Fig. 2.47) present in the symmetrical molecules simplifies NMR spectra (Fig. 2.44, and 2.48 green) because both fragments on each half of the molecule are equivalent.

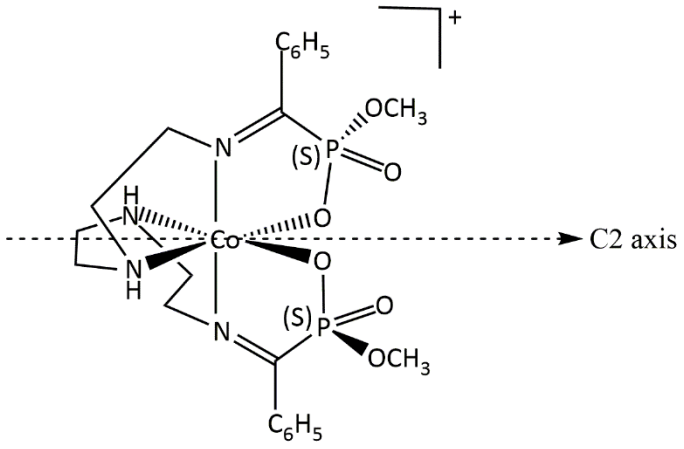

Figure 2.47 A C_2 axis illustrated on a phenyl trien system.

An overlaid spectrum showing the chromatographic fractions from where the diastereoisomers from procedure 3 were isolated has also been included as Fig. 2.48 and Fig. 2.49. Once again, these NMR spectra show that each band is dominated by the major pair of diastereoisomers present in that fraction with some contamination by the other isomer(s) present.

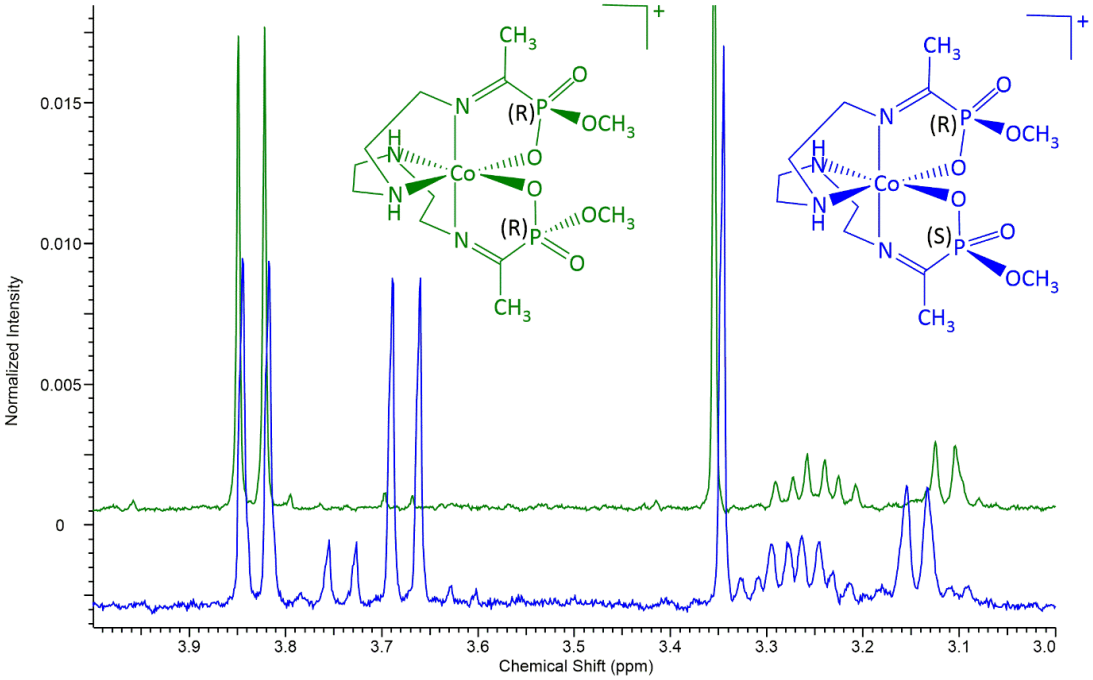

Figure 2.48 Overlaid spectra of ^{1}H NMR of chromatographic fractions: 1 (bottom); 2 (top) from procedure 3.

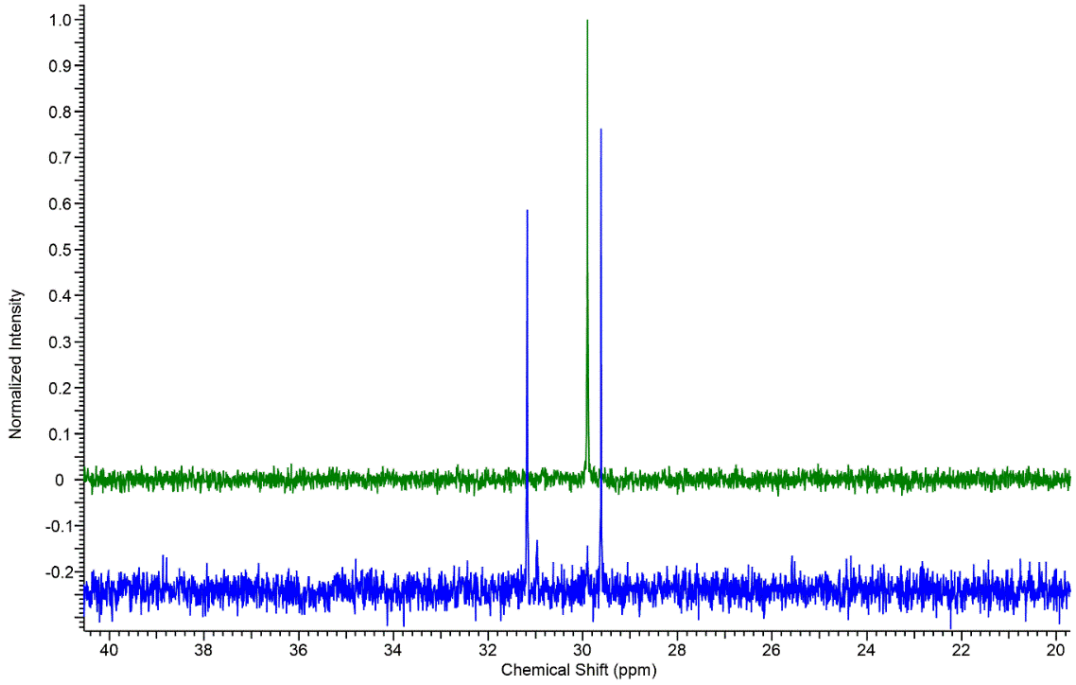

Figure 2.49 Overlaid spectra of ^{31}P{1H} NMR of chromatographic fractions: 1 (bottom); 2 (top) from procedure 3.

Ethane-1,2-diamine Based Di-Imine Phosphonate Complexes of Cobalt(III)

The compounds (**2.11, 2.12, 2.13**) made from complexes of the diamine ligand ethane-1,2-diamine, demonstrate the ability of donor atoms to change their relative locations around the central metal ion in order to adopt a geometry that will allow immediate dehydration and formation of a planar imine from the condensation reaction. The starting material had two leaving chlorido ligands *trans* to the central metal ion whereas the end isolated products have the oxygen ends of the incoming ligand swapped around to a *cis* presentation around the central metal ion.

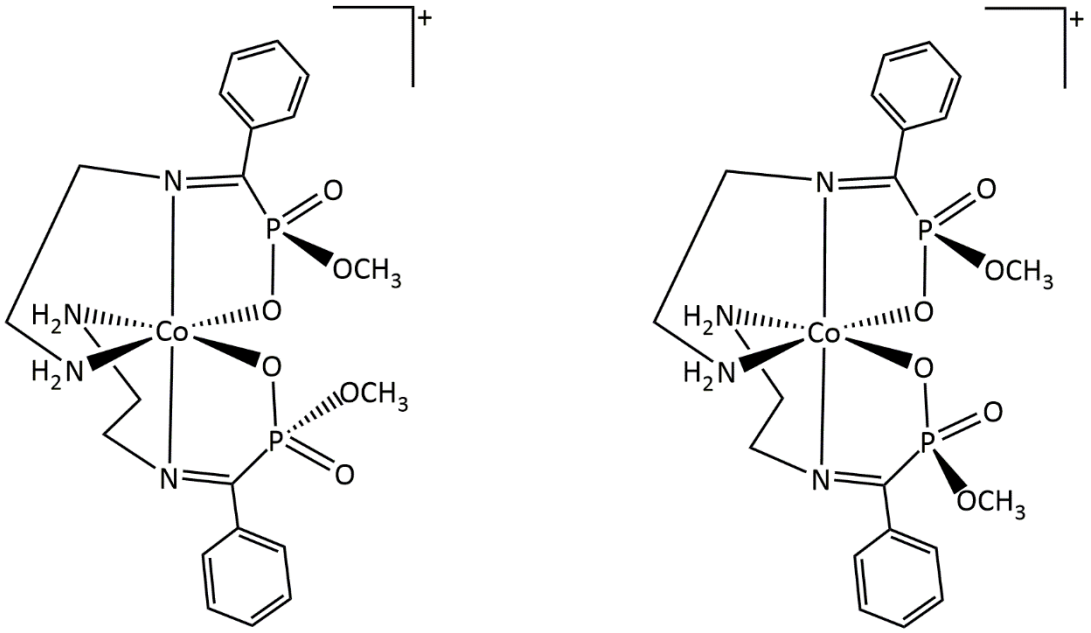

2.11 **2.12**

Λ*mm*(*RR*) Λ*mm*(*RS*)

Figure 2.50 Isolated isomers from the en polyamine ligand

Compounds from procedure 5 were made by reacting four equivalents of keto phosphonate acid with one equivalent of the pre-coordinated polyamine (ethane-1,2-diamine). Four pairs of diastereoisomers are expected for these di-imine complexes with respect to the cobalt(III) and phosphorus centres respectively: Δ*RS* & Δ*SR*, Δ*RR* & Δ*SS* and Λ*RS* & Λ*SR*, Λ*RR* & Λ*SS*, where Δ*RS* & Λ*SR* and Δ*SR* & Λ*RS* are enantiomers. Δ*RR* & Λ*SS* and Λ*RR* & Δ*SS* are also enantiomers. Once again, the expected outcome would be either a symmetrical molecule (Δ*RR* and Δ*SS*, Λ*RR* and Λ*SS*) or an unsymmetrical one (Δ*RS* and Δ*SR*, Λ*RS* and Λ*SR*).

Four resonance peaks were observed in the $^{31}P\{^{1}H\}$ NMR spectrum (Fig. 2.51) obtained from the product mixture. Based on NMR observations made so far in this chapter, the peak around 28 ppm has been assigned to a pair of unsymmetrical diastereoisomers with its associated peak at the 30 ppm region (one of the two). The other peak at the 30 ppm region was attributed to a pair of symmetrical diastereoisomers, leaving the minor peak around 29 ppm for another pair of (minor) symmetrical diastereoisomers. It appears from this spectrum that three pairs of diastereoisomers are in the product mixture with two of the diastereoisomers (one symmetrical and another unsymmetrical) dominating the mixture in a 1:1 ratio. ^{1}H NMR of the crude product mixture also showed a 1:1 integral ratio between the major components of the mixture. It is possible the minor component of this mixture has another form of the polydentate wrapping around the metal centre.

Given that the isolated compound **2.12** (Fig. 2.28) is a Λ*mm*(*RS*) diastereoisomer, the peak around 28 ppm of the $^{31}P\{^{1}H\}$ NMR spectrum with its 30 ppm associate, has been assigned to a Λ*mm*(*RS*) diastereoisomer (where its enantiomer (Δ*mm*(*SR*)) is also expected in the product mixture).

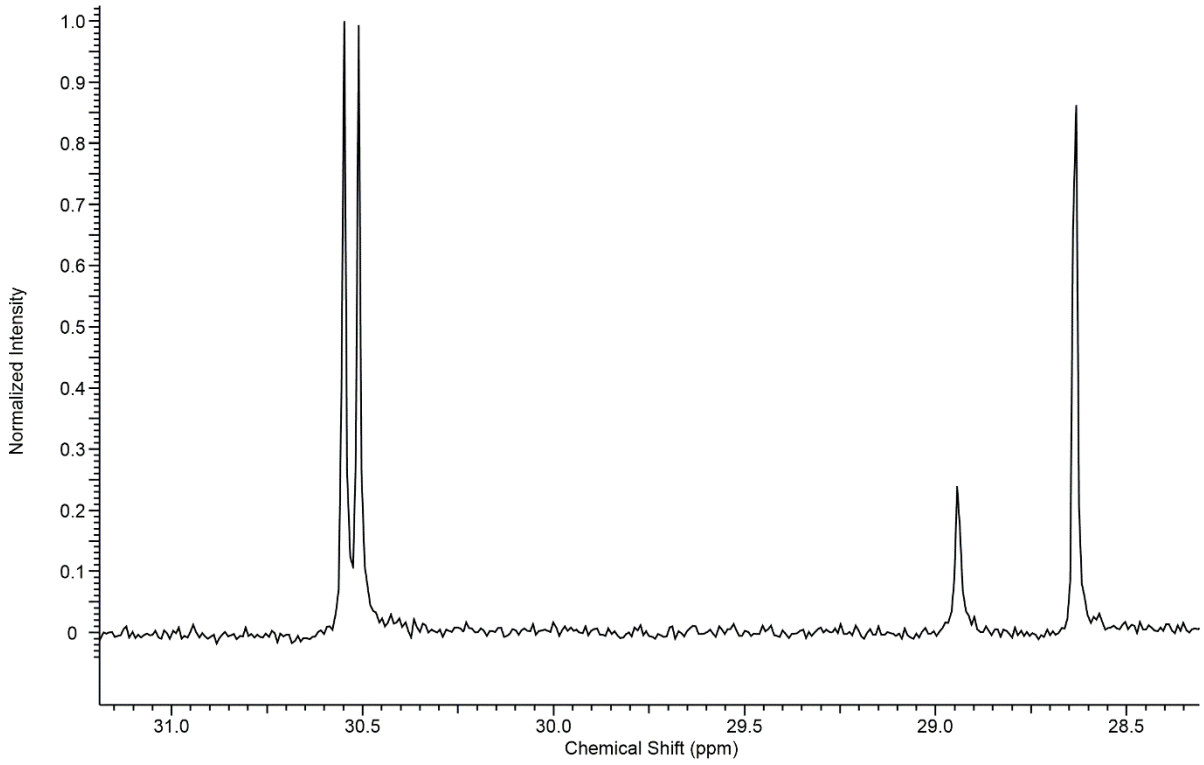

Figure 2.51 $^{31}P\{^{1}H\}$ NMR of the product mixture form procedure 5 showing four peaks with integral ratio of 1:1:0.3:1

Attempts to separate the isomers of this mixture failed. Since pairs of diastereoisomers have been isolated in this project from mixtures where they dominate, careful collections of front and back fractions were made off the column for the product mixture to see if some separation could be observed. ^{1}H NMR spectroscopy showed both fractions were still mixtures. The doublet at 3.5 ppm of the spectrum shown in Fig. 2.52 was assigned to an unsymmetrical pair of diastereoisomers (where the two phosphorus centres are in different chemical environments) with its associate doublet being one of the overlapped doublets at the 3.7 ppm region. The remaining overlapped doublet has been attributed to a pair of symmetrical diastereoisomers.

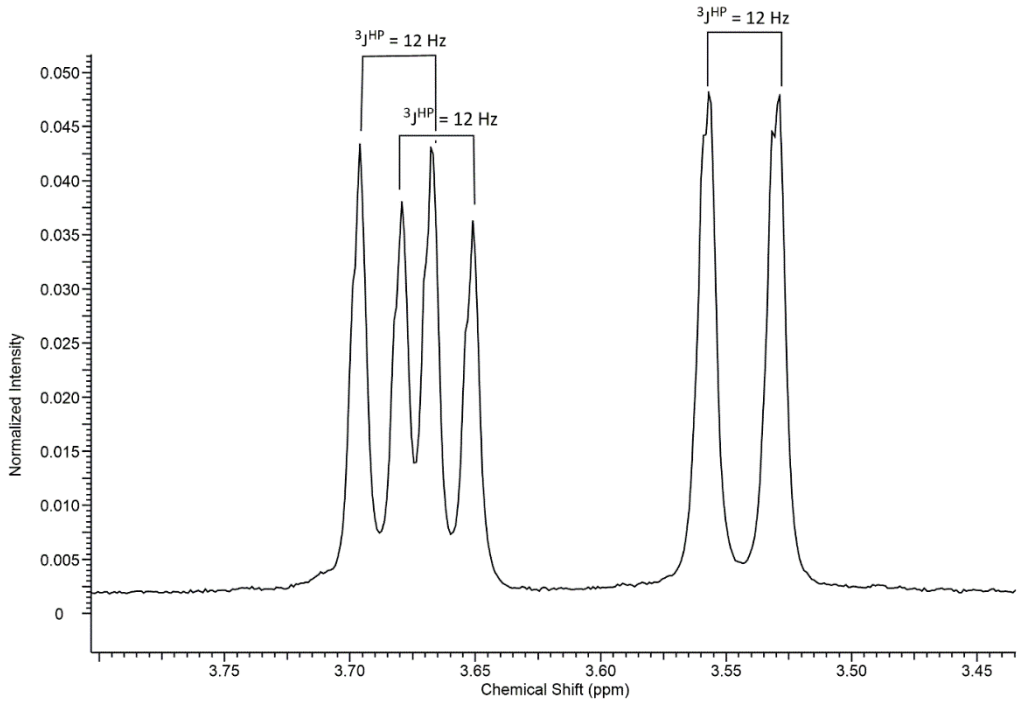

Figure 2.52 Methoxy region of the ^{1}H NMR spectrum from the front fraction of the product mixture from procedure 5.

The ^{1}H NMR shown as Fig. 2.52 resembles that in Fig. 2.45 from a trien system. Assuming that the wrapping of the en ligand is not assigned a different descriptor Λ, the system could be likened to the trien system where the symmetrical pair of diastereoisomers are expected to have an *RR* (or *SS*) configuration at its phosphorus centres (for a Δ isomer) going by the postulate that relates the chemical shift of the methoxy protons to the orientation of the methoxy group in space.

A symmetrical diastereoisomer Λ*mm*(*RR*) was isolated as compound **2.11** (Fig. 2.27) whereas an unsymmetrical diastereoisomer Λ*mm*(*RS*) was isolated as compound **2.12** (Fig. 2.28).

Compound **2.11** was isolated from the front fraction whereas **2.12** was isolated from the back fraction.

Compound **2.13** has the same absolute configuration as compound **2.11**. However, both compounds crystallised in different space groups.

Trien Based Di-Imine Carboxylato-Phosphonate Complexes of Cobalt(III)

Compound **2.14** was made by first reacting two equivalents of a keto carboxylate acid with one equivalent of the pre-coordinated polyamine (N′-[2-(2-aminoethylamino)ethyl]ethane-1,2-diamine). The resultant mono imine complex of cobalt(III) was then further reacted with two equivalents of a keto phosphonate acid to yield a di-imine bearing different ligands on each half of the octahedron. It is expected that the rich diversity of isomers from procedure 6 would resemble that of those from procedure 1 because previous research has demonstrated that the carboxylate analogues form only two isomers which are enantiomers. Hence two pairs of diastereoisomers are expected in the crude mixture from procedure 6: (Δ*R* and Δ*S*) and (Λ*R* and Λ*S*), where Δ*R* and Λ*S* are enantiomers. Δ*S* and Λ*R* are also enantiomers.

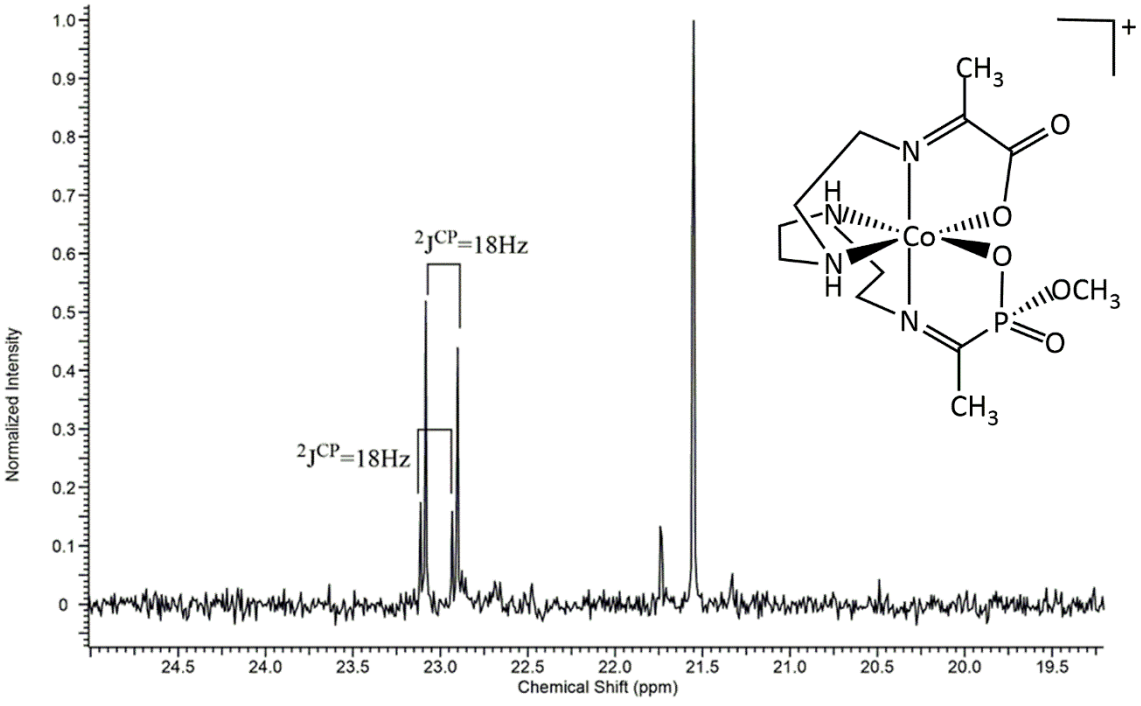

Figure 2.53 Methyl region of the $^{13}C\{^1H\}$ NMR spectrum from the front fraction of the product mixture from procedure 6 showing one enantiomer (Δ*mffm*(*R*)) of the dominant diastereoisomers.

Four sets of peaks can be seen in the methyl region of the $^{13}C\{^{1}H\}$ spectrum of the product mixture from procedure 6 shown in Fig. 2.53. Based on our discussion so far, there are two pairs of diastereoisomers present in the mixture. Each molecule has a methyl group on the carboxylate arm of the complex and another methyl group on its phosphonate arm. The two singlets have been assigned to the carboxylate methyl groups for the two diastereoisomers whereas the two sets of doublets have been assigned to the phosphonate methyl groups. As expected, the later methyl group resonance peaks are doublets because of the NMR active phosphorus nucleus on that arm of the complex. One pair of diastereoisomers dominates the mixture (the major isomer). The presence of a methoxy group on the phosphonate arm of the complex accounts for the downfield resonance of the doublets due to the presence of the electron withdrawing oxygen atom which causes deshielding from the applied magnetic field. The ^{1}H spectrum shown in Fig. 2.54 and the $^{31}P\{^{1}H\}$ spectrum (Fig. 2.55) confirm the presence of two pairs of diastereoisomers in the mixture in a 3:1 ratio, by integration, for both spectra. The methyl groups on the phosphonate arms of both pairs of diastereoisomers resonated with the same chemical shift of 2.8 ppm in the ^{1}H spectrum. Integration of the doublet at 2.8 ppm was equivalent to the sum of the two doublets in the methoxy region of the same spectrum (Fig. 2.54), hence the assignment.

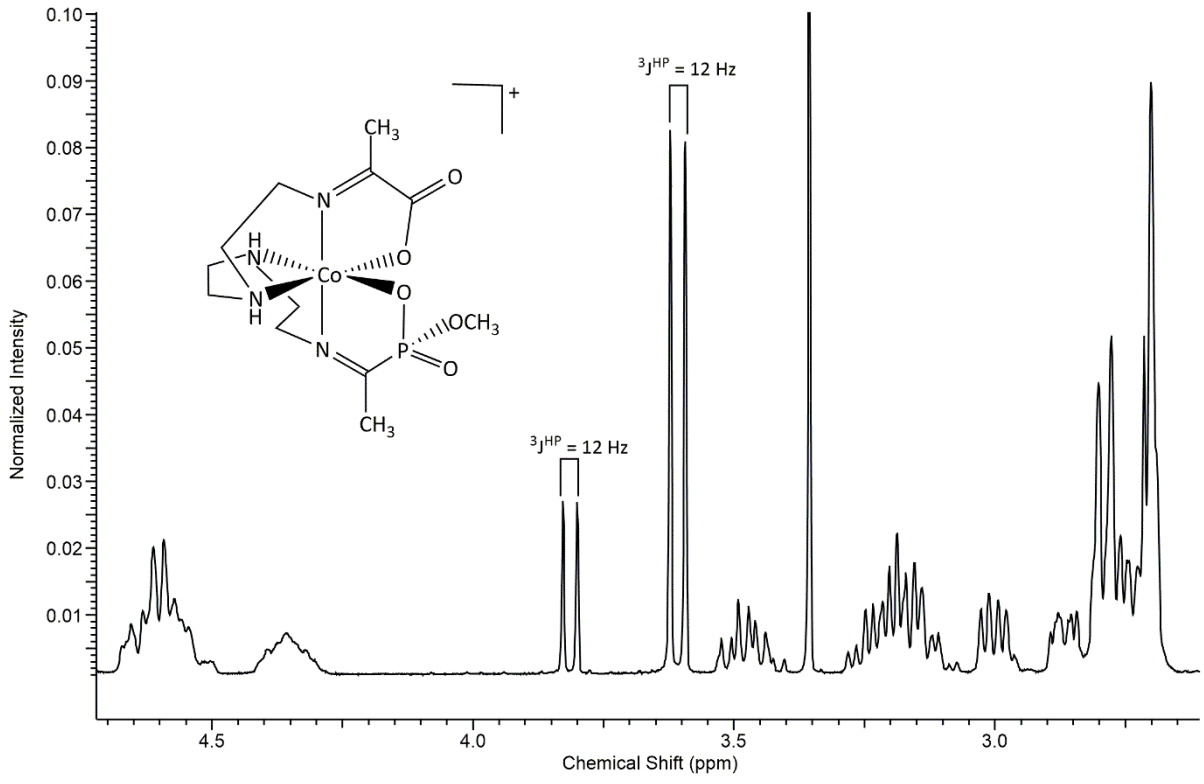

Figure 2.54 ^{1}H NMR spectrum of the front fraction of the product mixture from procedure 6 showing coupling constants for the methoxy protons with the ^{31}P nuclei and one enantiomer (Δ*mffm*(*R*)) of the isolated compound (**2.14**).

The main structure extracted from the asymmetric unit of the X-ray crystal structure of compound **2.14** has been shown in Figure 2.31. It has the Δ*mffm* wrapping of the polydentate ligand around its metal centre with an *R* configuration at the phosphorus stereogenic centre. It was isolated from the front fraction of a band from the column. The Δ*mffm* wrapping of the ligand around the metal ion is the same as that isolated from previous research[55] in the Hartshorn group.

Assuming that the isolated compound **2.14** (with the absolute configuration of (Δ*mffm*(*R*)) is the dominant compound (with its enantiomer) in fraction 1 of the product mixture, then the ^{1}H NMR spectrum shown in Fig. 2.54 would not support the hypothesis that the Δ*S* stereoisomers resonate slightly more upfield than the Δ*R* stereoisomers with respect to the phosphorus stereogenic centre. However, since the dominant compound has not always been the isolated one, the hypothesis may still hold. Following this hypothesis, one can argue that the second fraction of the product mixture is dominated by the Δ*R* stereoisomer (and its enantiomer). The spectrum shown in Fig. 2.56 highlights that.

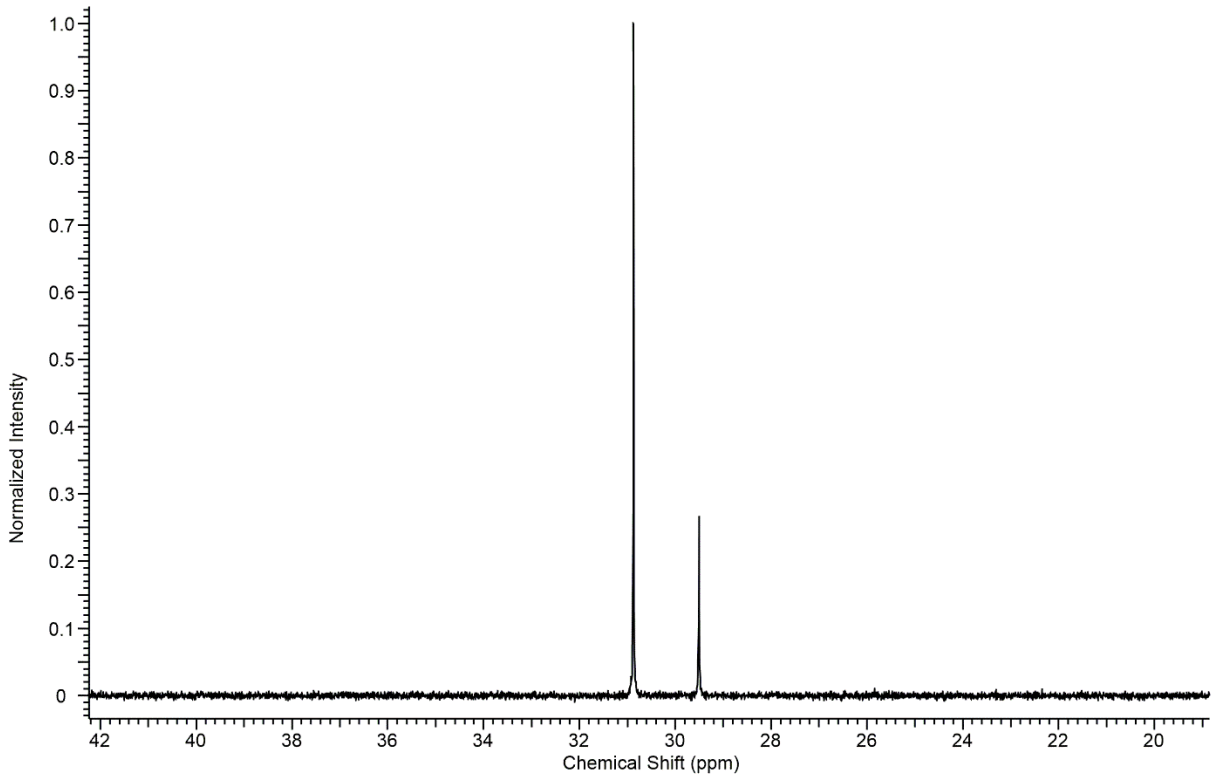

Figure 2.55 ^{31}P{^{1}H} NMR of the product mixture from procedure 6.

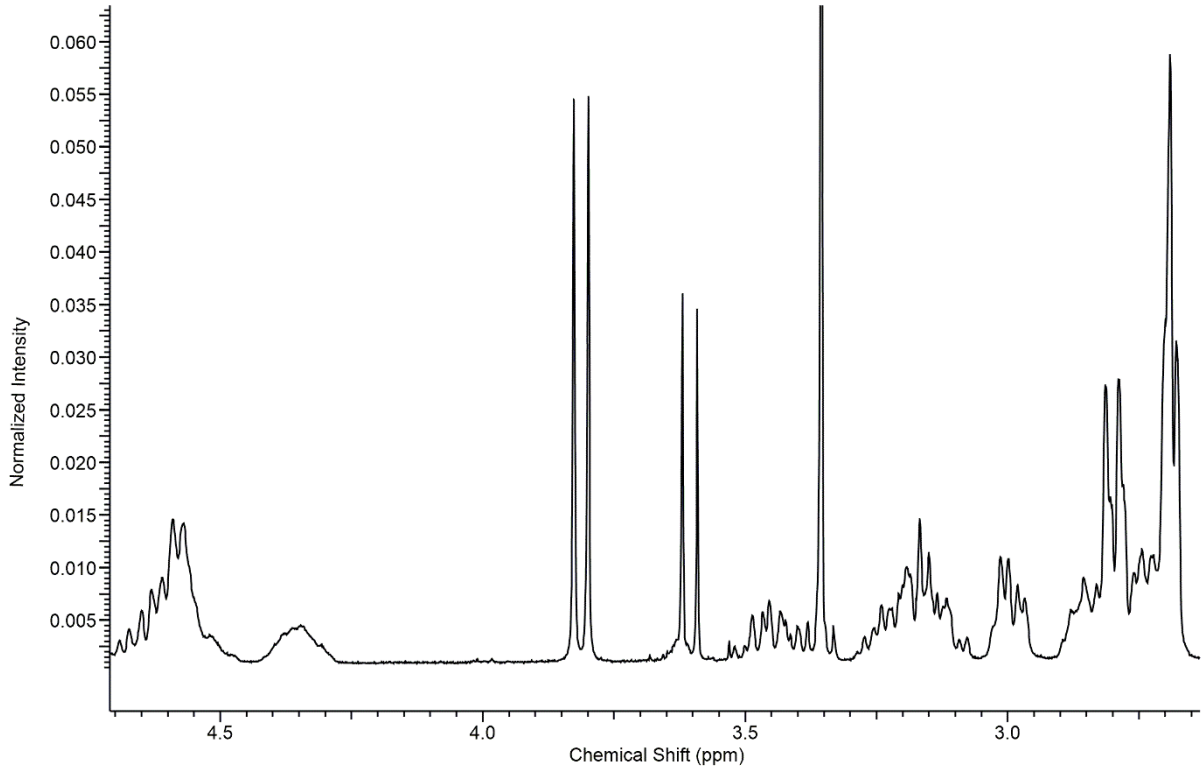

Figure 2.56 ^{1}H NMR spectrum of the back fraction of the product mixture from procedure 6.

2.4 Conclusions

The number of signals in the methylene and methoxy regions indicated whether one or two of the condensation reactions had occurred on a complex and highlighted the presence, or not, of a symmetry element in each molecule observed. Integration of the methoxy regions also provided a guide to the approximate number of pairs diastereoisomers present in a given product mixture.

The ^{1}H and ^{13}C{^{1}H} NMR spectra of the mixture of each crude product in this project are complicated. However, they significantly showed a limited number of isomers. The intricacy of these spectra has been attributed to the chemical similarity of the methylene protons and carbons in the polyamine backbone of each pair of diastereoisomers, giving rise to overlapping peaks. One of the most interesting parts of all ^{1}H NMR spectra obtained from crude products, is the presence of overlapping doublets around 2.7 and 3.6 ppm respectively. The protons of NH's were assigned in some complexes by comparing their spectra with those obtained from the cobalt(III) coordinated polyamine starting materials.

The polydentate wrapping around the cobalt(III) metal centres was a source of handedness where Δ and Λ descriptors have been used to express the helicity as discussed in chapter 1. The handedness expressed by a given X-ray structure has been highlighted in this chapter but that

is not without mentioning that the compounds reported here exist as racemic mixtures with both handedness equally present in a given product mixture as enantiomers.

For the tetraen derived mono imines, two pairs of diastereoisomers were expected in every crude mixture, considering the helicity of the wrapping of the polyamine ligand around the metal ion and the chirality at the phosphorus centres only: (Δ*R* and Δ*S*) and (Λ*R* and Λ*S*), where (Δ*R* and Λ*S*) and (Δ*S* and Λ*R*) are enantiomers. The possibility of having more isomers in the product mixtures because of the chirality at the meridional nitrogen (*mer*-N) atom *trans* to the imine donor was considered but was later ruled out after conducting a search of the Cambridge Crystallographic database. All the compounds isolated from the tetraen derivatives (**2.1** (Δ*mffm*$_a$(*R*)), **2.2** (Δ*mffm*$_a$(*R*)) and **2.3** Δ*mffm*$_a$(*S*)) presented in the *anti* configuration (with respect to their *mer*-NH's) confirmed by X-ray crystallographic techniques. This observation aligned with the literature[55] from previous research in the Hartshorn group and in most cobalt(III) octahedral complexes with related folds in the wider literature.[53, 104-122] It seems uncommon to have the *mer*-N-H pointing towards the rest of the polyamine fold.

For the tetraen derivatives, occurring in a Δ*R* configuration points the methoxy group away from N3 but towards N5. On the other hand, it was observed that the Δ*S* configuration presents with the methoxy group pointing towards N3 and away from N5. The proximity of the methoxy protons to a secondary amine group (N3) could contribute to shielding (and its consequent upfield resonance frequencies) of those protons from the applied magnetic field in NMR experiments. In contrast, the opposite effect could be the case for when the methoxy protons are pointed away from the secondary amine (N3), giving rise to deshielding and downfield resonance frequencies. There is therefore a current hypothesis that the Δ*S* (or its enantiomer: Λ*R*) stereoisomer of these complexes could result to an upfield chemical shift. Consequently, the Δ*R* (or its enantiomer: Λ*S*) stereoisomer of these complexes could result to a downfield chemical shift. The plethora of ^{1}H NMR spectra obtained from these compounds appear to support this hypothesis but further experiments may be required to form a theory.

The trien derivatives had double condensation sites. Therefore, four pairs of diastereoisomers were expected for the di-imine complexes: Δ*RS* & Δ*SR*, Δ*RR* & Δ*SS* and Λ*RS* & Λ*SR*, Λ*RR* & Λ*SS*, where Δ*RS* & Λ*SR* and Δ*SR* & Λ*RS* are enantiomers. Δ*RR* & Λ*SS* and Λ*RR* & Δ*SS* are also enantiomers. The helicity of the polyamine ligand around the cobalt(III) metal centre and the chirality of the phosphorus centre would yield either a symmetrical molecule (Δ*RR* & Δ*SS*,

Λ*RR* & Λ*SS*) or an unsymmetrical one (Δ*RS* & Δ*SR*, Λ*RS* & Λ*SR*), considering the presence or absence of a C_2 axis of rotation in a given molecule.

NMR revealed the methyl system was dominated by symmetrical diastereoisomers whereas the phenyl system was dominated by the unsymmetrical ones. Both the symmetrical (Δ*mffm*(*RR*)) and unsymmetrical (Δ*mffm*(*SR*)) compounds of the phenyl system were isolated and characterised by X-ray crystallography as **2.8** (Fig. 2.23) and **2.7** (Fig. 2.22) respectively.

Going by the original postulate of the observed ^{1}H NMR chemical shift being related to the configuration at the phosphorus stereogenic centre, it can then be argued that the methyl system (Fig. 2.48) is dominated by the (Δ*mffm*(*RR*)) diastereoisomer or its enantiomer (Λ*mffm*(*SS*)).

The en derived compounds provided classical examples for demonstrating the ability of donor atoms to change their relative locations around the central metal ion in order to adopt a geometry that will allow immediate dehydration and formation of a planar imine from the condensation reaction. The starting material had two leaving chlorido ligands *trans* to the central metal ion whereas the end isolated products have the oxygen ends of the incoming ligand swapped around to a *cis* presentation around the central metal ion.

Four pairs of diastereoisomers were expected for the en di-imine complexes with respect to the cobalt(III) and phosphorus centres respectively: Δ*RS* & Δ*SR*, Δ*RR* & Δ*SS* and Λ*RS* & Λ*SR*, Λ*RR* & Λ*SS*, where Δ*RS* & Λ*SR* and Δ*SR* & Λ*RS* are enantiomers. Δ*RR* & Λ*SS* and Λ*RR* & Δ*SS* are also enantiomers. Once again, the outcome was expected to be either a symmetrical molecule (Δ*RR* and Δ*SS*, Λ*RR* and Λ*SS*) or an unsymmetrical one (Δ*RS* and Δ*SR*, Λ*RS* and Λ*SR*). Three pairs of diastereoisomers were identified in the product mixture by NMR; where two of those (one symmetrical and another unsymmetrical) dominated the crude product mixture in a 1:1 integral ratio, prior to the attempted column chromatographic separation. If the different description for the en polydentate wrapping is ignored, the pair of symmetrical diastereoisomers could have Δ*RR* and Λ*SS* configurations going by the current hypothesis that relates the chemical shift of the methoxy protons to the orientation of the methoxy group in space.

A pair of symmetrical diastereoisomers Λ*mm*(*RR*) (and its enantiomer) was isolated as compound **2.11** (Fig. 2.27) whereas a pair of unsymmetrical diastereoisomers Λ*mm*(*RS*) (and its enantiomer) was isolated as compound **2.12** (Fig. 2.28).

The set of compounds made from condensing both a carboxylate and a phosphonate ligand onto a trien cobalt(III) system using procedure 6, were expected to have two pairs of diastereoisomers: (Δ*R* and Δ*S*) and (Λ*R* and Λ*S*), where Δ*R* and Λ*S* are enantiomers. Δ*S* and Λ*R* are also enantiomers. The isolated compound **2.14** (with the absolute configuration of (Δ*mffm*(*R*)) was not the dominant compound (with its enantiomer) in fraction 1 of the product mixture, judging by the current hypothesis using the ^{1}H NMR chemical shifts.

All of the compounds isolated in this chapter crystallised in centrosymmetric space groups with most of the crystal structures solved in the triclinic P$\bar{1}$ space group. The X-ray structures were all of octahedral geometry with cobalt(III) at the centre, save the two tetranuclear compounds (**2.5** and **2.9**) that had a cobalt(II) centre each. For the compounds made through double condensation reactions, there were usually two imine groups *trans* to each other around the metal ion, while two secondary amines (*cis* to each other) were in the same plane with two oxygens (also *cis* to each other) in the six-coordinate geometry. However, the compounds made from ethane-1,2-diamine, have two primary amines in place of the secondary amines adjacent to the two oxygens in the same plane. The singly condensed products differ by obviously having one oxygen , one imine group, three secondary amines and a primary amine coordinated to the central cobalt(III) ion.

There were cases where the free phosphonate oxygen (P=O) acted as a ligand. Two X-ray structures (Figures 2.19 (compound **2.5**) and 2.24 (compound **2.9**)) showed formation of O-Co bonds whereas Figure 2.26 (compound **2.10**) showed an O-Zn bond formation. However, the conditions which make the reactivity of the phosphonate oxygen favourable are not very clear at this stage. It seemed to happen in the presence of excess zinc chloride. One of the O-Co bonds formed in a methanolic solution whereas the other formed in a hydrochloric acid solution. The O-Co bonds formed in compounds **2.5** and **2.9** led to the tetranuclear complexes included in this chapter.

These tetranuclear complexes have a cobalt(II) ion at the centre of three phosphonate imine complexes of cobalt(III). The complex ligands were coordinated to the central metal ion in a distorted octahedral geometry. The arrangement of the complex ligands in space around the metal centre may well have contributed to the distortion of the octahedron. The two methoxy groups on the phosphonate arms of the complexes in compound **2.9** all pointed away from their relevant facial secondary amines. The methoxy group on P1 of compound **2.5** pointed away from N3 but the other methoxy group on P2 pointed towards N2.

Overall most of the single crystal X-ray structures presented with the *mffm* polydentate wrapping around the metal centre, except for ethane-1,2-diamine derivatives which had the *mm* descriptor from the tridentate en ligand. For the complexes derived from the tetraen ligand, some additional consideration had to be given to their meridional nitrogen (*mer*-N) atom's hydrogen. Compounds **2.1**, **2.2** and **2.3** all have their *mer*-NH's pointing away from the fold in an *anti*-style. Thus, the Hartshorn and House's nomenclature of $mffm_a$ has been assigned to each of the tetraen based isolated compounds. It can be postulated that the *anti* stereoisomer, where the hydrogen on the meridional nitrogen points away from the rest of the fold, is the most stable form for these complexes, especially because they were the same ones isolated from previous research in the group and in the wider literature.

The *R* form of the stereoisomers with respect to the phosphorus stereogenic centres (where cobalt(III) has Δ) were dominant across the complexes isolated. It appeared that the *S* stereoisomers resonated slightly more upfield than the *R* counterparts in the ^{1}H NMR spectra obtained.

The results of the experiments outlined in this chapter, align with findings from previous research that such condensation reactions can be conducted with starting material that is a mixture of stereoisomers to yield only a few isomers. The regiochemistry of the condensation reaction restricts its stereochemical outcome.

References

6. Spingler, B.; Scanavy-Grigorieff, M.; Werner, A.; Berke, H.; Lippard, S. J., Crystal Structure Determination of a (μ-Amido)(μ-hydroxo)(μ-superoxo) dicobalt (III) Complex from the Werner Collection. *Inorganic Chemistry* **2001,** *40* (5), 1065-1066.

27. Hartshorn, R. M.; House, D. A., A simple method for identifying and distinguishing between the diastereoisomers that result from wrapping polydentate ligands around octahedral metal ions. *Journal of the Chemical Society, Dalton Transactions* **1998,** (15), 2577-2588.

28. Sargeson, A.; Searle, G., The Absolute Configurations of Disubstituted Cobalt (III) Triethylenetetramine Complexes. *Inorganic Chemistry* **1965,** *4* (1), 45-52.

31. House, D.; Garner, C. S., Transition Metal Complexes of Tetraethylenepentamine. I. Preparation, Properties, and Geometric Configuration of α- and β-Chlorotetraethylenepentaminecobalt (III) Tetrachlorozincate (II) and the α Chromium (III) Analog. *Inorganic Chemistry* **1966,** *5* (12), 2097-2102.

33. Cahn, R.; Ingold, C.; Prelog, V., Convention for тг-complexes. *Angewandte Chemie International Edition. England* **1966,** *5*, 394.

39. Wilson-Coutts, S. M. The Synthesis and Configuration of Some Polydentate Amino Acid Complexes of Cobalt (III). A thesis submitted in partial fulfiment of the requirements for a Master of Science degree in Chemistry at the University of Canterbury, 2009.

45. Golding, B.; Harrowfield, J. M.; Sargeson, A., Intramolecular chelation via imines. Stereoselective synthesis of s-chloro-3-(2-aminoethyl)-1, 8-diamino-3, 6-diazaoctanecobalt (III) ion. *Journal of the American Chemical Society* **1974,** *96* (9), 3003-3004.

46. Bell, J. D.; Gainsford, A. R.; Golding, B. T.; Herlt, A. J.; Sargeson, A. M., X-Ray structure and stereoselective intramolecular synthesis of a novel quadridentate complex. *Journal of the Chemical Society, Chemical Communications* **1974,** (23), 980-981.

48. Gainsford, A.; Pizer, R.; Sargeson, A.; Whimp, P., Intramolecular carbinolamine and imine formation with cobalt (III)-amine complexes. Synthesis, structure, and reactivity. *Journal of the American Chemical Society* **1981,** *103* (4), 792-805.

49. Gainsford, A.; Sargeson, A., Stereoselective and regioselective condensation reactions of coordinated aminoacetone. *Australian Journal of Chemistry* **1978,** *31* (8), 1679-1688.

51. Sargeson, A. M.; Searle, G. H., The stereochemistry and preparation of triethylenetetraamine-disubstituted cobalt (III) complexes. *Inorganic Chemistry* **1967,** *6* (4), 787-796.

53. Browne, J. M.; Wikaira, J.; Fitchett, C. M.; Hartshorn, R. M., Polydentate ligand construction: intramolecular condensation reactions in the synthesis of imine-containing ligands. *Journal of the Chemical Society, Dalton Transactions* **2002,** (10), 2227-2234.

54. Browne, J. M.; Wikaira, J.; Hartshorn, R. M., Polydentate ligand construction: a re-examination of an intramolecular condensation reaction. *Journal of the Chemical Society, Dalton Transactions* **2001,** (23), 3513-3519.

55. Browne, J. M. Intramolecular Condensation Reactions of Cobalt (III) Complexes. A Thesis Submitted in Partial Fulfilment of the Requirements for the Degree of Master of Science in Chemistry at the University of Canterbury, University of Canterbury, 2000.

75. Browne, R. J.; Buckingham, D. A.; Clark, C. R.; Sutton, P. A., The Cobalt (III)-Promoted Synthesis of Small Peptides. *Advances in Inorganic Chemistry* **1999,** *49*, 307-373.

91. McLeod, D. A.; Brinkworth, R. I.; Ashley, J. A.; Janda, K. D.; Wirsching, P., Phosphonamidates and phosphonamidate esters as HIV-1 protease inhibitors. *Bioorganic Medicinal Chemistry Letters* **1991,** *1* (11), 653-658.

92. Etkin, N.; Dzwiniel, T. L.; Schweibert, K. E.; Stryker, J. M., Cobalt-mediated intermolecular allyl/alkyne [3+ 2+ 2] cycloaddition reactions. A practical metal template for convergent synthesis of functionalized seven-membered rings. *Journal of the American Chemical Society* **1998,** *120* (37), 9702-9703.

93. Thompson, M. C.; Busch, D. H., Reactions of coordinated ligands. IX. Utilization of the template hypothesis to synthesize macrocyclic ligands in situ. *Journal of the American Chemical Society* **1964,** *86* (18), 3651-3656.

94. Curtis, N., Macrocyclic coordination compounds formed by condensation of metal-amine complexes with aliphatic carbonyl compounds. *Coordination Chemistry Reviews* **1968,** *3* (1), 3-47.

95. Brubaker, G. R.; Schaefer, D. P.; Worrell, J. H.; Legg, J. I., Complexes of cobalt (III) with flexible tetradentate ligands. *Coordination Chemistry Reviews* **1971,** *7* (2), 161-195.

96. Coulter, G.; Krishnamurthy, M., Synthesis and characterization of some cobalt (III) complexes. *Journal of Inorganic and Nuclear Chemistry* **1977,** *39* (11), 1969-1970.

97. Sargeson, A. M.; Seale, G. H., Kinetics and stereochemistry of the aquation of some $[Co(trien)Cl_2]^+$ isomers. *Inorganic Chemistry* **1967,** *6* (12), 2172-2180.

98. Karaman, R.; Goldblum, A.; Breuer, E.; Leader, H., Acylphosphonic acids and methyl hydrogen acylphosphonates: Physical and chemical properties and theoretical calculations. *Journal of the Chemical Society, Perkin Transactions 1* **1989,** (4), 765-774.

99. Dixon, H. B.; Giddens, R. A.; Harrison, R. A.; Henderson, C. E.; Norris, W. E.; Parker, D. M.; Perham, R. N.; Slater, P.; Sparkes, M. J., A synthesis of acylphosphonic acids and of 1-aminoalkylphosphonic acids: the action of pyruvate

dehydrogenase and lactate dehydrogenase on acetylphosphonic acid. *Journal of enzyme inhibition* **1991,** *5* (2), 111-117.

100. CrysAlis, P., Oxford Diffraction Ltd. *Yarnton, England* **2009**.

101. Dolomanov, O. V.; Bourhis, L. J.; Gildea, R. J.; Howard, J. A.; Puschmann, H., OLEX2: a complete structure solution, refinement and analysis program. *Journal of Applied Crystallography* **2009,** *42* (2), 339-341.

102. Sheldrick, G. M., SHELXT–Integrated space-group and crystal-structure determination. *Acta Crystallographica Section A: Foundations and Advances* **2015,** *71* (1), 3-8.

103. Sheldrick, G. M., Crystal structure refinement with SHELXL. *Acta Crystallographica Section C: Structural Chemistry* **2015,** *71* (1), 3-8.

104. Glusker, J. P.; Carrell, H.; Job, R.; Bruice, T. C., Mechanism for chiral recognition of a prochiral center and for amino acid complexation to a cobalt (III) tetramine. Crystal structure, absolute configuration, and circular dichroism of lambda(-) 436- beta-2-[(2S, 9S)-2, 9-diamino-4, 7-diazadecanecobalt (III) aminomethylmalonate] perchlorate monohydrate. *Journal of the American Chemical Society* **1974,** *96* (18), 5741-5751.

105. Buckingham, D.; Cresswell, P.; Dellaca, R.; Dwyer, M.; Gainsford, G.; Marzilli, L.; Maxwell, I.; Robinson, W. T.; Sargeson, A.; Turnbull, K., Structure, conformational analysis, and properties of diastereoisomeric forms of. beta. 1-glycinatotriethylenetetraminecobalt (III) ions. *Journal of the American Chemical Society* **1974,** *96* (6), 1713-1725.

106. Clarkson, A. J.; Blackman, A. G.; Clark, C. R., Preparation, structures and reactions of isomeric $[Co(cyclen)(O_2C_2O_2)]^+$ and $[Co(cyclen)(O_2CCH_2CO_2)]^+$ complexes (cyclen= 1, 4, 7, 10-tetraazacyclododecane). *Journal of the Chemical Society, Dalton Transactions* **2001,** (5), 758-765.

107. Tsuboyama, S.; Shiga, Y.; Takasyo, Y.; Chijimatsu, T.; Kobayashi, K.; Tsuboyama, K.; Sakurai, T., Studies on metal complexes of chiral cyclen. Part 14. Configurational isomerism in a complex of cobalt (III). *Journal of the Chemical Society, Dalton Transactions* **1992,** (11), 1783-1789.

108. Tsuboyama, S.; Matsudo, M.; Tsuboyama, K.; Sakurai, T., Structures of [(R)- and (S)-prolinato](optically active cyclen) cobalt (III) complexes. *Acta Crystallographica Section C: Crystal Structure Communications* **1989,** *45* (6), 872-876.

109. Tsuboyama, S.; Tsuboyama, K.; Sakurai, T., Structure of $[Co(C_4H_5NO_4)(C_{16}H_{36}N_4)]ClO_4.2.5H_2O$.Corrigendum. *Acta Crystallographica Section C: Crystal Structure Communications* **1990,** *46* (4), 727-727.

110. Freeman, H. C.; Marzilli, L. G.; Maxwell, I. E., Crystal structure and absolute configuration of D- beta 2-(SSS)-(triethylenetetramine-(S)-prolinato) cobalt (III) tetrachlorozincate. *Inorganic Chemistry* **1970,** *9* (11), 2408-2415.

111. Muir, M. M.; Muir, J. A.; Saez, R.; Campana, C. F., Complexes with asymmetric tetraamine ligands. IV. Cobalt (III) complexes containing two chiral ligands. Structure of Λ-cis-β2-(SS)-[S-alaninato-2S, 5R, 9S-trimethyltriencobalt (III)] perchlorate hydrate. *Inorganica Chimica Acta* **1988,** *141* (1), 75-81.

112. Tashiro, S.; Ogura, Y.; Tsuboyama, S.; Tsuboyama, K.; Shionoya, M., Chiral recognition of α-Amino acids by an optically active (2s, 5s, 8s, 11s)-2, 5, 8, 11-tetraethyl cyclen Cobalt (III) complex. *Inorganic chemistry* **2010,** *50* (1), 4-6.

113. Muir, J. A.; Muir, M. M.; Saez, R.; Campana, C., Structure of a cobalt (III) complex with two opically active ligands. *Acta Crystallographica Section C: Crystal Structure Communications* **1987,** *43* (8), 1487-1490.

114. Cai, J.; Hu, X.; Feng, X.; Ji, L.; Bernal, I., Structures of three cis-β1 and three cis-β2 isomers of [Co (trien)(aminoacidato)]$^{2+}$ complexes. *Acta Crystallographica Section B: Structural Science* **2001,** *57* (1), 45-53.

115. Da Pieve, C.; Spingler, B., Nickel and cobalt complexes of 15, 15-disubstituted 1, 4, 7, 10, 13-pentaazacyclohexadecane-14, 16-dione ligands. *Inorganica Chimica Acta* **2012,** *380*, 230-235.

116. Buckingham, D. A.; Clark, C. R.; Rogers, A. J.; Simpson, J., The Synthesis, Separation and Structures of Three [Co (cyclen)((S)-AlaO)] $^{2+}$ Isomers. The Alkaline Hydrolysis of [Co (cyclen)((S)-AlaO)] $^{2+}$. *Australian Journal of Chemistry* **1998,** *51* (6), 461-470.

117. Anderson, B.; Bell, J.; Buckingham, D.; Cresswell, P.; Gainsford, G.; Marzilli, L.; Robertson, G.; Sargeson, A., Structures, chemistry, and relative energies of the [Co (trien)(glyO)]$^{2+}$ ions. 3 alpha -(RR, SS)-[Co (trien)(glyO)]$^{2+}$ and alpha -(RR, SS)-[Co (trien)(glyOEt) Cl]$^{2+}$ ions. *Inorganic Chemistry* **1977,** *16* (12), 3233-3244.

118. Chang, J. Y.-C.; Stevenson, R. J.; Lu, G.-L.; Brothers, P. J.; Clark, G. R.; Denny, W. A.; Ware, D. C., Syntheses of 8-quinolinolatocobalt (III) complexes containing cyclen based auxiliary ligands as models for hypoxia-activated prodrugs. *Dalton Transactions* **2010,** *39* (48), 11535-11550.

119. Hu, X.; Cai, J.; Chen, C.; Chen, X.-M.; Ji, L.-N., Conglomerate crystallization behavior of racemic [Co (N_4)(aminoacidato)]$^{2+}$ complexes. *Crystal Engineering* **2001,** *4* (2-3), 141-157.

120. Eduok, E. E.; Kashyap, R. P.; Nagl, A.; Bourne, S. A.; Watson, W. H., Amino acid complexes of [Co (III)(trien)]$^{+}$ [3]. *Journal of Chemical Crystallography* **1994,** *24* (9), 627-638.

121. Buckingham, D. A.; Clark, C. R.; Rogers, A. J.; Simpson, J., Synthesis and structures of five [Co (Mecyclen)(S-AlaO)]$^{2+}$ isomers: use of nOe and COSY ^{1}H NMR spectroscopy for structural assignment in solution. *Inorganic Chemistry* **1995,** *34* (14), 3646-3657.

122. Clarkson, A. J.; Blackman, A. G., Synthesis and Co (III) complexes of the new tetradentate mixed-donor tetraamine ligand N-{2-[(2-pyridin-2-ylethyl) amino] ethyl} ethane-1, 2-diamine (peda). *Polyhedron* **2006,** *25* (2), 373-378.

123. Bou-Moreno, R.; Cotton, S. A.; Hunter, V.; Leonard, K.; Platt, A. W.; Raithby, P. R.; Schiffers, S., Systematic structural studies on cobalt (II) complexes of tricyclohexylphosphine oxide and related ligands. *Polyhedron* **2011,** *30* (17), 2832-2836.

124. McClintock, L. F.; Cavigliasso, G.; Stranger, R.; Blackman, A. G., The donor ability of the chelated carbonate ligand: protonation and metallation of $[(L)Co(O_2CO)]^+$ complexes in aqueous solution. *Dalton Transactions* **2008,** (37), 4984-4992.

125. Schiff, H., Ann. 1864, 131, 118.(b) Layer, RW. *Chem. ReV* **1963,** *63*, 489-510.

126. Engelhardt, L.; Gainsford, A.; Gainsford, G.; Golding, B.; MacB, J., Harrowfield, AJ Herlt, AM Sargeson and AH White. *Inorg. Chem* **1988,** *27*, 4551.

Chapter 3. Polydentate Amino Acid Complexes of Cobalt(III)

3.1 Introduction

Reductive amination is a synthetic procedure employed in the conversion of aldehydes and ketones into primary (1°), secondary (2°), and tertiary amines (3°). The reaction takes place in two parts: nucleophilic addition of the carbonyl function to a nitrogen reactant to form an imine and the reduction of the imine to an amine using a reducing agent.

Chapter 2 of this thesis has dealt with the synthesis, isolation and characterisation of various phosphonate imine complexes of cobalt(III) (*e.g* **2** in Fig. 3.1), as analogues of carboxylate imines. This chapter shall report on the reduction of those imine complexes as well as some carboxylate systems already known in the literature[39, 52] to yield amine complexes similar to **3** in Fig. 3.1.

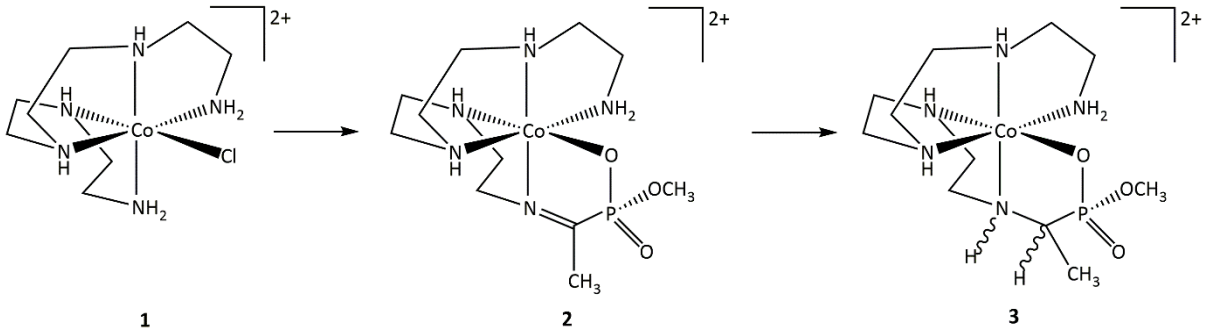

Figure 3.1 The condensation/reduction scheme to yield an amine complex.

The reducing agent used in this project was sodium borohydride ($NaBH_4$). The reduction of the imine has been reported to be achieved through hydride attack on the α-carbon atom, with protonation of the amine.[52, 57] This hydride attack can occur on either one of the two faces of the imine (Fig. 3.2) and the face chosen determines the configuration at the α-carbon atom[39, 52]. Protonation of the nitrogen atom can also occur on either face of the imine.

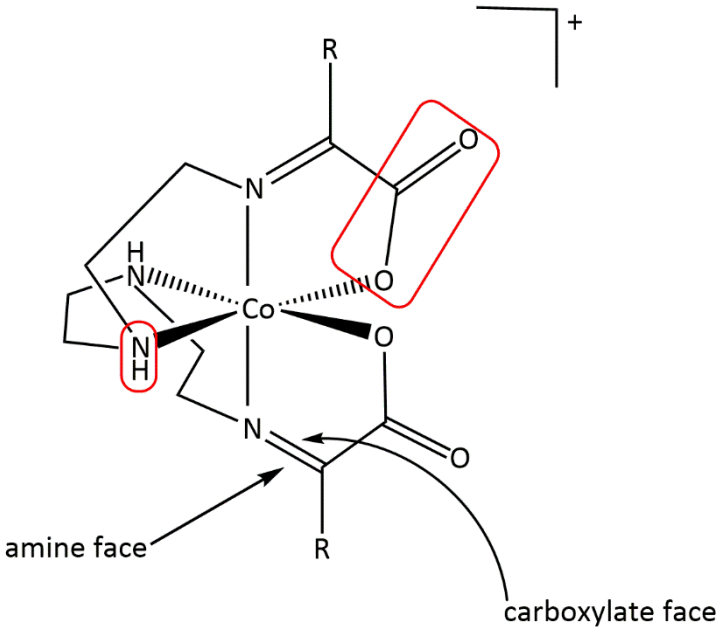

Figure 3.2 An illustration of the faces of the imine[39, 52]

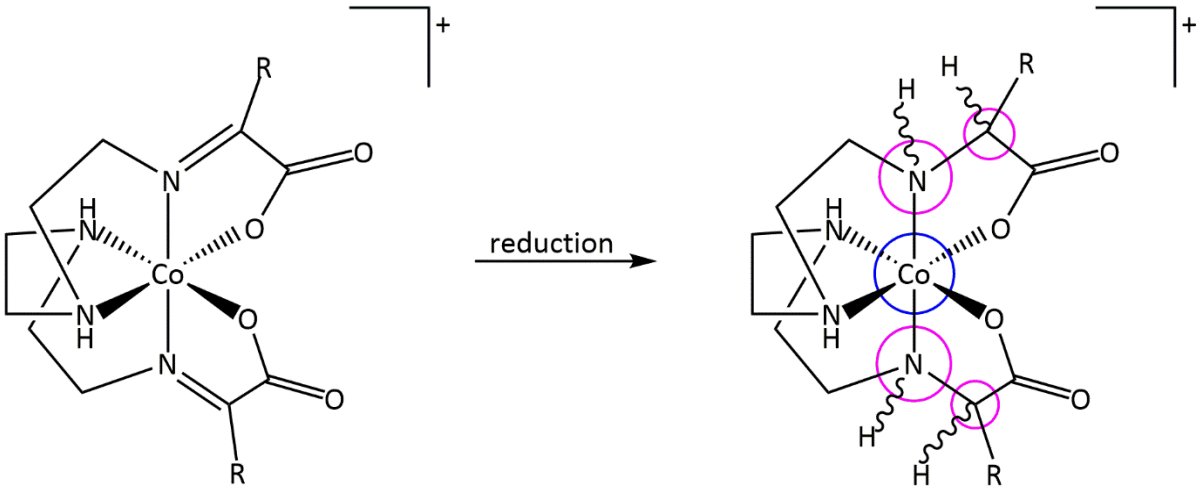

Figure 3.3 The new stereogenic centres (highlighted in purple) created by the reduction of a carboxylate system[39]

It is known that the maximum number of stereoisomers that a molecule can have is 2^n, where n is the number of chiral centres. So, for the complex shown as the product of the reduction reaction schematised in Fig. 3.3, a total number of 32 stereoisomers are expected from five chiral centres illustrated, but if there are meso isomers, the number would be less. The new stereogenic centres have been highlighted in purple.

For carboxylate systems prepared from symmetrical polyamines like (N′-[2-(2-aminoethylamino)ethyl]ethane-1,2-diamine): trien, if the C_2 axis of rotation is retained in the product molecule, the number of NMR signals observable from the mixture would be limited.[39, 52] However, for the phosphonate analogues also made from the trien polyamine, greater complexity is expected to be generated from the stereogenic phosphorus centre as shown in Fig. 3.4.

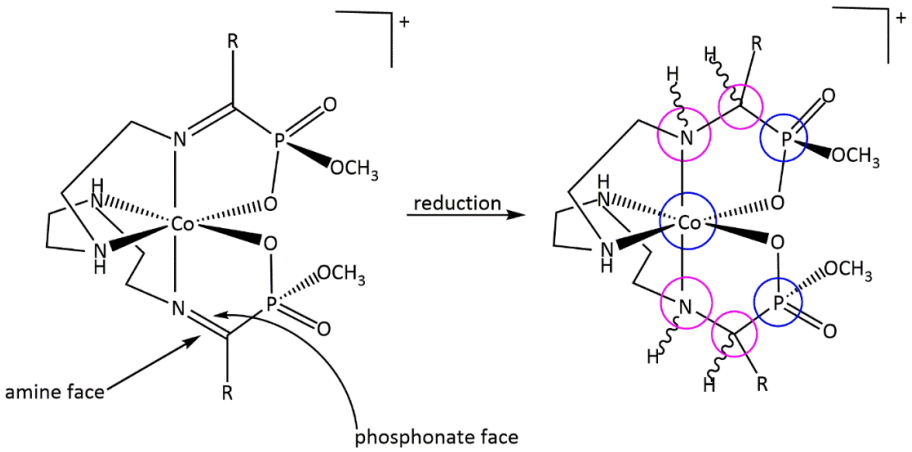

Figure 3.4 An illustration of the faces of the lower imine using a phosphonate system; new stereogenic centres following the reduction are highlighted in purple.

Considering the new stereogenic centres (Fig. 3.4) introduced by the reduction of the di-imine, 128 (2^7) stereoisomers are not expected due to the presence of the C_2 rotation axis which renders some combinations of absolute configuration equivalent (as shall be explained later). However, these phosphonate analogues are predicted to present more complicated systems than those from the carboxylates due to the additional phosphorus chiral centres in each molecule. Four more stereoisomers should be expected from the phosphonate systems considering the additional two stereogenic centres. Thus, two more pairs of diastereoisomers would be expected to be seen in the NMR spectra of these complexes.

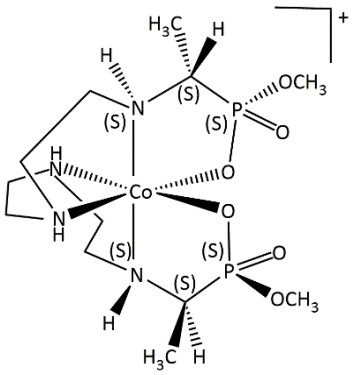

Δ*SSSSSS*

Figure 3.5 The Δ*SSSSSS* diastereoisomer of a trien polyamine system with phosphonates. The stereochemistry around the metal centre is Δ. The top half of the molecule has the stereochemistry S, S and S around the phosphorus, α-carbon atom and amine centres respectively. The lower half of the molecule is similar to the top half by the presence of the C_2 axis of rotation.

One of the diastereoisomers that could be formed from the imine reduction of a trien phosphonate system has been shown in Fig. 3.5. If chirality at the P centres is kept constant, and if epimerisation of the amine at the top half of the molecule and a C_2 rotation were performed, the molecules in Fig. 3.6 would be expected.[39, 52] However, if the original molecule (**1**) had the amine proton on the bottom half of the molecule inverted, the same molecule is obtained (**3**) as shown in Fig. 3.6 where the configuration is Δ*SSSSSR*.

It is true that some combinations of absolute configuration from a system containing molecules such as that shown in Fig. 3.5, will be equivalent owing to the limitation placed on the formation of all the possible diastereoisomers by the presence of a C_2 axis in some of the molecules in a given mixture[39, 52].

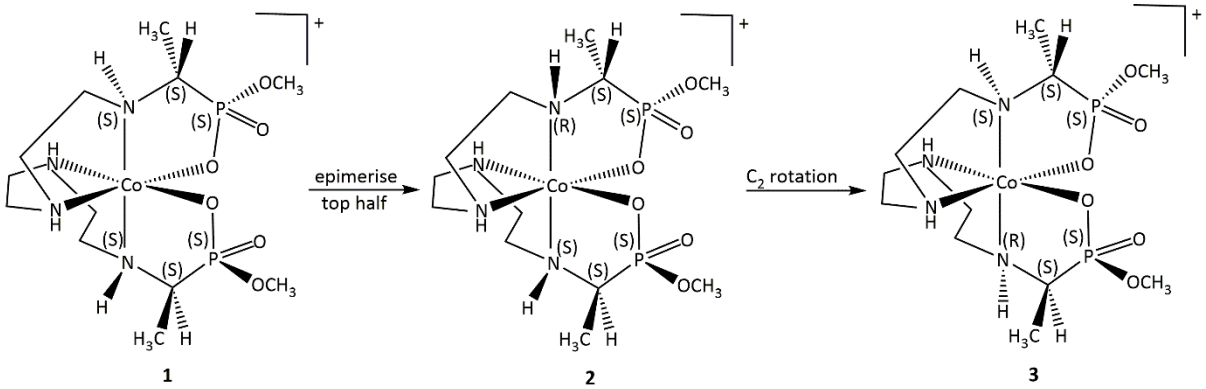

Δ*SSSSSS* Δ*SSRSSS* Δ*SSSSSR*

Figure 3.6 N-H epimerisation and rotation of the molecule[39, 52]

This idea has been extrapolated to the phosphonate systems. If the initial polydentate wrapping around the metal centre and the configurations at the phosphorus centres are retained, twenty stereoisomers (ten diastereoisomers) could therefore be formed from the reduction reaction of the trien systems[39, 52]. The ten diastereoisomers have been schematised in Fig. 3.7. The remaining ten diastereoisomers are each an enantiomer of one of these shown. Two more pairs of diastereoisomers would be expected from each of the ten diastereoisomers shown, if the presence of the two phosphorus centres in each molecule is considered.

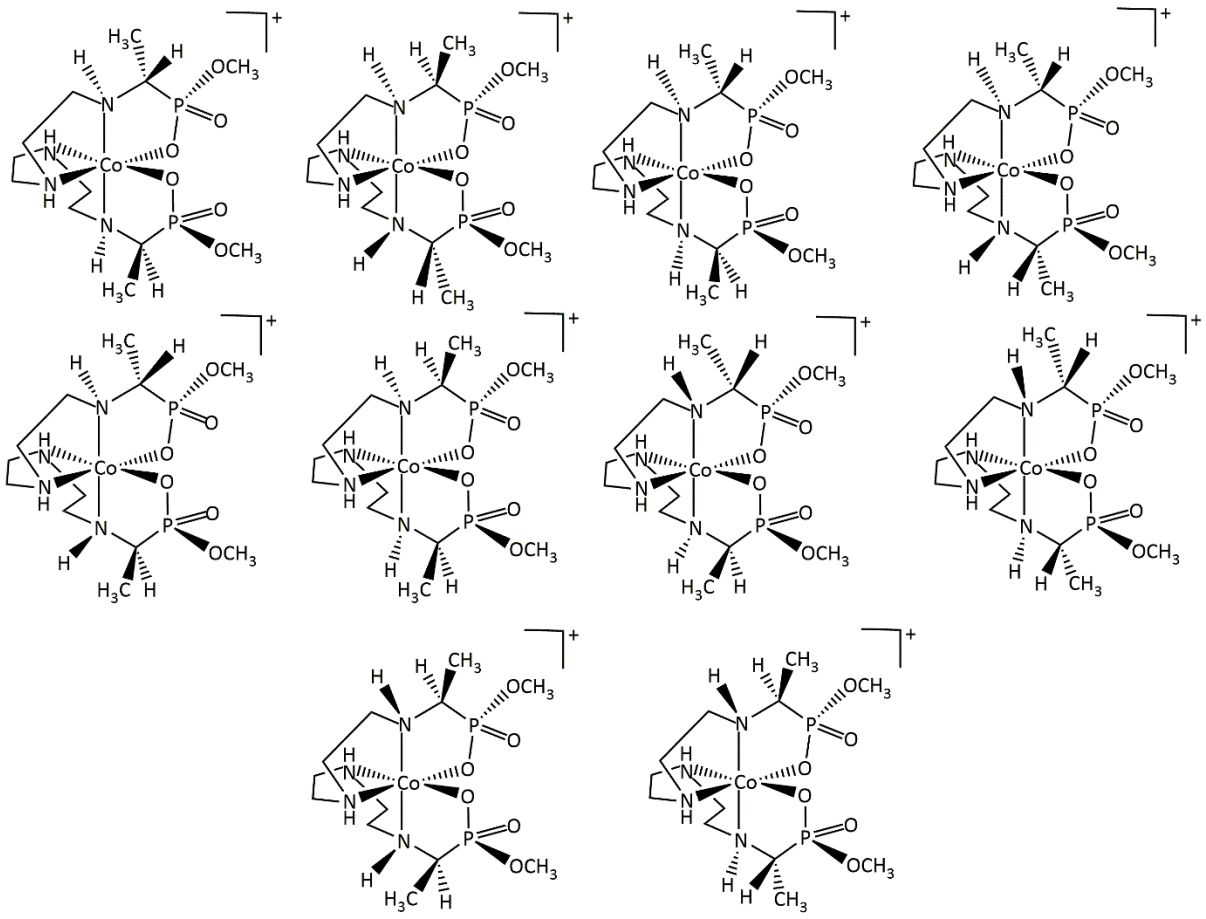

Figure 3.7 Diastereoisomers predicted from the reduction reaction of the trien systems with phosphonates with chirality at the P centres kept constant.

For systems generated from ethane-1,2-diamine (en), diastereoisomeric possibilities analogous to that outlined for the trien systems, are forecasted on the assumption that the donor atoms in the imines retain their positions after the reduction reaction. It has been demonstrated that the backbone does isomerise under some conditions. However, compounds made from (N′-[2-[2-(2-aminoethylamino)ethylamino]ethyl]ethane-1,2-diamine); (tetraen) as in Fig. 3.8, are

predicted to behave differently because of the absence of a C_2 axis in their molecules. At first the tetraen amines may be expected to be more complicated from the lack of a C_2 rotation axis on each molecule but those systems have fewer stereogenic centres, especially considering the ones created from the borohydride reduction. Ordinarily, 2^2 stereoisomers (or 2 diastereoisomers) are expected to form, only with respect to the newly created stereogenic centres. That is on the assumption that already existing stereogenic centres (cobalt(III), meridional secondary amine and phosphorus) would retain their configurations in the new molecules formed.

It has been reported[55, 57] that the process by which borohydride adds hydrogen to a double bond leads to the addition of dihydrogen in an *anti*-arrangement. This mechanism therefore relates the stereochemistry introduced at the reduced imine nitrogen to that of the adjacent α-carbon atom. However, epimerisation of the hydrogen on the meridional nitrogen atom cannot be excluded given that the reduction reaction is performed in a carbonate buffer[55]. It has been demonstrated[39, 52] that said epimerisation does not affect the isomer ratio observed after the reduction reaction. Thus, if the meridional nitrogen atom retains its original configuration (*anti* to the carboxylate group) and if the stereogenicity of the amine adjacent to the α-carbon atom is correlated to that nitrogen's stereogenicity, then only two diastereoisomers should form from the (N′-[2-[2-(2-aminoethylamino)ethylamino]ethyl]ethane-1,2-diamine) - tetraen systems (Fig. 3.8). However, more than two diastereoisomers have been observed in previous studies[39, 55] from these systems, where the minor isomers were as a result of epimerisation of the meridional N's proton.

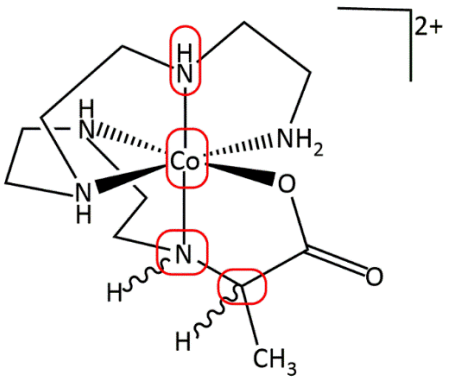

Figure 3.8 A tetraen polyamine system. Stereogenic centres where different configurations are possible have been highlighted red[39].

Previous studies[39, 52, 57] done with a range of imine-acidato ligands demonstrated the selectivity of the hydride attack. The borohydride attack occurred on the more hindered face (the amine face as in Fig. 3.9; same as Fig. 3.2) of the imine-acidato ligands.

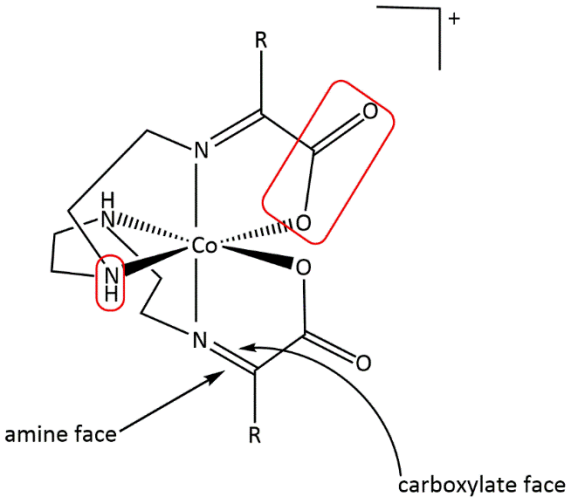

Figure 3.9 Illustrating faces of the imine using a carboxylate complex

Work done[50] with α-amino acid complexes of the type $[Co(en)_2(amino\ acid)]^{2+}$ using various hydride reagents also gave evidence of the facial selectivity. A di-hydrogen bonding interaction occurring between the amine proton of the polyamine backbone adjacent to the imine and a hydride on the borohydride anion was therefore postulated[39] on the argument that the interaction would favour the preference for the amine face during the hydride delivery (Fig. 3.10).

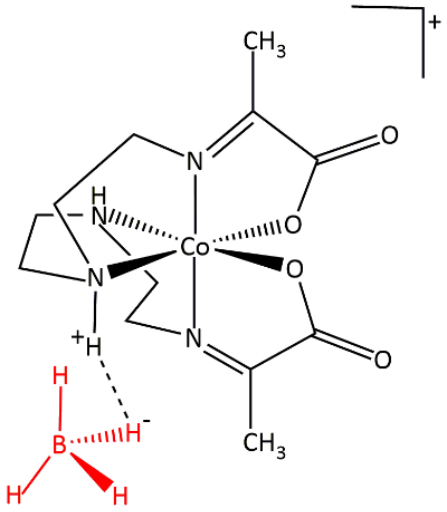

Figure 3.10 Schematic of hydride delivery as postulated by the Hartshorn group[39]. Red highlight shows the BH_4.

On the other hand, the delivery of the hydride occurring from the carbonyl face (Fig. 3.11) may be hindered by the electrostatic repulsion between the two δ^- fragments[39]

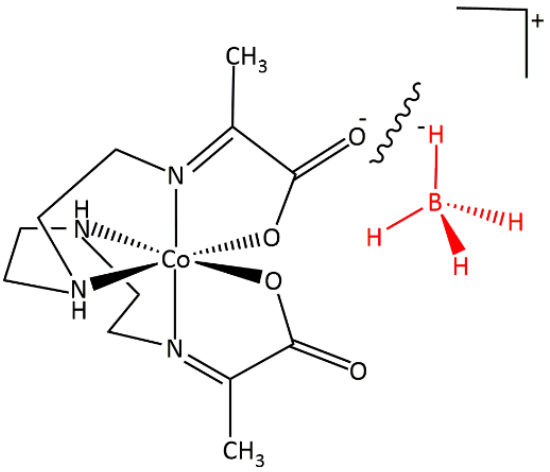

Figure 3.11 Schematic of the repulsion during hydride delivery from the carbonyl face[39].

X-ray crystallographic characterisation of some isolated products supported the hypothesis[39]. The structural solutions showed that the proton of each of the α-carbon atoms of the major isomer and the next most common one was placed on the amine face of the meridional ligand fragments. NMR results from previous research in the Hartshorn group[39, 52, 55] have shown that while only a few of the possible stereoisomers are formed in a remarkable yield in a given mixture, the symmetrical isomer (and its enantiomer) where the protons located on the two α-carbon atoms were located on the amine face of the meridional ligand fragment dominates the isomer mixture.

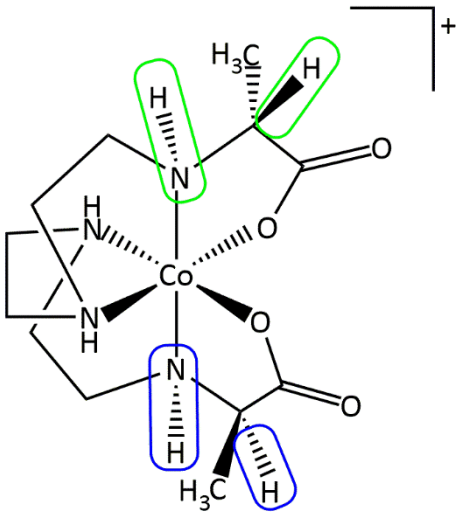

Figure 3.12 Schematic of the *anti*-configuration (green) and the *syn* configuration (blue) of protons using a trien carboxylate system

The asymmetric molecules are expected to be part of the minor isomers in the mixture. An asymmetric molecule (as in Fig. 3.12) was isolated from previous research[39] as one of the minor isomers. NMR spectra from the asymmetric molecules should have more resonance peaks than for those of the symmetrical molecules.

Phosphonate systems have been used in the current research as analogues of the carboxylates already studied in the literature[39, 55, 57]. Both phosphonate and carboxylate imine complexes of cobalt(III) have been converted to their amines through borohydride reduction in this project. Their syntheses, isolation and characterisation are reported in this chapter.

3.2 Experimental

3.2.1 Materials and Methods

The imine complexes made in chapter 2 of this project were used here. The carboxylate complexes were prepared according to the literature method[39]. All reagents used were obtained from Sigma-Aldrich (Merck) and were used without further purification, unless otherwise stated. Sephadex SPC25 120 cation exchange resin and Dowex 50WX2 100-200 mesh were washed before use for chromatography. Column dimensions are given as height x diameter. A Büchi rotary evaporator equipped with a diaphragm vacuum pump and water bath was used to concentrate solutions under reduced pressure.

Single crystal X-ray data of **3.2b**, **3.5**, **3.6** and **3.6b** were obtained. A suitable crystal was selected and mounted on a nylon loop in perfluorinated PEG on a SuperNova, Dual, Cu at zero, Atlas diffractometer. The crystals were kept at 120 K during data collection. Determination, refinement of cell parameters and absorption corrections were made using CrysAlisPro.[100] Using Olex2[101], each structure was solved with the ShelXT[102] structure solution program using Intrinsic Phasing and refined with the ShelXL[103] program using Least Squares minimisation on wR_2.

Numerical face indexed absorption corrections were done on all structures unless otherwise stated.

All non-hydrogen atoms were refined anisotropically, except in some cases where disorder was modelled. Hydrogen atoms bonded to carbon atoms were added in calculated positions and refined using a riding model with fixed isotropic thermal parameters (applying a multiplier factor of 1.2 or 1.5 to that of the parent atom, for aromatic carbons and for all other carbons,

respectively). However, the positions of hydrogen atoms bonded to nitrogen and oxygen atoms were located in the residual electron density map, the distance to the parent atom fixed at 0.86 Å using DFIX and their thermal parameters fixed by a multiplier factor of 1.5 that of the parent atom. Methyl groups were refined as an idealised tetrahedron and were free to rotate.

Unit cell parameters and details of the data collection for each crystal structure included in this chapter are given in Appendix 3.

3.2.2 General Procedure for the Synthesis of the Amino Complexes of Cobalt(III)

The reduction reactions were carried out in a carbonate buffer solution. The buffer solution was prepared by dissolving Na_2CO_3 (5.0 g; 0.05 mmol) and $NaHCO_3$ (5.0 g; 0.05 mmol) in 500 mL of distilled water. The $ZnCl_4$ salt of the imine complex (0.06 – 0.5 g) was dissolved in 50 mL of the carbonate buffer solution and stirred. An excess of $NaBH_4$ (1g – 12.5 g) was added and the stirring continued for a further 10 mins. The amount of $NaBH_4$ used was determined by the reactivity of the reagent. The product mixture was adsorbed onto a buffer equilibrated Na^+-form Dowex 50WX2 column (10 x 10 cm) under vacuum. The sides of the column were rinsed with a copious amount of water and the entire column washed with 500 mL of distilled water to get rid of all traces of $NaBH_4$. The eluate at this stage was collected in a Buchner flask connected to the column and was disposed of properly. The column's tap and vacuum were kept closed while adding water. The column was thereafter first washed with 0.1 M HCl to elute any small cations present and then eluted with 6 M HCl. The eluate was taken to dryness on a rotary evaporator at 40°C, desalted and characterised.

3.2.3 Desalting Procedure

Desalting was achieved by dissolving the dried sample (0.04 g – 0.3 g) in 50 mL aliquots of methanol. Since NaCl is sparingly soluble in methanol, the product dissolves, leaving the salt on the walls of the flask. The 50 mL aliquot is filtered and evaporated and the process repeated with less amount of methanol each time until the solution appears to have little or no salt in it. The crude material obtained after this procedure is usually still contaminated with NaCl.

For some compounds, Sephadex G-10 and G-25 columns were used for desalting.

3.2.4 Measurements

NMR spectra were measured on an Agilent NMRS-400 spectrometer. ^{1}H, $^{13}C\{^{1}H\}$ and $^{31}P\{^{1}H\}$ NMR were recorded in deuterium oxide solution. Chemical shifts are reported in parts per million (ppm) from 3-(trimethylsilyl)propionic 2,2,3,3-d_4 acid, sodium salt (TSP) (^{1}H, ^{13}C δ 0 ppm) as an internal standard and from 10% H_3PO_4 (^{31}P, δ 0 ppm) as an external standard in ^{31}P NMR. Electronic spectra were recorded in water using CARY100Bio UV-Visible spectrophotometer from 200-800 nm at room temperature whereas mass spectrometry measurements were obtained using an UltiMate 3000 mass spectrometer. Elemental analyses were performed by the Campbell Microanalytical Laboratory (University of Otago, NZ).

3.2.5 Syntheses

Procedure 1

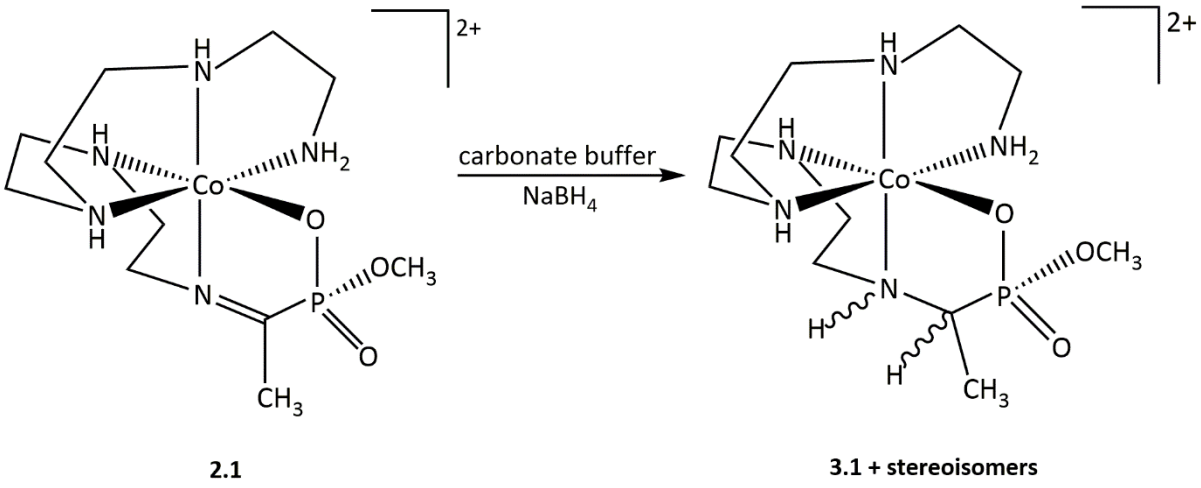

Figure 3.13 Reaction scheme for procedure 1

The orange $ZnCl_4$ salt of compound **2.1** (Δ*mffm*$_a$(*R*)) (0.06 g; 0.10 mmol) was dissolved in 50 mL of a carbonate buffer solution (5.0 g; 0.05 mmol of Na_2CO_3 and 5.0 g; 0.05 mmol of $NaHCO_3$ in 500 mL of H_2O) and stirred. Excess $NaBH_4$ (1 g; 30 mmol) was added and stirring continued for a further 10 mins. The slightly darker orange solution was adsorbed onto a buffer equilibrated Na^+-form Dowex (50WX2) column (10 x 10 cm) under vacuum. The sides of the column were rinsed with a copious amount of distilled water and the entire column washed with 500 mL of distilled water to get rid of all traces of $NaBH_4$. A clear eluate was collected at this stage in a Buchner flask connected to the column and was neutralised with some acid before being disposed of. The column tap and vacuum are kept closed while adding water. The

column is then first washed with 0.1 M HCl to elute any small cations present and then eluted with 6 M HCl. The eluant was taken to dryness on a rotary evaporator at 40°C, desalted and characterised.

^{1}H NMR (ppm): 1.57 – 1.68 (C**H**$_3$, multiplet of overlapping doublets), 2.45 – 2.58 (C**H**$_2$-NH, m), 2.62 - 2.77 (CH$_2$-CH$_2$-NH, m), 2.94 - 3.05 (C**H**$_2$-NH, m), 3.14 - 3.19 (C**H**$_2$-NH-CH$_2$, m), 3.46 – 3.53 (CH$_2$-NH-C**H**$_2$, m), 3.60 - 3.68 (C**H**$_2$-NH$_2$, m), 3.72 - 3.82 (OC**H**$_3$, overlapping doublets), 3.78 (OC**H**$_3$, d, $^{3}J^{HP}$ = 12 Hz); ^{31}P{^{1}H} NMR (ppm): 39.29, 40.13, 40.31, 42.16 (in the ratio of 1:7:4:4 in reverse order).

Electronic spectrum λ_{max} 476.00 nm; ESIMS for $[C_{11}H_{29}N_5O_3PCo]^{2+}$: *m/z* = 184.5 ($[M]^{2+}$ 100%), 185.0 ($[M]^{2+}$ 15%), 185.5 ($[M]^{2+}$ 2%).

Procedure 2

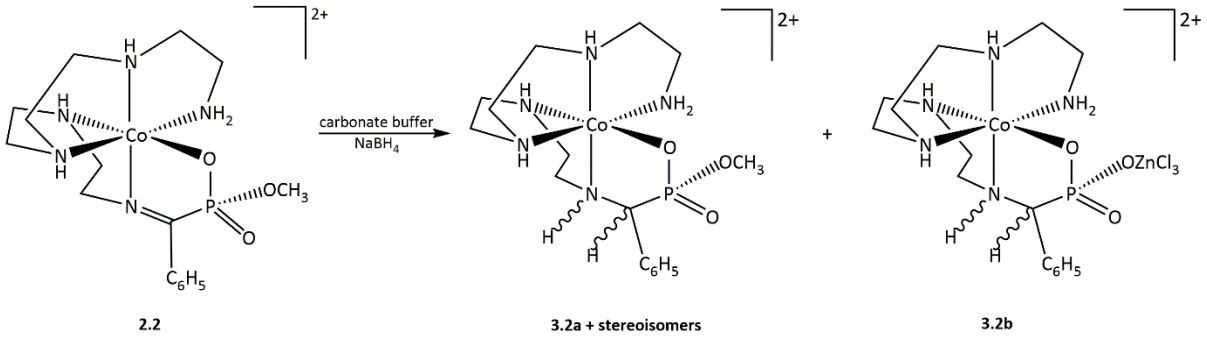

Figure 3.14 Reaction scheme for procedure 2

The orange $ZnCl_4$ salt of compound **2.2** (Δ*mffm*$_a$(*R*)) (0.50 g; 0.8 mmol) was dissolved in 50 mL of a carbonate buffer solution (5.0 g; 0.05 mmol of Na_2CO_3 and 5.0 g; 0.05 mmol of $NaHCO_3$ in 500 mL of H_2O) and stirred. Excess $NaBH_4$ (0.5 g; 15 mmol) was added and stirring continued for a further 10 mins. The red solution was adsorbed onto a buffer equilibrated Na^+-form Dowex (50WX2) column (10 x 10 cm) under suction. The sides of the column were rinsed with a copious amount of distilled water and the entire column washed with 500 mL of distilled water to get rid of all traces of $NaBH_4$. A clear eluate was collected at this stage in a Buchner flask connected to the column and neutralised with some acid before

being disposed of. The column tap and vacuum are kept closed while adding water. The column is then first washed with 0.1 M HCl to elute any small cations present and then eluted with

0.25 M – 3.0 M HCl. The eluant was taken to dryness on a rotary evaporator at 40°C, desalted and characterised. The desalted and characterised product mixture was re-dissolved in distilled water to give a purplish-red solution which was adsorbed onto a clean Sephadex SPC25 column to attempt separation with another salt solution. 0.05 M Na_2HPO_4 solution was used to elute two distinct bands. Eluates from these bands were desalted according to the desalting procedure and characterised. NMR showed both bands were still mixtures. The major mixture is reported below.

^{1}H NMR (ppm): 2.50 - 2.57 and 2.78 – 2.83 (C**H**$_2$-NH, m), 2.59 - 2.72 (C**H**$_2$-CH_2-NH, m), 2.92 – 3.09 (C**H**$_2$-NH, m), 3.17 - 3.34 (m, C**H**$_2$-NH-CH_2 and CH_2-NH-C**H**$_2$), 3.41 - 3.57 (C**H**$_2$-NH_2, m), 3.68 - 3.76 (OC**H**$_3$, overlapping doublets), 4.08 (OC**H**$_3$, d, $^3J^{HP}$ = 16 Hz), 7.47 - 7.52 (C_6**H**$_5$, m), 7.61 (C_6**H**$_5$, d, $^3J^{HH}$ = 8 Hz), 7.66 (C_6**H**$_5$, d, $^3J^{HH}$ = 4 Hz); ^{31}P{^{1}H} NMR (ppm): 29.93, 29.98, 30.51 (in the ratio of 1:0.91:0.18 in reverse order).

Electronic spectrum λ_{max} 497.36 nm; ESIMS for $[C_{16}H_{29}N_5O_3PCo]^{2+}$: Calculated *m/z* = 214.57 ($[M]^{2+}$ 100%), 215.07 ($[M]^{2+}$ 15%), 215.57 ($[M]^{2+}$ 2%). Found: *m/z* = 215.57 ($[M]^{2+}$ 100%), 216.07 ($[M]^{2+}$ 15%), 216.57 ($[M]^{2+}$ 2%) for $[C_{16}H_{29}N_5O_3PCo]^{2+}$ + 2H.

Crystals of **3.2b** were formed in an NMR tube and its mixture came from fraction 1 of a Sephadex G-25 column used for desalting the product mixture.

Crystal Data: $C_{30}H_{70}Cl_6Co_2N_{10}O_{13}P_2Zn_2$ (*M* =1302.20 g/mol): triclinic, space group P-1 (no. 2), *a* = 9.7293(4) Å, *b* = 9.8259(4) Å, *c* = 30.4424(17) Å, α = 94.625(4)°, β = 93.193(4)°, γ = 118.496(4)°, *V* = 2534.6(2) Å^3, *Z* = 2, *T* = 119.97(14) K, μ(CuKα) = 10.180 mm^{-1}, *Dcalc* = 1.706 g/cm^3, 9891 reflections measured (8.794° ≤ 2Θ ≤ 140.27°), 7385 unique (R_{int} = 0.0860, R_{sigma} = 0.0701) which were used in all calculations. The final R_1 was 0.1127 (I > 2σ(I)) and wR_2 was 0.3002 (all data).

Procedure 3

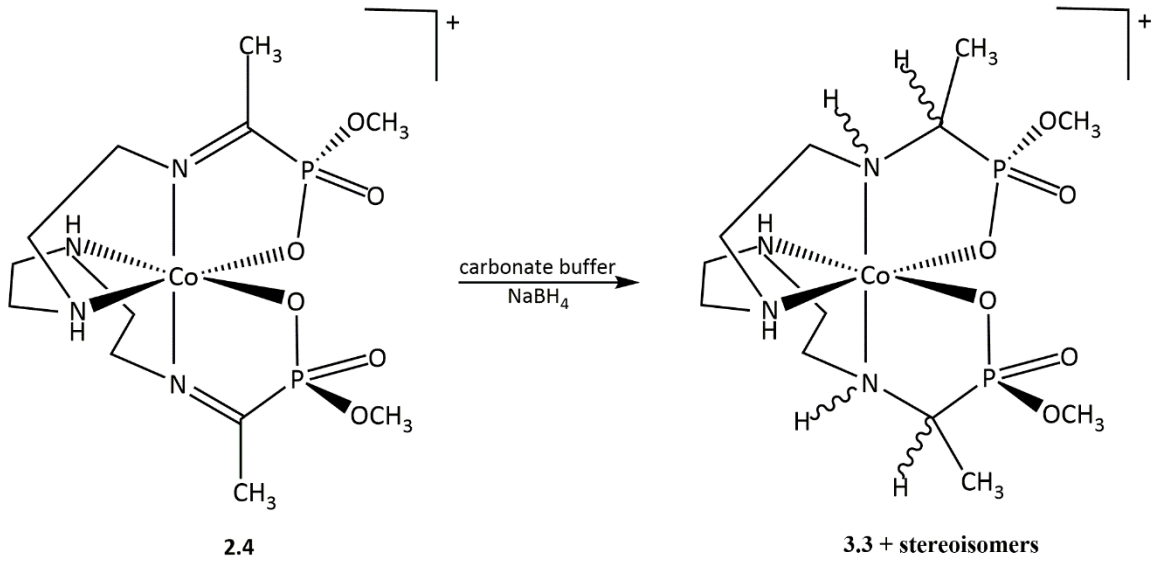

Figure 3.15 Reaction scheme for procedure 3

The red-orange $ZnCl_4$ salt of fraction 2 from procedure 3 in chapter 2 (0.50 g; 0.77 mmol) was dissolved in 50 mL of a carbonate buffer solution (5.0 g; 0.05 mmol of Na_2CO_3 and 5.0 g; 0.05 mmol of $NaHCO_3$ in 500 mL of H_2O) for 5 mins while stirring. Excess $NaBH_4$ (3.5 g; 90 mmol) was added and stirring continued for a further 10 mins. The purple solution was adsorbed onto a buffer equilibrated Na^+-form Dowex (50WX2) column (10 x 10 cm) under suction. The sides of the column were rinsed with a copious amount of distilled water and the entire column washed with 500 mL of distilled water to get rid of all traces of $NaBH_4$. A clear eluant was collected at this stage in a Buchner flask connected to the column and neutralised with some acid before being disposed of. The column tap and vacuum are kept closed while adding water. The column is then first washed with 0.1 M HCl to elute any small cations present and then eluted with 6 M HCl. The eluate was taken to dryness on a rotary evaporator at 40°C, desalted and characterised.

^{1}H NMR (ppm): 1.49 (C**H**$_3$, dd, $^3J^{HP}$ = 8 Hz (8 Hz)), 1.64 (C**H**$_3$, d, $^3J^{HP}$ = 8 Hz), 1.67 (C**H**$_3$, d, $^3J^{HP}$ = 8 Hz), 1.71 (C**H**$_3$, d, $^3J^{HP}$ = 8 Hz), 2.51 – 2.61 (C**H**$_2$-CH_2-NH, m), 3.00 – 3.12 and 3.21 – 3.28 (C**H**$_2$-NH, m), 3.42 – 3.60 (C**H**$_2$-NH, m), 3.62 - 3.67 (OC**H**$_3$, m) 3.68 (OC**H**$_3$, d, $^3J^{HP}$ = 12 Hz), 3.72 (OC**H**$_3$, d, $^3J^{HP}$ = 12 Hz); ^{31}P{^{1}H} NMR (ppm): 40.62, 40.70, 40.78, 41.81, 41.95 (in the ratio of 1:0.65:3:1:0.73 in reverse order).

Electronic spectrum λ_{max} 535.24 nm; ESIMS for $[C_{12}H_{30}N_4O_6P_2Co]^+$: *m/z* = 447.09 ($[M]^{1+}$ 100%), 448.09 ($[M]^{1+}$ 15%), 449.09 ($[M]^{1+}$ 2%).

Procedure 4

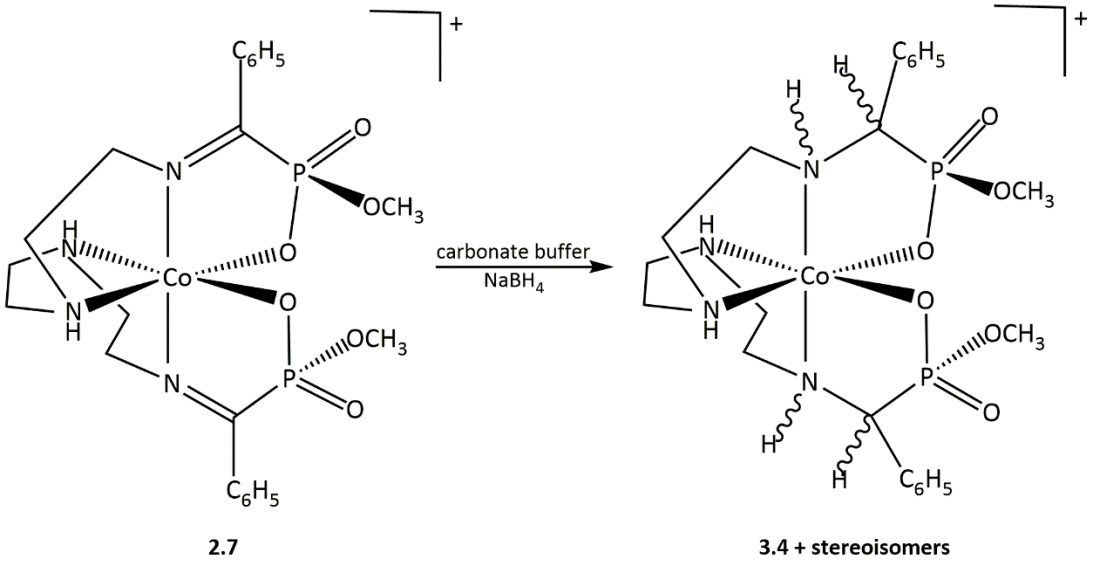

Figure 3.16 Reaction scheme for procedure 4

The red-orange $ZnCl_4$ salt of compound **2.7** (Δ*mffm*(*SR*)) (0.15 g; 0.2 mmol) was dissolved in 50 mL of a carbonate buffer solution (5.0 g; 0.05 mmol of Na_2CO_3 and 5.0 g; 0.05 mmol of $NaHCO_3$ in 500 mL of H_2O) and stirred. Excess $NaBH_4$ (1.2 g; 31.72 mmol) was added and stirring continued for a further 10 mins. The purple solution was adsorbed onto a buffer equilibrated Na^+-form Dowex (50WX2) column (10 x 10 cm) under suction. The sides of the column were rinsed with a copious amount of distilled water and the entire column washed with 500 mL of distilled water to get rid of all traces of $NaBH_4$. A clear eluate was collected at this stage in a Buchner flask connected to the column and neutralised with some acid before being disposed of. The column tap and vacuum were kept closed while adding water. The column was then first washed with 0.1 M HCl to elute any small cations present and then eluted with 0.5 – 3.0 M HCl. The eluate was taken to dryness on a rotary evaporator at 40°C, desalted and characterised. A dry sample of the mixture from this procedure was dissolved in 100 mL of distilled water and adsorbed onto a Sephadex SPC 25 column. The column was washed with 100 mL of distilled water and eluted with 0.05 M NaCl. Two bands eluted. The eluates were

taken to dryness on a rotary evaporator at 40°C, desalted and characterised. NMR showed the bands were still mixtures.

^{1}H NMR (ppm): 2.61 - 2.67 (C**H**$_2$-CH$_2$-NH, m), 3.21 - 3.31 (C**H**$_2$-NH, m), 3.28 (C**H**$_2$-NH, m), 3.44 (OC**H**$_3$, d, $^{3}J^{HP}$ = 12 Hz), 3.51 (OC**H**$_3$, d, $^{3}J^{HP}$ = 8 Hz), 3.53 (OC**H**$_3$, d, $^{3}J^{HP}$ = 8 Hz), 3.59 (OC**H**$_3$, d, $^{3}J^{HP}$ = 8 Hz), 4.82 (C**H**, d, $^{2}J^{HP}$ = 20 Hz), 4.89 (C**H**, d, $^{2}J^{HP}$ = 16 Hz), 7.57 - 7.63 (C$_6$**H**$_5$, m), 7.75 (C$_6$**H**$_5$, d, $^{3}J^{HH}$ = 8 Hz); ^{31}P{^{1}H} NMR (ppm): 34.85, 34.94, 35.33, 35.42 (in the ratio of 0.24:1:4.26:0.88 in reverse order).

Electronic spectrum λ_{max} 572.83 nm; ESIMS for $[C_{22}H_{34}N_4O_6P_2Co]^+$: *m/z* = 571.13 ($[M]^{1+}$ 100%), 572.13 ($[M]^{1+}$ 25%), 573.13 ($[M]^{1+}$ 5%).

Procedure 5

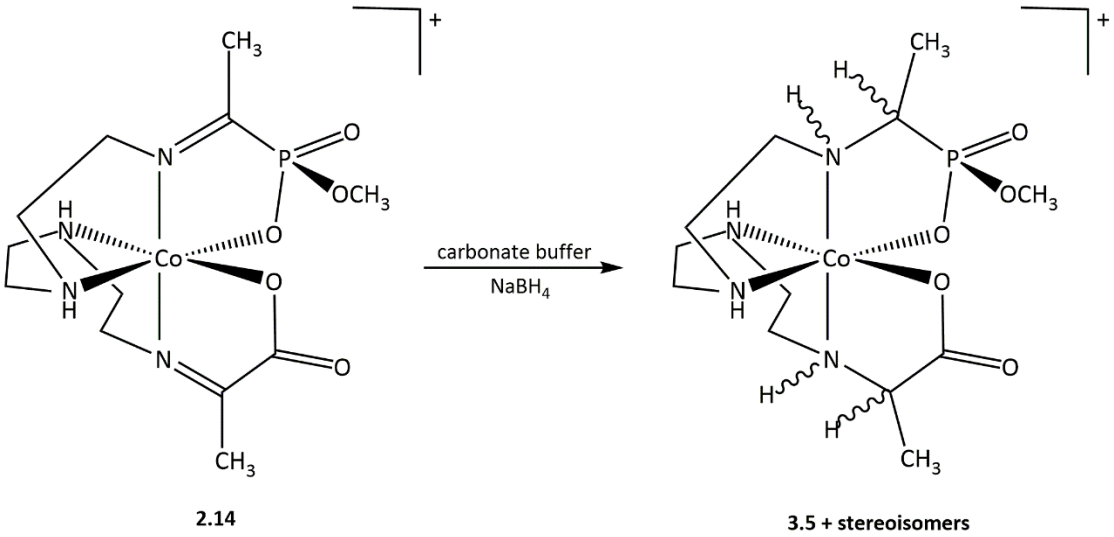

Figure 3.17 Reaction scheme for procedure 5

The red $ZnCl_4$ salt of compound **2.14** (Δ*mffm*(*R*)) (2.42 g; 4.03 mmol) was dissolved in 250 mL of a carbonate buffer solution (5.0 g: 0.05 mmol of Na_2CO_3 and 5.0 g; 0.05 mmol of $NaHCO_3$ in 500 mL of H_2O) and stirred. Excess $NaBH_4$ (12.5 g; 330 mmol) was added and stirring continued for a further 10 mins. The beetroot red solution was adsorbed onto a buffer equilibrated Na^+-form Dowex (50WX2) column (10 x 10 cm) under suction. The sides of the column were rinsed with a copious amount of distilled water and the entire column washed with 1 L of distilled water to get rid of all traces of $NaBH_4$. A clear eluate was collected at this stage in a Buchner flask connected to the column and neutralised with some acid before being

disposed of. The column tap and vacuum were kept closed while adding water. The column was then first washed with 0.1 M HCl to elute any small cations present and then eluted with 6 M HCl. The eluate was taken to dryness on a rotary evaporator at 40°C, desalted using a 0.45 µM sieve for the methanol (100 mL) solution and characterised. The sample was hygroscopic.

^{1}H NMR (ppm): 1.45 (C**H**$_3$, d, J = 4 Hz), 1.50 (C**H**$_3$, d, J = 8 Hz), 1.53 (C**H**$_3$, d, J = 8 Hz), 1.57 (C**H**$_3$, d, J = 8 Hz), 1.59 (C**H**$_3$, d, J = 8 Hz), 1.61 – 1.68 (C**H**$_3$, overlapping doublets), 1.70 (C**H**$_3$, d, J = 8 Hz), 2.41 – 2.46 (C**H**$_2$-CH$_2$-NH, m), 2.53 – 2.69 (C**H**$_2$-NH, m), 2.86 – 3.06 (C**H**$_2$-NH, m), 3.13 – 3.28 (C**H**$_2$-NH, m), 3.39 – 3.45 (C**H**$_2$-NH, m), 3.49 (OC**H**$_3$, d, $^{3}J^{HP}$ = 12 Hz), 3.53 (OC**H**$_3$, d, $^{3}J^{HP}$ = 12 Hz), 3.60 (OC**H**$_3$, d, $^{3}J^{HP}$ = 12 Hz), 3.68 – 3.71 (OC**H**$_3$, m), 3.73 (OC**H**$_3$, d, $^{3}J^{HP}$ = 12 Hz), 3.92 – 3.96 (C**H**, m), 4.08 – 4.15 (C**H**, m), 5.96 – 6.76 (N**H** broad, m), 7.12 – 7.62 (N**H**, broad, m); ^{31}P{^{1}H} NMR (ppm): 40.42, 40.55, 40.99, 41.49, 41.52, 42.22, 43.75 (in the ratio of 1:0.8:0.5:0.6:0.7:5.82:7.29 in reverse order).

Electronic spectrum λ_{max} 502.17 nm; ESIMS for $[C_{12}H_{27}N_4O_5PCo]^+$: *m/z* = 397.10 ($[M]^{1+}$ 100%), 398.10 ($[M]^{1+}$ 15%), 399.10 ($[M]^{1+}$ 2%).

Tiny red crystals of compound **3.5** formed in a flask holding the filtrate after trituration of a procedure 11 experiment in chapter 4 of this thesis. After filtration to recover the powdered product in chapter 4, it was noticed that the filtrate was intensely coloured. The dark red solution was safely stored pending characterisation. At the point of preparing a sample for characterisation of the filtrate, crystals were observed.

Crystal Data: $C_{14}H_{31}CoF_3N_4O_9PS$ (*M* =578.39 g/mol): orthorhombic, space group Pbca (no. 61), *a* = 15.9745(18) Å, *b* = 12.7365(8) Å, *c* = 22.7611(13) Å, *V* = 4631.0(7) Å^3, *Z* = 8, *T* = 120.00(10) K, µ(CuKα) = 8.024 mm^{-1}, *Dcalc* = 1.659 g/cm^3, 16933 reflections measured (7.768° ≤ 2Θ ≤ 152.362°), 4737 unique (R_{int} = 0.0897, R_{sigma} = 0.0755) which were used in all calculations. The final R_1 was 0.0995 (I > 2σ(I)) and wR_2 was 0.3252 (all data).

Procedure 6

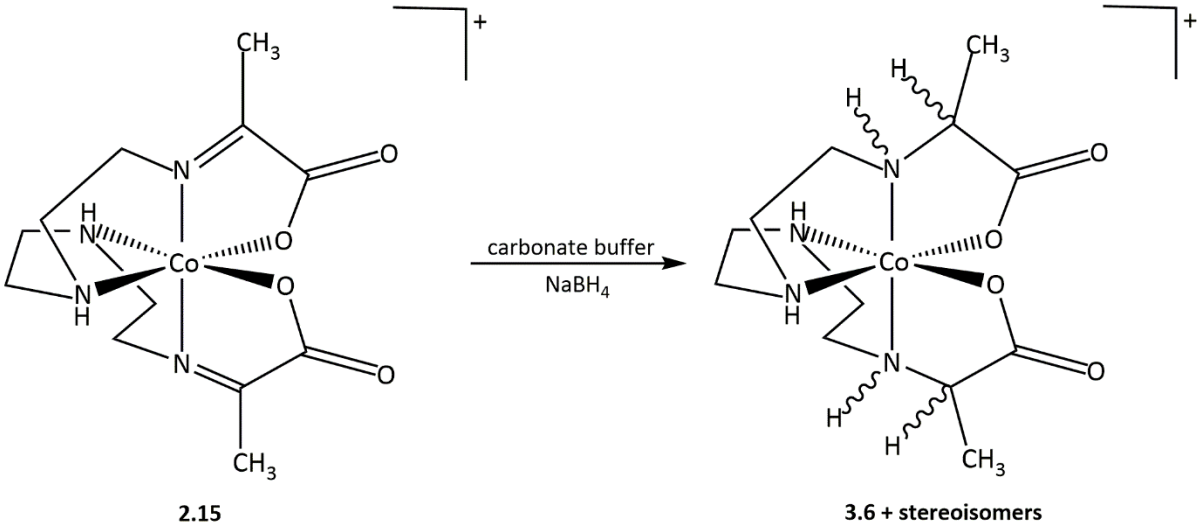

Figure 3.18 Reaction scheme for procedure 6

The orange $ZnCl_4$ salt of compound **2.15** (2.0 g; 3.63 mmol) was dissolved in 50 mL of a carbonate buffer solution (5.0 g; 0.05 mmol of Na_2CO_3 and 5.0 g; 0.05 mmol of $NaHCO_3$ in 500 mL of H_2O) and stirred. Excess $NaBH_4$ (5.0 g; 130 mmol) was added and stirring continued for a further 10 mins. The dark red solution was adsorbed onto a buffer equilibrated Na^+-form Dowex (50WX2) column (10 x 10 cm) under suction. The sides of the column were rinsed with a copious amount of distilled water and the entire column washed with 1 L of distilled water to get rid of all traces of $NaBH_4$. A clear eluate was collected at this stage in a Buchner flask connected to the column and neutralised with some acid before being disposed of. The column tap and vacuum were kept closed while adding water. The column was then first washed with 0.1 M HCl to elute any small cations present and then eluted with 6 M HCl. Some of the desired product eluted with the 0.1 M HCl wash but was kept aside. The 6 M HCl eluate was taken to dryness on a rotary evaporator at 40°C, desalted following the desalting procedure and characterised.

^{1}H NMR (ppm): 1.54 (C**H**$_3$, d, J^{HH} = 8 Hz), 1.59 (C**H**$_3$, d, J^{HH} = 8 Hz), 1.64 (C**H**$_3$, d, J^{HH} = 8 Hz), 2.45 (C**H**$_2$-NH, m), 2.68 (C**H**$_2$-NH, m), 2.79 – 2.91 (C**H**$_2$-CH_2-NH, m), 3.05 – 3.28 (CH_2-C**H**$_2$-NH, m), 3.41 (C**H**$_2$-NH, m), 3.56 (CH_2-C**H**$_2$-NH, m), 3.81 – 3.92 (C**H**, m), 4.00 - 4.12 (C**H**, m), 6. 00 (N**H**-CH_2, broad, m), 6.15- 6.22 (N**H**-CH_2, broad, m), 7.00 – 7.50 (N**H**, broad, m).

Electronic spectrum λ_{max} 488.07 nm; ESIMS for $[C_{12}H_{24}N_4O_4Co]^+$: *m/z* = 347.11 ($[M]^{1+}$ 100%), 348.11 ($[M]^{1+}$ 15%), 349.11 ($[M]^{1+}$ 2%).

Crystals of **3.6** formed in the product mixture at 18°C in a methanolic solution.

Crystal Data: $C_{12}H_{28}ClCoN_4O_6$ (*M* =418.76 g/mol): monoclinic, space group $P2_1/c$ (no. 14), *a* = 10.2796(3) Å, *b* = 12.7146(3) Å, *c* = 13.2413(4) Å, β = 96.262(3)°, *V* = 1720.33(8) Å^3, *Z* = 4, *T* = 120.02(10) K, μ(CuKα) = 9.592 mm^{-1}, *Dcalc* = 1.617 g/cm^3, 6274 reflections measured (8.654° ≤ 2Θ ≤ 152.634°), 3492 unique (R_{int} = 0.0357, R_{sigma} = 0.0470) which were used in all calculations. The final R_1 was 0.0359 (I > 2σ(I)) and wR_2 was 0.0960 (all data).

Crystals of **3.6b** formed as a salt of the triflate anion during the trituration stage of a chapter 4 procedure.

Crystal Data: $C_{26}H_{48}Co_2F_6N_8O_{14}S_2$ (*M* =992.70 g/mol): triclinic, space group $P\bar{1}$ (no. 2), *a* = 12.0378(5) Å, *b* = 12.8059(4) Å, *c* = 14.3205(5) Å, α = 101.598(3)°, β = 114.318(4)°, γ = 90.875(3)°, *V* = 1958.70(14) Å^3, *Z* = 2, *T* = 120.01(10) K, μ(CuKα) = 8.550 mm^{-1}, *Dcalc* = 1.683 g/cm^3, 15236 reflections measured (6.956° ≤ 2Θ ≤ 153.392°), 8015 unique (R_{int} = 0.0396, R_{sigma} = 0.0497) which were used in all calculations. The final R_1 was 0.0877 (I > 2σ(I)) and wR_2 was 0.2614 (all data).

Procedure 7

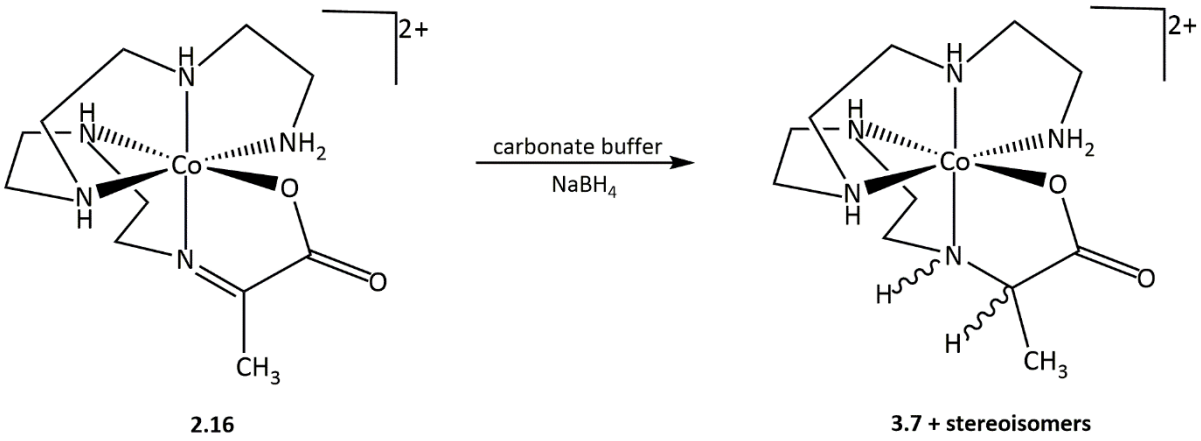

Figure 3.19 Reaction scheme for procedure 7

The orange chloride salt of compound **2.16** (1.18 g; 3.04 mmol) was dissolved in 200 mL of a carbonate buffer solution (5.0 g; 0.05 mmol of Na_2CO_3 and 5.0 g; 0.05 mmol of $NaHCO_3$ in

500 mL of H_2O) and stirred. Excess $NaBH_4$ (3.0 g; 79.28 mmol) was added and stirring continued for a further 10 mins. The red solution was adsorbed onto a buffer equilibrated Na^+-form Dowex (50WX2) column (10 x 10 cm) under vacuum. The sides of the column were rinsed with a copious amount of distilled water and the entire column washed with 1 L of distilled water to get rid of all traces of $NaBH_4$. A clear eluate was collected at this stage in a Buchner flask connected to the column and neutralised with some acid before being disposed of. The column tap and vacuum were kept closed while adding water. The column was then first washed with 0.1 M HCl to elute any small cations present and then eluted with 6 M HCl. The 6 M HCl eluate was taken to dryness on a rotary evaporator at 40°C, desalted following the desalting procedure and characterised.

^{1}H NMR (ppm): 1.54 (C**H**$_3$, d, J^{HH} = 8 Hz), 1.57 (C**H**$_3$, d, J^{HH} = 8 Hz), 2.53 – 2.58 (C**H**$_2$-NH, m), 2.75 – 2.80 (C**H**$_2$-NH, m), 2.88 – 2.98 (C**H**$_2$-CH_2-NH, m), 3.02 – 3.20 (C**H**$_2$-NH, m), 3.24 – 3.31 and 3.38 – 3.45 (C**H**$_2$-NH-CH_2, m), 3.46 – 3.55 (CH_2-NH-C**H**$_2$, m), 3.57 – 3.69 (C**H**$_2$-NH_2, m), 3.89 – 3.97 (C**H**, m), 5.85 – 6.22 (N**H**, m), 6.60 – 7.38 (N**H**, broad, m).

Electronic spectrum λ_{max} 485.73 nm; ESIMS for $[C_{11}H_{26}N_5O_2Co]^{2+}$: *m/z* = 159.57 ($[M]^{2+}$ 100%), 160.07 ($[M]^{2+}$ 40%), 160.57 ($[M]^{2+}$ 2%).

Procedure 8

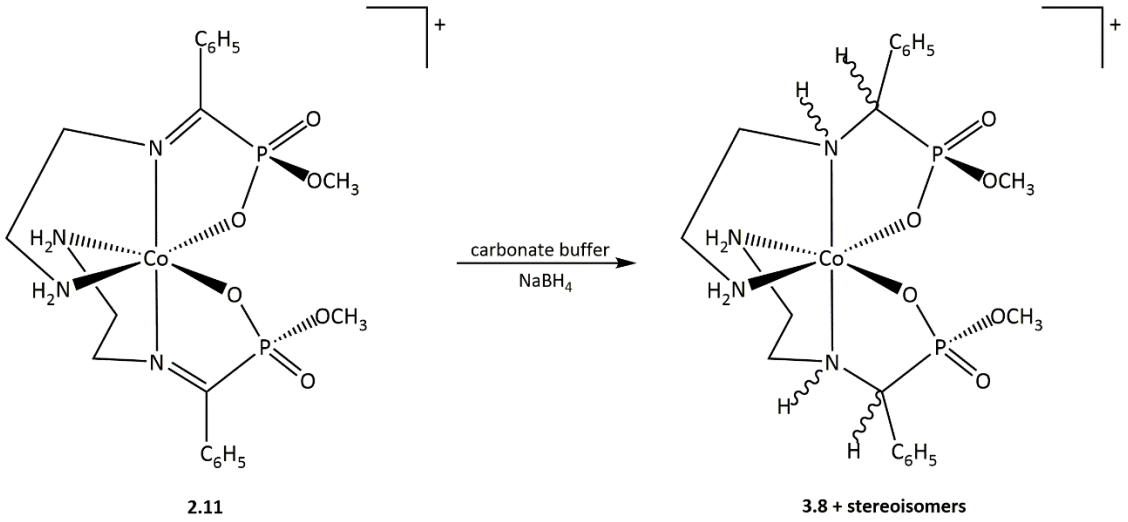

Figure 3.20 Reaction scheme for procedure 7

The red-orange $ZnCl_4$ salt of compound **2.11** (Λ*mffm*(*RR*)) (0.5 g; 0.67 mmol) was dissolved in 50 mL of a carbonate buffer solution (5.0 g; 0.05 mmol of Na_2CO_3 and 5.0 g; 0.05 mmol of $NaHCO_3$ in 500 mL of H_2O) and stirred. Excess $NaBH_4$ (2.0 g; 53 mmol) was added and

stirring continued for 2 mins only (a very reactive batch of $NaBH_4$ was used here). The purple solution was adsorbed onto a buffer equilibrated Na^+-form Dowex (50WX2) column (10 x 10 cm) under suction. The sides of the column were rinsed with a copious amount of distilled water and the entire column washed with 1 L of distilled water to get rid of all traces of $NaBH_4$. A clear eluate was collected at this stage in a Buchner flask connected to the column and neutralised with some acid before being disposed of. The column tap and vacuum were kept closed while adding water. The column was then first washed with 0.1 M HCl to elute any small cations present and then eluted with 5 M HCl. The 5 M HCl eluate was taken to dryness on a rotary evaporator at 40°C, desalted following the desalting procedure and characterised.

^{1}H NMR (ppm): 2.70 (C**H**$_2$-NH$_2$, broad), 2.88 – 3.04 (C**H**$_2$-NH$_2$, m), 3.28 – 3.38 (OC**H**$_3$, m), 3.43 (OC**H**$_3$, d, $^3J^{HP}$ = 12 Hz), 3.49 – 3.56 (OC**H**$_3$, m), 3.62 (OC**H**$_3$, d, $^3J^{HP}$ = 8 Hz), 4.37 – 4.43 (C**H**$_2$-NH, m), 7.52 -7.61 (C$_6$**H**$_5$, m), 7.73 (C$_6$**H**$_5$, m); ^{31}P{^{1}H} NMR (ppm): 36.52, 36.98, 37.38, 38.53.

Electronic spectrum λ_{max} 568.17 nm; ESIMS for $[C_{20}H_{32}N_4O_6P_2Co]^+$: *m/z* = 545.11 ($[M]^{1+}$ 100%), 546.11 ($[M]^{1+}$ 20%), 547.11 ($[M]^{1+}$ 2%)

3.3 Results and Discussion

3.3.1 Crystal Structure Determinations of the Amino Acid Complexes

All the X-ray structures described in this section have the Δ*mffm* configuration of the polydentate wrapping around the cobalt(III) metal centre, with the tetraen derivatives having an extra *a* descriptor to have the Δ*mffm*$_a$ configuration, where *a* represents the configuration (*anti*) of the hydrogen on the meridional nitrogen atom with respect to the rest of the polyamine fold (as have been described in section 1.2 of chapter 1). The Δ/Λ descriptors have been shown for the structures as well as their *R*/*S* ones.

Compound 3.2b

The crystal structure (Fig. 3.21) of the red plates of **3.2b** was solved in the triclinic space group P$\bar{1}$. The crystals formed in an NMR tube and the mixture came from fraction 1 of a Sephadex G-25 column used for desalting the product mixture. The structure has an $OZnCl_3$ in place of the methyl ester (methoxy) group.

The completeness (79%) of the data set used to solve for compound **3.2b** is lower than the acceptable standard. This was primarily because the data set was collected in a crystal system

with symmetry higher than actually was required for the structural solution. The structure has only been shown to model connectivity of the atoms in that molecule.

The structure of **3.2b** (Fig. 3.21) relates to that of compound **2.2** (Fig. 3.22) from which it was synthesised. Both structures have been solved in the triclinic space group P$\bar{1}$. Considering the enantiomer shown, the absolute configuration of $\Delta mffm_a(S)$ (where $\Delta mffm_a$ refers to the wrapping of the polyamine around the metal ion, including the orientation (*anti*) of the proton at the meridional nitrogen atom with respect to the fold, and *S* represents the chirality at the phosphorus centre) would have been retained after the reduction of **2.2** to give **3.2b** save for the replacement of the CH_3 group on O2 with $ZnCl_3$. The CIP based priority thus changes with O2 counted before O1 to give a ΔS configuration at the phosphorus stereogenic centre. The asymmetric unit (Fig. 3.23) contains both enantiomers ($\Delta mffm_a(S)$ and $\Lambda mffm_a(R)$). Table 3.1 shows some selected bond lengths between both compounds for comparison. The two molecules in the asymmetric unit are related to each other by a mirror plane. One of the molecules is shown in Fig. 3.21.

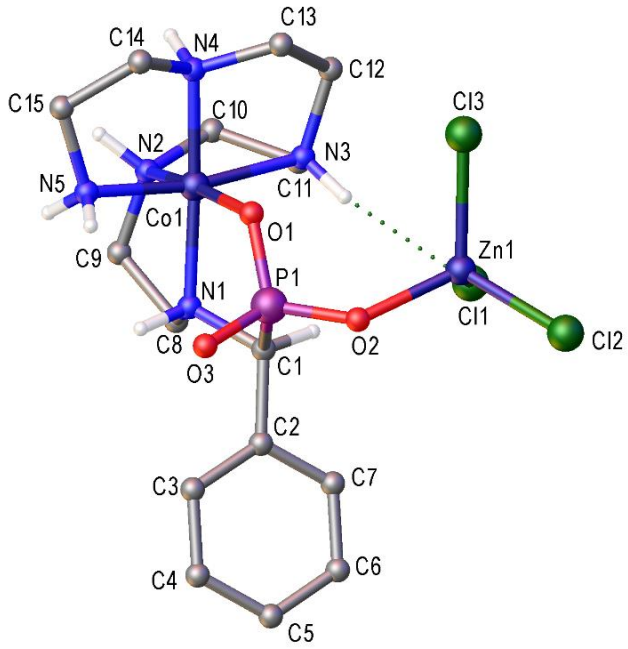

Figure 3.21 One of the molecules ($\Delta mffm_a(S)$) in the asymmetric unit of the structural solution for compound **3.2b**. Most hetero atoms have been omitted for clarity.

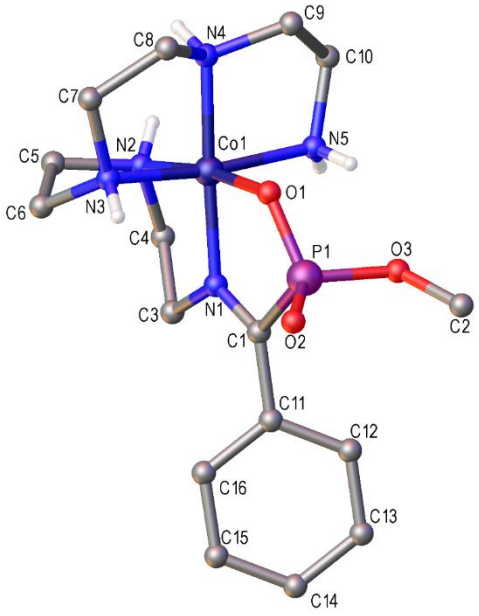

Figure 3.22 The crystal structure **2.2** (Δ*mffm*$_a$(*R*) diastereoisomer) from procedure 2. Non-hetero atoms and $ZnCl_4$ have been omitted for clarity.

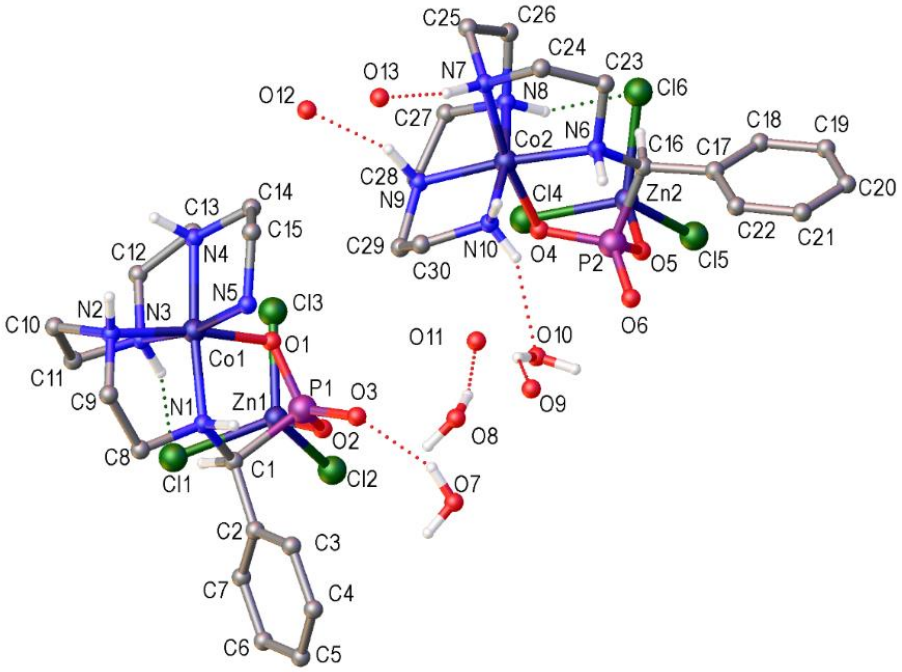

Figure 3.23 The asymmetric unit of the structural solution for a derivative of **3.2** from procedure 2. Most hydrogen atoms have been omitted for clarity.

Bond lengths (Å)	**3.2b** **$[C_{15}H_{28}N_5O_3PCoZnCl_3]$**	**2.2** **$[C_{16}H_{29}N_5O_3PCo]^{2+}$**
N-C	1.468 (15) – 1.546 (15)	1.284 (4) – 1.509 (4)
Co-O	1.938 (8) and 1.937 (8)	1.948 (2)
Co-N	1.942 (10) – 2.002 (11)	1.935 (3) – 1.972 (3)
P-O	1.498 (8) – 1.539 (7)	1.480 (2) – 1.579 (2)
P-C	1.843 (11) – 1.853 (12)	1.832 (4)

Table 3.1 Selected bond lengths from structural models

Nine resonance peaks are expected in the methylene region of the $^{13}C\{^1H\}$ spectrum from each molecule of compound **3.2b**, including the **C**H peak of the α-carbon atom. The $^{13}C\{^1H\}$ spectrum obtained from dissolving the crystals of this compound had nine major signals as well as some minor ones in the region. Two new peaks were found at 67 and 68 ppm respectively and both have been assigned to the **C**H of the α-carbon atom on each isomer. The number of minor lines in that region suggested there could be at least two pairs of diastereoisomers in the crystals' mixture.

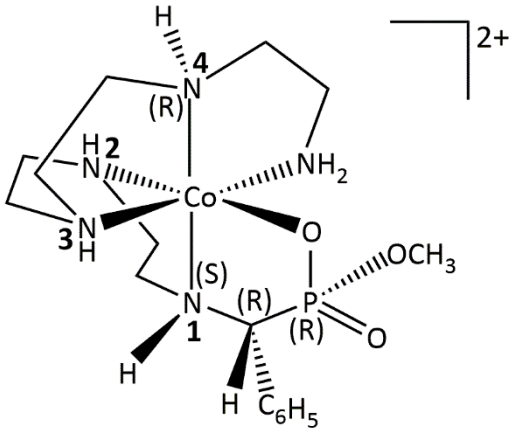

Figure 3.24 Numbering of the nitrogen atoms start from the phosphonate end of the molecule.

Browne[55] suggested that for the tetraen systems, if the meridional nitrogen atom N4 (as in Fig. 3.24) retained its original configuration (*anti* to the carboxylate group) and if the chirality of the amine adjacent to the α-carbon atom was correlated to the meridional nitrogen's chirality, then only two pairs of diastereoisomers (two pairs of enantiomers; Δ*RSR* & Λ*SRS* and Δ*SSR* & Λ*RRS*) should form.

The chemistry can be extended to these phosphonate analogues. Hence, if the wrapping of the polyamine backbone and the configuration around the phosphorus stereogenic centre are retained, and if epimerization of the proton on the meridional nitrogen atom N4 (counting from the α-carbon) does not occur, then only two pairs of diastereoisomers (for example, Fig. 3.25) would be expected from the product mixture.

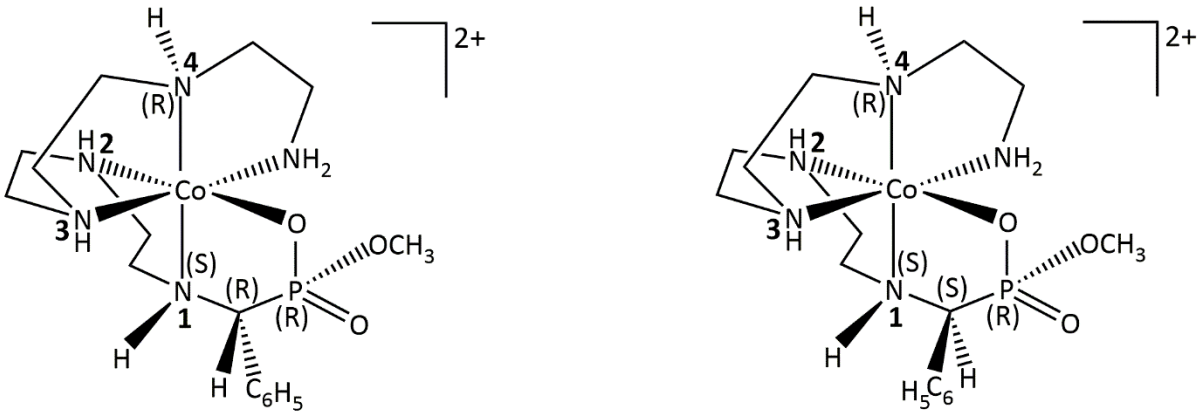

ΔRRSR *ΔRSSR*

Figure 3.25 The two diastereoisomers expected from the phosphonate tetraen systems if all other chiral centres are kept constant except the α-C centre. Their enantiomers will also be present in the mixtures.

The $^{31}P\{^{1}H\}$ NMR spectrum (Fig. 3.26) shows two major components (1:0.9 ratio) are in the product mixture from procedure 2 with two minor ones (0.15 and 0.16 integral values).

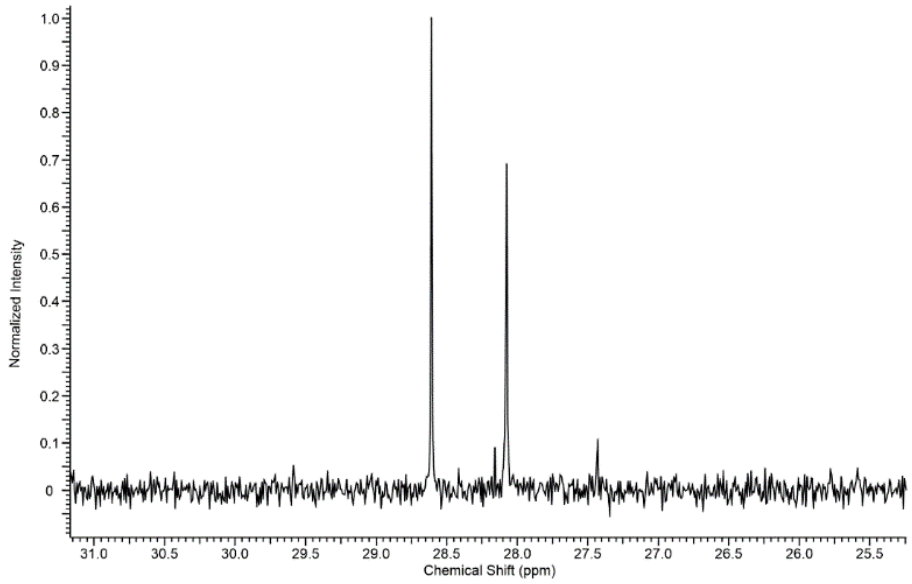

Figure 3.26 $^{31}P\{^{1}H\}$ NMR spectrum of product mixture from procedure 2

Compound 3.5

Tiny red crystals of one of compound **3.5**'s isomers formed in a flask holding the filtrate after trituration of a procedure 11 experiment in chapter 4 of this thesis. After filtration to recover the powdered product in chapter 4, it was noticed that the filtrate was intensely coloured. The dark red solution was safely stored pending characterisation. At the point of preparing a sample for characterisation of the filtrate, crystals were observed. One of the crystals was mounted for X-ray analysis and the structural model is shown as Fig. 3.27. However, the data set obtained was too noisy (Fig. 3.28) with most of the data points in the noise region. The structural model has been included to show connectivity and for comparison. The counter-ion for this crystal structure is a triflate anion derived from the methyl triflate used for the esterification of the amines before the peptide linkage step.

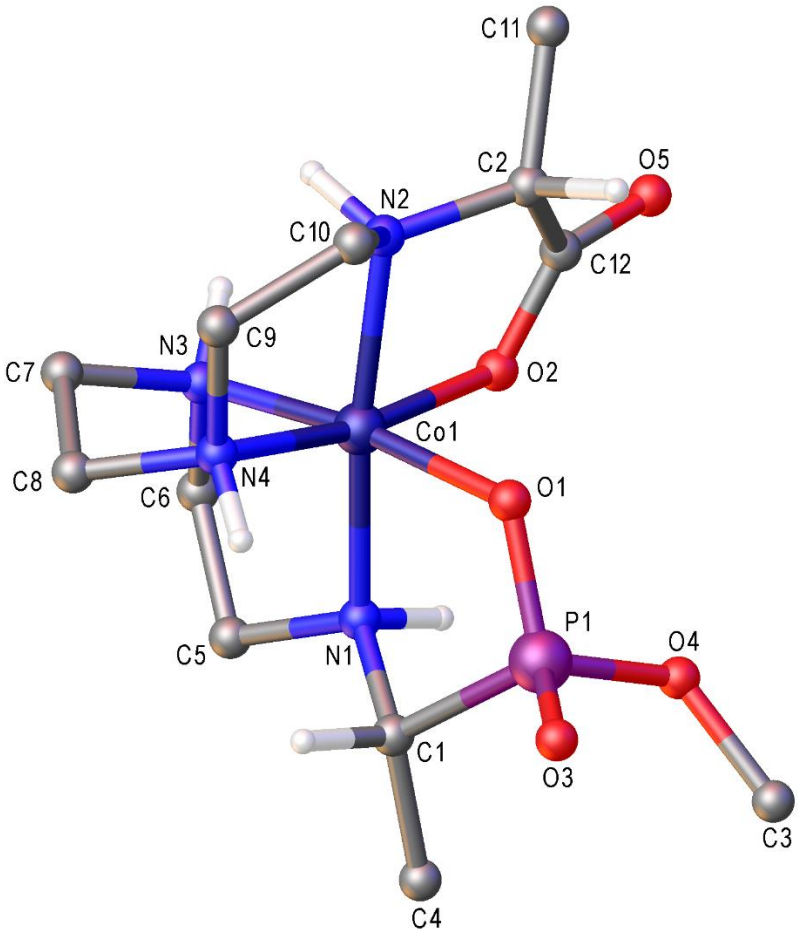

Figure 3.27 The crystal structure of the Δ*RSRRR* diastereoisomer of **3.5** (counting from the top half of the molecule at C2, N2, N1, C1 and P1). Most hydrogen atoms and the triflate anion have been omitted for clarity.

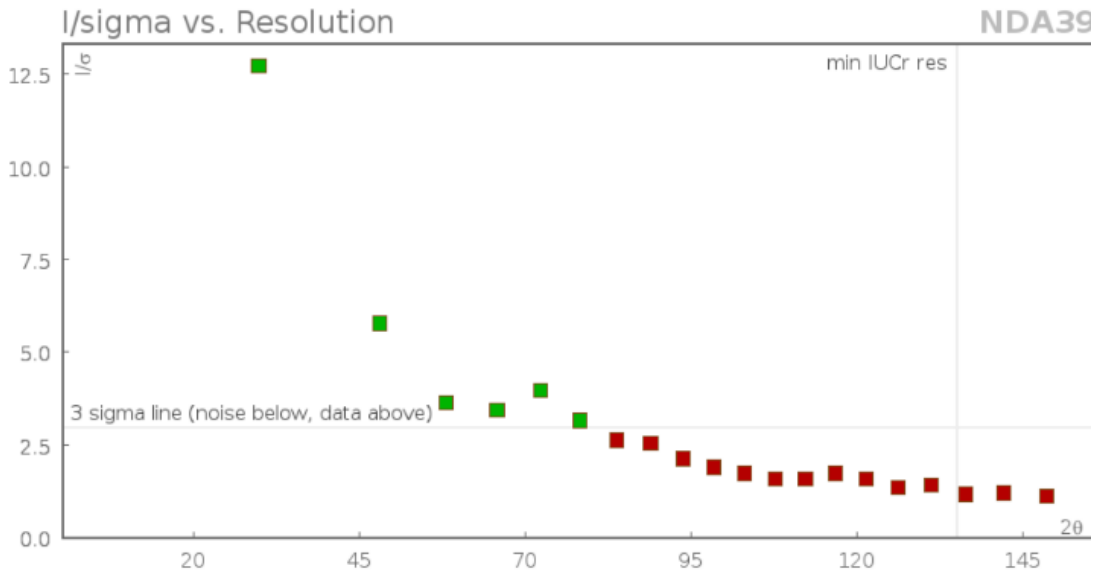

Figure 3.28 I/σ vs. resolution profile for the data set of compound **3.5** (Fig.3.27)

The crystal structure shown in Fig. 3.27 is a Δ*RRRR* diastereoisomer (its enantiomer is also present in the mixture). The X-ray structure shows that the proton of the α-carbon atom on the carboxylate group of the complex has been added on the phosphonate face of the complex. It means that the reduction of the carboxylate had gone with the hydride attack from the phosphonate face.

On the contrary, the proton on the α-carbon atom of the phosphonate group has been added on the amine face of the complex. The amine-faced addition is the dominant form of hydride attack from previous research where it was statistically shown to be 92% selective[39, 52]. Even when en systems were used in the past[50, 57] for systems such as those shown in Fig. 3.29, the borohydride attack occurred from the more hindered face of the imine acid ligands.

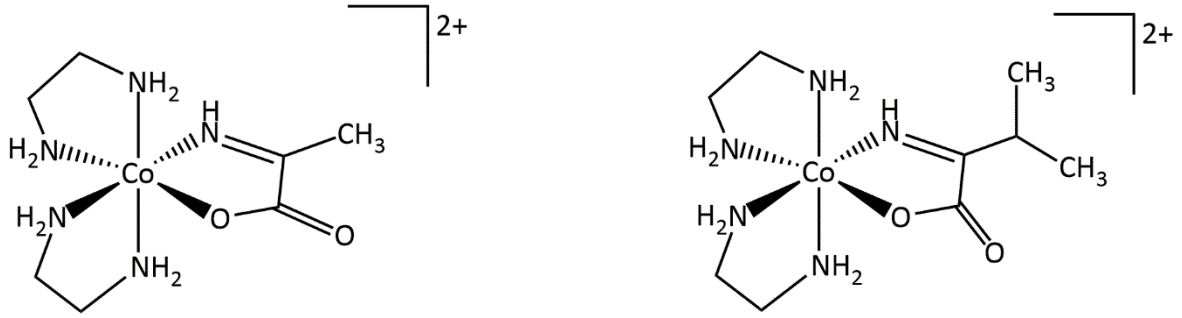

Figure 3.29 Complexes used by Hartshorn[50] to investigate selectivity in hydride reduction reactions.

The $^{31}P\{^{1}H\}$ NMR spectrum from procedure 5's product mixture showed two major resonance peaks (integral ratio of 3.4:2.5) and five minor ones (each with the integral value of ~1). If the polyamine backbone retains its configuration throughout the reaction and the phosphorus centre does so too, it can then be assumed that the face through which the hydride was added during the reduction reaction determines which isomers are formed. In terms of isomer distribution, the carbonate buffer (in which the reduction reaction is carried out) promotes epimerisation of the N-H protons, leading to the generation of more isomers as a result of dynamic equilibrium. Also, since a typical molecule from the product mixture of procedure 5 would be asymmetrical, the expected number of stereoisomers could be as many as 2^4 (16) or 8 diastereoisomers from the newly generated stereogenic centres. Eight resonance peaks were observed in the $^{31}P\{^{1}H\}$ NMR spectrum (Fig. 3.30) from the product mixture.

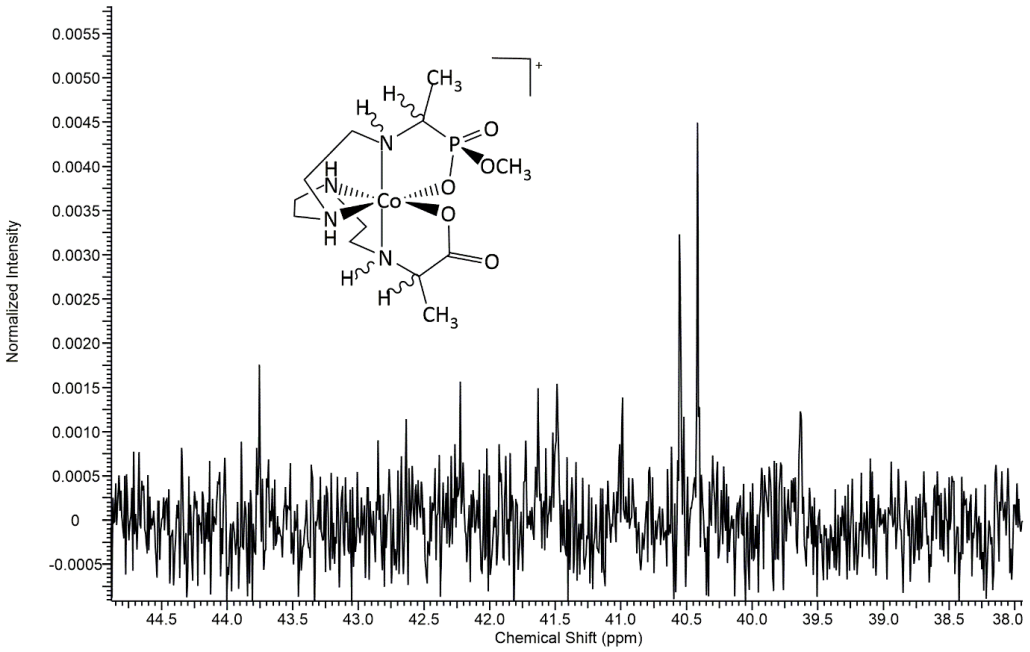

Figure 3.30 $^{31}P\{^{1}H\}$ NMR of the product mixture from procedure 5 showing two major isomers and some minor ones.

It has been observed by NMR that only one or two pairs of diastereoisomers usually dominate these product mixtures with the other diastereoisomers present in minor quantities.

The $^{13}C\{^{1}H\}$ NMR spectrum for this product mixture was noisy, however, 8 major signals (46.39 – 60.80 ppm) were observed in the **C**H_2-NH and **C**-N region as expected from one typical molecule. The region appeared to have sets of peaks for each major signal indicating the presence of other stereoisomers in the sample mixture. Two major signals were observed in the **C**=O region of the spectrum whereas the **C**H_3 region (Fig. 3.31) was more complicated. The complexity of the methyl region can be attributed to the different chemical environment at

each arm of the complex (one carboxylate, the other phosphonate). The multiplicity of the set of peaks at the 18 ppm region of the $^{13}C\{^{1}H\}$ NMR spectrum (Fig. 3.31) is generated from the coupling effect of the methyl protons to the NMR active phosphorus nuclei. The coupling constant of each doublet in the 18 ppm region was 36 Hz. The unavailability of $^{13}C\{^{1}H\}$ NMR spectra of great resolution for the amines reported in this project, made it difficult to draw conclusions with this $^{13}C\{^{1}H\}$ NMR spectrum.

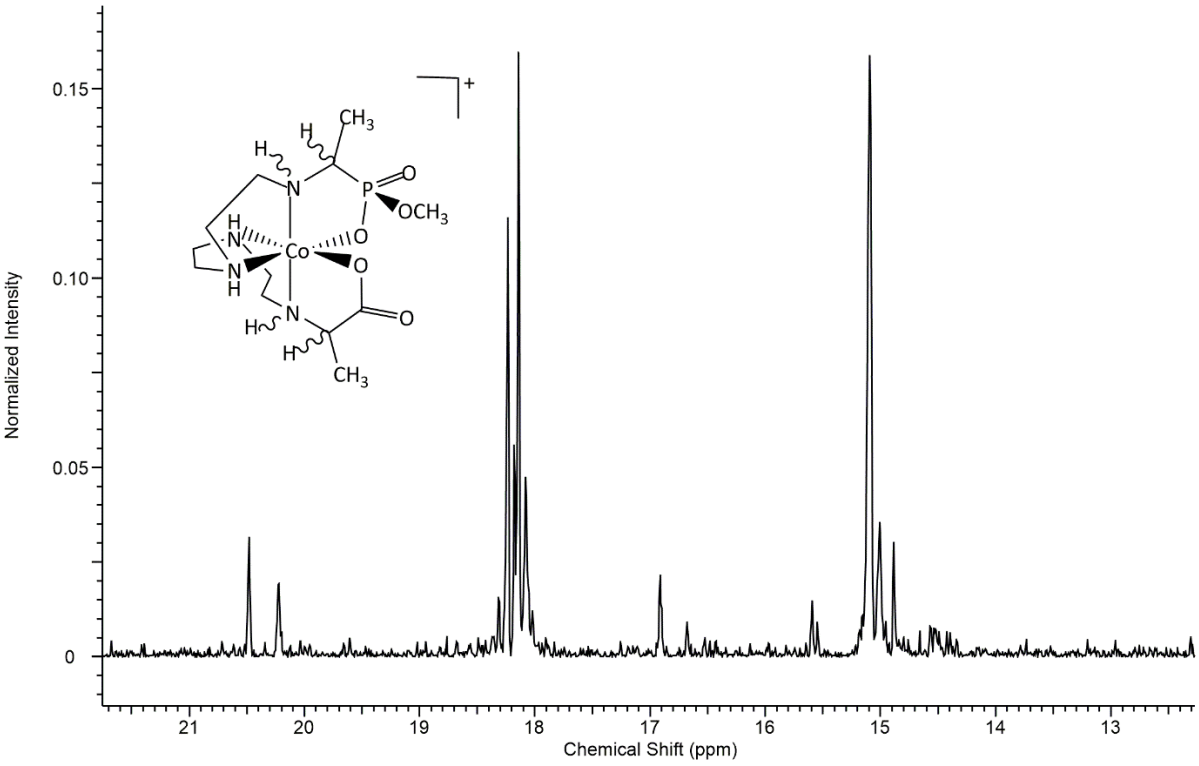

Figure 3.31 The methyl region of the $^{13}C\{^{1}H\}$ NMR spectrum from the product mixture of procedure 5.

The ^{1}H NMR spectrum obtained from the same product mixture from procedure 5 (discussed in section 3.3.2) helped to confirm that two pairs of diastereoisomers dominate the product mixture from procedure 5.

Compound 3.6a

Crystals of **3.6a** formed in the product mixture at 18°C in a methanolic solution. The crystal structure of the red plates of **3.6a** was solved in the monoclinic space group $P2_1/c$ and is shown in Figure 3.32.

The structure shown in Fig. 3.32 is a known structure.[39, 52] The structural determination parameters differ only slightly, the major one being that data set for both structures were collected at different temperatures (see table 3.2). The unit cell parameters between both structures are very similar.

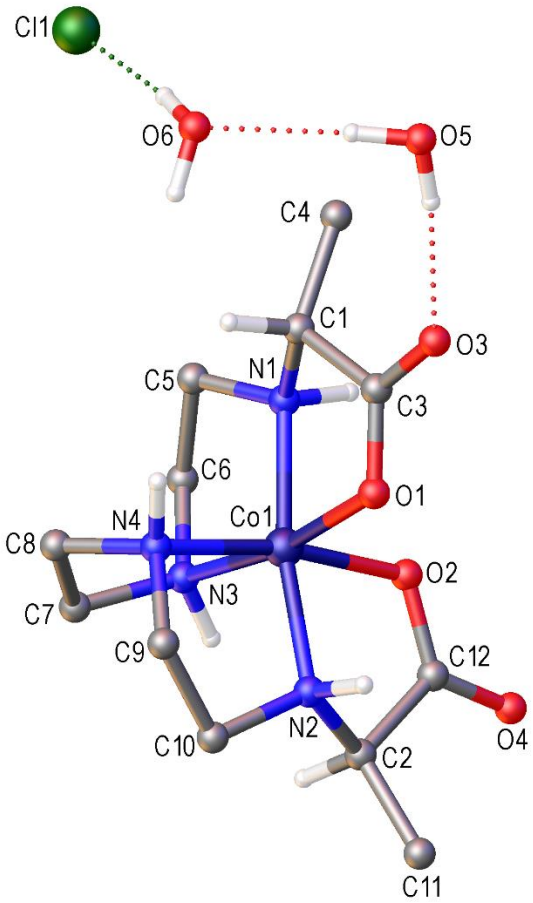

Figure 3.32 The crystal structure of **3.6a** from procedure 6. Most hydrogen atoms have been omitted for clarity.

The protons on both α-carbon atoms are located on the amine face of the meridional ligand fragment as in the literature[39, 52]. ^{1}H and $^{13}C\{^{1}H\}$ NMR spectra obtained from the mixture containing compound **3.6a** correspond with spectra obtained in the literature before the chromatographic separation to isolate the major component of their mixture. There were six resonance peaks observed in the $^{13}C\{^{1}H\}$ NMR spectrum and the ^{1}H spectrum is shown in Fig. 3.33.

The major isomer isolated in the literature is structurally similar to the model shown in Fig.3.32 in terms of bond lengths and angles, counter ion, solvent molecules etc.

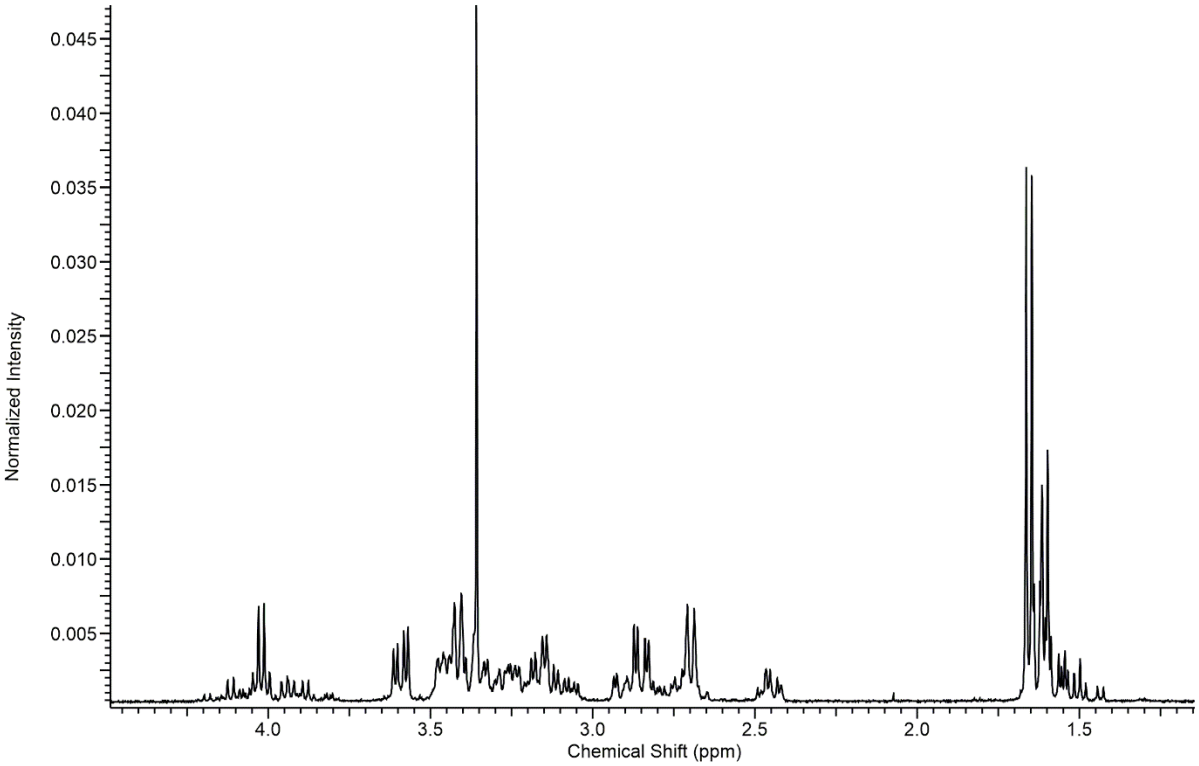

Figure 3.33 A region of the 1H NMR spectrum of the product mixture from procedure 6.

The cluster of signals seen in the methyl region (1.6 ppm) of the spectrum shown in Fig. 3.33 resembles that generated from previous study in the literature.[39, 55] The most intense doublet has been assigned to the major isomer whereas the other doublets have been attributed to the minor isomers of the mixture.

Compound 3.6b

The X-ray structure of the red crystals of **3.6b** was solved in the triclinic space group P$\bar{1}$ and is shown in Figure 3.34. It bears two triflate anions from the esterification process of chapter 4. Compound **3.6a**'s anion is a chloride.

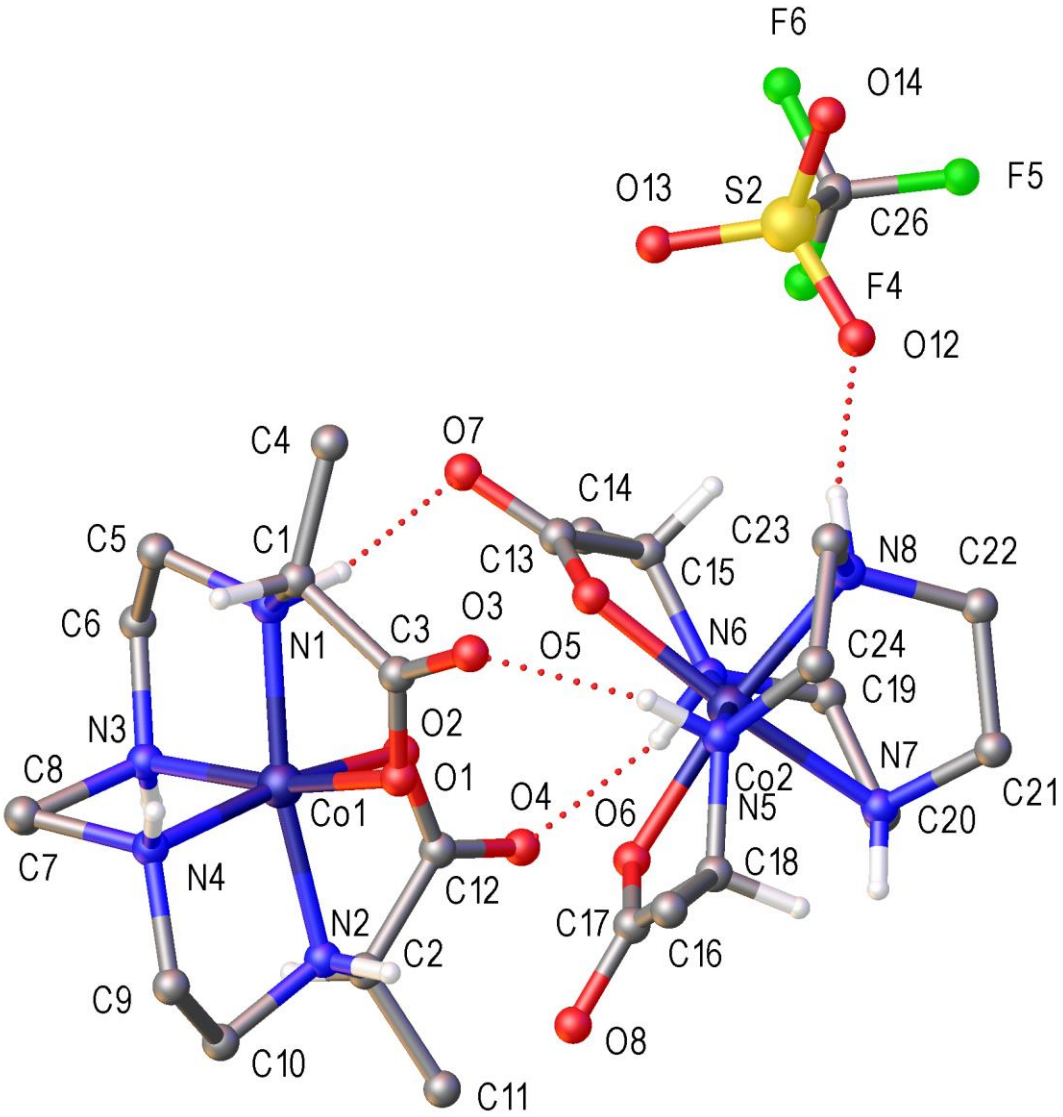

Figure 3.34 The crystal structure of **3.6b** from procedure 6 of chapter 4. Most hydrogen atoms and a triflate anion have been omitted for clarity.

One of the anions was bound to one of the complexes through a hydrogen bond between the hydrogen of N8 and O12 of the anion. Three other hydrogen bond interactions were observed between the two complexes. They were O3---H-N5, O4---H-N6 and O7---H-N1 respectively. The other triflate anion had disordered fluorine atoms which have been modelled to have thermal parameters as close to their neighbouring atoms as possible by applying ISOR[101, 103].

The structures shown in Fig. 3.34 with respect to the cobalt(III) complexes are known structures.[39, 52] Both of them have similar bond lengths and angles between each other and are

also comparable with the literature structure[39]. However, the counter ions as well as the unit cell parameters are different from the literature structure as expected. While the structural solution for the known compound has been reported in the monoclinic space group of $P2_1/c$, the solution here is in the triclinic $P\bar{1}$ space group. Other contrasting features have been included in table 3.2.

	$C_{12}H_{28}ClCoN_4O_6$ (known compound)	$C_{12}H_{28}ClCoN_4O_6$ (compound **3.6a**)	$C_{26}H_{48}Co_2F_6N_8O_{14}S_2$ (compound **3.6b**)
Crystal system	monoclinic	monoclinic	triclinic
Space group	$P2_1/c$	$P2_1/c$	$P\bar{1}$
Unit cell dimensions			
a (Å)	10.2882(17)	10.2796(3)	12.0378(5)
b (Å)	12.738(2)	12.7146(3)	12.8059(4)
c (Å)	13.267(2)	13.2413(4)	14.3205(5)
α (°)	90	90	101.598(3)
β (°)	96.273(6)	96.262(3)	114.318(4)
γ (°)	90	90	90.875(3)
Temperature (K)	293(2)	120.02(10)	120.01(10)
Wavelength	0.71073	1.54184	1.54184
Volume/$Å^3$	1728.2(5)	1720.33(8)	1958.70(14)

Table 3.2 Comparing between X-ray structures of present and existing models

3.3.2 Formation of the Amine Complexes

The amine complexes reported in this project were produced through reduction reactions performed in a carbonate buffer solution using sodium borohydride as the reducing agent. The general procedure usually involved a minimum of 26-fold excess of sodium borohydride being reacted with the imine acid complex for 10 mins. The reactivity of sodium borohydride was found to differ through different batches and the reducing agent also loses its reactivity over time. So, in some instances up to 300-fold excess of the reducing agent has been used. Care was taken in observing the colour change of the reacting mixture as colour was a very good indicator as to when the reduction reaction has reached completion. Excessive reaction times lead to the decomposition of the complex and less reaction time may yield partially reduced

compounds as has been reported in the literature[39]. The product mixture is quickly adsorbed onto a Na^+ form Dowex 50WX2 column (that has been pre-equilibrated with the carbonate buffer) under suction. The column is thereafter washed with excess distilled water in order to get rid of any unreacted borohydride. If the entire column process is delayed, the borohydride reaction continues to decompose the complex in the matrix of the column as was observed during the course of this project. It is important to carry out these reduction reactions in 2 g maximum reactant quantity per batch because it takes a few minutes to finish up the reaction in the column.

The columns were eluted with 6 M HCl to recover the product mixtures. Lower concentrations of HCl can be used but it amounts to collecting a large volume of fractions which need to be evaporated to dryness before characterisation or further use. Since lower HCl concentrations did not give separation of the mixtures on the Dowex 50WX2 columns, higher concentrations of HCl solutions were used to elute the columns.

Attempts were made to separate the isomers from the reduction reactions described in this section using Sephadex SPC 25 columns but they were unsuccessful. NMR spectra of samples prepared from the fractions obtained from those chromatographic procedures showed that each fraction was still a mixture of isomers. The salt used in the mobile phase was also changed to disodium hydrogenphosphate (Na_2HPO_4) but NMR experiments still confirmed the fractions collected were mixtures.

Assigning the NMR Spectra

$^{13}C\{^1H\}$ spectra obtained for most compounds in this chapter were not completely assigned to all possible isomers in the mixture because of their complexity in addition to the low signal to noise ratio observed for most of the carbon spectra. Partial assignments have been done where possible by stating the number of major resonance peaks above the noise level; most minor peaks could not be therefore be accurately accounted for in order to avoid assigning a signal to a peak that was only noise.

The complexity of the spectra was not unexpected. The greater number of stereogenic centres in the molecules described in this chapter compared with their imine starting materials, would give rise to more complicated spectra (as is evident in the ^1H and $^{31}P\{^1H\}$ from these systems) than those of their imine precursors. The $^{31}P\{^1H\}$ spectra provide a guide as to the number of

diastereoisomers in a given product mixture. Integration of the ^{1}H NMR spectra gives information about the isomer distribution in each mixture.

^{1}H NMR spectra for these amino acid complexes of cobalt(III) with phosphonates and carboxylates, were very useful for their characterisation. The first indication that the reduction reaction was successfully carried out was usually the appearance of a new set of peaks at the 1.6 ppm region of the spectrum. For the pyruvate derived complexes, the methyl group of the imine precursor resonates as a singlet in the ^{1}H NMR spectrum around the 2.6 ppm region. That signal splits into a doublet after the reduction reaction by reason of the introduction of a proton to the α-carbon atom by the reducing agent. This was also the case for the phosphonate derived systems even though the multiplicity of the new set of peaks was more complicated from the presence of the NMR active ^{31}P nuclei proximate to the α-carbon atom in those complexes. Referring to the spectra of related compounds in the literature and also within these new compounds, coupling constants were used to deconvolute relevant spectra where possible.

Doublets of doublets were expected for the methyl protons of the phosphonate derived complexes, from both $^{3}J^{HH}$ and $^{3}J^{HP}$ coupling effects caused by the H on the α-carbon atom and by the ^{31}P respectively. The coupling constants helped in the deconvolution of these spectra but the most difficult aspect was that the $^{3}J^{HH}$ values of the methyl protons on carboxylate groups were sometimes similar with the $^{3}J^{HP}$ values for the methyl protons of the phosphonate groups. The appearance of these new sets of peaks was obviously accompanied by the disappearance of the methyl resonance peaks around 2.6 ppm region of the spectrum.

There was also the usual intricacy of the methylene region of the spectrum as have been observed in this project in alignment with the literature.[39, 52] This is mainly contributed by the overlap from the presence of inequivalent protons in the polyamine backbone of these complexes as well as the multiplicity caused by the adjacent protons. Spectra have therefore been assigned as confidently as possible with the help of COSY (where possible) and reference to the literature.[39, 52]

The amines were usually a mixture even after column chromatography, as shown by NMR. These mixtures are thought to be composed majorly of stereoisomers rather than other contaminants. Previous study in the Hartshorn group[39] also reported the salt contamination even though a careful re-submission to a new column often dealt with this problem. Different resins were trialled in the attempt to achieve purer mixtures but the salt was still an issue, hence the lack of elemental analysis results in this chapter. CHN analysis results obtained for most of

the amines showed salt contamination. It was therefore reasoned that the mixtures can be worked with since the next step of the project being the esterification process should be selective, reacting only with the complexes, leaving the salt behind.

Tetraen Based Mono-Amine Complexes of Cobalt(III)

Compounds from procedures 1, 2 and 7 were made by reacting the imine acid precursor with the (N′-[2-[2-(2-aminoethylamino)ethylamino]ethyl]ethane-1,2-diamine); (tetraen) pre-coordinated polyamine backbone with excess of sodium borohydride. The complexes formed (**3.1**, **3.2** or **3.7** and their diastereoisomers), are expected to have two new stereogenic centres in each molecule (Fig. 3.35). The carboxylate systems have two other pre-existing stereogenic centres whereas the phosphonate ones have three.

Based on previous studies[39, 55] done with the tetraen system, if the meridional nitrogen atom retains its original configuration (*anti* to the carboxylate group) and if the chirality of the amine adjacent to the α-carbon atom is correlated to that atom's chirality, then only two pairs of diastereoisomers are expected.[39, 55] If the carboxylate chemistry is extended to these phosphonate systems , then two pairs of diastereoisomers are expected from the product mixture, if the original configuration at the phosphorus centre is retained in the final products.

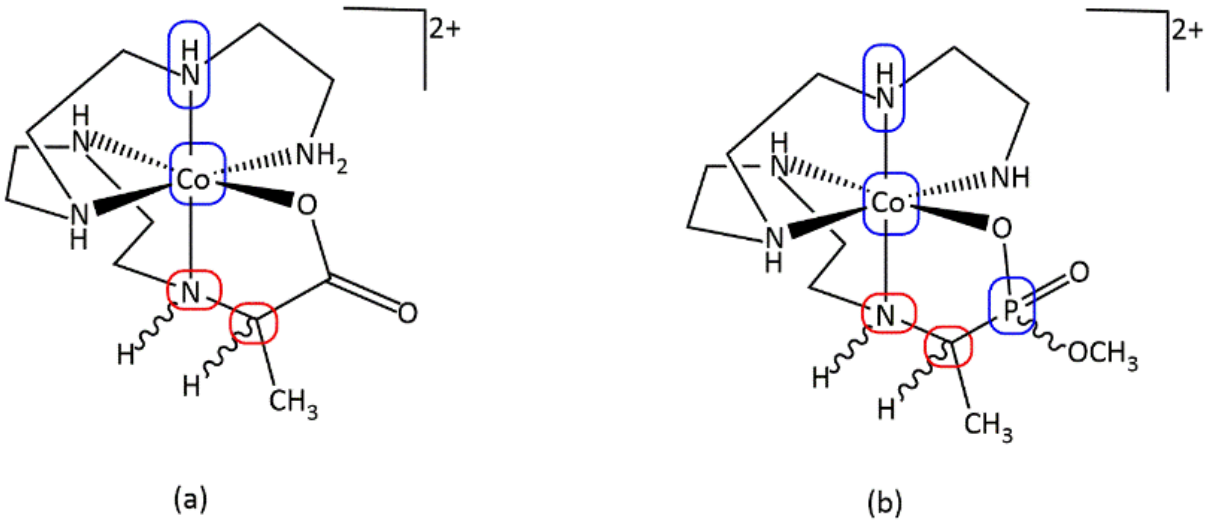

Figure 3.35 Tetraen systems with a: carboxylates; b: phosphonates. New stereogenic centres are highlighted in red while blue highlights already existing stereogenic centres before the reduction reaction.

The two expected diastereoisomers (their enantiomers will also be present in each mixture) from the phosphonate systems have been schematised in Fig. 3.36.

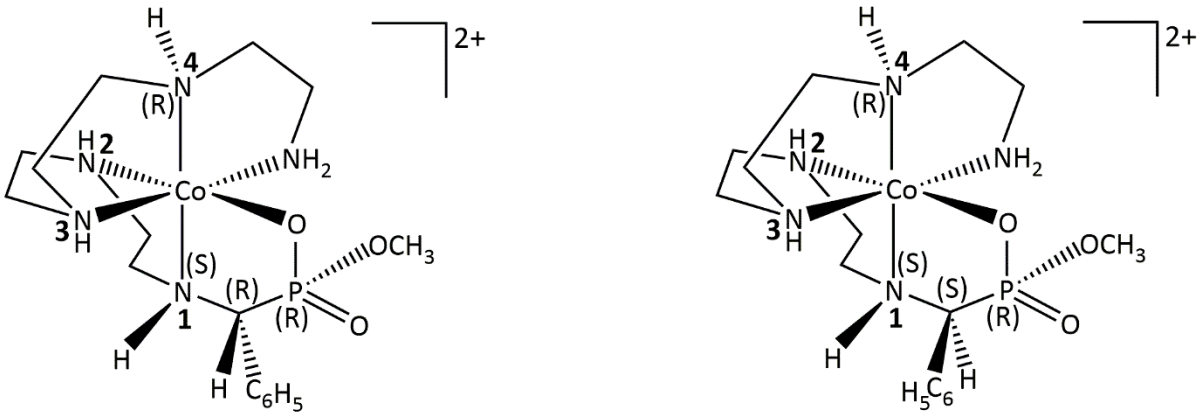

ΔRRSR *ΔRSSR*

Figure 3.36 The two diastereoisomers expected from the phosphonate tetraen systems if all other chiral centres are kept constant except the α-C centre.

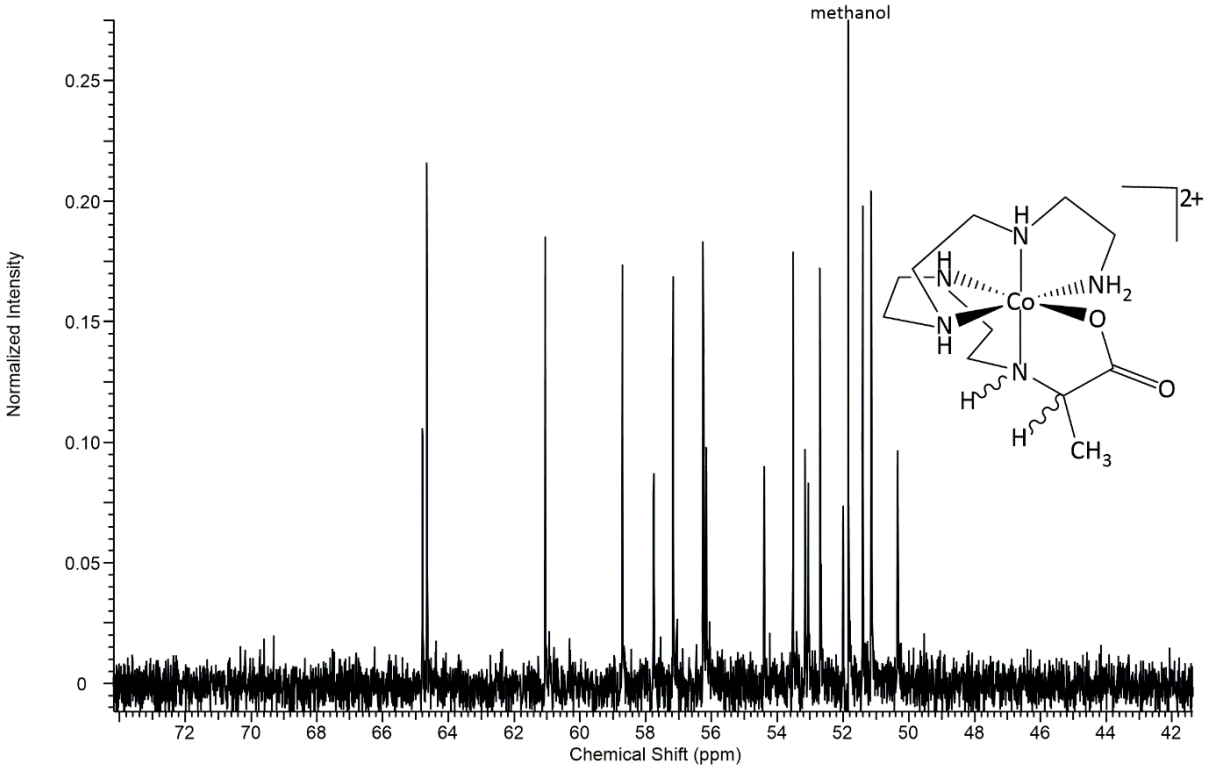

Figure 3.37 **C**H_3 and **C**H region of the $^{13}C\{^1H\}$ NMR spectrum from procedure 7.

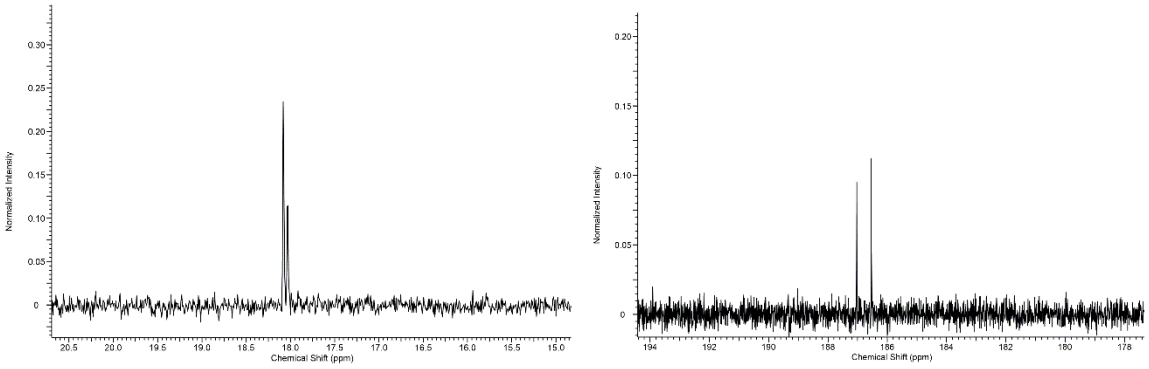

Figure 3.38 **Right**: Carbonyl region of procedure 7's $^{13}C\{^{1}H\}$ NMR spectrum showing two diastereoisomers in the product mixture. **Left**: Methyl region of procedure 7's $^{13}C\{^{1}H\}$ NMR spectrum showing two diastereoisomers in the product mixture.

Fig. 3.37 shows the (**C**H_2) methylene and **C**H (α-carbon atom) region of the spectrum from compound **3.7** and its stereoisomers. Nine signals are expected in that region of the $^{13}C\{^{1}H\}$ spectrum for one compound. Nine major resonance peaks have been observed for the major component of the product mixture from procedure 7 (and eight signals for the minor isomer). The other parts of this spectrum (Fig. 3.38) showed two lines each for both the **C**H_3 (18.03 and 18.08) and the **C**=O (186.54 and 187.03 ppm) groups respectively. A combination of the $^{13}C\{^{1}H\}$ spectrum and the ^{1}H spectrum (Fig. 3.39) confirm that two major components dominate the product mixture from procedure 7. They are predicted to be Δ*RSR* (and Λ*SRS*) and Δ*SSR* (and Λ*RRS*) pairs of diastereoisomers.

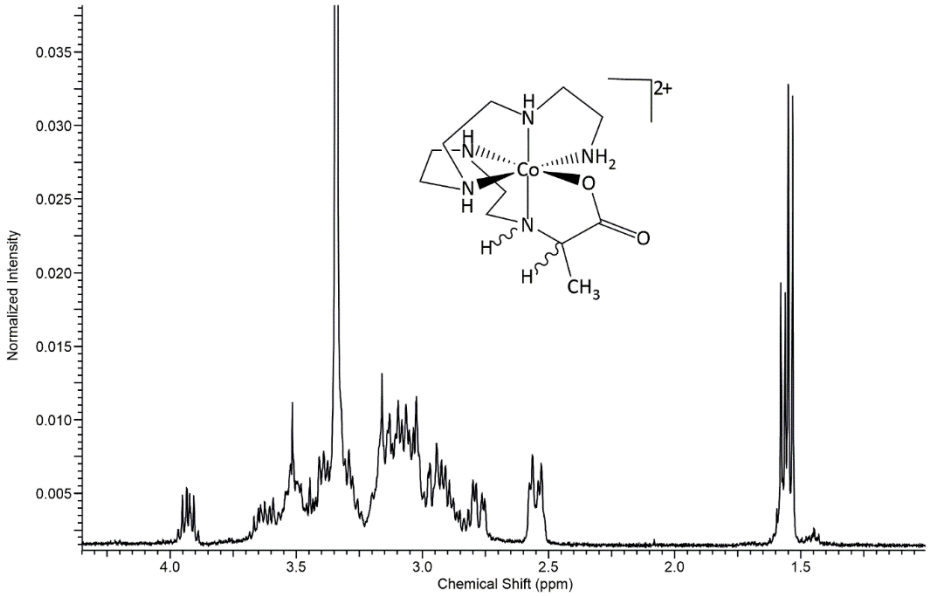

Figure 3.39 A portion of the ^{1}H NMR spectrum from procedure 7 showing two major components in the product mixture.

These results are in alignment with the postulation in the Hartshorn group[39, 55] that only two pairs of diastereoisomers should form from the tetraen systems.

The $^{13}C\{^{1}H\}$ and ^{1}H NMR spectra obtained from procedure 2's product mixture were too noisy. However, nine major resonance peaks were still observed in the $^{13}C\{^{1}H\}$ spectrum as expected from a typical molecule of the amine complex. Due to the noise, it was hard to figure out the presence of other isomers or not especially in the methylene and α-carbon atom region of the spectrum. The aromatic region showed a complexity of peaks too (Fig. 3.40). There appears to be two overlapped doublets at 131.75 ppm and two other ones of proportionate intensity at 131.59 and 131.07 ppm respectively. All these peaks have collectively been assigned to the carbon atoms of the phenyl ring in compound **3.2** and its stereoisomers. The three obvious doublets in that region all have the same coupling constant of 5 Hz each.

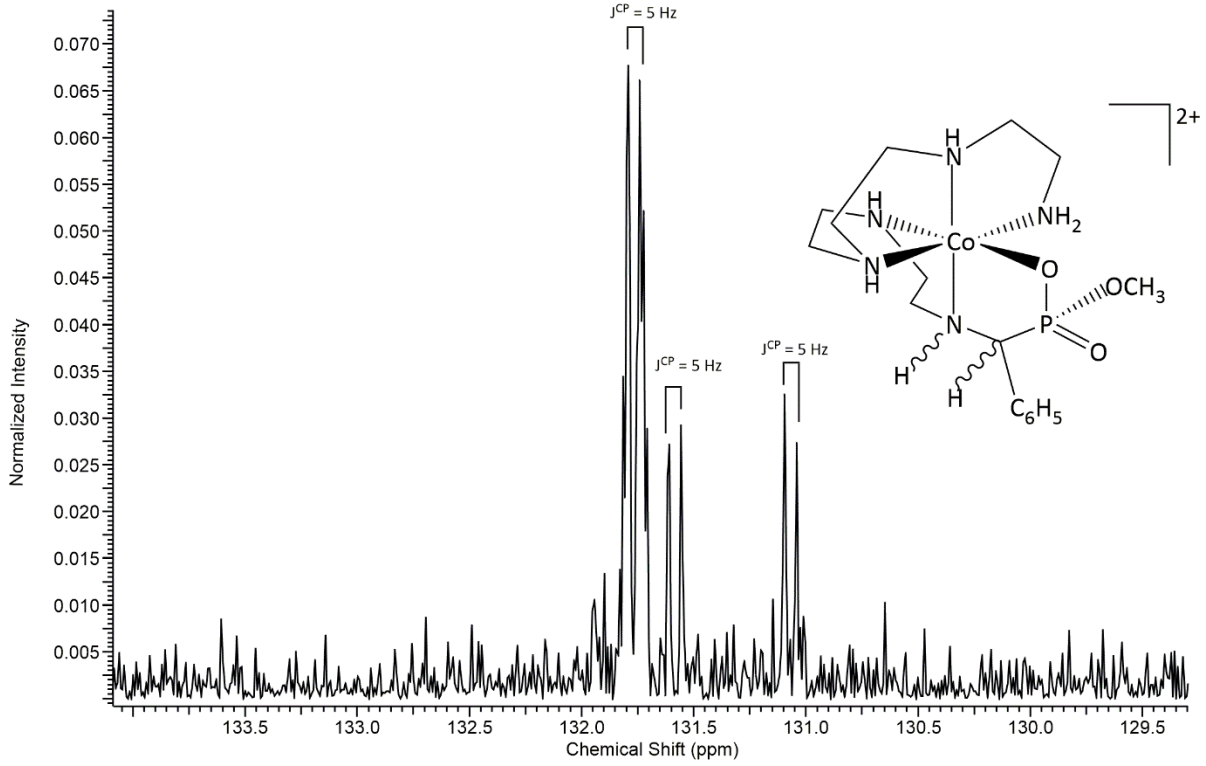

Figure 3.40 Aromatic region of the $^{13}C\{^{1}H\}$ spectrum from procedure 2's product mixture (shown in power spectrum mode to minimise noise).

Figure 3.41 is the $^{31}P\{^{1}H\}$ NMR spectrum of compound **3.2** and its stereoisomers, showing two major resonance peaks.

It can therefore be deduced that two pairs of stereoisomers dominate the product mixture from procedure 2. They would have the absolute configurations of Δ*RRSR* (& Λ*SSRS*) and Δ*RSSR* (& Λ*SRRS*) as have been schematised in Fig. 3.36.

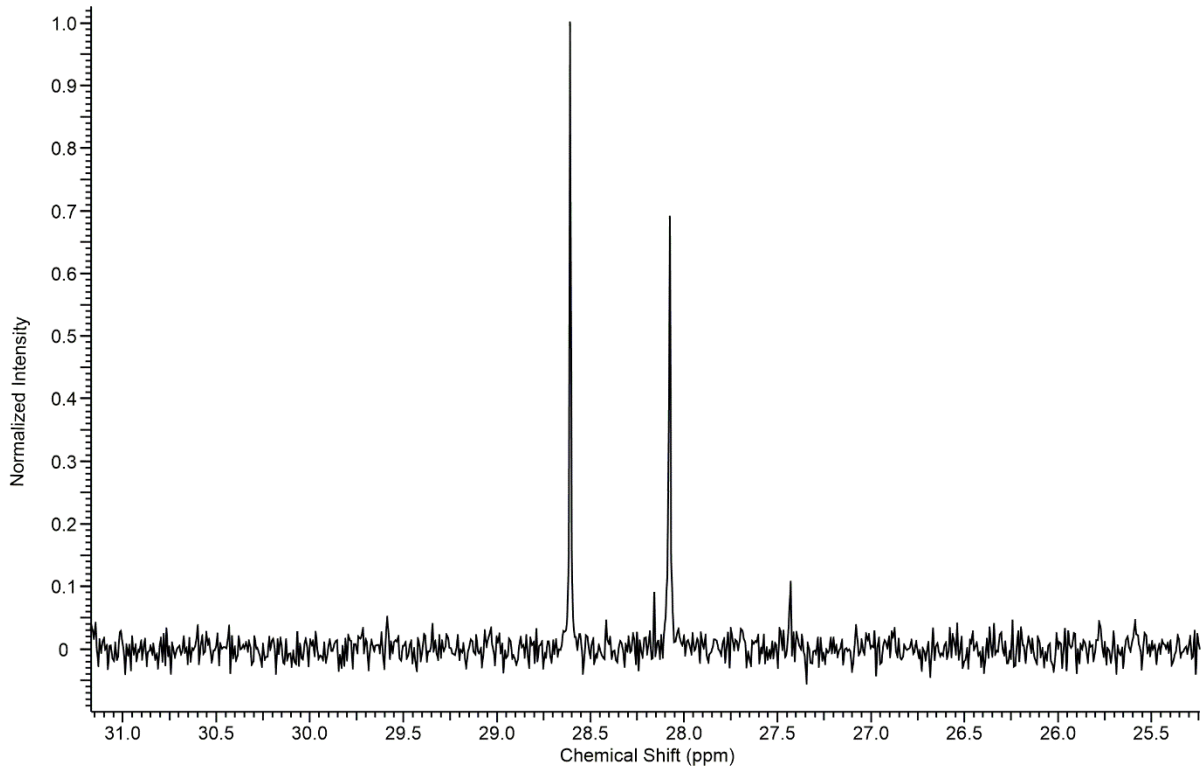

Figure 3.41 $^{31}P\{^{1}H\}$ NMR spectrum of product mixture from procedure 2 showing two major isomers dominating the mixture.

The $^{31}P\{^{1}H\}$ NMR spectrum shown in Fig. 3.41 is consistent with signals observed in the sample's ^{1}H NMR spectrum. The methoxy region of the ^{1}H spectrum has a doublet with the $^{3}J^{HP}$ value of 16 Hz at 4 ppm. Slightly upfield at 3.7 ppm was a cluster of about three doublets (assigned as a multiplet). One main doublet could be extracted from the cluster also with a $^{3}J^{HP}$ value of 16 Hz. Overall, it appeared the product mixture from procedure 2 was dominated by two major pairs of diastereoisomers.

The ESIMS result of the product mixture from procedure 2 has been included as Fig. 3.42.

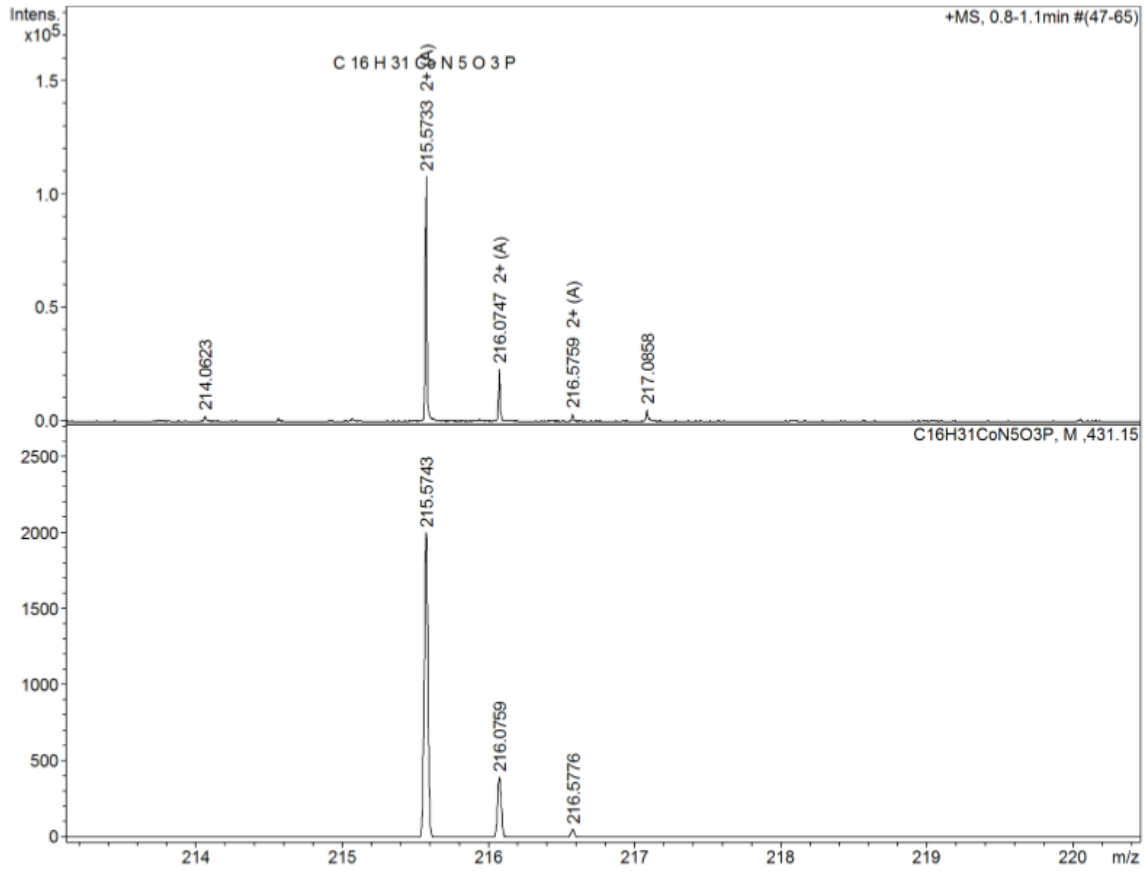

Figure 3.42 Mass spectrometry spectrum from the product mixture of procedure 2. Top: experimental. Bottom: calculated.

The $^{31}P\{^{1}H\}$ NMR spectrum (Fig. 3.44) obtained from a sample of the product mixture for compound **3.1** and its stereoisomers showed four lines well above the noise signals. These have been assigned to four compounds (Fig. 3.43) in the product mixture. These four compounds are most likely stereoisomers because they have resonated in the same region of the NMR spectrum and the mass spectrometry results were as expected.

Given the conditions under which the borohydride reduction is carried out, there is likelihood of epimerisation of the meridional nitrogen atom's proton in the carbonate buffer as has been demonstrated from previous studies[39, 52] in the Hartshorn group. Fig. 3.43 provides the schematics for four stereoisomers that could be generated simply through this epimerisation and from the chirality at the α-C centre too. Every other stereogenic centre has been kept constant.

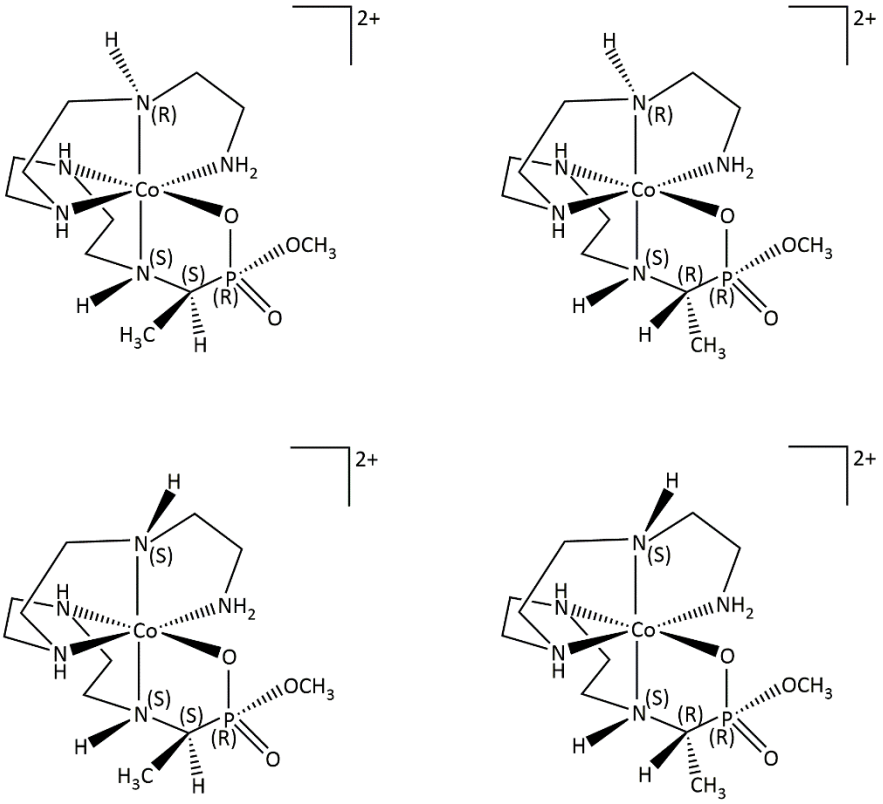

Figure 3.43 Schematic of the four expected diastereoisomers from the tetraen phosphonate systems, with the helicity around the metal centre, chirality at N1 (adjacent to the α-C) and chirality at the phosphonate stereogenic centre kept constant.

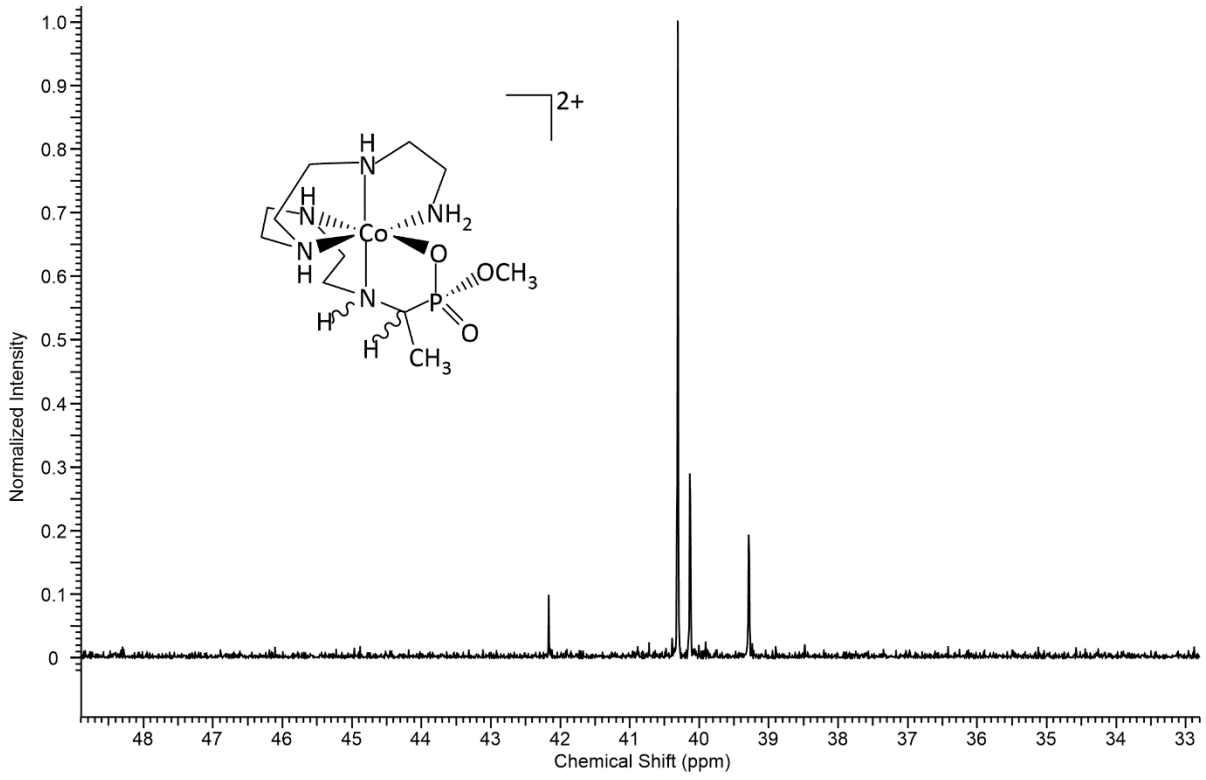

Figure 3.44 $^{31}P\{^{1}H\}$ NMR spectrum of product mixture from procedure 1 showing four stereoisomers.

Integration of these signals gave a 1:1.5:3:0.3 from upfield to downfield. Four chemically different phosphorus species are consistent with four doublets which were observed both for the methyl and methoxy regions of the ^{1}H NMR spectrum from this procedure, with one isomer dominating the mixture.

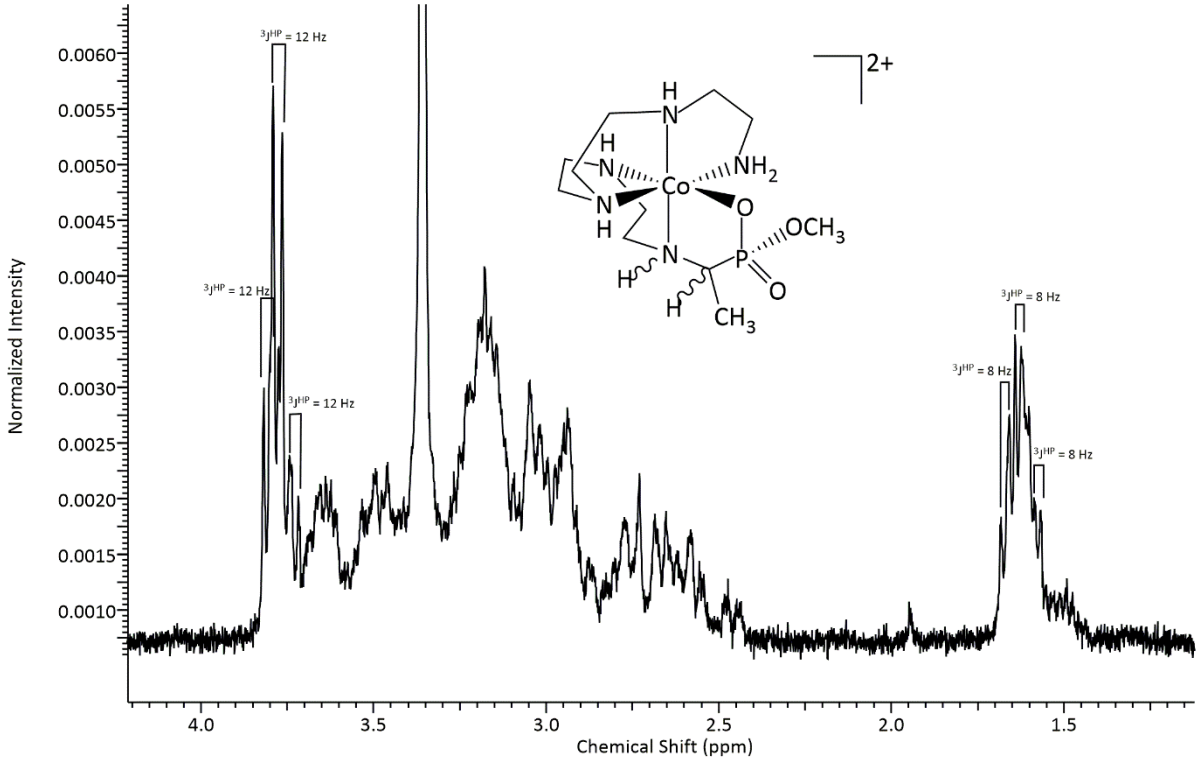

Figure 3.45 ^{1}H NMR of procedure 1's product mixture showing coupling constants

Integration of the spectrum shown in Fig. 3.45 showed a 1:1 ratio between the methyl protons and the methoxy ones, as expected. There was a rough value of 7:1 between the methylene protons and the methyl ones. The expected integral ratio was 8:1. It is possible the missing signals were hidden by peak overlap. Three doublets can be extracted from the methyl region (1.6 ppm) of the spectrum, leaving at least one more doublet in the multiplet. The same applied to the methoxy region of the spectrum. The integral ratio between the three extracted doublets at the methoxy region was 1:2:1. The ^{31}P{^{1}H} NMR of the same product mixture (Fig. 3.44) has four lines, confirming the presence of another isomer, which has been attributed to the overlapped doublet somewhat visible in the ^{1}H NMR spectrum in both the methyl and methoxy regions.

Even though there are four compounds in the product mixture from procedure 1, that is still a limited number compared with thirty-two (2^5) possible diastereoisomers that could ordinarily be generated from a system with five stereogenic centres.

The occurrence of the resonance peaks (methyl and methylene nuclei) from the current phosphonate systems in the same region of the ^1H and $^{13}C\{^1H\}$ NMR spectra with those of the carboxylates, indicates that the isomers produced in the present project must be related in terms of stereochemistry with those from previous research in the Hartshorn group.

Trien Based Di-Amino Complexes of Cobalt(III)

Compounds from procedures 3, 4 and 6 were made by reacting excess sodium borohydride with isolated imine complexes of cobalt(III) precoordinated with the polyamine (N′-[2-(2-aminoethylamino)ethyl]ethane-1,2-diamine); trien. The complexes formed (**3.3**, **3.4**, **3.6** and their stereoisomers) are expected to have four new stereogenic centres as shown in Fig. 3.46 introduced by the borohydride reduction.

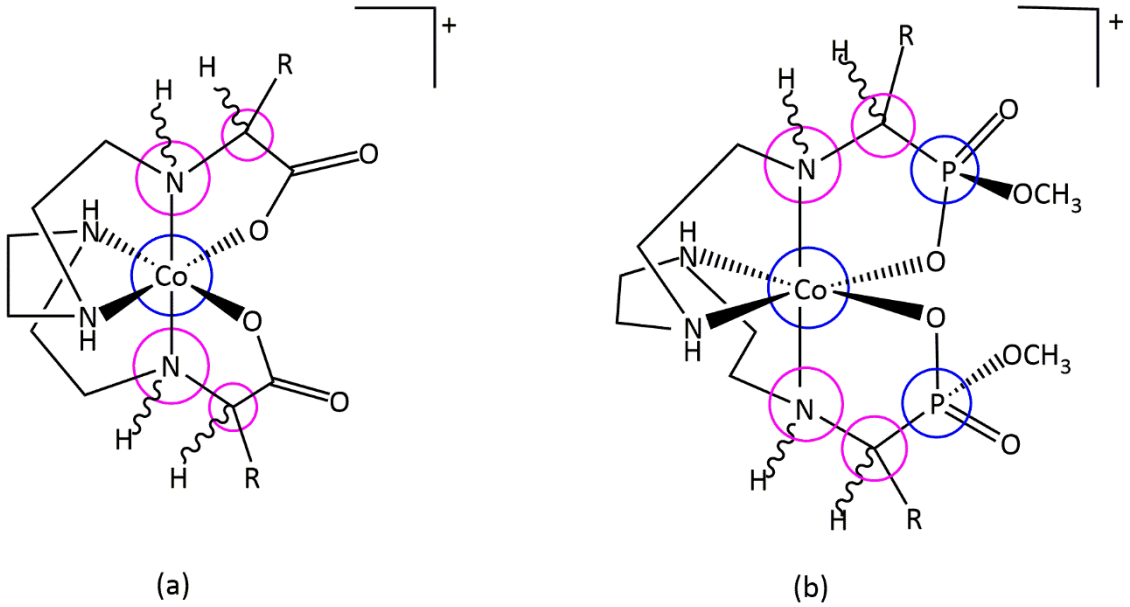

Figure 3.46 Trien systems with a: carboxylates; b: phosphonates. New stereogenic centres are highlighted in purple while blue highlights already existing stereogenic centres before the reduction reaction.

The trien polyamine from which the carboxylate and phosphonate systems in this section were prepared is symmetrical. If the C_2 axis of rotation is retained in the product molecule, the

number of stereoisomers observed in the NMR spectra would be limited.[39, 52] It has been stated earlier that some combinations of absolute configuration from a symmetrical trien system such as that shown in Fig. 3.47, will be equivalent owing to the limitation placed on the formation of all the possible diastereoisomers by the presence of a C_2 axis in some of the molecules in a given mixture[39, 52].

If the initial polydentate wrapping around the metal centre and the configurations at the phosphorus centres are retained, twenty stereoisomers (ten diastereoisomers) could therefore be formed from the reduction reaction of the trien systems[39, 52]. The ten diastereoisomers have been schematised in Fig. 3.7. The remaining ten stereoisomers are each an enantiomer of one of those shown in Fig. 3.7. Two more pairs of diastereoisomers are expected to be formed for each stereoisomer if the phosphorus centres are not kept constant, making a total of forty stereoisomers (twenty diastereoisomers).

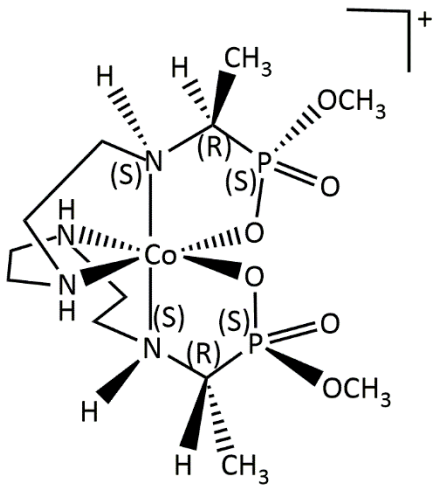

Δ*mffm*(*SRSSRS*)

Figure 3.47 The Δ*mffm*(*SRSSRS*) diastereoisomer of a trien polyamine system with phosphonates. The stereochemistry around the metal centre is Δ*mffm*. The top half of the molecule has the stereochemistry *S*, *R* and *S* around the phosphorus, α-carbon atom and amine centre respectively. The lower half of the molecule is similar to the top half by the presence of a C_2 axis of rotation.

The NMR spectra shown in Fig. 3.48 - 3.50 indicate the presence of multiple stereoisomers in the product mixture of **3.4** prepared from procedure 4.

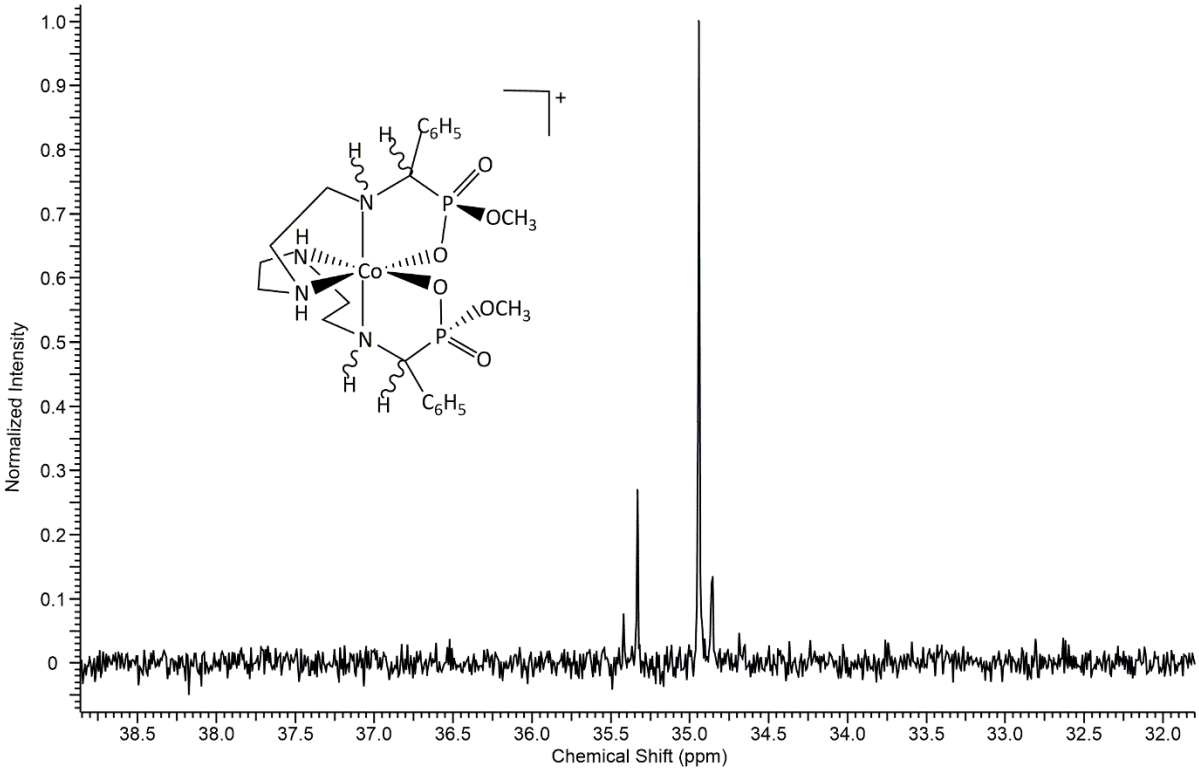

Figure 3.48 $^{31}P\{^{1}H\}$ NMR spectrum of the product mixture of **3.4** from procedure 4 showing four pairs of diastereoisomers.

At least four resonance peaks (integral values in the ratio of 0.93:4.5:1:0.23 from upfield to downfield) can be seen in the $^{31}P\{^{1}H\}$ NMR spectrum shown as Fig. 3.48. The peak at 34.94 ppm dominates the product mixture. The cluster of these signals in the same region of the spectrum demonstrates that the components of the mixture are most likely stereoisomers. These diastereoisomers all appear to have some symmetry in their molecules (for example a C_2 axis of rotation) since there are no signals with the same integral value or their phosphorus environments must all be similar. Mass spectrometry showed the expected M/Z ratio was obtained and the isotope distribution map displayed the right charge of +1 for each complex ion.

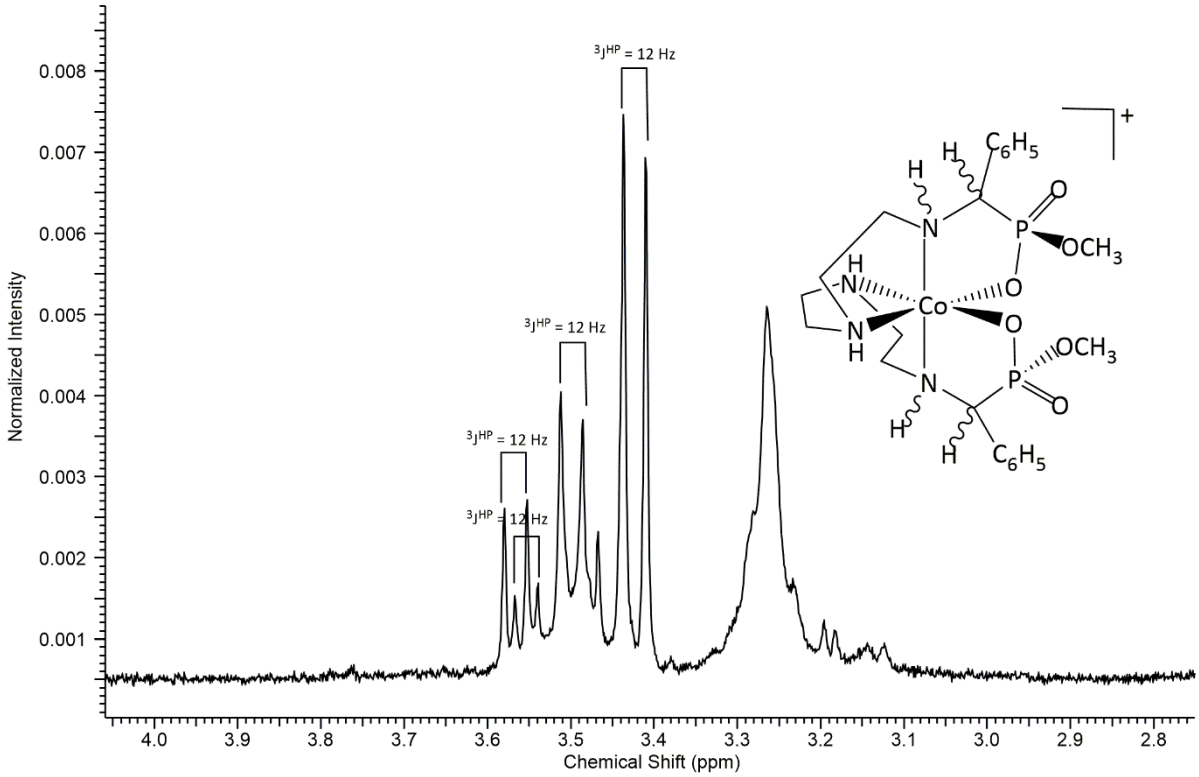

Figure 3.49 A region of the ^{1}H NMR spectrum of the product mixture of **3.4** showing four methoxy doublets and their coupling constants.

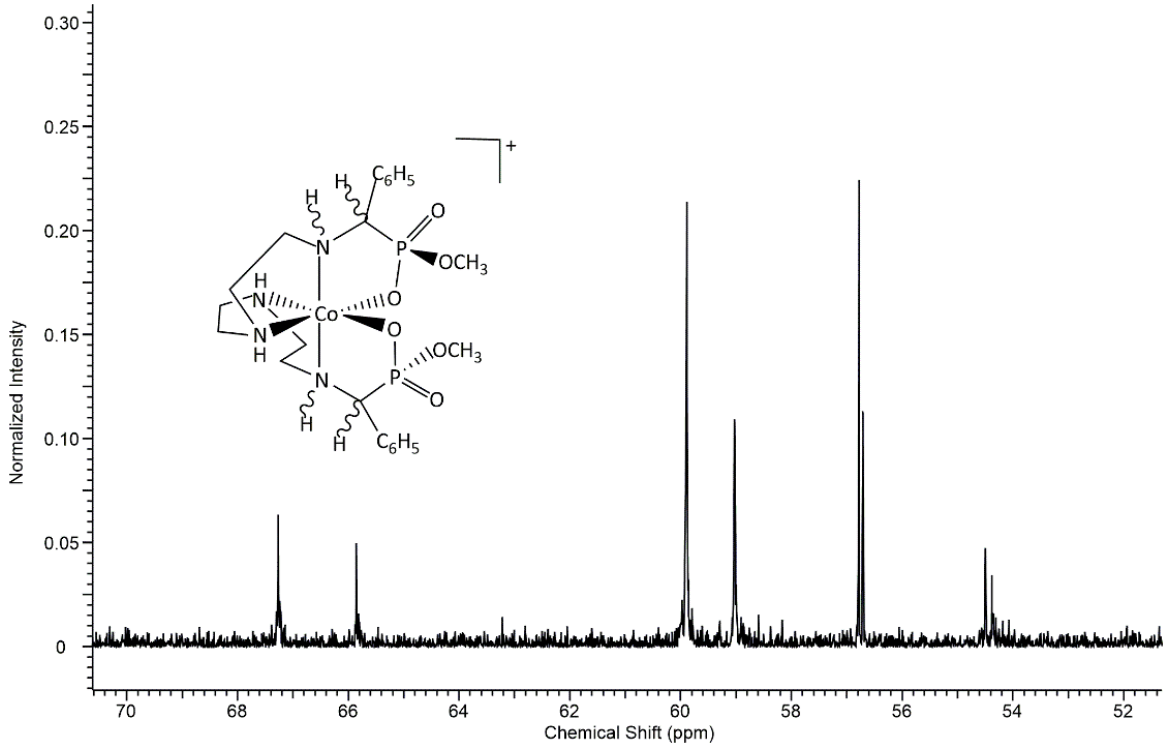

Figure 3.50 **C**H$_2$ and **C**H region of the ^{13}C{^{1}H} NMR spectrum of a product mixture from another procedure 4 experiment.

Two sets of signals were observed in the **C**H_2 (methylene) and **C**H (α-carbon atom) region of the $^{13}C\{^1H\}$ NMR spectrum (Fig. 3.50) acquired from another experiment using procedure 4. Four resonance signals are expected from a symmetrical molecule of the product mixture of procedure 4 in that region of the $^{13}C\{^1H\}$ NMR spectrum. There are two signals at 54 ppm, two at 56 ppm, two at 59 ppm and two at the 66 ppm regions respectively. Having only four resonance peaks in that region of the spectrum indicates that the product molecules formed were symmetrical. Having symmetrical molecules is consistent with the ^1H NMR shown in Fig. 3.49 with four methoxy doublets of unequal integration. However, the carbon environments of some of the diastereoisomers must be equivalent that only two signals are observed in the $^{13}C\{^1H\}$ NMR. This is not surprising given the resolution obtainable from $^{13}C\{^1H\}$ NMR experiments where the decoupling parameter improves sensitivity by focusing the otherwise multiplets into a single sharp peak, with added sensitivity gained due to the nuclear overhauser effect (NOE).

The number of signals in an NMR spectrum indicates the number of diastereoisomers present in the product mixture but symmetry in molecules can reduce this number. There may at least be four pairs of diastereoisomers in the product mixture from procedure 4.

There is also another possibility of the presence of unsymmetrical molecules in the product mixtures obtained from these trien systems. If a given complex is unsymmetrical, then a total of 8 signals would be observed in the **C**H_2 and **C**H region of the $^{13}C\{^1H\}$ NMR spectrum for the benzoyl phosphonate derivatives made from procedure 4. The minor isomers isolated from previous research[39] in the group had asymmetric molecules. If asymmetric molecules were the case here, the peak integrals should be equal. Since the peak integrals are not equal in the ^1H NMR spectrum shown in Fig. 3.49, it can be concluded that the molecules in the product mixture are symmetrical.

Considering the **C**H_2 and **C**H region shown in Fig. 3.50, the resemblance in terms of chemical shifts (54, 56, 59 and 66 ppm) of the carbon atoms of the $^{13}C\{^1H\}$ NMR spectrum for compound **3.4** and its stereoisomers to that in the literature (53, 58, 60, 64 ppm) for the major isomers isolated from the carboxylate systems, can be a clue that the isomers present in the product mixture of **3.4** could have the protons on their α-carbon atoms on the amine faces of their meridional ligand fragments. It can therefore be argued that the hydride attack was selectively on the amine face of the complexes derived from procedure 4 using these phosphonate analogues as it was for the carboxylate systems. The minor isomers (asymmetric

molecules) isolated from previous research[39] in the Hartshorn group had resonance peaks from 47 – 64 ppm in the **C**H_2 and **C**H region of their $^{13}C\{^1H\}$ NMR spectrum.

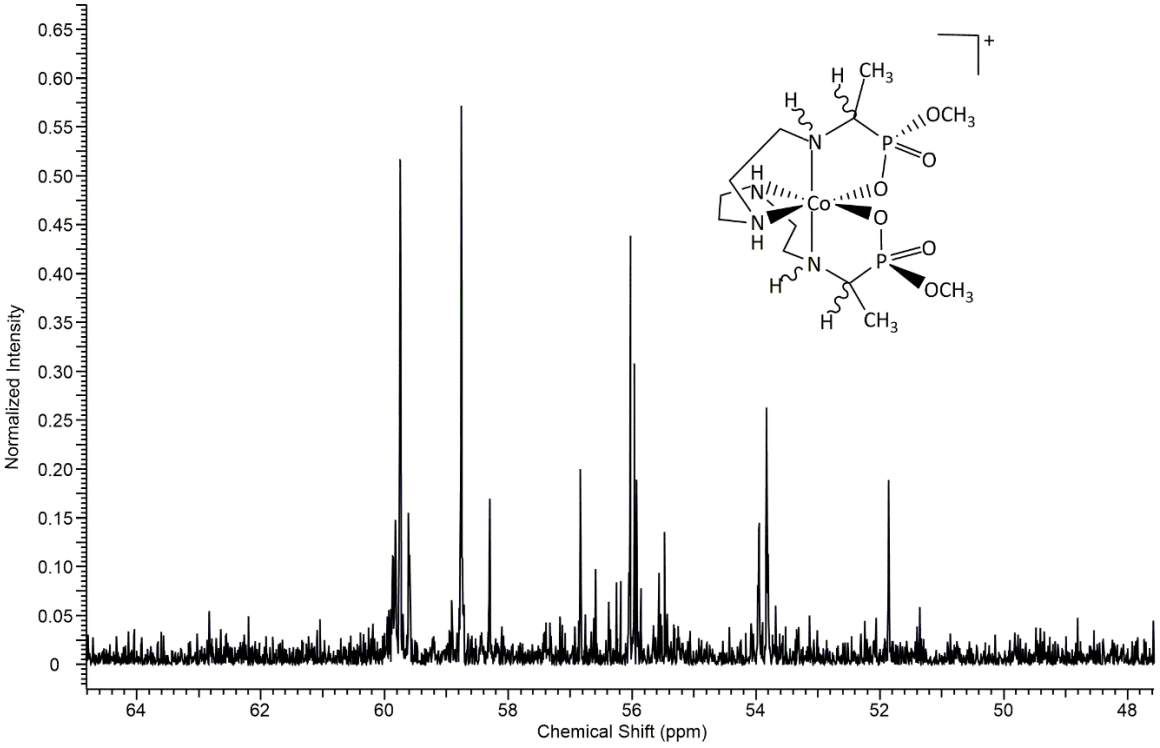

Figure 3.51 A region of the $^{13}C\{^1H\}$ NMR spectrum of the product mixture of **3.3** from procedure 3

The **C**H_2 and **C**H region of the $^{13}C\{^1H\}$ NMR spectrum shown in Fig. 3.51 was acquired from a sample of the product mixture of **3.3** from procedure 3. It was very noisy hence the application of power spectrum mode to minimise the noise for visual purposes. A symmetrical molecule (possessing a C_2 axis of rotation) as have been explained earlier, would have only four resonance peaks in the methylene and α-carbon region of its $^{13}C\{^1H\}$ NMR spectrum. There are four major peaks observed in that region of the spectrum shown in Fig. 3.51. Those signals have been assigned to a symmetrical molecule in the product mixture.

If a molecule from this system is not symmetrical, eight resonance peaks would be expected in this region of the spectrum. A careful look at the spectrum shown in Fig. 3.51 reveals some other minor signals in that region. These signals have been assigned to an unsymmetrical isomer because there are more than four of them. From a combination of spectral data, it appears that the product mixture of **3.3** is made up of one major pair of symmetrical stereoisomers and two minor unsymmetrical pairs of stereoisomers.

With respect to the major peaks observed in Fig. 3.51, it can also be argued that this major pair of symmetrical diastereoisomers of the mixture has had its hydride attack occurring on the amine face of the complex. This is because of the resemblance of its $^{13}C\{^{1}H\}$ NMR spectrum in terms of chemical shifts with those isolated and characterised in the literature as the amine-faced product. Fig. 3.52 shows the methyl region of the $^{13}C\{^{1}H\}$ NMR spectrum of **3.3** and it reveals the major symmetrical molecule dominates the mixture. The splitting pattern (a doublet) of the carbon signal is expected from the coupling effect of the NMR active neighbouring phosphorus atom.

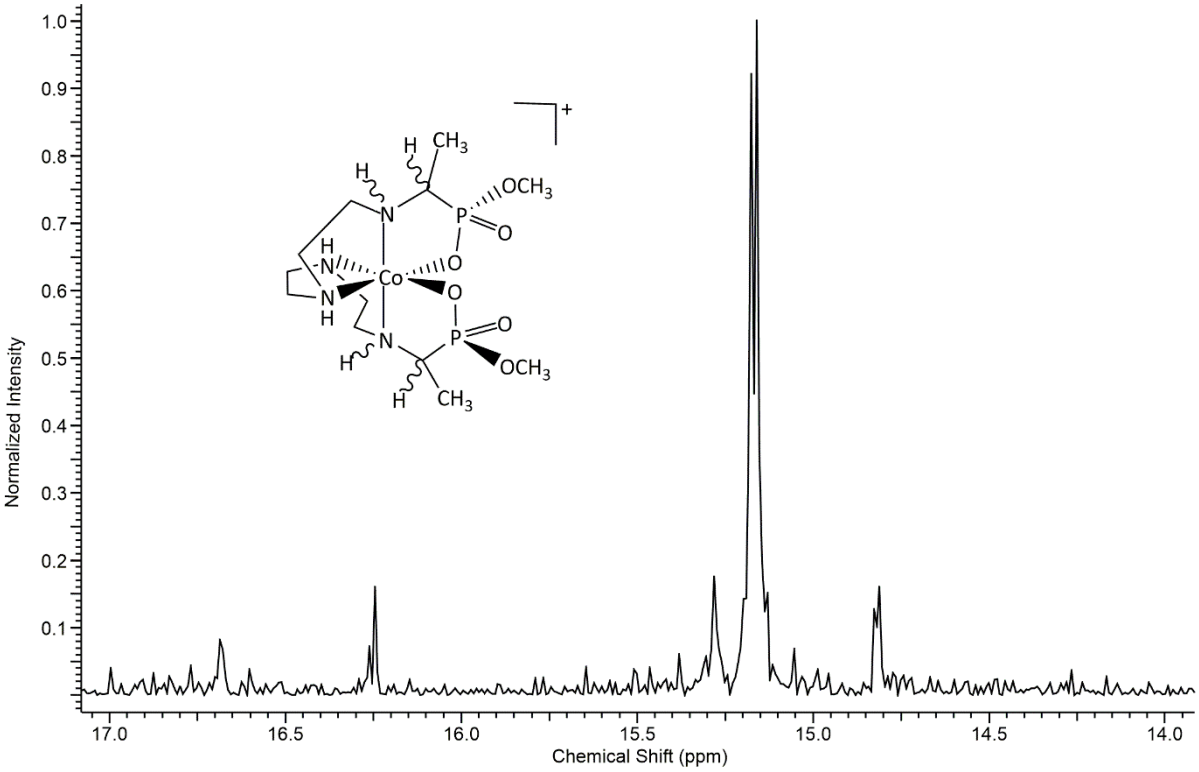

Figure 3.52 Methyl region of the $^{13}C\{^{1}H\}$ NMR spectrum of the product mixture of **3.3** from procedure 3

The $^{31}P\{^{1}H\}$ NMR spectrum from a sample of the product mixture from procedure 3 showed multiple signals. Four of these were assigned to four diastereoisomers in the product mixture. The noisy spectrum could not allow for a complete assignment to be done. However, it was outstanding that a major isomer was dominant in the mixture. Comparing the chemical shift of this major isomer's carbon atom (15 ppm) with that of the major isomer isolated and characterised in the literature (17 ppm), provides more support to the argument that the hydride attack is highly selective with most of it occurring on the amine face of these complexes. The

$^{13}C\{^{1}H\}$ NMR spectrum from a sample of the product mixture of **3.5** (a carboxylate-phosphonate complex) disclosed two overlapping doublets around 18 ppm for the protons of the methyl group. The overlap indicates similar chemical environments for all the methyl protons in the sample mixture. X-ray of the isolated compound **3.5** revealed the proton on the α-carbon atom of the phosphonate group had been added on the amine face of the complex, supporting the hypothesis for the facial selectivity of the hydride attack. A detailed discussion of the carboxylate-phosphonate system can be found in the sections that follow.

The ^{1}H NMR spectrum (Fig. 3.53) obtained from a sample of the product mixture of **3.3** was too complicated. It showed multiple isomers were present in the product mixture. A complete assignment was not possible. The slightly upfield chemical shifts (1.5 ppm) observed for some of the methyl protons, apart from the others (1.7 ppm) confirms the presence of two minor but outstanding unsymmetrical molecules in the product mixture. The ^{1}H spectrum also indicates the presence of one dominant and symmetric molecule in the methoxy region of the spectrum.

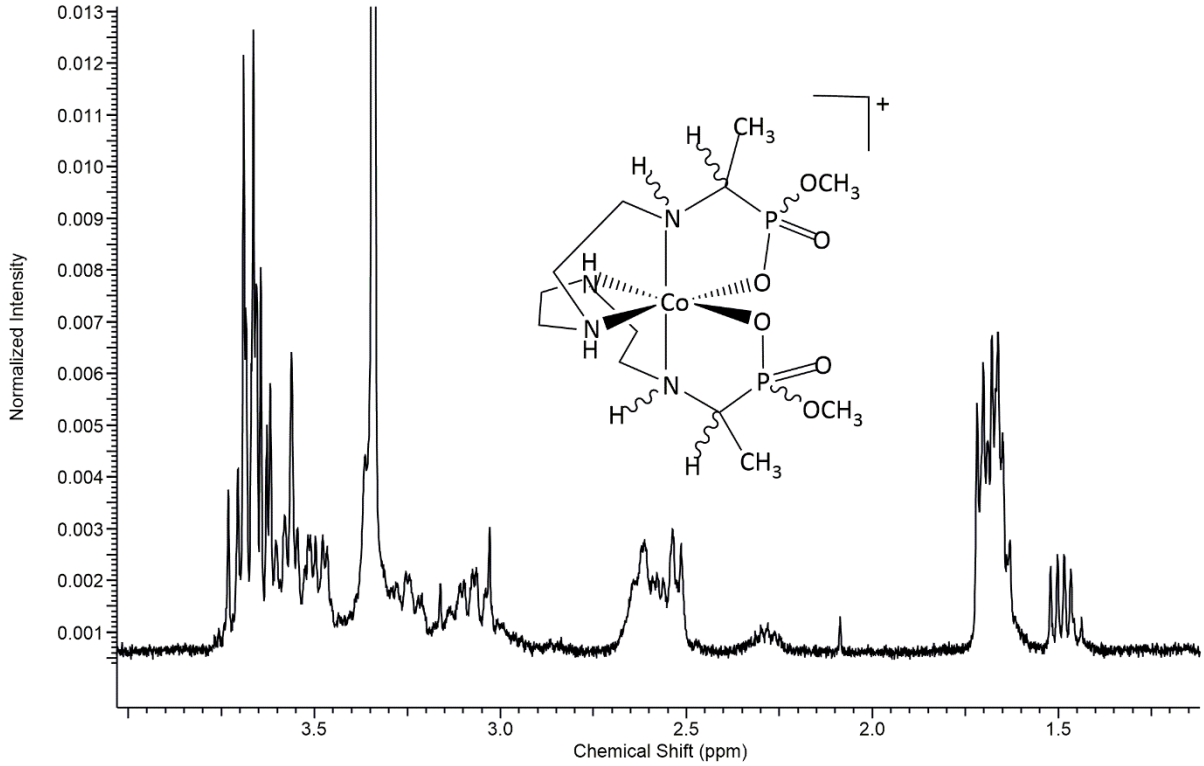

Figure 3.53 1H NMR of the product mixture of **3.3** from procedure 3

The intricacy introduced by the presence of more stereogenic centres in these trien systems has been highlighted by the NMR spectrum shown in Fig. 3.53. The methyl region (1.5 -1.7 ppm) is clustered by doublets. At least four doublets can be observed in that region; two major ones

and two minor ones. The integral values between the methyl region and the methoxy region (3.6 – 3.7 ppm) had a ratio of 1:1 as expected. However, it was difficult to integrate the individual doublets at the methoxy region. It can be concluded, however, that a major pair of symmetrical diastereoisomers dominate the product mixture of **3.3** from procedure 3.

Ethane-1,2-diamine Based Di-Amino Complexes of Cobalt(III)

Compounds from procedure 8 were made by reacting excess sodium borohydride with isolated imine complexes of cobalt(III) precoordinated with the diamine ligand ethane-1,2-diamine (en). The complexes formed (**3.8** and its stereoisomers) are expected to have four new stereogenic centres as shown in Fig. 3.54 introduced by the borohydride reduction.

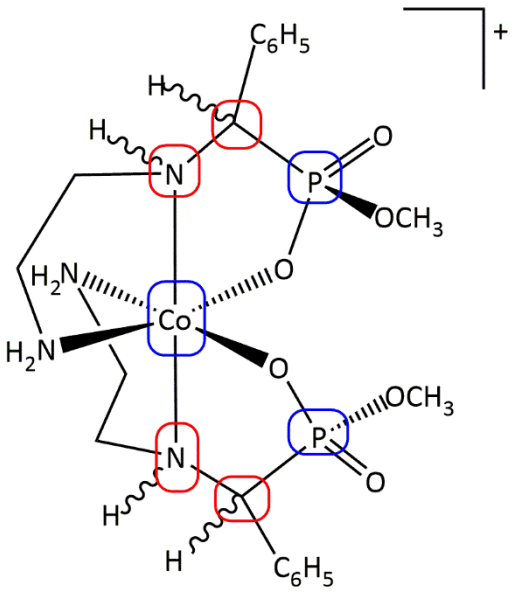

Figure 3.54 A molecule from procedure 8. New stereogenic centres are highlighted in red while blue highlights already existing stereogenic centres before the reduction reaction.

These en based systems are expected to behave like the trien based analogues. Once again, if the initial polydentate wrapping around the metal centre and the configurations at the phosphorus centres are retained, twenty stereoisomers (ten diastereoisomers) could be formed from the reduction reaction of these en systems assuming that a C_2 axis of rotation exists in given molecule.[39, 52]

The imine precursor used for procedure 8 was the symmetrical compound **2.10** from chapter 2 of this thesis. It is therefore expected that the symmetry would be retained in the product

molecules. If that was the case then, fewer isomers would be observed in the NMR spectrum. However, the ^{1}H NMR spectrum shows multiple number of stereoisomers were present in the product mixture.

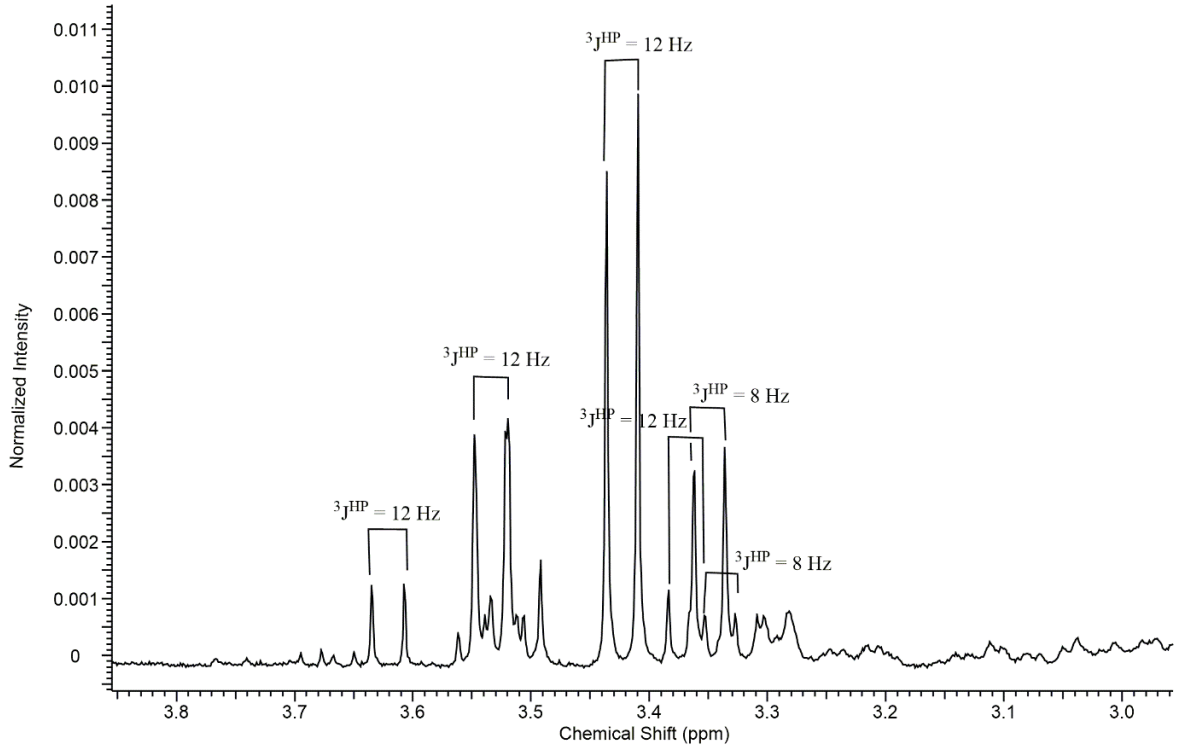

Figure 3.55 Methoxy region of the ^{1}H NMR spectrum from procedure 8 showing coupling constants.

If an asymmetric molecule, with respect to the chirality at the phosphorus centres, is in the mixture, the two methoxy groups would have their protons resonating at slightly different chemical shifts. However, both peaks (doublets) from these two different methoxy groups would have similar intensities (integral values). The spectrum shown in Fig. 3.55 shows two minor doublets at 3.35 and 3.54 ppm respectively with approximately 1:1 integral ratio. Two pairs of diastereoisomers, among others, can be identified based on their coupling constants as well as their integral values, in the methoxy region of the spectrum. One of the pairs of diastereoisomers should be symmetrical with both methoxy groups' protons resonating as one tall doublet at 3.4 ppm with an integral value of 2 relative to the two other doublets (integral value of 1 each). The two doublets of equal intensity have been assigned to an unsymmetrical pair of diastereoisomers. There are yet other doublets in the intricate spectrum. The product mixture from procedure 8 must be made up of some combination of both symmetric and asymmetric molecules, where the asymmetry could be generated from the different chiral centres present in a given molecule.

The similarities between the NMR spectra of these en based amino complexes with those from the trien systems can be translated to mean that their mixtures contain similar components in terms of stereochemistry at chiral centres.

Trien Based Di-Amino Carboxylato-Phosphonate Complexes of Cobalt(III)

Compounds from procedure 5 were made by reacting excess sodium borohydride with isolated imine complexes of cobalt(III) precoordinated with the polyamine (N′-[2-(2-aminoethylamino)ethyl]ethane-1,2-diamine); trien. The complexes formed (**3.5** and their stereoisomers) are expected to have four new stereogenic centres as shown in Fig. 3.56 introduced by the borohydride reduction. An isomer of compound **3.5** was isolated and characterised using single crystal X-ray diffraction (section 3.3.1). The hydride on its carboxylate end had been added through the phosphonate face of the di-imine complex. On the other hand, the hydride attack on the imine on the phosphonate end of the molecule had occurred through the amine face of the complex.

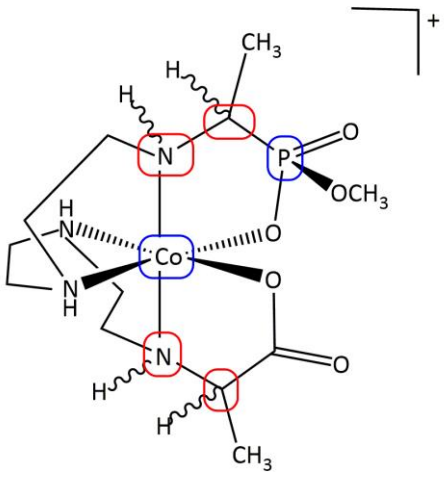

Figure 3.56 A molecule from procedure 5. New stereogenic centres are highlighted in red while blue highlights already existing stereogenic centres before the reduction reaction.

Compound **3.5** and its stereoisomers are expected to behave not differently from the other trien based compounds described earlier. The trien polyamine's symmetry does not count in these systems because each arm of the complex is different from the other. Thus, each molecule is expected to be unsymmetrical. This asymmetry does not, however, remove completely the limitations placed on the possible number of outcomes from different combinations of the configurations that could be generated from the many stereogenic centres in one given molecule of the complex. However, if the original configurations around the already existing

stereogenic centres are preserved in the new molecules created from the reduction reaction, then fewer isomers could result from procedure 5. If the wrapping of the polyamine around the metal ion and the chirality at the phosphorus stereogenic centre are kept constant, then at least twelve diastereoisomers (Fig. 3.57) are formed.

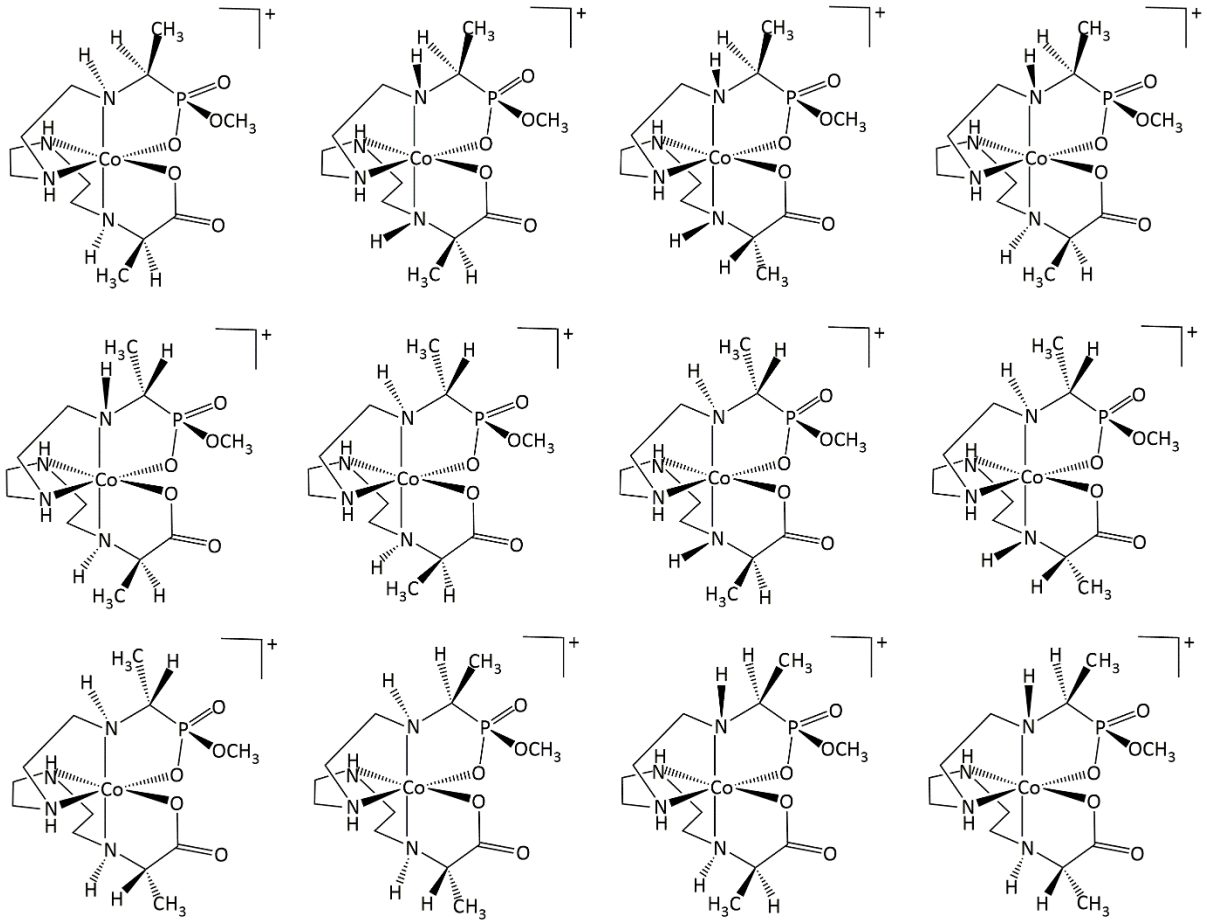

Figure 3.57 Twelve diastereoisomers predicted for the trien based carboxylate-phosphonate systems. Polydentate wrapping around the metal ion and chirality at the phosphorus centre have been kept constant.

Hence it is expected that the NMR spectra for these compounds would be complicated. The complexity should emerge from the similarity of methylene protons from the polyamine backbone as well as the multiplicity of the splitting pattern that could be generated from having two different chemical environments on each arm of the complex with potential for possible overlap of resonance peaks in the same region of a spectrum.

Figure 3.58 shows the methyl region of the $^{13}C\{^{1}H\}$ NMR spectrum acquired from a sample of the product mixture of **3.5**. The doublets around 18 ppm have been assigned to the carbons

of the methyl group on the phosphonate arm of the complex. The reason was because the expected splitting pattern for a carbon atom close to a phosphorus atom is a doublet and the comparison to spectra for complexes containing only phosphonates. There appears to be at least two sets of doublets overlapped in that region of the spectrum. The singlet at 15 ppm has been assigned to carbons of the methyl group on the carboxylate arm of the complex. The decoupled ($^{13}C\{^{1}H\}$) experiment meant that coupling effects from protons were not observed. Due to the noise in that spectrum, minor peaks have not been assigned to avoid errors. The spectrum (Fig. 3.58) has been shown in the power spectrum mode in order to minimise the noise for visual purposes.

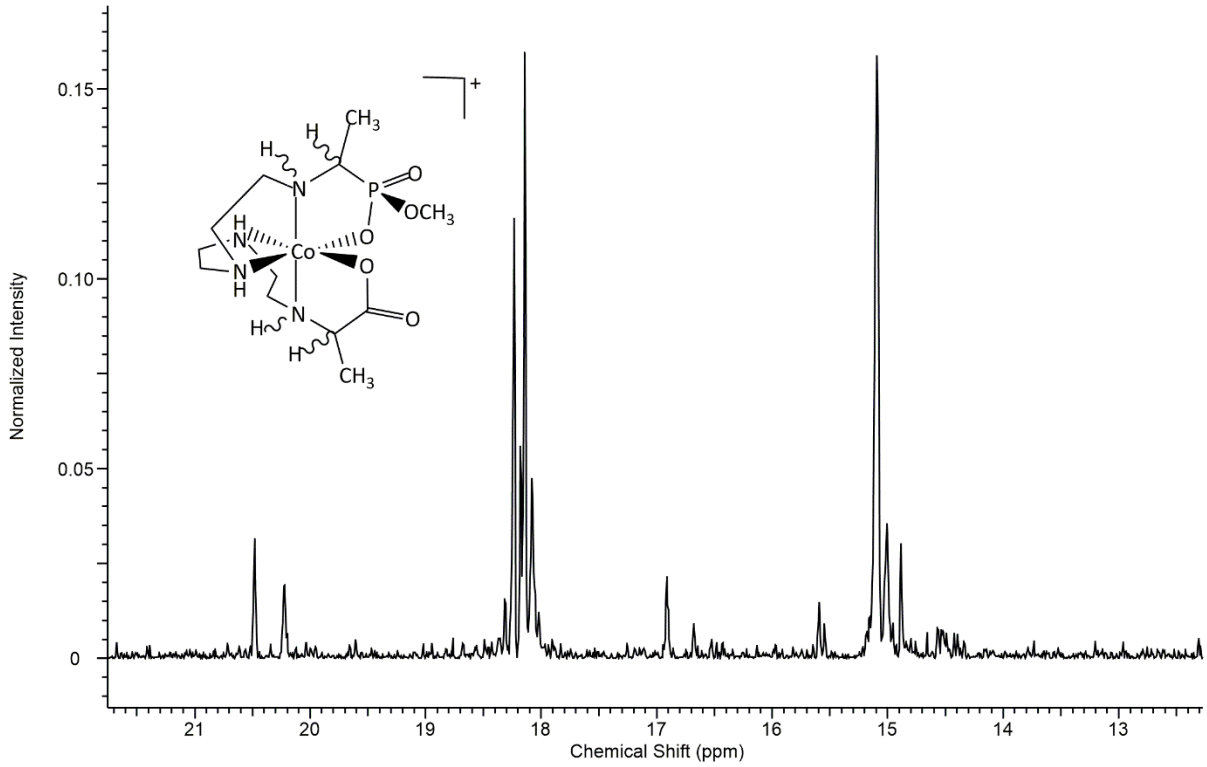

Figure 3.58 Methyl region of the $^{13}C\{^{1}H\}$ NMR spectrum of the product mixture from procedure 5 showing the presence of multiple isomers. Shown in power spectrum mode to minimise noise.

The rest of the $^{13}C\{^{1}H\}$ NMR spectrum had the expected number of resonance signals above the noise level among minor ones. Eight major peaks were observed in the methylene (**C**H_2) and α-carbon (**C**H) region of the spectrum. There appeared to be two sets of peaks for each signal region even though the spectrum was noisy. The carbonyl (**C**=O) region had five signals. The $^{31}P\{^{1}H\}$ NMR spectrum was also noisy but five resonance peaks were observed above the noise level. It is hard to provide more information on the number of isomers that were in the

product mixture with the available tools. It can thus be reported that the mixture from procedure 5 has multiple isomers.

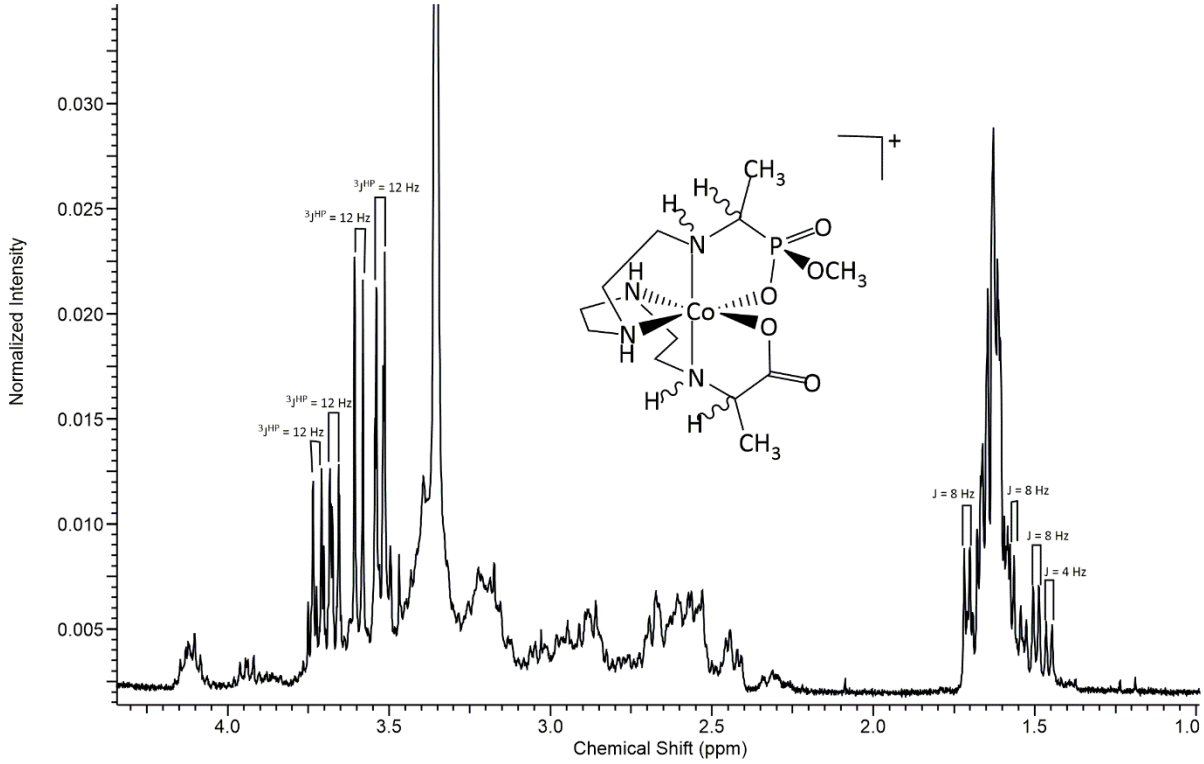

Figure 3.59 A region of the ^{1}H NMR spectrum of the product mixture from procedure 5 showing the presence of multiple isomers.

Fig. 3.59 shows a region of the ^{1}H NMR spectrum of a sample from the product mixture of procedure 5. This spectrum confirms that there are multiple isomers in the mixture as predicted. Four isomers can be identified easily with the doublets' coupling constants (J), even though it was hard to isolate the methyl groups on each end (either carboxylate or phosphonate) of the molecule as they had similar J values. The literature $^{3}J^{HH}$ was 6.9 Hz. There are other doublets overlapped in both the methyl and methoxy regions of the spectrum. Overall, it seems there are not as many as twelve diastereoisomers in the product mixture.

The spectrum obtained from mass spectrometry was as expected for this mixture.

The crystal structure of an isomer of **3.5** was obtained from another experiment and the crystals were insufficient for an NMR experiment. The isomer shown in Fig. 3.27 shows that the hydride attack had occurred on the phosphonate face of the complex at one of the imines while the other imine has the hydride added from the amine face of the complex. It is hard to decipher

whether that structure represents the major or minor component of the product mixture from procedure 5 without comparing their NMR spectra.

3.4 Conclusions

The imine complexes synthesised in chapter 2 of this thesis were converted to their amine derivatives through reduction. Some carboxylate complexes were also synthesized. Sodium borohydride was the reducing agent used for all the procedures described in this chapter. The reduction chemistry mimicked that from previous studies, especially the studies done in the Hartshorn group.

^{1}H NMR spectra for these amino acid complexes of cobalt(III) with phosphonates and carboxylates, were very useful for their characterisation. The first indication that the reduction reaction was successfully carried out was usually the appearance of a new set of peaks at the 1.6 ppm region of the spectrum. For the pyruvate derived complexes, the methyl group of the imine precursor resonates as a singlet in the ^{1}H NMR spectrum around the 2.6 ppm region. That signal splits into a doublet after the reduction reaction by reason of the introduction of a hydrogen to the α-carbon atom by the reducing agent. Appearance of new sets of peaks upfield (around 1.6 ppm) was also the case for the phosphonate derived systems even though the multiplicity of these new sets of peaks was more complicated from the presence of the NMR active ^{31}P nuclei proximate to the α-carbon atom in those complexes. Protons of the methyl group of the phosphonate systems were expected to appear as doublet of doublets from coupling to the newly introduced hydrogen atom (on the α-carbon atom) and also to the phosphorus nucleus. However, the peak overlap (from stereoisomers) in that region of the ^{1}H NMR spectrum for those complexes did not allow for complete assignment.

The X-ray structures isolated in this section had the Δ*mffm* configuration of the polydentate wrapping around the cobalt(III) metal centre, with the tetraen derivatives having an extra *a* descriptor to have the Δ*mffm*$_a$ configuration, where *a* represents the configuration (*anti*) of the hydrogen on the meridional nitrogen atom with respect to the rest of the polyamine fold.

A combination of the ^{13}C{^{1}H} spectrum and the ^{1}H spectrum (Fig. 3.39) confirmed that two major components dominate the product mixture of **3.7**. They have been predicted to be Δ*mffm*(*RSR)* (and Λ*mffm*(*SRS)*) and Δ*mffm*(*SSR)* (and Λ*mffm*(*RRS)*) pairs of diastereoisomers. Two pairs of diastereoisomers were also found to dominate the product mixture of **3.2**. They were expected to have the absolute configurations of Δ*mffm(RRSR)* (and Λ*mffm(SSRS)*) and

Δ*mffm*(*RSSR)* (and Λ*mffm*(*SRRS)*) as have been schematised in Fig. 3.36. A combination of spectra obtained from a sample of the product mixture for compound **3.1** and its stereoisomers led to the conclusion that were four compounds in the product mixture. These four compounds are expected to have the following absolute configurations: Δ*mffm*(*RSSR)*, Δ*mffm*(*RRSR)*, Δ*mffm*(*RSSS)*, Δ*mffm*(*RRSS)* and their enantiomers (schematised in Fig. 3.43).

The X-ray structure of **3.5** showed that the hydrogen of the α-carbon atom on the carboxylate group of the complex was added on the phosphonate face of the complex. It meant that the reduction of the carboxylate imine had gone with the hydride attack from the phosphonate face. On the contrary, but in consistence with the literature, the hydrogen on the α-carbon atom of the phosphonate group was added on the amine face of the complex thereby providing support evidence that the amine-faced addition is the dominant form of hydride attack from previous research where it was shown to be 92% selective.

$^{13}C\{^{1}H\}$ NMR spectrum from a sample of the product mixture of **3.5** disclosed two overlapping doublets around 18 ppm for the protons of the methyl group. The overlap indicated similar chemical environments for all the methyl protons in the sample mixture. The occurrence of the resonance peaks (methyl and methylene nuclei) from the current phosphonate systems in the same region of the ^{1}H and $^{13}C\{^{1}H\}$ NMR spectra with those of the carboxylates, indicated that the isomers produced in the present project could be related in terms of stereochemistry with those in the literature. Therefore, it was postulated that the hydride attack has dominantly occurred from the more hindered face of the phosphonate tetraen systems or from the amine faces of the majority of the other systems.

References

39. Wilson-Coutts, S. M. The Synthesis and Configuration of Some Polydentate Amino Acid Complexes of Cobalt (III). A thesis submitted in partial fulfiment of the requirements for a Master of Science degree in Chemistry at the University of Canterbury, 2009.

50. Hartshorn, R. M. Reactions of chelated ligands. A thesis submitted in partial fulfilment of the requirements for the degree of Doctor of Philosophy in Chemistry at the Australian National University 1989.

52. Wilson-Coutts, S. M.; Browne, J. M.; Marsh, L. C.; Polson, M. I.; Hartshorn, R. M., High diastereoselectivity in borohydride reductions of coordinated imines. *Dalton Transactions* **2012,** *41* (5), 1591-1596.

55. Browne, J. M. Intramolecular Condensation Reactions of Cobalt (III) Complexes. A Thesis Submitted in Partial Fulfilment of the Requirements for the Degree of Master of Science in Chemistry at the University of Canterbury, University of Canterbury, 2000.

57. Pearce, D. A.; Hartshorn, R. M.; Sargeson, A. M., Facile reduction of coordinated α-imino acids to amino acids by dithionite and borohydride. *Journal of the Chemical Society, Dalton Transactions* **2002,** (8), 1747-1752.

100. CrysAlis, P., Oxford Diffraction Ltd. *Yarnton, England* **2009**.

101. Dolomanov, O. V.; Bourhis, L. J.; Gildea, R. J.; Howard, J. A.; Puschmann, H., OLEX2: a complete structure solution, refinement and analysis program. *Journal of Applied Crystallography* **2009,** *42* (2), 339-341.

102. Sheldrick, G. M., SHELXT–Integrated space-group and crystal-structure determination. *Acta Crystallographica Section A: Foundations and Advances* **2015,** *71* (1), 3-8.

103. Sheldrick, G. M., Crystal structure refinement with SHELXL. *Acta Crystallographica Section C: Structural Chemistry* **2015,** *71* (1), 3-8.

Chapter 4. Synthesis and Reactivity of Chelated Carboxylate Ester and Phosphonate Ester Complexes

4.1 Introduction

Amides (RC(O)NR′R″) are the fundamental connections within protein architectures and as such represent an important synthetic target. Classically, the amide functional group (the peptide bond) is made *via* the dehydrative coupling of carboxylic acids and amines.

The chemical synthesis of peptides is not a rapid process in the absence of peptide-forming enzymes.[127] However, the synthetic utility of the chemical method (in the absence of enzymes) allows for a wide variation with the inclusion of non-naturally occurring amino acids and other 'spacer' reagents thereby producing new reagents of biochemical and pharmacological usefulness.[75] In order to speed up the process of the chemical synthesis (Fig.4.1), some form of activation is required. This activation is achieved using common activating agents like (**2**) dicyclohexylcarbodiimide (DCC) or diisopropylcarbodiimide (DIC), often in conjunction with additives such as N-hydroxysuccinimide (HOSu) or 1-hydroxybenzotriazole (HOBt).

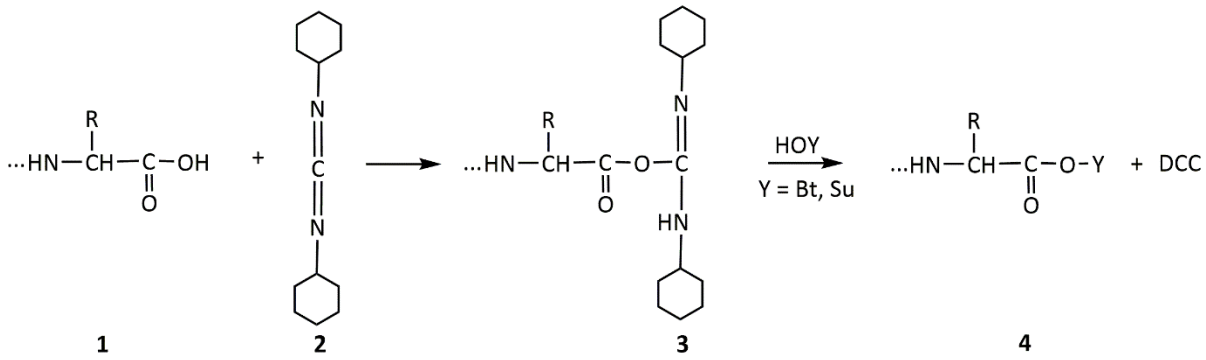

Figure 4.1 Scheme for the chemical synthesis of peptides[75]

All such chemical methods are known to involve some racemization of chiral centres and efforts are made to reduce this to the barest minimum[75].

These coupling reagents react with the carboxyl group of (**1**) to form a highly reactive O-acyl isourea intermediate (**3**) that is converted to its N-acyl derivative (**4**), which is less prone to racemization under the experimental conditions. A nucleophilic attack from the deprotected primary amino group on the N-terminus of the growing peptide chain forms the nascent peptide bond (Fig. 4.2).

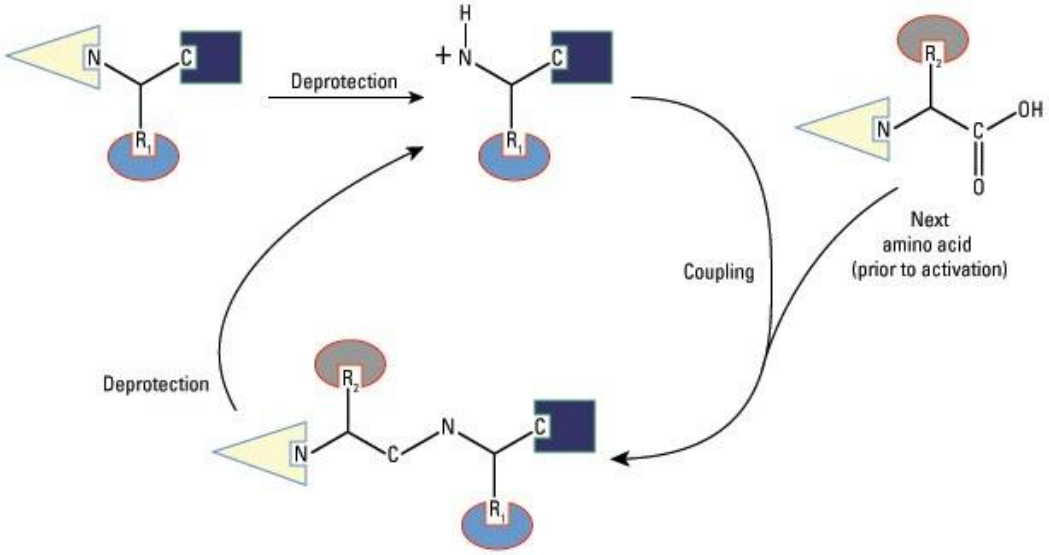

Figure 4.2[128] The N-terminal protecting group on the C-terminal amino acid of the peptide to be synthesized is first deprotected. After removing the unbound protecting groups, the next amino acid is activated at the C-terminal end by a coupling agent (e.g., DCC; not shown), which facilitates peptide bond formation between the deprotected N-terminus of the first amino acid and the activated C-terminus of the incoming amino acid. The new N-terminus of the growing peptide is then deprotected and coupled to the next amino acid. This cycle of deprotection and coupling is repeated until the full-length peptide is formed.

Carbodiimides form such a reactive intermediate that racemization of the amino acid can occur. Therefore, reagents that react with the O-acylisourea intermediate are often added, (HONSu or HOBt), which forms a less-reactive intermediate that reduces the risk of racemization.

Additionally, side reactions caused by carbodiimides have led to the examination of other coupling agents, including benzotriazol-1-yl-oxy-tris(dimethylamino)phosphonium hexafluorophosphate (BOP) and 2-(1H-benzotriazol-1-yl)-1,1,3,3-tetramethyluronium hexafluorophosphate (HBTU), which both require activating bases to mediate amino acid coupling.[128]

Some groups of scientists[63, 64, 66, 75, 129] discovered that peptides could also be synthesised through a cobalt(III) chelated amino acid ester reactant (**6**) as schematised in Fig. 4.3. The chelated ester is synthesised through the esterification of a cobalt(III) amino acid complex (**5**) using methyl triflate ($CF_3SO_3CH_3$). Another amino acid (or peptide) is coupled to the carbonyl-C of (**6**) through a nucleophilic attack by the N-terminal of the incoming amino acid (or peptide) to form a small peptide (**7**).

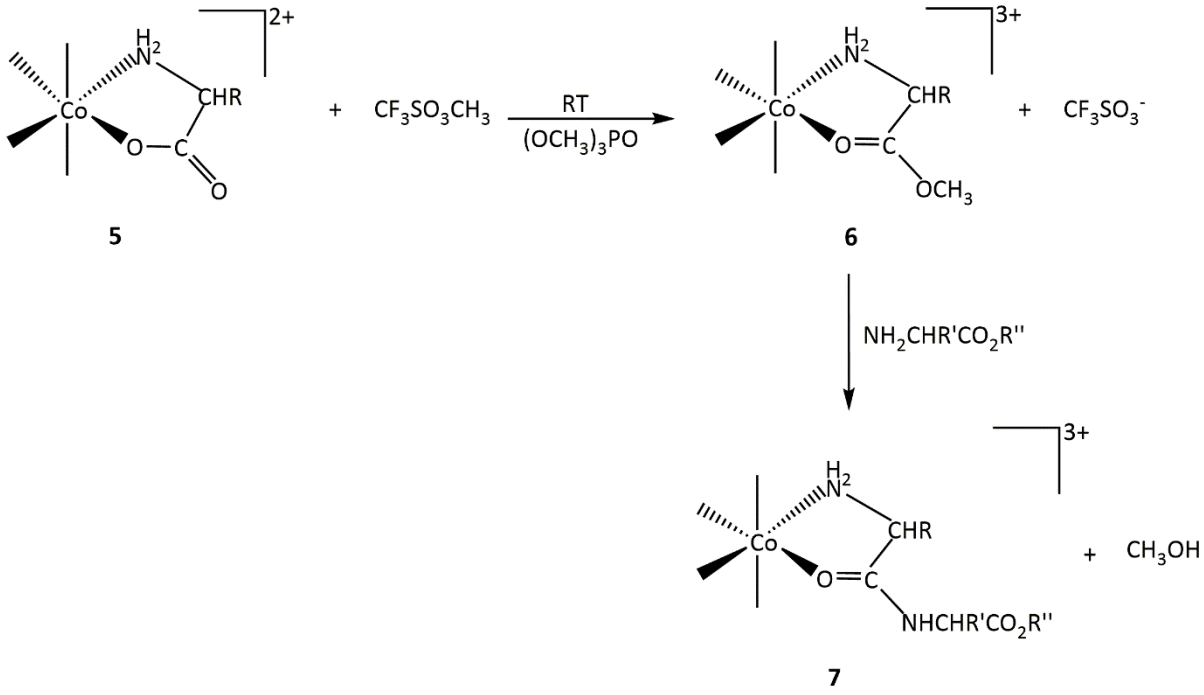

Figure 4.3 Reaction scheme for the cobalt(III)-promoted synthesis of small peptides[63, 64]

Peptide synthesis on the metal was discovered when β_2–[Co(trien)(glyOEt)Cl]$(ClO_4)_2$ was treated with glyOEt in an non-aqueous environment.[63] The significance of using cobalt(III) stems from the relative kinetic inertness it offers. This provides a greater likelihood for the identification of reaction intermediates which could facilitate the differentiation of reaction pathways and subsequently help establish reaction mechanisms. The ester chelate (**6**) has been reported to condense readily with amino acid esters and small peptides[63, 64] as in Fig. 4.4.

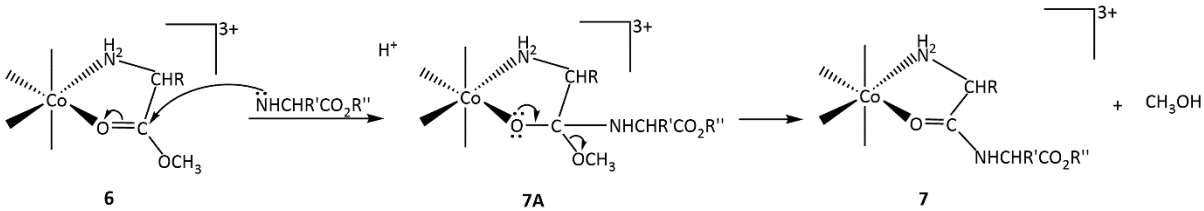

Figure 4.4 Cobalt(III)-mediated peptide synthesis coupling reaction.[66]

The use of $Co(NH_3)_5$ centre as a protecting group in solution-phase peptide synthesis was first proposed in 1978 by Isied and Kuehn[130]. No activation of the peptide-forming step is required.

Kinetic studies[67] demonstrated that the rate of the coupling reaction of the coordinated amino acid ester is enhanced by about 10^6 times more than that of the uncoordinated amino acid ester. The metal ion accounts for this enhancement by its electron withdrawing effect which makes the carbon of the carbonyl group more electrophilic so that it can undergo nucleophilic attack by an incoming nucleophile. The metal ion also enhances C-H acidity at the α-carbon atom through the additional binding of the amine nitrogen.

This cobalt(III) method does not only provide an alternative route to peptide synthesis, it also provides both N-terminal protection (necessary for preventing any attack on the incoming amino acid carbonyl-C) and carbonyl-O activation (for directing the nucleophilic attack by the N-terminal of the incoming amino acid to the carbonyl-C of the complex) in one system and makes coloured compounds which are generally water soluble (essential for biological applications). The metal ion and the ligands can be removed by chemical or electrochemical reduction methods.[75]

The synthetic potential of amino acid ester chelates (such as (**6**) in Fig. 4.5) was first perceived by the isolation of $[Co(en)_2(GlyOMe)](ClO_4)_3$ in 1967[64]. Initial attempts to prepare the cobalt(III) complexes by direct acid-catalysed esterification of $[Co(N)_4(AAO)]^{n+}$ species proved partially successful with prolonged treatment, or heating, leading to decomposition of the complex. Later, it was discovered that alkylation, using either FSO_3CH_3 or $CF_3SO_3CH_3$ provided an efficient general route to methyl ester complexes.[75] These chelated esters act as intermediates in the cobalt(III) promoted peptide synthesis.

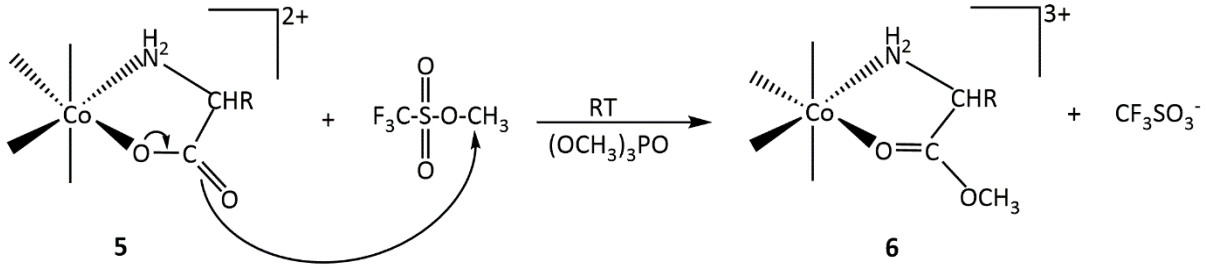

Figure 4.5 Formation of a chelated ester using methyl triflate.

In the absence of other nucleophiles, water attacks the positive centre, the carbonyl carbon, resulting in hydrolysis of the ester and formation of a 2+ species[72, 73] (Fig. 4.6) followed by the expulsion of the alkoxyl group. The hydrolysis of the chelated ester is also subject to general

nucleophilic or general base catalysis[73] and ^{18}O exchange data (Fig. 4.6) was used to establish that it is the acyl-oxygen that breaks[69, 75] in systems such as $[Co(en)_2(NH_2CH_2CO_2R)]^{2+}$.

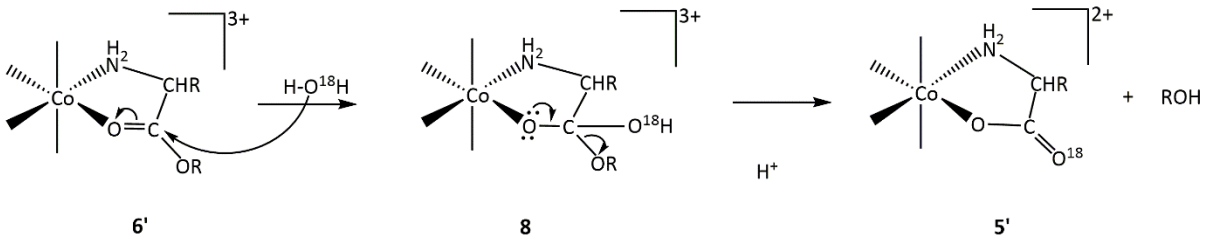

Figure 4.6 Cobalt(III)-promoted hydrolysis of an ester chelate by the nucleophilic attack of water[47] through a tetrahedral intermediate (**8**).

In 1951 Kroll[131] discovered that Cu^{2+} (and to a lesser extent Co^{2+} and Ni^{2+}) catalysed the hydrolysis of amino acid esters. Even though that early discovery prompted a lot of research in that area, exact descriptions of those exchange-labile systems were lacking.[75] Exploring the nature of the hydrolytic process became very important since it could highlight possible relationships to similar enzymatic processes which occur in biological systems. Investigations into the possibility of using chelated esters of the type shown as (**6**) for the N-terminal synthesis of peptides as well as for probing the mechanisms of ester hydrolysis and exchange begun in the early 1960s.

Precise mechanistic information has been provided by Browne et al.,[75] for studies done using exchange-inert complexes, particularly those containing cobalt(III) centres of the type *cis*-$[Co(N)_4(OH/H)(AAOR)]^{2+/3+}$ and $[Co(N)_4(AAOR)]^{3+}$ ($(N)_4 = (en)_2$, AA = Gly, β-Ala, R = Me, Et, i-Pr).

It was established[75] that the cobalt(III) centre, though generally regarded as lacking the polarizing power of a proton, accelerates OH^- catalysed hydrolysis by *ca*. 100-fold if attached to the N-terminus of an amino acid ester, as in $[Co(NH_3)_5(GlyOEt)]^{3-}$. The metal ion also directly activates the carbonyl function and also enhances C-H acidity at the α-carbon atom (by at least 10^6 times[75]) through the additional binding of the amine nitrogen. Such coordination results in substantial electron withdrawal from the carbonyl group which reflects in accelerated rates observed[75] for both OH^- catalysed and spontaneous hydrolyses by *ca*. 10^6. The hydrolysis occurs with little or no stereochemical change (S↔ R) at the α-carbon atom.[75]

Studies have shown that hydrolysis of the directly activated esters of the type shown as (**6′**) where R is methyl, ethyl or isopropyl ester, is accelerated by about 10^6 times by the cobalt(III) metal centre.[47, 63-75]

Reaction	k/mol^{-1} dm^3 s^{-1}; E_a/kJ mol^{-1}; s^{-1}; $\Delta S^{\ddagger}$/J K^{-1} mol^{-1}
	A. Esters
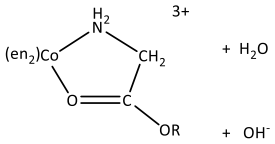	6.9 x 10^{-4} (R = Me) 2.0 x 10^{-5} (R = Pr'); E_a, 67; $\Delta S^{\ddagger}$, -122 2.3 x 10^{-5} (R = t-Bu) 8 x 10^5 (R = Pr'); E_a, 73; $\Delta S^{\ddagger}$, 164
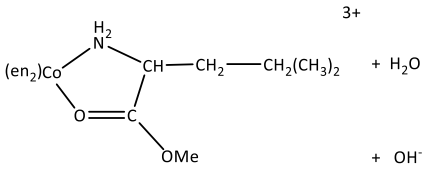	1.4 x 10^{-4} (Λ(S)) 5.8 x 10^{-5} (Δ(S)) 3 x 10^6 (Λ(S)) 1.4 x 10^6 (Δ(S))
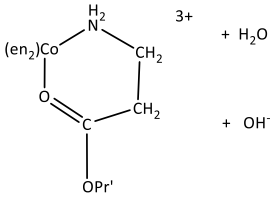	8.3 x 10^{-7} 4 x 10^4 (addition of OH- rate determining)

Table 4.1 Rate Constants for The Cobalt(III)-Promoted Hydrolysis of Coordinated Amino Acid Esters[67]

Table 4.1[67] gives the rates for the nucleophilic attack by water (k_{H2O}) and hydroxide (k_{OH}) paths along with provided activation parameters. Other bases in aqueous solutions do catalyse hydrolysis.[65, 73] They do so by direct attack at the carbonyl centre rather than by general base-catalysed solvent addition.[65]

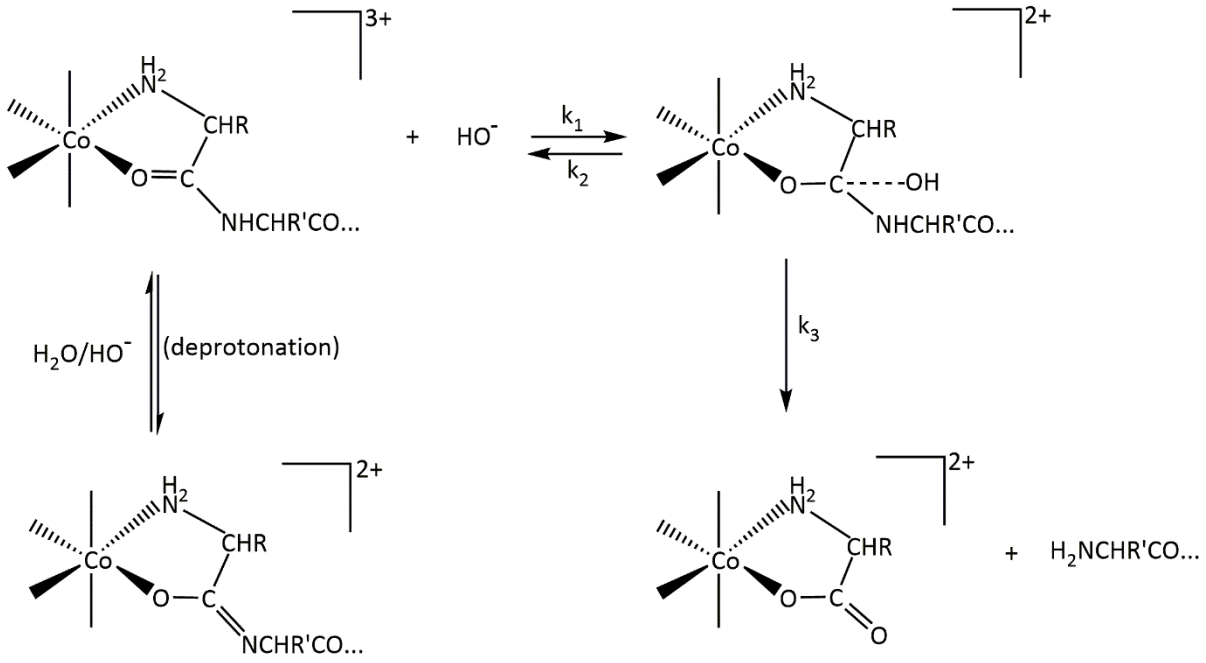

Figure 4.7 Full scheme of possible (and isolated) species in the cobalt(III)-promoted hydrolysis of amides[65]

Sutton and Buckingham observed that at pH 7-8, loss of HO^- (k_2) competes with loss of amine (k_3).[67]

In this present study, different polyamine ligands have been precoordinated to a cobalt(III) metal centre to produce synthetic amino acid compounds of the carboxylate and phosphonate groups. These amines were esterified using methyl triflate to form chelated esters. Carboxylate and phosphonate examples such as shown in Fig. 4.8 have been investigated.

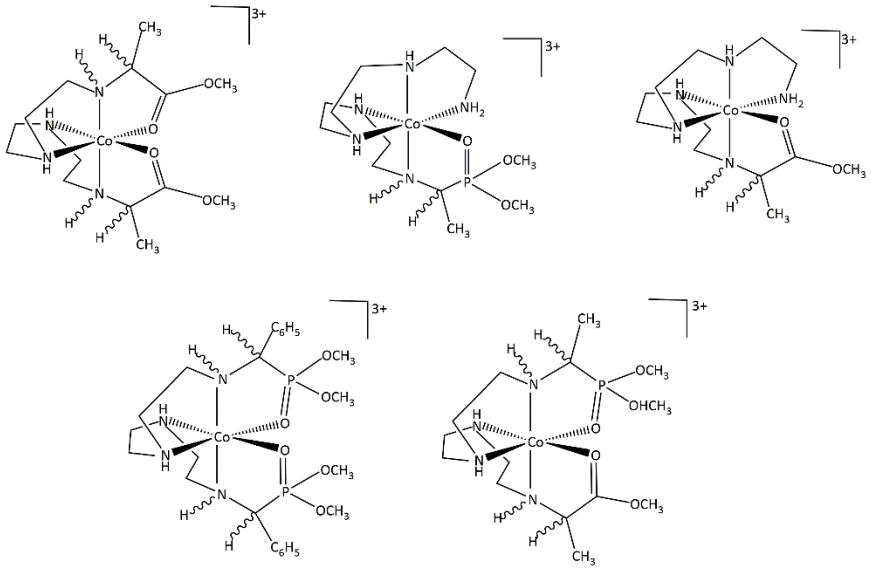

Figure 4.8 Some of the chelated carboxylate ester and phosphonate ester complexes synthesised in this project.

The reactivity of these cobalt(III) systems is expected to mimic those in the literature, by being active towards the addition of a nucleophile, thereby enabling small peptides to be formed through the chelated ester intermediates.

The chelated carboxylate ester and phosphonate ester complexes synthesised in this project were coupled with some amines including benzylamine, diamines like ethane-1,2-diamine, amino acid methyl esters, amino acid ethyl esters and a novel dipeptide made in the Hartshorn laboratory. These chelated ester intermediates and their small peptides have been reported in the sections that follow.

4.2 Experimental

4.2.1 Materials and Methods

Reagent grade chemicals (or better) were used without further purification, unless otherwise specified. Trimethyl phosphate was dried using 4 Å molecular sieves. Sephadex SPC 25 120 cation exchange resin and Sephadex G-10 were washed with distilled water before use for chromatographic separations and purification, where applicable. The trituration procedure as outlined in section 4.2.3 was used to precipitate compounds out of solution.

4.2.2 General Procedure for Esterification of the Phosphonate and Carboxylate Amino Acid Complexes of Cobalt(III)

For a complex with only one chelated ester site, four equivalents of methyl trifluoromethanesulfonate is reacted with one equivalent of the phosphonate (or carboxylate) cobalt(III) polyamine complex (typically on a 0.04 – 1 g scale). In the same vein, eight equivalents of methyl trifluoromethanesulfonate was used to treat those complexes with two chelate ester sites. The reaction is carried out in the minimum amount (2 – 9 mL) of trimethyl phosphate. The reaction mixture is then heated at 50^{o} C for 90 – 120 mins. During the reaction period, a drying tube filled with 4 Å molecular sieves was used to keep moisture away as much as is possible within a fume hood. Isolation of the products was done through trituration (section 4.2.4) of the product mixture using dry diethyl ether (or ACS grade where the dry solvent was not available). The resulting powder is usually hygroscopic and was stored in a desiccator over P_2O_5 upon silica gel.

4.2.3 General Procedure for Peptide Linkage of the Phosphonate and Carboxylate Amino Acid Chelated Esters of Cobalt(III)

For a complex with only one ester chelate, a minimum of two equivalents of an amino acid salt of choice, an amine or a diamine, were reacted with one equivalent of the phosphonate (or carboxylate) cobalt(III) polyamine complex (typically on a 0.06 – 0.5 g scale). In the same vein, a minimum of four equivalents of amino acid salts, amine or diamines was used to treat those complexes with two chelate rings. The reactions were carried out in methanol (typically 10 – 20 mL) heated at 50^{o} C for 60 - 120 mins. Some of the reactions have only been stirred for 5 - 30 mins. During the reaction period, a drying tube filled with 4 Å molecular sieves was used to keep moisture away as much as is possible within a fume hood. Isolation of the products was done through trituration (section 4.2.4) of the product mixture using dry diethyl ether (or ACS grade where the dry solvent was not available). The resulting powder is recovered through filtration and is stored in a desiccator over P_2O_5 upon silica gel.

4.2.4 The Trituration Procedure

At the end of the esterification or amide reaction, a solution is obtained, the colour of which depends on that of the starting cobalt(III) amino phosphonate (or carboxylate) complex obtained from chapter 3 of this thesis. The reaction mixture is allowed to cool before the trituration. An excess (150 – 250 mL) of diethyl ether is added to the solution and stirred vigorously with a magnetic flea (using a magnetic stirrer). After about 2 minutes of stirring, the suspension formed is allowed to settle. The diethyl ether layer becomes clear and is decanted off. The process is repeated until a powder is formed.

4.2.5 Measurements

NMR spectra were measured on an Agilent NMRS-400 spectrometer or JEOL JNM-ECZ series (400 and 600 MHz). ^{1}H and ^{31}P{^{1}H} NMR were recorded in deuterated methanol. Chemical shifts are reported in parts per million (ppm) from 3-(trimethylsilyl)propionic 2,2,3,3-d4 acid, sodium salt (TSP) (^{1}H, δ 0) as an internal standard or CD_3OD ((^{1}H, δ 3.31) and from 10% H_3PO_4 (^{31}P, δ 0) as external standard in ^{31}P{^{1}H} NMR. Mass spectrometry measurements were obtained using an UltiMate 3000 Mass Spectrometer.

4.2.6 Syntheses

Procedure 1

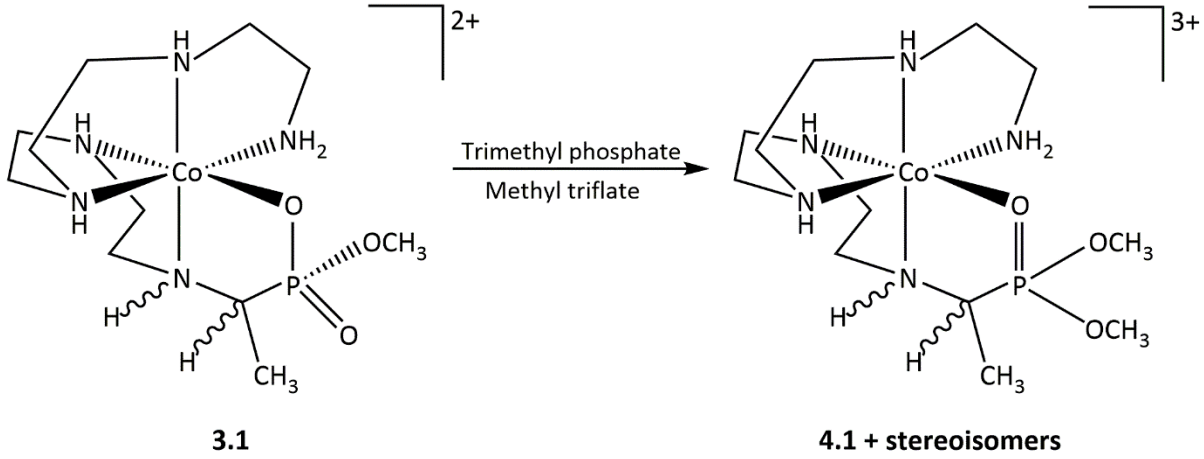

Figure 4.9 Reaction scheme for procedure 1

3.1 (0.24 g; 0.55 mmol) was dissolved in trimethyl phosphate ($P(O)(OCH_3)_3$) (3 mL). The reaction vessel was fitted with a drying tube filled with 4 Å molecular sieves. A 4-fold excess of methyl trifluoromethanesulfonate ($CF_3SO_2OCH_3$) (0.36 g; 2.2 mmol) was added. The mixture was heated at 50°C for 90 minutes, while stirring. The reaction mixture was allowed to cool before the trituration. Dry diethyl ether (150 mL) was used to triturate the mixture until a powder was obtained according to the procedure outlined in section 4.2.4.

^{1}H NMR: 1.61 (C**H**$_3$, dd, $^3J^{HP}$ = 16 Hz, $^3J^{HH}$ = 8 Hz), 1.76 (C**H**$_3$, dd, $^3J^{HP}$ = 16 Hz, $^3J^{HH}$ = 8 Hz), 2.50 – 2.76 (C**H**$_2$-NH, m), 2.91 – 3.20 (C**H**$_2$-NH, m), 3.35 (C**H**, q), 3.42 (C**H**, q), 3.59 (C**H**$_2$-NH_2, m), 3.72 (OC**H**$_3$, d, $^3J^{HP}$ = 12 Hz), 3.83 (OC**H**$_3$, d, $^3J^{HP}$ = 12 Hz), 4.13 (OC**H**$_3$, d, $^3J^{HP}$ = 8 Hz, major), 4.14 (OC**H**$_3$, d, $^3J^{HP}$ = 8 Hz, major), 4.56, 4.73, 5.09, 5.56, 5.90, 6.75, 6.86, 7.31 (N**H**, each peak broad); $^{31}P\{^1H\}$: 38.23, 38.54, 38.24, 40.87, 48.87 (major).

ESIMS: Calcd. for $[C_{12}H_{32}CoN_5O_3P]^{3+}$: 384.16; M/Z = 128.05. Found: 382.14 for $[C_{12}H_{30}CoN_5O_3P]^{1+}$; $[M\text{-}2H]^+$

Procedure 2

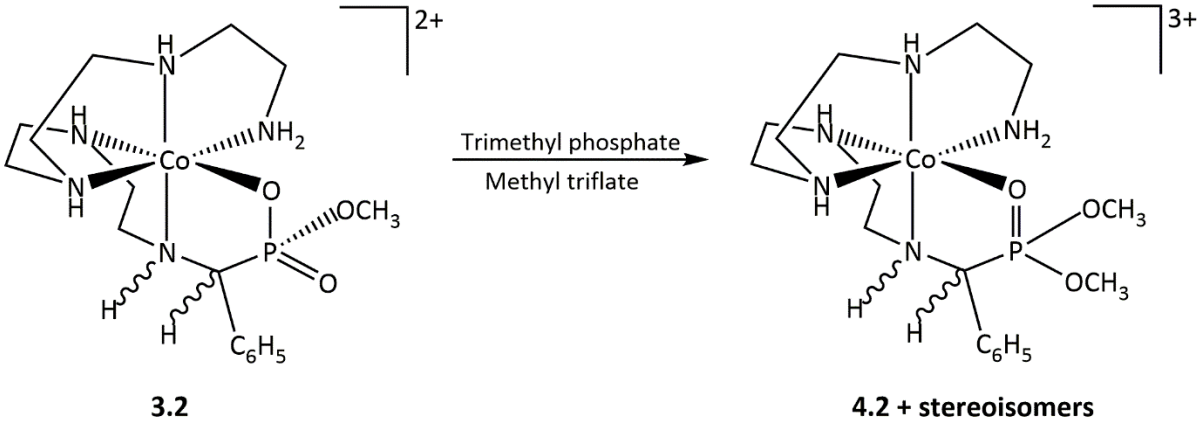

Figure 4.10 Reaction scheme for procedure 2

3.2 (0.10 g; 0.17 mmol) was dissolved in trimethyl phosphate ($P(O)(OCH_3)_3$) (2 mL). The reaction vessel was enclosed with a drying tube filled with 4 Å molecular sieves. A 4-fold excess of methyl trifluoromethanesulfonate ($CF_3SO_2OCH_3$) (0.11 g; 0.68 mmol) was added. The mixture was heated at 50°C for 90 mins. Dry diethyl ether (150 mL) was used to triturate the mixture until a powder was obtained according to the procedure outlined in section 4.2.4.

^{1}H NMR: 2.60 (C**H**$_2$-NH, m), 2.63 (C**H**$_2$-CH$_2$-NH, m), 2.67 (C**H**$_2$-NH, m), 2.71 (C**H**$_2$-CH$_2$-NH, m), 2.91 (C**H**$_2$-NH, m), 2.99 (C**H**$_2$-NH, m), 3.02 (C**H**$_2$-NH, m), 3.08 (C**H**$_2$-NH-CH$_2$, m), 3.12 (C**H**$_2$-NH-CH$_2$, m), 3.23 (CH$_2$-NH-C**H**$_2$, m), 3.37 (OC**H**$_3$, d, J^{HP} = 12 Hz), 3.47 (C**H**, m), 3.51 (C**H**, m), 3.56 (OC**H**$_3$, d, J^{HP} = 12 Hz), 3.69 (OC**H**$_3$, d, J^{HP} = 12 Hz), 4.09 (C**H**, m), 4.23 (N**H**, m), 4.54 (N**H**, m), 4.74, 5.07 (N**H**, m), 5.41, 5.78, 5.95, 6.42, 6.69, 6.99, 7.15 (N**H**, each peak broad), 7.45-7.54 (C$_6$**H**$_5$, m), 7.62-7.72 (C$_6$**H**$_5$, m); ^{31}P{^{1}H}: 33.87, 35.08 (major), 35.21 (major).

ESIMS: Calcd. for $[C_{17}H_{34}CoN_5O_3P]^{3+}$: 446.17; M/Z = 148.72. Found: 444.16 for $[C_{17}H_{32}CoN_5O_3P]^{1+}$; $[M-2H]^+$

Procedure 3

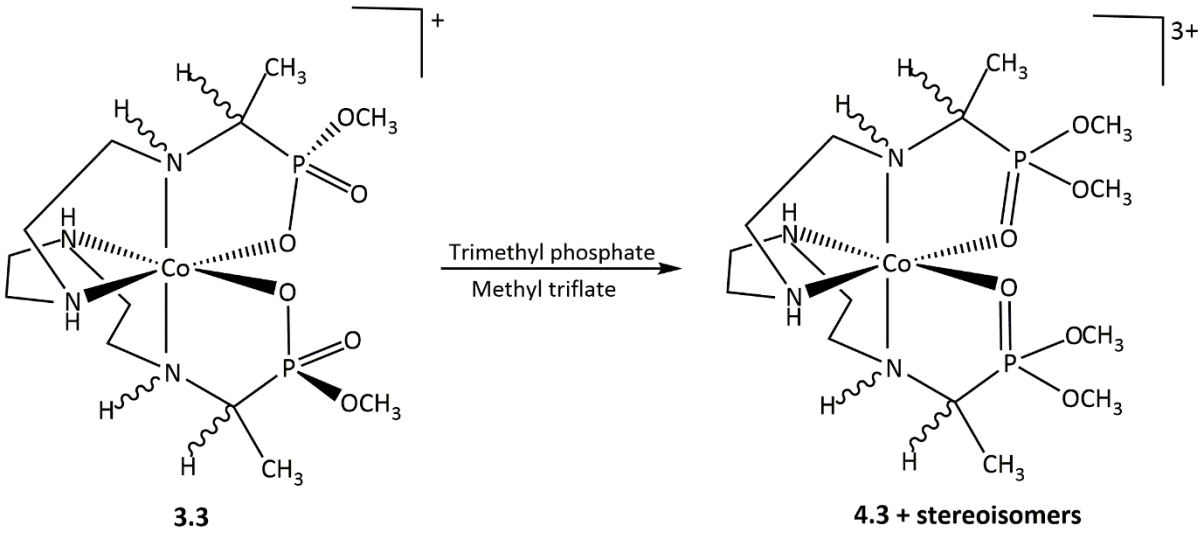

Figure 4.11 Reaction scheme for procedure 3

3.3 (0.28 g; 0.58 mmol) was dissolved in trimethyl phosphate ($P(O)(OCH_3)_3$) (3 mL). The reaction vessel was enclosed with a drying tube filled with 4 Å molecular sieves. An 8-fold excess of methyl trifluoromethanesulfonate ($CF_3SO_2OCH_3$) (0.76 g; 4.64 mmol) was added. The mixture was heated at 50°C heat for 90 mins. Dry diethyl ether (150 mL) was used to triturate the mixture until a powder was obtained according to the procedure outlined in section 4.2.4.

^{1}H NMR: 1.60 (C**H**$_3$, overlapping doublets), 1.68 (C**H**$_3$, dd, $^3J^{HP}$ = 16 Hz, $^3J^{HH}$ = 8 Hz), 2.70 (C**H**$_2$-NH, m), 2.73 (C**H**$_2$-NH, m), 3.13 (C**H**$_2$-NH, m), 3.34 (C**H**$_2$-NH, m), 3.38 (C**H**$_2$-NH, m), 3.58 (OC**H**$_3$, d, J^{HP} = 12 Hz), 3.68 (OC**H**$_3$, d, J^{HP} = 12 Hz), 3.98 (OC**H**$_3$, d, J^{HP} = 8 Hz), 4.02 (OC**H**$_3$, d, J^{HP} = 8 Hz), 4.11 (OC**H**$_3$, d, J^{HP} = 8 Hz), 4.13 (OC**H**$_3$, d, J^{HP} = 8 Hz).

ESIMS: Calcd. for $[C_{14}H_{36}CoN_4O_6P_2]^{3+}$: 477.14; M/Z = 159.05. Found: 475.13 for $[C_{14}H_{34}CoN_4O_6P_2]^{1+}$; $[M\text{-}2H]^+$

Procedure 4

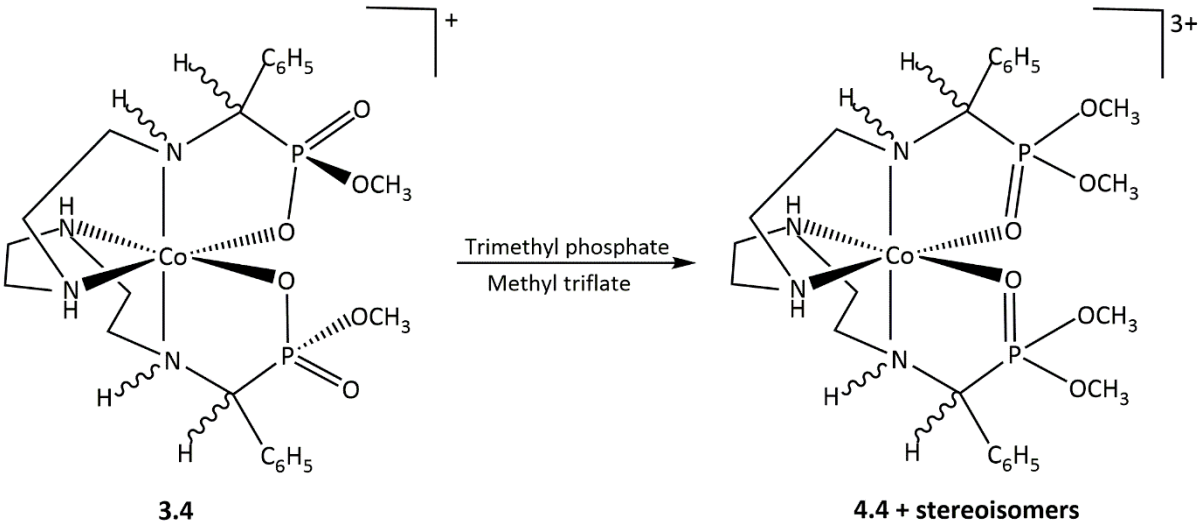

Figure 4.12 Reaction scheme for procedure 4

3.4 (0.04 g; 0.07 mmol) was dissolved in trimethyl phosphate ($P(O)(OCH_3)_3$) (2 mL). The reaction vessel was enclosed with a drying tube filled with 4 Å molecular sieves. An 8-fold excess of methyl trifluoromethanesulfonate ($CF_3SO_2OCH_3$) (0.09 g; 0.56 mmol) was added. The mixture was heated at 50°C for 90 minutes. Dry diethyl ether (150 mL) was used to triturate the mixture until a powder was obtained according to the procedure outlined in section 4.2.4.

^{1}H NMR: 3.11 (C**H**$_2$-NH, m), 3.23 (C**H**$_2$-NH, m), 3.33 (C**H**$_2$-NH, m), 3.40 – 3.51 (OC**H**$_3$, m), 3.57 (OC**H**$_3$, d, J^{HP} = 12 Hz), 3.62 (OC**H**$_3$, d, J^{HP} = 8 Hz), 3.70 – 3.76 (OC**H**$_3$, m), 3.96 (OC**H**$_3$, d, J^{HP} = 8 Hz), 4.09 (OC**H**$_3$, d, J^{HP} = 12 Hz), 4.10 (OC**H**$_3$, d, J^{HP} = 12 Hz), 4.18 (OC**H**$_3$, d, J^{HP} = 12 Hz), 7.52 (C$_6$**H**$_5$, m), 7.58 (C$_6$**H**$_5$, m), 7.73 (C$_6$**H**$_5$, m), 7.82 (C$_6$**H**$_5$, m); ^{31}P{^{1}H}: 34.34, 34.60, 44.24, 44.71.

Procedure 5

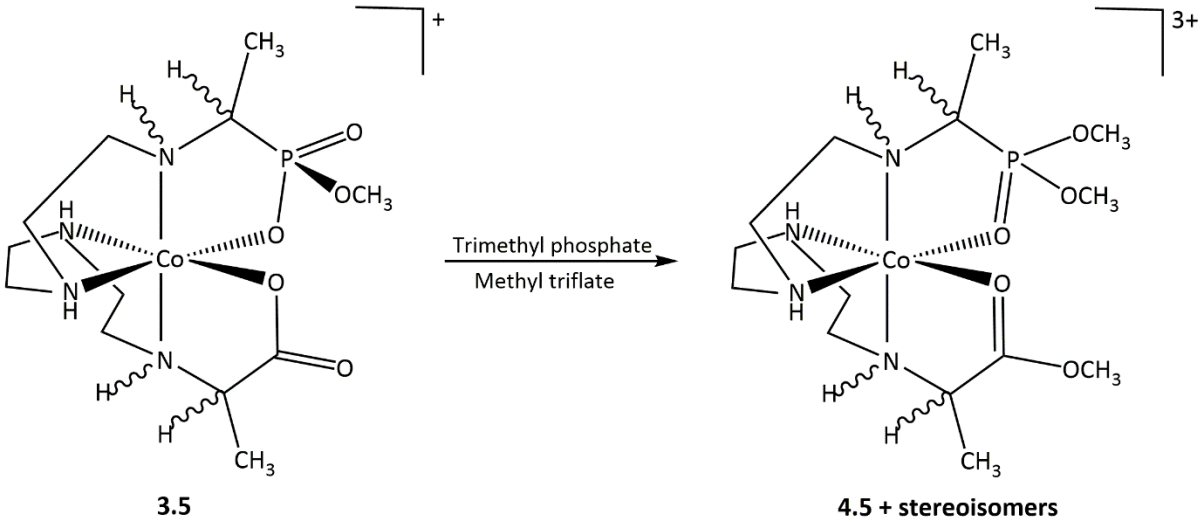

Figure 4.13 Reaction scheme for procedure 5

3.5 (1.24 g; 2.86 mmol) (dried over P_2O_5) was dissolved in trimethyl phosphate ($P(O)(OCH_3)_3$) (9 mL). The reaction vessel was enclosed with a drying tube filled with 4 Å molecular sieves. An 8-fold excess of methyl trifluoromethanesulfonate ($CF_3SO_2OCH_3$) (3.77 g; 22.88 mmol) was added. The mixture was heated at 50°C for 120 mins. A dry diethyl ether/methanol mixture (90:10) (250 mL) was used to triturate the mixture until a powder was obtained according to the procedure outlined in section 4.2.4.

^{1}H NMR: 1.47 (C**H**$_3$, overlapping doublets), 1.62 (C**H**$_3$, d, J^{HP} = 8 Hz), 1.65 (C**H**$_3$, d, J^{HH} = 4 Hz), 1.71 (C**H**$_3$, d, J^{HP} = 8 Hz), 1.74 (C**H**$_3$, d, J^{HP} = 8 Hz), 1.76 (C**H**$_3$, d, J^{HH} = 4 Hz), 1.78 (C**H**$_3$, d, J^{HP} = 8 Hz), 1.84 (C**H**$_3$, d, J^{HH} = 8 Hz), 1.87 (C**H**$_3$, d, J^{HP} = 8 Hz), 1.99 (C**H**$_3$, d, J^{HP} = 8 Hz), 2.16 (C**H**$_2$-CH_2-NH, m), 2.19 (C**H**$_2$-CH_2-NH, m), 2.35 - 2.37 (C**H**$_2$-CH_2-NH, m), 2.39 - 2.41 (C**H**$_2$-CH_2-NH, m), 2.46 (C**H**$_2$-CH_2-NH, m), 2.49 (C**H**$_2$-CH_2-NH, m), 2.55 (C**H**$_2$-CH_2-NH, m), 2.59 (C**H**$_2$-CH_2-NH, m), 2.62 (C**H**$_2$-CH_2-NH, m), 2.78 (C**H**$_2$-NH, m), 2.81 (C**H**$_2$-NH, m), 2.84 (C**H**$_2$-NH, m), 2.89 (C**H**$_2$-NH, m), 2.91 (C**H**$_2$-NH, m), 3.01 (C**H**$_2$-NH, m), 3.17 (C**H**$_2$-NH, broad), 3.20 (C**H**$_2$-NH, m), 3.43 (C**H**$_2$-NH, m), 3.47 (C**H**$_2$-NH, m), 3.50 (C**H**$_2$-NH, broad), 3.57 (OC**H**$_3$, d, J^{HP} = 12 Hz), 3.65 (OC**H**$_3$, d, J^{HP} = 8 Hz), 3.66 (OC**H**$_3$, d, J^{HP} = 12 Hz), 3.82 (OC**H**$_3$, d, J^{HP} = 4 Hz), 3.86 (OC**H**$_3$, d, J^{HP} = 12 Hz), 3.90 (OC**H**$_3$, d, J^{HP} = 12 Hz), 3.94 - 3.96 (OC**H**$_3$, m), 4.00 (OC**H**$_3$, d, J^{HP} = 12 Hz), 4.04 (OC**H**$_3$,s, on carboxylate chelate), 4.11 – 4.16 (OC**H**$_3$, 6 overlapped singlets, on carboxylate chelate), 4.18 (OC**H**$_3$, s, on carboxylate chelate),

4.22 (OC**H**$_3$, d, J^{HP} = 12 Hz), 4.26 (OC**H**$_3$, s, on carboxylate chelate), 4.38 (C**H**, q), 4.66 (**H**, q), 4.76 (C**H**, m), 5.81 (N**H**-CH_2, broad), 6.00 (N**H**-CH_2, broad), 6.11 (N**H**-CH_2, broad), 6.37 (N**H**-CH_2, broad), 6.43 (N**H**-CH_2, broad), 6.50 (N**H**-CH_2, broad), 6.59 (N**H**-CH_2, broad), 6.73 (N**H**-CH_2, broad), 7.04 (N**H**-CH_2, broad), 7.19 (N**H**, broad), 7.24 (N**H**, broad), 7.54 (N**H**, broad), 7.78 (N**H**, broad), 7.95 (N**H**, broad), 8.76 (N**H**, broad); $^{31}P\{^1H\}$: 38.17, 39.15, 39.52, 39.57, 48.00, 48.03, 48.04, 48.25, 51.71, 51.74, 51.79.

ESIMS: Calcd. for $[C_{14}H_{33}CoN_4O_5P]^{3+}$: 427.15; M/Z = 142.38. Found: 425.14 for $[C_{14}H_{31}CoN_4O_5P]^{1+}$; $[M-2H]^+$ and 561.08 for $([C_{13}H_{30}CoN_4O_5P]^{2+}(CF_3SO_3^-))^{1+}$; $[M-CH_3]^{2+}(CF_3SO_3^-))^{1+}$

Procedure 6

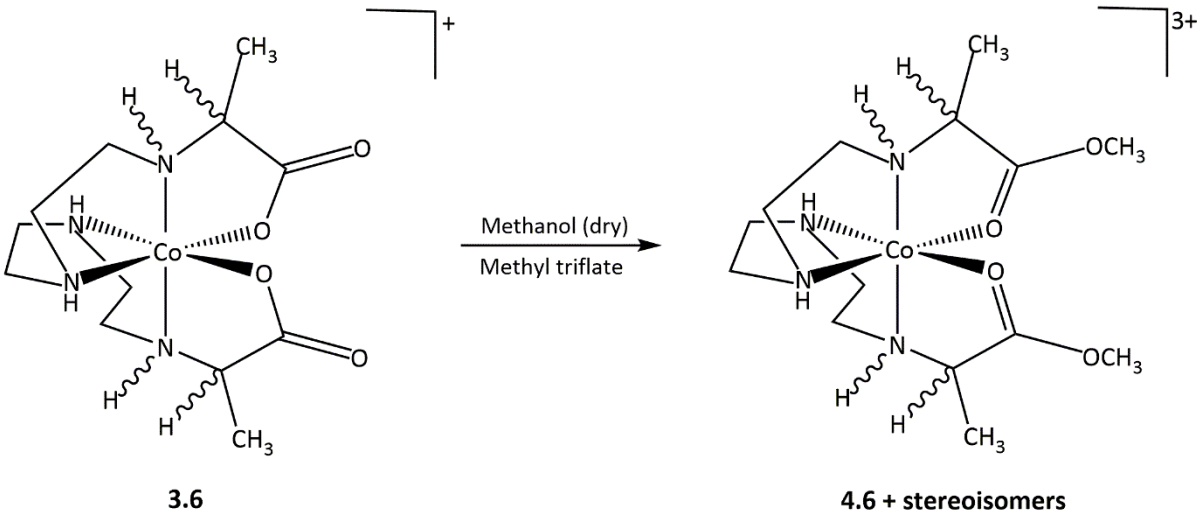

Figure 4.14 Reaction scheme for procedure 6

3.6 (0.50 g; 1.31 mmol) was dissolved in dry methanol (10 mL). The reaction vessel was enclosed with a drying tube filled with 4 Å molecular sieves. An 8-fold excess of methyl trifluoromethanesulfonate ($CF_3SO_2OCH_3$) (1.72 g; 10.48 mmol) was added. The mixture was heated at 50°C for 120 mins. Dry diethyl ether (150 mL) was used to triturate the mixture until a powder was obtained according to the procedure outlined in section 4.2.4.

^{1}H NMR: 1.50 (C**H**$_3$, d, J^{HH} = 8 Hz), 1.52 (C**H**$_3$, d, J^{HH} = 8 Hz), 1.57 - 1.60 (C**H**$_3$, overlapping doublets), 1.61 -1.63 (C**H**$_3$, overlapping doublets), 1.64 (C**H**$_3$, d, J^{HH} = 8 Hz), 1.67 – 1.69 (C**H**$_3$, overlapping doublets), 1.70 (C**H**$_3$, d, J^{HH} = 8 Hz), 1.72 – 1.75 (C**H**$_3$, m), 1.77 (C**H**$_3$, d, J^{HH} = 8 Hz), 1.79 (C**H**$_3$, d, J^{HH} = 8 Hz), 1.80 (C**H**$_3$, d, J^{HH} = 8 Hz), 2.15 (C**H**$_2$-NH, m), 2.19 (C**H**$_2$-NH, m), 2,42 - 2.48 (C**H**$_2$-NH, m) 2.62 – 2.65 (C**H**$_2$-CH$_2$-N-C, m), 2.67 (C**H**$_2$-CH$_2$-N-C, m), 2.86 (C**H**$_2$-CH$_2$-N-C, m), 2.89 (C**H**$_2$-CH$_2$-N-C, m) 3.01 (C**H**$_2$-N-C, m), 3.03 (C**H**$_2$-N-C, m), 3.05 (C**H**$_2$-N-C, m), 3.11 (C**H**$_2$-N-C, m), 3.20 (C**H**$_2$-NH, m), 3.24 (C**H**$_2$-NH, m), 3.39 (C**H**$_2$-NH, m), 3.81 - 3.86 (C**H**, m), 3.90 - 3.97 (C**H**, m), 4.08 (OC**H**$_3$, s), 4.10 (OC**H**$_3$, s), 4.11 (OC**H**$_3$, s), 4.74 (C**H**, m).

ESIMS: Calcd. for $[C_{14}H_{30}CoN_4O_4]^{3+}$: 377.16; M/Z = 125.72. Found: 375.14; M/Z = 187.57 for $[C_{14}H_{28}CoN_4O_4]^{2+}$; $[M\text{-}2H]^{+}$ and 347.11 for $([C_{12}H_{24}CoN_4O_4]^{1+}$ $[M\text{-}2(CH_3)]^{1+}$ for compound **3.6**.

Procedure 7

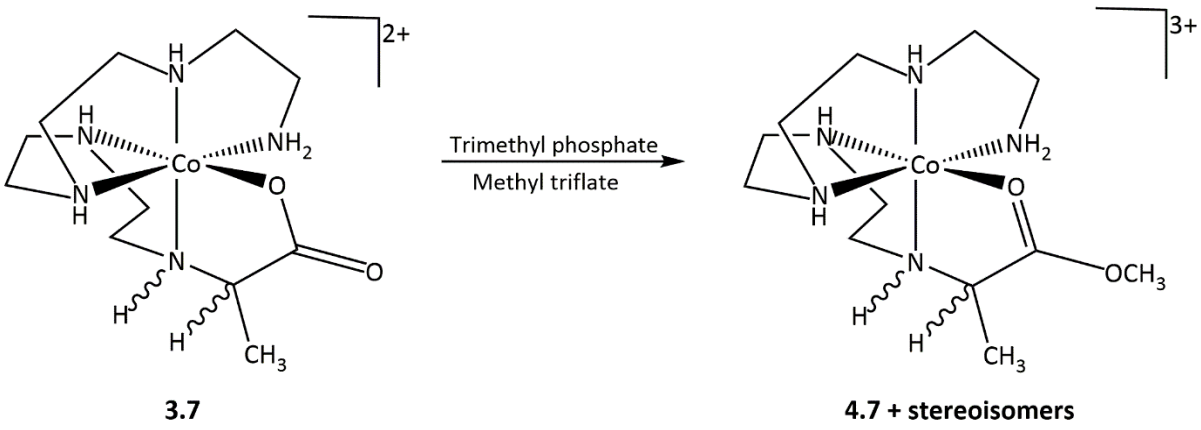

Figure 4.15 Reaction scheme for procedure 7

3.7 (1.0 g; 2.17 mmol) was dissolved in trimethyl phosphate ($P(O)(OCH_3)_3$) (3 mL). The reaction vessel was enclosed with a drying tube filled with 4 Å molecular sieves. A 4-fold excess of methyl trifluoromethanesulfonate ($CF_3SO_2OCH_3$) (1.42 g; 8.68 mmol) was added. The mixture was heated at 50°C for 90 mins. Dry diethyl ether/methanol mixture (90:10) (250 mL) was used to triturate the mixture until a red-orange powder was obtained according to the procedure outlined in section 4.2.4.

^{1}H NMR: 1.54 - 1.59 (C**H**$_3$, overlapping doublets), 1.73 - 1.79 (C**H**$_3$, overlapping doublets), 2.41 (C**H**$_2$-NH, m), 2.44 (C**H**$_2$-NH, m), 2.47 (C**H**$_2$-NH, m), 2.51 (C**H**$_2$-NH, m), 2.64 (C**H**$_2$-NH, m), 2.68 (C**H**$_2$-NH, m), 2.71 (C**H**$_2$-CH$_2$-NH, m), 2,73 - 2.81 (C**H**$_2$-CH$_2$-NH, m), 2.86 (C**H**$_2$-NH, m), 2.90 (C**H**$_2$-NH, m), 2.93 - 3.02 (C**H**$_2$-NH, m), 3.04 - 3.18 (C**H**$_2$-NH-CH$_2$, m), 3.20 - 3.26 (C**H**$_2$-NH-CH$_2$, m), 3.35 - 3.50 (CH$_2$-NH-C**H**$_2$, m), 3.52 - 3.57 (C**H**$_2$-NH$_2$, m, broad), 3.64 - 3.68 (C**H**$_2$-NH$_2$, m), 3.71 (OC**H**$_3$, s), 3.74 (OC**H**$_3$, s), 3.77 (OC**H**$_3$, s), 3.79 (OC**H**$_3$, s), 4.34 (C**H**, q), 4.72 (C**H**, q).

ESIMS: Calcd. for $[C_{12}H_{29}CoN_5O_2]^{3+}$: 334.17; M/Z = 111.39. Found: 332.15; M/Z = 166.07 for $[C_{12}H_{27}CoN_5O_2]^{2+}$; $[M-2H]^{+}$

Procedure 8

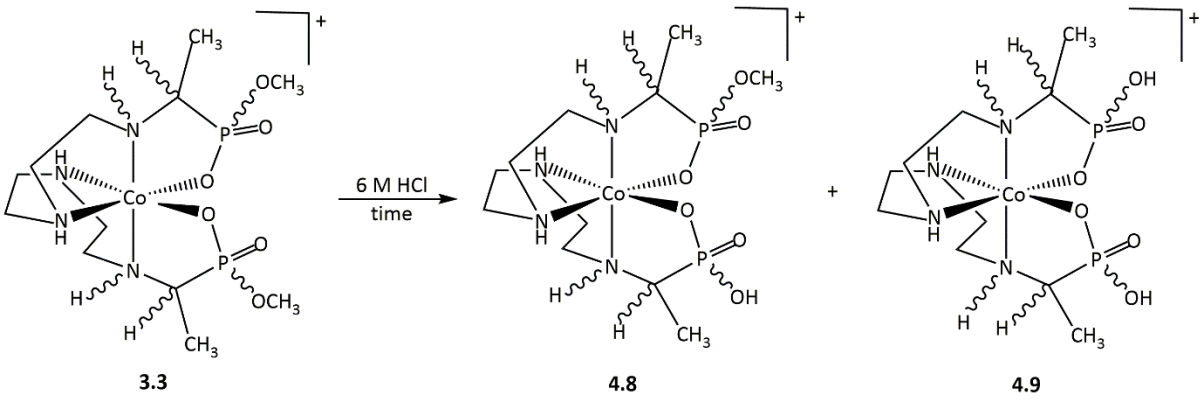

Figure 4.16 Reaction scheme for procedure 8

A sample containing a mixture from a preparation using procedure 3 of chapter 3, was treated with 6 M HCl (20 mL) and heated at 60°C to monitor (by ^{1}H NMR and MS) the ester hydrolysis over a period. Mass spectrometry of the reaction mixture was obtained at 24 hr, 48 hr and 72 hr intervals respectively. The NMR spectra assigned below were from a sample prepared from the 72 hr reaction mixture.

^{1}H NMR: 1.50 (C**H**$_3$, dd, $^{3}J^{HP}$ = 16 Hz, $^{3}J^{HH}$ = 8 Hz), 1.68 (C**H**$_3$, dd, $^{3}J^{HP}$ = 16 Hz, $^{3}J^{HH}$ = 4 Hz), 2.53 (C**H**$_2$-NH, m), 2.58 - 2.63 (C**H**$_2$-NH, m), 3.05 – 3.14 (C**H**$_2$-CH$_2$-N-C, m), 3.21 - 3.36 (C**H**$_2$-N-C, m), 3.48 – 3.54 (OC**H**$_3$, m), 3.60 (C**H**$_3$OH (by-product of

hydrolysis)), 3.65 - 3.69 (OC**H**$_3$, m), 5.79 (N**H**, broad), 6.99 N**H**, broad, m); $^{31}P\{^1H\}$: 38.99.

ESIMS: Calcd. for $[C_{12}H_{30}CoN_4O_6P_2]^{1+}$: 447.09. Found: 447.09 and 433.08 for $[C_{11}H_{28}CoN_4O_6P_2]^{1+}$ and 419.06 for $[C_{10}H_{26}CoN_4O_6P_2]^{1+}$

Procedure 9

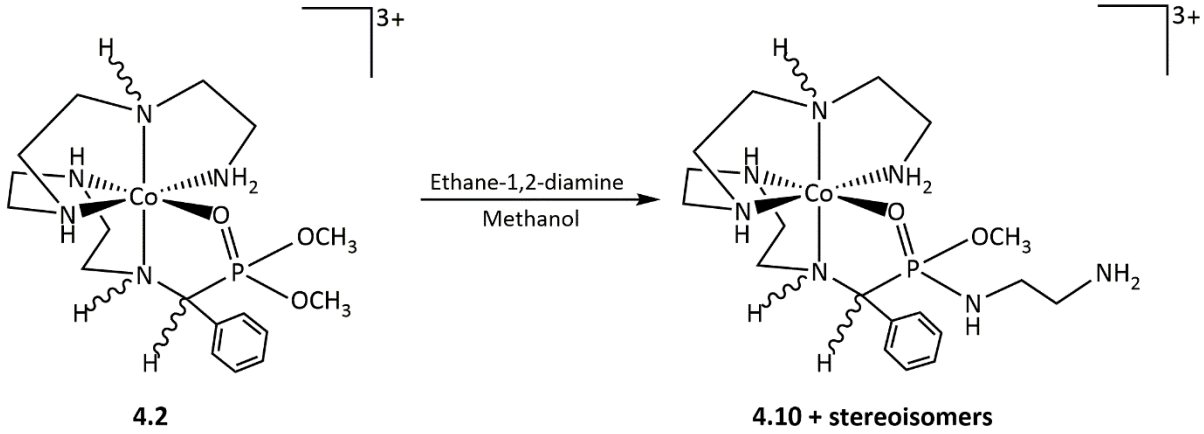

Figure 4.17 Reaction scheme for procedure 9

4.2 (0.06 g; 0.067 mmol) was dissolved in methanol (10 mL) (dried with 4 Å molecular sieves) to give a red-orange solution. 2 equivalents of ethane-1,2-diamine (0.01 g; 0.13 mmol) were dissolved in dry methanol (10 mL). Both solutions were mixed together and heated at 50°C for 1 hour. There was no observable colour change. The reaction was quenched by adding two drops of glacial acetic acid. The quenched reaction mixture was triturated with excess diethyl ether (150 mL) according to the trituration procedure outlined in section 4.2.4. A magenta coloured powder was recovered through filtration and was dried in a desiccator over P_2O_5 before characterisation.

^{1}H NMR (400 MHz, D_2O (ppm)): 1.92 (C**H**$_2$, broad), 2.45 (C**H**$_2$-NH, m), 2.50 (C**H**$_2$-CH$_2$-NH, m), 2.54 – 2.57 (C**H**$_2$-NH and C**H**$_2$-NH-CH$_2$, m), 2.59 -2.69 (C**H**$_2$-NH and C**H**$_2$-NH-CH$_2$, m), 2.72 – 2.82 (C**H**$_2$-NH and C**H**$_2$-NH-CH$_2$, m), 2.91 – 2.95 (C**H**$_2$-NH and C**H**$_2$-NH-CH$_2$, m), 2.98 - 3.09 (C**H**$_2$-NH and C**H**$_2$-NH-CH$_2$, m), 3.16 - 3.19 (C**H**$_2$-NH$_2$ on en), 3.31 - 3.35 (C**H**$_2$-NH on en), 3.49 (P-OC**H**$_3$, d, $^3J^{HP}$ = 8 Hz), 3.53 – 3.57 (C**H**, m), 3.60 (P-OC**H**$_3$, d, $^3J^{HP}$ = 12 Hz), 3.68 – 3.77 (C**H**$_2$-NH$_2$, m), 3.83 (P-OC**H**$_3$, d, $^3J^{HP}$ = 12 Hz), 4.05 – 4.09 (N**H**, m), 4.18 –

4.26 (N**H**, m), 4.52 – 4.59 (N**H**, m), 7.49 – 7.67 (C_6**H**$_5$, m); $^{31}P\{^1H\}$ NMR (ppm): 29.98, 30.51, 34.74, 34.87, 35.37, 35.76.

Procedure 10

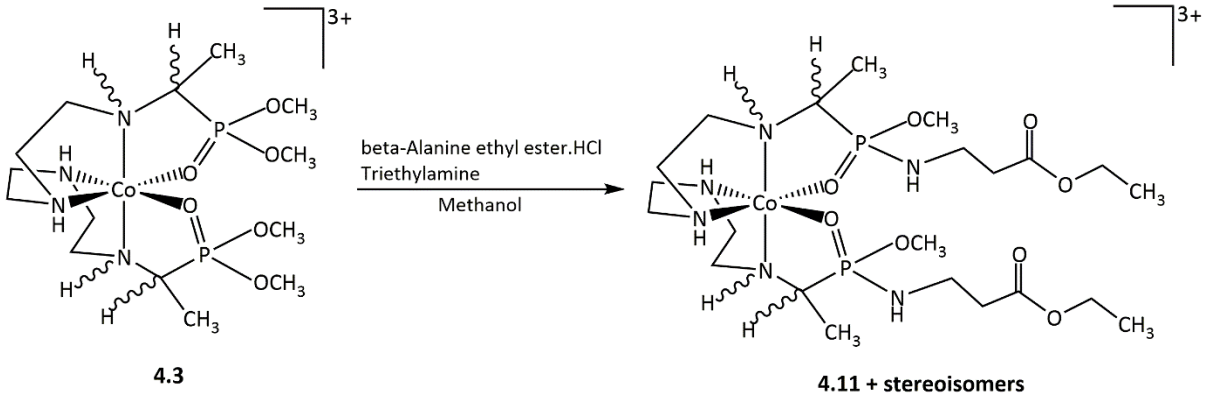

4.3 **4.11 + stereoisomers**

Figure 4.18 Reaction scheme for procedure 10

4.3 (0.26 g; 0.28 mmol) was dissolved in dry methanol (10 mL) to give a purple solution. 8 equivalents of β-alanine ethyl ester·HCl (0.34 g; 2.24 mmol) were dissolved in dry methanol (10 mL). Triethylamine (0.14 g; 1.4 mmol) was added to neutralise the acid. Both solutions were mixed together and stirred for 15 mins. There was no observable colour change. The reaction was quenched by adding 0.05 mL of glacial acetic acid. The quenched reaction mixture was triturated with excess acetonitrile (200 mL) according to the trituration procedure outlined in section 4.2.4. A purple coloured powder was recovered through filtration and was dried in a desiccator over P_2O_5 before characterisation.

^{1}H NMR (600 MHz, D_2O (ppm)): 1.11 (C**H**$_3$ on AA, t, J^{HH} = 8 Hz), 1.15 (C**H**$_3$ on AA, m)1.27 (C**H**$_3$ on AA, t, J^{HH} = 8 Hz), 1.46 – 1.58 (C**H**$_3$, m), 2.04 (C**H**$_3$COOH), 2.19 – 2.24 (C**H**$_2$-NH, m), 2.52 (C**H**$_2$, m), 2.70 (C**H**$_2$, m), 2.79 – 2.86 (C**H**$_2$-CH_2-NH, m), 2.98 -3.04 (C**H**$_2$-C=O on AA, m), 3.01 (C**H**, q, J^{HH} = 4 Hz), 3.09 (C**H**$_2$, m), 3.11 – 3.36 (C**H**$_2$ on AA, m), 3.37 (C**H**$_2$-NH on AA, t, J^{HH} = 8 Hz), 3.53 (P-OC**H**$_3$, d, J^{HP} = 8 Hz), 3.55 (P-OC**H**$_3$, d, J^{HP} = 8 Hz), 3.74 – 3.76 (C**H**, m), 3.91 (P-OC**H**$_3$, d, J^{HP} = 8 Hz), 4.10 (C**H**$_2$-NH, m), 4.20 – 4.29 (C**H**, m), 4.84 – 4.96 (C**H**, m), 7.47 – 7.93 (P-N**H**, m); $^{31}P\{^1H\}$ NMR (ppm): 42.34, 42.47, 42.63, 43.25, 44.58, 44.88.

Procedure 11

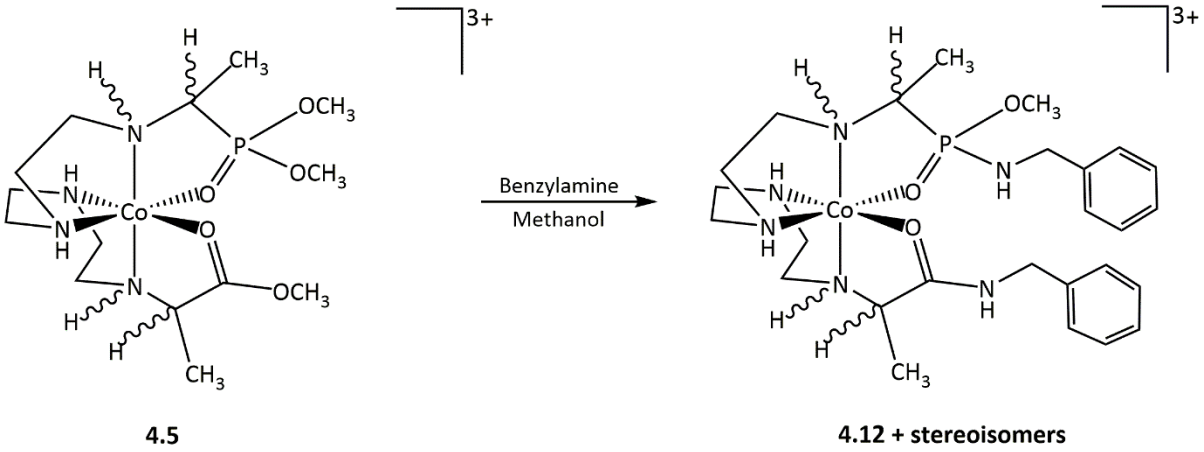

Figure 4.19 Reaction scheme for procedure 11

4.5 (0.5 g; 0.57 mmol) was dissolved in methanol (100 mL) (dried with 4 Å molecular sieves) to give a dark red suspension. 4 equivalents of benzylamine (0.25 g; 2.29 mmol) were added directly to the suspension. A darker red solution was formed. This solution was heated at 50°C for 1 hour. There was no observable colour change. The reaction was quenched by adding three drops of glacial acetic acid. The quenched reaction mixture was triturated with excess diethyl ether (250 mL) according to the trituration procedure outlined earlier. A red coloured powder was recovered through filtration and was dried in a desiccator over P_2O_5 before characterisation. However, the filtrate remained intensely red coloured and thus was allowed to settle. The diethyl ether layer decanted off and an attempt was made to isolate the constituents of the residue through column chromatography. This residue was dissolved in 1 L of distilled water and adsorbed onto a Sephadex SPC 25 column. The column was washed with 1 L of distilled water. A dark red band formed and was eluted with 0.3 M ammonium acetate solution. The eluate was evaporated to dryness on a rotary evaporator before characterisation. The characterisation details of the dry eluate are reported.

^{1}H NMR (400 MHz, D_2O (ppm)): 1.49 (C**H**$_3$, td, $^3J^{HP}$ = 16 Hz, $^3J^{HH}$ = 8 Hz), 1.59 – 1.72 (C**H**$_3$, m), 1.63 (C**H**$_3$, dd, $^3J^{HP}$ = 16 Hz, $^3J^{HH}$ = 8 Hz), 2.41 (C**H**$_2$-CH_2-NH, m), 2.44 (C**H**$_2$-CH_2-NH, m), 2.53 – 2.70 (C**H**$_2$-CH_2-NH, m), 2.77 – 2.95 (C**H**$_2$-NH, m), 3.05 – 3.44 (C**H**$_2$-NH, m), 3.55 (OC**H**$_3$, d, $^3J^{HP}$ = 12 Hz), 3.61 (OC**H**$_3$, d, $^3J^{HP}$ = 12 Hz), 3.66 – 3.78 (C**H** and OC**H**$_3$, m), 3.96 (C**H**, q, J^{HH} = 8 Hz), 4.05 (C**H**, q, J^{HH} = 8 Hz), 4.20 (C**H**$_2$ on benzylamine, s), 7.48

($C_6\underline{\mathbf{H}}_5$ on benzylamine); $^{31}P\{^1H\}$ NMR (ppm): 39.64, 40.43, 40.52, 40.96, 41.50, 41.62, 41.75, 42.21, 43.32, 43.49, 43.75, 44.74, 45.61.

Procedure 12

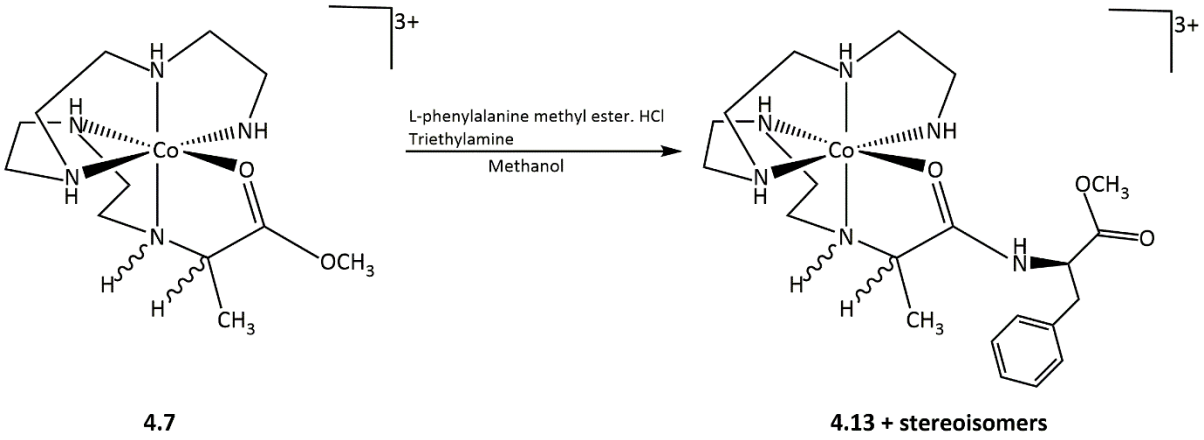

4.7 **4.13 + stereoisomers**

Figure 4.20 Reaction scheme for procedure 12

4.7 (0.5 g; 0.64 mmol) was dissolved in dry methanol (20 mL) to give a red-orange suspension. 8 equivalents of L-phenylalanine methyl ester·HCl (1.08 g; 5.0 mmol) were dissolved in dry methanol (15 mL). Triethylamine (0.30 g; 3.0 mmol) was added to neutralise the acid. Both solutions were mixed together to form a bright red solution which was stirred for 5 mins. The reaction was quenched by adding 0.1 mL of glacial acetic acid to yield a slurry product mixture. This crude mixture was purified using column chromatography. The crude product mixture was evaporated to dryness (for the purpose of characterisation) before dissolving in 500 mL of distilled water. This dilute solution was adsorbed onto a Sephadex SPC 25 column. The column was washed with 500 mL of distilled water before elution with 0.3 – 0.5 M ammonium acetate solution. Three bands formed. The third one was eluted with 1.0 M ammonium acetate solution. The eluates were evaporated to dryness on a rotary evaporator before characterisation. Details for the third band are reported below.

^1H NMR (400 MHz, D_2O (ppm)): 1.54 ($C\underline{\mathbf{H}}_3$, d, $^3J^{HH}$ = 8 Hz), 1.56 ($C\underline{\mathbf{H}}_3$, d, $^3J^{HH}$ = 4 Hz), 1.61 ($C\underline{\mathbf{H}}_3$, d, $^3J^{HH}$ = 8 Hz), 1.66 - 1.74 ($C\underline{\mathbf{H}}_3$, m), 2.27 ($C\underline{\mathbf{H}}_2$ on phenylalanine, m), 2.36 ($C\underline{\mathbf{H}}_2$ on phenylalanine, m), 2.53 – 2.97 ($C\underline{\mathbf{H}}_2$-NH and $C\underline{\mathbf{H}}_2$-$CH_2$-NH, m), 2.99 – 3.15 ($C\underline{\mathbf{H}}_2$-NH, m), 3.18 – 3.31 ($C\underline{\mathbf{H}}_2$-NH-$CH_2$, m), 3.34 – 3.52 ($CH_2$-NH-$C\underline{\mathbf{H}}_2$, m), 3.63 – 3.79 ($C\underline{\mathbf{H}}_2$-$NH_2$, m), 3.84 ($OC\underline{\mathbf{H}}_3$ on phenylalanine, s), 3.90 ($C\underline{\mathbf{H}}$ on phenylalanine, m), 4.00 ($C\underline{\mathbf{H}}$ on phenylalanine, m), 4.44 ($C\underline{\mathbf{H}}$, m), 4.56 ($C\underline{\mathbf{H}}$, m), 6.78 ($N\underline{\mathbf{H}}$, broad), 7.31 – 7.43 ($C_6\underline{\mathbf{H}}_5$ on phenylalanine, m).

ESIMS: Calcd. for $[C_{21}H_{38}CoN_6O_3]^{3+}$: 481.23; M/Z = 160.41. Found: 160.07 for $[C_{21}H_{37}CoN_6O_3]^{2+}$; [M-1H], 525.21 for $[C_{20}H_{34}CoN_6O_3]^{2+}\cdot(CH_3COO^-)$; [M-$CH_3$]$^{2+}$($CH_3COO$-) and 465.20 for $[C_{20}H_{34}CoN_6O_3]^{2+}$; [M-$CH_3$ & -1H]; M/Z = 232.60.

Procedure 13

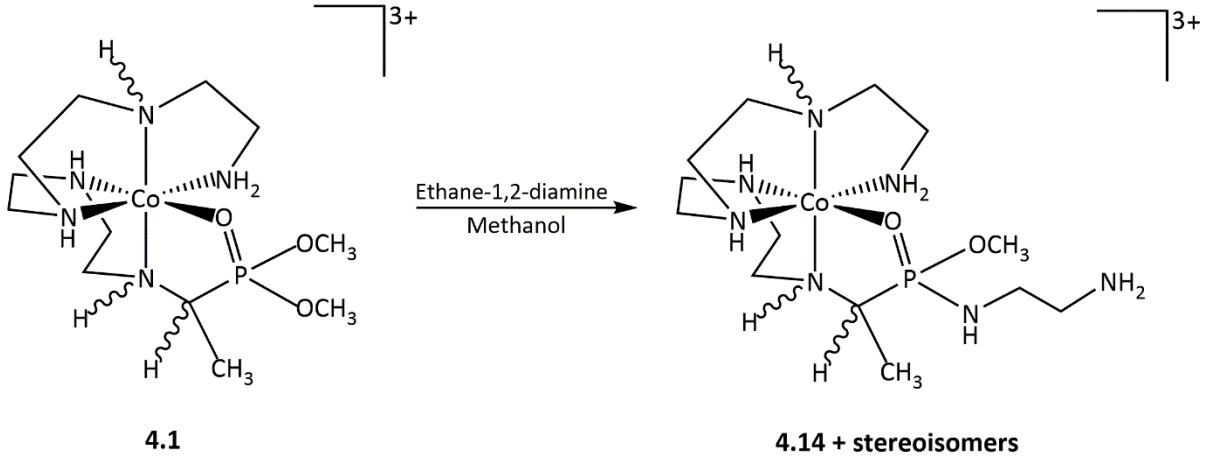

4.1 **4.14 + stereoisomers**

Figure 4.21 Reaction scheme for procedure 13

4.1 (0.1 g; 0.12 mmol) was dissolved in methanol (20 mL). A light orange solution was formed. 2 equivalents of ethane-1,2-diamine (0.02 g; 0.3 mmol) were dissolved in dry methanol (5 mL). Both solutions were mixed together to give a red-orange solution which was stirred for 30 mins. There was no observable colour change. The reaction was quenched by adding two drops of glacial acetic acid. The quenched reaction mixture was triturated with excess dry diethyl ether according to the trituration procedure outlined in section 4.2.4. An orange coloured powder was recovered through filtration and was dried in a desiccator over P_2O_5 before characterisation.

^{1}H NMR (400 MHz, D_2O (ppm)): 1.27 (C**H**$_3$, d, $^3J^{HH}$ = 4 Hz), 1.31 (C**H**$_3$, d, $^3J^{HH}$ = 4 Hz), 1.92 (C**H**$_2$-NH_2 on en), 2.04, (C**H**$_2$-NH on en), 2.08 (C**H**$_2$-NH on en), 2.79 (C**H**$_2$-CH_2-NH and C**H**$_2$-NH on cobalt(III), m), 2.85 – 2.93 (C**H**$_2$-NH and C**H**$_2$-NH-CH_2 on cobalt(III), m), 2.95 – 2.99 (CH_2- NH-C**H**$_2$, m), 3.04 (C**H**$_2$-NH_2 on en), 3.08 – 3.12 (C**H**$_2$-NH_2 on cobalt(III), m), 3.54 - 3.63 (P-OC**H**$_3$, m), 3.81 (C**H**, m), 3.94 (C**H**, m); ^{31}P{^{1}H} NMR (ppm): 42.87.

Procedure 14

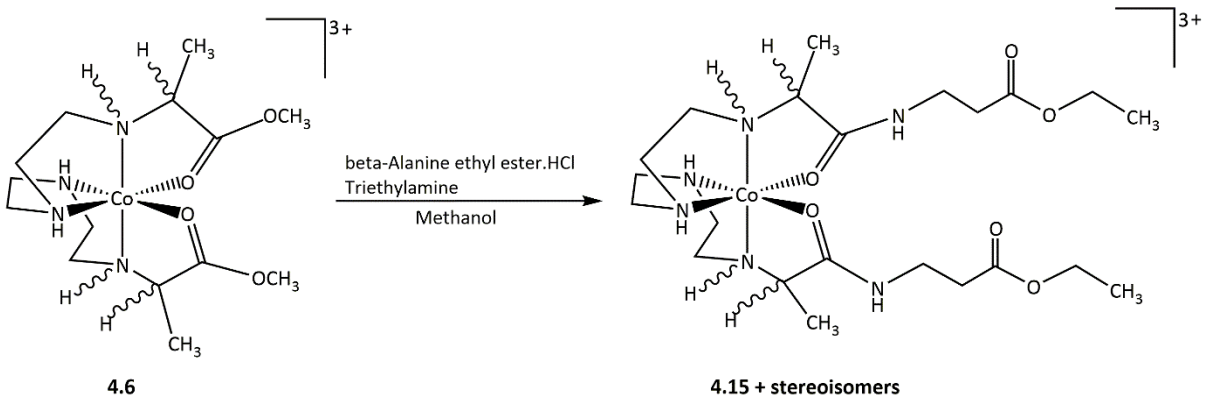

Figure 4.22 Reaction scheme for procedure 14

4.6 (0.24 g; 0.29 mmol) was dissolved in dry methanol (50 mL). 8 equivalents of β-alanine ethyl ester·HCl (0.36 g; 2.32 mmol) were dissolved in dry methanol (10 mL). Triethylamine (0.23 g; 2.32 mmol) was added to neutralise the acid. The reaction mixture of the three components was red in colour. The reaction vessel was fitted with a drying tube filled with 4 Å molecular sieves and the mixture was heated at 50°C for 1 hr. The reaction was quenched by adding two drops of glacial acetic acid. The quenched reaction mixture was triturated with excess dry diethyl ether according to the trituration procedure outlined in section 4.2.4. A red coloured powder was recovered through filtration and was dried in a desiccator over P_2O_5 before characterisation.

^{1}H NMR (400 MHz, D_2O (ppm)): 1.24 – 1.31 (C**H**$_3$, overlapping triplets), 1.59 – 1.66 (C**H**$_3$, overlapping doublets), 1.68 – 1.78 (C**H**$_3$, overlapping doublets), 2.56 (C**H**$_2$-C=O on AA, t, J^{HH} = 8 Hz), 2.67 – 2.71 (C**H**$_2$ on cobalt(III), m), 2.79 – 2.88 (C**H**$_2$-C=O on AA, m), 3.18 (C**H**$_2$-NH on AA, m), 3.30 (C**H**$_2$-NH on AA, t, J^{HH} = 8 Hz), 3.41 – 3.48 (C**H**$_2$ on cobalt(III), m), 3.91 – 3.98 (C**H** on cobalt(III), m), 4.01 – 4.05 (C**H** on cobalt(III), m), 4.16 – 4.25 (CH_3-C**H**$_2$ on AA, m), 4.47 – 4.67 (C**H**$_2$-NH on AA, m).

ESIMS: Calcd. for $[C_{22}H_{44}CoN_6O_6]^{3+}$: 547.27; M/Z = 182.42. Found: 182.42 for $[C_{22}H_{44}CoN_6O_6]^{3+}$ and 272.62 for $[C_{22}H_{42}CoN_6O_6]^{+}$; $[M\text{-}2H]^{+}$.

Procedure 15

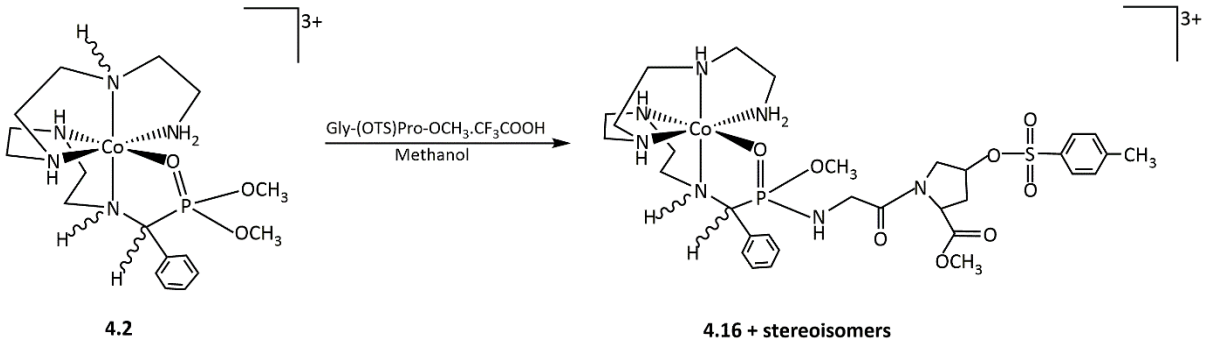

Figure 4.23 Reaction scheme for procedure 15

4.2 (0.38 g; 0.43 mmol) was dissolved in dry methanol (20 mL) to give a red-orange solution. Gly-(OTS)Pro-OCH_3.CF_3COOH (1.60 g; 3.42 mmol) was dissolved in dry methanol (10 mL). Both solutions were mixed together and heated at 50°C for 2 hours. There was no observable colour change. The reaction was quenched by adding two drops of glacial acetic acid. The quenched reaction mixture was triturated with excess diethyl ether (200 mL) according to the trituration procedure outlined in section 4.2.4. A red-orange powder was recovered through filtration and was dried in a desiccator over P_2O_5 before characterisation.

^{1}H NMR (600 MHz, D_2O (ppm)): 2.20 – 2.25 (Pro-C**H**$_2$, m), 2.48 (Tosyl-C**H**$_3$, s), 2.53 – 2.56 (C**H**$_2$-NH on cobalt(III), m), 2.62 – 2.72 (C**H**$_2$-CH_2-NH and C**H**$_2$-NH on cobalt(III), m), 2.84 – 3.15 (C**H**$_2$-NH on cobalt(III), m), 3.22 – 3.29 (C**H**$_2$-NH-CH_2, m), 3.33, 3.34, 3.35 (C**H**$_2$-NH_2 and Pro-C**H**$_2$, m), 3.49 – 3.53 (C**H**, m), 3.56, 3.57, 3.58, 3.59 (P-OC**H**$_3$, m), 3.76 (Pro-OC**H**$_3$, s), 3.79 – 3.86 (Gly-C**H**$_2$, m), 3.92 (Pro-OC**H**$_3$, s), 3.94 – 4.08 (Gly-C**H**$_2$, m), 4.57 – 4.67 (Pro-C**H**, m), 7.54 (Tosyl-**H**, d, J^{HH} = 12 Hz), 7.57 (Tosyl-**H**, d, J^{HH} = 12 Hz), 7.68 (Phenyl-**H**, d, J^{HH} = 6 Hz), 7.88 (Phenyl-**H**, d, J^{HH} = 6 Hz); ^{31}P{^{1}H} NMR (ppm): 35.54 (**P**-OCH_3), 36.53 (**P**-OCH_3); ^{13}C{^{1}H} NMR (600 MHz (ppm)): 23.78 (Tosyl-**C**H_3), 37.53 (Pro-**C**H_2), 43.25 (Pro-**C**H_2), 55.07 (Pro-O**C**H_3), 56.21 (Pro-O**C**H_3), 58.61 (P-O**C**H_3), 60.64 (P-O**C**H_3), 69.01 (**C**H_2-NH_2), 130.71 (Tosyl-**C**H), 132.35 (Tosyl-**C**H), 133.36 (**C**$_6H_5$), 134.11 (**C**$_6H_5$).

ESIMS: Calcd. for $[C_{31}H_{50}CoN_7O_8PS]^{3+}$: 770.25; M/Z = 256.75. Found: 414.13 for $C_{31}H_{50}CoN_7O_8PS]^{3+}\cdot(CH_3COO^-)$.

Procedure 16

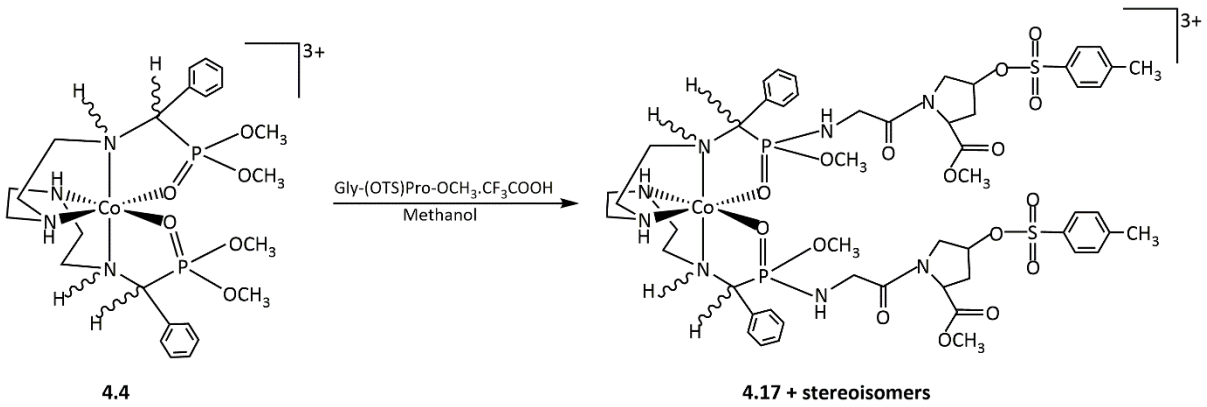

Figure 4.24 Reaction scheme for procedure 16

4.4 (0.31 g; 0.30 mmol) was dissolved in 20 mL of dry methanol to give a purple solution. Gly-(OTS)Pro-OCH_3.CF_3COOH (1.03 g; 2.19 mmol) was dissolved in 10 mL of dry methanol. Both solutions were mixed together and heated at 50°C for 1 hour. There was no observable colour change. The reaction was quenched by adding two drops of glacial acetic acid. The quenched reaction mixture was triturated with excess dry diethyl ether according to the trituration procedure outlined in section 4.3.4. A purple powder was recovered through filtration and was dried in a desiccator over P_2O_5 before characterisation.

^{1}H NMR (600 MHz, D_2O (ppm)): 2.23 (Pro-C**H**$_2$, m), 2.46 (Tosyl-C**H**$_3$, s), 3.13 - 3.29 (C**H**$_2$-CH_2-NH and C**H**$_2$-NH on cobalt(III), m), 3.35 (OC**H**$_3$, s), 3.37 (C**H**$_2$-NH on cobalt(III), m), 3.56 – 3.70 (Pro-C**H**$_2$, m), 3.76 (Pro-OC**H**$_3$, s), 3.80 (OC**H**$_3$), 3.83 (P-OC**H**$_3$, d, $^3J^{HP}$ = 12 Hz), 3.91 (OC**H**$_3$), 3.98 (Gly-C**H**$_2$, m), 4.02 (Gly-C**H**$_2$, m), 4.62 (Pro-C**H**, m), 7.52 (Tosyl-**H**, m), 7.56 (Phenyl-**H**, m), 7.85 (Tosyl-**H**, m), 7.66 (Phenyl-**H**, m); ^{31}P{^{1}H} NMR (ppm): 34.56 (**P**-OCH_3), 34.84 (**P**-OCH_3), 35.94 (**P**-OCH_3), 36.10 (**P**-OCH_3), 36.84 (**P**-OCH_3), 37.04 (**P**-OCH_3), 37.54 (**P**-OCH_3);^{13}C{^{1}H} NMR (600 MHz (ppm)): 23.82 (Tosyl-**C**H_3), 37.56 (Pro-**C**H_2), 43.27 (Pro-**C**H_2), 51.81 (P-O**C**H_3), 54.69 (H_2**C**-NH on cobalt(III)), 55.07 (Pro-O**C**H_3), 56.23 (Pro-O**C**H_3), 56.24 (H_2**C**-NH on cobalt(III)), 59.92 (P-O**C**H_3), 60.67 (Pro-**C**H_2), 60.96 (P-O**C**H_3), 69.03 (Pro-**C**H), 72.56 (Pro-**C**H), 80.21 (Pro-**C**H), 81.91 (Pro-**C**H), 83.62 (Pro-**C**H_2), 121.54 (**C**$_6H_5$, *meta*), 123.65 (**C**$_6H_5$, *ortho*), 131.90 (**C**$_6H_5$, *para*), 130.71 (Tosyl-**C**H), 133.40 (Tosyl-**C**H), 134.12 (Tosyl-**C**H), 150.03 (Tosyl-**C**H), 168.65 (Gly ester-**C**=O), 176.02 (Pro ester-**C**=O).

4.3 Results and Discussion

4.3.1 The cobalt(III) chelated carboxylate and phosphonate ester complexes

^{1}H NMR was very useful for providing evidence of successful synthesis of the chelated ester complexes described in this project and also helped to elucidate their inherent reactivity to yield hydrolysed derivatives and short peptides or amides. The hydrolytic vulnerability of these chelated ester complexes coupled with the isomeric complexity of their mixtures made interpretation of integral values and complete assignments of signals obtained from their ^{1}H NMR spectra harder.

Mass spectrometry data for some of the chelated ester complexes and their relevant short peptides or amides did not give the expected charges (and isotope distribution pattern) for the complex cations. Reasons are not clear at this stage as to why that was the case.

New resonance peaks are expected for the methyl esters. The protons were predicted to resonate as singlets around the 4.1 ppm region of the ^{1}H NMR spectrum for the carboxylate systems according to the literature[66]. On the other hand, the phosphonate systems were expected to behave a little differently. Protons of the new methyl ester group in the phosphonate systems should resonate as doublets because of the NMR active ^{31}P nuclei to which the group is bonded.

Apart from the additional resonance peaks for the methyl esters, it was foreseen that these new cobalt(III) chelated methyl ester compounds would have spectra that resemble those of their precursors (compounds **3.1** – **3.7** from chapter 3). The methyl systems are predicted to retain their signature (methyl protons) doublets around the 1.6 ppm region of the ^{1}H NMR spectrum, with the methoxy protons resonating from 3.5 ppm to downfield. Once again, the methoxy protons should be singlets for the carboxylate systems but doublets for the phosphonate analogues. Derivatives of the phenyl systems should have signals in the aromatic region (7 – 8 ppm) of the ^{1}H NMR spectrum as well.

Two different sets of resonance peaks were usually observed for these new chelated ester complexes, one of which disappears after some time as evidenced by ^{1}H NMR. The observations were particularly obvious in the methyl and methoxy regions of the ^{1}H NMR spectrum.

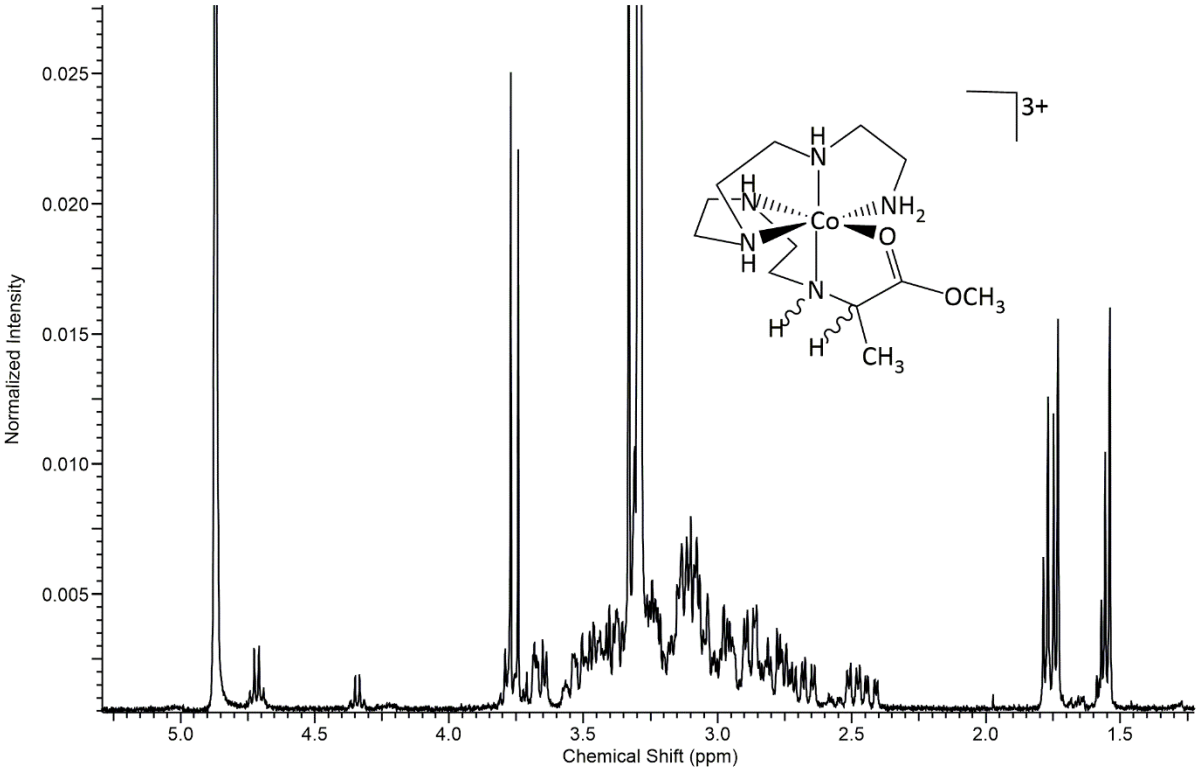

Figure 4.25 ^{1}H NMR spectrum of the product mixture from procedure 7.

Fig. 4.25 shows the ^{1}H NMR from procedure 7. No other peaks were observed further downfield. Two sets of peaks were detected for the methyl protons (around 1.6 ppm). Quartets are forecasted as the multiplicity pattern for the α-C-**H** protons given their C**H**$_3$ and N**H** neighbours. Thus, the quartets at 4.3 and 4.7 ppm have both been assigned to α-C-**H** protons on two different sets of diastereoisomers. Next to the quartets and upfield are the singlets of the methoxy (OCH_3) protons around the 3.7 ppm region of the spectrum. The two singlets could mean that there are two major pairs of diastereoisomers dominating the product mixture. If the other chiral centres in a given molecule from this mixture are kept constant and considering only the α-carbon centre and the amine adjacent to it, then four pairs of diastereoisomers (Fig. 4.26) are expected from the product mixture.

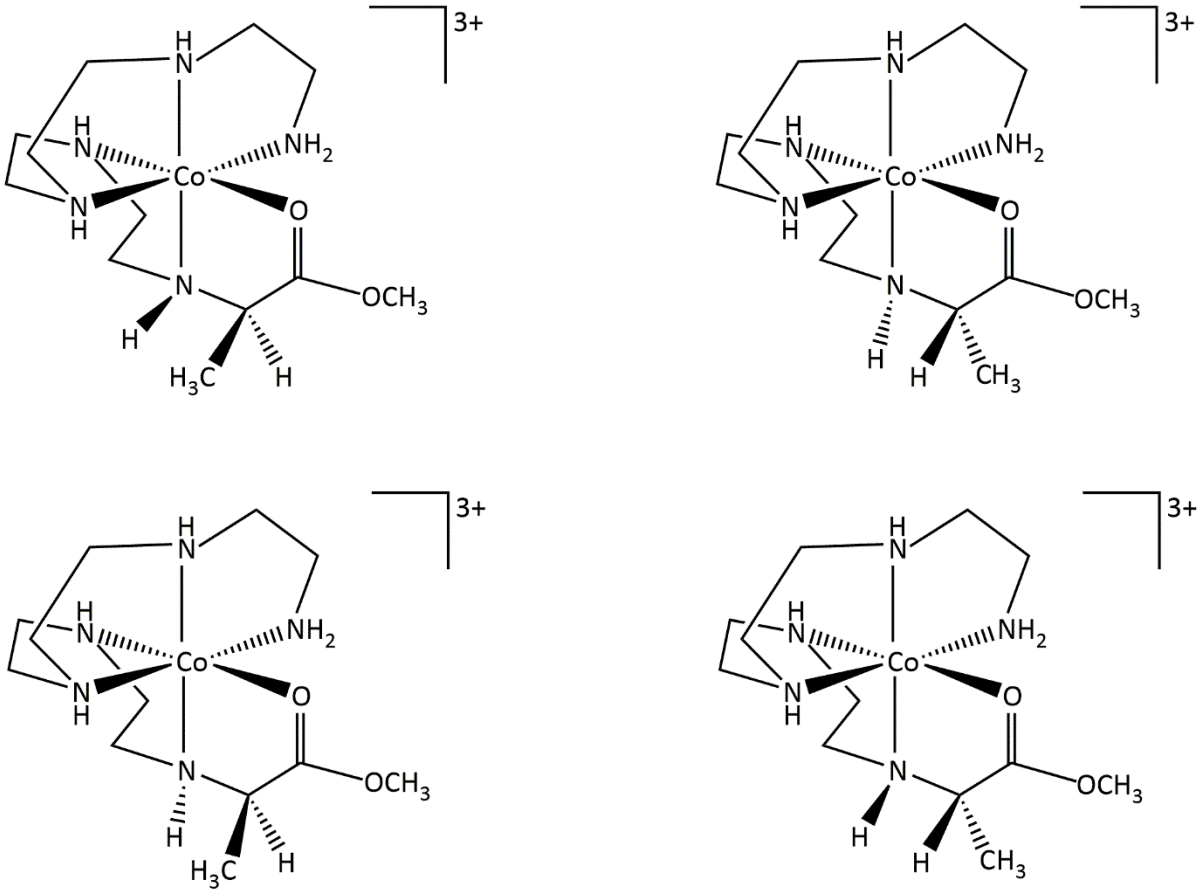

Figure 4.26 Four possible diastereoisomers (and their enantiomers) expected in the product mixture form procedure 7, if the other stereogenic centres are kept constant.

However, if it is more favourable for one pair of diastereoisomers to be formed over the other with respect to the α-carbon centre only, then the possible number of pairs of diastereoisomers narrows down to two. Two pairs of diastereoisomers could therefore be expected from the product mixture from procedure 7.

During the synthesis of these new chelated cobalt(III) ester complexes, two possibilities exist in the mixture realised at the end of the experiment: (1) not all starting materials were transformed into esters (2) all starting materials were made into esters but then hydrolysed. For the reason of the existence of these possibilities, an excess of methyl triflate was used in each procedure to ensure that the esterification of all starting materials occurs completely. It was envisaged that even upon hydrolysis, the presence of the excess methylating agent would keep the reaction going to revert the hydrolysed species back to esters. These chelated ester complexes are isolated through the trituration procedure outlined in section 4.2.4 as triflate salts in powder form. For an NMR experiment, some of this powder is dissolved in a deuterated

solvent of choice (CD_3OD in this case) for analysis. In solution, hydrolysis is inevitable given that the chelated esters are expected to be very reactive. The rest of the powdered product is stored in a desiccator over P_2O_5.

Therefore, the two sets of peaks observed in the initial ^1H NMR obtained from a sample of the product mixture (as in Fig. 4.25) indicate the presence of two different sets of species in solution; one where the esters have been made and remain intact and another where hydrolysis has already started taking place. The two major singlets at 3.74 and 3.77 ppm respectively, in the methoxy region of the spectrum shown as Fig. 4.25 indicate that two pairs of diastereoisomers dominate the product mixture, with respect to complexes that have the chelated ester groups intact.

Another ^1H NMR spectrum (Fig. 4.27) for the product mixture of procedure 7 was obtained after 72 hours. Interestingly, one of the sets of signals previously observed in the spectrum in Fig. 4.25 disappeared but the methoxy signals were not completely gone. Integration showed a 1:3 ratio between the methoxy protons and the methyl ones in the spectrum shown as Fig. 4.27, giving evidence to the hydrolysis. Also, the quartets due to the α-C-H protons were gone too. If the disappearance of the signals of the α-C-H protons is interpreted to mean that solvent exchange had taken place between the protons of the α-C centre and deuterons of the NMR solvent, then the signals from the methyl protons would be singlets (as opposed to doublets). Wilson-Coutts et al[52] reported that ^1H NMR experiments conducted two weeks after sample dissolution in deuterated carbonate buffer indicated exchange had occurred at the α-C centre with solvent deuterons; as doublets in the methyl region became singlets.

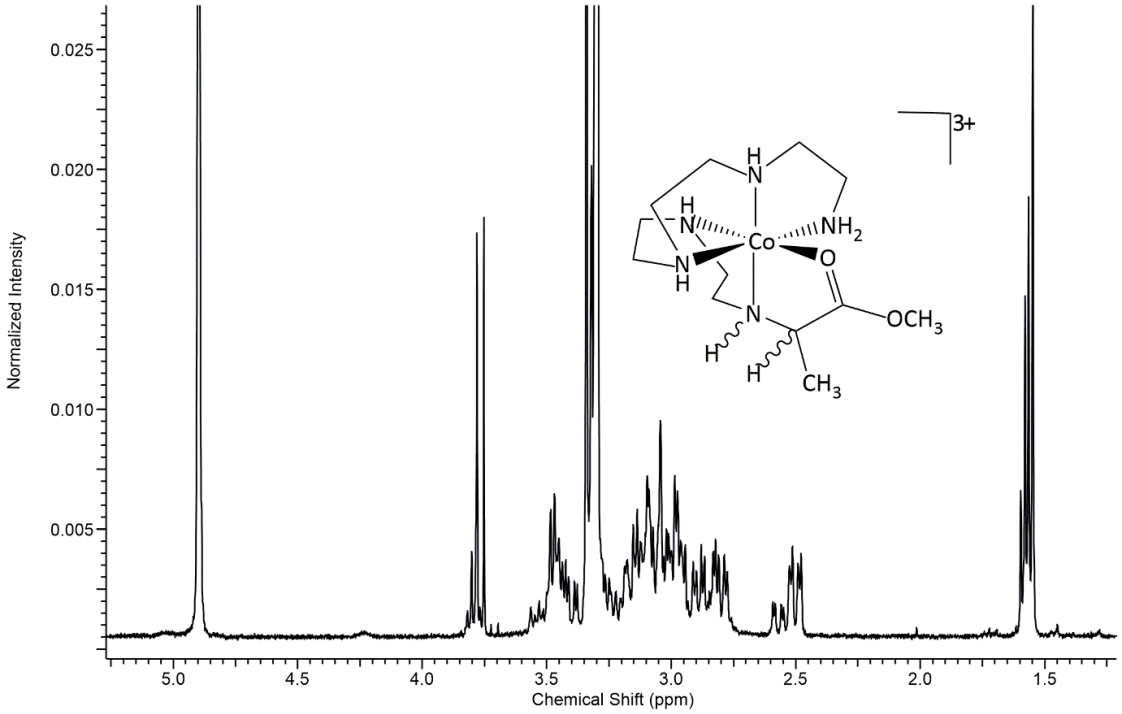

Figure 4.27 ^{1}H NMR spectrum of the product mixture from procedure 7 after 72 hours.

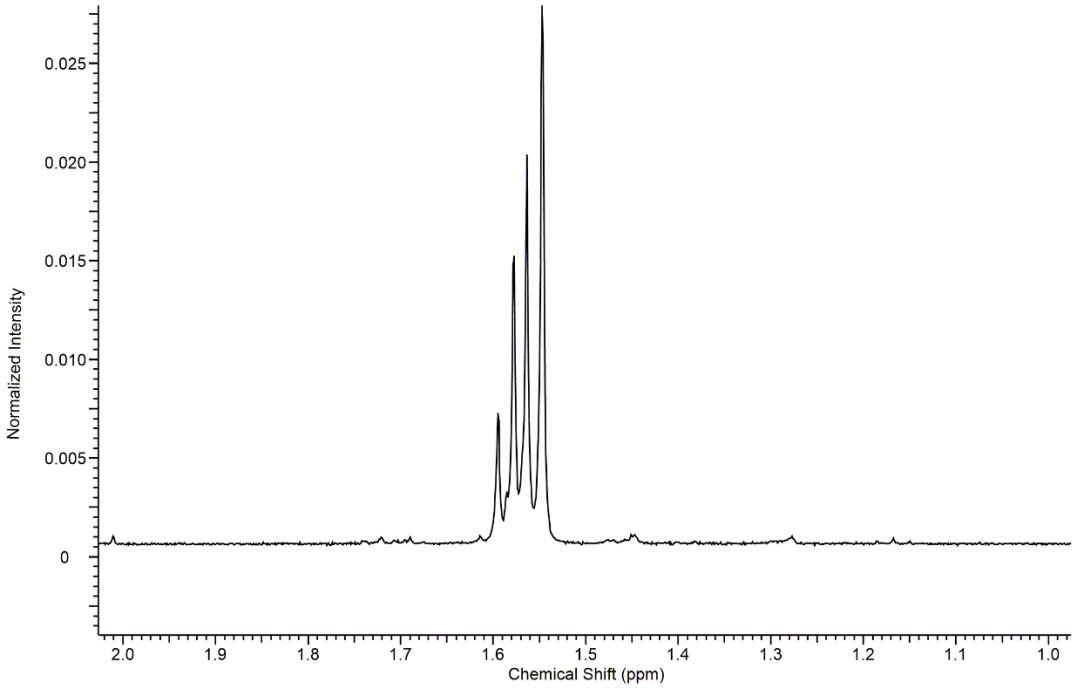

Fig. 4.27b Enlargement of the methyl region of the spectrum shown in Fig. 4.27.

The splitting pattern in the methyl region of the spectrum shown in Fig. 4.27b does not look like singlets. The COSY NMR spectrum obtained from the product mixture after 72 hours revealed the presence of the α-C-H protons in the species present at 3.48, 3.79 and 3.80 ppm respectively, each coupled to methyl protons at 1.58, 1.56 and 1.55 ppm

respectively. Thus, even though epimerisation at the α-carbon centre was considered, it could not be concluded.

The ^{1}H NMR spectrum obtained from the starting material for procedure 7 has been shown in Fig. 4.28 for comparison.

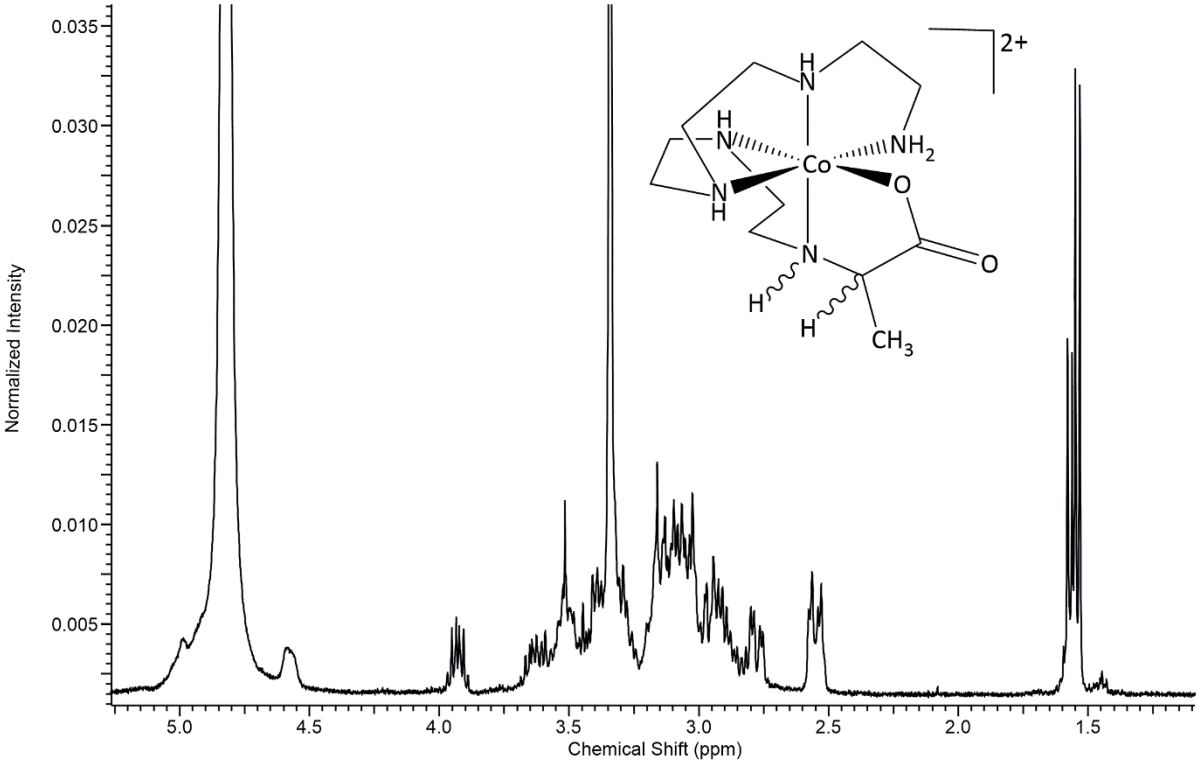

Figure 4.28 A region of the ^{1}H NMR spectrum of the starting material for procedure 7.

Comparing the spectrum from the starting material used for procedure 7 and that from the product mixture of procedure 7 after 72 hours, shows the two mixtures are not the same. At this stage, it can be concluded that epimerisation is not occuring at most of the α-carbon centres. One of the reasons for that conclusion is because ^{1}H NMR showed signals (quartets) for the α-C-H protons were retained even when the methoxy and methyl protons' signals decayed over time. The occurrence of doublets as the splitting pattern for the methyl protons (adjacent to the α-C-H protons) was another indication that the proton of the α-carbon atom was still intact.

All the products from the esterification procedures followed in this chapter showed similar characteristics in solution with respect to hydrolysis. Spectra obtained over time have shown a decay of the methoxy peaks and the consequent disappearance of the methyl peaks

accompanying them thereby confirming hydrolysis of these systems in water/moisture. The NMR spectra show water peaks from the deuterated solvents.

A consistent pattern was observed from mass spectrometry where the new species 'fly' with some protons lost. For most of the products two protons were lost. It was observed that if the sample for the MS analysis was prepared a while before the experiment runs, that the chelated esters could not be found. Knowing that these chelated ester complexes hydrolyse very easily, a method termed 'spiking' was used by the departmental instrument technician (Dr. Amanda Inglis) to 'catch' these short-lived species. Spiking involves preparing a concentrated sample in a choice solvent (dry methanol was used here) which will be diluted at the point of analysis. That way, there would be less water available and the presence of excess solvent to push the equilibrium to the ester product and not hydrolysed product.

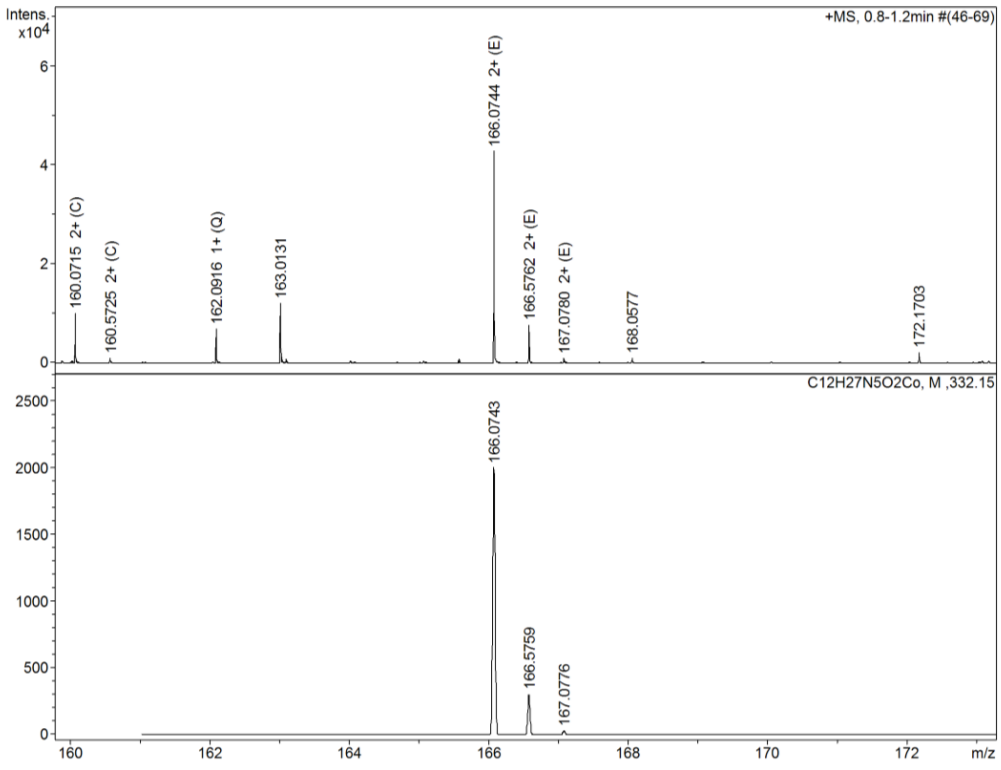

Figure 4.29 ESIMS of procedure 7 showing a +2 species. Top: experimental, bottom: calculated.

Compound **4.7** (and its stereoisomers) from procedure 7 has (have) the chemical formula of $[C_{12}H_{29}N_5O_2Co]^{3+}$ with a monoisotopic mass of 334.17 and an M/Z ratio of 111.39

as a 3+ species. As a 2+ species (where it has lost 2 H's), its M/Z ratio is 166.07 as shown in the spectrum in figure 4.29. If a 3+ species loses two protons, it would become a 1+ species. It is not clear at this stage why the calculated 1+ peak carries a 2+ charge in the spectrum.

This same argument applies to compound **4.1** (and its stereoisomers) which have the molecular formula of $[C_{12}H_{32}N_5O_3PCo]^{3+}$ and a monoisotopic mass of 384.16 and an M/Z ratio of 128.05. The expected spectra have been obtained and are shown in Figs. 4.30 – 4.32. Figure 4.30 shows where one molecular ion of a 2+ charged complex (after losing 1 H), 'flies' with one of its counter ions ($CF_3SO_3^-$) to give a 1+ species.

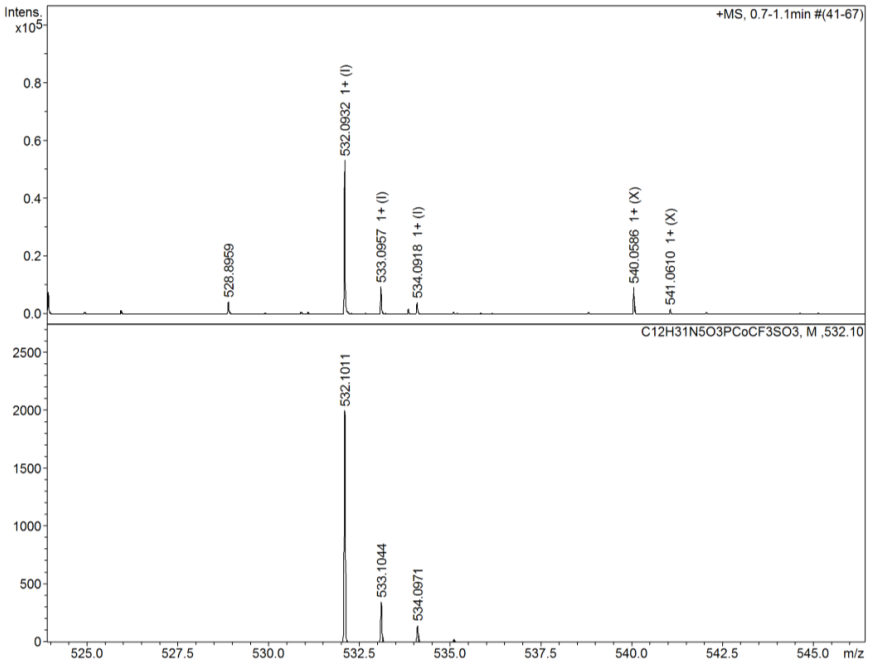

Figure 4.30 ESIMS of procedure 1 showing a +1 species. Top: experimental, bottom: calculated.

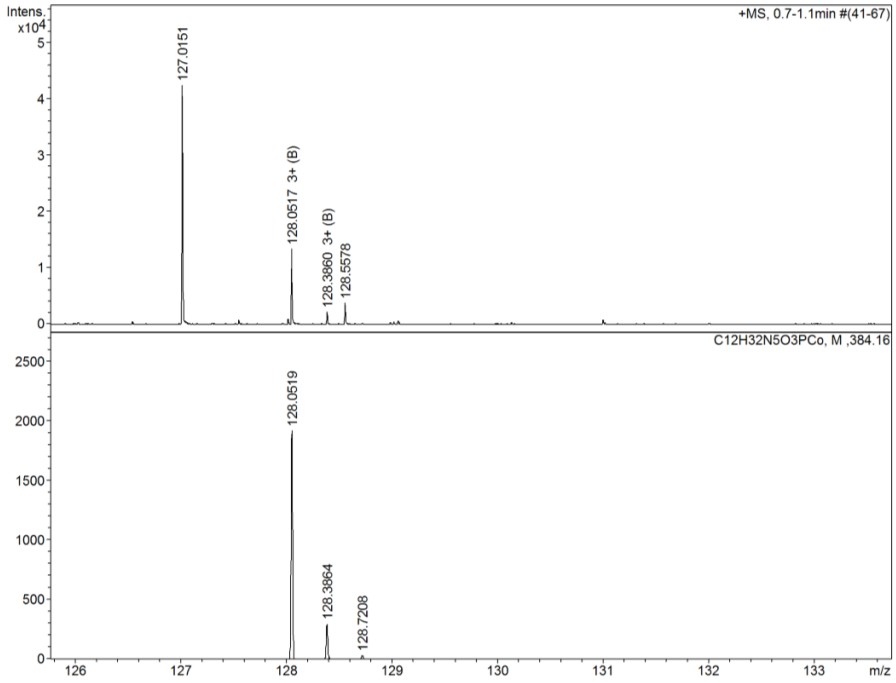

Figure 4.31 ESIMS of procedure 1 showing a +3 species. Top: experimental, bottom: calculated.

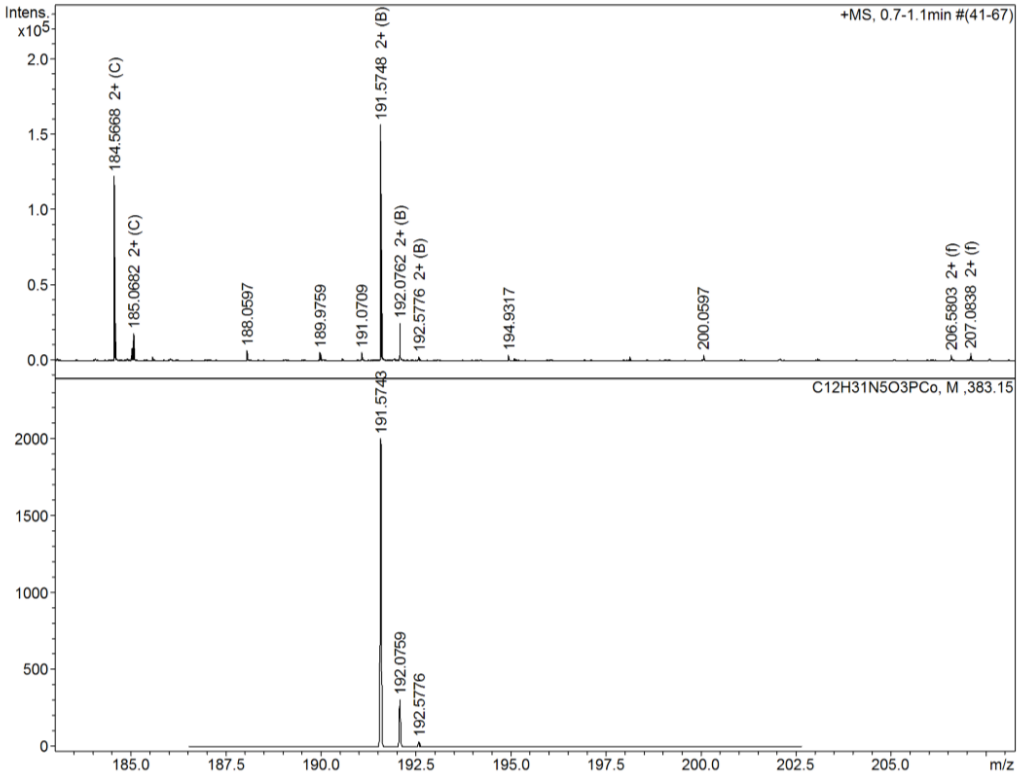

Figure 4.32 ESIMS of procedure 1 showing a +2 species. Top: experimental, bottom: calculated.

It appears from ^{1}H NMR and MS that the hydrolysis reaction occurs side-by-side with the esterification reaction. This aligns with observations in the literature.[47, 63-75] The unbalanced integral values found between the methyl protons and those of the methoxy ones give a good indication that not all the molecules present in the NMR tube mixture bear two esters on their phosphonate arms.

One of the molecules expected in the product mixture of procedure 6 has been shown as Fig. 4.33. The methoxy and methyl regions of the ^{1}H spectrum from the procedure are shown as Figs. 4.34 and 4.35 respectively.

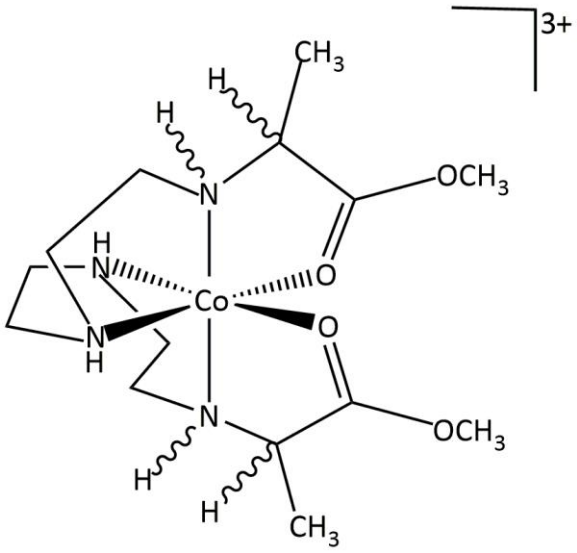

Figure 4.33 One of the expected molecules from the product mixture of procedure 6

If a C_2 axis of rotation exists in a given molecule from the product mixture of procedure 6, four pairs of diastereoisomers would be expected to be generated considering only two of all the stereogenic centres present; the α-carbon centre and the secondary amine adjacent to it. On the other hand, if no symmetry element is present in a given molecule, then as many as eight pairs of diastereoisomers could be produced from four stereogenic centres only; the α-carbon centre and the secondary amine adjacent to it on both ends of the molecule. It is predicted that the product mixture could be a mixture of both symmetrical and unsymmetrical stereoisomers.

The methoxy protons of the chelated carboxylate ester complexes prepared in this project resonate between 3.71 and 4.11 ppm region of the ^{1}H NMR spectrum as singlets (*e.g* Fig. 4.34), as in the literature.[66] Three singlets were observed in the methoxy region from the ^{1}H NMR spectrum (Fig. 4.34) of procedure 6. There is a tall peak of about 50%

intensity, which is flanked on both sides by two peaks of about 25% and 20% intensities respectively. The tall middle peak could be attributed to a symmetrical molecule whose methoxy protons all resonate in the same frequency. It is very tempting to assign the two other resonance peaks to an unsymmetrical molecule but that would depend on the analysis from the methyl region of this spectrum.

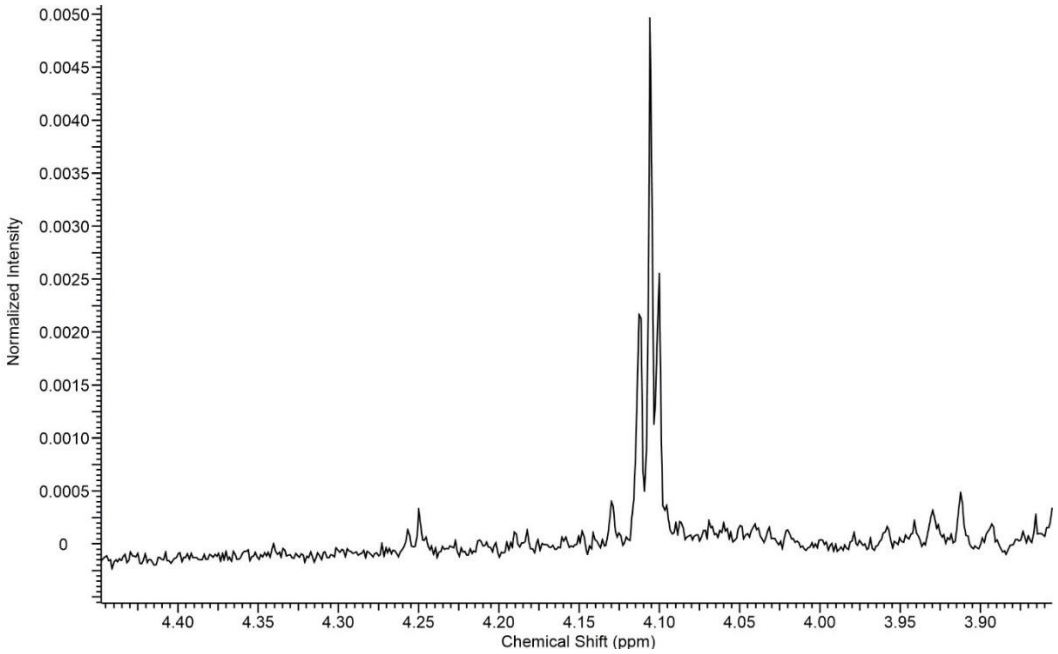

Figure 4.34 Methoxy region of ^{1}H NMR of product from procedure 6

The methyl region of the product mixture from procedure 6 has been shown as Fig. 4.35. This spectrum was obtained soon after the NMR sample was prepared in deuterated methanol (CD_3OD). The region is quite clustered with doublets of the methyl protons coupled to the proton on the same α-carbon atom. There are two doublets at 1.6 and 1.7 ppm respectively with roughly the same intensities (based on integral values). They appear to be from an unsymmetrical molecule. That would match the two other peaks flanking the major peak at 4 ppm of the same spectrum, confirming the presence of unsymmetrical molecules in the product mixture. The cluster of peaks from 1.76 – 1.81 ppm may well contain two doublets from a symmetrical molecule in the overlap.

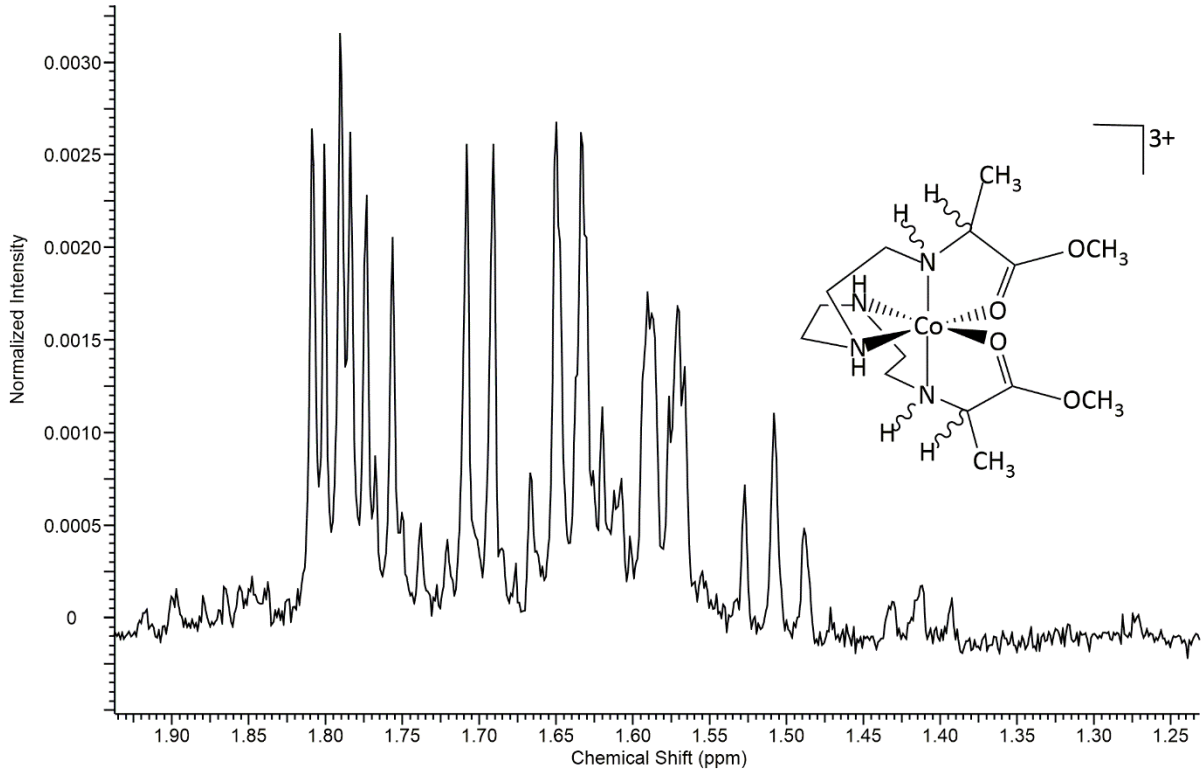

Figure 4.35 Methyl region of ^{1}H NMR from procedure 6

After about 72 hours, another ^{1}H NMR experiment was carried out using the same sample (in the same NMR tube) and the methyl region as recorded has been shown in Fig. 4.36. It looks very much like the starting material and that is not unexpected as hydrolysis reverts the molecule back to its starting material, compound **3.6** (methyl region of its ^{1}H shown in Fig. 4.37). Procedure 6's ESIMS can be recalled as follows: Calcd. for $[C_{14}H_{30}CoN_4O_4]^{3+}$: 377.16; M/Z = 125.72. Found: 375.14; M/Z = 187.57 for $[C_{14}H_{28}CoN_4O_4]^{2+}$; $[M\text{-}2H]^{+}$ and 347.11 for $([C_{12}H_{24}CoN_4O_4]^{1+}$ $[M\text{-}2(CH_3)]^{1+}$ for compound **3.6** (starting material).

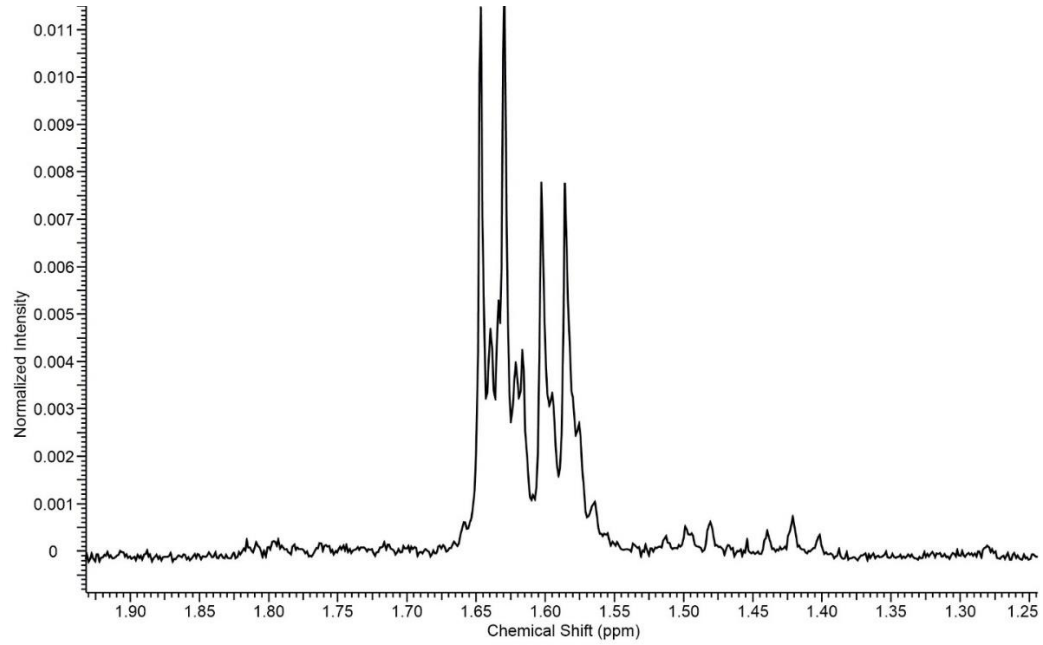

Figure 4.36 Methyl region of the 1H spectrum of procedure 6 product after 72 hours.

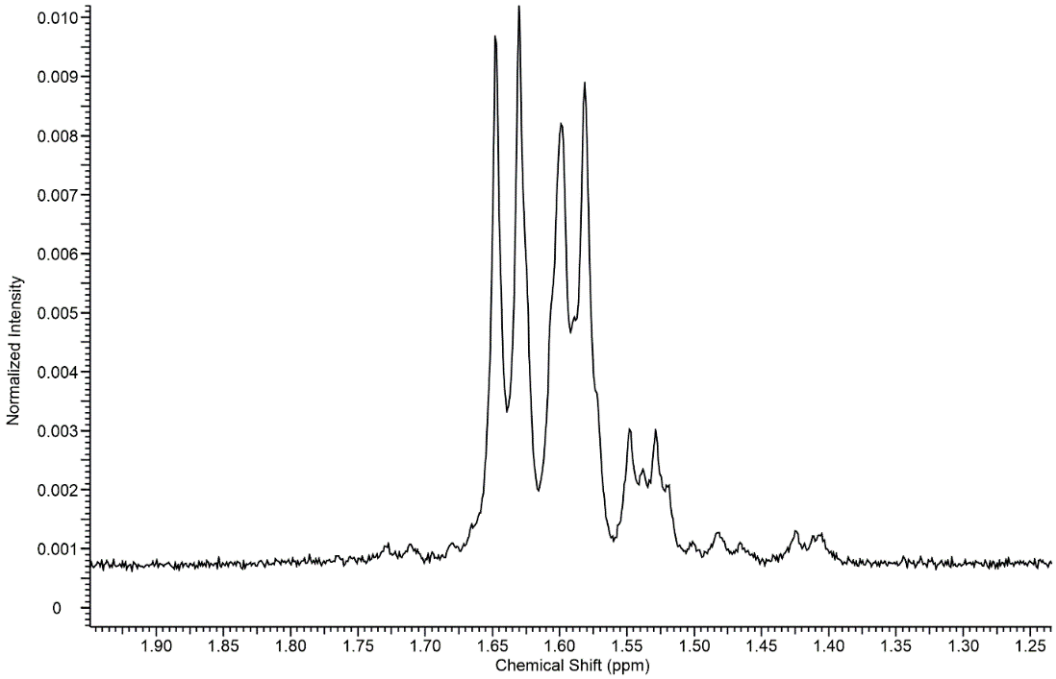

Figure 4.37 Methyl region of the 1H NMR spectrum of compound 3.6's (starting material) product mixture.

The shifted resonance peaks observed after 72 hours from the spectrum shown in Fig. 4.36 (compared with the spectrum of the starting material shown in Fig. 4.37) aligns with the aforementioned hypothesis that epimerisation of the proton on the amine adjacent to the α-carbon atom must be occurring in the solution of the product mixture with the deuterated NMR solvent. This epimerisation leads to isomerisation which

would introduce new stereoisomers into the product mixture thereby generating new (or shifted) signals in the NMR spectrum.

Solvent exchange with the deuterons of the NMR solvent (CD_3OD) also occurs; evident from the multiplicity of the α-C-H protons observed as quartets as opposed to quintets. The methoxy resonance peaks disappeared after 72 hours.

Fig. 4.38 shows a part of the ^{1}H NMR of the product mixture from procedure 1, a phosphonate system. The main highlights of that spectrum are the sets of doublets upfield (1.5 – 1.8 ppm) and downfield (around 4.1 ppm) which demonstrate that the new methoxy group was added successfully. Each doublet of doublets (1.5 – 1.8 ppm) resonates from the methyl group in a given molecule whose signal is split by both the α-carbon ^{1}H and the ^{31}P nuclei. The two doublets around 4.1 ppm are from the chemically different methoxy groups on the phosphorus centre.

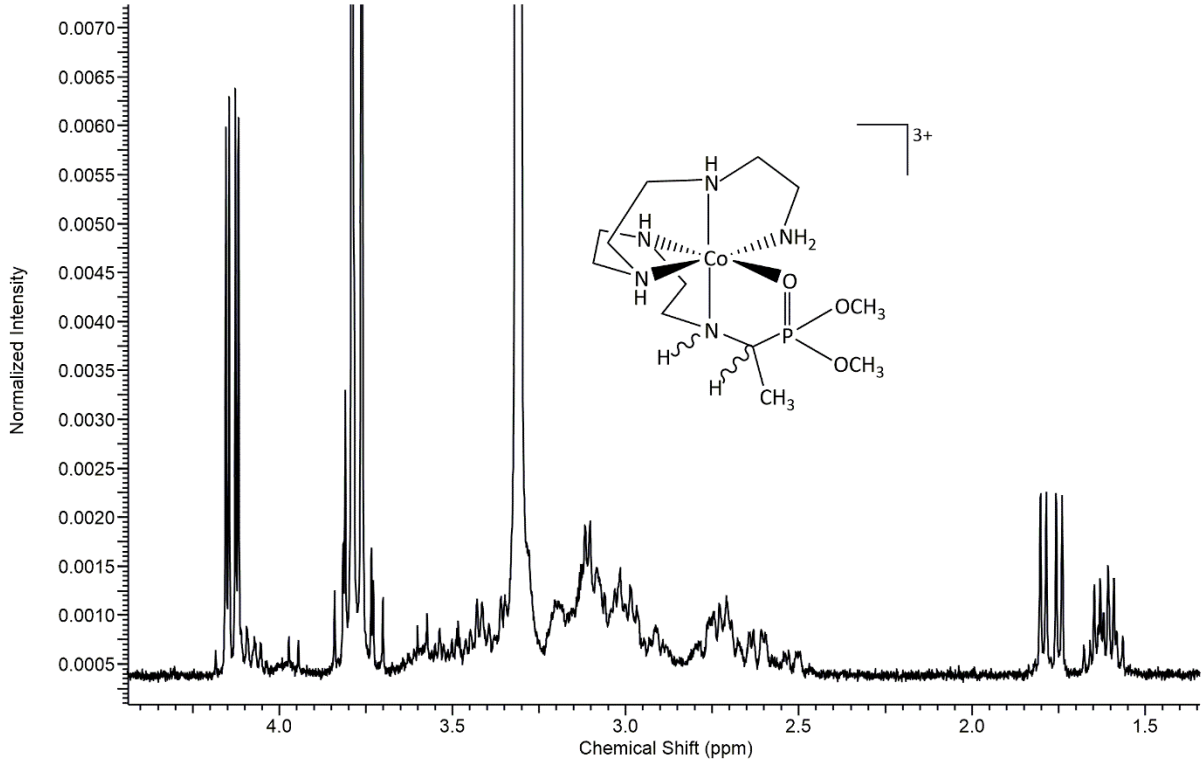

Figure 4.38 A region of the 1H NMR of the product mixture from procedure 1

Following the trend observed in the carboxylate systems, two sets of compounds are predicted in the product mixture from procedure 1: (1) one set of complexes where the phosphorus centre

has two ester groups attached to it ((**4.1**) in Fig. 4.39), (2) another set of complexes with only the pre-existing ester group at the phosphorus centre; a situation where hydrolysis had occurred at the phosphorus centre to form the complex shown as **9** in Fig. 4.39, which could eventually revert to its amine precursor (**3.1**) or its isomer.

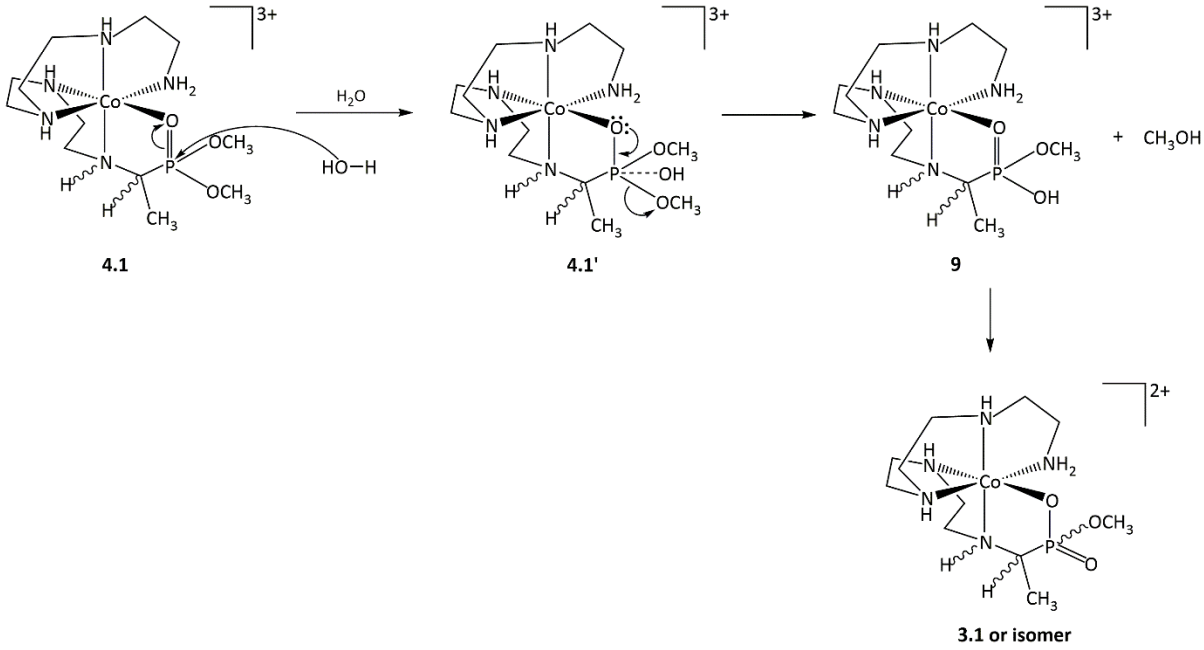

Figure 4.39 Schematic of the expected hydrolysis through a trigonal bipyramidal intermediate in the phosphonate systems.

The two sets of doublets (doublet of doublet; integral values of 1:1) around 1.7 ppm in Fig. 4.38 have been assigned to molecules where two ester groups are attached to the phosphorus centre. The protons on the methyl group would be coupled to both H and P nuclei, thereby experiencing some combination of $^{3}J^{HH}$ and $^{3}J^{HP}$ coupling effects to give a doublet of doublet. Two signals are expected from each set of diastereotopic methoxy protons. The two doublets at the 4.1 ppm region of the spectrum (Fig. 4.38) have been assigned to the two chemically different ester groups at the phosphorus stereogenic centre. The coupling constants of these new methoxy doublets are 8 Hz each. Integration showed a 2:1 ratio between the major methoxy protons (4.1 ppm) and the major methyl ones (1.7 ppm), as expected.

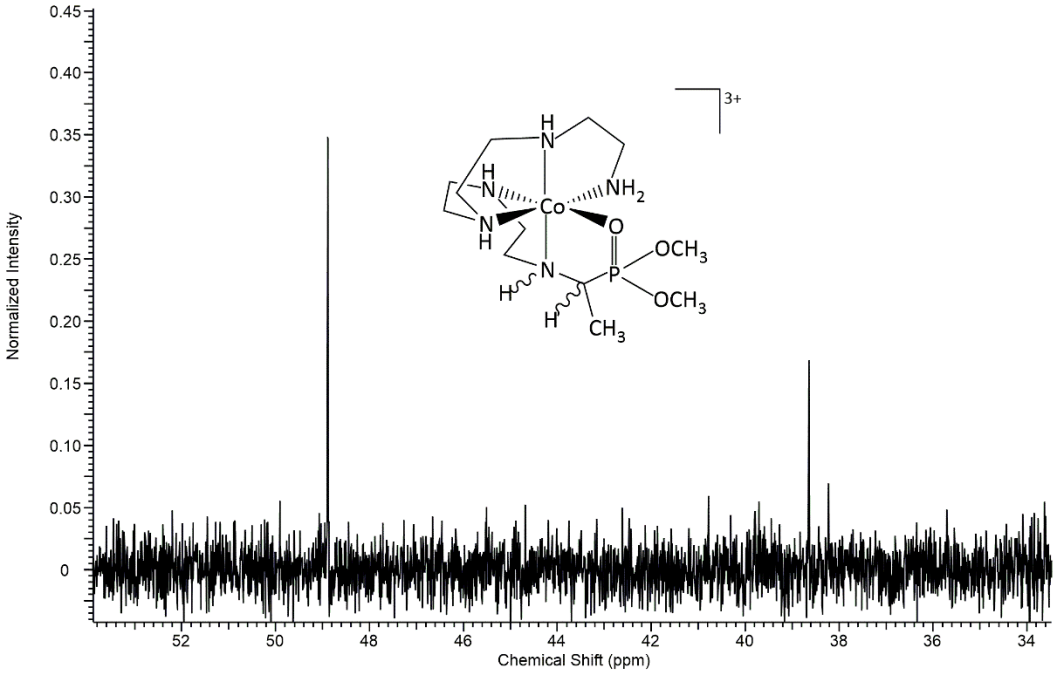

Figure 4.40 $^{31}P\{^{1}H\}$ NMR from the product mixture of procedure 1 showing two sets of signals.

One pair of diastereoisomers dominate the product mixture in the spectrum shown as Fig. 4.38 and they are chelated ester complexes. A major peak at 48.87 ppm was also observed in the $^{31}P\{^{1}H\}$ NMR spectrum (Fig. 4.40) for the product mixture (from procedure 1) with three minor ones, validating the ^{1}H NMR spectrum.

This assignment was also supported by the disappearance of these peaks (at 1.7 ppm) with those of the methoxy protons (also in a 1:1 integral ratio) consequently after hydrolysis had taken place as can be seen in the spectrum shown as Fig. 4.41. Upon disappearance of the methoxy signals, the spectrum shows an increase in the peak intensities of the methyl protons at 1.6 ppm. This increase was also confirmed through integration of the spectrum. The overlapped signals appear to be dominated by a major doublet of doublets and another minor set of same multiplicity.

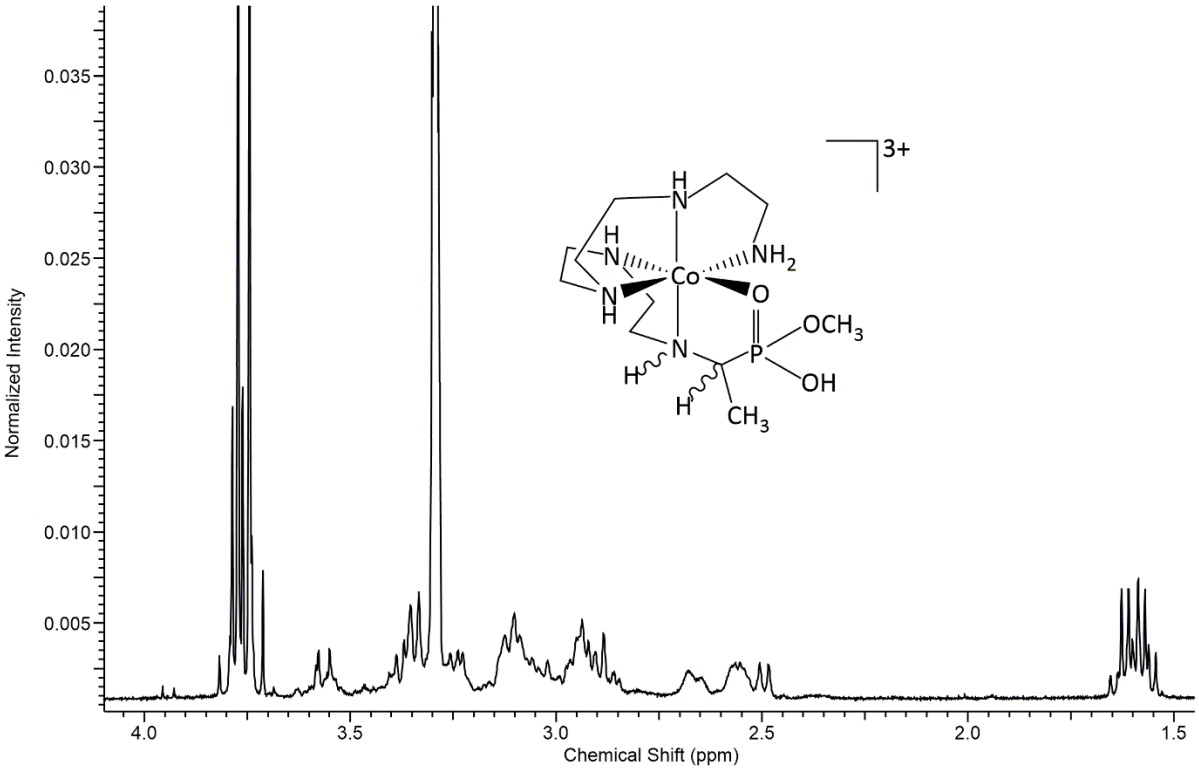

Figure 4.41 A region of the ^{1}H NMR of the product mixture from procedure 1 after 24 hrs

Another observation made from the NMR spectrum shown as Fig. 4.41 is its simplicity compared with that in Fig. 4.38. Not only did the signals from the methyl and methoxy protons disappear from the spectrum, those from protons of the methylene groups as well as protons of the amine groups were also lost after 24 hours. The disappearance of signals coupled with the increased integral value of the methyl protons after 24 hours suggests hydrolysis of these chelated ester systems and isomerisation of the complexes in solution over time.

Previous research on the carboxylate systems demonstrated[52] that the initial configuration at the α-carbon centre is retained through to isolation while exchange occurred at the amine sites between protons and the solvent ions. The solvent exchange of amine protons resulted in the loss of signals at the 6 ppm and 7.5 ppm regions for the carboxylate compounds studied[52]. However, the α-C-H signal at 4 ppm was still present[52] as well as the doublets for the methyl protons. If the α-carbon centre's proton had been exchanged, it will result to singlets in the methyl region of the ^{1}H NMR spectrum, since the hydrogen-deuterium coupling would not be observed.

Four possible pairs of diastereoisomers that could be generated from the chirality at the α-carbon atom and the amine adjacent to it, have been schematised in Fig. 4.42.

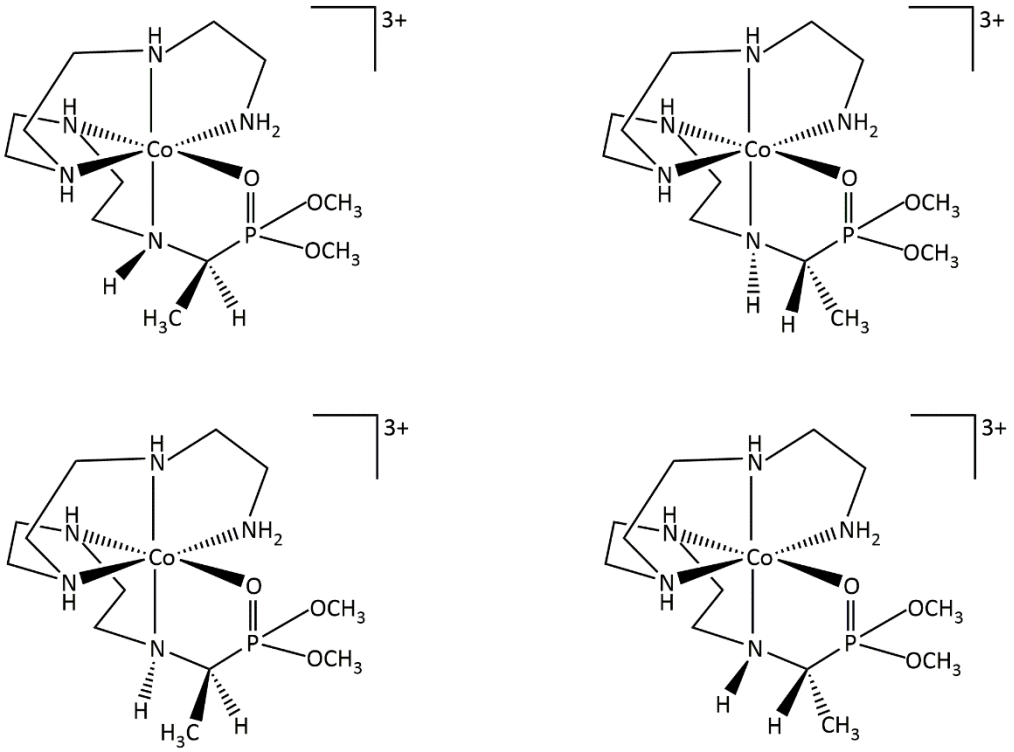

Figure 4.42 Schematic of four diastereoisomers (and their enantiomers) that could be generated from epimerisation at the α-carbon centre and the amine adjacent to it.

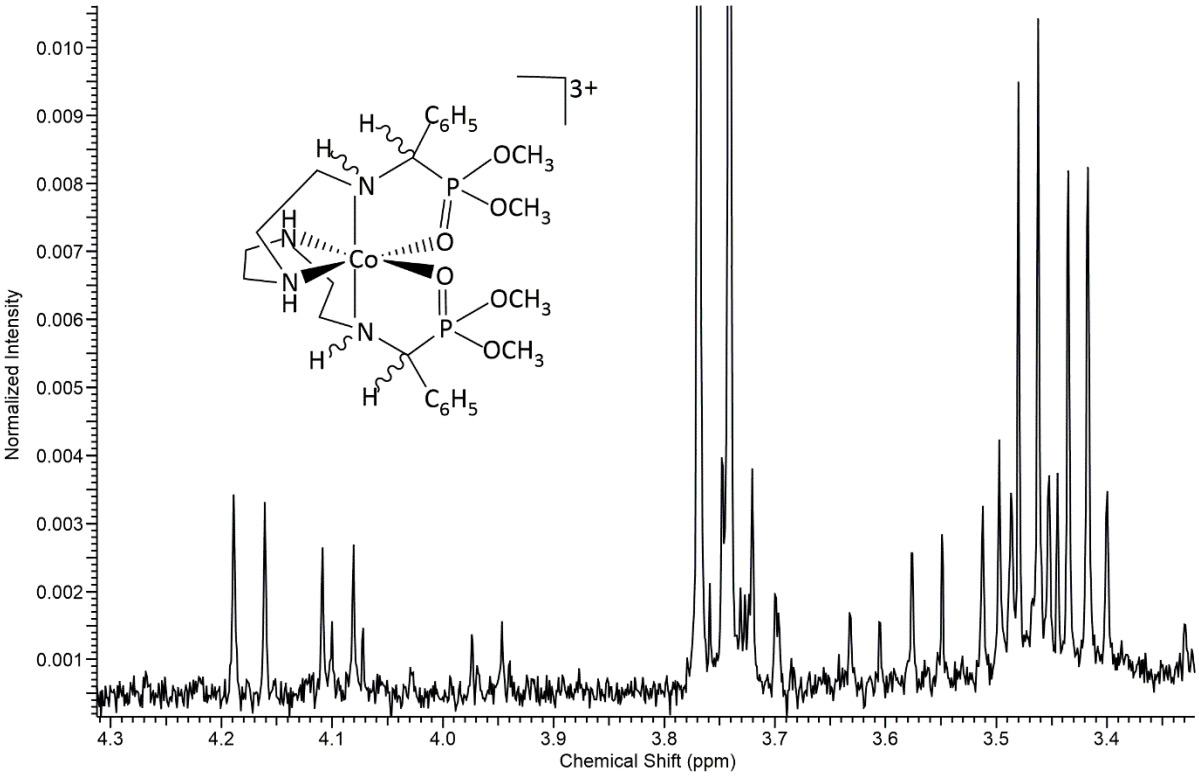

Figure 4.43 Methoxy region of the ^{1}H NMR of the product mixture from procedure 4 before complete hydrolysis and isomerisation.

Figure 4.43 shows yet another very complicated ^{1}H NMR spectrum from procedure 4. The synthesis was done with a sample (**3.4**) dominated by symmetrical molecules (based on its ^{1}H NMR spectrum: Fig. 4.45). It has therefore been assumed that the symmetry would be retained in most of the compounds in the product mixture. Symmetrical molecules are expected to have their methoxy protons resonating in the same frequency due to being in similar chemical environments. Focusing on the new signals downfield from 3.9 ppm in Fig. 4.43 and using integral values, there are two new pairs of symmetrical diastereoisomers and one pair of unsymmetrical diastereoisomers. The other (associated) peaks assigned to the pre-existing methoxy protons of these new compounds can be seen in the 3.5 and 3.6 ppm region of the same spectrum. They look like those from two symmetrical molecules judging by a combination of integration and the pattern observed so far from the ^{1}H NMR of the complexes reported in this project.

The presence of unsymmetrical molecules in the product mixture from procedure 4 cannot be ruled out. If two resonance peaks are generated from an unsymmetrical molecule, they would be expected to have equal integral values. The two minor doublets at 3.9 and 4.1 ppm have matching intensities with a 1:1 integral ratio.

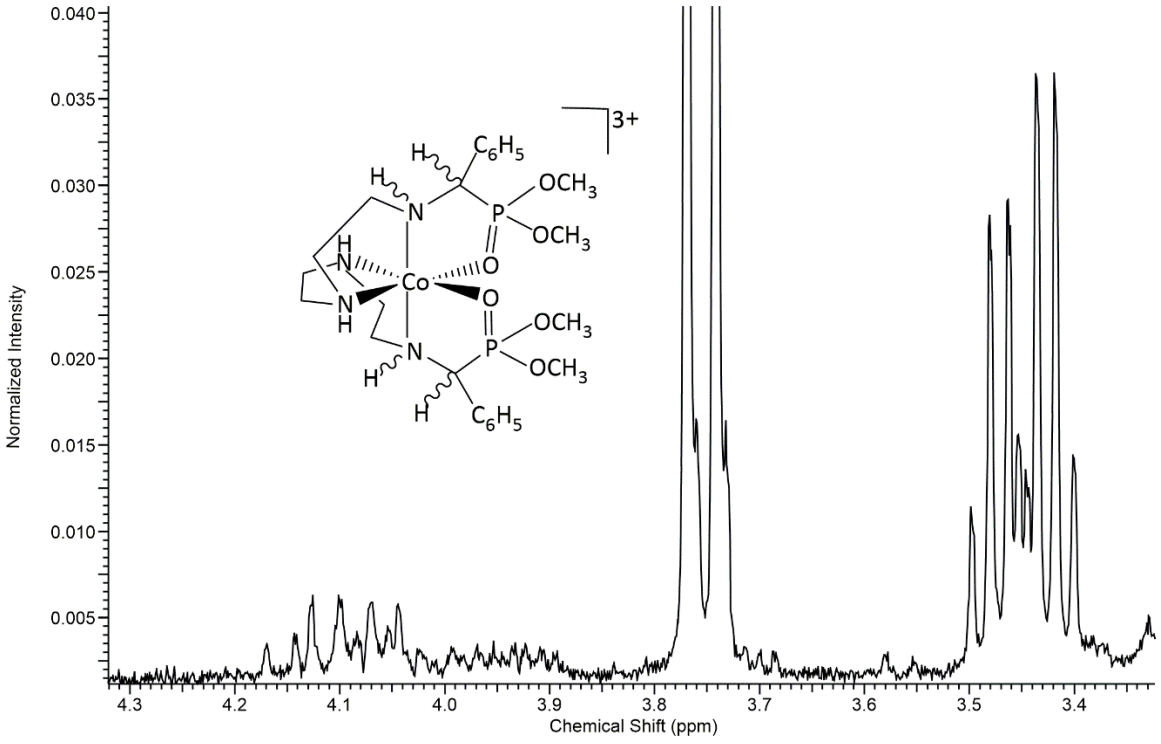

Figure 4.44 Methoxy region of the ^{1}H NMR of the product mixture from procedure 4 close to complete hydrolysis.

Another possibility yet exists for some new stereoisomers which could be generated from epimerisation of the protons of the NH adjacent to the α-carbon atom of the amine. All these combinations of isomers give rise to a complicated NMR spectrum, as seen in Fig. 4.43, for example. The protons of the α-carbon atom have been masked by the solvent (trimethyl phosphate) peak in Fig. 4.43. The disappearance of the α-CH signals alongside the methoxy signals in Fig. 4.44 over time validates the claim of isomerisation.

Once again, the presence of stereoisomers amidst hydrolysis products, makes complete assignment of the spectrum daunting. There are overlapping peaks, some may be not even distinguishable. However, there is striking evidence of the presence of new OCH_3 resonance peaks which confirm that the new ester group was successfully added to the cobalt(III) complex. The methoxy region of the ^1H NMR spectrum obtained from the starting material for procedure 4 has been shown in Fig. 4.45 for comparison. The product mixture obtained after the esterification reaction (and after hydrolysis) does not match the mixture of the starting material.

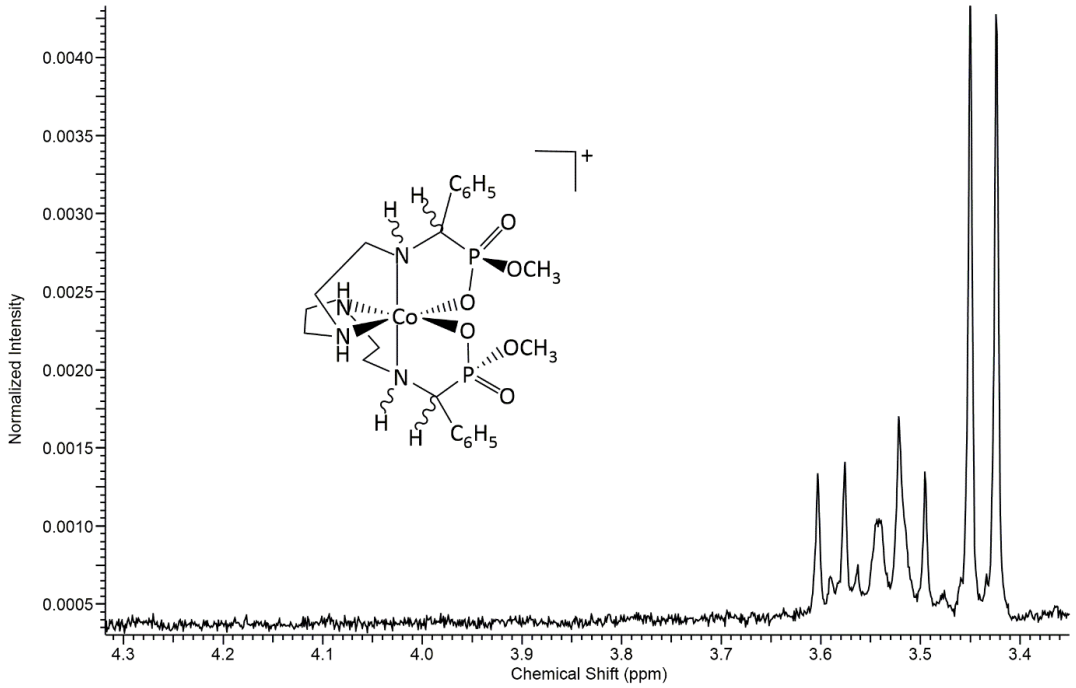

Figure 4.45 Methoxy region of the ^1H NMR of the starting material for procedure 4.

The methyl region (1.5 – 1.9 ppm) of the ^1H spectrum (Fig. 4.46) obtained from the product mixture from procedure 5 was also complicated. The lack of a symmetry element (like a C_2 axis of rotation) in a given molecule of the mixture must contribute to the complexity observed

in the NMR signals. However, the two sets of signals observed in that region followed the trend observed so far for the other characterised chelated ester complexes synthesised in this project.

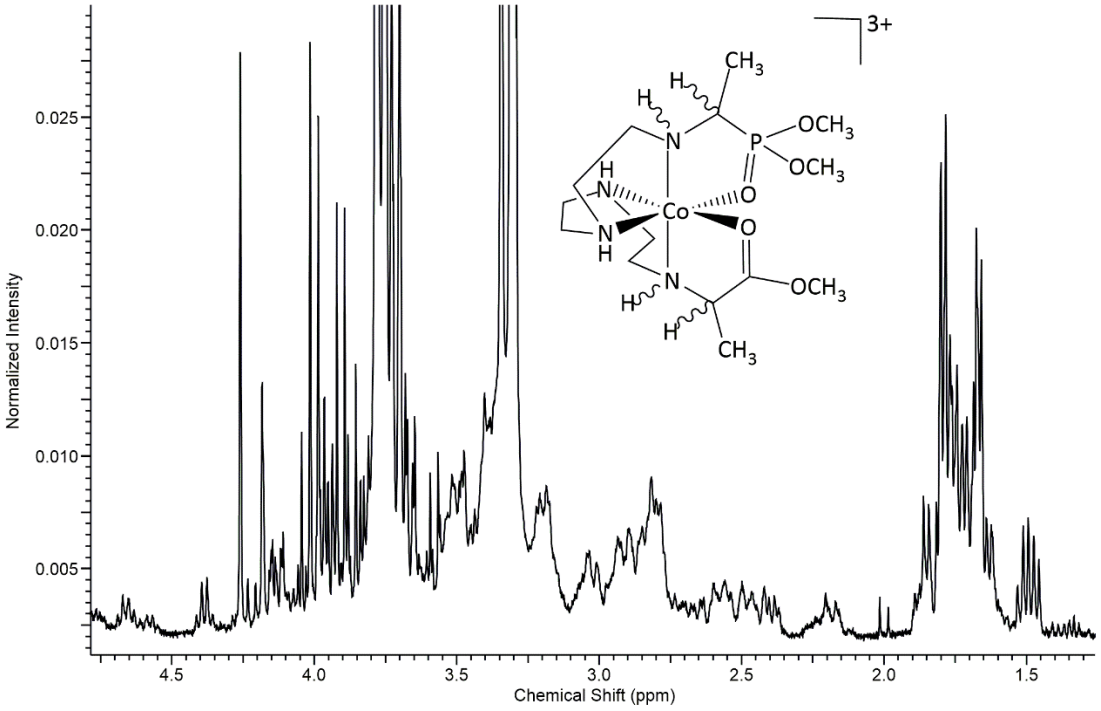

Figure 4.46 Methoxy region of the ^{1}H NMR of the product mixture from procedure 5 before complete hydrolysis and isomerisation.

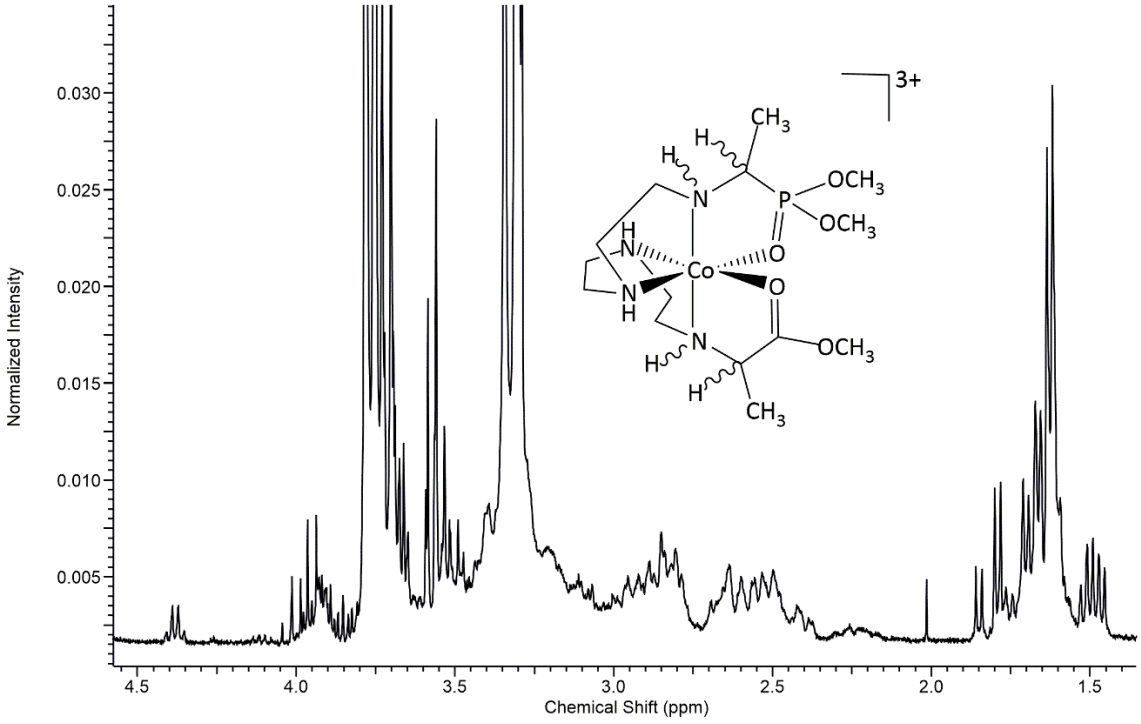

Figure 4.47 Methoxy region of the ^{1}H NMR of the product mixture from procedure 5 partly through hydrolysis and isomerisation.

It could be argued that the less intense cluster of peaks is from the methyl protons on the phosphonate end of a minor pair of diastereoisomers where hydrolysis and NH epimerisation had already occurred whereas the cluster next to it is from both the carboxylate and phosphonate ends of the molecules in the mixture. The methyl protons on the carboxylate end are expected to resonate as doublets in the 1.6 ppm region of an ^{1}H NMR spectrum. However, the methyl protons on the phosphonate end of the complex have been observed to resonate as doublets of doublets due to both $^{3}J^{HH}$ and $^{3}J^{HP}$ coupling effects. The multiplicity of the signals was hard to figure out from the overlap dominant in that region.

The methoxy protons on the carboxylate end of the complex from the product mixture of procedure 5 are expected to resonate as singlets above the 4 ppm region of a ^{1}H NMR spectrum. The spectrum shown as Fig. 4.46 shows three outstanding singlets at 4.04, 4.18 and 4.26 ppm respectively. Those have been assigned to the methoxy protons on one major and two minor pairs of diastereoisomers. There is yet another cluster of singlets overlapped by other signals from 4.11 – 4.16 ppm. The methoxy protons on the phosphonate end of the complex have been assigned through the coupling constants of the doublets in that region of the spectrum; the main ones being at 3.9 and 4.0 ppm respectively. Two outstanding quartets at 4.4 and 4.6 ppm have been assigned to C-H protons (on the α-carbon atom). Assignment of the other C-H protons (on the α-carbon atom) was aided by a COSY spectrum which showed the other quartets were hidden at 3.96, 4.09 and 4.13 respectively.

The trend of peak decay and consequent disappearance was also observed with the chelated ester complexes made from procedure 5. Fig. 4.46 shows the spectrum obtained soon after sample preparation while Fig. 4.47 shows the spectrum obtained from the sample a little less than 24 hours from its preparation. It can be observed with respect to the methoxy region of the spectrum especially, that the peak intensities are lower in the spectrum of Fig. 4.47 than in that of Fig. 4.46. That follows the earlier discussion on the effects of hydrolysis as well as NH epimerisation on these chelated phosphonate ester complexes of cobalt(III). While integration indicated the loss of methoxy signals, the sum of the integral values from the methyl signals stayed the same.

There is a likelihood that the molecules present in these systems could be isomerising over time to a more favourable configuration with respect to the amine adjacent to the α-carbon centre. However, given the conditions under which these observations of peak

disappearance and shifting have been made, the quest is still on to understand all the factors that contribute to this epimerisation. In the literature[52], the NH isomerisation was studied in basic conditions. One of the factors under consideration is that of an increased positive charge on the metal complex as a 3+ cation in its full ester form, which would increase the acidity of the NH protons making them more prone to epimerisation.

4.3.2 Hydrolysis of trien based amino phosphonate complex

Metal ion promoted hydrolysis of α-amino esters is a matter of significance.[73] In this study, MS and ^{1}H NMR data provide evidence for the hydrolysis observed on the chelated ester groups of a trien-based cobalt(III) phosphonate amino acid complex. A closer look at the spectrum shown as Fig. 4.48 revealed that there were fewer resonance peaks in the methoxy region of the spectrum as opposed to being completely non-existent. Peak intensities (integral values) of the major and well resolved resonance peaks at both the methyl (1.6 – 1.7 ppm) and methoxy (3.6 ppm) regions of the spectrum also supported the hydrolysis. Better resolution of the spectrum obtained after 72 hours of reaction can be attributed to the decrease in the number of protons which are all in different chemical environments (caused by the loss of methoxy groups and their protons).

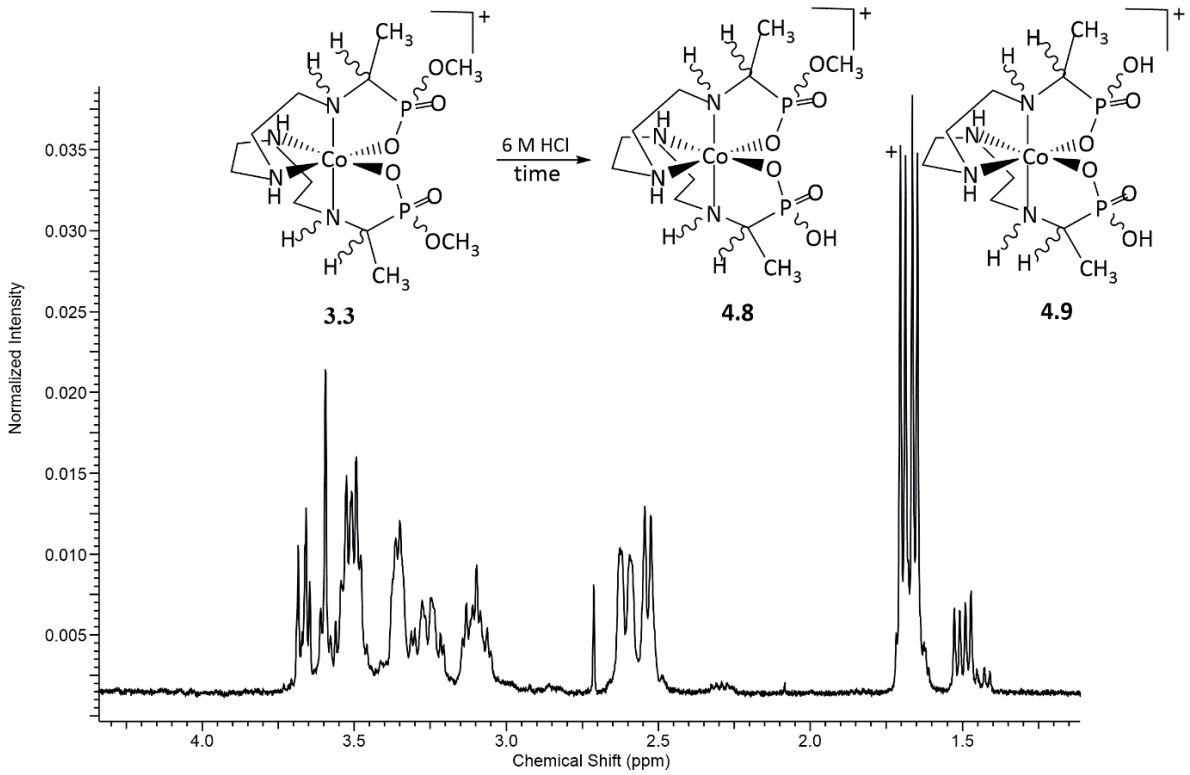

Figure 4.48 A region of the ^{1}H NMR spectrum of the product mixture of procedure 8 showing three possible components.

The methoxy protons resonate around the 3.6 ppm region (Fig. 4.49) for this mixture. It has been explained that the more electronegative oxygen atom of the alkoxy group deshields the protons hence their downfield chemical shifts. They are coupled by the ^{31}P NMR active nuclei to split into doublets. The presence of N**H** resonance peaks downfield of the spectrum could be an indication that the α-carbon protons should still be intact but overlapped and hidden by other peaks upfield from 4 ppm. The splitting pattern of doublets for the methyl protons provide more evidence to support the presence of the protons of the α-carbon atoms at both ends of the molecule. That would support the proposition that epimerisation is not occurring at the α-carbon atoms of the compounds synthesised in this project under the prevailing conditions.

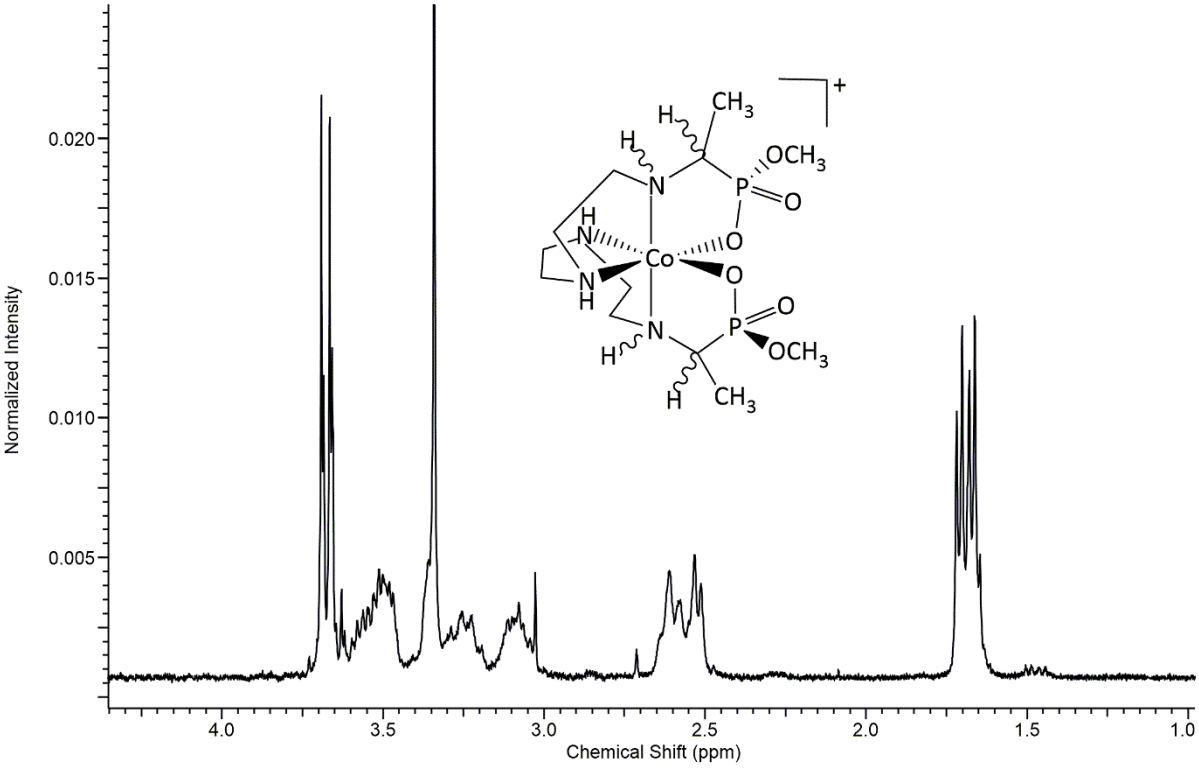

Figure 4.49 A region of the ^{1}H NMR spectrum of the starting material for procedure 8.

During the method development for the isolation of the isomers from a given reaction mixture of the imine-phosphonate complexes of cobalt(III) made in this project, a procedure whereby a 0.5 – 1.0 M HCl solution was used to elute the bands off a Dowex 50WX2 (100 – 200 mesh) column, resulted in hydrolysis (observed in NMR and MS) of the ester chelate as highlighted in this section. Single crystals of a mono-hydrolysed molecule (hydrolysed on one of its chelated ester groups), from the product mixture of chapter 2's procedure 3, were grown by

vapour diffusion of acetone into a 0.1 M HCl solution of the mixture. Dark red, irregular shaped, crystals formed. The crystals were grown from a fraction 1 mixture and the structural model of one of its single crystals is shown in Fig. 4.50 (same as Fig. 2.21 for compound **2.6** in chapter 2 of this thesis).

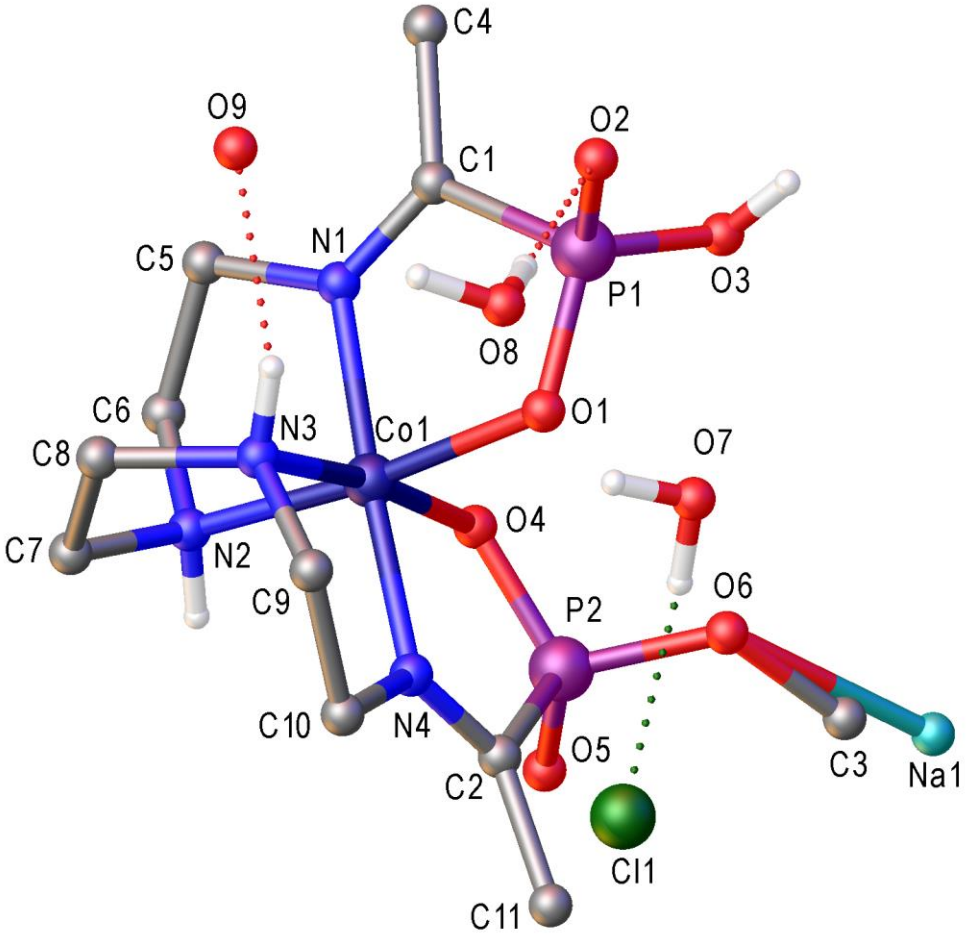

Figure 4.50 Crystal structure from chapter 2 showing a hydrolysed ester chelate of a cobalt(III) imine phosphonate complex. Most hydrogens have been omitted for clarity.

Solving the crystallographic model shown in Fig. 4.50 prompted the study of the hydrolysis of the chelated ester complexes of the phosphonate amino acids of cobalt(III) in this project as outlined in procedure 8 of this chapter. Evidence of acid catalysed hydrolysis of cobalt(III) chelated ester complexes abounds in the literature.[47, 63-67, 69-71, 73-75, 132]

The ester hydrolysis was also monitored by mass spectrometry. Fig. 4.51 shows the three most likely species that could be contained in a mixture during the period of the hydrolysis reaction. When the imine complex is formed bearing two phosphonate arms with a methoxy group on each arm (chelated esters in this context), the calculated monoisotopic mass is 447.09. This mass reduces to 433.08 when one of the phosphonate arms loses its methoxy group (chelated ester) to take on a hydroxyl group. The peak at 419.06 matches the experimental value for the monoisotopic mass of a complex that has been fully hydrolysed.

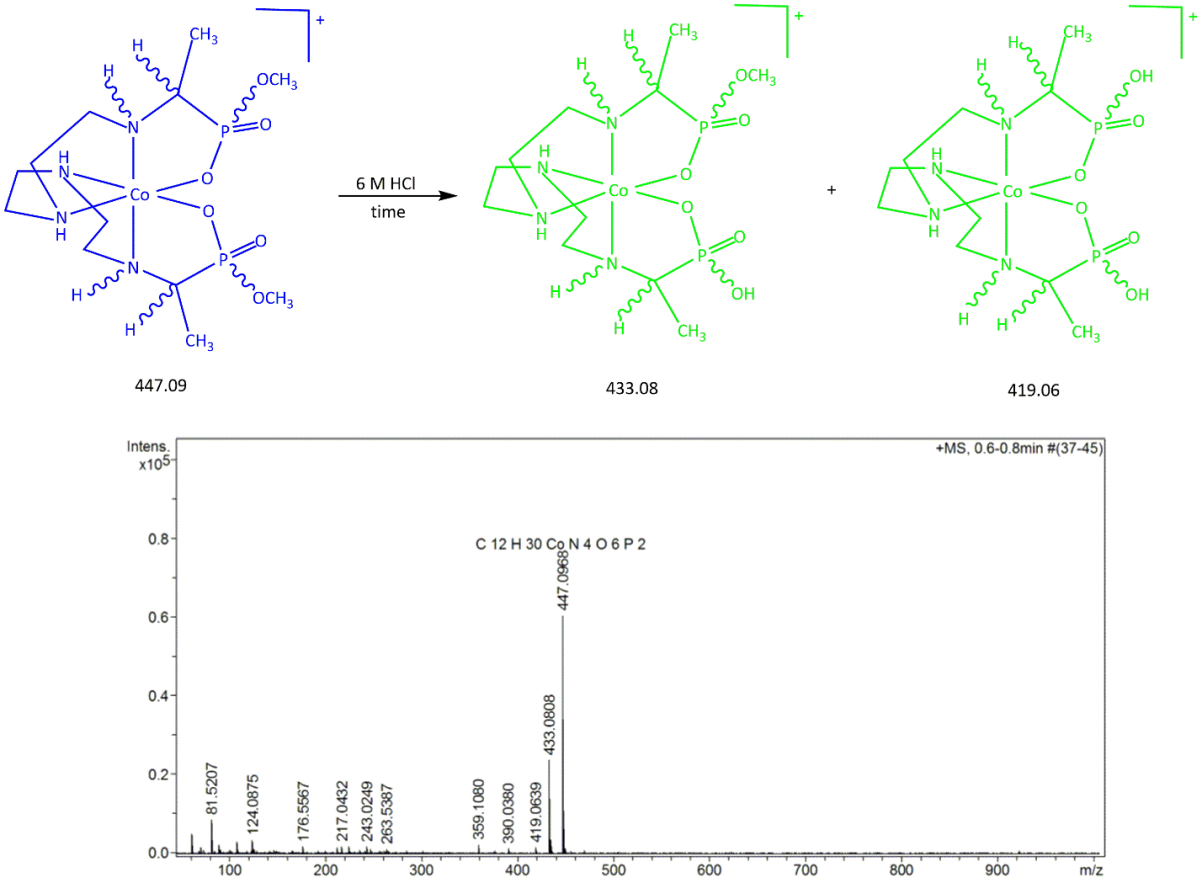

Figure 4.51 Mass Spectrum after one hour of reaction (procedure 8).

One hour after the start of the hydrolysis reaction, the species with the monoisotopic mass of 447.09 dominated the reaction mixture. That corresponds with the mass of the cobalt(III) complex with two chelated ester groups, where the methoxy groups are still

intact (Fig. 4.51). Figs. 4.52 - 4.54 show how the mixture tends towards producing fully hydrolysed molecules over time.

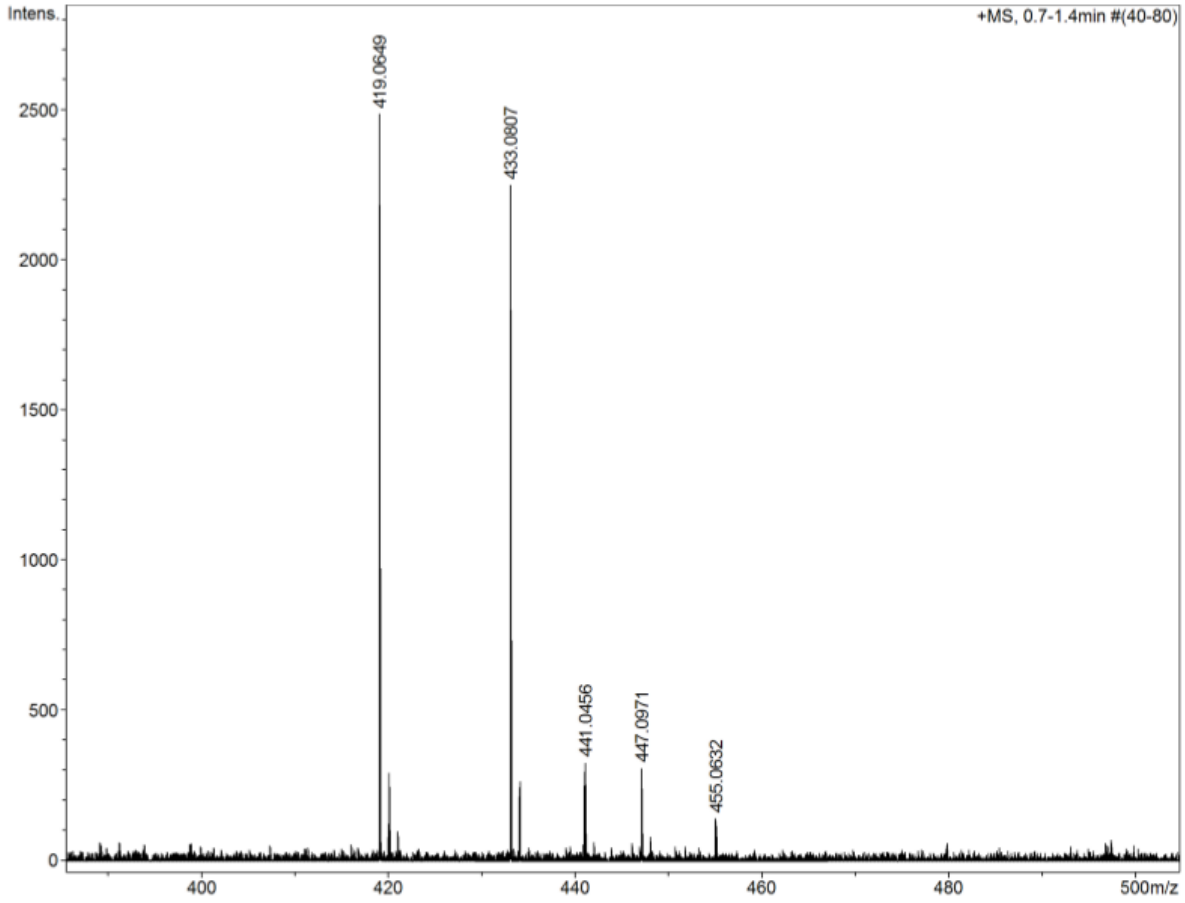

Figure 4.52 Mass spectrum of procedure 8 after 24 hours of reaction

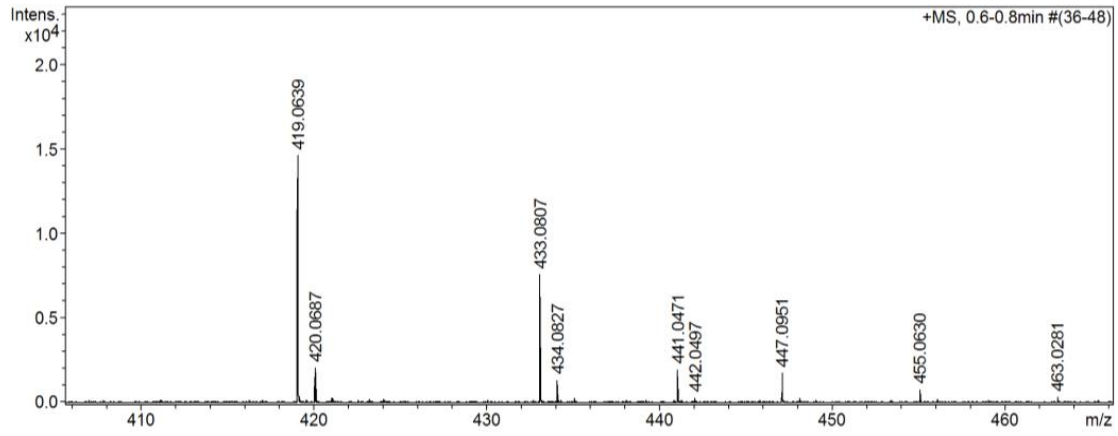

Figure 4.53 Mass spectrum of procedure 8 after 48 hours of reaction

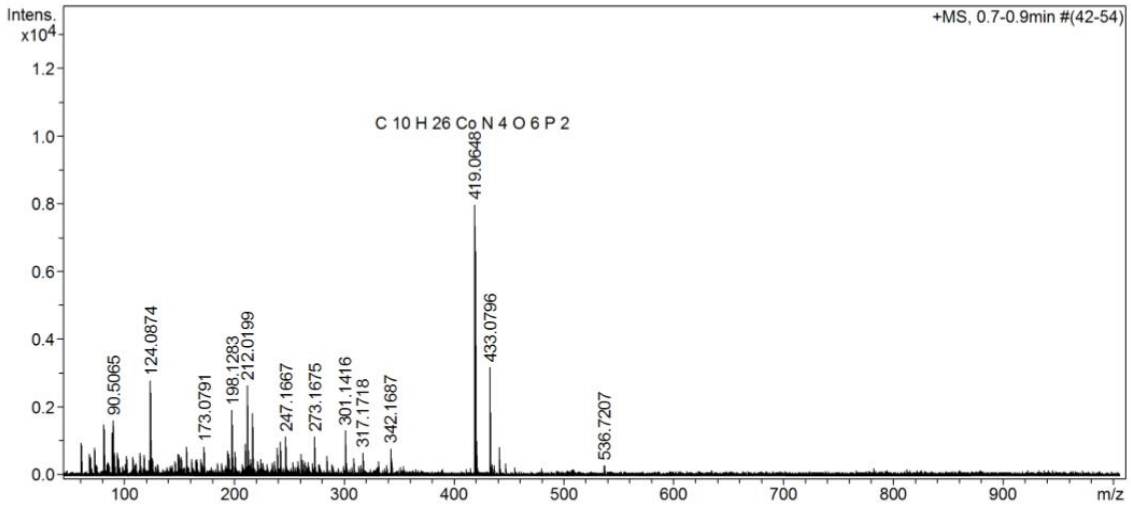

Figure 4.54 Mass spectrum of procedure 8 after 72 hours of reaction

After the hydrolysis was observed, the use of hydrochloric acid was avoided and subsequent column chromatographic separations were carried out using Sephadex SPC 25 resin with NaCl solution as the eluent.

4.3.3 The cobalt(III)-mediated peptides and amides.

NMR spectra for this section were collected over different instruments. Care has been taken to state the frequency of the applied magnetic field used for each NMR characterisation. Some $^{31}P\{^{1}H\}$ NMR spectra have not been included where there was insufficient sample for the experiment. The complexity of these spectra made it difficult to achieve complete assignment. Most of the spectra were assigned by making reference to their starting materials.

Ethane-1,2-diamine (en) was coupled to **4.2** to form **4.10** and its stereoisomers. A portion of the ^{1}H NMR spectrum has been shown as Fig. 4.55. The spectrum was expected to be closely related to that from the starting material, since the new ligand (en) does not look very different from the meridional fragment at the other end of the polyamine backbone of the complex.

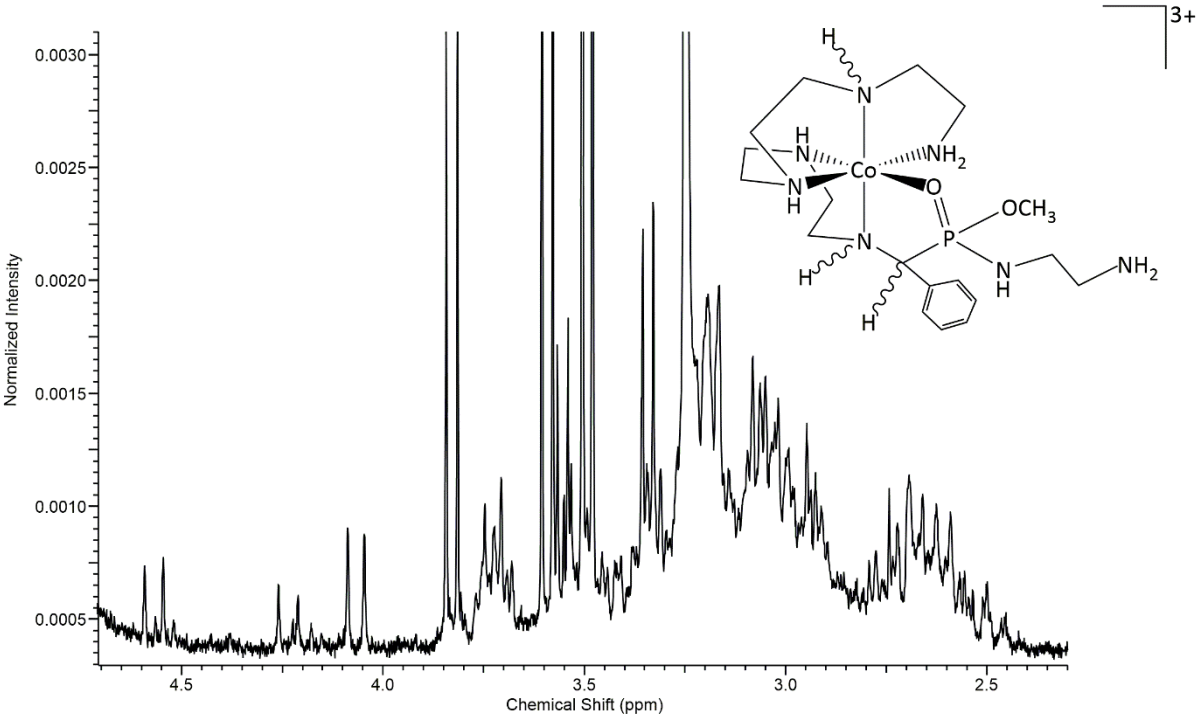

Figure 4.55 A portion of the ^{1}H NMR spectrum of the product mixture from procedure 9

Two sets of peaks were observed in the $^{31}P\{^{1}H\}$ NMR spectrum from procedure 9. That sparked some curiosity as to whether all of the starting material reacted or not. The $^{31}P\{^{1}H\}$ NMR spectra of neither the immediate starting material nor of the ones before it matched the current spectrum shown as Fig. 4.56. Yingchun and Frank[133] observed two separate signals of about 0.038 ppm difference in chemical shifts in the ^{31}P NMR spectrum of a solution of racemic 4-acetylphenyl cyclohexyl methylphosphonate in $CDCl_3$ during their test for the potential of

N-acyl L-amino acid derivatives as chiral solvating agents for the differentiation of chiral phosphorus compounds. Most of the other phosphorus containing compounds were found to resonate from 28 – 45 ppm on the ^{31}P NMR spectrum.

Stereoisomers may account for the different chemical shifts observed in these current systems hence the sets of peaks observed in their NMR spectrum, including the ^{31}P spectrum.

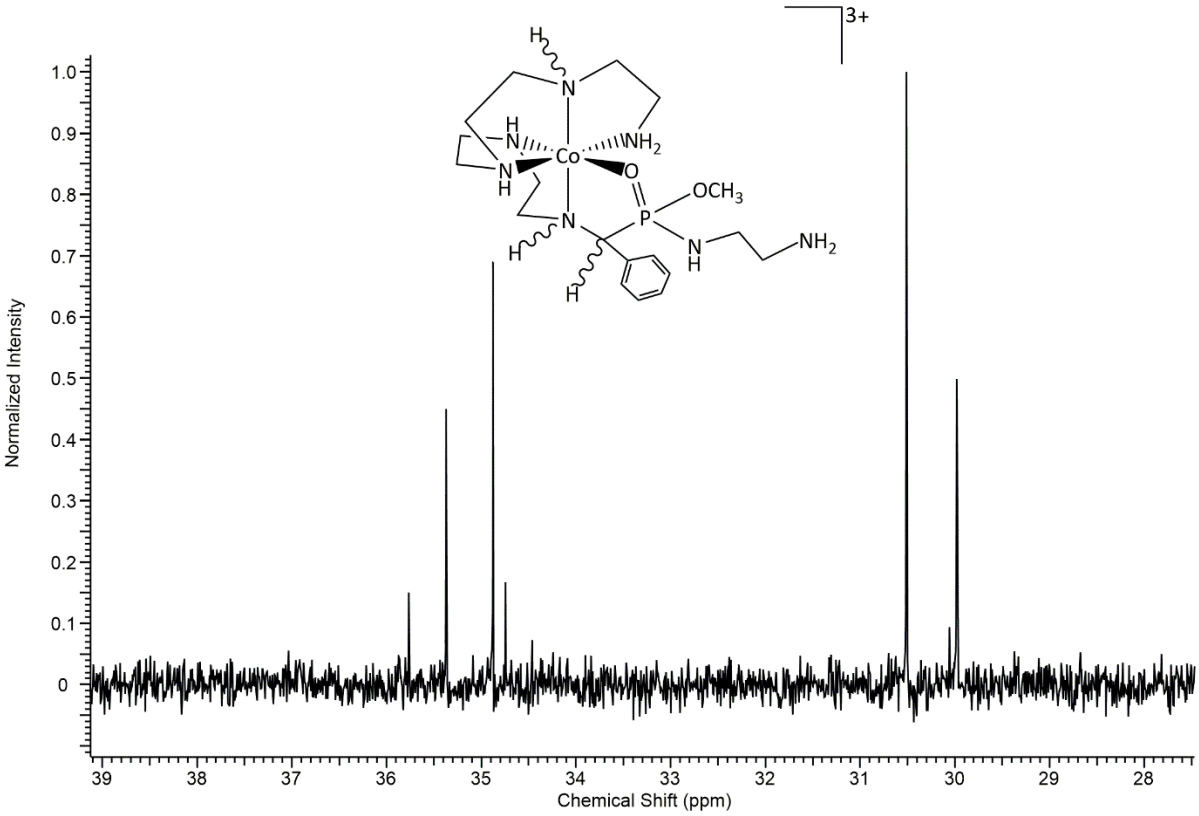

Figure 4.56 The $^{31}P\{^{1}H\}$ NMR spectrum of the product mixture from procedure 9

The $^{31}P\{^{1}H\}$ NMR spectrum (Fig. 4.57) obtained from the product mixture of procedure 10 appeared to also have two sets of peaks although not hugely separated compared with the spectrum in Fig. 4.56. It can be argued that the stereoisomers are the cause of the separation in terms of chemical shifts. This is not surprising given that the functional group to which an NMR active nucleus is proximate to, affects the applied magnetic field either to cause an upfield chemical shift (through shielding) or a downfield signal (through deshielding).

There could also be some hydrolysed materials in the mixture.

Six pairs of diastereoisomers are expected from the product mixture from procedure 10, given the six stereogenic centres present, assuming no C_2 axis of rotation exists in a molecule. At least six resonance peaks were observed from the spectrum shown as Fig. 4.57.

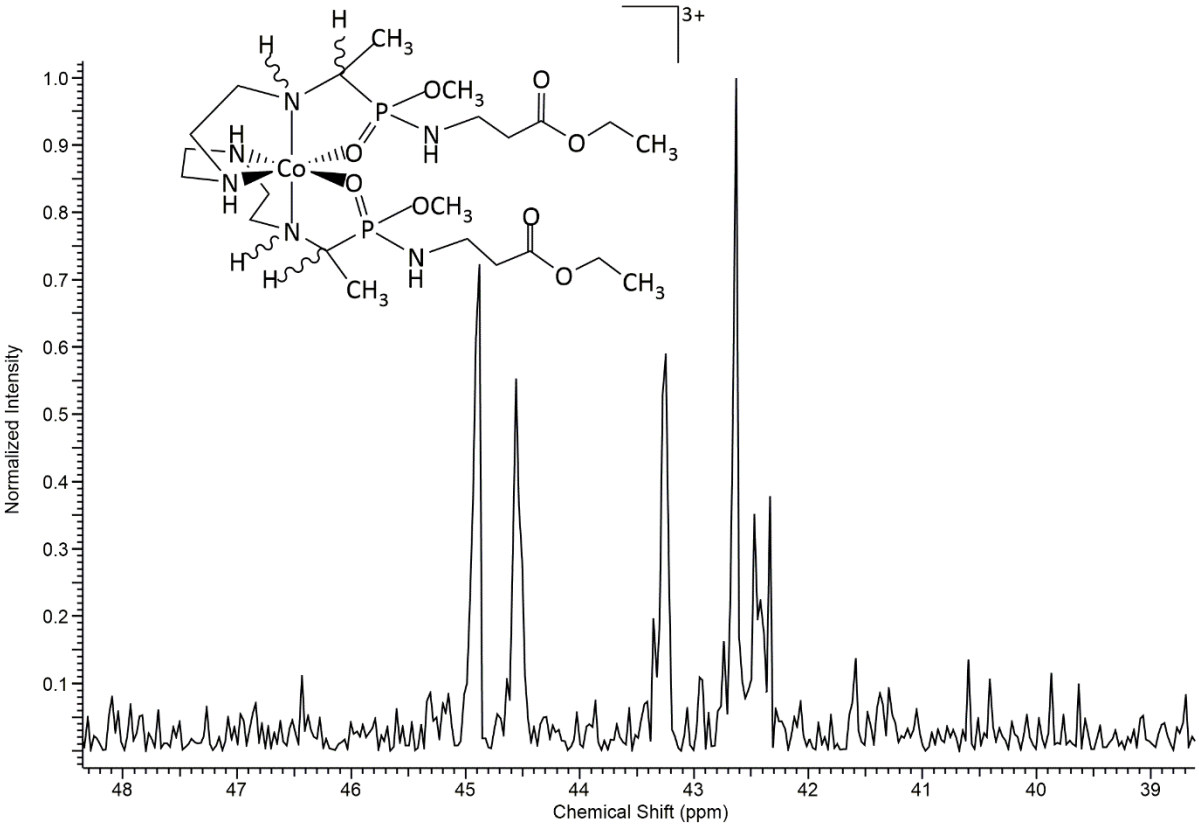

Figure 4.57 $^{31}P\{^{1}H\}$ NMR spectrum of the product mixture from procedure 10

Benzylamine was used for the coupling reaction in procedure 11. ^{1}H NMR spectrum for the complex formed was expected to resemble that of its starting material (**4.5** and its stereoisomers), apart from the newly introduced aromatic groups of benzylamine. A new broad peak due to the N**H**s of benzylamine can be seen in Fig. 4.59 as well as the aromatic protons' signals in Fig. 4.60. The COSY spectrum (Fig. 4.58) aided the assignment of the ^{1}H NMR spectrum.

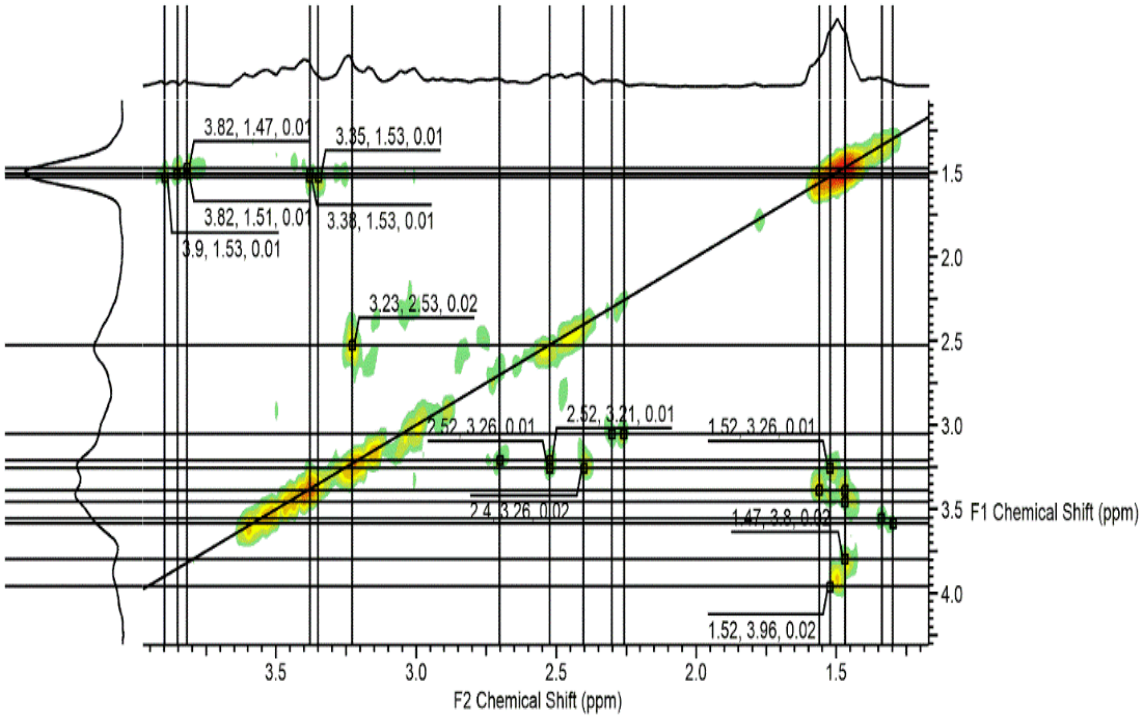

Figure 4.58 A part of the COSY NMR spectrum of the product mixture from procedure 11

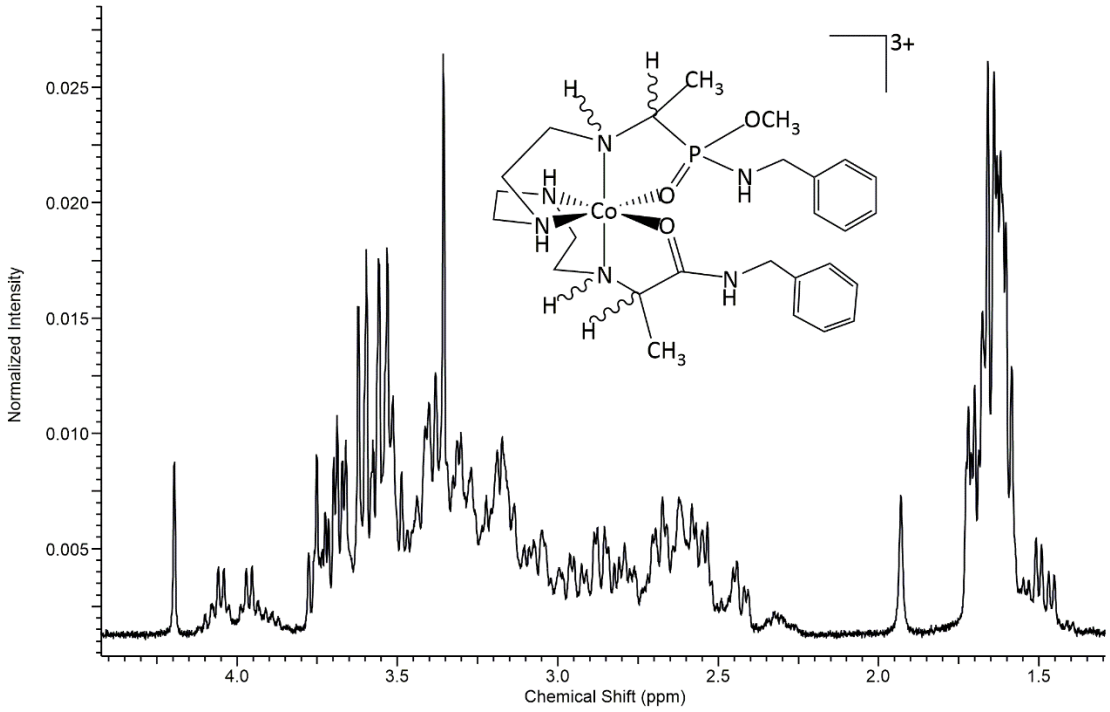

Figure 4.59 A portion of ^{1}H NMR spectrum of the product mixture from procedure 11

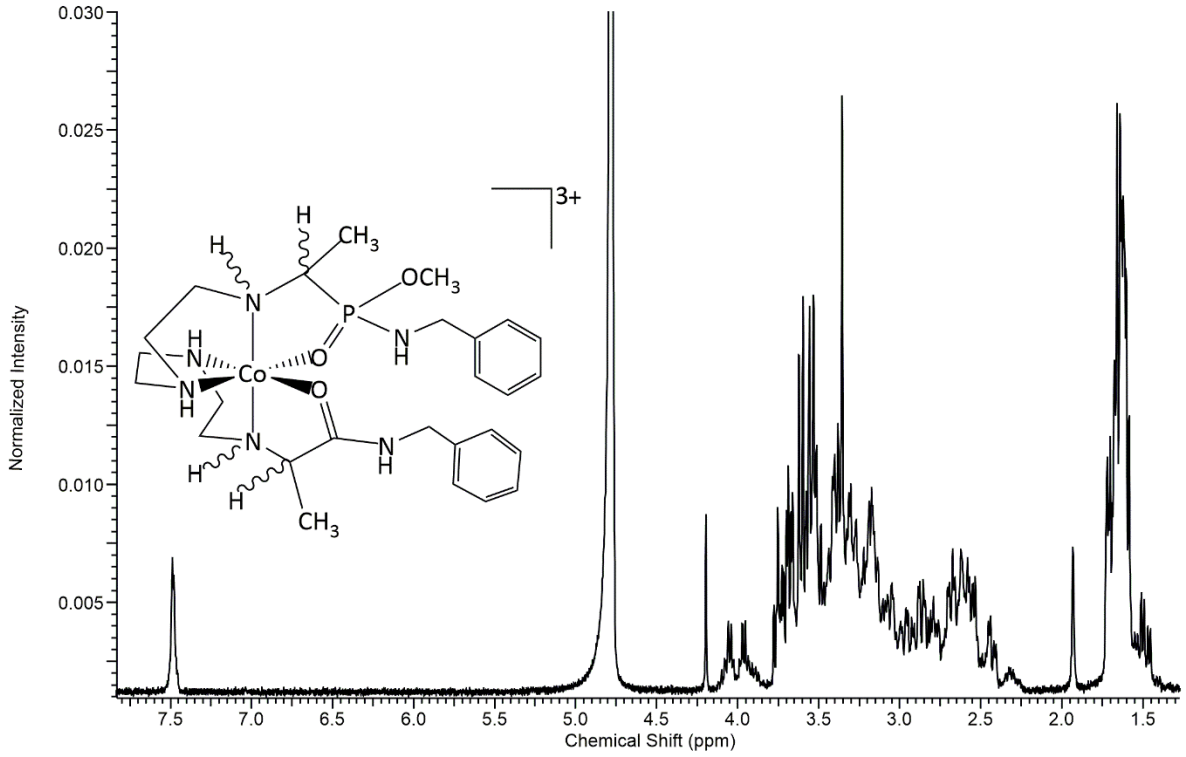

Figure 4.60 The ^{1}H NMR spectrum of the product mixture from procedure 11

The outstanding quartets in Fig. 4.59 or 4.60 have been assigned to the α-carbon protons at each end of the molecule. Other quartets appear to be hidden beneath the outstanding ones in an overlap as multiplets. The COSY spectrum revealed there are α-C-H protons also hidden in the overlapped peaks from 3.26 – 3.96 ppm. Those signals would be for the different stereoisomers in the product mixture. At least five pairs of diastereoisomers are expected in the product mixture from procedure 11considering only five stereogenic centres apart from the metal centre. The COSY and ^{1}H NMR show there are more than five pairs of diastereoisomers in solution. The secondary amine of each of the benzylamine groups should account for these extra stereoisomers due to its chirality. Therefore, there could be as many as seven pairs of diastereoisomers assuming that the wrapping of the polyamine around the metal centre remains constant. However, the ^{31}P{^{1}H} NMR spectrum (Fig. 4.61) shows fourteen resonance peaks, two of which dominate the mixture.

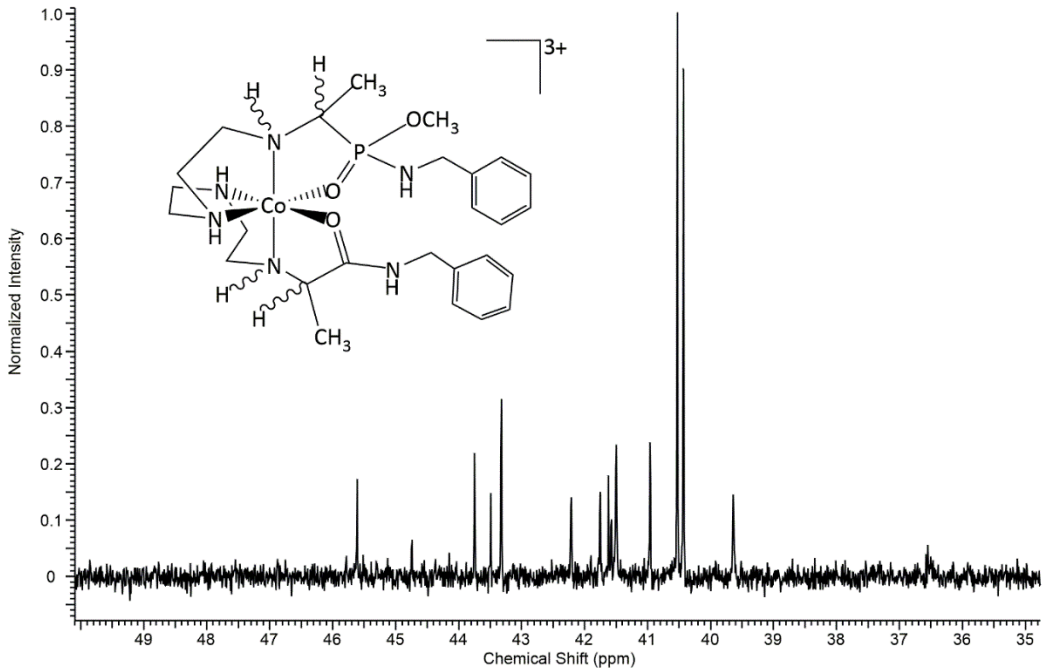

Figure 4.61 $^{31}P\{^{1}H\}$ spectrum from procedure 11

The cluster of the resonance peaks in the same region of the $^{31}P\{^{1}H\}$ spectrum is a good indication that the product mixture most likely contains isomers, especially after this product mixture was purified using column chromatographic technique. Table 2 shows the chemical shifts obtained from the $^{31}P\{^{1}H\}$ NMR spectra of the amides/peptides synthesised in this section.

Compound (and its stereoisomers)	$^{31}P\{^{1}H\}$ NMR chemical shifts in ppm
4.10	29.98, 30.51, 34.74, 34.87, 35.37, 35.76
4.11	42.34, 42.47, 42.63, 43.25, 44.58, 44.88
4.12	39.64, 40.43, 40.52, 40.96, 41.50, 41.62, 41.75, 42.21, 43.32, 43.49, 43.75, 44.74, 45.61
4.13	NA (carboxylate system)
4.14	42.87
4.15	NA (carboxylate system)
4.16	35.54, 36.53
4.17	34.56, 34.84, 35.94, 36.10, 36.84, 37.04, 37.54

Table 4.2 $^{31}P\{^{1}H\}$ NMR chemical shifts of the amides/peptides reported in this section.

There was no observable difference between the spectra obtained from the powder recovered directly from the trituration procedure for compound **4.12** (and its stereoisomers) and that obtained after column chromatography. The column chromatography step is therefore not required to attain purity of these compounds.

The spiked ESIMS for compound **4.12** showed a peak of interest at 212.12 (Fig. 4.62). The expected complex ion of 3+ charge has the chemical formula of $[C_{26}H_{43}CoN_6O_3P]^{3+}$. If this complex loses two protons as usual, it will generate a 1+ species. If this 1+ complex ion 'flies' with an acetate anion as follows: $[C_{26}H_{41}CoN_6O_3P]^{1+}\cdot(CH_3COO^-)$, a neutral species with the formula of $C_{28}H_{44}CoN_6O_5P$ could be formed. That neutral species would then have to gain a proton to become a 1+ species with the chemical formula: $C_{28}H_{44}CoN_6O_5P$. This 1+ species should have a monoisotopic mass of 635.25. The experimental and calculated masses do not quite match. The experimental isotope pattern observed from the spectrum shown in Figure 4.62 corresponds to a 1+ species. However, the calculated isotope pattern (below the experimental one) shows the correct distribution map that would be generated from the correct molecular ion if it were a 3+ species. This is one of the cases where the MS data does not fit with other characterisation parameters. So, the peak at 212.12 has not been assigned to the expected complex as described here. However, ^{1}H and $^{31}P\{^{1}H\}$ NMR spectra provide evidence that the desired product was made.

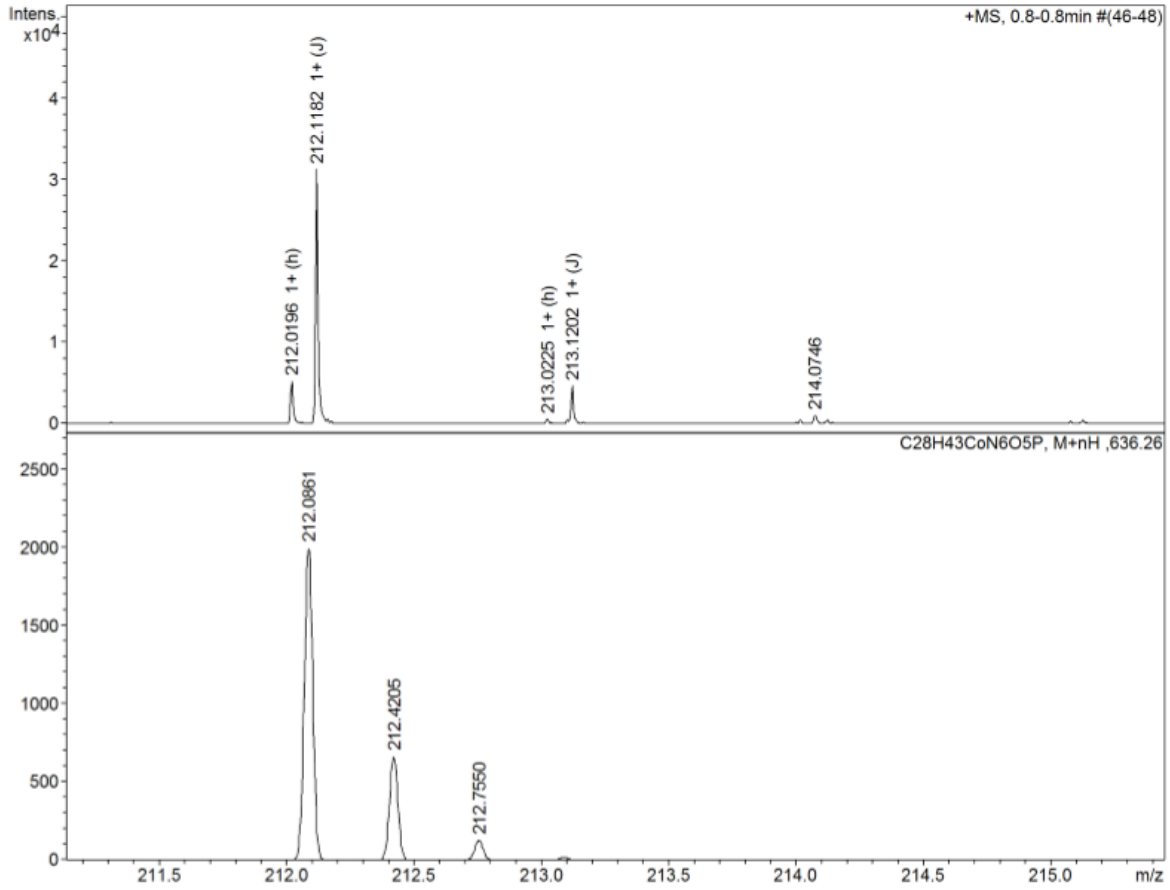

Figure 4.62 ESIMS of compound **4.12** showing experimental (top) and simulated (bottom) isotope distribution maps.

The M/Z ratio found (Fig. 4.63) for compound **4.13** and its stereoisomers is 159.57 for $[C_{21}H_{37}N_6O_3Co]^{2+}$; [M-1H]. The calculated M/Z ratio was 160.41 for $[C_{21}H_{38}N_6O_3Co]^{3+}$. There was also a peak at 465.20 (Fig. 4.64) for the hydrolysed species where the methyl of the methoxy group was lost during the ionization process in the spectrometer.

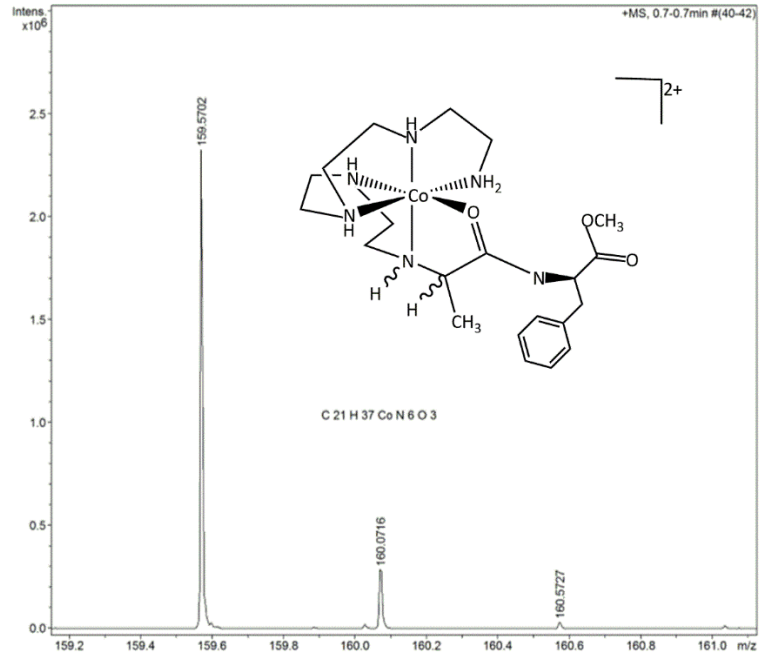

Figure 4.63 Mass spectrum of the product mixture of procedure 12 showing some [M-1H] species.

The monoisotopic mass of 465.20 for $[C_{20}H_{34}N_6O_3Co]^+$; [M-1H(-CH_3)] corresponds with the complex insert in Fig. 4.64 where the methyl group of the amino acid end of the molecule has been hydrolysed.

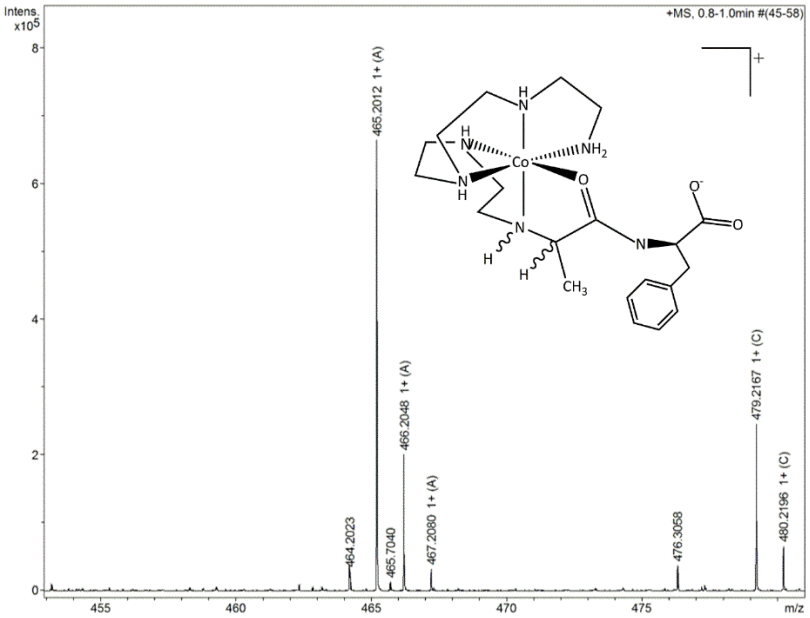

Figure 4.64 Evidence of hydrolysis for the product mixture from procedure 12 (compound **4.13** and isomers) by mass spectrometry.

Compounds **4.16** and **4.17** (and their stereoisomers) were synthesised using some Gly-(OTS)Pro dipeptide obtained from the Hartshorn laboratory (prepared by Shirley P. Celestine; a PhD student). The diversity of the peaks in especially the $^{13}C\{^{1}H\}$ and $^{31}P\{^{1}H\}$ NMR spectra of those compounds could have been complicated some more from the ability of some of the bonds in the Gly-(OTS)Pro dipeptide to rotate thereby forming conformational isomers known as rotamers. The cluster of peaks from the 35 to 38 ppm region observed in the $^{31}P\{^{1}H\}$ NMR spectrum (Fig. 4.65) of compound **4.17** and its stereoisomers is a good indication that the product mixture from procedure 16 is most likely made up of stereoisomers and not otherwise. This rich diversity of resonance peaks observed in the phosphorus NMR was a helpful guide in the assignment of the proton NMR of this mixture.

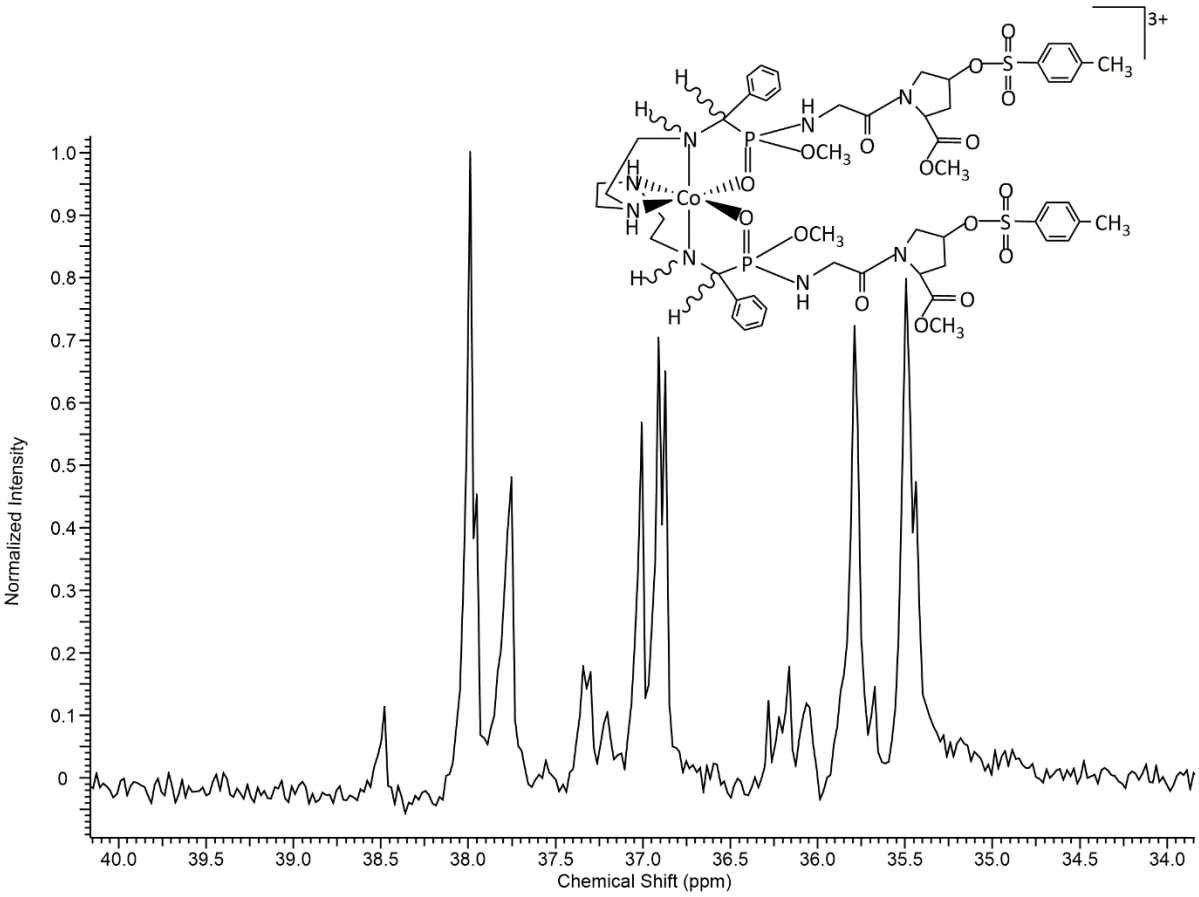

Figure 4.65 $^{31}P\{^{1}H\}$ NMR spectrum of the product mixture from procedure 16 for compound **4.17** and its stereoisomers.

Peaks corresponding to the di-peptide part of the molecule were confidently assigned with reference to the spectra of the di-peptide starting material.

4.4 Conclusions

Peptide synthesis on the metal which was discovered when β_2–[Co(trien)(glyOEt)Cl]$(ClO_4)_2$ was treated with glyOEt in an non aqueous environment[63], has been employed to prepare new carboxylate and phosphonate systems. The relative kinetic inertness offered by cobalt(III) infers a higher likelihood for the identification of reaction intermediates which could facilitate the differentiation of reaction pathways and subsequently help establish reaction mechanisms. The route to the cobalt(III) peptides is through the ester chelate (**6**). The chelated ester has been reported to condense readily with amino acid esters and small peptides[63, 64] as in Fig. 4.4. The mechanism of the reaction includes a tetrahedral intermediate[63] (**7A**), for the carboxylates.

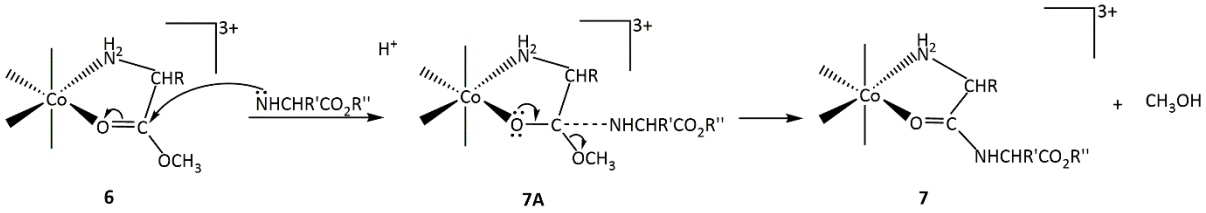

The phosphonate analogues have been hypothesised to go through a trigonal bipyramidal intermediate to yield the peptide or amide.

No activation of the peptide-forming step is required. Kinetic studies[67] demonstrated that the rate of the coupling reaction of the coordinated amino acid ester is enhanced by about 10^6 times more than that of the uncoordinated amino acid ester. The metal ion accounts for this enhancement by its electron withdrawing effect which makes the carbon of the carbonyl group more electrophilic so that it can undergo nucleophilic attack by an incoming nucleophile. The metal ion also enhances C-H acidity at the α-carbon atom through the additional binding of the amine nitrogen.

Therefore, this cobalt(III) method does not only provide an alternative route to peptide synthesis, it also provides both N-terminal protection (necessary for preventing any attack on the incoming amino acid carbonyl-C) and carbonyl-O activation (for directing the nucleophilic attack by the N-terminal of the incoming amino acid to the carbonyl-C of the complex) in one system and makes coloured compounds which are generally water soluble (essential for biological applications). The metal ion and the ligands can be removed by chemical or electrochemical reduction methods.[75]

The reactivity of these cobalt(III) systems was expected to mimic those in the literature, by being active towards the addition of a nucleophile, thereby enabling small peptides to be

formed through the chelated ester intermediates. The cobalt(III) chelated esters prepared in this section behaved like those in the literature by being very prone to hydrolysis as have been confirmed both by NMR and MS. This reactivity was essential for the formation of the amides or short peptides. The N-terminal of an incoming amino acid or amine carries out a nucleophilic attack on the cobalt(III) activated carbonyl-C to form the new peptide bond.

The chelated carboxylate ester and phosphonate ester complexes synthesised in this project were successfully coupled with some amines including benzylamine, diamines like ethane-1,2-diamine, amino acid methyl esters, amino acid ethyl esters and a novel dipeptide made in the Hartshorn laboratory.

References

47. Buckingham, D.; Dekkers, J.; Sargeson, A.; Wein, M., Hydrolysis and aminolysis of metal ion activated esters. Nucleophilic paths and properties of the tetrahedral intermediate. *Journal of the American Chemical Society* **1972,** *94* (11), 4032-4034.

52. Wilson-Coutts, S. M.; Browne, J. M.; Marsh, L. C.; Polson, M. I.; Hartshorn, R. M., High diastereoselectivity in borohydride reductions of coordinated imines. *Dalton Transactions* **2012,** *41* (5), 1591-1596.

63. Buckingham, D. A.; Marzilli, L. G.; Sargeson, A. M., Peptide bond formation and subsequent hydrolysis at a cobalt (III) center. *Journal of the American Chemical Society* **1967,** *89* (11), 2772-2773.

64. Buckingham, D. A.; Marzilli, L. G.; Sargeson, A. M., N-Terminal addition of glycine to amino acid and peptide esters activated by the cobalt (III) ion. *Journal of the American Chemical Society* **1967,** *89* (17), 4539-4540.

65. Buckingham, D. A.; Davis, C.; Foster, D.; Sargeson, A. M., Cobalt (III)-promoted hydrolysis of chelated glycine amides, glycylglycine, and glycylglycine esters. Kinetics and mechanism. *Journal of the American Chemical Society* **1970,** *92* (19), 5571-5579.

66. Clark, C.; Tasker, R.; Buckingham, D.; Knighton, D.; Harding, D.; Hancock, W., Cobalt (III)-mediated peptide synthesis. 1. Cobalt (III)-activated amino acid methyl esters and the synthesis of dipeptides. *Journal of the American Chemical Society* **1981,** *103* (23), 7023-7025.

67. Sutton, P. A.; Buckingham, D. A., Cobalt (III)-promoted hydrolysis of amino acid esters and peptides and the synthesis of small peptides. *Accounts of Chemical Research* **1987,** *20* (10), 357-364.

68. Bodanszky, M., Synthesis of peptides by aminolysis of nitrophenyl esters. *Nature* **1955,** *175* (4459), 685-685.

69. Buckingham, D. A.; Foster, D.; Sargeson, A., Cobalt (III)-promoted hydrolysis of chelated glycine esters. Kinetics, anion competition, and oxygen-18 exchange studies. *Journal of the American Chemical Society* **1968,** *90* (22), 6032-6040.

70. Collman, J. P.; Kimura, E., Formation of peptide bonds in the coordination sphere of cobalt (III). *Journal of the American Chemical Society* **1967,** *89* (24), 6096-6103.

71. Lawson, P. J.; McCarthy, M. G.; Sargeson, A. M., Cobalt (III)-promoted syntheses of the amino acids (RS)-2-cyclopropylglycine and (R)-and (S)-proline. *Journal of the American Chemical Society* **1982,** *104* (24), 6710-6716.

72. Wu, Y.-L.; Busch, D. H., Reactions of coordinated ligands. XX. Cobalt (III)-promoted hydrolysis of glycine tert-butyl ester. *Journal of the American Chemical Society* **1970,** *92* (11), 3326-3332.

73. Alexander, M. D.; Busch, D. H., Reactions of Coordinated Ligands. XIII. Cobalt (III)-Promoted Hydrolysis of Glycine Esters. *Journal of the American Chemical Society* **1966,** *88* (6), 1130-1138.

74. Baraniak, E.; Buckingham, D.; Clark, C.; Moynihan, B.; Sargeson, A., Cobalt (III)-promoted hydrolysis of esters. Hydrolysis of chelated and monodentate. beta.-alanine isopropyl ester and interconversions via hydrolysis intermediates. *Inorganic Chemistry* **1986,** *25* (19), 3466-3478.

75. Browne, R. J.; Buckingham, D. A.; Clark, C. R.; Sutton, P. A., The Cobalt (III)-Promoted Synthesis of Small Peptides. *Advances in Inorganic Chemistry* **1999,** *49*, 307-373.

127. Schellenberger, V.; Jakubke, H. D., Protease-catalyzed kinetically controlled peptide synthesis. *Angewandte Chemie International Edition in English* **1991,** *30* (11), 1437-1449.

128. Peptide Synthesis. https://www.thermofisher.com/nz/en/home/life-science/protein-biology/protein-biology-learning-center/protein-biology-resource-library/pierce-protein-methods/peptide-synthesis.html#strategies (accessed Dec 11, 2019).

129. D. R. Knighton, D. R. K. H., M. J. Friar, W. S. Hancock, G. D. Reynolds, C. R. Clark, C. R. Clark, R. F. Tasker, D. A. Buckingham, Cobalt(III)-mediated peptide synthesis. 2. Synthesis of tetrapeptides and [leu5]-enkephalin *Journal of the American Chemical Society* **1981,** *103* (23), 7025-7026

130. Isied, S. S.; Kuehn, C. G., Peptide formation in the presence of a metal ion protecting group. Pentaammine cobalt (III)-peptide complexes. *Journal of the American Chemical Society* **1978,** *100* (21), 6752-6754.

131. Kroll, H., The Participation of Heavy Metal Ions in the Hydrolysis of Amino Acid Esters1. *Journal of the American Chemical Society* **1952,** *74* (8), 2036-2039.

132. Collman, J. P.; Buckingham, D. A., Hydrolytic cleavage of N-terminal peptide bonds by a cobalt chelate. *Journal of the American Chemical Society* **1963,** *85* (19), 3039-3040.

133. Li, Y.; Raushel, F. M., Differentiation of chiral phosphorus enantiomers by ^{31}P and ^{1}H NMR spectroscopy using amino acid derivatives as chemical solvating agents. *Tetrahedron: Asymmetry* **2007,** *18* (12), 1391-1397.

Chapter 5. Conclusions and Future Work

5.1 Conclusions

During the syntheses of the imine phosphonate cobalt(III) complexes described in chapter 2 of this thesis, the number of signals in the methylene and methoxy regions indicated whether one or two of the condensation reactions had occurred on a complex and highlighted the presence, or not, of a symmetry element in each molecule observed. Integration of the methoxy regions also provided a guide to the approximate number of pairs of diastereoisomers present in a given product mixture. The ^{1}H and ^{13}C{^{1}H} NMR spectra of the mixture of each crude product significantly showed a limited number of isomers. The carboxylate systems would yield one product and its enantiomer whereas these phosphonate systems would have only one more pair of diastereoisomers for every stereogenic phosphorus centre in a given molecule. This project provided more evidence to support the stereoselectivity and regioselectivity of the condensation reactions between cobalt(III) coordinated polyamines and other carbonyl containing compounds to give imines.

The polydentate wrapping around the cobalt(III) metal centres was a source of handedness where Δ and Λ descriptors have been used to express the helicity as discussed in chapter 1. The handedness expressed by a given X-ray structure has been highlighted in this chapter but that was not without mentioning that the compounds reported here exist as racemic mixtures with both handedness equally present in a given product mixture as enantiomers.

For the tetraen derived mono imines, two pairs of diastereoisomers were expected in every crude mixture, considering the helicity of the wrapping of the polyamine ligand around the metal ion and the chirality at the phosphorus centres only: (Δ*R* and Δ*S*) and (Λ*R* and Λ*S*), where (Δ*R* and Λ*S*) and (Δ*S* and Λ*R*) are enantiomers. The three compounds isolated and characterised by X-ray crystallography from the tetraen derivatives were **2.1** (Δ*mffm*$_a$(*R*)), **2.2** (Δ*mffm*$_a$(*R*)) and **2.3** Δ*mffm*$_a$(*S*)). They all presented in the *anti* configuration with respect to the position of the hydrogen on their meridional nitrogen atom; an observation that aligned with the literature[55] from previous research in the Hartshorn group and in most cobalt(III) octahedral complexes with related folds in the wider literature.[53, 104-122]

It was also discovered that occurring in a Δ*R* configuration points the methoxy group away from N3 but towards N5 for the tetraen derivatives. On the other hand, it was observed that the Δ*S* configuration presented with the methoxy group pointing towards N3 and away from N5. The proximity of the methoxy protons to a secondary amine group (N3) could contribute to shielding (and its consequent upfield resonance frequencies) of those protons from the applied

magnetic field in NMR experiments. In contrast, the opposite effect could be the case for when the methoxy protons are pointed away from the secondary amine (N3), giving rise to deshielding and downfield resonance frequencies. A hypothesis was therefore put forward that, the Δ*S* (or its enantiomer: Λ*R*) stereoisomer of these complexes could result to an upfield chemical shift. Consequently, the Δ*R* (or its enantiomer: Λ*S*) stereoisomer of these complexes could result to a downfield chemical shift. The plethora of ^{1}H NMR spectra obtained from these new compounds supported this hypothesis but further experiments may be required to form a theory.

The trien derivatives had double condensations sites. Therefore, four pairs of diastereoisomers were expected for the di-imine complexes: Δ*RS* & Δ*SR*, Δ*RR* & Δ*SS* and Λ*RS* & Λ*SR*, Λ*RR* & Λ*SS*, where Δ*RS* & Λ*SR* and Δ*SR* & Λ*RS* are enantiomers. Δ*RR* & Λ*SS* and Λ*RR* & Δ*SS* are also enantiomers. Once again, the helicity of the polyamine ligand around the cobalt(III) metal centre and the chirality of the phosphorus centres would yield either a symmetrical molecule (Δ*RR* & Δ*SS*, Λ*RR* & Λ*SS*) or an unsymmetrical one (Δ*RS* & Δ*SR*, Λ*RS* & Λ*SR*), considering the presence or absence of a C_2 axis of rotation in a given molecule.

NMR revealed the methyl system was dominated by symmetrical diastereoisomers whereas the phenyl system was dominated by the unsymmetrical ones. Both the symmetrical (Δ*mffm*(*RR*)) and unsymmetrical (Δ*mffm*(*SR*)) compounds of the phenyl system were isolated and characterised by X-ray crystallography as **2.8** (Fig. 2.23) and **2.7** (Fig. 2.22) respectively.

Going by the original postulate of the observed ^{1}H NMR chemical shift being related to the configuration at the phosphorus stereogenic centre, it could be argued that the methyl system (Fig. 2.48) was dominated by the (Δ*mffm*(*RR*)) diastereoisomer or its enantiomer (Λ*mffm*(*SS*)).

The ethane-1,2-diamine derived compounds provided classical examples for demonstrating the ability of donor atoms to change their relative locations around the central metal ion in order to adopt a geometry that will allow immediate dehydration and formation of a planar imine from the condensation reaction. The starting material had two leaving chlorido ligands *trans* to the central metal ion whereas the end isolated products had the oxygen ends of the incoming ligand swapped around to a *cis* presentation around the central metal ion.

Four pairs of diastereoisomers were expected for the en di-imine complexes with respect to the cobalt(III) and phosphorus centres respectively: Δ*RS* & Δ*SR*, Δ*RR* & Δ*SS* and Λ*RS* & Λ*SR*, Λ*RR* & Λ*SS*, where Δ*RS* & Λ*SR* and Δ*SR* & Λ*RS* are enantiomers. Δ*RR* & Λ*SS* and Λ*RR* & Δ*SS* are also enantiomers. Once again, the outcome was expected to be either a symmetrical

molecule (Δ*RR* and Δ*SS*, Λ*RR* and Λ*SS*) or an unsymmetrical one (Δ*RS* and Δ*SR*, Λ*RS* and Λ*SR*). Three pairs of diastereoisomers were identified in the product mixture by NMR; where two of those (one symmetrical and another unsymmetrical) dominated the crude product mixture in a 1:1 integral ratio. Going by the current hypothesis that relates the chemical shift of the methoxy protons to the orientation of the methoxy group in space and ignoring the different description for the en polydentate wrapping, the pair of symmetrical diastereoisomers were predicted to have Δ*RR* and Λ*SS* configurations. A pair of symmetrical diastereoisomers Λ*mm*(*RR*) (and its enantiomer) was isolated as compound **2.11** (Fig. 2.27) whereas a pair of unsymmetrical diastereoisomers Λ*mm*(*RS*) (and its enantiomer) was isolated as compound **2.12** (Fig. 2.28) from the en derivatives.

The set of compounds made from condensing both a carboxylate and a phosphonate ligand onto a trien cobalt(III) system using procedure 6, were expected to have two pairs of diastereoisomers: (Δ*R* and Δ*S*) and (Λ*R* and Λ*S*), where Δ*R* and Λ*S* are enantiomers. Δ*S* and Λ*R* are also enantiomers. The isolated compound **2.14** (Δ*mffm*(*R*)) was not the dominant compound (with its enantiomer) in fraction 1 of the product mixture, judging by the current hypothesis using the ^{1}H NMR chemical shifts.

There were cases where the free phosphonate oxygen (P=O) acted as a ligand in these complexes. Two X-ray structures (Figures 2.19 (**2.5**) and 2.24 (**2.9**)) showed formation of O-Co bonds whereas Figure 2.26 (compound **2.10**) showed an O-Zn bond formation. However, the conditions which make the reactivity of the phosphonate oxygen favourable are not very clear. It seemed to happen in the presence of excess zinc chloride. One of the O-Co bonds formed in a methanolic solution whereas the other formed in a hydrochloric acid solution. The O-Co bonds formed in compounds **2.5** and **2.9** led to the tetranuclear complexes isolated during the course of this project. The tetranuclear complexes had a cobalt(II) ion at the centre of three phosphonate imine complexes of cobalt(III). The complex ligands were coordinated to the central metal ion in a distorted octahedral geometry.

The imine complexes synthesised in chapter 2 of this thesis were converted to their amine derivatives through borohydride reduction in chapter 3. Some carboxylate complexes were also synthesized.

^{1}H NMR spectra for these amino acid complexes of cobalt(III) with phosphonates and carboxylates, were very useful for their characterisation. The first indication that the reduction reaction was successfully carried out was usually the appearance of a new set of peaks at the

1.6 ppm region of the spectrum. For the pyruvate derived complexes, the methyl group of the imine precursor resonated as a singlet in the ^{1}H NMR spectrum around the 2.6 ppm region. That signal splits into a doublet after the reduction reaction by reason of the introduction of a hydrogen to the α-carbon atom by the reducing agent. Appearance of new sets of peaks upfield (around 1.6 ppm) was also the case for the phosphonate derived systems even though the multiplicity of those new sets of peaks was more complicated from the presence of the NMR active ^{31}P nuclei proximate to the α-carbon atom in those complexes. Protons of the methyl group of the phosphonate systems were expected to appear as doublet of doublets from coupling to the newly introduced hydrogen atom (on the α-carbon atom) and also to the phosphorus nucleus. However, the peak overlap (from stereoisomers) in that region of the ^{1}H NMR spectrum for those complexes did not allow for complete assignment.

A combination of the ^{13}C{^{1}H} spectrum and the ^{1}H spectrum confirmed that two major components dominated the product mixture of **3.7**. They were predicted to be Δ*mffm*(*RSR)* (and Λ*mffm*(*SRS)*) and Δ*mffm*(*SSR)* (and Λ*mffm*(*RRS)*) pairs of diastereoisomers. Two pairs of diastereoisomers were also found to dominate the product mixture of **3.2**. They were expected to have the absolute configurations of Δ*mffm(RRSR)* (and Λ*mffm(SSRS)*) and Δ*mffm*(*RSSR)* (and Λ*mffm*(*SRRS)*) as have been schematised in Fig. 3.36. A combination of spectra obtained from a sample of the product mixture for compound **3.1** and its stereoisomers led to the conclusion that were four compounds in the product mixture. Those four compounds were expected to have the following absolute configurations: Δ*mffm*(*RSSR)*, Δ*mffm*(*RRSR),* Δ*mffm*(*RSSS)*, Δ*mffm*(*RRSS)* and their enantiomers (schematised in Fig. 3.43).

The X-ray structure of **3.5** showed that the hydrogen of the α-carbon atom on the carboxylate group of the complex was added on the phosphonate face of the complex. It meant that the reduction of the carboxylate imine had gone with the hydride attack from the phosphonate face. On the contrary, but in consistence with the literature, the hydrogen on the α-carbon atom of the phosphonate group was added on the amine face of the complex thereby providing support evidence that the amine-faced addition is the dominant form of hydride attack from previous research where it was shown to be 92% selective.

^{13}C{^{1}H} NMR spectrum from a sample of the product mixture of **3.5** disclosed two overlapping doublets around 18 ppm for the protons of the methyl group. The overlap indicated similar chemical environments for all the methyl protons in the sample mixture. The occurrence of the resonance peaks (methyl and methylene nuclei) from the current phosphonate systems in the

same region of the ^{1}H and $^{13}C\{^{1}H\}$ NMR spectra with those of the carboxylates, indicated that the isomers produced in the present project could be related in terms of stereochemistry with those in the literature. Therefore, it was postulated that the hydride attack has dominantly occurred from the more hindered face of the phosphonate tetraen systems or from the amine faces of the majority of the other systems.

Chapter 4 of this thesis dealt with the esterification of the cobalt(III) amino acid complexes made in chapter 3 and the reactivity of those chelated esters. Peptide bonds were formed through condensation reactions between the chelated esters and small peptides, as well as with other amino acids and amines to yield cobalt(III) amides.

Peptide synthesis on the metal which was discovered when β_2–$[Co(trien)(glyOEt)Cl](ClO_4)_2$ was treated with glyOEt in an non aqueous environment[63], has been employed to prepare new carboxylate and phosphonate systems. The route to the cobalt(III) peptides is through the ester chelate (**6**). The chelated ester has been reported to condense readily with amino acid esters and small peptides[63, 64] as in Fig. 4.4. The mechanism of the reaction includes a tetrahedral intermediate[63] (**7A**), for the carboxylates.

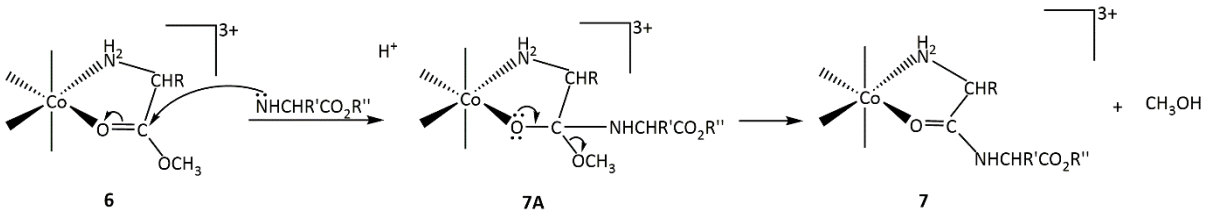

Taking a cue from the carboxylate systems, it was postulated that these phosphonate analogues would undergo a nucleophilic attack on their phosphoryl centre from the N-terminal of an incoming species to give a trigonal bipyramidal intermediate that will lead to the final product.

No activation of the peptide-forming step is required. Kinetic studies[67] demonstrated that the rate of the coupling reaction of the coordinated amino acid ester is enhanced by about 10^6 times more than that of the uncoordinated amino acid ester. The metal ion accounts for this enhancement by its electron withdrawing effect which makes the carbon of the carbonyl group more electrophilic so that it can undergo nucleophilic attack by an incoming nucleophile. The metal ion also enhances C-H acidity at the α-carbon atom through the additional binding of the amine nitrogen.

Therefore, this cobalt(III) method does not only provide an alternative route to peptide synthesis, it also provides both N-terminal protection (necessary for preventing any attack on

the incoming amino acid carbonyl-C) and carbonyl-O activation (for directing the nucleophilic attack by the N-terminal of the incoming amino acid to the carbonyl-C of the complex) in one system and makes coloured compounds which are generally water soluble (essential for biological applications). The metal ion and the ligands can be removed by chemical or electrochemical reduction methods.[75]

The reactivity of these new cobalt(III) systems was expected to mimic those in the literature, by being active towards the addition of a nucleophile, thereby enabling small peptides to be formed through the chelated ester intermediates. The cobalt(III) chelated esters behaved like those in the literature by being very prone to hydrolysis as was confirmed both by NMR and MS. The reactivity was essential for the formation of the amides or short peptides of cobalt(III). The N-terminal of an incoming amino acid or amine carries out a nucleophilic attack on the cobalt(III) activated carbonyl-C or phosphoryl-P to form the new peptide bond. The chelated carboxylate ester and phosphonate ester complexes synthesised in this project were thus successfully coupled with some amines including benzylamine, diamines like ethane-1,2-diamine, amino acid methyl esters, amino acid ethyl esters and a novel dipeptide made in the Hartshorn laboratory.

5.2 Future Work

The most difficult situation encountered during the course of this research was that of separating the isomers formed after a chemical reaction, given the systems investigated. Due to the similarities between these isomers, it would normally be hard to achieve total separation of the individual components of each product mixture on a single column. Some of the distinct fractions collected in this project from column chromatographic techniques were further subjected to yet another column chromatography to attempt more separation but the fractions collected were confirmed to still be a mixture of stereoisomers through NMR and MS techniques. An attempt could be made at separating and isolating enantiomers[138] from their mixtures by using bromocamphorsulfonate (BCS)[134-136] or tartrate salts as eluent in Sephadex ion exchange chromatography. Otherwise, the tartrate salts[137, 138] could be used to attempt crystallisation of diastereoisomeric salts (where the salts of the cationic enantiomers have different solubilities) as has been used in the Hartshorn group to resolve ruthenium phendione complexes.

If enantiomers are isolated, their optical activities can be measured and then used in the future as references. That way, when an enantiomer is used as a reactant in a chemical reaction, say borohydride reduction, optical tests would reveal if the configurations at stereogenic centres were retained or inverted. Then product mixtures could be completely assigned with less assumptions.

Alternatives methods (if available) for the imine bond reduction should also be sought. Hydrogenation[139] could be tested for reducing the imine bond(s) to amine(s) under conditions that will not reduce the metal ion.

Another approach that could reduce the stereochemical complexity of the amides and short peptides prepared in this project is to release the ligand from the metal ion. Releasing the ligand would not only reduce stereochemical complexity but would also provide samples for biological studies using the complicated ligands synthesised thereof. The amide or short peptide is decomplexed from around the metal centre through the reduction of the cobalt(III) ion to cobalt(II) ion making the ligands labile. That could be achieved by warming the cobalt(III) complex with CN^-, by reacting with zinc amalgam at pH 1-2, by electrolytic reduction using a potential of about -1.0 V or by using $NaBH_4$ in neutral or alkaline conditions[66].

Preliminary studies in the Hartshorn group (carried out by two summer students: Brooke Matthews and Jerram Wood) has begun with respect to the ligand release. That was achieved by reacting the complex with $NaBH_4$ until the colour of the reaction mixture changes to black. The product mixture was quickly adsorbed onto an acidified (H^+) Dowex 50WX2 column and washed with 3 M HCl before elution.

However, the chelating nature of the ligands could pose a problem during the decomplexation as have been encountered already. Initially Matthews discovered that the $[Co(A_2trien)]^+$ was able to reform because the cobalt(II) had not been removed and was oxidised by atmospheric oxygen back to cobalt(III). Therefore, the chief modification used by Wood was an additional elution using 3 M HCl to elute the cobalt(II) ions produced by the reduction while retaining the ligand on the column.

While the free ligand (A_2trien) was isolated without any trace of $[Co(A_2trien)]^+$ in at least one of Wood's experiments, confirmed by the mass spectrometry data obtained, there was a significant drawback. Various side products were observed, although at least one side product was also present in Brooke's work. Wood therefore presented two possible solutions to this new problem. The first was "to perhaps accept that the side reactions will happen and develop a way of separating the side products and the desired ligand. However, it is far more desirable to isolate the ligand from the cobalt without the side products. Potentially, this could be done by ensuring that the material is exposed to conditions which might cause self-condensation or other undesirable reactions to occur for as little time as possible. This could be done perhaps by ensuring rapid addition of the 3 M HCl to the column after addition of the black solution which results from reduction of the cobalt(III), with elution of this in as prompt a manner as possible, followed by the copious volume of water and then the 0.1% ammonia solution. This could perhaps minimize the side reactions occurring during this part of the experiment".

Obviously, more work needs to be done to finesse the reaction conditions necessary to achieve optimum decomplexation of these novel ligands. One of them could be doing the reduction with dithionite in conditions with a pH over 5.5, probably under an N_2 atmosphere, filtering off any solids, followed by appropriate steps to get rid of the other sulphur by-products.

The free ligands could find several applications in medicine. The phosphonate moiety represents a source of inorganic phosphate to microorganisms that live in environments that lack this nutrient[77]. As a substitute for a natural phosphate metabolite, phosphonate esters are capable of inhibiting the regular metabolism of an organism simply by non-participation in a

normal phosphate cleavage process[140]. The pyruvate analogues acetylphosphonate and methyl acetyl phosphonate both inhibit the reaction of pyruvate oxidase with its normal substrate, pyruvate[141]. Some phosphonate analogues of cyclophostin are inhibitors of acetylcholinesterase (AChE)[80]. The phosphonamidate moiety can inhibit the human immunodeficiency virus type-1 protease (HIV-1 PR)[91]. Sulfur containing amino acids such as are known to contribute substantially to the maintenance and integrity of cellular systems by influencing cellular redox state and cellular capacity to detoxify toxic compounds, free radicals and reactive oxygen species.[142]

Some interesting amino acids or peptides which could be incorporated into these new systems include but are not limited to (1) excitatory amino acids such as glutamate and aspartate which are major transmitters of the cerebral cortex and hippocampus[143] and (2) sulfur containing amino acids such as methionine and cysteine which contribute substantially to the maintenance and integrity of cellular systems by influencing cellular redox state and cellular capacity to detoxify toxic compounds, free radicals and reactive oxygen species.[142]

Possible ligands that could be generated from the decomplexation of the systems synthesised in this project include but are not limited to the following:

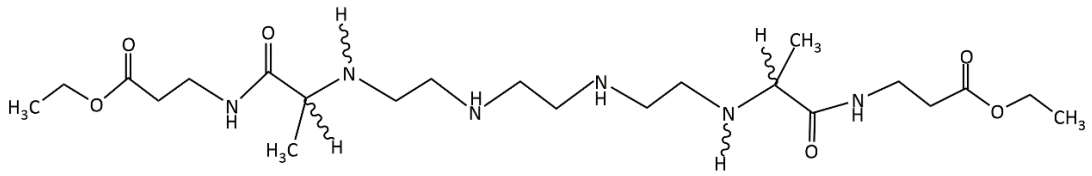

Figure 5.1 Expected free ligand from **4.15** mixture

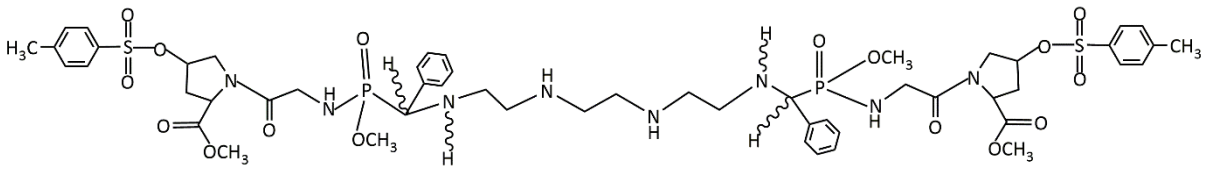

Figure 5.2 Expected free ligand from **4.17** mixture

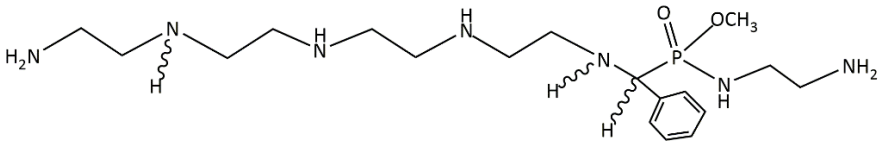

Figure 5.3 Expected free ligand from **4.10** mixture

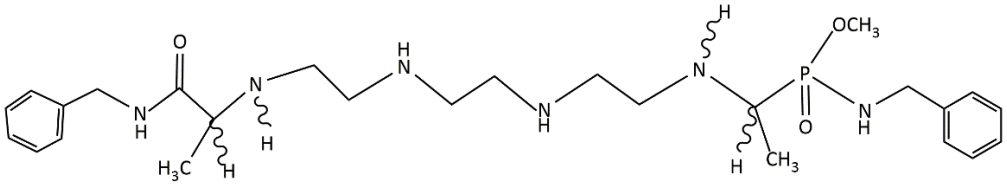

Figure 5.4 Expected free ligand from **4.12** mixture

References

53. Browne, J. M.; Wikaira, J.; Fitchett, C. M.; Hartshorn, R. M., Polydentate ligand construction: intramolecular condensation reactions in the synthesis of imine-containing ligands. *Journal of the Chemical Society, Dalton Transactions* **2002,** (10), 2227-2234.

55. Browne, J. M. Intramolecular Condensation Reactions of Cobalt (III) Complexes. A Thesis Submitted in Partial Fulfilment of the Requirements for the Degree of Master of Science in Chemistry at the University of Canterbury, University of Canterbury, 2000.

63. Buckingham, D. A.; Marzilli, L. G.; Sargeson, A. M., Peptide bond formation and subsequent hydrolysis at a cobalt (III) center. *Journal of the American Chemical Society* **1967,** *89* (11), 2772-2773.

64. Buckingham, D. A.; Marzilli, L. G.; Sargeson, A. M., N-Terminal addition of glycine to amino acid and peptide esters activated by the cobalt (III) ion. *Journal of the American Chemical Society* **1967,** *89* (17), 4539-4540.

66. Clark, C.; Tasker, R.; Buckingham, D.; Knighton, D.; Harding, D.; Hancock, W., Cobalt (III)-mediated peptide synthesis. 1. Cobalt (III)-activated amino acid methyl esters and the synthesis of dipeptides. *Journal of the American Chemical Society* **1981,** *103* (23), 7023-7025.

67. Sutton, P. A.; Buckingham, D. A., Cobalt (III)-promoted hydrolysis of amino acid esters and peptides and the synthesis of small peptides. *Accounts of Chemical Research* **1987,** *20* (10), 357-364.

75. Browne, R. J.; Buckingham, D. A.; Clark, C. R.; Sutton, P. A., The Cobalt (III)-Promoted Synthesis of Small Peptides. *Advances in Inorganic Chemistry* **1999,** *49*, 307-373.

77. Horsman, G. P.; Zechel, D. L., Phosphonate biochemistry. *Chemical Reviews* **2016,** *117* (8), 5704-5783.

80. Dutta, S.; Malla, R. K.; Bandyopadhyay, S.; Spilling, C. D.; Dupureur, C. M., Synthesis and kinetic analysis of some phosphonate analogs of cyclophostin as inhibitors of human acetylcholinesterase. *Bioorganic Medicinal Chemistry* **2010,** *18* (6), 2265-2274.

91. McLeod, D. A.; Brinkworth, R. I.; Ashley, J. A.; Janda, K. D.; Wirsching, P., Phosphonamidates and phosphonamidate esters as HIV-1 protease inhibitors. *Bioorganic Medicinal Chemistry Letters* **1991,** *1* (11), 653-658.

104. Glusker, J. P.; Carrell, H.; Job, R.; Bruice, T. C., Mechanism for chiral recognition of a prochiral center and for amino acid complexation to a cobalt (III) tetramine. Crystal structure, absolute configuration, and circular dichroism of lambda(-) 436- beta-2-[(2S, 9S)-2, 9-diamino-4, 7-diazadecanecobalt (III) aminomethylmalonate] perchlorate monohydrate. *Journal of the American Chemical Society* **1974,** *96* (18), 5741-5751.

105. Buckingham, D.; Cresswell, P.; Dellaca, R.; Dwyer, M.; Gainsford, G.; Marzilli, L.; Maxwell, I.; Robinson, W. T.; Sargeson, A.; Turnbull, K., Structure, conformational analysis, and properties of diastereoisomeric forms of. beta. 1-glycinatotriethylenetetraminecobalt (III) ions. *Journal of the American Chemical Society* **1974,** *96* (6), 1713-1725.

106. Clarkson, A. J.; Blackman, A. G.; Clark, C. R., Preparation, structures and reactions of isomeric $[Co(cyclen)(O_2C_2O_2)]^+$ and $[Co(cyclen)(O_2CCH_2CO_2)]^+$ complexes (cyclen= 1, 4, 7, 10-tetraazacyclododecane). *Journal of the Chemical Society, Dalton Transactions* **2001,** (5), 758-765.

107. Tsuboyama, S.; Shiga, Y.; Takasyo, Y.; Chijimatsu, T.; Kobayashi, K.; Tsuboyama, K.; Sakurai, T., Studies on metal complexes of chiral cyclen. Part 14. Configurational isomerism in a complex of cobalt (III). *Journal of the Chemical Society, Dalton Transactions* **1992,** (11), 1783-1789.

108. Tsuboyama, S.; Matsudo, M.; Tsuboyama, K.; Sakurai, T., Structures of [(R)- and (S)-prolinato](optically active cyclen) cobalt (III) complexes. *Acta Crystallographica Section C: Crystal Structure Communications* **1989,** *45* (6), 872-876.

109. Tsuboyama, S.; Tsuboyama, K.; Sakurai, T., Structure of $[Co(C_4H_5NO_4)(C_{16}H_{36}N_4)]ClO_4.2.5H_2O$.Corrigendum. *Acta Crystallographica Section C: Crystal Structure Communications* **1990,** *46* (4), 727-727.

110. Freeman, H. C.; Marzilli, L. G.; Maxwell, I. E., Crystal structure and absolute configuration of D- beta 2-(SSS)-(triethylenetetramine-(S)-prolinato) cobalt (III) tetrachlorozincate. *Inorganic Chemistry* **1970,** *9* (11), 2408-2415.

111. Muir, M. M.; Muir, J. A.; Saez, R.; Campana, C. F., Complexes with asymmetric tetraamine ligands. IV. Cobalt (III) complexes containing two chiral ligands. Structure of Λ-cis-β2-(SS)-[S-alaninato-2S, 5R, 9S-trimethyltriencobalt (III)] perchlorate hydrate. *Inorganica Chimica Acta* **1988,** *141* (1), 75-81.

112. Tashiro, S.; Ogura, Y.; Tsuboyama, S.; Tsuboyama, K.; Shionoya, M., Chiral recognition of α-Amino acids by an optically active (2s, 5s, 8s, 11s)-2, 5, 8, 11-tetraethyl cyclen Cobalt (III) complex. *Inorganic chemistry* **2010,** *50* (1), 4-6.

113. Muir, J. A.; Muir, M. M.; Saez, R.; Campana, C., Structure of a cobalt (III) complex with two opically active ligands. *Acta Crystallographica Section C: Crystal Structure Communications* **1987,** *43* (8), 1487-1490.

114. Cai, J.; Hu, X.; Feng, X.; Ji, L.; Bernal, I., Structures of three cis-β1 and three cis-β2 isomers of $[Co (trien)(aminoacidato)]^{2+}$ complexes. *Acta Crystallographica Section B: Structural Science* **2001,** *57* (1), 45-53.

115. Da Pieve, C.; Spingler, B., Nickel and cobalt complexes of 15, 15-disubstituted 1, 4, 7, 10, 13-pentaazacyclohexadecane-14, 16-dione ligands. *Inorganica Chimica Acta* **2012,** *380*, 230-235.

116. Buckingham, D. A.; Clark, C. R.; Rogers, A. J.; Simpson, J., The Synthesis, Separation and Structures of Three [Co (cyclen)((S)-AlaO)] $^{2+}$ Isomers. The Alkaline

Hydrolysis of [Co (cyclen)((S)-AlaO)] $^{2+}$. *Australian Journal of Chemistry* **1998,** *51* (6), 461-470.

117. Anderson, B.; Bell, J.; Buckingham, D.; Cresswell, P.; Gainsford, G.; Marzilli, L.; Robertson, G.; Sargeson, A., Structures, chemistry, and relative energies of the [Co (trien)(glyO)]$^{2+}$ ions. 3 alpha -(RR, SS)-[Co (trien)(glyO)]$^{2+}$ and alpha -(RR, SS)-[Co (trien)(glyOEt) Cl]$^{2+}$ ions. *Inorganic Chemistry* **1977,** *16* (12), 3233-3244.

118. Chang, J. Y.-C.; Stevenson, R. J.; Lu, G.-L.; Brothers, P. J.; Clark, G. R.; Denny, W. A.; Ware, D. C., Syntheses of 8-quinolinolatocobalt (III) complexes containing cyclen based auxiliary ligands as models for hypoxia-activated prodrugs. *Dalton Transactions* **2010,** *39* (48), 11535-11550.

119. Hu, X.; Cai, J.; Chen, C.; Chen, X.-M.; Ji, L.-N., Conglomerate crystallization behavior of racemic [Co (N_4)(aminoacidato)]$^{2+}$ complexes. *Crystal Engineering* **2001,** *4* (2-3), 141-157.

120. Eduok, E. E.; Kashyap, R. P.; Nagl, A.; Bourne, S. A.; Watson, W. H., Amino acid complexes of [Co (III)(trien)]$^{+}$ [3]. *Journal of Chemical Crystallography* **1994,** *24* (9), 627-638.

121. Buckingham, D. A.; Clark, C. R.; Rogers, A. J.; Simpson, J., Synthesis and structures of five [Co (Mecyclen)(S-AlaO)]$^{2+}$ isomers: use of nOe and COSY ^{1}H NMR spectroscopy for structural assignment in solution. *Inorganic Chemistry* **1995,** *34* (14), 3646-3657.

122. Clarkson, A. J.; Blackman, A. G., Synthesis and Co (III) complexes of the new tetradentate mixed-donor tetraamine ligand N-{2-[(2-pyridin-2-ylethyl) amino] ethyl} ethane-1, 2-diamine (peda). *Polyhedron* **2006,** *25* (2), 373-378.

134. Jörgensen, S., Ueber Metalldiaminverbindungen. *Journal für Praktische Chemie* **1889,** *39* (1), 1-26.

135. Werner, A., Information on asymmetric cobalt atoms XII. Optical activity with carbon compounds. *Berichte Der Deutschen Chemischen Gesellschaft* **1914,** *47*, 3087-3094.

136. Werner, A., Information on the assymetric cobalt atom. IX. *Berichte Der Deutschen Chemischen Gesellschaft* **1913**, 3674-3683.

137. Lindner, W.; Rath, M.; Stoschitzky, K.; Uray, G., Enantioselective drug monitoring of (R)-and (S)-propranolol in human plasma via derivatization with optically active (R, R)-O, O-diacetyl tartaric acid anhydride. *Journal of Chromatography B: Biomedical Sciences Applications* **1989,** *487*, 375-383.

138. Whelpton, R.; Jonas, G.; Buckley, D. G., High-performance liquid chromatographic resolution of the enantiomers of thioridazine, its metabolites and related compounds. *Journal of Chromatography B: Biomedical Sciences Applications* **1988,** *426*, 223-228.

139. Blaser, H. U.; Spindler, F., Catalytic asymmetric hydrogenation of C-N functions. *Organic Reactions* **2004**, 1-102.

140. Engel, R., Phosphonates as analogues of natural phosphates. *Chemical Reviews* **1977,** *77* (3), 349-367.

141. O'Brien, T. A.; Kluger, R.; Pike, D. C.; Gennis, R. B., Phosphonate analogues of pyruvate. Probes of substrate binding to pyruvate oxidase and other thiamin pyrophosphate-dependent decarboxylases. *Biochimica et Biophysica Acta (BBA)-Enzymology* **1980,** *613* (1), 10-17.

142. Townsend, D. M.; Tew, K. D.; Tapiero, H., Sulfur containing amino acids and human disease. *Biomedicine pharmacotherapy* **2004,** *58* (1), 47-55.

143. Greenamyre, J. T.; Young, A. B., Excitatory amino acids and Alzheimer's disease. *Neurobiology of aging* **1989,** *10* (5), 593-602.

Appendices

Appendix 1 X-ray information for some starting materials

Table A1.1 Crystal data and structure refinement for $[Co(trien)Cl_2]ZnCl_4$.

Identification code	nda2a10052018
Empirical formula	$C_6H_{18}Cl_4CoN_4Zn_{0.5}$
Formula weight	379.66
Temperature/K	120.01(10)
Crystal system	orthorhombic
Space group	Pnma
a/Å	12.6958(3)
b/Å	26.8039(8)
c/Å	7.8416(2)
α/°	90
β/°	90
γ/°	90
Volume/Å^3	2668.47(12)
Z	8
ρ_{calc}g/cm^3	1.890
μ/mm^{-1}	18.212
F(000)	1536.0
Crystal size/mm^3	0.203 × 0.108 × 0.016
Radiation	CuKα (λ = 1.54184)
2Θ range for data collection/°	11.758 to 153.384
Index ranges	$-10 \leq h \leq 15$, $-31 \leq k \leq 33$, $-9 \leq l \leq 9$
Reflections collected	10134
Independent reflections	2842 [R_{int} = 0.0496, R_{sigma} = 0.0406]
Data/restraints/parameters	2842/0/153
Goodness-of-fit on F^2	1.024
Final R indexes [I>=2σ (I)]	R_1 = 0.0393, wR_2 = 0.0988

Final R indexes [all data]	R_1 = 0.0433, wR_2 = 0.1028
Largest diff. peak/hole / e Å^{-3}	0.93/-0.52

Refinement model description

This complex crystallised with half of the tetrachlorozincate molecule in its asymmetric unit. Hydrogen bonding interactions were observed between the tetrachlorozincate anion and the complex through two chloride atoms on the ZnCl4 and protons on N3 and one of the protons on N1.

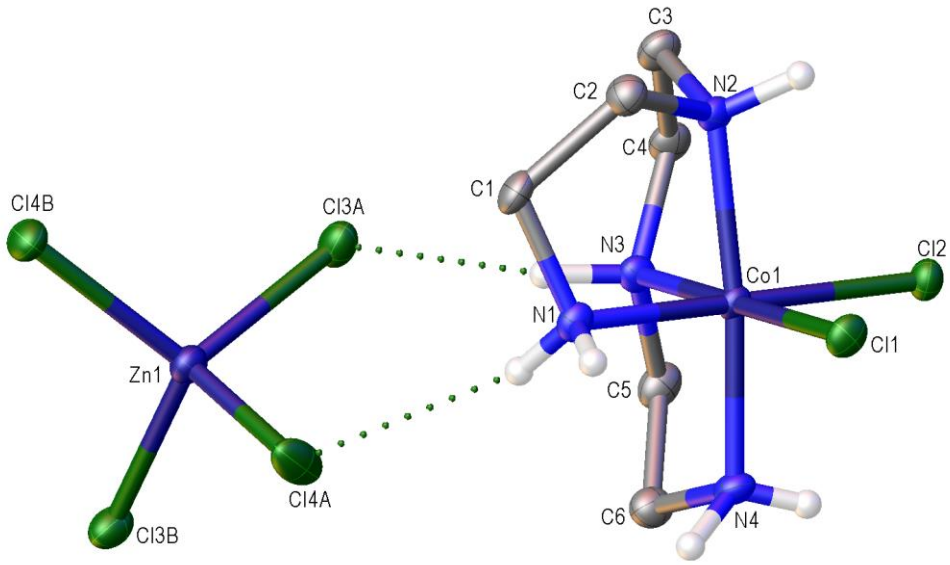

Figure A1.1 Crystal structure of [Co(trien)Cl_2]$ZnCl_4$

Selected bond lengths (Å): Co1-Cl1, 2.2728 (9); Co1-Cl2, 2.2641(9); Co1-N2, 1.970 (3); Co1-N1, 1.947 (3); Co1-N3, 1.940 (3); Co1-N4, 1.960 (3); N2-C2, 1.492 (4); N2-C3, 1.506; N1-C1, 1.485; N3-C5, 1.478 (4); N3-C4, 1.483 (4); N4-C6, 1.497 (4).

Table A1.2 Crystal data and structure refinement for $[Co(tetraen)Cl]Cl_2$.

Identification code	nda3a
Empirical formula	$C_8H_{27}Cl_3CoN_5O_2$
Formula weight	390.62
Temperature/K	120.01(10)
Crystal system	tetragonal
Space group	$P4_1$
a/Å	14.6548(5)
b/Å	14.6548(5)
c/Å	7.3690(4)
α/°	90
β/°	90
γ/°	90
Volume/Å^3	1582.59(13)
Z	4
ρ_{calc}g/cm^3	1.639
μ/mm^{-1}	13.226
F(000)	816.0
Crystal size/mm^3	0.129 × 0.084 × 0.035
Radiation	CuKα (λ = 1.54184)
2Θ range for data collection/°	8.532 to 153.202
Index ranges	$-18 \leq h \leq 18$, $-18 \leq k \leq 18$, $-9 \leq l \leq 8$
Reflections collected	7953
Independent reflections	2978 [R_{int} = 0.1387, R_{sigma} = 0.1517]
Data/restraints/parameters	2978/1/182
Goodness-of-fit on F^2	1.056
Final R indexes [I>=2σ (I)]	R_1 = 0.1021, wR_2 = 0.2425
Final R indexes [all data]	R_1 = 0.1223, wR_2 = 0.2882
Largest diff. peak/hole / e Å^{-3}	1.96/-1.16
Flack parameter	-0.067(14)

Refinement model description

This complex crystallised with two molecules of water in its asymmetric unit. Hydrogen bonding interactions were observed between the complex and its two chloride counter ions through one of the protons on N1 and the proton of N4 respectively.

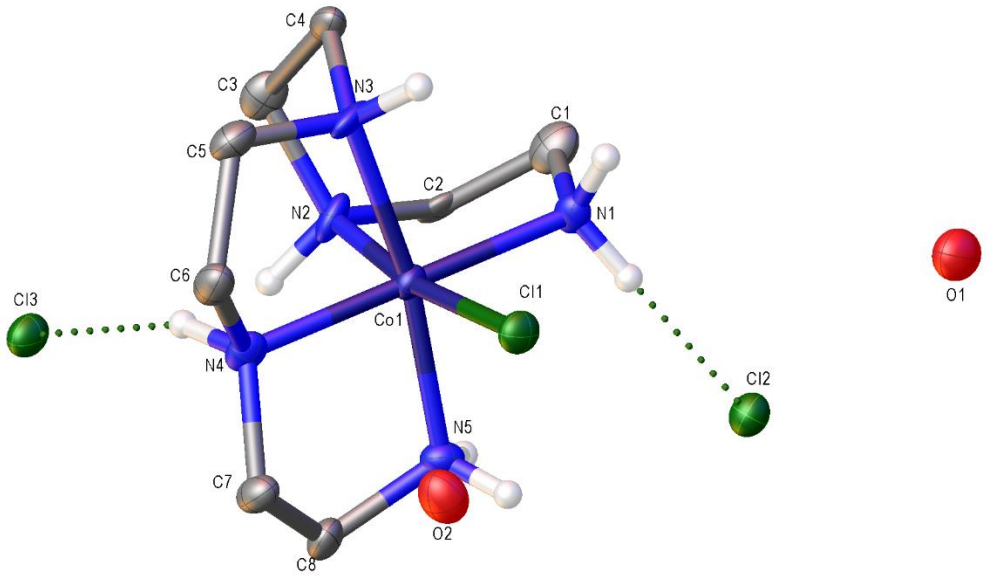

Figure A1.2 Crystal structure of [Co(tetraen)Cl]Cl_2

Selected bond lengths (Å): Co1-Cl1, 2.265 (3); Co1-N2, 1.975 (12); Co1-N1, 1.966 (11); Co1-N3, 1.982 (11); Co1-N4, 1.962 (12); Co1-N5, 1.986 (11); N2-C2, 1.514 (17); N2-C3, 1.485 (18); N1-C1, 1.486 (17); N3-C5, 1.471 (19); N3-C4, 1.491 (18); N4-C6, 1.457 (18); N5-C8, 1.482 (16); N4-C7, 1.487 (16).

Appendix 2 X-ray information for chapter 2 complexes

Table A2.1 Crystal data and structure refinement for compound **2.1**

Identification code	nda15a 260318
Empirical formula	$C_{11}H_{27}Cl_4CoN_5O_4PZn$
Formula weight	590.44
Temperature/K	120.01(10)
Crystal system	triclinic
Space group	$P\bar{1}$
a/Å	8.1037(5)
b/Å	10.2097(8)
c/Å	14.1124(7)
α/°	101.636(5)
β/°	91.405(4)
γ/°	111.759(6)
Volume/Å^3	1055.79(13)
Z	2
ρ_{calc}g/cm^3	1.857
μ/mm^{-1}	13.188
F(000)	600.0
Crystal size/mm^3	0.127 × 0.052 × 0.041
Radiation	CuKα (λ = 1.54184)
2Θ range for data collection/°	6.432 to 142.566
Index ranges	$-7 \leq h \leq 9$, $-12 \leq k \leq 12$, $-16 \leq l \leq 17$
Reflections collected	7094
Independent reflections	4047 [R_{int} = 0.0546, R_{sigma} = 0.0589]
Data/restraints/parameters	4047/5/246
Goodness-of-fit on F^2	1.048
Final R indexes [I>=2σ (I)]	R_1 = 0.0408, wR_2 = 0.1025
Final R indexes [all data]	R_1 = 0.0465, wR_2 = 0.1062
Largest diff. peak/hole / e Å^{-3}	0.68/-0.72

Refinement model description

No solvent molecules were found in the asymmetric unit of this complex.

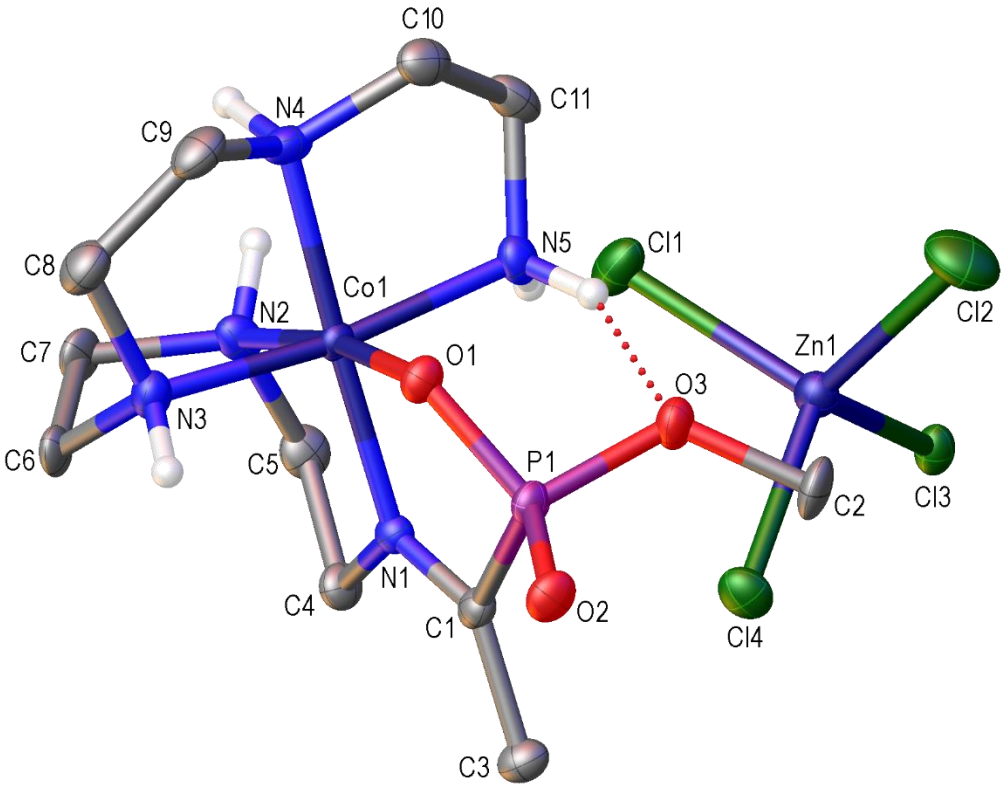

Figure A2.1 The asymmetric unit of compound **2.1**. Non-hetero atoms have been omitted for clarity.

Table A2.2 Crystal data and structure refinement for compound **2.2**

Identification code	nda5recollected A
Empirical formula	$C_{16}H_{29}Cl_4CoN_5O_3PZn$
Formula weight	636.51
Temperature/K	120.00(10)
Crystal system	monoclinic
Space group	$P2_1/n$
a/Å	14.0250(7)
b/Å	12.6934(6)
c/Å	17.1301(9)
α/°	90
β/°	109.877(6)
γ/°	90
Volume/Å^3	2867.9(3)
Z	4
ρ_{calc}g/cm^3	1.474
μ/mm^{-1}	9.730
F(000)	1296.0
Crystal size/mm^3	0.158 × 0.14 × 0.038
Radiation	CuKα (λ = 1.54184)
2Θ range for data collection/°	7.072 to 144.094
Index ranges	$-17 \leq h \leq 11$, $-15 \leq k \leq 15$, $-20 \leq l \leq 21$
Reflections collected	20367
Independent reflections	5634 [R_{int} = 0.0393, R_{sigma} = 0.0358]
Data/restraints/parameters	5634/0/301
Goodness-of-fit on F^2	1.066
Final R indexes [I>=2σ (I)]	R_1 = 0.0305, wR_2 = 0.0751
Final R indexes [all data]	R_1 = 0.0374, wR_2 = 0.0780
Largest diff. peak/hole / e Å^{-3}	0.36/-0.47

Refinement model description

This complex crystallized with a poorly ordered tetrahydrofuran (THF) in the asymmetric unit. The model was therefore refined with dummy atoms in place of THF. These atoms were removed, and a solvent mask applied before refinement using the OLEX2 program. Void size and electrons removed were of the THF.

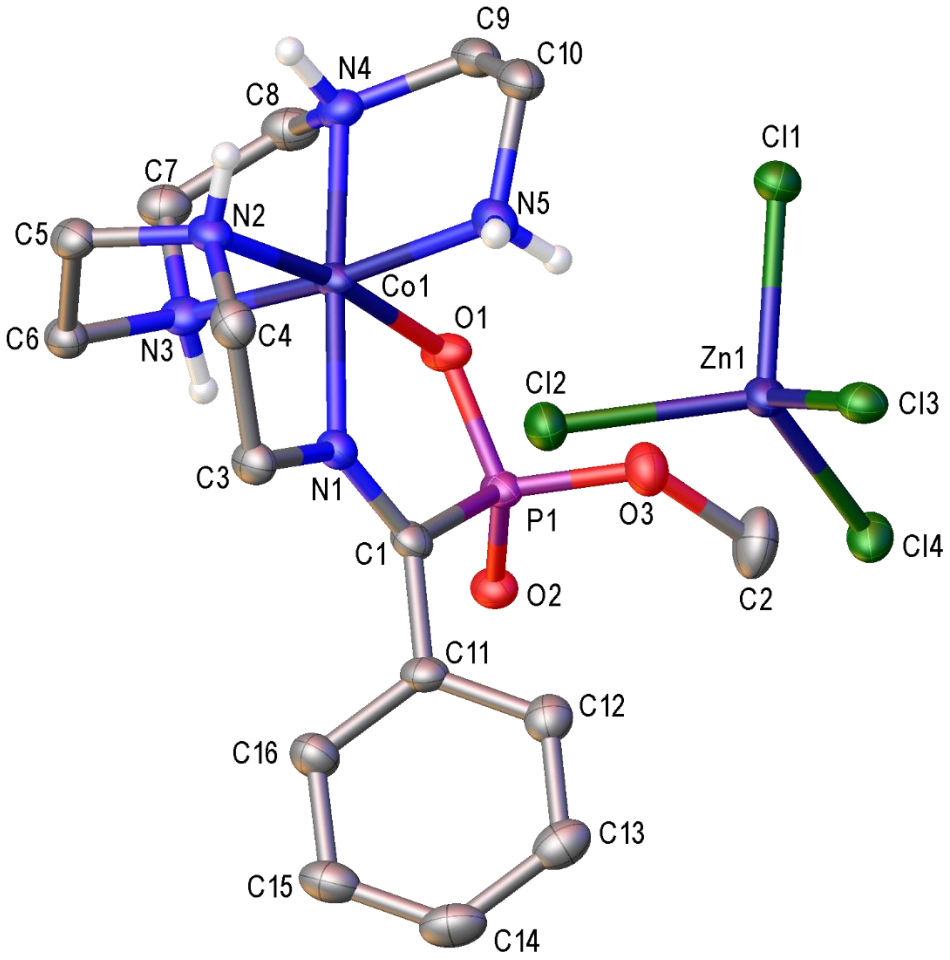

Figure A2.2 The asymmetric unit of compound **2.2**. Non-hetero atoms have been omitted for clarity.

Table A2.3 Crystal data and structure refinement for compound **2.3**

Identification code	nda13Ra 040319
Empirical formula	$C_{16}H_{31}Cl_4CoN_5O_4PZn$
Formula weight	683.54
Temperature/K	120.00(10)
Crystal system	triclinic
Space group	PĪ
a/Å	9.2402(4)
b/Å	11.9830(5)
c/Å	13.8865(4)
α/°	114.763(4)
β/°	102.300(3)
γ/°	90.166(4)
Volume/Å^3	1356.78(10)
Z	2
ρ_{calc}g/cm^3	1.673
μ/mm^{-1}	10.387
F(000)	698.0
Crystal size/mm^3	0.179 × 0.111 × 0.042
Radiation	CuKα (λ = 1.54184)
2Θ range for data collection/°	7.214 to 153.484
Index ranges	$-11 \leq h \leq 11$, $-15 \leq k \leq 15$, $-17 \leq l \leq 17$
Reflections collected	24037
Independent reflections	5622 [R_{int} = 0.0464, R_{sigma} = 0.0370]
Data/restraints/parameters	5622/7/329
Goodness-of-fit on F^2	1.105
Final R indexes [I>=2σ (I)]	R_1 = 0.0391, wR_2 = 0.1054
Final R indexes [all data]	R_1 = 0.0463, wR_2 = 0.1093
Largest diff. peak/hole / e Å^{-3}	1.09/-0.39

Refinement model description

This complex crystallised with one molecule of water in its asymmetric unit. A molecule of methanol which occupied two positions half of the time was also located in the asymmetric unit but its hydrogen atoms could not be located. Dummy atoms were therefore used in place of methanol. These atoms were removed and a solvent mask applied before refinement. Void size and electrons removed were of methanol.

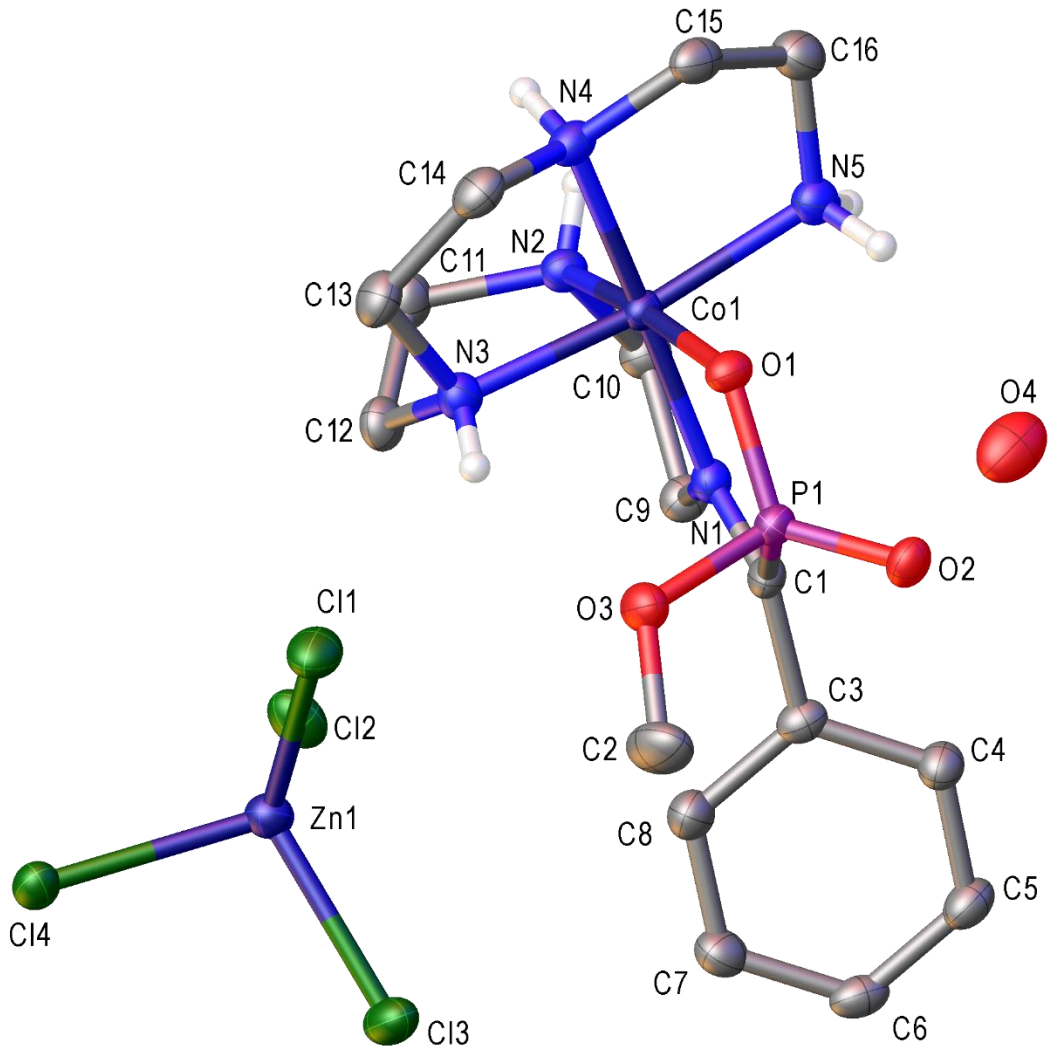

Figure A2.3 The asymmetric unit of compound **2.3**. Non-hetero atoms have been omitted for clarity.

Table A2.4 Crystal data and structure refinement for compound **2.5**.

Identification code	nda25a
Empirical formula	$C_{39}H_{90}Cl_{13}Co_4N_{12}O_{21}P_6Zn_3$
Formula weight	2141.75
Temperature/K	120.02(10)
Crystal system	trigonal
Space group	R3c
a/Å	15.3143(4)
b/Å	15.3143(4)
c/Å	57.5472(19)
α/°	90
β/°	90
γ/°	120
Volume/Å^3	11688.2(7)
Z	6
ρ_{calc}g/cm^3	1.826
μ/mm^{-1}	13.393
F(000)	6510.0
Crystal size/mm^3	0.289 × 0.217 × 0.129
Radiation	CuKα (λ = 1.54184)
2Θ range for data collection/°	7.34 to 143.98
Index ranges	$-18 \leq h \leq 14$, $-14 \leq k \leq 18$, $-70 \leq l \leq 55$
Reflections collected	18552
Independent reflections	4031 [R_{int} = 0.0590, R_{sigma} = 0.0334]
Data/restraints/parameters	4031/4/307
Goodness-of-fit on F^2	1.099
Final R indexes [I>=2σ (I)]	R_1 = 0.0493, wR_2 = 0.1345
Final R indexes [all data]	R_1 = 0.0527, wR_2 = 0.1527
Largest diff. peak/hole / e Å^{-3}	1.23/-1.89
Flack parameter	0.049(8)

Refinement model description

One molecule of methanol crystallised with this complex. This well-ordered methanol was bound to the main structure through a hydrogen bond (2.087 (2) Å). A -1 charge could not be accounted for while trying to balance the charges between the complex and its counter-ions. However, the cobalt atom has been confidently assigned a +3 charge. One of the reasons for choosing the +3 charge is by charge balance, requiring an additional H on the complex. The hydrogens on N2 and N3 were located in the electron density map.

The Flack parameter for this structure is 0.049(8). However, absolute configuration resolution is not one of the goals of this research. Therefore, no further interpretation would be given to this feature.

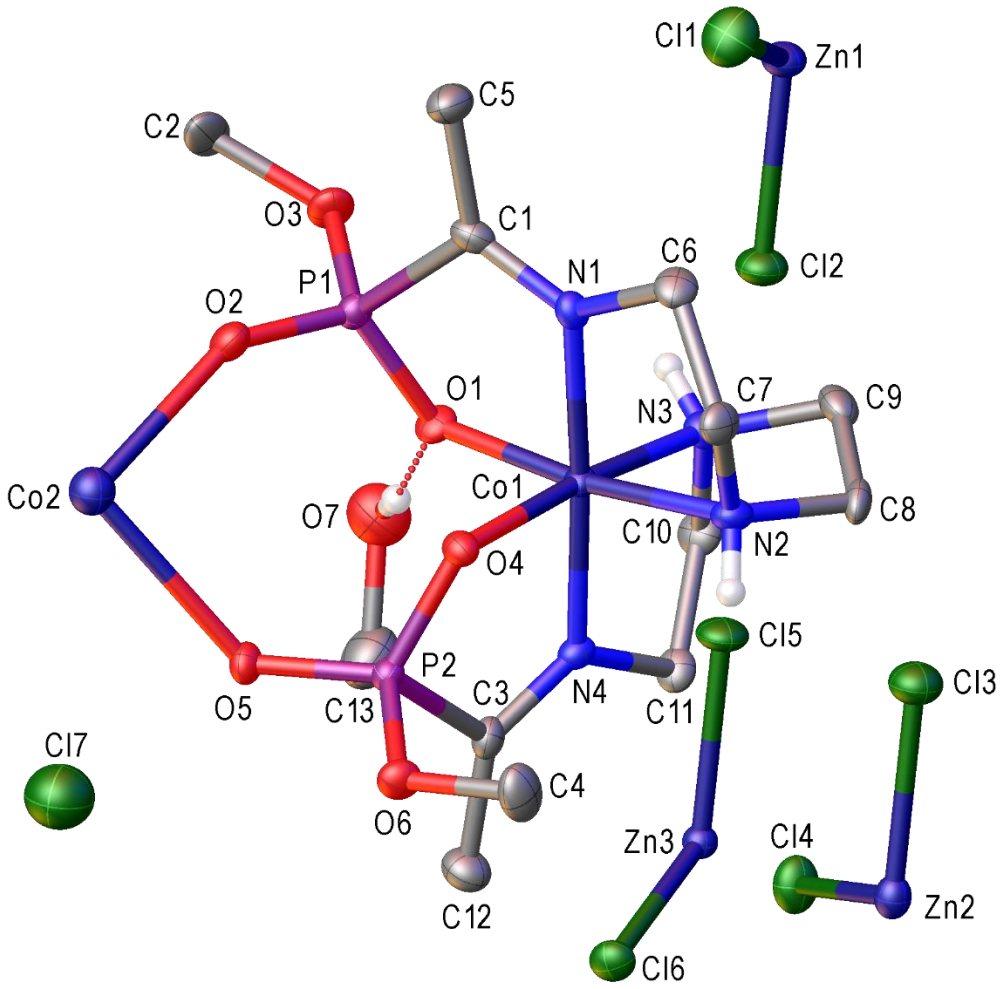

Figure A2.4 The asymmetric unit of compound **2.5**. Non-hetero atoms have been omitted for clarity.

Table A2.5 Crystal data and structure refinement for compound **2.6**.

Identification code	nda1a130318
Empirical formula	$C_{10.75}H_{31.25}ClCoN_4Na_{0.25}O_{10}P_2$
Formula weight	538.71
Temperature/K	120.00(12)
Crystal system	triclinic
Space group	PĪ
a/Å	7.9320(3)
b/Å	10.4761(6)
c/Å	13.6775(6)
α/°	83.882(4)
β/°	87.529(4)
γ/°	73.459(4)
Volume/Å^3	1083.21(9)
Z	2
ρ_{calc}g/cm^3	1.652
μ/mm^{-1}	9.306
F(000)	561.0
Crystal size/mm^3	0.232 × 0.149 × 0.044
Radiation	CuKα (λ = 1.54184)
2Θ range for data collection/°	8.848 to 147.484
Index ranges	$-9 \leq h \leq 9$, $-11 \leq k \leq 13$, $-17 \leq l \leq 17$
Reflections collected	21835
Independent reflections	4366 [R_{int} = 0.0616, R_{sigma} = 0.0382]
Data/restraints/parameters	4366/10/308
Goodness-of-fit on F^2	1.016
Final R indexes [I>=2σ (I)]	R_1 = 0.0398, wR_2 = 0.0975
Final R indexes [all data]	R_1 = 0.0418, wR_2 = 0.0989
Largest diff. peak/hole / e Å^{-3}	0.61/-0.40

Refinement model description

Four water molecules were located in the asymmetric unit of this crystal. Two of these were bound to the complex through hydrogen bonding. The third molecule of water was interacting with the chloride anion only. Some disorder has been modelled in the structure to show the hydrolysed product and a sodium salt of the desired product. Two compounds have co-crystallised. One is the OMe, the other is ONa, in a 75:25 ratio.

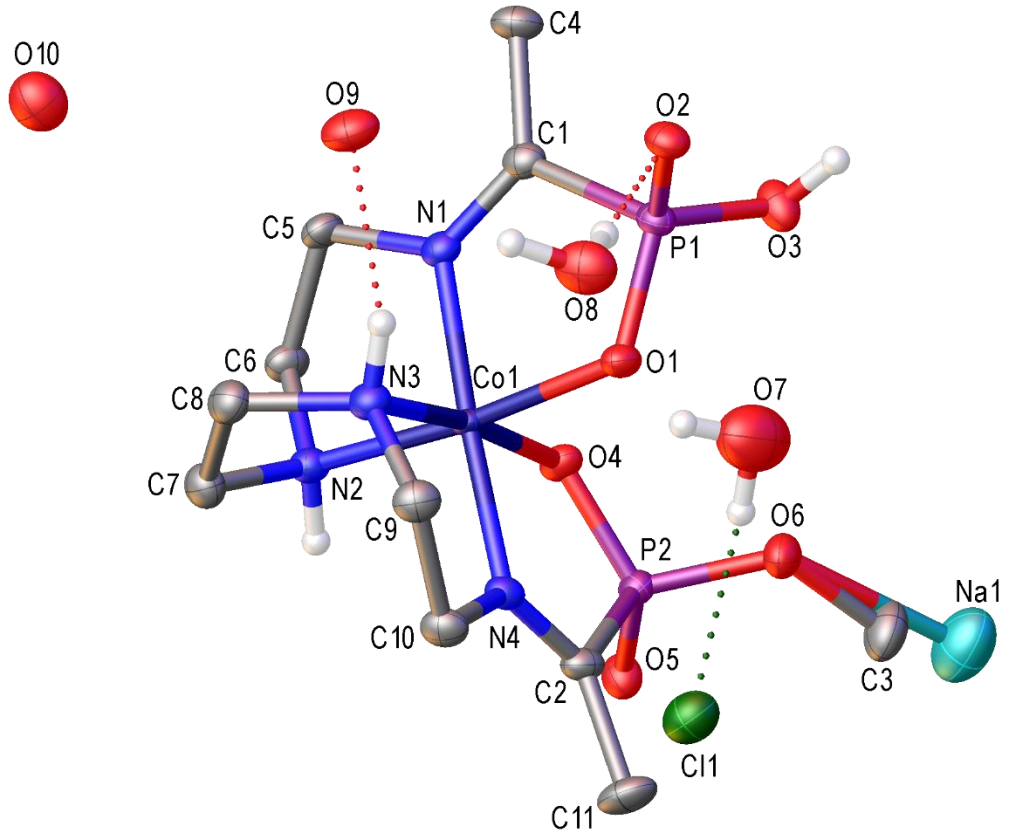

Figure A2.5 The asymmetric unit of compound **2.6**. Non-hetero atoms have been omitted for clarity.

Table A2.6 Crystal data and structure refinement for compound **2.7**.

Identification code	nda21 repeat
Empirical formula	$C_{11}H_{17}Cl_{0.5}Co_{0.5}N_2O_4P$
Formula weight	319.42
Temperature/K	120.01(10)
Crystal system	triclinic
Space group	P-1
a/Å	10.916(5)
b/Å	11.057(5)
c/Å	12.931(10)
α/°	69.11(6)
β/°	68.43(6)
γ/°	78.12(4)
Volume/Å^3	1351.0(16)
Z	4
ρ_{calc}g/cm^3	1.570
μ/mm^{-1}	7.480
F(000)	664.0
Crystal size/mm^3	0.084 × 0.05 × 0.035
Radiation	CuKα (λ = 1.54184)
2Θ range for data collection/°	7.73 to 152.85
Index ranges	$-12 \leq h \leq 13$, $-12 \leq k \leq 13$, $-14 \leq l \leq 16$
Reflections collected	6547
Independent reflections	4521 [R_{int} = 0.2341, R_{sigma} = 0.4843]
Data/restraints/parameters	4521/6/351
Goodness-of-fit on F^2	0.802
Final R indexes [I>=2σ (I)]	R_1 = 0.1010, wR_2 = 0.2308
Final R indexes [all data]	R_1 = 0.3497, wR_2 = 0.4582
Largest diff. peak/hole / e Å^{-3}	0.35/-0.36

Refinement model description

The crystal structure shown in Fig. A2.6 is unreliable. It has not been used for bond lengths and angles in the discussion section. It has only been included for connectivity.

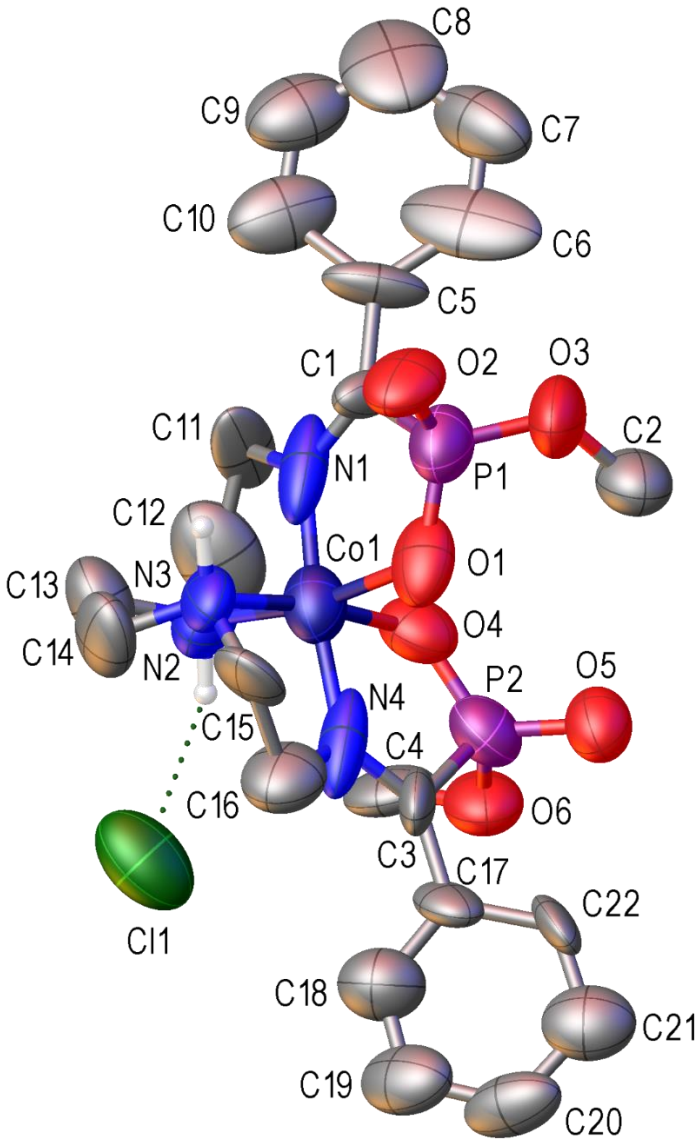

Figure A2.6 The asymmetric unit of compound **2.7**. Non-hetero atoms have been omitted for clarity.

Table A2.7 Crystal data and structure refinement for compound **2.8**

Identification code	nda9R2 B050318
Empirical formula	$C_{22}H_{30}Cl_4CoN_4O_6P_2Zn$
Formula weight	774.54
Temperature/K	120.01(10)
Crystal system	monoclinic
Space group	$P2_1/c$
a/Å	12.2218(11)
b/Å	21.1027(17)
c/Å	14.5092(14)
α/°	90
β/°	113.241(11)
γ/°	90
Volume/Å^3	3438.5(6)
Z	4
ρ_{calc}g/cm^3	1.496
μ/mm^{-1}	8.716
F(000)	1572.0
Crystal size/mm^3	0.15 × 0.132 × 0.04
Radiation	CuKα (λ = 1.54184)
2Θ range for data collection/°	7.844 to 147.55
Index ranges	$-12 \leq h \leq 15$, $-26 \leq k \leq 26$, $-18 \leq l \leq 17$
Reflections collected	31523
Independent reflections	6948 [R_{int} = 0.0978, R_{sigma} = 0.0813]
Data/restraints/parameters	6948/2/376
Goodness-of-fit on F^2	1.036
Final R indexes [I>=2σ (I)]	R_1 = 0.0915, wR_2 = 0.2550
Final R indexes [all data]	R_1 = 0.1179, wR_2 = 0.2903
Largest diff. peak/hole / e Å^{-3}	1.38/-1.36

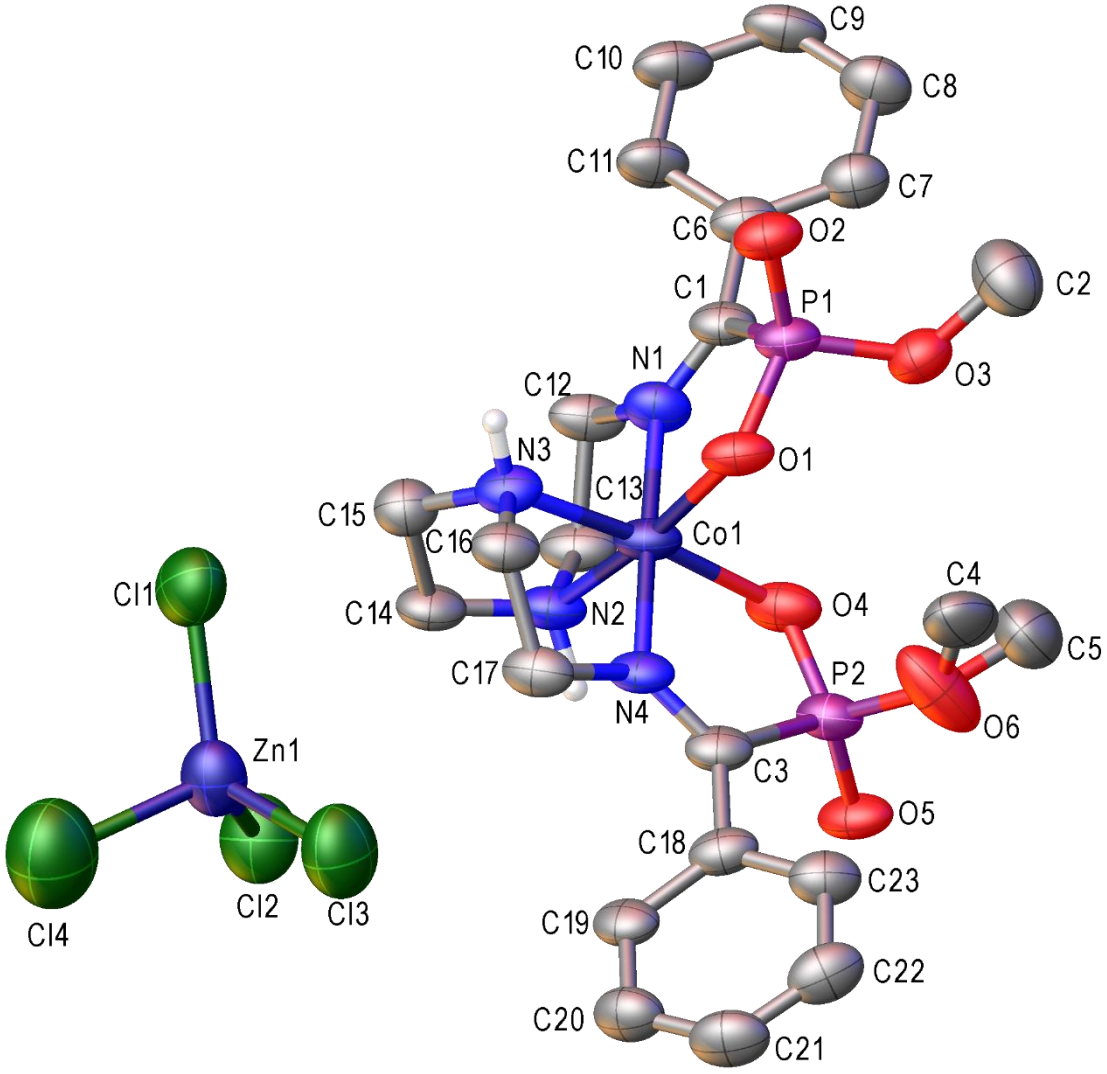

Figure A2.7 The asymmetric unit of compound **2.8**. Non-hetero atoms have been omitted for clarity.

Table A2.8 Crystal data and structure refinement for compound **2.9**

Identification code	nda16x180418
Empirical formula	$C_{66}H_{90}Cl_{12}Co_4N_{12}O_{18}P_6Zn_3$
Formula weight	2382.57
Temperature/K	120.01(10)
Crystal system	trigonal
Space group	R3c
a/Å	15.3774(10)
b/Å	15.3774(10)
c/Å	75.3092(18)
α/°	90
β/°	90
γ/°	120
Volume/Å^3	15422(2)
Z	6
ρ_{calc}g/cm^3	1.539
μ/mm^{-1}	9.966
F(000)	7236.0
Crystal size/mm^3	0.203 × 0.131 × 0.028
Radiation	CuKα (λ = 1.54184)
2Θ range for data collection/°	7.04 to 144.276
Index ranges	$-18 \leq h \leq 17$, $-13 \leq k \leq 18$, $-93 \leq l \leq 78$
Reflections collected	16210
Independent reflections	5600 [R_{int} = 0.0347, R_{sigma} = 0.0340]
Data/restraints/parameters	5600/3/369
Goodness-of-fit on F^2	1.029
Final R indexes [I>=2σ (I)]	R_1 = 0.0709, wR_2 = 0.2162
Final R indexes [all data]	R_1 = 0.1050, wR_2 = 0.2610
Largest diff. peak/hole / e Å^{-3}	0.70/-0.90
Flack parameter	0.241(16)

Refinement model description

This crystal structure is disordered over several positions. Attempts to constrain the highly distorted thermal ellipsoids using EADP of like atoms led to refinement instability. Solving the structure in lower symmetry space groups also proved unsuccessful.

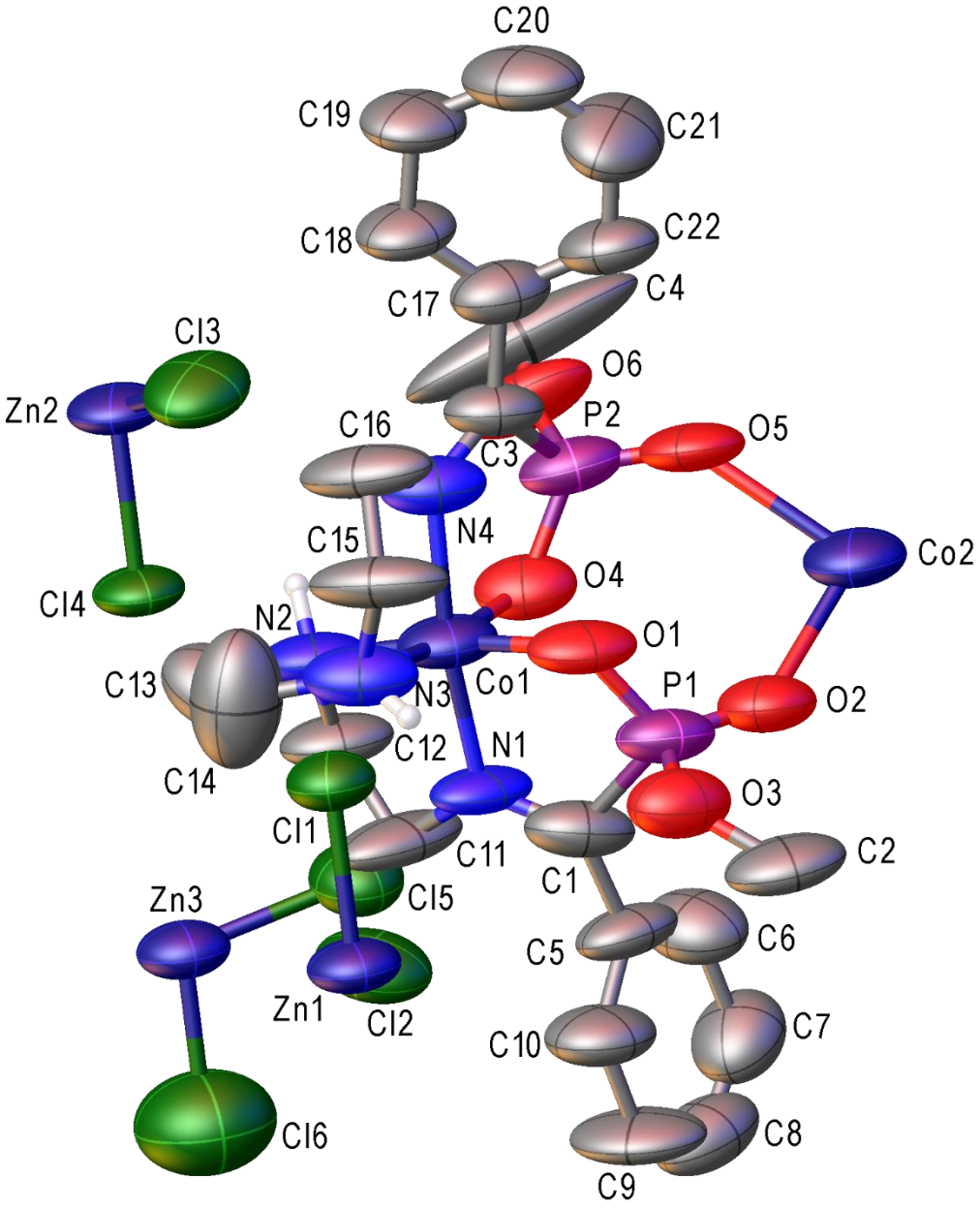

Figure A2.8 The asymmetric unit of compound **2.9** Non-hetero atoms have been omitted for clarity.

Table A2.9 Crystal data and structure refinement for compound **2.10**

Identification code	nda28a 270318
Empirical formula	$C_{22}H_{30}Cl_3CoN_4O_{6.4}P_2Zn$
Formula weight	745.49
Temperature/K	120.00(10)
Crystal system	monoclinic
Space group	$P2_1/n$
a/Å	11.7896(7)
b/Å	22.3431(13)
c/Å	12.2658(6)
α/°	90
β/°	96.699(5)
γ/°	90
Volume/Å^3	3209.0(3)
Z	4
ρ_{calc}g/cm^3	1.543
μ/mm^{-1}	8.577
F(000)	1517.0
Crystal size/mm^3	0.237 × 0.196 × 0.057
Radiation	CuKα (λ = 1.54184)
2Θ range for data collection/°	7.914 to 145.966
Index ranges	$-14 \leq h \leq 14$, $-26 \leq k \leq 27$, $-15 \leq l \leq 10$
Reflections collected	31474
Independent reflections	6407 [R_{int} = 0.0813, R_{sigma} = 0.0549]
Data/restraints/parameters	6407/66/471
Goodness-of-fit on F^2	1.053
Final R indexes [I>=2σ (I)]	R_1 = 0.0698, wR_2 = 0.1891
Final R indexes [all data]	R_1 = 0.0876, wR_2 = 0.2018
Largest diff. peak/hole / e Å^{-3}	1.12/-0.62

Refinement model description

Only 60% of methanol was found in the asymmetric unit. There were also 1.4(H_2O) molecules distributed over three positions, all poorly ordered. Most of these disordered solvent molecules were assigned dummy atoms, which were deleted thereafter and a solvent mask applied to buffer their effects. Only one water molecule has been modelled. The two phenyl rings present in this structure were both disordered in two different positions. They have been modelled as having partial occupancy of 50% per time in each of the positions shown in Figure A2.9. RIGU and ISOR from the OLEX2 software were employed to tidy up this structure. Therefore, the unit cell contains non-integer number of atoms in its empirical formula.

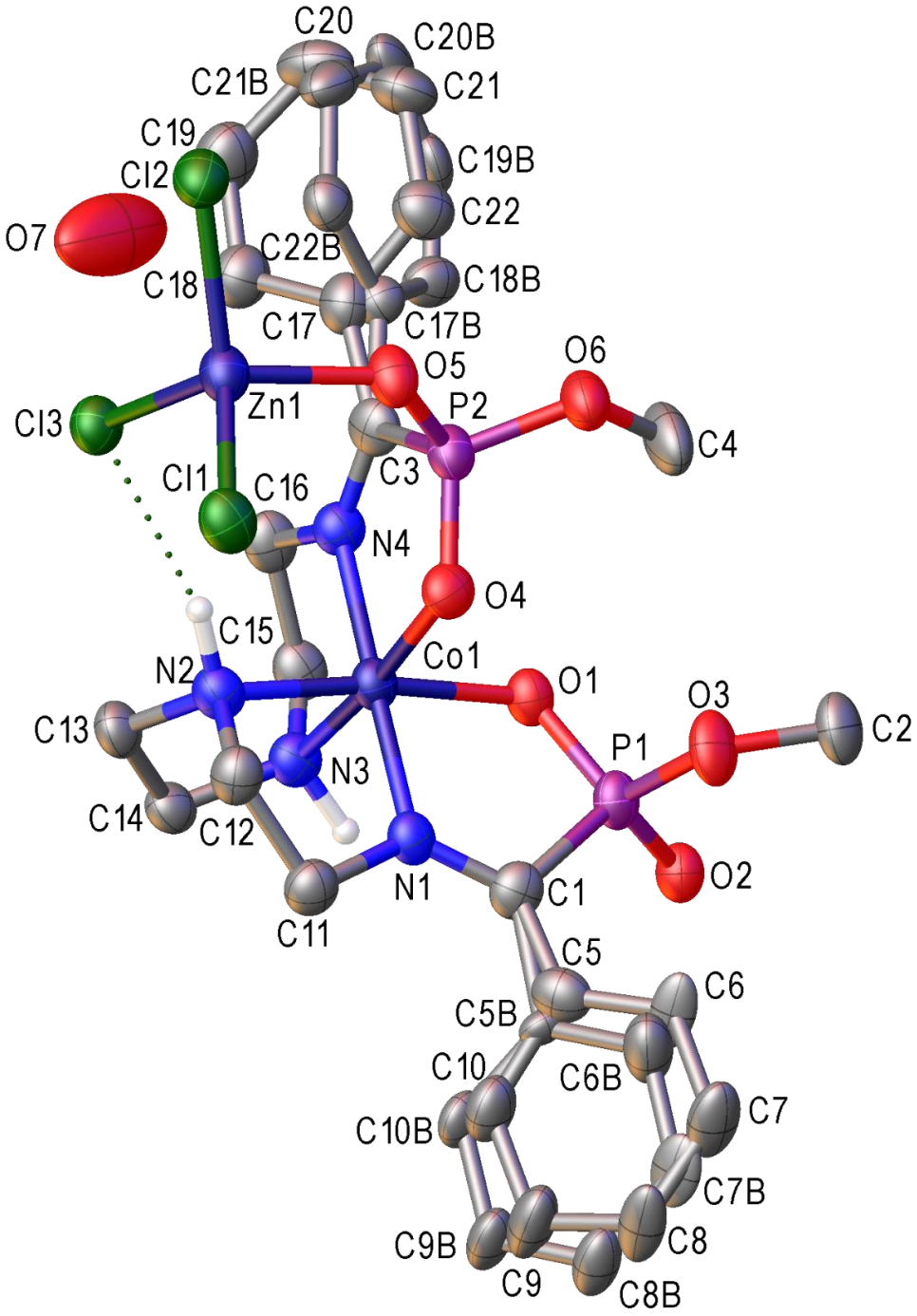

Figure A2.9 The asymmetric unit of compound **2.10** Non-hetero atoms have been omitted for clarity.

Table A2.10 Crystal data and structure refinement for compound **2.11**

Identification code	nda20b 060418
Empirical formula	$C_{20}H_{30}ClCoN_4O_7P_2$
Formula weight	594.80
Temperature/K	120.00(10)
Crystal system	monoclinic
Space group	$P2_1/c$
a/Å	14.7930(4)
b/Å	11.6061(3)
c/Å	14.8838(5)
α/°	90
β/°	104.573(3)
γ/°	90
Volume/Å^3	2473.17(13)
Z	4
ρ_{calc}g/cm^3	1.597
μ/mm^{-1}	8.093
F(000)	1232.0
Crystal size/mm^3	0.183 × 0.15 × 0.123
Radiation	CuKα (λ = 1.54184)
2Θ range for data collection/°	9.786 to 153.778
Index ranges	$-18 \leq h \leq 17$, $-14 \leq k \leq 14$, $-18 \leq l \leq 18$
Reflections collected	33260
Independent reflections	5188 [R_{int} = 0.0434, R_{sigma} = 0.0233]
Data/restraints/parameters	5188/6/321
Goodness-of-fit on F^2	1.045
Final R indexes [I>=2σ (I)]	R_1 = 0.0383, wR_2 = 0.0961
Final R indexes [all data]	R_1 = 0.0429, wR_2 = 0.0993
Largest diff. peak/hole / e Å^{-3}	0.73/-0.51

Refinement model description

This complex crystallised with one molecule of water in the asymmetric unit.

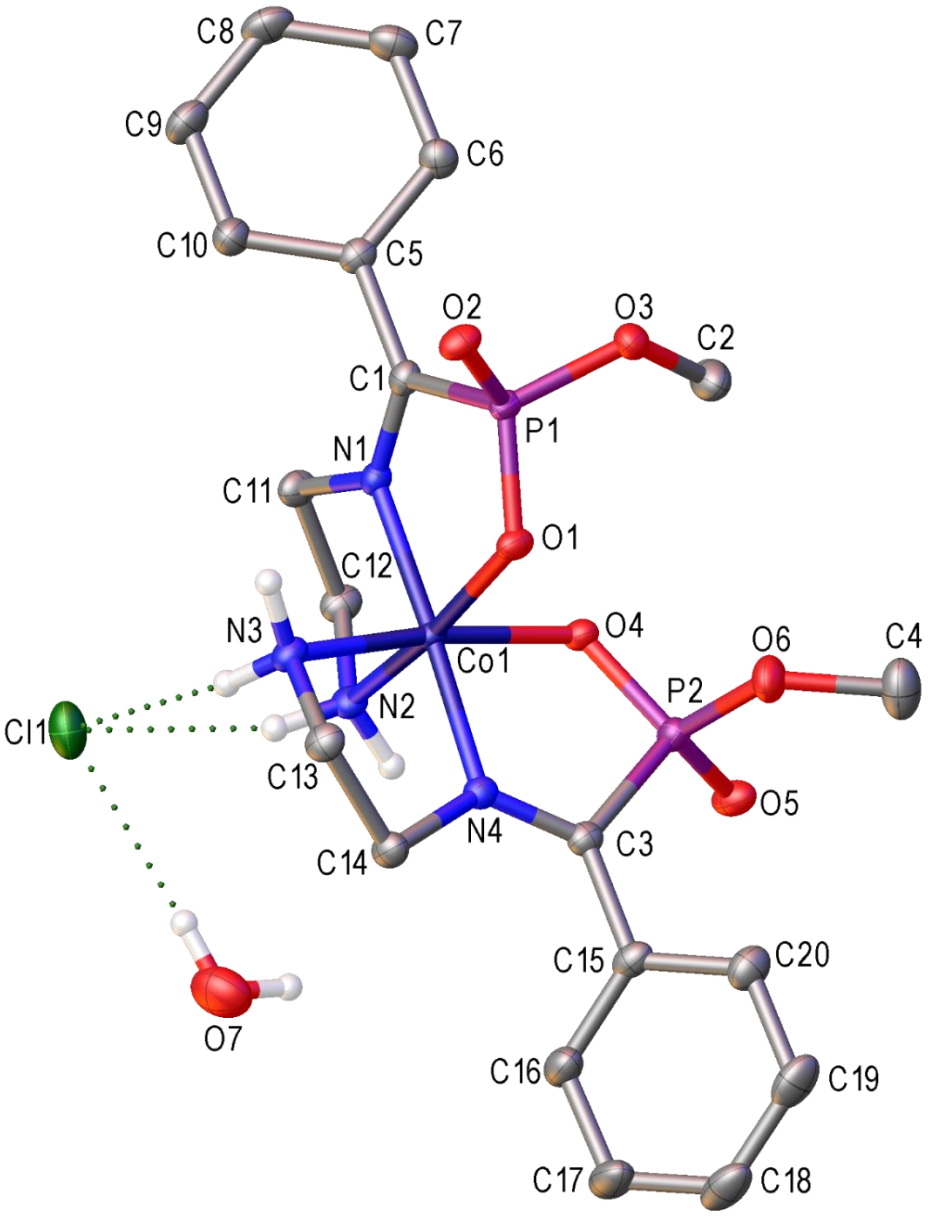

Figure A2.10 The asymmetric unit of compound **2.11** Non-hetero atoms have been omitted for clarity.

Table A2.11 Crystal data and structure refinement for compound **2.12**

Identification code	nda32 07032019
Empirical formula	$C_{20}H_{30}ClCoN_4O_7P_2$
Formula weight	594.80
Temperature/K	120.01(10)
Crystal system	triclinic
Space group	PĪ
a/Å	9.0001(3)
b/Å	9.5389(3)
c/Å	15.3957(4)
α/°	86.716(2)
β/°	76.364(3)
γ/°	82.605(3)
Volume/Å^3	1273.30(7)
Z	2
ρ_{calc}g/cm^3	1.551
μ/mm^{-1}	7.860
F(000)	616.0
Crystal size/mm^3	0.284 × 0.201 × 0.108
Radiation	CuKα (λ = 1.54184)
2Θ range for data collection/°	9.352 to 121.548
Index ranges	$-10 \leq h \leq 9$, $-10 \leq k \leq 10$, $-17 \leq l \leq 11$
Reflections collected	6527
Independent reflections	3840 [R_{int} = 0.0482, R_{sigma} = 0.0361]
Data/restraints/parameters	3840/6/329
Goodness-of-fit on F^2	1.078
Final R indexes [I>=2σ (I)]	R_1 = 0.0456, wR_2 = 0.1238
Final R indexes [all data]	R_1 = 0.0476, wR_2 = 0.1253
Largest diff. peak/hole / e Å^{-3}	0.69/-0.51

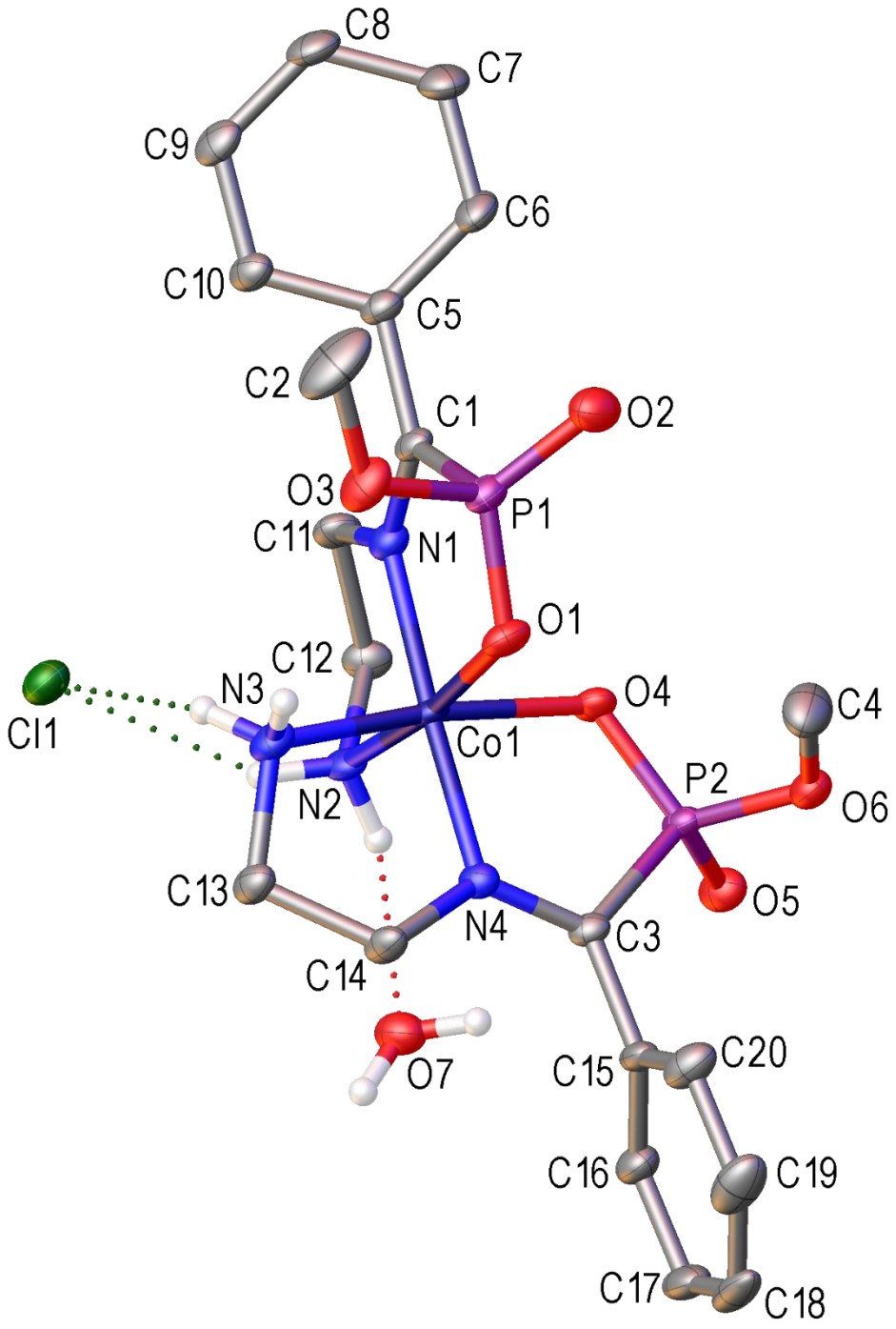

Figure A2.11 The asymmetric unit of compound **2.12** Non-hetero atoms have been omitted for clarity.

Table A2.12 Crystal data and structure refinement for compound **2.13**

Identification code	nda34a 070319
Empirical formula	$C_{21}H_{32}ClCoN_4O_7P_2$
Formula weight	608.82
Temperature/K	120.00(10)
Crystal system	triclinic
Space group	$P\bar{1}$
a/Å	10.7865(6)
b/Å	11.5463(7)
c/Å	12.4136(5)
α/°	103.013(4)
β/°	98.655(4)
γ/°	114.250(5)
Volume/Å^3	1321.05(13)
Z	2
ρ_{calc}g/cm^3	1.531
μ/mm^{-1}	7.589
F(000)	632.0
Crystal size/mm^3	0.153 × 0.093 × 0.058
Radiation	CuKα (λ = 1.54184)
2Θ range for data collection/°	7.6 to 154.712
Index ranges	$-13 \leq h \leq 12$, $-14 \leq k \leq 14$, $-15 \leq l \leq 15$
Reflections collected	20145
Independent reflections	5344 [R_{int} = 0.0917, R_{sigma} = 0.0638]
Data/restraints/parameters	5344/5/345
Goodness-of-fit on F^2	1.166
Final R indexes [I>=2σ (I)]	R_1 = 0.0658, wR_2 = 0.1807
Final R indexes [all data]	R_1 = 0.0881, wR_2 = 0.2283
Largest diff. peak/hole / e Å^{-3}	0.61/-1.27

Refinement model description

This complex crystallised with one molecule of methanol (disordered) in the asymmetric unit.

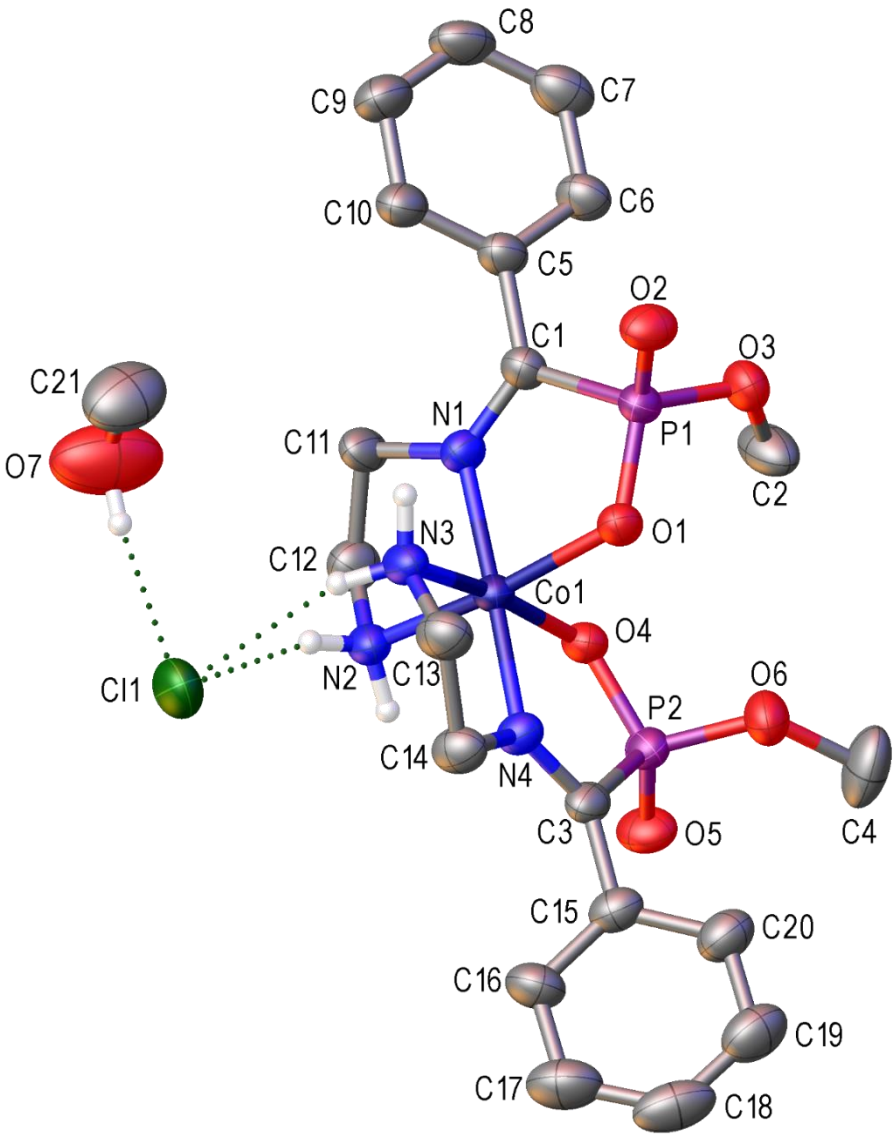

Figure A2.12 The asymmetric unit of compound **2.13**. Non-hetero atoms have been omitted for clarity.

Table A2.13 Crystal data and structure refinement for compound **2.14**

Identification code	nda35z240418
Empirical formula	$C_{24.75}H_{49.25}Cl_4Co_2N_8O_{10.75}P_2Zn$
Formula weight	1018.29
Temperature/K	120.00(10)
Crystal system	monoclinic
Space group	$P2_1/n$
a/Å	21.196(2)
b/Å	12.4743(4)
c/Å	26.969(3)
α/°	90
β/°	144.03(2)
γ/°	90
Volume/Å^3	4188.8(15)
Z	4
ρ_{calc}g/cm^3	1.615
μ/mm^{-1}	10.388
F(000)	2088.0
Crystal size/mm^3	0.22 × 0.171 × 0.046
Radiation	CuKα (λ = 1.54184)
2Θ range for data collection/°	8.226 to 139.048
Index ranges	$-25 \leq h \leq 23$, $-14 \leq k \leq 14$, $-30 \leq l \leq 32$
Reflections collected	45134
Independent reflections	7795 [R_{int} = 0.0808, R_{sigma} = 0.0428]
Data/restraints/parameters	7795/3/489
Goodness-of-fit on F^2	1.136
Final R indexes [I>=2σ (I)]	R_1 = 0.1512, wR_2 = 0.3272
Final R indexes [all data]	R_1 = 0.1547, wR_2 = 0.3288
Largest diff. peak/hole / e Å^{-3}	1.55/-2.11

Refinement model description

The asymmetric unit of this crystal contains two molecules. One of them was well ordered whereas the other (the bottom structure of Figure A2.13) has some disorder on its phosphonate arm. The disorder has been modelled as two phosphonate arms on the same half of the complex. The phosphorus atom labelled P2B has a higher occupancy of 75% while P2A is only there 25% of the time. The methanol has 75% occupancy. Some isotropic non-hydrogen atoms have been used for the model in Fig. A13 because fitting those atoms into thermal ellipsoids led to refinement instability. EADP was applied on C21 and C22 to improve the shape of their ellipsoids. The disorder in the bottom structure (Fig. A2.13) accounts for the high R factor.

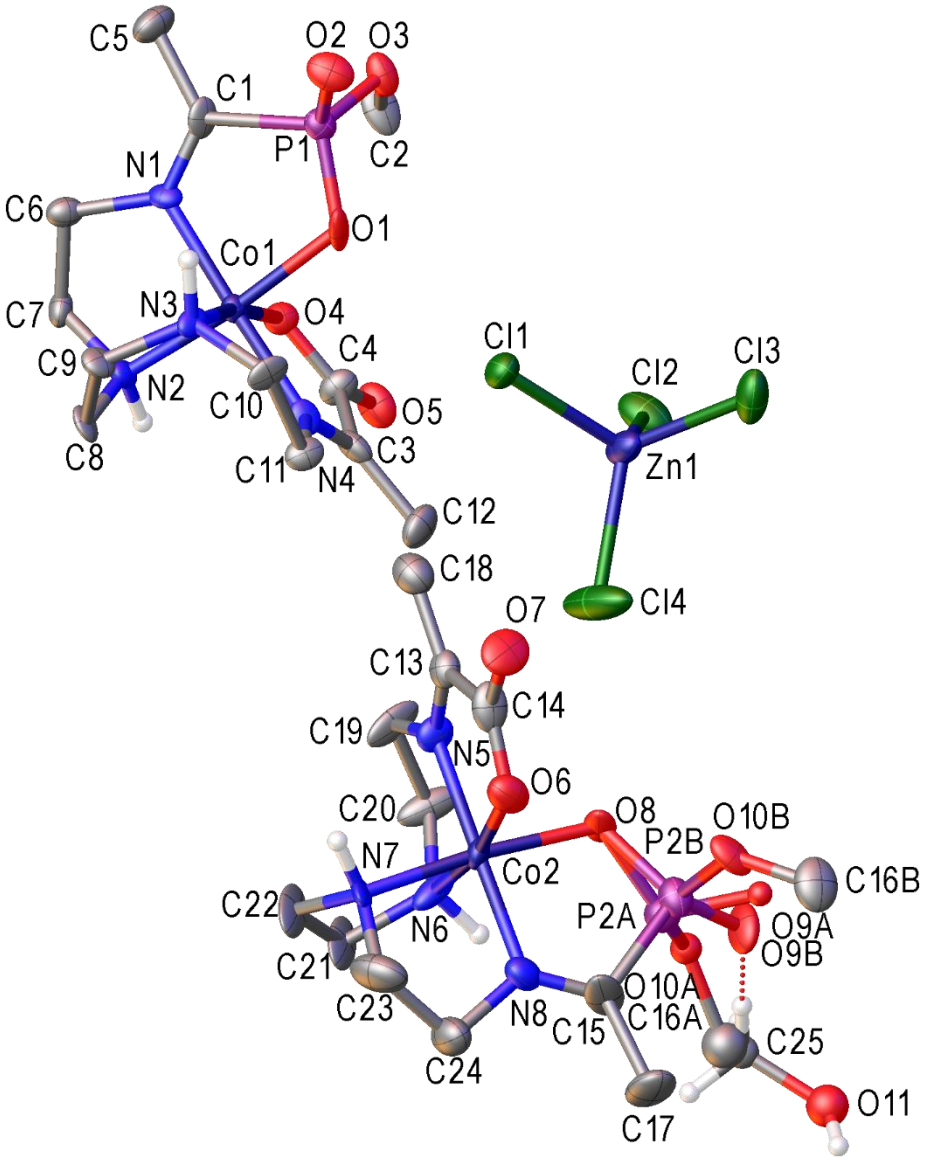

Figure A2.13 The asymmetric unit of compound **2.14** Non-hetero atoms have been omitted for clarity.

Table A2.14 Crystal data and structure refinement for 2,6-lutidine.

Identification code	ndagreenxtal 080319
Empirical formula	$C_7H_9Cl_2NZn_{0.5}$
Formula weight	210.74
Temperature/K	120.00(10)
Crystal system	orthorhombic
Space group	Pbcn
a/Å	16.7833(10)
b/Å	8.7561(5)
c/Å	12.9850(9)
α/°	90
β/°	90
γ/°	90
Volume/Å^3	1908.2(2)
Z	8
ρ_{calc}g/cm^3	1.467
μ/mm^{-1}	6.889
F(000)	856.0
Crystal size/mm^3	0.164 × 0.112 × 0.088
Radiation	CuKα (λ = 1.54184)
2Θ range for data collection/°	10.542 to 103.252
Index ranges	$-16 \leq h \leq 15$, $-8 \leq k \leq 8$, $-10 \leq l \leq 13$
Reflections collected	2382
Independent reflections	1046 [R_{int} = 0.0244, R_{sigma} = 0.0377]
Data/restraints/parameters	1046/0/98
Goodness-of-fit on F^2	1.091
Final R indexes [I>=2σ (I)]	R_1 = 0.0560, wR_2 = 0.1508
Final R indexes [all data]	R_1 = 0.0663, wR_2 = 0.1591
Largest diff. peak/hole / e Å^{-3}	0.57/-0.85

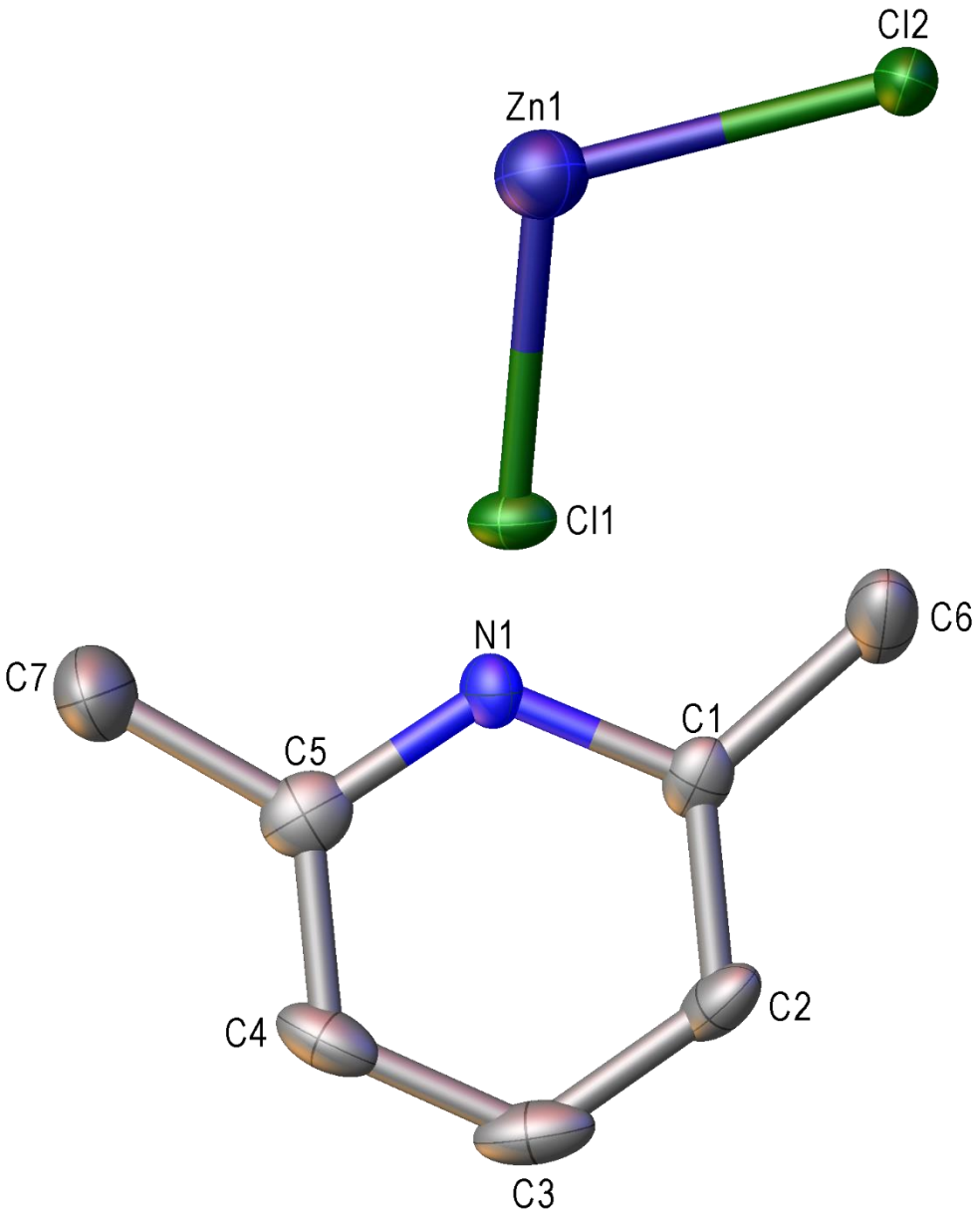

Figure A2.14 The asymmetric unit of 2,6-lutidine. Non-hetero atoms have been omitted for clarity.

Appendix 3 X-ray information for chapter 3 complexes

Table A3.1 Crystal data and structure refinement for compound **3.2b**.

Identification code	nda41b
Empirical formula	$C_{30}H_{70}Cl_6Co_2N_{10}O_{13}P_2Zn_2$
Formula weight	1302.20
Temperature/K	119.97(14)
Crystal system	triclinic
Space group	$P\bar{1}$
a/Å	9.7293(4)
b/Å	9.8259(4)
c/Å	30.4424(17)
α/°	94.625(4)
β/°	93.193(4)
γ/°	118.496(4)
Volume/Å^3	2534.6(2)
Z	2
ρ_{calc}g/cm^3	1.706
μ/mm^{-1}	10.180
F(000)	1340.0
Crystal size/mm^3	0.113 × 0.083 × 0.03
Radiation	CuKα (λ = 1.54184)
2Θ range for data collection/°	8.794 to 140.27
Index ranges	$-9 \leq h \leq 11$, $-11 \leq k \leq 9$, $-25 \leq l \leq 36$
Reflections collected	9891
Independent reflections	7385 [R_{int} = 0.0860, R_{sigma} = 0.0701]
Data/restraints/parameters	7385/3/607
Goodness-of-fit on F^2	1.118
Final R indexes [I>=2σ (I)]	R_1 = 0.1127, wR_2 = 0.2965
Final R indexes [all data]	R_1 = 0.1168, wR_2 = 0.3002
Largest diff. peak/hole / e Å^{-3}	3.79/-1.25

Refinement model description

The completeness (79%) of the data set used to solve for compound **3.2b** is lower than the acceptable standard. This was primarily because the data set was collected in a crystal system with higher symmetry than actually was required for the structural solution. Therefore, the structure has not been used for bond lengths and angles in the discussion section. It has only been shown to model connectivity of the atoms in that molecule.

Two molecules were found in the asymmetric unit, both of them related by a mirror plane. Seven water molecules were also located in the asymmetric unit. The two molecules showed no interactions between each other even when the extended packing view was checked. However, each molecule had some hydrogen bonding interaction with some of the water molecules. There was an intra-hydrogen bonding interaction between of the chlorides on the $ZnCl_3$ arm of each complex and a facial secondary amine.

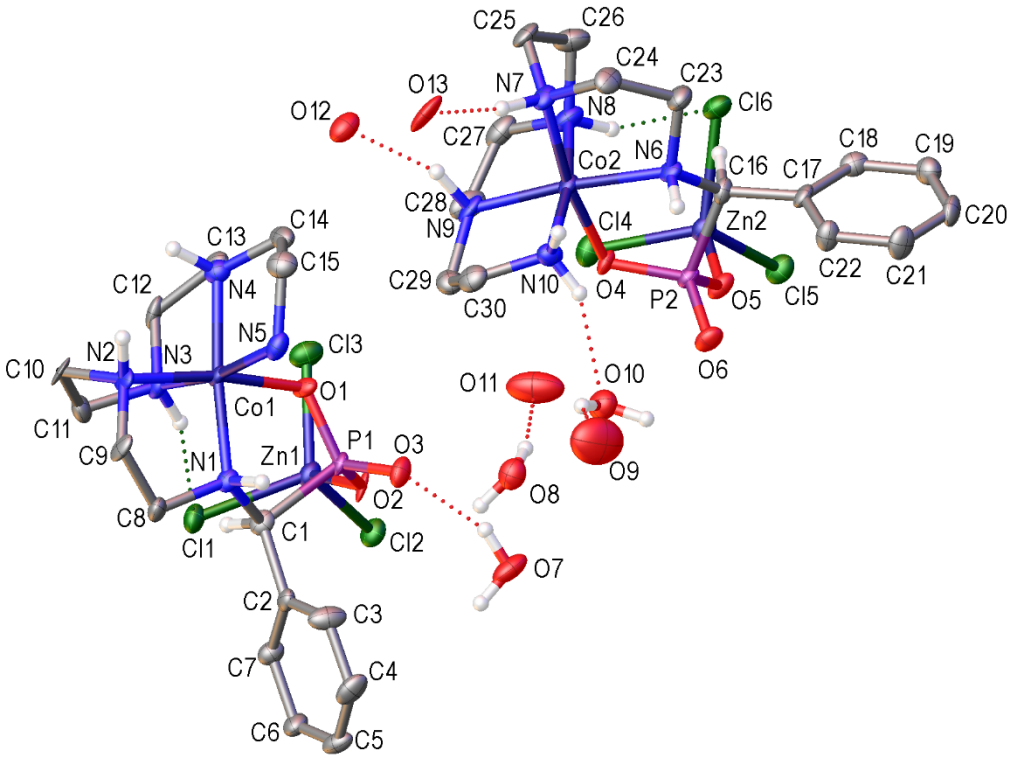

Figure A3.1 The asymmetric unit of **3.2b**. Non-hetero atoms have been omitted for clarity.

Table A3.2 Crystal data and structure refinement for compound **3.5**.

Identification code	NDA39C
Empirical formula	$C_{14}H_{31}CoF_3N_4O_9PS$
Formula weight	578.39
Temperature/K	120.00(10)
Crystal system	orthorhombic
Space group	Pbca
a/Å	15.9745(18)
b/Å	12.7365(8)
c/Å	22.7611(13)
α/°	90
β/°	90
γ/°	90
Volume/Å^3	4631.0(7)
Z	8
ρ_{calc}g/cm^3	1.659
μ/mm^{-1}	8.024
F(000)	2400.0
Crystal size/mm^3	0.027 × 0.041 × 0.113
Radiation	CuKα (λ = 1.54184)
2Θ range for data collection/°	7.768 to 152.362
Index ranges	$-13 \leq h \leq 19$, $-15 \leq k \leq 11$, $-28 \leq l \leq 28$
Reflections collected	16933
Independent reflections	4737 [R_{int} = 0.0897, R_{sigma} = 0.0755]
Data/restraints/parameters	4737/0/311
Goodness-of-fit on F^2	1.104
Final R indexes [I>=2σ (I)]	R_1 = 0.0995, wR_2 = 0.2612
Final R indexes [all data]	R_1 = 0.1492, wR_2 = 0.3252
Largest diff. peak/hole / e Å^{-3}	0.96/-1.06

Refinement model description

One molecule of the triflate anion was located in the asymmetric unit of this crystal. The anion was disordered over most of its hetero atoms. Attempts to use the data set after absorption correction failed to yield good solutions. That was primarily because most of the data was noisy(see the I/σ vs. resolution profile attached in Fig. A3.3). So, once the absorption correction was done; outliers applied as well as removing bad reflections, one gets left with nothing for a structural solution. The crystal size shown here is as have been directly measured from the crystal movie window.

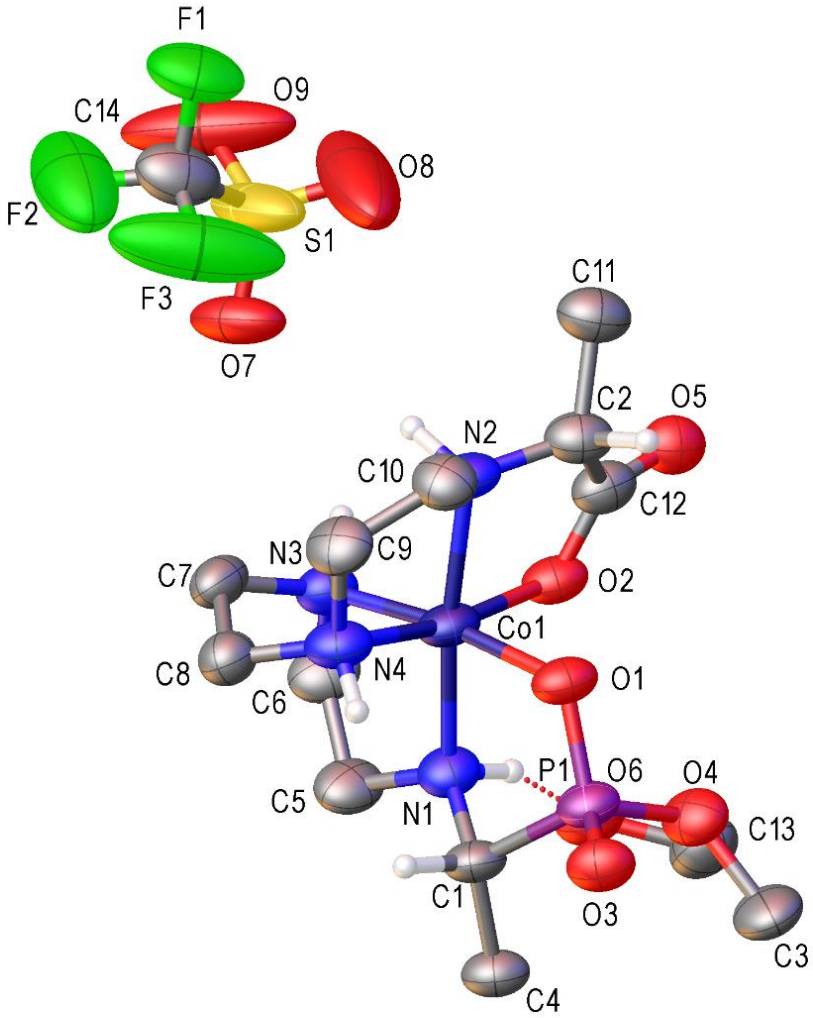

Figure A3.2 The asymmetric unit of **3.5**. Non-hetero atoms have been omitted for clarity.

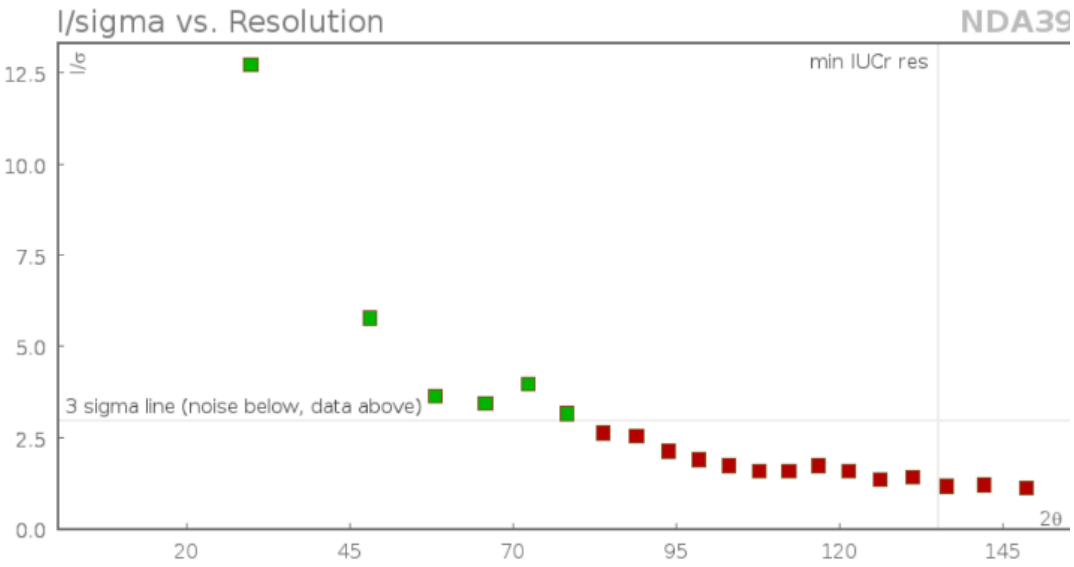

Figure A3.3 I/σ vs. resolution profile of **3.5**'s structural model.

Table A3.3 Crystal data and structure refinement for compound **3.6**.

Identification code	nda22A
Empirical formula	$C_{12}H_{28}ClCoN_4O_6$
Formula weight	418.76
Temperature/K	120.02(10)
Crystal system	monoclinic
Space group	$P2_1/c$
a/Å	10.2796(3)
b/Å	12.7146(3)
c/Å	13.2413(4)
α/°	90
β/°	96.262(3)
γ/°	90
Volume/Å^3	1720.33(8)
Z	4
ρ_{calc}g/cm^3	1.617
μ/mm^{-1}	9.592
F(000)	880.0
Crystal size/mm^3	0.215 × 0.118 × 0.066
Radiation	CuKα (λ = 1.54184)
2Θ range for data collection/°	8.654 to 152.634
Index ranges	$-12 \leq h \leq 11$, $-15 \leq k \leq 8$, $-16 \leq l \leq 15$
Reflections collected	6274
Independent reflections	3492 [R_{int} = 0.0357, R_{sigma} = 0.0470]
Data/restraints/parameters	3492/8/225
Goodness-of-fit on F^2	1.047
Final R indexes [I>=2σ (I)]	R_1 = 0.0359, wR_2 = 0.0928
Final R indexes [all data]	R_1 = 0.0404, wR_2 = 0.0960
Largest diff. peak/hole / e Å^{-3}	0.47/-0.69

Refinement model description

Two water molecules were located in the asymmetric unit of this crystal. Both of them were bound to the complex through O3. Actually, one of the water molecules was directly bound to O3 of the complex through a hydrogen bond on one of its hydrogens while its other hydrogen bound to the O6 of the other water molecule. The model also showed a hydrogen bond interaction between O6 of the second water molecule and the chloride counter ion of the molecule.

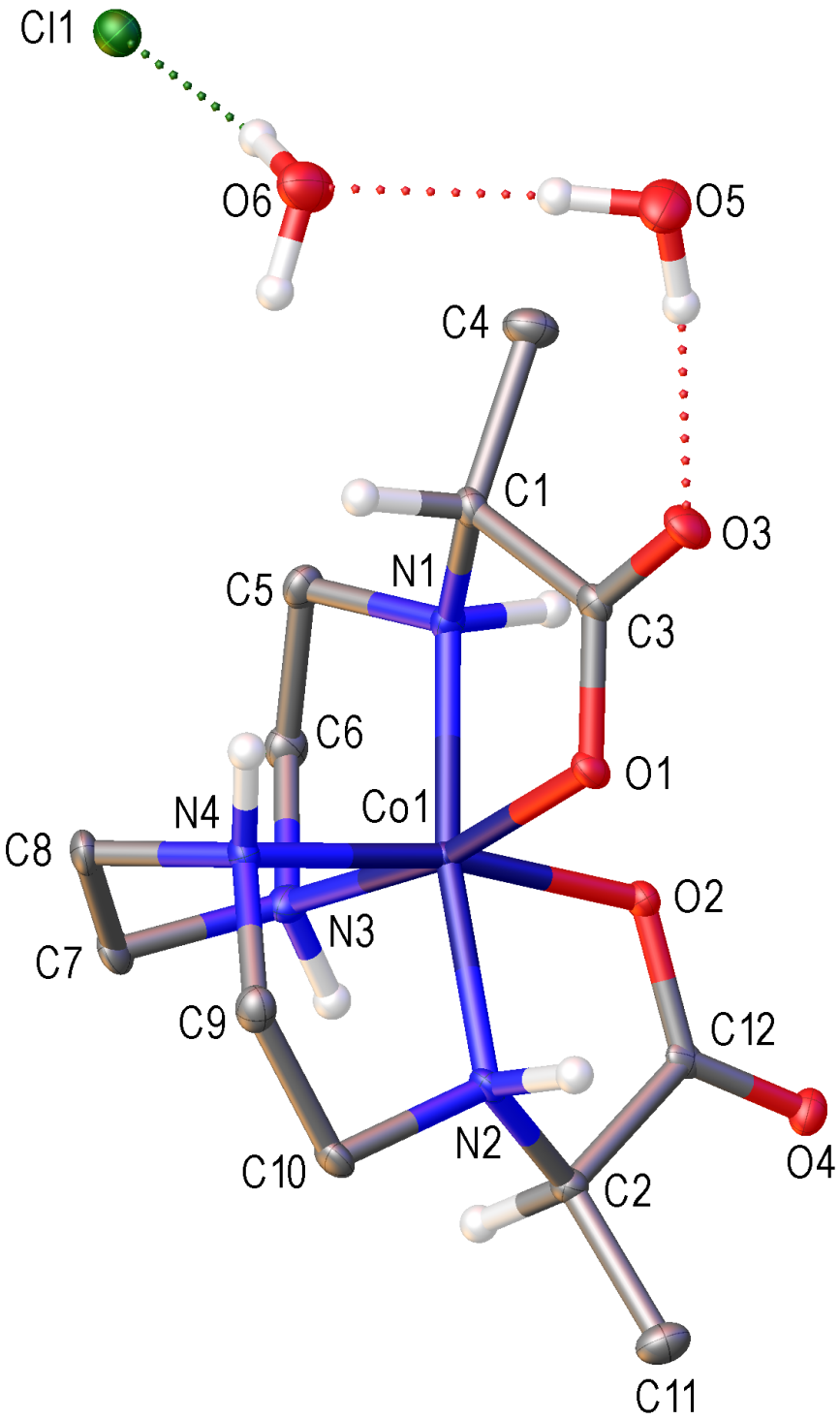

Figure A3.4 The asymmetric unit of compound **3.6**. Most hydrogen atoms have been omitted for clarity.

Table A3.4 Crystal data and structure refinement for compound **3.6b**.

Identification code	nda33a
Empirical formula	$C_{26}H_{48}Co_2F_6N_8O_{14}S_2$
Formula weight	992.70
Temperature/K	120.01(10)
Crystal system	triclinic
Space group	$P\bar{1}$
a/Å	12.0378(5)
b/Å	12.8059(4)
c/Å	14.3205(5)
α/°	101.598(3)
β/°	114.318(4)
γ/°	90.875(3)
Volume/Å^3	1958.70(14)
Z	2
ρ_{calc}g/cm^3	1.683
μ/mm^{-1}	8.550
F(000)	1024.0
Crystal size/mm^3	0.259 × 0.138 × 0.11
Radiation	CuKα (λ = 1.54184)
2Θ range for data collection/°	6.956 to 153.392
Index ranges	$-11 \leq h \leq 14$, $-15 \leq k \leq 15$, $-18 \leq l \leq 17$
Reflections collected	15236
Independent reflections	8015 [R_{int} = 0.0396, R_{sigma} = 0.0497]
Data/restraints/parameters	8015/26/555
Goodness-of-fit on F^2	1.047
Final R indexes [I>=2σ (I)]	R_1 = 0.0877, wR_2 = 0.2487
Final R indexes [all data]	R_1 = 0.0958, wR_2 = 0.2614
Largest diff. peak/hole / e Å^{-3}	2.30/-1.57

Refinement model description

Two triflate anions were located in the asymmetric unit of this crystal. One of the anions was bound to one of the complexes through a hydrogen bond between the hydrogen of N8 and O12 of the anion. Three other hydrogen bond interactions were observed between the two complexes. They were O3---H-N5, O4---H-N6 and O7---H-N1 respectively. The other triflate anion had disordered fluorine atoms which have been modelled to have thermal parameters as close to their neighbouring atoms as possible by applying ISOR[101, 103]. The disorder is believed to contribute to the high R factor of this structural model given that its R_{int} value is 0.0396.

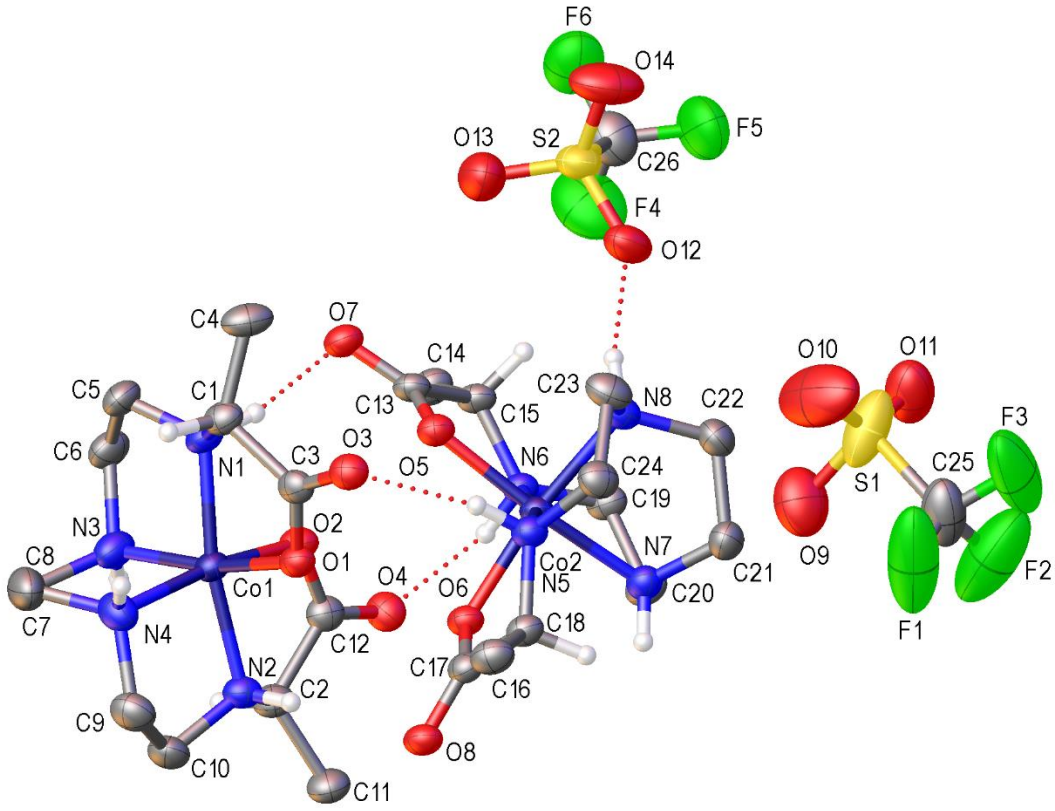

Figure A3.5 The asymmetric unit of compound **3.6b**. Most hydrogen atoms have been omitted for clarity.

101. Dolomanov, O. V.; Bourhis, L. J.; Gildea, R. J.; Howard, J. A.; Puschmann, H., OLEX2: a complete structure solution, refinement and analysis program. *Journal of Applied Crystallography* **2009,** *42* (2), 339-341.

103. Sheldrick, G. M., Crystal structure refinement with SHELXL. *Acta Crystallographica Section C: Structural Chemistry* **2015,** *71* (1), 3-8.